EEG connectivity in infants at risk for Autism Spectrum Disorder

Rianne Haartsen

Supervised by:

Professor Mark H. Johnson

Dr. Emily J.H. Jones

Thesis submitted for the degree of:

Doctor of Philosophy

Birkbeck, University of London

2019

Birkbeck, University of London, Malet Street, London, WC1E 7HX

Declaration

I, Rianne Haartsen, hereby declare that all the work, with a few exceptions, presented in this thesis is entirely my own.
This PhD project aimed to examine associations between EEG connectivity at infancy and familial risk, diagnostic outcome, and severity of traits of Autism Spectrum Disorder at toddlerhood. This project requires longitudinal datasets, and therefore utilises data from the British Autism Study of Infant Siblings (BASIS). The exceptions consist of the preprocessing of EEG, behavioural, and questionnaire data from 2 cohorts in the BASIS study and data collected at Utrecht University. For one of the cohorts of the BASIS study, raw EEG data were collected by other researchers, but the preprocessing, cleaning, and analysing of the EEG data was done by myself. The details of these exceptions are clearly stated in *Section 2.5 Description of datasets and statement of contribution*, and throughout this thesis.

Based on the work presented in this thesis, I published 2 peer reviewed articles:
Chapter 1:
Haartsen, R., Jones, E.J.H., & Johnson, M.H. (2016). Human brain development over the early years. *Current opinion in behavioral sciences, 10,* 149 – 154.
Chapter 4:
Haartsen, R., Jones, E.J.H., Orekhova, E.V., Charman, T., Johnson M.H., & The BASIS team (In Press). Functional EEG connectivity in infants associates with later restricted and repetitive behaviours in autism: a replication study. *Translational Psychiatry.*

Signed:

Rianne Haartsen

24th of January, 2019

Abstract

Autism Spectrum Disorder (ASD) is characterized by social and communication difficulties, and restricted and repetitive behaviours, and is typically diagnosed during toddlerhood. Electroencephalographic (EEG) connectivity during infancy may predict later diagnostic outcome, and dimensional traits, although results vary with differences in methods. The aim of this thesis is to examine how infant EEG connectivity relates to familial risk, and later categorical and dimensional outcomes of ASD. A previous study found alpha band hyperconnectivity in 14-month-old infants who developed ASD compared to infants who did not develop ASD at 36 months. Chapter 3 shows that methods used in this previous study indeed provide reliable results. Chapter 4 describes the replication study using identical methods to the previous study. Although the difference between groups was not replicated, the association between alpha connectivity and restricted and repetitive behaviours during toddlerhood was replicated. Chapter 5 tested the hypothesis that social and communication difficulties relate to theta connectivity in response to social and non-social stimuli. Theta connectivity was increased during social compared to non-social stimuli. Network topologies differed between groups with high and low familial risk, but not between categorical outcome groups. Theta connectivity was not associated with dimensional traits at toddlerhood. Chapter 6 showed that graph organisation was not related to familial risk, or diagnostic or dimensional outcomes at toddlerhood. Finally, Chapter 7 combined measures from previous chapters and examined how these relate to dimensional outcomes at childhood. Graph organisation at infancy showed a stronger association with dimensional outcomes at childhood than other connectivity measures. Overall, the results in this thesis illustrate the variability in developmental trajectories in ASD, while emphasizing the complexity of the disorder and use of a dimensional approach to ASD. Chapter 8 further discusses contributions and implications for research of EEG connectivity as early predictive marker for ASD.

Acknowledgments

I would first of all like to thank my supervisors Professor Mark H. Johnson and dr. Emily J.H. Jones. I'm incredibly grateful for their guidance and encouragement while becoming an independent researcher, and developing my own critical thinking. I would further like to thank Elena V. Orekhova for teaching me how to do connectivity analyses, and Greg Pasco and Tony Charman for answering all my questions with regard to clinical questionnaires, interviews, and behavioural assessments. I would also like to thank Professor Michelle de Haan and dr. Elizabeth Milne for examining this PhD thesis, and drs. Charlotte Tye and Virginia Carter Leno for helping me prepare for the PhD examination.

This work would not have been possible without the BASIS network and all the participating families. Thank you to JJ and Chloë who taught me how to collect data for the infant visits of the BASIS study. Also thanks to Anna Gui, and Elizabeth Shephard who were involved in the follow-up assessments of the BASIS cohorts. Furthermore, many thanks to Professor Chantal Kemner, dr. Carlijn van den Boomen, and Bauke van der Velde in Utrecht for their guidance and discussions when I was on my secondment at Utrecht University, the Netherlands. Also thanks to the research group and participating families at the Kinder Kennis Centrum. This work has been supported by a grant from the European Community's Horizon 2020 Program under grant agreement n° 642996 (BRAINVIEW). I would further like to thank all the PIs and ESRs within the BRAINVIEW network. It has been amazing to be part of BRAINVIEW and I have gained more experience and knowledge during the last 3 years and the training weeks.

I would like to thank all my friends, and colleagues: thank you to Anna, Maheen, Elena, Tessel, and Judit for all your support during our coffee breaks, lunch breaks and dinners, to Fernanda and Joanneke for listening to all my frustrations and worries and lifting up my spirits, and to all my colleagues at the CBCD. Finally, I am very thankful for my parents and siblings, Yvonne and Bas, for their unconditional support and encouragement to seize every opportunity, even if it is abroad.

Table of Contents

List of Tables

List of Figures

List of Abbreviations

ADOS	Autism Diagnostic Observational Schedule
ADI-R	Autism Diagnostic Interview - Revised
ASD	Autism Spectrum Disorder
BCT	Brain Connectivity Toolbox
CI	Circumscribed Interests (subtype of Restricted and Repetitive Behaviours symptom core domain)
C_{wnorm}	Normalised clustering coefficient
dACC	dorsal anterior cingulate cortex
DAWBA	Development and Wellbeing Assessment
dbWPLI	Debiased Weighted Phase Lag Index
DSM-V	Diagnostic and Statistical Manual of Mental Disorders, 5th Edition
EEG	Electroencephalography
FA	Fractional Anisotropy
FEF	Frontal Eye Field
FFT	Fast Fourier Transform
fMRI	functional Magnetic Resonance Imaging
fNIRS	functional Near-Infrared Spectroscopy
FT	Fourier Transform
HR infants	Infants with an older sibling who has a diagnosis of ASD, which poses the infant at higher risk for developing the disorder at later age as well
HR-ASD infants	High-risk infants who develop ASD at a later age
HR-Atyp infants	High-risk infants who do not develop typically, but are not meeting criteria for ASD at a later age
HR-no ASD infants	High-risk infants who do not develop ASD at a later age
HR-TD infants	High-risk infants who develop typically at a later age

ICA	Independent Component Analysis
IS	Insistence on Sameness (subtype of Restricted and Repetitive Behaviours symptom core domain)
LFP	Local Field Potential
LR infants	Infants with an older sibling who is typically developing, which poses the infant a low risk for developing ASD at a later age
L_{wnorm}	Normalised path length
MEG	Magnetoencephalography
MRI	Magnetic Resonance Imaging
MSEL	Mullen Scales of Early Learning
MSEL ELC scores	Mullen Scales of Early Learning Early Learning Composite scores
NBS	Network Based Statistics
PAC	Phase Amplitude Coupling
PCA	Principal Component Analysis
PLI	Phase Lag index
RBS	Repetitive Behavior Scale
RMB	Repetitive Motor Behaviours (subtype of Restricted and Repetitive Behaviours symptom core domain)
RRB	Restricted and Repetitive Behaviours
SL	Synchronization likelihood
SRS-2	Social Responsiveness Scale, Second version
SCQ	Social Communication Questionnaire
SWI	Small-Worldness Index
TD	Typically developing
VABS-II	Vineland Adaptive Behavior Scale, Second version

Chapter 1: Introduction

1.1. The importance of studying ASD

Autism Spectrum Disorder (ASD) is a developmental disorder that is diagnosed during toddlerhood and childhood, and is characterised by difficulties in social communication and interaction, and restricted and repetitive behaviours (American Psychological Association, 2013). ASD was first described by Kanner (Kanner, 1943) and Asperger (Asperger, 1944). The disorder was then thought of as rare, but now about 1 in every 68 children is diagnosed with ASD in the United States. Males receive a diagnosis 4 times more often than females (Christensen et al., 2016). The disorder has serious impact on the daily life of the diagnosed individuals and those in the families around them. Recent findings showed that individuals with ASD are at higher risk for fatal unintentional injury than individuals without ASD, especially for individuals younger than 15 years (Guan & Li, 2017).

Reliable diagnoses can be currently made after behavioural symptoms have emerged, which is typically during toddlerhood between 2 and 3 years of age (Charman & Baird, 2002). Diagnoses of ASD are largely stable during later life, even though developmental trajectories during childhood vary between individuals (Lord, Bishop, & Anderson, 2015; Lord, Luyster, Guthrie, & Pickles, 2012). The specific set of symptoms varies widely between individuals who have received an ASD diagnosis, demonstrating the heterogeneity of the disorder. Early diagnosis however is important in ASD as this can help towards early treatment or intervention that in turn can improve later outcome in terms of symptom severity and cognitive skills (Green et al., 2015, 2017; Pickles et al., 2016; Webb, Jones, Kelly, & Dawson, 2014).

Early diagnoses are currently based on subjective observations of ASD behaviours that do not emerge until after infancy. Previous research in ASD however suggests that atypicalities in neural processing might arise before the onset of the disorder during toddlerhood, and that these atypicalities could be used as objective markers for ASD (Jeste, Frohlich, & Loo, 2015; Jones, Gliga, Bedford, Charman, & Johnson, 2014). Research into markers for ASD has the potential to inform on later categorical outcomes (whether an infant will develop ASD or not) and dimensional traits (the severity and the nature of the ASD symptoms experienced by the individual), stratification of individuals into subgroups of ASD, and treatment (selection of the treatment, predicting treatment response, or monitoring the effectiveness of the treatment). Furthermore, research on ASD markers could improve understanding of underlying mechanisms of ASD (Loth, Charman, Collier, & Williams, 2016; Singh & Rose, 2009; Walsh, Elsabbagh, Bolton, & Singh, 2011). Finally, replication of previous findings in independent cohorts can facilitate further validation of markers of ASD (Button et al., 2013; Open Science Collaboration, 2015).

Recent studies have suggested that EEG connectivity might be a potential neural marker for ASD (O'Reilly, Lewis, & Elsabbagh, 2017; Schwartz, Kessler, Gaughan, & Buckley, 2016). The aim of this PhD project is to examine the relation between EEG connectivity during infancy and later ASD diagnosis and dimensional traits. The following introduction will provide a more detailed account introducing 1) Autism Spectrum Disorders; symptomatology, diagnosis, and aetiology, 2) Early development of ASD, 3) Brain connectivity in typical development, and finally 3) Brain connectivity in ASD.

1.2. Symptomatology of ASD

According to the Diagnostic and Statistical Manual of Mental Disorders 5th Edition (DSM-V), ASD is characterized difficulties in 2 main core domains: 1) difficulties during reciprocal social interactions, and 2) restricted and repetitive behaviours and interests (American Psychological Association, 2013) (Fig. 1.1).

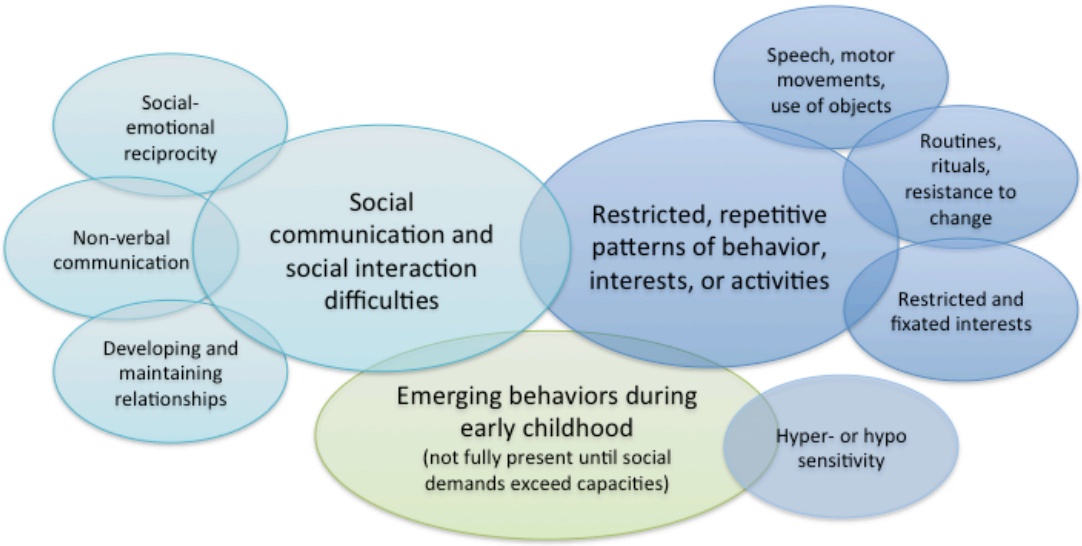

Figure 1.1. Overview of ASD symptoms as defined by the DSM-V
ASD symptoms are defined in 2 main domains: 1) social communication and social interaction difficulties (light blue on the left), and 2) restricted, repetitive patterns of behaviour, interests, or activities (dark blue on the right). Each of the symptoms can be divided into subtypes of these symptoms. These behaviours start to emerge during childhood.

Some individuals with ASD diagnosis may experience difficulties during reciprocal interactions, for example with turn taking in a conversation or matching their behaviours to the social context. Spontaneous sharing of interests and emotions, and understanding gestures or body language are other behaviours that may be difficult for individuals with ASD. The use of appropriate eye contact,

intonations, or emotional affect could also be affected. Verbal language can furthermore be delayed, and might be characterised by repetitive use of specific words or phrases. Younger children with ASD frequently show less variation in their imaginative and pretend play, and less spontaneous social imitative play. Furthermore, establishing friendships and relationships with peers could be difficult (American Psychological Association, 2013).

The second core feature of ASD is restricted and repetitive behaviours and interests. Different subsets of these behaviours exist. Repetitive motor behaviours involve hand and finger mannerisms or repetitive movements with the whole body (rocking). Use of objects in a restrictive and repetitive way is also observed in individuals with ASD; for example, flapping hands or spinning wheels on cars. Individuals with ASD may display a preference and insistence on sameness. They find sudden changes in their personal routine or environment difficult to cope with. Some individuals might have specific non-functional rituals during their daily life. Individuals with ASD might have restrictive interests for specific topics, unusual preoccupations, or unusual attachment to objects, also referred to by the umbrella term 'circumscribed interests' (American Psychological Association, 2013).

In addition to the two core features of ASD, individuals with ASD might also experience other features that are commonly observed in ASD. For example, atypicalities in gross movements, such as poor motor coordination, clumsiness, abnormal gait and posture, and tiptoe walking. Sensory atypicalities are also common. Individuals with ASD might for example be hyper- or hyporeactive to loud sounds, certain visual stimuli (e.g. bright lights), or the feeling of certain textures. Finally, a few individuals with ASD have a special skill that is superior to

their other abilities, for example art, mathematics, or music (American Psychological Association, 2013).

It is important to note that not all individuals with a diagnosis of ASD experience the same symptoms mentioned above. Some individuals might experience more social communication difficulties, whereas other might experience more difficulties in the restricted and repetitive behaviours domain. Thus, ASD is a disorder characterised by heterogeneity.

1.2.1. Clinical diagnosis of ASD

According to the DSM-V criteria, an individual suspected to have ASD must meet 3 of the criteria for deficits in social communication and social interaction in different contexts, and at least 2 of the criteria for restricted and repetitive behaviours and interests. The symptoms must have a clear impact on daily life (American Psychological Association, 2013). Another criterion is that the symptoms have to be displayed from an early age. The criteria acknowledge that the symptoms might not fully emerge until the social demands are exceeding the current abilities of the individual, often around 4 or 5 years of age. For example, difficulties with friendships and relationships might not emerge until childhood and therefore makes assessing this criterion difficult in young toddlers.

Early clinical diagnoses are given only to children from 2 years of age and older, and are usually defined as a 'working diagnosis'. A working diagnosis of ASD is based on careful consideration of the severity of ASD symptoms, cognitive abilities, and developmental history of the target child, among others, by a multidisciplinary team (Charman & Baird, 2002; Pasco, 2011; Risi et al., 2006). All relevant information is reviewed including results from direct measures in the form of behavioural assessments with the target child, and indirect measures in

the form of interviews and questionnaires with the parents. In particular at young ages, clinical expertise may be more accurate than cut-off scores for these instruments measuring ASD symptoms. Difficulties with social communication are more apparent than restricted and repetitive behaviours in 2-year-olds compared to in 4 to 5-year-olds. The working diagnosis for young individuals however is always made with reference to the DSM criteria.

1.2.2. Aetiology of ASD

Over the last few decades ASD research has significantly increased as new research techniques and methods were being developed. This increase in knowledge has revealed that ASD is an incredibly complex disorder with multiple pathways resulting in the same behavioural phenotype defined as ASD. Researchers have focused on different levels of explanations for ASD behaviours, such as genetic and environmental factors, cognitive theories, and explanations at the level of the brain.

1.2.2.1. Genetic and environmental factors

ASD is a behavioural phenotype, defined based on behaviours. Studies in twins and families show that ASD is heritable, which suggests involvement of a genetic component (Hallmayer et al., 2011). Individuals with a first-degree relative with a diagnosis are at increased risk of developing ASD as well. There is also an increased risk for them experiencing sub-threshold ASD traits (Bolton et al., 1994). However, heritability in these studies is not 100%, which suggests additional involvement of environmental factors, or genetic-environmental interactions. The specific mechanism of genetic involvement in ASD is incredibly complex, and largely unknown. In a few rare cases, ASD behaviours are the result of a specific single gene or genetic mutation associated with a known genetic disorder, such as

Fragile X syndrome, tuberous sclerosis, or neurofibromatosis. In the other individuals with ASD diagnosis, complex interactions between multiple genes with additive effects and environmental factors likely underlie their symptoms (De La Torre-Ubieta, Won, Stein, & Geschwind, 2016; Geschwind, 2009; Willsey & State, 2015).

Human and animal studies have previously linked environmental factors to risk for ASD diagnosis. The identified associations depend on the nature, timing, and duration of the environmental factors. For example, increased parental ages, medication intake (valproate, antidepressants), toxic chemicals (traffic-related air pollution, pesticides) during prenatal periods have been related to increased risk for ASD. Prenatal stress via maternal factors crossing the placenta, and maternal infections leading to altered immune system responses in the foetus have been linked to increased risk for ASD also. In contrast, prenatal nutrition such as intake of folic acid was associated with decreased risk for ASD diagnosis (Mandy & Lai, 2016). It has been suggested that both genetic mutations and the environmental factors alter the expression of genes in different cell types via epigenetic mechanisms such as DNA methylation. These alterations in the expression of genes impact multiple downstream pathways implicated in ASD, including synaptic and neuronal functioning, brain functioning, and cognitive functioning (Chaste & Leboyer, 2012; Grayson & Guidotti, 2016; Mitchell, Schneper, & Notterman, 2016).

1.2.2.2. Cognitive theories

While evidence from genetic and environmental studies suggests there is a broad range of possible aetiologies of ASD, research has been aiming to canalize this broad aetiology into a more coherent phenotype. One approach is to explain ASD aetiology at a cognitive level. Cognitive theories initially aimed to account for ASD

by defining one aspect that accounts for specificity, uniqueness, and universality in the disorder. The most widely studied cognitive accounts of ASD are the Theory of Mind Deficit, Executive Dysfunctioning, and Weak Central Coherence Theory (Rajendran & Mitchell, 2007). The social motivation theory (Chevallier, Kohls, Troiani, Brodkin, & Schultz, 2012) and predictive processing theory (Pellicano & Burr, 2012) have gained research interest also.

The Theory of Mind (ToM) Deficit theory suggests that individuals with ASD have difficulties inferring others' mental states and intentions (e.g. 1st order belief; I think he thinks, and 2nd order belief: I think he thinks she thinks). The majority of children with ASD failed to pass a 1st order false belief task (Baron-Cohen, Leslie, & Frith, 1985), and none a 2nd order false belief task (Baron-Cohen, 1989). These observations led to the proposal that ASD is characterized by a delay in the development of Theory of Mind. Further research however showed that high-functioning individuals with ASD performed at ceiling levels for these false belief tasks, but they still had difficulties inferring mental states from pictures of faces or eyes, or vocalizations in more advanced Theory of Mind tests. Difficulties with inferring others' mental states were therefore further characterized as mindblindness rather than a deficit of Theory of Mind. While Theory of Mind can be either present or absent, mindblindness accounts for different levels of this skill, including individuals passing on more advanced Theory of Mind tests (Rajendran & Mitchell, 2007).

The theory of Executive Dysfunctioning is another widely studied theory, and suggests individuals with ASD experience impairments in executive functions (Rajendran & Mitchell, 2007). Executive functions (EFs) are a set of functions used during goal-directed behaviours, such as working memory, planning, inhibition,

impulse control, and control of attention (Diamond, 2013; Hill, 2004b; Johnson, 2012). Individuals with ASD have been found to perform worse on tasks involving planning multiple actions in sequence. They further display less mental flexibility and perseveration when switching between tasks, whereas performance on tasks involving inhibition of ones actions is similar compared to typically developing individuals (Hill, 2004a, 2004b; Ozonoff, Pennington, & Rogers, 1991).

The other widely studied early cognitive theory is the weak central coherence (WCC) theory (Frith & Happé, 1994). This theory suggests that individuals with ASD have difficulties integrating information drawn from different levels, and processing global information that reflects the gist or overall meaning of the message. This theory was proposed after findings of individuals with ASD outperforming typically developing individuals on tasks that involve locating smaller shapes imbedded in larger drawings, and reproducing graphic designs with blocks (Frith & Happé, 1994; Rajendran & Mitchell, 2007). Further research showed that individuals with ASD were able to process information on a global level when instructed to. The WCC theory was refined suggesting that individuals with ASD have a bias towards processing information in a detailed, piecemeal fashion, rather than a deficit in global processing (Happé & Frith, 2006).

The social motivation theory hypothesizes that ASD is characterized by a disruption in social motivation (Chevallier et al., 2012). This theory is based on findings of diminished orienting or preference for social over non-social stimuli, diminished enjoyment and drive for social interactions, and use of fewer strategies and attempts for maintaining social relationships. The behavioural impairments are possibly a result of a deficit in the attribution of reward value to social stimuli, and the representation of these social rewards in which the orbitofrontal-striatal-

amygdala circuit is involved. More importantly, the theory suggests that diminished social motivation or attention to social stimuli creates a downstream cascading effect on social development. Diminished social motivation leads to deprivation of social learning opportunities and therefore difficulties with later social cognition. According to the social motivation hypothesis, ASD is characterized by an early onset of diminished social motivation.

Finally, another line of research in ASD has proposed that individuals with ASD experience difficulties predicting events as a result of difficulties with integrating prior information and forming predictions based on that prior information. It has been suggested that this might underlie abnormal sensory processing, and being overwhelmed by sensory information. Individuals with ASD might therefore avoid unpredictable environments and situations, for example during social interactions that are characterised by unpredictable events. Furthermore, difficulties with predictions might relate to the insistence on sameness in routines and environment often observed in ASD. Repetitive motor behaviours similarly would require fewer predictions since motor plans and expected sensory experiences have already been created before, thus making them more predictable (Lawson, Rees, & Friston, 2014; Pellicano & Burr, 2012; van Boxtel & Lu, 2013; Van de Cruys et al., 2014).

Although several cognitive theories of ASD have been proposed, none of these seem to give a perfect account for the underlying mechanisms of ASD. The proposed cognitive difficulties are not always apparent in each individual with an ASD diagnosis. Furthermore, some of the difficulties are also evident in other (developmental) disorders. Another line of research has therefore focused on explanations of ASD at brain levels.

1.2.2.3. Explanations at the level of the brain

Research examining brain structure and function has led to theories suggesting that abnormalities in the brain underlie ASD. Results from post mortem studies suggest that early brain overgrowth might play a role in ASD. In individuals with ASD, there is initial overgrowth of brain volume during the early years of life followed by slowing or arrest of this growth during childhood. This overgrowth in frontal and temporal brain regions might arise from an excess of neurons (Courchesne et al., 2007). Indeed, individuals with ASD showed increased density of minicolumns in temporal and frontal regions with smaller and more dispersed neurons. The alternations in the minicolumns might be compensated for by increased numbers of connections and white matter volume between these columns (Hutsler & Casanova, 2015). Together, these findings suggest altered trajectories of whole brain development in ASD.

In addition to alterations in whole brain development, alterations in synaptic processes have been related to ASD also. Studies using animal models of ASD exhibited dysfunction of glutamatergic and GABAergic receptors in synapses. ASD-like behaviours in mice could be 'rescued' or reduced by glutamate antagonists and GABA agonists, and depended on the brain areas or circuits affected (Kim, Lim, & Kaang, 2016). Human studies have shown abnormalities in glutamate levels in individuals with ASD also (Bejjani et al., 2012; Joshi et al., 2013; Naaijen et al., 2017). These findings have led to the excitation-inhibition (E/I) imbalance hypothesis, which suggests that the ratio between excitatory and inhibitory neurons in the cortex and neural circuits is altered in individuals with ASD (Nelson & Valakh, 2015; Rubenstein & Merzenich, 2003; Uzunova, Pallanti, & Hollander, 2016). The imbalance could arise from an increase in signalling by

excitatory glutamatergic receptors, a decrease in signalling by inhibitory GABAergic receptors, or a combination of both. If there is an E/I imbalance, the cortex would be more excitable or weakly inhibited, resulting in more noise and poor signal-to-noise ratios, and finally a decrease in functional differentiation of neural processes (Rubenstein & Merzenich, 2003). Different mechanisms of E/I imbalances may underlie different subgroups of individuals with ASD that may respond differently to therapeutic treatments targeting this imbalance (Uzunova et al., 2016).

Both alterations in E/I balance and overgrowth in the brain may also affect brain connectivity: the E/I imbalance likely affects neural circuits embedded in larger brain networks (Rubenstein & Merzenich, 2003), and overgrowth in the frontal and temporal brain regions arising from an excess of neurons may relate to altered functional connectivity in these regions (Courchesne et al., 2007). Indeed, another influential theory of aetiology in ASD suggests that brain connectivity is altered in ASD. This theory was proposed by Just and colleagues who found that individuals with ASD exhibited lower correlations between activations in key language areas than individuals without ASD (Just, Cherkassky, Keller, & Minshew, 2004). They hypothesized that underconnectivity between cortical regions results in difficulties with the integration and coordination of information, for example during social interactions where different aspects of communication need to be integrated, during the performance of novel tasks where efficient coordination is crucial, or during the change of plans or strategies where involvement of the prefrontal cortex is needed. Possibly lack of functional connectivity or synchronisation between cortical regions provides a biological basis for a bias

towards a detailed rather than global processing style as suggested by the weak central coherence theory (Happé & Frith, 2006).

After this initial proposal, studies examining connectivity in ASD displayed mixed findings showing overall overconnectivity, underconnectivity, or varying patterns depending on brain region (Ecker, Bookheimer, & Murphy, 2015). Further refinements of the theory were suggested. For example, Belmonte and colleagues suggested that connections between more distant areas are underconnected, whereas connections among nearby areas are overconnected in individuals with ASD compared to typically developing individuals (Belmonte et al., 2004). Several studies found supporting evidence for underconnectivity in long-range connections, but findings for short-range connections showed evidence for over-connectivity, under-connectivity, or a mixture of both (O'Reilly et al., 2017; Vissers, X Cohen, & Geurts, 2012).

Furthermore, alterations in brain connectivity patterns may also be related to developmental stage. Studying developmental pathways as opposed to static end states in children and adults is important for the understanding of developmental disorders such as ASD (Karmiloff-Smith, 1998). Recent reviews of connectivity studies across different age groups revealed whole brain overconnectivity during toddlerhood, and whole brain underconnectivity during later childhood, adolescence, and adulthood (Hoppenbrouwers, Vandermosten, & Boets, 2014; Uddin, Supekar, & Menon, 2013). Overconnectivity during toddlerhood may arise from delayed or aberrant pruning or increased myelination in young individuals with ASD. In addition, developmental changes during puberty may impact brain connectivity resulting in under-connectivity during adolescence and adulthood. It is possible that alterations in brain connectivity even occur

before childhood, for example during infancy, when one considers that genetic and environmental factors can impact brain development during pre- and perinatal periods via downstream pathways also (Grayson & Guidotti, 2016).

1.2.2.4. Considering development: ASD as an adaptive response

The perspective of ASD proposed by Johnson and colleagues adopts a developmental framework of ASD also. They suggest the ASD phenotype is the result of an adaptive response to atypical neural processing during critical periods occurring during the first years of life. Altered, atypical neural processing during early development might arise from E/I imbalances, and genetic and environmental factors during pre-and perinatal periods, which in turn may lead to excessive noise masking the signal. Appropriate signal-to-noise ratios are crucial for information processing and cortical specialization of brain regions during development. The adaptive response compensating for atypical neural processing of the environment may arise from several mechanisms of whole brain adaptation: 1) use of alternative redundant processing pathways, 2) re-organisation of neural networks to optimize brain functioning, 3) change in developmental trajectories via prolonged brain plasticity or developmental delays, and 4) selecting environments that match the atypical neural processing mechanisms, also called niche construction (Johnson, 2011, 2017; Johnson, Jones, & Gliga, 2015).

This theory emphasizes the importance of studying early development of ASD, as atypical neural processing and adaptive responses are most likely to occur during the first years of life rather than adulthood. Examining developmental trajectories and occurring adaptive processes will further facilitate understanding of underlying mechanisms of ASD, and the heterogeneity present within groups of individuals with ASD.

1.3. Research in the Early Development of ASD

Investigating ASD during early development before the onset of ASD behaviours during toddlerhood is important for early detection and intervention, but also for the understanding of underlying mechanisms. Studies aiming to investigate the early development of ASD typically use the high-risk infant sibling design, and have revealed both behavioural and neural findings.

1.3.1. The design of high-risk infant sibling studies

Studies focusing on the first few years of postnatal life when investigating the development of ASD use retrospective and prospective designs. Retrospective designs are studies that investigate behaviour during early life after the diagnosis has been made (Szatmari et al., 2016; Zwaigenbaum, Bryson, & Garon, 2013), for example by means of previously recorded home videos, or parental interviews. The main problem with these methods is that they are based on memories and occurrences that might not be representative of the child's daily life. Home video recordings are more often taken during special occasions, and might show a lack of consistency across individual recordings. The recollection of events by the parents may be inaccurate, or biased during the parental interview.

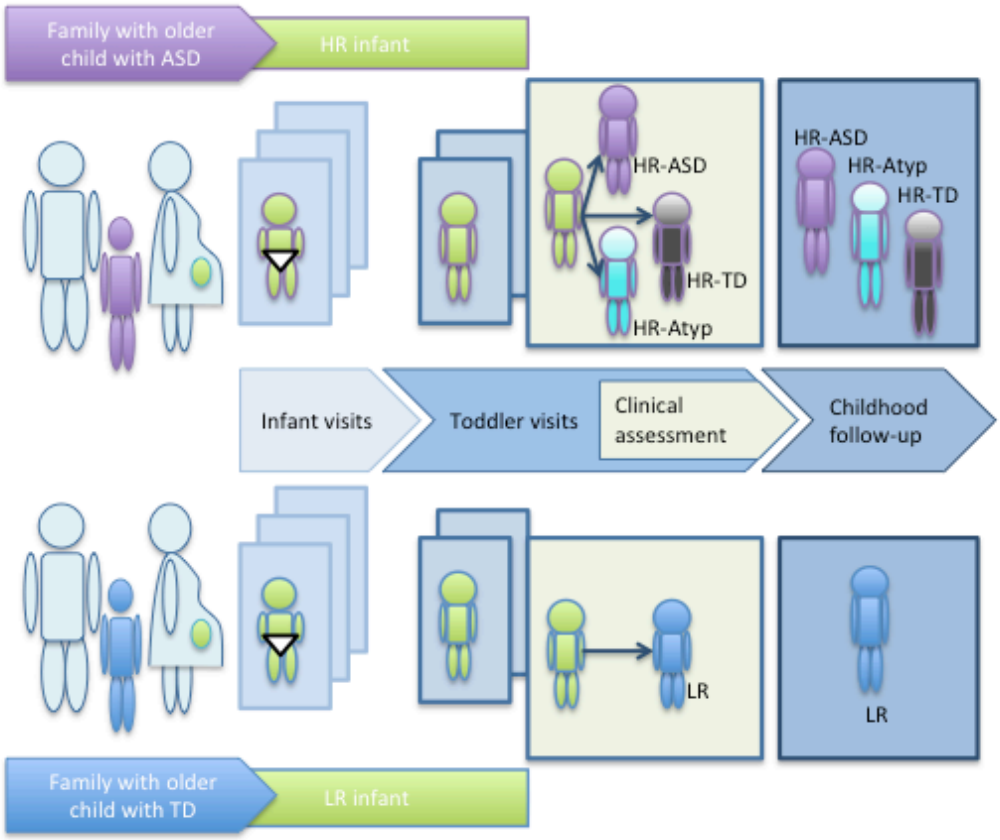

Figure 1.2. Overview of the high-risk infant sibling design

The high-risk infant sibling design is a prospective longitudinal design that involves multiple visits to the lab during infancy and toddlerhood. High-risk (HR) infants have an older sibling with ASD, whereas low-risk (LR) siblings have an older sibling showing typical development. A clinical assessment during the 36-month-old visit is used to examine whether the infants shows typical development, atypical development, or is meeting criteria for ASD. Continued follow-ups into childhood can further inform on developmental trajectories of ASD.

In contrast to retrospective designs, prospective designs investigate behaviour during early life before a diagnosis is made. In these longitudinal prospective studies younger infant siblings of children with an ASD diagnosis are repeatedly invited to visit the lab where their cognitive and neural functioning, and developmental skills are assessed with a battery of behavioural and neuroimaging tasks (Szatmari et al., 2016). Younger siblings of children with ASD have a higher

familial risk of developing the disorder themselves at a later age compared to siblings of children who are typically developing: the population risk of developing ASD at a later ages increases from 1% to 20% if an older sibling has an ASD diagnosis (Ozonoff et al., 2015). Infant sibling studies hence focus on investigating early development of these younger infant siblings. The infants with older siblings with a diagnosis are initially described as high-risk (HR) infants, while younger siblings of children with a typical development are described as low-risk (LR) infants (see Fig. 1.2).

Infant sibling studies typically continue until after toddlerhood, as a reliable diagnosis for ASD can be made when the child is 2 or 3 years old (Charman & Baird, 2002). Therefore, a clinical assessment is included during the 2 or 3-year-old visit. Experienced clinicians review information from different assessments to determine whether the toddler is meeting ASD criteria for a research ASD diagnosis. HR infants who meet ASD criteria are included in the HR-ASD infant group. Toddlers who are not meeting ASD criteria are included in the HR-no ASD infant group. This group can be further divided into 2 groups: a) toddlers who are not meeting ASD criteria nor showing developmental delays or other concerning behaviours are termed high-risk infants with typical development (HR-TD group), and b) toddlers who do not meet ASD criteria, but are showing concerning behaviour are categorized as high-risk infants with atypical development (HR-Atyp group). This group typically includes toddlers who show elevated ASD traits but score below threshold, or show developmental delays in cognitive skills, expressive or receptive language skills (e.g. (Cheung, Bedford, Johnson, Charman, & Gliga, 2016), and see Fig. 1.2).

The longitudinal prospective design also allows for different comparisons. In risk analyses, the HR group is compared with the LR group. These risk analyses provide information about aspects associated with risk for ASD. First-degree relatives of individuals with ASD tend to show increased levels of ASD symptoms compared to LR individuals, although the severity of symptoms is not high enough to meet criteria for diagnosis, also named the broader autism phenotype (BAP) (Bolton et al., 1994; Charman et al., 2017). These risk analyses can be performed before the clinical assessment data are available. When outcome data are available, analyses including this information can provide information about aspects associated later outcome. Comparison between the HR-TD and HR-ASD groups for example can inform on whether there might be protective factors that are related to typical development as opposed to an ASD diagnosis, or risk factors that relate to ASD diagnosis. Comparison between the HR-Atyp and HR-ASD groups can inform on whether certain factors are specific to ASD, or more common in atypical development.

1.3.2. Findings from high-risk infant sibling studies

Previous studies using the prospective high-risk ASD sibling design have shown that both behavioural and neural markers begin to emerge during the first and second year of life. These markers are evident across multiple levels, including behaviour, brain anatomy, and brain functioning.

1.3.2.1. Behavioural findings from high-risk infant sibling studies

Although clear behavioural atypicalities do not emerge before toddlerhood, some atypical behaviour can already be observed during infancy. Smiling, vocalising, attending to faces, and following gaze all appear typical around 6 months of age, but are less frequent in HR-ASD group than other groups around the first birthday.

The HR-ASD group also displays less frequent sharing of interests, initiation of joint attention, and a smaller variety of gestures. Language expression and understanding might be delayed as well at 6 and 14 months, although no differences between HR-ASD and LR or HR-no ASD groups have also been reported (Bedford et al., 2012; Hudry et al., 2014; Jones et al., 2014; Landa, Holman, & Garrett-Mayer, 2007; Ozonoff et al., 2010; Paul, Fuerst, Ramsay, Chawarska, & Klin, 2011; Zwaigenbaum et al., 2005).

Restricted and repetitive behaviours are already present around the first birthday (Wolff et al., 2014). The HR-ASD group displays more frequent arm waving, and atypical visual exploration than LR and HR-no ASD groups (Loh et al., 2007; Ozonoff, Macari, Young, Goldring, & Thompson, 2008). Few other studies however have looked further into restricted and repetitive behaviours as they become more evident later during development.

Other behavioural studies have focused on attentional control and visual preferences using eye-tracking techniques. One study found that the HR-ASD group displayed longer disengagement latencies during visual orienting than HR-no ASD and LR groups at 7 months of age (Elison et al., 2013), whereas another study found the same pattern at 14 months, but not at 7 months of age (Elsabbagh et al., 2013). Furthermore, while speed and flexibility of attentional control typically improve over time between 7 and 14 months of age, no such increase was observed in the HR-ASD and HR-Atyp groups. A similar pattern of attenuated developmental trajectory was observed for working memory and response inhibition in the HR group compared to the LR group between 12 and 14 months of age (St. John et al., 2016).

Findings from eye-tracking studies further revealed a preference for geometric images in young children with ASD. Toddlers between 14 and 42 months of age who fixated on geometric dynamic images more than 69% of the looking time rather than movies of children doing yoga all had a diagnosis of ASD (Pierce, Conant, Hazin, Stoner, & Desmond, 2011). A replication study with a larger cohort in 10 to 49-month-olds revealed that toddlers with ASD spend more time fixation on geometric dynamic images than toddlers with developmental delay, high-risk toddlers showing typical development, and toddlers with other developmental atypicalities (premature birth, prenatal drug exposure). Toddlers with elevated ASD traits but not meeting criteria for and ASD diagnosis showed no difference with the group with an ASD diagnosis in time spent fixating on the geometric images. Finally, the percentage of fixation time on the geometric images increased with age and is less informative in toddlers above 4 years of age (Pierce et al., 2016). However, a recent study using a high-risk infant sibling design and a gaze-contingent eye-tracking paradigm revealed a different pattern of results at 27 months of age: the HR-ASD group displayed longer looking times and more frequent second looks to face stimuli than toy stimuli. This pattern was identical to those in the LR and HR-no ASD groups. There were no differences in the frequency of initial looks to the face or toy stimuli when compared to the LR an HR-no ASD groups (Vernetti et al., 2018). Differences in developmental levels or control over the movies presented may account for the differences in findings between the studies by Pierce and colleagues and by Vernetti and colleagues.

Atypicalities or delays in motor skill development can also be observed, but might not be evident throughout development. For example, delays in gross motor, fine motor, and postural control development have been observed from 3 to 6

months of age (Bhat, Galloway, & Landa, 2012; Flanagan, Landa, Bhat, & Bauman, 2012). The HR group showed less frequent grasping during free play at 6 months of age, but not at 10 months of age compared to the LR group (Libertus, Sheperd, Ross, & Landa, 2014). Another study reported group differences in fine motor skills at 14 months, but not 7 or 24 months of age, and differences in gross motor skills at 24 months of age only (Leonard, Elsabbagh, Hill, & Team, 2014). Differences in fine motor skills from 12 to 18 months of age have also been observed (Ozonoff et al., 2010).

While differences in behaviours have been observed between risk groups and outcome groups, these differences are not all consistent across time, or across studies. Gender may play a role in these associations between these early markers and later severity of ASD traits also, where associations are stronger in males than females (Bedford et al., 2016; Messinger et al., 2015). This demonstrates the heterogeneity of behaviours, and developmental trajectories during early development in ASD (Jones et al., 2014). Furthermore, this suggests that early behaviours might not be reliable as early markers for later ASD diagnosis or dimensional traits. It is possible that atypicalities in brain structure and functioning provide a clearer picture as early markers during the development of ASD.

1.3.2.2. Neural findings from high-risk infant sibling studies

Previous studies have found that differences in brain structure and functioning between HR-ASD infants and HR-no ASD or LR infants are better visible at early ages than behavioural differences.

1.3.2.2.1. Brain volume in early ASD

The developmental trajectory of total brain volume in ASD is characterized by 3 different stages; 1) an abnormally accelerated overgrowth during the first years of life, 2) a slowed or arrested growth between young childhood and preadolescence, and 3) an accelerated decline in brain volume between adolescence and middle age (Courchesne, Campbell, & Solso, 2011). The overgrowth occurs across specific regions, such as the frontal lobe, the occipital lobe, and the amygdala. Furthermore, findings from magnetic resonance imaging (MRI) studies and studies measuring head circumference across the life span consistently show this early overgrowth (Courchesne et al., 2007).

Infant sibling MRI studies focusing on the first postnatal years have further revealed that differences in brain structures between the HR-ASD and other groups start to emerge during the first postnatal year, and become more prominent during the second postnatal year. At 6 months of age, the HR-ASD group displays similar total brain volumes compared to LR, HR-TD, and HR-Atyp groups (Hazlett et al., 2017; Shen et al., 2013). The surface area at this age however is larger in the HR-ASD group than LR and HR-no ASD groups, and at 12 months of age also. Between 6 and 12 months an accelerated expansion of the surface areas occurs, in particular in the middle occipital gyri, right cuneus, and right lingual gyrus. The accelerated growth rates in these areas are higher for the HR-ASD group than the other groups (Hazlett et al., 2017).

During the second postnatal year there is an accelerated growth of total brain volume in the HR-ASD group compared to HR-no ASD and LR groups. Studies have found both increases of brain volumes in HR-ASD groups (Shen et al., 2013), and no differences between groups (Hazlett et al., 2017) at the 12-month-old time

point. In contrast, at 24 months of age there are consistent findings of greater total brain volumes in the HR-ASD group compared to the other groups. The rate of surface expansion during the first postnatal year was positively related to the growth rate of total brain volume during the second postnatal year. The HR-ASD group furthermore displayed larger head circumference and volumes of extra-axial cerebral spinal fluid during the 2 first postnatal years, whereas cortical thickness was similar across HR-ASD, HR-no ASD, and LR groups. The amount of elevated extra-axial fluid and total brain volume growth during the second postnatal year were both related to more social communicative difficulties at 24 and 36 months (Hazlett et al., 2017; Shen et al., 2013). These findings are consistent with the hypothesis that ASD is characterised by atypical early brain development discussed earlier (section 1.2.2.3).

1.3.2.2.2. Brain functioning in early ASD

In addition to differences in brain structures, differences in brain functioning between the HR-ASD group and other groups have also been found as early as 4-6 months of age, in particular during social processing. Brain regions implicated in the social brain showed a diminished haemodynamic response to social visual and vocal stimuli in a group of HR infants compared to a group of LR infants (Braukmann et al., 2017; Lloyd-Fox et al., 2013). The LR group showed more widespread responses to social stimuli, while only a few channels showed differential responses in the HR-no ASD group, and none in the HR-ASD group. The reductions in activation in response to social stimuli were further related to increased ASD traits across the whole group. This suggests that brain functioning in young infants is related to categorical outcomes and dimensional traits (Lloyd-Fox et al., 2017).

Further differences between the HR-ASD and other groups during social processing have been found for face processing in EEG event-related potential research. At 6 months of age, the HR-ASD group displayed faster neural responses while viewing faces than HR-no ASD and LR groups. This effect was however not evident at 12 months of age (Jones et al., 2016). Another study found that around 10 months of age the HR group showed slower neural responses when viewing a face with direct eye gaze compared the LR group (Elsabbagh, Volein, Csibra, et al., 2009). Further, HR-no ASD and LR groups displayed different neural responses to faces with direct and averted eye gazes, whereas the HR-ASD group showed no such differences in responses to faces with different gazes (Elsabbagh et al., 2012).

Other methods of EEG analyses also point towards atypical brain functioning in ASD. Analyses of spectral power reflect the strength of oscillatory activity at different frequencies from the populations of neurons in the brain. Oscillations at different frequencies have been related to different cognitive functions. The borders of the bands of these frequencies differ with age, where the frequencies in the bands are lower in younger infants and toddlers than the frequencies in adolescents and adults (Marshall, Bar-Haim, & Fox, 2002; Saby & Marshall, 2012). For example, theta frequencies (3-6 Hz in infants) have been related to the processing of emotional information, the executive control of attention (Jones, Venema, Lowy, Earl, & Webb, 2015), and attentional gating (Orekhova, Stroganova, Posikera, & Elam, 2006; Orekhova, Stroganova, & Posikera, 1999). Alpha band frequencies (6-9 Hz in infants) have been related to attentional processes and inhibition (Klimesch, Sauseng, & Hanslmayr, 2007), and specifically inhibition of attention shifting in infants (Orekhova, Stroganova, & Posikera, 2001; Stroganova, Orekhova, & Posikera, 1999) but also voluntary motor control (Saby &

Marshall, 2012), somatosensory stimulation (Stroganova et al., 1999), and inhibition of irrelevant movements (Orekhova et al., 2001). Gamma band frequencies (20-60 Hz in infants) have been related to perceptual binding and memory. Finally, other defined frequency bands are delta (1-3 Hz) and beta (13-30 Hz), but these are less well researched in infants (Saby & Marshall, 2012).

Power differences between children with ASD and without ASD diagnosis vary with the age, and frequency band selected. At 14-months of age, no differences were observed between the HR-ASD group, and the LR and HR-no ASD groups for the alpha frequency band across the whole scalp (Orekhova et al., 2014). During childhood, differences seem to become more apparent. One group of 6-11-year-olds with an ASD diagnosis displayed *increases* in theta and beta power across the midline when compared to peers with typical development (Coben, Clarke, Hudspeth, & Barry, 2008). Another group of 4-12-year-olds with ASD displayed *increases* in delta and alpha power in frontal regions, whereas beta and alpha power displayed *decreases* in central regions when compared to typically developing age-matched children (Elhabashy, Raafat, Afifi, Raafat, & Abdullah, 2015).

In sum, previous research has revealed atypical brain anatomy and activity in infants with a later ASD diagnosis as young as 5 months. One possibility is that these alterations are related to the adaptive response occurring during the first years of life in ASD, as hypothesized by Johnson and colleagues. As previously mentioned, they suggest that whole brain adaptation occurs via alterations in brain connectivity during early development. If atypicalities in neural processing arise from prenatal and perinatal factors, and adaptive responses to these atypicalities are likely to occur during the first postnatal years, then changes in

brain connectivity are also likely to occur during this time period (Johnson, 2017). The next section focuses on brain connectivity during typical and atypical development of ASD.

1.4. Brain connectivity in individuals with typical development and with a diagnosis of ASD

Several researchers have suggested that ASD is characterised by altered brain connectivity (Belmonte et al., 2004; Johnson, 2017; Just et al., 2004; Uddin, Supekar, & Menon, 2013). It is possible that these alterations already occur during early development. Before further going into detail in connectivity in ASD, I will introduce different forms of brain connectivity, and typical development of brain connectivity (also see (Haartsen, Jones, & Johnson, 2016) for a review on early brain development).

1.4.1. Different forms of brain connectivity

Brain connectivity encompasses different forms of connectivity: structural, functional, and effective connectivity. Structural connectivity indicates how brain regions are physically connected. This involves a structural connection, for example by bundles of axons or white matter connections, which is typically measured using diffusion tensor imaging (Park & Friston, 2013).

In contrast, functional connectivity informs on how similar or how synchronized the activations in different brain regions are. This measure gives an indication how different brain areas interact or communicate with each other. Efficient coupling or synchronization between populations of neurons in different brain regions improves information flow (Peterson & Voytek, 2015). For efficient

coupling, populations of neurons would have to oscillate at the same frequency, with a consistent predictable phase delay between groups, and a conduction delay that allows for precisely timed arrival of the information when the receiving neurons are excitable (Fries, 2005, 2015). Neural synchronisation across brain regions is furthermore important for the development of cortical networks (Uhlhaas, Roux, Rodriguez, Rotarska-Jagiela, & Singer, 2010). Functional connectivity can be measured with different neuroimaging methods; such as functional MRI, functional near-infrared spectroscopy (fNIRS), magnetoencephalography (MEG), and electroencephalography (EEG) methods, which are able to measure neural synchronisation at different time scales.

Brain regions that have strong structural connections also tend to have strong functional connections (Bullmore & Sporns, 2009). Functional connectivity however can also arise in the absence of a direct structural connection between the brain regions (Chu et al., 2015; Honey et al., 2009). Functional connectivity fluctuates over time during rest, and is modulated by different task demands, but the underlying structural anatomy remains largely stable (Wang et al., 2014). It is assumed that the flexibility of functional connectivity plays a role in global integration of segregated information processing. Short-range connections are involved in local or segregated information processing, whereas long-range connections have the flexibility and ability to facilitate the integration of different information processing modules depending on the task demands at hand (Park & Friston, 2013).

Lastly, effective connectivity investigates the direction of information flow between brain regions. While structural and functional connectivity measure undirected connectivity, effective connectivity allows for interpretation of the

direction of the signal and indicates which signal is leading and which signal is following (Bastos & Schoffelen, 2016; Hillebrand et al., 2016; van Diessen et al., 2015). This method can be applied to fMRI, MEG, and EEG data.

Brain connectivity can be defined as whole brain connectivity (values are averaged across the whole brain), as connectivity across specific regions of interest (e.g. regions involved networks with specific functions), or in terms of organisation using graph theory measures (Bullmore & Sporns, 2009; Rubinov & Sporns, 2010). Graph theory measures reflect the amount of segregation and integration across networks, and can inform us about the organization of the network as opposed to whole brain connectivity that informs on the overall strength of connections.

According to graph theory, networks consist of nodes (brain regions, or electrode positions) and edges (links between nodes). The values of the edges represent the strength of the connections between the nodes, which can be the strength of the physical connection, or the amount of synchronisation between regions, or directed connectivity values. The degree of a node reflects the number of other nodes it is connected to. Both local and global graph theory measures exist, for example the clustering coefficient, and characteristic path length. An optimal network would be characterised by balanced integration and segregation, also known as 'small-world' network.

1.4.2. Brain connectivity during typical development

Typical development of both structural and functional connectivity shows rapid changes between a few weeks after conception and 2 years after birth.

1.4.2.1. Structural brain connectivity

The development of structural connectivity starts before birth. Connections between the cortex and subcortical region involving major pathways between the cortex and striatum, pons and spinal cord are established during the fetal period (9-23 weeks post conception (WPC)). The corpus callosum also begins to form. Then, during the early preterm (24-28 WPC), connections between the subcortical regions continue to extend into central, frontal, temporal, and occipital regions in the cortex, in particular connections between the thalamus and cortical layer IV crucial for sensory functioning. During the late preterm period (29-34 WPC), there is a rapid development of structural connections, in particular of long pathways connecting associative areas. Synaptogenesis and pruning occur also, and will continue to do so throughout the first year after birth. Myelination of the associative cortico-cortical pathways furthermore develops while following a specific order: starting at the centre of the brain and extending outwards, from proximal pathways to distal pathways, from sensory to motor pathways, from projection to associative pathways, and from occipital to parietal, and then to temporal and frontal poles (Dubois, Kostovic, & Judas, 2015).

Studies in preterm infants have shown that structural connectivity continues to develop between 27 and 38 WPC. Structural networks become more distinct with age, and are stable between 38 and 46 WPC (Ball et al., 2013). A rich-club organisation characterised by clusters of highly connected regions and long-range connections between these clusters is already present at birth. The clustering of the networks, the strength of long-range connections, and thereby the efficiency of the networks increase with increasing age (30-40 WPC (Ball et al., 2014), and 27 – 45 WPC (Brown et al., 2014)). The growth rates of the networks

associated with age depend on their location; connections in frontal and occipital lobes show higher growth rates than connections within other areas (Brown et al., 2014).

After birth, structural networks continue to develop. The networks become even stronger, more efficient, and better integrated with increasing age. The networks grow more robust and less vulnerable to attacks or random failure between birth and adulthood. In other words, the networks become more stable and less plastic during development. With increasing stability and efficiency, plasticity of the networks decreases (Huang et al., 2015). Development of the networks seems to follow a trade-off between minimizing the cost of the network and maximizing network integration. The optimal result of this trade-off changes over time. Overall, structural connectivity exhibits a developmental shift from local networks towards more globally distributed networks across age (Vértes & Bullmore, 2015).

1.4.2.1. Functional brain connectivity

Similar to structural connectivity, functional connectivity shows rapid developmental changes during early development. Functional connectivity can be measured with fMRI, which has a high spatial resolution and allows for precise interpretation of the source of brain activity, or with MEG/EEG methods, which have a high temporal resolution and allow for the investigation of fast neural coupling.

1.4.2.1.1. fMRI connectivity

Synchronisation across different brain regions is evident from before term age. This evidence comes from fMRI studies conducted with preterm neonates who are asleep. Different brain areas that are synchronised during these resting states

compose a functional resting state network. Functional resting state networks measured in this way have been found as early as 26 weeks post menstrual age (Smyser & Neil, 2015).

The functional resting state networks are characterized by involvement in different cognitive functions and show different developmental trajectories. Networks involved in primary motor and sensory areas appear more adult like than other networks at term age and show minimal further development after the first postnatal year, for example the primary sensory-motor network and the auditory/ language network. Other networks that are involved in higher order processing appear incomplete and premature at term age, but show fast development during the first postnatal year, such as the attention network and default mode network, which is active during rest. Networks involved in decision-making and executive functioning show the lowest developmental rates; these are the fronto-parietal networks, and the salience network (Alcauter et al., 2014; Gao, Alcauter, Elton, et al., 2015; Gao, Alcauter, Smith, Gilmore, & Lin, 2015; Hoff, Van den Heuvel, Benders, Kersbergen, & De Vries, 2013; Smyser & Neil, 2015) . Overall, the resting state networks show rapid development during the first postnatal years, and show more fine-tuning and higher specialization with increasing age.

Furthermore, connections between the thalamus, which is involved in the relay of sensory information to the cortex, and other regions involved in the sensory-motor network, salience network, and default mode network are already present at birth. These connections show further rapid development and increased specialization during the first two postnatal years (Toulmin et al., 2015). Infants with stronger functional connectivity between the thalamus and salience network

at 12 months, showed better working memory performance at 12 and 24 months (Alcauter et al., 2014).

1.4.2.1.2 MEG/EEG connectivity

While fMRI methods have the advantage of high spatial resolution, MEG/EEG methods have the advantage of high temporal resolution. MEG/EEG methods can show how different brain regions are synchronized in different frequency bands like delta, theta, alpha, beta, and gamma. Higher connectivity values reflect stronger synchronization whereas lower values reflect weaker synchronization (Bastos & Schoffelen, 2016; van Diessen et al., 2015). As with functional fMRI connectivity, functional MEG/ EEG connectivity also shows developmental changes. EEG connectivity overall increases with age from infancy until late adolescence in the delta, theta, alpha, and beta band for short electrode distances (1/2-16 years of age (Thatcher, North, & Biver, 2008), and 1-25 years of age (Peters et al., 2013)). The most rapid increase in EEG synchronisation occurs during the first 4 postnatal years. Connectivity between electrodes at long distances however decreases with age. It has been argued that these results reflect increases in local integration, and segregation between distant areas with increasing age.

Furthermore, the developmental trajectory shows a rapid growth period every 2-5 years displaying a curvilinear trajectory before adulthood rather than a linear trajectory (Thatcher et al., 2008). Indeed, decreases in connectivity have been found from 5 to 7 years of age across the theta, alpha, and beta band, which would coincide with the period after the first rapid growth period in life. Clustering and path length, reflecting local and global network organisation, increase over time as well, suggesting that networks become increasingly organised with age.

Overall synchronization likelihood is higher in girls than in boys, and the decrease over time was larger in girls than boys (Boersma et al., 2011). Another study showed a non-linear developmental trajectory as well: overall EEG connectivity increased with age across childhood and adolescence, and continued to increase into middle adulthood for theta, alpha, and beta frequencies. During middle adulthood, around 50 years of age, global EEG connectivity displayed a peak, before declining again after 55 years of age. Clustering and path length further increased between childhood and adolescence (Smit et al., 2012).

In short, brain connections increase in strength with age, with concurrent networks emerging during development. Brain networks become more distinct and organised with age, showing local clustering via increased strength of small-range connections, and global integration via stronger long-range connections. This developmental pathway is similar for structural and functional networks, although the rate and timing of development of the networks varies. Structural connectivity shows most rapid changes during early development, whereas functional connectivity continues to develop during childhood and adolescence as well.

1.4.3. Brain connectivity during the early development of ASD

The hypothesis that ASD is characterized by altered brain connectivity has led to several studies comparing structural and functional brain connectivity measures between individuals with and without ASD diagnosis. The nature of the abnormality in brain connectivity in ASD however remains unclear, in particular during early postnatal life.

1.4.3.1 Structural connectivity in ASD

Findings from structural connectivity studies have overall shown differences in connectivity between HR-ASD and HR-no ASD groups. At 6 months of age, most large white matter fiber tracts connecting association cortices exhibited higher fractional anisotropy (FA) values in the HR-ASD than HR-no ASD group. During the following months, FA in the tracts decreased further; the HR-ASD group showed slower rates of decrease in FA than the HR-no ASD group. Diffusivity in the tracts was similar across groups at 12 months of age, while at 24 months of age FA in the tracts was lower for the HR-ASD group than the HR-no ASD group. This trajectory of development was evident in most large white matter tracts, with the exception of the tract originating from the thalamus and radiating into the anterior cortex. The latter tract showed similar FA values across groups at 6 and 12 months, but lower FA in the HR-ASD than HR-no ASD group (Wolff et al., 2012).

In addition to differences in large white matter tracts, differences have also been found in the corpus callosum that connects the two hemispheres during the first year of life. The midsaggital area and the thickness of the anterior part of the corpus callosum were larger in the HR-ASD group than the HR-no ASD and LR group. The differences between groups were most pronounced at 6 months, decreased at 12 months, and not significant at 24 months of age. The thickness of the corpus callosum connecting the two hemispheres at both 6 and 12 months was positively associated with repetitive behaviours at 24 months of age (Wolff et al., 2015). Also, lower radial diffusivity in the splenium of the corpus callosum in LR group was related to more difficulties in attentional control, but this association was not observed in the HR-ASD group of 7-month-old infants (Elison et al., 2013). Finally, higher levels of FA in the genu of the corpus callosum at 6 months of age were associated with more severe repetitive behaviours, and sensory

responsiveness measured parental questionnaires at the age of 24 months. No associations were found with severity of social communication symptoms (Wolff et al., 2017).

Structural connectivity differences continue to exist during toddlerhood, and might even be ASD specific. Toddlers with ASD displayed higher FA values and larger volumes in frontal white matter tracts than their TD peers, whereas there were no differences between groups for posterior tracts. These differences in frontal tracts between groups were most prominent in young 1 to 3-year-old toddlers, but were absent in 3 to 4-year-old toddlers. The same developmental pattern occurred in the corpus callosum overall. The frontal part of the corpus callosum, however, showed smaller age related increases in toddlers with ASD than TD toddlers throughout toddlerhood. Higher diffusivity and volume in frontal tracts in *younger* HR-ASD was associated with higher levels of symptom severity, whereas lower FA values and volume in *older* HR-ASD toddlers was related to higher levels of symptom severity (Solso et al., 2016). Finally, comparisons between toddlers with ASD and with a developmental disorder other than ASD (language disorder or intellectual disability) revealed hyperconnectivity in the ASD group, in particular among frontal-temporal connections and connections between the basal ganglia (Conti et al., 2017).

Thus, studies from structural connectivity show converging evidence of altered connectivity during early infancy and toddlerhood, which is also related to severity of symptoms. Although functional connectivity is related to structural connectivity, findings from functional connectivity studies show a less consistent pattern.

1.4.3.2. Functional connectivity in ASD

Functional connectivity during early infancy in individuals with later ASD diagnosis has not been extensively investigated yet. One recent study showed that it is possible to predict diagnostic outcome at 24 months from fMRI connectivity data collected at 6 months in HR infants with 96.6% accuracy, by using of classification analyses and machine learning (Emerson et al., 2017). Associations between early fMRI networks and dimensional traits however remain un-investigated. MEG/EEG connectivity in contrast has been more widely examined, although results vary across different age groups and ranges. Similarly to the findings from spectral power studies, findings from studies in adults and children seem to be more consistent than in infants (Mohammad-Rezazadeh, Frohlich, Loo, & Jeste, 2016; Schwartz et al., 2016).

Infancy

At 6 months of age, LR and HR groups display similar levels of gamma EEG connectivity. At 12 months, the HR-ASD group displayed *decreased* gamma connectivity compared to the HR-no ASD group in frontal and temporal-central areas, which in turn displayed decreased connectivity compared to the LR group. Also, the LR group at this age displayed higher leftward-lateralized gamma connectivity, while the HR group showed higher rightward-lateralized gamma connectivity. In the HR-ASD group, more leftward lateralisation at 12 months of age was related to increased ASD symptom severity measured with clinical observations at 24 and 36 months of age (Keehn, Vogel-Farley, Tager-Flusberg, & Nelson, 2015; Righi, Tierney, Tager-Flusberg, & Nelson, 2014).

Further, at 14 months of age, whole brain alpha band connectivity was *increased* in the HR-ASD group compared to the LR and HR-no ASD groups. Increases in connectivity were strongest in fronto-central areas, which were also

related to increased severity of restricted and repetitive behaviours at 36 months of age measured with parental interviews, but not to social communication difficulties. No differences between groups were observed for theta band connectivity (Orekhova et al., 2014).

Toddlerhood

In toddlers, differences in connectivity have been reported also. In 2-5-year-olds with ASD, whole brain beta band connectivity was *lower* compared to toddlers with typical development, but similar across groups for the broad band (.1-30 Hz) and the theta-alpha frequency band (Boersma et al., 2013). *Increased* connectivity for delta, theta, and alpha frequency band in 2-5-year-olds with ASD compared to TD peers has also been found (García Domínguez, Stieben, Pérez Velázquez, & Shanker, 2013). Another study found that connectivity findings depended on the state of the infant (awake or asleep), and the connectivity measure used, with findings of *increased, decreased* connectivity for the ASD compared to the TD group, and *no differences* between groups across the alpha, theta, delta, or beta bands (Buckley et al., 2015).

Not only whole brain connectivity, but also the organization of brain graphs seems affected. For example, *increases* in connectivity in the ASD group compared to the TD group were most prominent in short-range connections for delta and theta frequencies, but were also present in connections across long distances (García Domínguez et al., 2013). Graph theory metrics further support a disruption in organisation of brain graphs. Normalised path lengths in the broad band were *increased*, whereas normalised clustering and small-worldness were *decreased* in the theta-alpha band in the group of ASD toddlers compared to the TD group (Boersma et al., 2013).

Childhood and adolescence

Results from studies in children and those covering large age ranges between infancy and adolescence mainly report reduced levels of connectivity in children with ASD compared to TD children. For example, compared to age-matched TD children, 5.5-8.5-year-old children with ASD exhibited *reduced* connectivity in the delta and theta band across 2 different measures of connectivity (Isler, Martien, Grieve, Stark, & Herbert, 2010). Connectivity was also *lower* in 6-11-year-olds with ASD in the delta, theta, and alpha band, across frontal, temporal, and posterior regions, and across both long and short-distance connections (Coben et al., 2008). Other studies have also found hypoconnectivity for groups with ASD compared to TD; in the alpha range for 2-12 year olds (Dickinson, DiStefano, Lin, et al., 2018; Duffy & Als, 2012), in the delta, theta, and alpha range for 4-12 year olds within hemispheres (Elhabashy et al., 2015), and in the alpha band for posterior areas in 0 to 17-year-olds (Takagaki, Russell, Lippert, & Motamedi, 2015).

Findings of *no differences* between ASD and TD groups of children also exist for different age groups: in 6-14 year-olds (Lazarev, Pontes, Mitrofanov, & deAzevedo, 2010), in 6-16-year-olds (Vakorin et al., 2016), between hemispheres for the alpha band in 4-12-year-olds (Elhabashy et al., 2015), for theta and alpha bands in 1-25-year-olds (Peters et al., 2013), or for delta, theta, alpha, beta, or gamma bands in 6-year-olds (Takahashi et al., 2017). Of course, there are also findings of *increased* connectivity in the ASD group compared to the TD group, although these are less extensive: for example between hemispheres for 4-12-year-olds in one study (Elhabashy et al., 2015).

Connectivity in children with ASD furthermore is differently modulated by task demands than connectivity in typically developing children. Boys with ASD

showed a leftward asymmetry in connectivity in response to light flashes, whereas this asymmetry was not present in 6-14 year old TD boys (Lazarev et al., 2010). Children with ASD exhibited smaller increases in connectivity in the theta range during a demanding executive functioning task than the TD group (7-16-year-olds) across lower frequencies from 8 to 34 Hz (Perez Velazquez et al., 2009).

Differences in connectivity organisation are also present during childhood and adolescence. In the study focusing on 1-25-year-olds, no differences in small-worldness between the ASD and TD group were found. The ratio between long and short-range coherence however was decreased in theta and alpha bands in the ASD group, which implies local overconnectivity and long-range underconnectivity in ASD (Peters et al., 2013). Another study found that decreases in short-range connections, and both increases and decreases in long-range connections distinguished best between ASD and TD groups with 2-12-year-olds, which is inconsistent with the short-range overconnected and long-range underconnected hypothesis (Duffy & Als, 2012). Further, a group of 3-11 year old children with ASD displayed increases in normalised clustering and path length, and decreases in small-worldness across delta, theta, alpha, beta, and gamma frequency bands (Han et al., 2017). In contrast, another study found increased small-worldness in gamma and delta ranges in a group of 6-year-olds with ASD compared to a group with TD (Takahashi et al., 2017). Overall, this suggests that graph organisation is atypical during childhood and adolescence.

Finally, connectivity atypicalities in ASD appear to be related to cognitive functioning, and developmental trajectories. Low functioning children with an IQ below 70 displayed increased theta band connectivity in both long and short

connections compared to high functioning children (8-17-year-olds) (Han et al., 2013).

Adulthood

During adulthood, individuals with ASD overall show decreases in lower frequencies in MEG/EEG connectivity compared to typically developing individuals, most frequently in the alpha range, but also in the gamma range (Barttfeld et al., 2013; Catarino et al., 2013; Kenet et al., 2012; Khan et al., 2013), No differences between groups have also been reported (Mathewson et al., 2012), although interesting associations with dimensional traits were revealed in this study: increased social difficulties were related to increased theta coherence in ASD, whereas less social difficulties were related to increased gamma coherence in TD individuals. Connectivity in both long and short-range connections were reduced (Khan et al., 2013). Higher short-range connectivity and lower long-range connectivity in adults were furthermore related to higher symptom severity in the ASD group (Barttfeld et al., 2011). As for the organisation of the graphs, path lengths were increased, whereas both clustering and small-worldness were decreased (Barttfeld et al., 2013).

To summarise, findings from MEG/EEG connectivity studies across different age ranges showed mixed findings: increases, decreases, and no differences in connectivity between groups with ASD diagnosis or typical development have been found. Findings possibly differ due to the variety of methods used. Different studies tend to focus on different age groups, different paradigms, and different measures of functional connectivity across different frequency bands. In particular for studies during infancy, analyses focusing on familial risk or later diagnostic outcome hamper comparisons between studies. Further, most studies focus on

associations between connectivity and groups with different later outcomes, while few consider associations with later dimensional traits also. Associations with outcome group may inform on later diagnosis, whereas associations with dimensional traits may allow for individual prediction of symptoms across different domains (Mohammad-Rezazadeh et al., 2016; O'Reilly et al., 2017; Schwartz et al., 2016). Examining connectivity during early development in ASD is important since altered connectivity patterns may occur during the first 2 postnatal years as an adaptive response mechanism to atypical neural processing arising from pre- and perinatal factors (Johnson, 2017).

1.5. Aim of the current project

The aim of the current PhD project is to examine how EEG connectivity during infancy is related to later diagnosis and dimensional traits of ASD. It has been suggested that altered EEG connectivity might be a marker for ASD (Jeste et al., 2015; Orekhova et al., 2014). While ASD behaviours do not clearly emerge before toddlerhood, neural markers such as connectivity might develop during infancy prior to the behavioural markers. If altered connectivity is implicated in the adaptive developmental trajectory of ASD in response to atypical neural processing, these alterations are likely to occur during the first 2 years of life (Johnson, 2017). It is thus possible that alterations in EEG connectivity are already evident after the first year of life. A few infant studies indeed suggest that whole brain EEG connectivity is altered in groups of HR-ASD infants compared to HR-no ASD and LR groups, although findings are not in consensus and further research is needed. Findings of associations between EEG connectivity and ASD may depend on the measure and paradigm used, frequency band of interest, connectivity

metrics derived, and the measure of ASD outcomes. Further research is needed to disentangle these different aspects of associations between early EEG connectivity and later ASD outcomes.

Research on EEG connectivity as markers for ASD could further increase understanding of underlying mechanisms by examining brain-behaviour relationships (Insel et al., 2010). Since spectral power in different frequency bands has been associated with different cognitive functions, it is possible that EEG connectivity in different frequency bands is related to different domains of symptoms (social and communication difficulties, or restricted and repetitive behaviours). Furthermore, whole brain connectivity and graph organisation measure different aspects of brain connectivity and may show different associations with later ASD outcomes. In toddlers, whole brain connectivity did not relate to ASD diagnosis, whereas graph metrics did show such an association. It remains unknown how whole brain connectivity and graph organisation in infancy relate to later ASD outcomes.

Research on early markers could also facilitate early detection of ASD or atypical development. Examining both associations with later ASD diagnosis and dimensional traits could help predicting whether an individual might develop ASD at a later age or not, but may also allow to inform on the profile of symptoms an individual might experience at later age (Insel et al., 2010). Early diagnosis may further help towards early intervention, with a possible positive impact on later outcomes (Dawson et al., 2012; Green et al., 2015, 2017; Pickles et al., 2016; Webb et al., 2014). Finally, these markers may help coping with the heterogeneity of ASD by stratifying individuals into more homogeneous subgroups (Loth et al., 2016). It is likely that the previously reported mixed findings arise from the heterogeneity

in ASD. Possibly, different alterations in EEG connectivity patterns are associated with different subgroups of ASD, who also show different behavioural profiles. This stratification may further facilitate early diagnosis and intervention.

While previous findings provide a strong background for EEG connectivity as early marker for ASD, replication and further validation are important in the search for markers as well. Objective measures functioning as markers should be both reliable and reproducible (Strimbu & Tavel, 2011). High test-retest reliability is particularly important for individual prediction of dimensional traits. Replication of previous results in an independent cohort using a similar paradigm and methods would further support the use of EEG connectivity as marker for ASD. However, reliability studies in infant EEG connectivity and replication studies in infants at risk for ASD are scarce. In the context of the current mixed findings with regard to EEG connectivity in infants, it is important to select one specific paradigm to focus on. Further research examining test-retest reliability of this paradigm and EEG connectivity measures, and attempting to replicate previous results, before further extending previous findings, is an important step in the search for markers of ASD.

The current PhD project aims to contribute to research on early markers of ASD by focusing on the question how EEG connectivity during infancy is related to later diagnosis and dimensional traits of ASD. As previous findings have been inconsistent, I am selecting one infant paradigm that has been previously used in one of EEG connectivity studies (Orekhova et al., 2014), and is included in the pre-existing datasets from a high-risk infant sibling study: the BASIS study (British Autism Study of Infant Siblings). Different measures of EEG connectivity may further have contributed to the variability in findings. I will therefore first examine

test-retest reliability for different connectivity measures in young typically developing infants in a test-retest reliability study (Chapter 3). The results of this study will be help to infer the most reliable measurements for EEG connectivity in infants that can also be used to help answer the main question of this thesis.

The second step is to examine the reproducibility of EEG connectivity in infants at risk for ASD. To this end, I attempt to replicate previous findings from the EEG connectivity study by Orekhova and colleagues in a new independent cohort (Chapter 4). Previous findings revealed hyperconnectivity across the alpha band in the HR-ASD group compared to the LR and HR-no ASD group at 14 months of age, and associations between connectivity and restricted and repetitive behaviours at 36 months of age in the HR-ASD group. Replication of these previous findings will provide support for the hypothesis of altered connectivity during early development of ASD. Furthermore, this study may help reveal underlying mechanisms of altered connectivity and later restricted and repetitive behaviours.

Third, examining associations between social and communication difficulties and other measures of EEG connectivity may further help to reveal underlying mechanisms. For example, theta frequency band has been related to the processing of social information. Early atypical connectivity in the theta band might relate to social communication and interaction difficulties. I will therefore continue examining how connectivity in the theta band during social and non-social processing is related to risk and later diagnosis, and severity of ASD traits at 36 months of age (Chapter 5). These results will further help extend previous findings by focusing on theta connectivity and social difficulties rather than alpha connectivity and restricted and repetitive behaviours.

Fourth, in addition to atypicalities in whole brain connectivity, alterations might also exist in the organisation of the connectivity graphs during infancy. I will therefore examine associations between graph theory metrics in the alpha and theta band, and risk and outcome, and dimensional ASD traits at 36 months of age next (Chapter 6). These findings may reveal how different aspects of EEG connectivity in particular whole brain connectivity and organisation of connectivity patterns are related to ASD.

Finally, associations between early EEG connectivity and later ASD traits may depend on the developmental period. The severity of ASD traits at 3 years of age may change during childhood. As mentioned before, traits are typically most visible during childhood, thus after the clinical assessment at toddlerhood in most high-risk infant sibling studies. The expression of ASD traits may worsen or improve after the 3-year-old time point. It is possible that associations of infant EEG connectivity measures with ASD traits at childhood are different from those with ASD traits at toddlerhood. In the last experiment, I will combine the EEG connectivity measures calculated in the previous chapters, and examine how these relate to later ASD traits during mid-childhood (Chapter 7). These findings may reveal further underlying mechanisms of ASD that may occur across different developmental periods.

Together, the results of this project will further our understanding of EEG connectivity during infancy, and how this associates with risk and diagnosis, and dimensional traits of ASD at later ages. This may further help our understanding of underlying mechanisms of early development of ASD, as different aspects of infant EEG connectivity, and different measures of later traits of ASD are examined.

1.6. Summary of Chapter 1

ASD is a developmental disorder, typically diagnosed during toddlerhood or childhood. It has been suggested that ASD is characterized by altered brain connectivity patterns, possibly as result of an adaptive response to atypical neural processing during early development. Alterations in EEG connectivity might function as an early marker for ASD diagnosis and dimensional traits. Research into potential early markers of ASD could increase our understanding of underlying mechanisms, and help toward early diagnosis and intervention.

Previous studies in young infants who develop ASD at a later age have shown increases, decreases, and no differences in EEG connectivity compared to groups of infants without a later ASD diagnosis. This variability of results possibly arises from differences in age groups, paradigms, frequency bands of interest, or the measure of functional connectivity used. Further studies examining test-retest reliability of these measures, and reproducibility of previous results are needed to further research of early markers of ASD. In addition, extending previous findings by examining different aspects of EEG connectivity and their association with ASD risk and diagnosis, and later ASD traits will help reveal underlying mechanisms of ASD. The overall aim of the current project is to examine the relation between EEG connectivity in young infants at low and high familial risk for ASD, and later ASD diagnosis and dimensional ASD traits during toddlerhood and childhood. The next chapter will focus on the methods used to achieve this goal.

Chapter 2: The Methodology of Electroencephalography (EEG)

2.1. Introduction

Electroencephalography (EEG) is the main neuroimaging method used in this thesis. The EEG method measures synchronisation of neural populations. This chapter provides a general introduction of EEG by discussing what EEG measures, and the different methods of analyses of the EEG signal, such as frequency analyses, and connectivity analyses.

2.2. The importance of measuring neural synchrony

Synchronised neural oscillations are involved in cognitive processes, including the encoding of information during memory and perceptual processing, learning, modulating attentional systems, motor behaviour, information transfer, and the consolidation of memories (Lopes da Silva, 2013; Pfurtscheller & Lopes Da Silva, 1999). These oscillations furthermore play an important role in the establishment of neural networks (Uhlhaas, Roux, Rodriguez, Rotarska-Jagiela, & Singer, 2010). Previous studies have shown that changes in synchronised neural activity are activity and experience dependent, and have been related to changes in myelination both during early development and adolescence (Benders et al., 2015; Dubois, Kostovic, & Judas, 2015; Smyser & Neil, 2015; Uhlhaas et al., 2009). Synchronised activity is thus thought to reflect functional network development, and network reorganisation. Focusing on synchronised neural activity during development is therefore important for understanding atypical neural development for example in ASD.

In addition, it has been hypothesized that synchronised neural oscillations are important for neuronal communication. Neural oscillations are related to

alternating periods of excitability and inhibition of the neuronal populations. Strong synchronization allows for efficient information transfer so that encoded information arrives at the precise moment the receiving neural population is most excitable. This mechanism relies on the high predictability of oscillatory rhythms. When oscillations are predictable, the next phase-dependent excitable period can be precisely predicted, and arrival of the encoded information can be properly coordinated. Oscillatory entrainment of neural populations creates a phase relationship that allows for this efficient neural communication. This entrainment can occur at and between different frequencies, depending on the oscillatory strength and phase relations between the receiving and sending neural populations. Dynamic changes in neural synchronisation and information transfer may be related to cognition. Overall this suggests that precise temporal coupling between oscillatory signals is important for efficient information transfer, and thus effective and functional connectivity (Fries, 2005, 2015; Maris, Fries, & van Ede, 2016; Peterson & Voytek, 2015).

Synchronised neural activity occurs mostly at frequencies between 1 and 80 Hz (Uhlhaas et al., 2010). In order to measure the amount of neural synchronisation and coupling at high frequencies, a neuroimaging technique measuring brain signals with high temporal precision is essential. Indeed, the high temporal resolution of EEG makes this a suitable method to examine precise neural communication or coupling between different neural signals across the whole brain, or EEG connectivity. Two main groups of paradigms for measuring EEG connectivity exist: task-dependent paradigms, and resting-state paradigms. Task-dependent experiments involve a task, where usually a sensory (visual, auditory, tactile etc.) stimulus is presented, and a response is required from the

participant. In contrast, resting state paradigms measure the participants' EEG signal while at rest. In eyes open paradigms, participants are asked to fixate on a fixation cross presented at the screen while resting. In the eyes closed paradigms, participants are asked to close their eyes and rest (M. X. Cohen, 2014; Luck, 2014). Thus neural synchronisation has been related to cognitive processes and early brain development, and may be a mechanism for neural communication. EEG is a suitable measure for neural synchronisation due to its high temporal resolution, but also due to its well-known origin of the signal, and applicability in infant studies, which will both be discussed in the next sections.

2.2.1. The origin of the EEG signal

The EEG sensors measure changes in electrical currents with respect to the reference electrode that arise from electrical currents traveling along the neural membranes. Once a neuron depolarizes or is activated by a signal transfer from another neuron, ions of Na^+ and Ca^{2+} flow into the neuron leading to a change in voltage deflection within the neuron with respect to outside the neuron. This Na^+ and Ca^{2+} influx leads to a local extracellular sink. To balance out this sink in voltage, return currents or passive currents appear in the extracellular environment. This event creates a dipole that is defined as two opposite charges with infinitely small distance. The potential (measured in Volts) of this dipole decreases with increasing distance: $1/r^2$, where r reflects the distance (Buzsáki, Anastassiou, & Koch, 2012) (Fig. 2.1A).

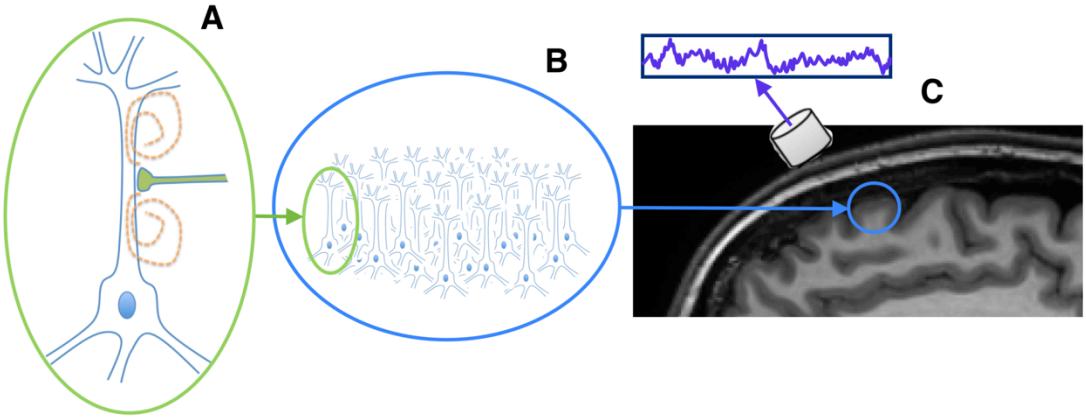

Figure 2.1. The origin of the EEG signal

The EEG signal arises from electric currents moving along the neural membrane (A) in populations of parallel-aligned pyramidal neurons (B) near the surface of the cortex where the signal travels through the scalp and is measured by EEG sensors (C).

Extracellular currents like these occur at various sorts of neurons and neural processes, such as interneurons, spikes, and glial cells. The superposition or additions of all these extracellular processes give rise to the local field potential (LFP) that can be measured at the scalp by the EEG sensors. Charges in the same direction add up (+1 and +1 = +2), whereas charges in opposite directions cancel out (+1 and -1 = 0). Some neurons are more likely to contribute to LFPs measured by EEG than others since the strength of the potential decreases with increasing distance. Specifically, dendritic postsynaptic potentials of pyramidal cells are thought to mostly contribute to the EEG signal, due to their shape, position in the cortex, and temporal fluctuations. First, pyramidal neurons are characterized by long thick dendrites that allow for strong dipoles along the dendrites axes. These also give rise to an open field where the sink and return currents are maximally separated in such a way that the extracellular current changes can be measured from larger distances (Buzsáki et al., 2012; Lopes da Silva, 2013).

Second, pyramidal neurons are ordered in parallel alignment. The synapses providing input are perpendicular to the dendrites. The cortical folding in humans further increases the density of pyramidal neurons in the gyri near the surface of the brain. This arrangement of neurons in the cortex facilitates the superposition process of potentials contributing to the local field potential (Buzsáki et al., 2012) (Fig. 2.1B & C).

Third, temporal fluctuations by means of timely synchronized activations of many neurons will increase the superposition of the potentials and considerably contribute to the LFP. The power of the LFP is inversely related to the temporal frequency of the neuronal activity. It has been suggested that slow oscillations are less attenuated with increasing distance between source and recording site than faster oscillations. Larger dendrites tend to synchronize at lower frequencies. Further, activations of neurons with larger dendrites within a short time period will lead to slower oscillations with larger amplitudes as opposed to recruitment neurons with shorter dendrites and higher frequency oscillations with lower amplitudes. As pyramidal neurons have long thick dendrites, this makes them a strong contributor to the LFPs and their recording at the scalp by EEG sensors (Buzsáki et al., 2012).

2.2.2. The EEG system and experimental set up

The changes in electrical fields are measured by an EEG system. The EEG system consists of several sensors or electrodes that are in contact with the scalp via a net or cap applied to the participants' head (Fig 2.2A). The number of electrodes used varies; commonly 32, 64 or 128, but fewer or more electrodes are also possible depending on the research question and experimental design at hand. Since air is a bad conductor of the electrical signal, the electrodes need to be in contact with the

scalp, either via conductive gel (systems as Biosemi, Acticap) or via sponges soaked in water with conductive salts (systems as Electric Geodesic Inc. (EGI)) (M. X. Cohen, 2014; Johnson et al., 2001). Furthermore, the sampling rate, or the rate at which the electrical field is measured, can differ as well depending on the design and research question. Sampling rates in practice vary between 500 and 2000 Hz, but 256 Hz, 512 Hz, or 2048 Hz are also frequently used (M. X. Cohen, 2014).

The EEG experimental set up involves a recording computer, an EEG recording system, and usually a stimulus computer (Fig. 2.2.B). Ideally, the EEG experiment takes place in a shielded room to prevent electrical interference with the EEG signal from other apparatus. A video camera and microphone will aid monitoring and communication with the participant during the experiment. Depending on the task, stimuli are presented on the stimulus computer while the EEG signal of the participant is recorded. Event markers marking the timing of the stimulus events are simultaneously sent to the EEG recording system to mark the events. These markers will allow the researcher to match the stimulus events to those occurring in the EEG signal in later data analyses (M. X. Cohen, 2014).

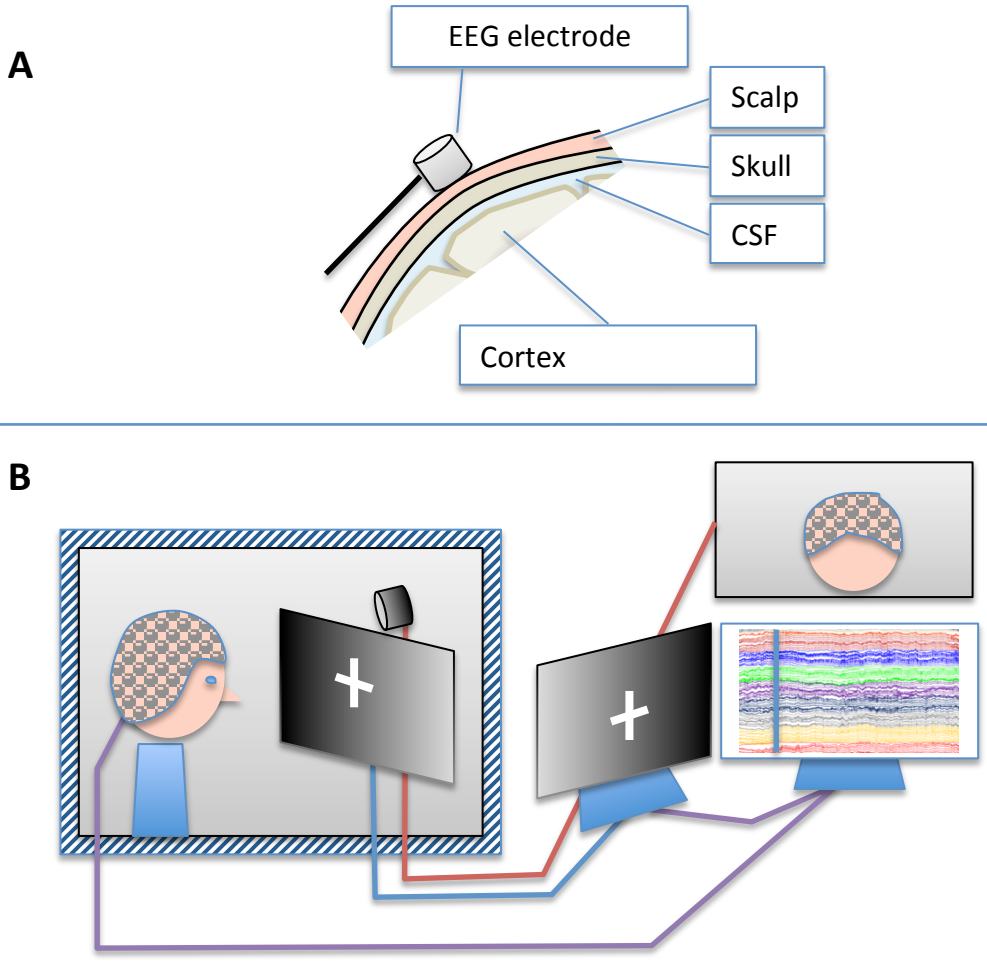

Figure 2.2. Measuring the EEG signal

The EEG signal is measured with EEG electrodes touching the scalp (A). The EEG signal is typically recorded in a shielded room (B). Abbreviations: cerebral spinal fluid (CSF), electroencephalography (EEG).

2.2.3. The problem of volume conduction for EEG

Volume conduction is the transmission of an electric charge through a volume, for example brain tissue or bone. The volume conducted electrical field arises from the extracellular return currents. The degree to which an electrical charge is conducted throughout the brain onto the scalp depends on resistance of the tissues, the homogeneity of the tissues, and the shape of the extracellular space.

Volume conduction causes an electrical field spread between the skull and scalp. As a result, changes in the electrical fields measures by the EEG electrodes are more spread and smeared out across the scalp, and multiple electrodes pick up signals from common sources (Figure 2.3). Therefore, the EEG method does not provide an accurate spatial localisation of the effect. It is possible to draw conclusions about the rough topography however (frontal, central, temporal, parietal, occipital areas, left and right hemispheres). Still, one should be aware that there is common pick up by multiple sensors from the same source, and each sensor picks up a mixture of activations from different sources which is a problem when estimating functional EEG connectivity at sensor level (Buzsáki et al., 2012; M. X. Cohen, 2014).

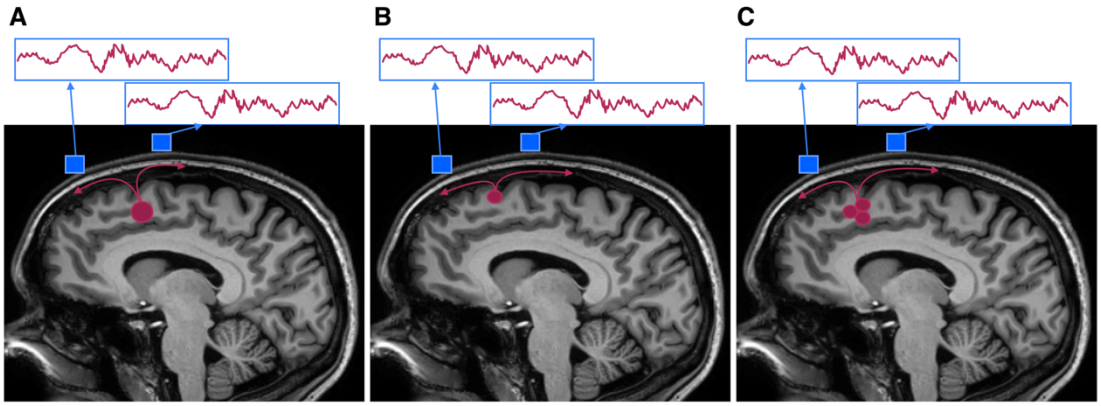

Figure 2.3. Volume conduction

Volume conduction of the EEG signal through the brain leads to field spread and common pickup of a source by multiple electrodes. The inverse problem refers to the same signal that would arise from a stronger dipole (A), a weaker dipole nearer to the cortical surface (B), or multiple weaker dipoles (C), among other possible solutions.

Localisation methods can identify the origin of the EEG signals by localising the sources of the electrical currents, and thereby circumventing the volume conduction effects. These methods infer the properties of the current sources from the electrical fields recorded at the scalp, while attempting to solve 'the inverse mapping problem'. For example, an EEG signal might arise from a strong dipole, a weaker dipole near the cortical surface, or from multiple dipoles (Fig. 2.3A, B, and C). Thus there are an infinite number of possible solutions to the inverse problem. When a suitable solution is found, it is still always possible that there are other solutions that would result in the same electrical field recorded at the scalp. In order to solve the inverse problem, 'the forward problem' needs solving first: potentials measured at the scalp are calculated based on source models, and head models. Source models estimate the location of the source current(s), which can be represented by one or multiple dipoles. Head models contain information on the conductivities of tissues in the head. Spherical head models assume three homogeneous spherical volumes reflecting the scalp, skull, and brain. More realistic head models also take into account the individual differences in thickness of the scalp, skull, and surfaces of the brain (boundary element methods), and differences in conductivity of different tissues (direction of conduction, white matter, cerebral spinal fluid, bone, skin). These realistic head models are based on individual MRI scans (Baillet, Mosher, & Leahy, 2001; van Diessen et al., 2015). Different source localisation methods exist, for example LORETA, current source dipole modelling, or beam forming.

Source localisation methods are commonly used in adults, but only few studies have applied these methods in infants (Bathelt, O'Reilly, & de Haan, 2014; Xie, Mallin, & Richards, 2017). Localisation methods are successful in only half of

the participants. First, there is a lack of appropriate head models for infants. Adult models cannot be applied in infant studies as infants' heads have different shapes and skull thickness. Infants' skulls are thinner and have a smaller density than adult skulls, and are not even present at some places in young infants (at fontanels and sutures between skull bones), so that currents can freely travel through the head. The conductivity for different tissues is also higher in adults than infants. The spherical head models are therefore even less appropriate here as infants do not have a perfect spherical head, and skull thickness and density are not homogeneous across the head. Databases for anatomical models from infant MRI scans have only recently been developed. Infant MRI scans however might not always be available for the appropriate age group, or might only be based on a small number of infants. Thus the individual properties of the infant brains would not be accounted for (Johnson et al., 2001; Lew et al., 2013; Reynolds & Richards, 2009; Richards, Sanchez, Phillips-Meek, & Xie, 2016).

The second reason that source localisation is not widely applied in infants is that these methods typically involve independent component analysis (ICA) or principal component analysis (PCA). These methods extract components from the raw EEG data that 'unmix' the data which each component accounting for the smaller amounts of variance in the data. It is assumed that the sum of these components reflects the recorded EEG signal. ICA and PCA both assume that a) the EEG signal is a linear combination of the activations of underlying sources, b) sources are spatially fixed and remain in the same region, and c) temporal activations of different sources are statistically independent in time. For PCA, components are extracted if they are normally distributed, whereas ICA does not assume a normal distribution. After extracting a small number of components that

reduces the complex EEG data, source localisation can be done on these components (Johnson et al., 2001; Reynolds & Richards, 2009). However, the researcher will have to select the components for source localisation out of the many components that result from PCA/ICA analyses. Noise might furthermore influence the results. Components might be fitted to the data while simultaneously accounting for noise and true brain signal. This makes it difficult to disentangle the noise from the EEG signal. Also, the assumption of spatial stability might not be appropriate when applied across long segments of data. Finally, these methods typically require large amounts of artefact-free data that are often not available in infant studies (M. X. Cohen, 2014; Johnson et al., 2001). In short, due to volume conduction, spatial resolution of EEG is limited and source localisation techniques are not widely applied in infants. However, there are other advantages to this method for infant research.

2.2.4. EEG in comparison with other neuroimaging methods

The main advantage of EEG is the high temporal resolution, and strong link between the EEG signal and neurophysiological mechanisms in the brain. This allows for precise quantification of the dynamic coupling between neural oscillations. The technique can be applied during task-related, and resting-state paradigms, and in both adults and infants. Infant EEG is typically recorded using the EGI system with sponges, which reduces preparation time compared to conductive gel systems (M. X. Cohen, 2014; Johnson et al., 2001). Furthermore, resting-state paradigms for infants are different from those applied in adults, as following verbal instructions is problematic for infants. The infant version of resting state EEG paradigms therefore involve a person blowing bubbles in front of the infant (live) (Righi et al., 2014; Stroganova et al., 1999), or women singing

nursery rhymes, toys spinning around, or toys being spun around by a hand (live or video recordings) (Jones et al., 2015). Finally, EEG allows for more freedom of movement during recordings, thus the awake infants are less restrained in the resting-state paradigms.

Other measures of brain functioning however exist along EEG, such as magnetoencephalography (MEG), functional magnetic resonance (fMRI), and functional near-infrared spectroscopy (fNIRS). Each of these methods has its own advantages and disadvantages with regards to spatial resolution, temporal resolution, and freedom of movement (Fig. 2.4). MEG measures changes in magnetic fields that arise from local potentials that also induce the electric currents measured by EEG. The resulting magnetic field arises along the neuron from primary intercellular currents. Due to this orientation, only the magnetic fields of tangential neurons are measurable with MEG. The electric field, in contrast, arises from both radial and tangential neurons. The apparatus measuring the MEG signal has a stationary helmet containing superconducting quantum interference devices that record changes in the magnetic field. The main advantage of MEG however is the higher spatial resolution when compared to EEG. Magnetic fields are less influenced by volume conduction, since the magnetic permeability across different tissues is constant. Thus there is less field spread across the scalp, and oscillations originating from subcortical structures are likely to be recorded. The temporal resolutions for EEG and MEG are similar. However, the MEG involves a stationary device that limits the participants' freedom of movement. This is especially an issue for infants, as these move around frequently when awake. MEG in infant research is therefore commonly used in resting state research while the infants are sleeping (Baillet et al., 2001; Lopes da Silva, 2013).

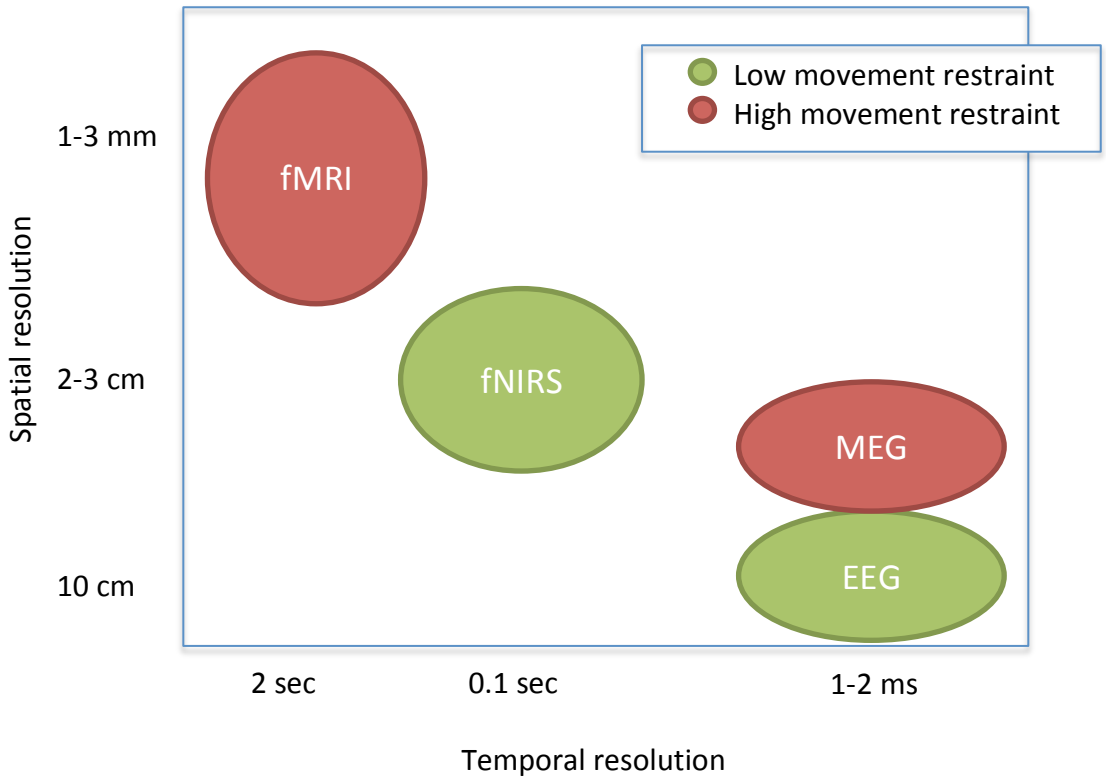

Figure 2.4. Comparison of different neuroimaging methods

The x-axis represents the amount of temporal resolution, while the y-axis represents the amount of spatial resolution. The degree of freedom to move around is reflected in different colours.

The fMRI method does not allow for movement either, as movement by participants lying in the scanner creates large artefacts. fMRI studies are therefore usually conducted in sleeping or sedated infants. fMRI measures blood oxygenation level dependent (BOLD) changes that arise from changes in deoxygenated haemoglobin and the blood flow when neurons are activated. The BOLD response peaks around 6 seconds after stimulus presentations in adults. It should be noted that changes in the BOLD signal in infants might arise from different neurovascular mechanisms than those in adults. Thus fMRI is a more indirect measure of brain activity than EEG or MEG. The temporal resolution of

fMRI (about .5 Hz) is lower, but the spatial resolution of fMRI is higher than of EEG/MEG methods, where fMRI has the ability to detect changes in 1-3 mm voxels or smaller with stronger scanners (Aslin, Shukla, & Emberson, 2015; Harris, Reynell, & Attwell, 2011).

Lastly, fNIRS is now more commonly applied in infant studies. This method measures changes in oxygenated and de-oxygenated blood. After neural firing, there is a local increase in de-oxygenated blood, followed by a compensatory increase of oxygenated blood, and finally a decrease of de-oxygenated blood. fNIRS emitters send near-infrared light into the brain, while fNIRS sensors measure the amount of light refracted by both oxygenated and de-oxygenated blood in the cortex about 1 cm below the surface. The adult fNIRS response peaks after 6 seconds, and returns back to baseline after 10 seconds after stimulus onset. However, the infant fNIRS response and the underlying mechanisms remain unclear. The sampling rate of the fNIRS method is about 10 Hz, which is higher than fMRI but lower than EEG/MEG. The spatial resolution of fNIRS is about 2-3 cm, which is higher than EEG/MEG, but lower than the fMRI method. Finally, fNIRS does not limit movement of the infant as much as MEG or fMRI, and can thus be used in infants while awake (Aslin et al., 2015; Wilcox & Biondi, 2015).

In short, the main advantages of EEG are the strong link with neurophysiological mechanisms, the high temporal resolution, and freedom of movement during recording when compared to MEG, fMRI, or fNIRS. This makes the method especially suitable for infant research. The main disadvantage is the low spatial resolution, but this is a small issue if the research question mainly concerns temporal aspects of the brain responses.

2.3. EEG analyses methods

The EEG signal can be analysed with different methods, depending on the research question and experimental design: frequency analyses, and connectivity analyses. Before these analyses are performed, EEG data are usually cleaned using manual and/ or automatic artefact rejection. Artefacts from eye blinks, eye movements, muscle contractions, jumps in the signal, or flat lines among others are removed from the signal. Single electrodes that show a noisy or flat signal may be excluded from further analyses, or be interpolated based on the signals from neighbouring electrodes. Further filtering can be applied to remove the mean, slow wave drifts, high frequency noise, or line noise from electrical apparatus in the signal. Different toolboxes and analyses tools exist for analysing EEG data such as EEGlab, and FieldTrip (M. X. Cohen, 2014; Delorme & Makeig, 2004; Oostenveld, Fries, Maris, & Schoffelen, 2011). After preprocessing, frequency analyses are applied to the data where the resulting values are used to calculate EEG connectivity.

2.3.1. Frequency analyses

Frequency analyses provide information on the characteristics of the frequencies that comprise the EEG signal, such as power, amplitude, and the phase of the signal at a specific frequency. For efficient neural communication, neural populations should oscillate in the same frequencies. Different frequency bands have been related to different perceptual and cognitive processes.

2.3.2.1. Frequency bands

Frequency analyses provide frequency spectra that reflect power at specific frequencies (e.g. power at 8 Hz reflect power for signals with 8 cycles per second). A typical frequency spectrum shows an inverse relation between power and the frequencies of the oscillations; lower oscillations exhibit higher power, whereas

higher oscillations exhibit lower power (Fig. 2.5). This is probably due to the fact that amplitudes of higher frequencies are more attenuated across longer distances than amplitudes of lower frequencies. Also, lower frequency signals tend to be more in phase with each other than higher frequencies.

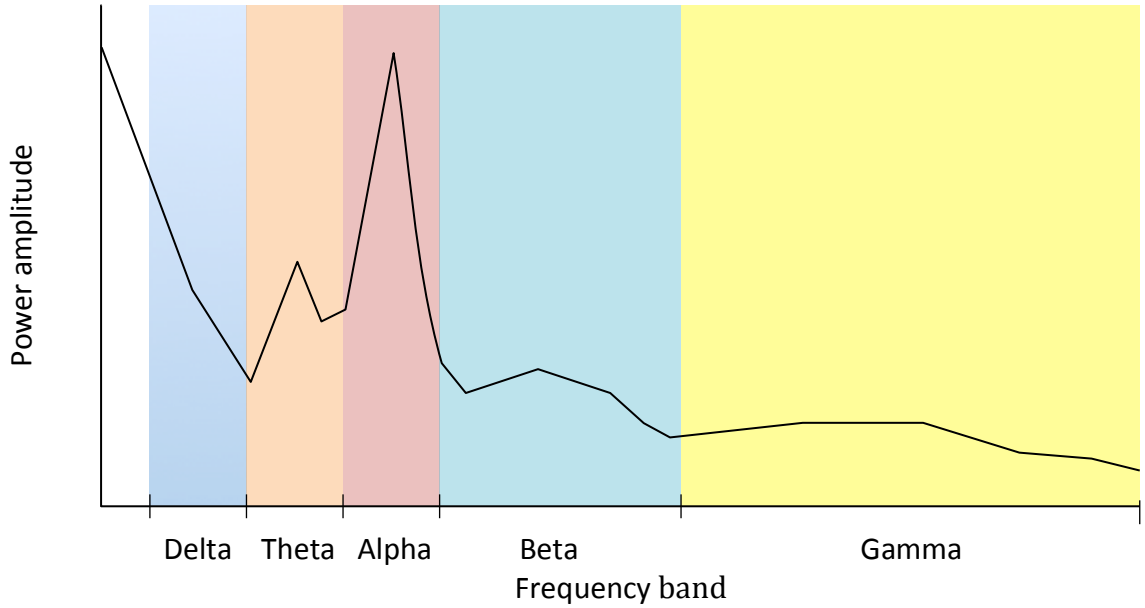

Figure 2.5. Shape of a typical frequency spectrum for EEG data
Peaks are typically observed in the theta and alpha bands. The specific borders between the frequency bands differ between subjects, and across different ages.

Another possible explanation is that only a small amount of neurons can be activated within a short time. The activation of a small number of neurons at lower frequencies would be more efficient than the activation of a small number of neurons at higher frequencies that are attenuated with increasing distances (Buzsáki et al., 2012).

Lower frequencies are characterized by a high signal-to-noise ratio, and are less susceptible to muscle and ocular artefacts (Goncharova, McFarland, Vaughan, & Wolpaw, 2003; Muthukumaraswamy, 2013; Shackman, McMenamin, Maxwell, Greischar, & Davidson, 2010). Two clear peaks can often be distinguished in the

power spectrum: one in the theta band, and another one in the alpha band (M. X. Cohen, 2014)(Fig. 2.10). Different frequency bands have been defined in previous EEG research: delta, theta, alpha, beta, and gamma frequency bands. Different bands have been related to different cognitive functions, and borders vary with age. For example, delta oscillations (1-3 Hz in infants, 1-4 Hz in adults) have been related to sleep, whereas beta oscillations (10-25 Hz in infants, 13-30 Hz in adults) have been associated with muscle contractions and movements. Gamma oscillations (20-60 Hz in infants, 30-100 Hz in adults) have been related to memory, familiarity, and the formation of representations of events, also called 'perceptual binding' of different features of an object into one coherent concept (Saby & Marshall, 2012). Theta and alpha frequency oscillations have also been extensively investigated in infants.

The theta frequency band (3-6 Hz in infants, 4-8 Hz in adults) plays a role in the executive control of attention (Orekhova, Stroganova, Posikera, & Elam, 2006; Orekhova, Stroganova, & Posikera, 1999), the processing of emotional information, and learning and memory (Saby & Marshall, 2012). Theta increases in spectral power have also been observed in response to social stimuli when compared to responses to non-social stimuli (Dawson et al., 2012; Jones, Dawson, Kelly, Estes, & Jane Webb, 2017; Jones et al., 2015).

The alpha frequency band (6-9 Hz in infants, 8-12 Hz in adults) has been related to cortical inhibition and top down modulation. Alpha power decreases in task-relevant areas, while simultaneously increasing in task-irrelevant areas (Klimesch et al., 2007). It has been suggested that via this inhibition mechanism alpha oscillations play a role in visual attention, inhibition of attention shifting, voluntary motor control, and sensory motor stimulation after observing different

topologies of alpha band power increases and decreases (Lopes da Silva, 2013). Studies in infants show that alpha power is related to attentional control (Jones et al., 2015; Orekhova, Stroganova, & Posikera, 2001; Stroganova et al., 1999), and action observation and execution (Marshall & Meltzoff, 2011; Marshall, Young, & Meltzoff, 2011; Orekhova et al., 2006; Southgate, Johnson, Osborne, & Csibra, 2009). The alpha band peaks a lower frequencies at younger ages than at older ages (Marshall et al., 2002; Saby & Marshall, 2012). Alpha peaks at posterior electrodes occur at 3-5 Hz around 3 months of age, and at 6-7 Hz around 12 months of age. Alpha peaks at central electrodes occur at 6-7 Hz at 5 months of age, 7-8 Hz at 10 months, 8 Hz at 14 to 24 months, and 9 Hz at 51 months of age (Marshall et al., 2002). Other studies defined the alpha band as 6 to 9 Hz in 6 and 12-month-old infants (Jones et al., 2015), or 7-8 Hz in 14-month-old infants (Orekhova et al., 2014).

In summary, spectral power in different frequency bands has been related to different functional properties. The specific borders of the frequency bands are lower for infants than for adults. Not only power analyses, but also EEG connectivity analyses could be investigated within the different frequency bands.

2.3.2.2. Performing frequency analyses

Fourier once stated that each signal could be decomposed into a sum of sine and cosine waves. Frequency analyses transform the data from the time domain (sample of the signal for each time point) to the frequency domain. The frequency domain represents amplitude, power, and phase for different frequency across a certain amount of time. Frequencies are the number of cycles within 1 second in the unit of Hertz (Hz): 5 Hz reflects a signal with 5 cycles within 1 second (Fig. 2.6). Different versions of Fourier analyses exist, such as Fourier transform, Fast

Fourier Transform, short-time Fourier Transform (M. X. Cohen, 2014; Smith, 1999).

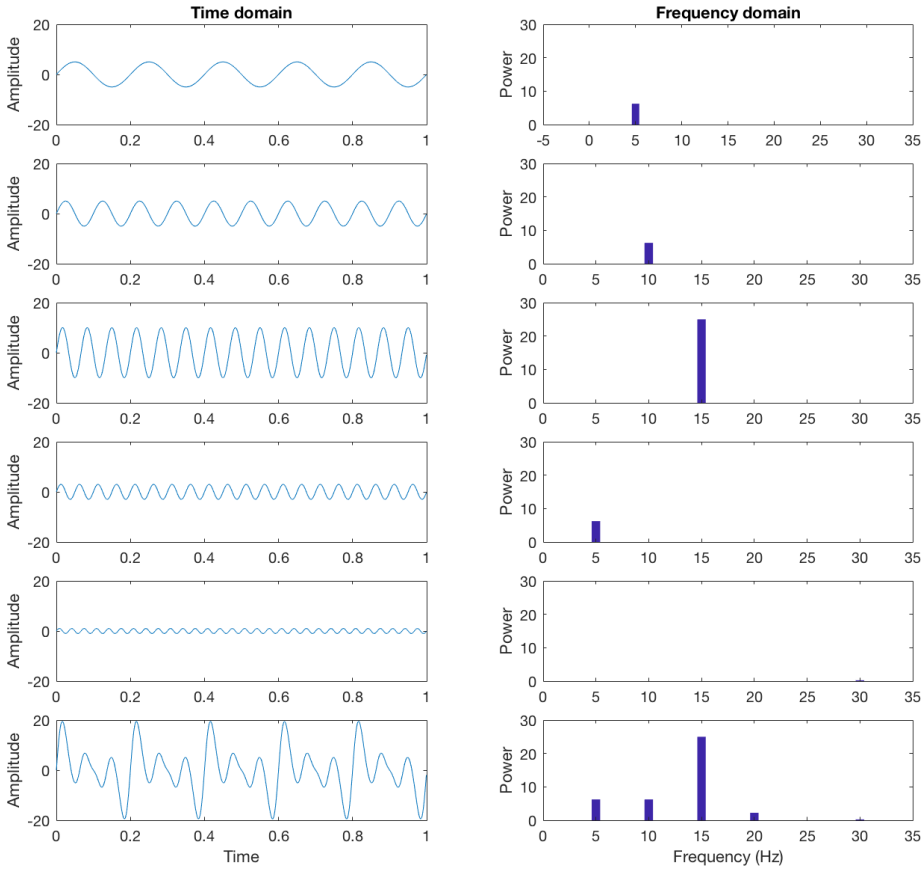

Figure 2.6. Signals in the time and frequency domain

Signals with different frequencies are represented in the time domain (left), and frequency domain (right). Signals containing 1 frequency with different amplitudes are presented in the different rows. A signal can also be composed of different frequencies (sum of previous signals in 6th row).

The Fourier transform is defined as the dot product between a continuous signal and a sine. The dot product represents the similarity or covariance between the two signals or vectors, for example time series a and b, and is calculated as:

$$dot\ product_{ab} = \sum_{i=1}^{n} a_i b_i$$

where n is the number of elements in a and b (n_a and n_b must be the same). In other words, the first element in a is multiplied with the first element in b, the second element in a is multiplied with the second element in b, et cetera until the end of the time series. Then all the results are summed. Convolution in the time domain is defined as the dot product between the time domain signal and another signal (also termed kernel) while being shifted over time. The dot product requires full overlap of the signal and kernel to be computed. To ensure that the entire signal is convoluted, the end and beginning of the signal are padded with zeros. After the calculation of the dot products, these values are trimmed again (M. X. Cohen, 2014).

In the Fourier transform this kernel is a sine or a cosine. Both are a periodic function, but their phases are shifted by 90° (Fig. 2.7). A periodic wave can be defined as:

$$A\sin(2\pi ft + \varphi) \qquad \text{or} \qquad A\cos(2\pi ft + \varphi)$$

where A is the amplitude wave, f it the frequency of the wave, t is the time, and φ is the phase angle offset (phase at $t = 0$). Multiple sine waves with different frequencies can be created to extract the similarities between the raw EEG signal and the sine wave. The result of the Fourier transform is Fourier coefficients for different frequencies that together compose the frequency spectrum. The discrete time Fourier transform is calculated over a signal that consists of samples taken at time intervals as opposed to a continuous signal. This transform is defined as the dot product between the EEG signal and a complex sine wave that contains a cosine (real) component and a sine (imaginary) component. The Fast Fourier transform (FFT) is another version of the Fourier transform that is characterized

by the fast computation. Also here, the result consists of Fourier coefficients for different frequencies (M. X. Cohen, 2014; Smith, 1999).

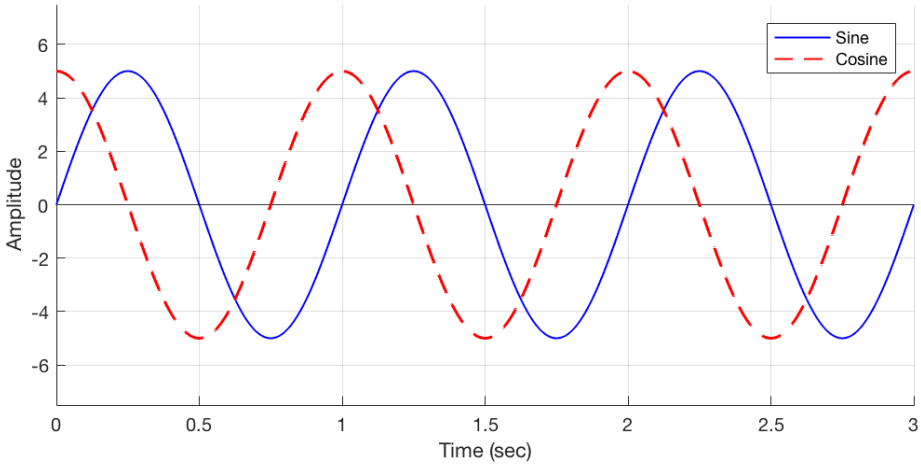

Figure 2.7. Example of sine and cosine

Examples of a sine (solid blue line) and a cosine (dashed red line) of 1 Hz.

The range and the resolution of the frequencies for the Fourier coefficients depend on the number of samples in the signal and the sampling rate. The first frequency is a flat line at 0 Hz, also called the direct current component (DC). This signal is the mean offset of the entire signal. According to the Nyquist theorem, 2 samples per cycle are required for a periodic signal to be sampled appropriately. The highest frequency that can be measured is therefore defined as F_s / 2, where F_s is the sampling rate. The frequency spectrum then consists of $N/2 + 1$ equally spaced frequencies, where N is the amount of samples in the data, and the +1 represents the DC. For example, if a signal contains 1000 samples and the sampling rate is 1000 Hz, the Fourier coefficients can be computed for frequencies 0 to 1000/2 = 500 Hz, in 1000/2+1= 5001 equally spaced sampled frequencies between 0 and 500 Hz: 0 Hz, 1 Hz, 2 Hz, 3 Hz, … ,499 Hz, 500 Hz.

The Fourier coefficient for a given frequency *f* is defined as:

$$X_f = \sum_{k=1}^{n} x_k \, e^{-i\,2\pi f(k-1)n^{-1}}$$

where X_f is the Fourier coefficient at frequency f, n is the number of data points in time series x. The Fourier coefficients reflect the amplitude, power, and phase of the signal at the frequencies, and can take the form of complex numbers for a Cartesian notation, or of magnitude and angle for a polar notation.

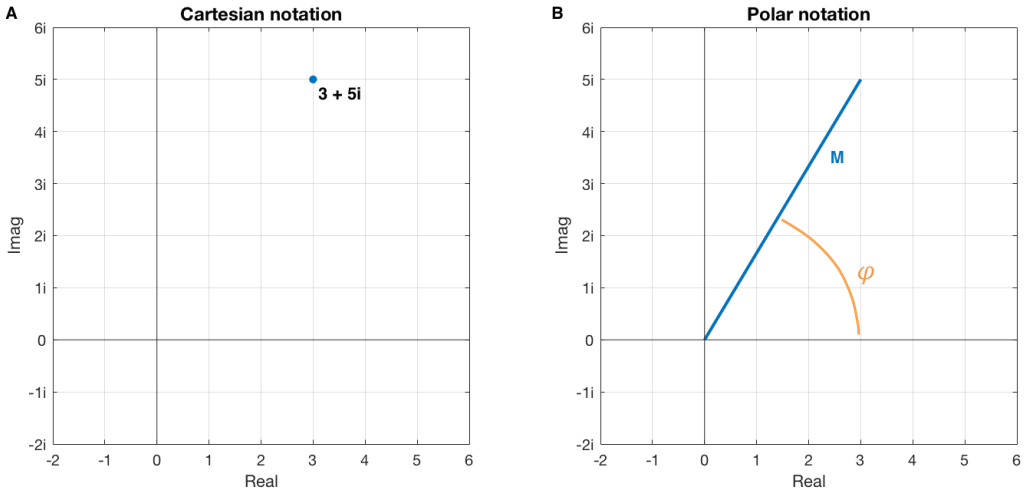

Figure 2.8. Cartesian and Polar representations
Cartesian notation (A) consists of complex numbers. Polar notation (B) consists of magnitude M and phase *φ*.

For the Cartesian notation, the complex numbers consist of a real and an imaginary part. The imaginary part is characterized by *i*, which is the square root of -1. An example of a complex number is 3 + 5i. The coefficient can be plotted in a plane where the real part (amplitude of cosine wave) is plotted on the horizontal axis, and the imaginary part (amplitude of sine wave) is plotted on the vertical axis (Fig 2.8A). The polar notation consists of the magnitude *M* and the angle *φ* (Fig 2.8B). These can be derived from the complex number from the Cartesian notation, as follows:

$$M = \sqrt{Re^2 + Im^2}$$

$$\varphi = \arctan(\frac{Im}{Re})$$

where *Re* is the real component, *Im* the imaginary component, M the magnitude, and φ the phase angle that is expressed in radians. The polar notation of 3 + 5i would be M = 5.83, and φ = 1.03 rad. Similarly, complex values can be derived from the magnitude and phase angle, so that:

$$Re = M\cos(\varphi)$$

$$Im = M\sin(\varphi)$$

From this also follows:

$$Re + Im = M\cos(\varphi) + M\sin(\varphi)$$

$$Re + Im = M[\cos(\varphi) + \sin(\varphi)]$$

$$a + ib = M[\cos(\varphi) + \mathrm{i}\sin(\varphi)]$$

The Fourier transform is used to transform signals from the time domain into the frequency domain. Similarly, a signal in the frequency domain can be transformed to the time domain via the inverse Fourier Transform:

$$x_k = \sum_{k=1}^{n} X_k\, e^{i\,2\pi f(k-1)n^{-1}}$$

where x_k is the time series for frequency *f*, X_k is the Fourier coefficient at frequency *f*, *n* is the number of data points in time series. The inverse Fourier transform is especially useful during filtering of the signal, where specific frequencies are attenuated. For example, some research might be interested in specific frequency bands or want to attenuate 50 Hz line noise from the apparatus in the EEG room or high frequency noise from the data. Band-pass, band-stop, and high- or low-pass filters can be applied to the data. However, convolution with the specific frequencies in the time domain is time consuming. Computation time is

considerable decreased when data are transformed to the frequency domain with the FFT, multiplied with the frequency domain filter, and finally transformed back into the time domain with the inverse Fourier transform (M. X. Cohen, 2014).

One thing to keep in mind is that the Fourier transform assumes the signal is stationary: the signal is periodic, and the mean, variance and frequency structure are the same over time. If this assumption is violated for example during long EEG recordings, the frequency spectrum shows less clear peaks, and the energy is spread across a larger number of frequencies as to account for the complex structure. Therefore, other frequency methods such as wavelet convolution, or short time FFT might be used. The short time FFT can be used across short lengths of time during which the signal is more likely to remain stationary than during longer lengths of time (M. X. Cohen, 2014; Smith, 1999).

When the FFT is calculated over short time segments, the resolution of the frequencies is lower (1 sec segments result in a 1 Hz resolution). Spectral leakage will occur from the frequencies that are not sampled. As a way to control spectral leakage, tapers can be applied to the signal. Tapers attenuate the signal at the beginning and end of the recording, and thereby smooth the frequency spectrum. The Hanning window for example tapers the signal to 0, while the Hamming window tapers the signal as well, but not to 0. A Gaussian window also tapers the signal to 0, but becomes narrow and might taper the signal too much (Fig. 2.9). Although no zero-padding of the signal is needed when one applies tapers to the data, the disadvantage of this method is that there is a data loss of the tapered data. Overlapping epochs (50-90%) are therefore commonly used. Single tapers are particularly suitable for research focusing on low frequencies (< 30 Hz). Multiple tapers that each taper the data in different ways are more suitable for

research focusing on higher frequencies (>30 Hz), since the tapers will smoothen the frequency spectrum and help increase the signal to noise ratio. The use of multiple tapers is more suitable to higher frequencies, as more tapers will provide smoother results (M. X. Cohen, 2014).

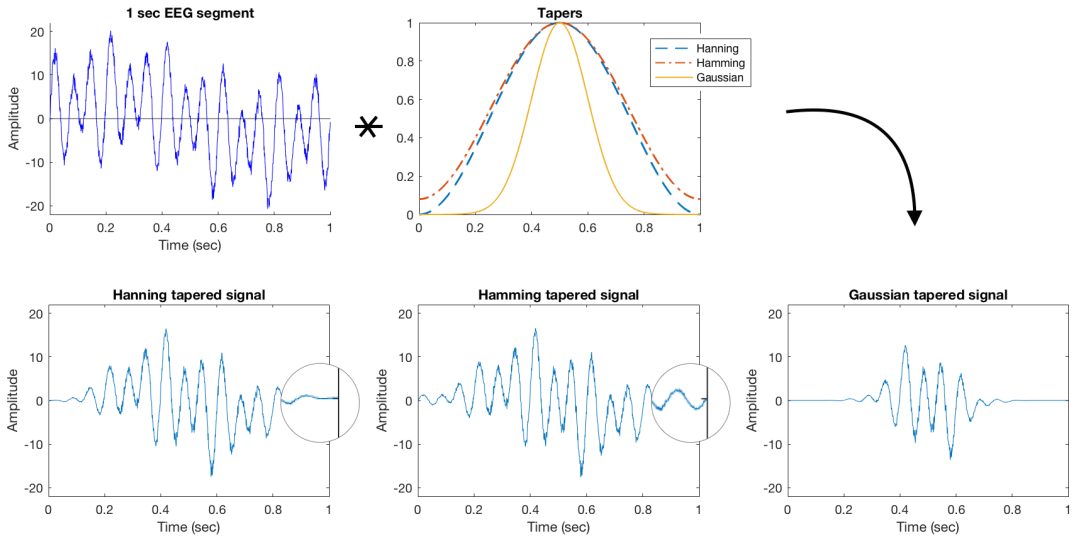

Figure 2.9. Tapers

A short segment EEG signal (upper left) can be tapered with a Hanning, Hamming, or Gaussian taper (upper right). The tapered signal is attenuated at the beginning and end of the segment.

2.3.3. EEG connectivity

While spectral power analyses reflect the amount of synchronisation in a population of neurons, EEG connectivity analyses reflect the amount of synchronisation between different populations of neurons across different distances. EEG connectivity analyses further allow for the investigation of phase relationships between the neural signals of different populations, which should be consistent for efficient neural communication. These analyses help to further

quantify different aspects of synchronised neural activity that are important for the development of brain networks during early development.

2.3.3.1 Measures of EEG connectivity

Functional EEG connectivity specifies how similar the EEG signals are across different channels. Signals that are very similar reflect high connectivity, whereas signal that are very dissimilar reflect low connectivity (M. X. Cohen, 2014). This is in contrast with spectral power analyses that focus on the signals of individual channels. Connectivity analyses result in connectivity matrices that contain 1 connectivity value for each possible electrode pair. For example, if the EEG dataset contains 116 channels, the connectivity matrix contains 116x116 values (Fig. 2.10). A series of functional EEG connectivity measures have been proposed, such as coherence, imaginary part of coherency, phase lag index, and the debiased weighted phase lag index, among others (van Diessen et al., 2015) (see Appendix A2.1 for measures used in previous EEG connectivity studies). Each of these measures has advantages and disadvantages that should be considered within the context of the study conducted. Coherence and phase lag index measures are used most often and will be further discussed here.

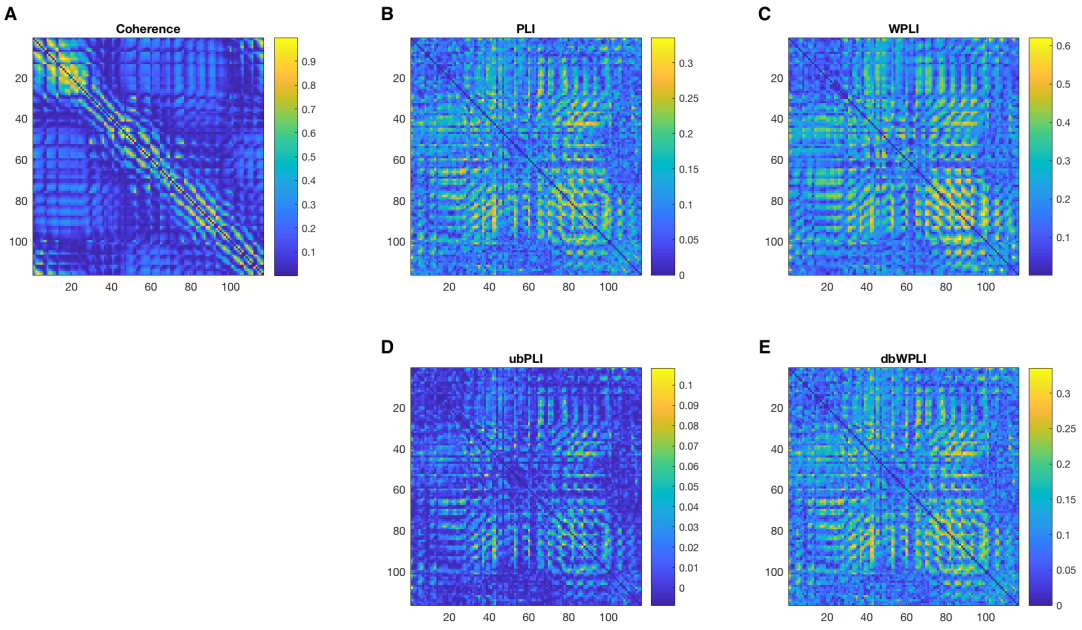

Figure 2.10. Functional connectivity matrices

Functional connectivity matrices for 7-8 Hz calculated with coherence (A), PLI (B), WPLI (C), ubPLI (C), and dbWPLI (E).

2.3.3.1.1 Coherence and Coherency

Coherence is one of the measures that is most frequently used (Coben et al., 2008; Duffy & Als, 2012; Y. M. Y. Han et al., 2013; Isler et al., 2010; Kenet et al., 2012; Khan et al., 2013; Lazarev et al., 2010; Mathewson et al., 2012; Perez Velazquez et al., 2009; Peters et al., 2013; Righi et al., 2014; Thatcher et al., 2008). Coherence measures the linear correlation between the amplitude of two signals in the frequency domain. Coherence is the absolute value of coherency.

Coherency is defined as the cross-spectral density function normalized by the individual auto spectral density functions, or power spectra (Nolte et al., 2004; Nunez et al., 1997). Raw EEG signals from two channels, e.g. channel *i* and *j*, that contain information in the time domain are typically first transformed to the frequency domain using the Fourier transform (Smith, 1999). For each epoch *n*, for

each channel *i*, the complex Fourier coefficient $X_{in}(f)$ is calculated. The auto spectral density from channel *i* for epoch *n* is defined as:

$$G_{iin}(f) = X_{in}(f).X_{in}^{*}(f)$$

where * reflects the complex conjugate. The conjugate is calculated by multiplying the imaginary part by -1: the conjugate of 3 + 5i is 3 – 5i. The Fourier coefficient of channel *i* for epoch *n* is multiplied by the complex conjugate of the Fourier coefficient of the same channel *i* for the same epoch *n*. The auto spectral density is calculated for each epoch and then averaged across all *N* epochs to increase accuracy:

$$\hat{G}_{ii}(f) = \frac{1}{N}\sum_{n=1}^{N} G_{iin}(f)$$

Using the same functions, the auto spectral density for channel j could be calculated: $\hat{G}_{jj}$.

The cross spectral density for 2 channels *i* and *j* is defined as:

$$G_{ijn}(f) = X_{in}(f).X_{jn}^{*}(f)$$

Now, the Fourier coefficient of channel *i* for epoch *n* is multiplied by the complex conjugate of the Fourier coefficient of the other channel *j* for the same epoch *n*. The cross spectral densities are calculated for each epoch, and then averaged across epochs, resulting in $\hat{G}_{ij}(f)$. Then coherency can be calculated as cross-spectral density normalized by the individual auto spectral density:

$$Coherency_{ij}(f) = \frac{\hat{G}_{ij}(f)}{(\hat{G}_{ii}(f)\hat{G}_{jj}(f))^{1/2}}$$

Coherence is the absolute value of coherency, thus:

$$Coherence_{ij}(f) = |\, Coherency_{ij}(f) \,|$$

Values for coherence range between 0 and 1, where 0 reflects no connectivity and 1 reflects high connectivity. It has been suggested that coherence gives an indication of the amount of firing neurons (Thatcher, Biver, & North, 2004).

One major issue with using coherence and coherency measures is their sensitivity to volume conduction. Coherence between electrodes located at a short distance will therefore be overestimated (Fig. 2.10A). The interpretation of these results based on analysis of the sensor signals is problematic as it is impossible to disentangle true connectivity from the volume conduction effects. Source localisation techniques as discussed in section 2.2.3 might provide a solution for adult data, but not for infant data. Other methods to avoid volume conduction and field spread effects have been proposed. Some research focuses on investigating coherence between electrodes with large distances, while ignoring short distance electrodes (Mathewson et al., 2012). Others have incorporated inter-electrode distance as a variable in their calculations as to account for the differences in distance. Nolte and colleagues suggested to focus on the imaginary component of coherency while ignoring the real component (Nolte et al., 2004).

The crucial assumption here is that the observed signal at the electrodes at the scalp has no time lag with the underlying source activity (Stinstra & Peters, 1998). The phase lag between the two signals caused by volume conduction would be 0 (in phase, Fig. 2.11A top row) or 180° (opposite phase, Fig. 2.11A, third row). In the former case, the real component has its maximum positive value, whereas in the latter case, the real component has its maximum negative value. The imaginary component has a value of 0 in both cases. Any effects from volume conduction would result in changes in the real component of the cross spectrum, but no

changes in the imaginary component (Fig. 2.11B). Thus, the imaginary part of coherency is insensitive to volume conduction.

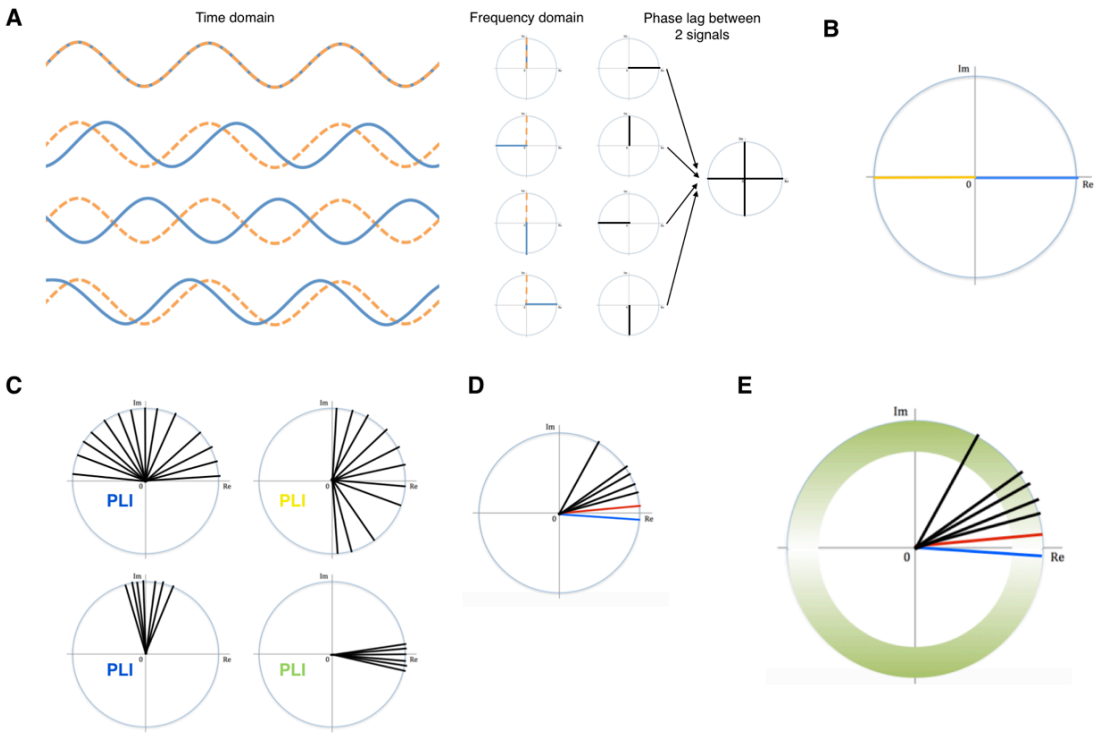

Figure 2.11. Imaginary part of coherency and phase lag indices

Two signals in phase or opposite phase (first and third row in A) create 0 or 180° phase lag, respectively (blue and yellow line in B). The phase lag index is based on the distribution and the phase angle of the phase lags rather than the clustering (C: blue reflects high, green intermediate, and yellow low PLI values). The PLI however is sensitive to noise with small phase lags that affect the distribution (D; phase lag in red, phase lead in blue). The WPLI weights the imaginary component of the cross-spectrum by the magnitude of the imaginary component (higher for phase angles in dark green than lighter green around the real axis (E).

The magnitude of the imaginary component reflects the strength of the synchronization or connectivity between two signals, and can be positive or negative reflecting leads or lags, respectively. Thus, the advantage of using the imaginary part of coherency above coherence is its relatively insensitivity to

volume conduction effects. The imaginary part of coherency is however dependent on the amplitude and magnitude of the phase delays of the signals. This means that the imaginary part of coherency is most effective when the phase delays between signals are 90°, but shows poor performance in identifying the connectivity values when signals are in phase or in opposite phase. Thus even when the signals are in phase, the imaginary part of coherency would be small.

2.3.3.1.2 Phase Lag Index measures

The phase lag index (PLI) is another measure of functional EEG connectivity (Stam, Nolte, & Daffertshofer, 2007). In contrast to the imaginary part of coherency, the PLI does not depend on the magnitude of the phase delay between 2 signals. The PLI is based on the consistency of the phase lag between signals. If volume conduction effects are characterized by zero time lags, any non-zero time lags cannot be explained by volume conduction and thus more likely reflect true connectivity. The consistency of the phase lag between two signals is derived from the asymmetry of the distribution of the phase differences between the two signals. The distribution of phase differences is considered asymmetrical if the probability of the phase difference being between –180° and 0° is different from the probability of the phase difference being between 0° and 180° (Fig. 2.11C left column). If the probabilities are equal for differences between –180° and 0°, and between 0° and 180°, the distribution is flat and considered symmetric (Fig. 2.11C right column). This is also the case when the median of the phase differences is or is close to 0° or 180°. For symmetric distributions of the phase differences, the PLI would have a value of 0 indicating that there is no coupling. If the distribution of phase differences is asymmetrical, thus the median of the phase differences is

different from 0° or 180°, the PLI would have a non-zero value. The PLI can be calculated with the following formula:

$$PLI = |\langle sign[\Delta\varphi(t_k)]\rangle|$$

where $\Delta\varphi(t_k)$ is a series of the phase differences between electrodes across time, and k is the trial. The PLI can also be acquired from the Fourier transform, as defined by (Vinck, Oostenveld, Van Wingerden, Battaglia, & Pennartz, 2011):

$$PLI = |E\ \{sgn(\Im\{X\})\}|$$

where $sgn(\Im\{X\})$ is the sign of imaginary component of the cross-spectrum, and E{.} is the expected value operator.

PLI values range from 0 to 1 with 0 reflecting no coupling, and 1 reflecting perfect phase coupling. Values closer to 1 indicate higher connectivity, whereas values closer to 0 indicate lower connectivity. Information on whether the signal is leading or lagging is lost, but can be calculated by not taking the absolute value in the last step of the calculation. Simulations have revealed that the PLI is better at detecting coupling than the imaginary component of coherence. Furthermore, the PLI is less affected by simulated volume conduction effects (Fig. 2.10B (Stam et al., 2007)).

Although the PLI shows improved performance in the detection of phase coupling compared to the imaginary part of coherence, it is sensitive to noise and volume conduction causing small phase differences jumping around the real axis. Any small phase lags added by noise can turn a phase lag into a phase lead, and vice versa (Fig. 2.11D). To this end, Vinck and colleagues (2001) introduced the weighted phase lag index (WPLI) that weights the imaginary component of the cross-spectrum $sgn(\Im\{X\})$ of the PLI by the magnitude of the imaginary

component of coherency $|\Im\{X\}|$. The WPLI can be calculated by the following formula:

$$WPLI = \frac{|E\{\Im\{X\}\}|}{E\{|\Im\{X\}|\}} = \frac{|E\{|\Im\{X\}|sgn(\Im\{X\})\}|}{E\{|\Im\{X\}|\}}$$

where $\Im\{X\}$ is the imaginary component of the cross-spectrum, and E{.} is the expected value operator. The phase differences with a small imaginary component, thus close to the real axis and with 0° or 180° phase difference, will result in smaller WPLI values. In contrast, phase differences with a large imaginary component, thus close to the imaginary axis and with 90° or -90° phase difference, will results in larger WPLI values. Noise causes the cross spectra to jump around the real axis. As the WPLI assigns less weight to the cross spectra close to the real axis, these changes have less influence on the WPLI compared to PLI that does not apply any weighting (Fig. 2.11E).

Analyses with simulated data show that the WPLI is more robust to noise increases than the PLI (Vinck et al., 2011). Additionally, the WPLI is better able to detect small changes in phase synchronization than the PLI. Thus in contexts with high noise levels, the WPLI will be able to detect small phase differences, whereas the PLI will not pick up on those. The simulations also showed that the PLI and WPLI display a sample size bias, where connectivity is overestimated when small numbers of epochs are used. The bias decreases when the WPLI is calculated across a larger number of epochs. To avoid this bias, Vinck and colleagues also proposed the unbiased PLI (ubPLI) and debiased WPLI (dbWPLI). These are defined with the following formulas:

$$ubPLI = E\{sign(\Im\{Z_j\}) * sign(\Im\{Z_k\})\}$$

$$dbWPLI = \frac{\sum_{j=1}^{N}\sum_{k\neq j}\Im\{X_j\}\Im\{X_{jk}\}}{\sum_{j=1}^{N}\sum_{k\neq j}|\Im\{X_j\}\Im\{X_{jk}\}|}$$

In other words, the ubPLI is calculated by the average of all pairwise products of signs. The dbWPLI is calculated as the sum of all pairwise products of all imaginary components, divided by the sum of all pairwise products of the magnitudes of the imaginary components. The results of the simulation analyses showed that the dbWPLI is negatively biased for small numbers of epochs, but this bias becomes very small with more than 30 epochs (Vinck et al., 2011) .

2.3.3.1.3 Advantages and disadvantages of Phase Lag Indices

The main advantage of the phase lag indices is their relative insensitivity to volume conduction effects. In the context of infant research, EEG data are often noisy, and only a small amount of artefact-free data is available for further analyses. The weighting and debiasing of the dbWPLI measure are therefore important. The weighting however also poses a disadvantage of the WPLI and dbWPLI. The effects of noise with small phase lags are minimized, as are the small phase lags caused by 'true brain connectivity'. The result is that connectivity between electrodes at short distances is underestimated.

Moreover, the phase lag indices are measures of undirected connectivity. It is not possible to conclude whether one signal is driving the other, only that there is increased or decreased coupling across the signals. Other measures like Granger causality, partial directed coherence, or phase slope index do reflect the directionality of the information flow. These measures however have not often been applied to infant data yet, possibly because they require source data that are not often available in infant data (Sperdin et al., 2018; van Diessen et al., 2015).

2.4. Further connectivity analyses

After calculating the connectivity strengths between each of the different electrodes, the result contains a connectivity matrix for each of the frequencies in the Fourier transformed data. Connectivity matrices across different frequencies can be averaged to obtain one matrix for a specific frequency band. Different methods for further analyses exist, such as global brain connectivity, network analyses, and graph theory analyses.

2.4.1. Global brain connectivity

Global brain connectivity is calculated by averaging the connectivity values across electrode pairs, excluding the values on the diagonal that reflect connectivity with the same electrodes (Fig. 2.12A). For undirected connectivity, global connectivity is calculated by averaging all connectivity values below the diagonal (the values above and below the diagonal are identical). It is also possible to calculate the average connectivity for one electrode with all other electrodes by averaging the values across the columns excluding the values on the diagonal, for example $(dbWPLI^{E1-E2} + dbWPLI^{E1-E3} + \ldots + dbWPLI^{E1-E116})/115$. The averaged connectivity for each electrode can be plotted in a topoplots as to give an indication of the overall connectivity across the brain.

Alternatively, global connectivity can be calculated across selected electrode pairs, for example across specific regions or hemispheres, or across specific electrode pairs that have been identified as showing significant differences between conditions or groups in network analyses (discussed in the next section). Values for excluded electrode pairs are set to 0 in the connectivity matrix, so that averaging across all non-zero values with result in global connectivity across

selected electrode pairs (Fig. 2.12B). Global connectivity values can be further used to test for differences between groups or experimental conditions.

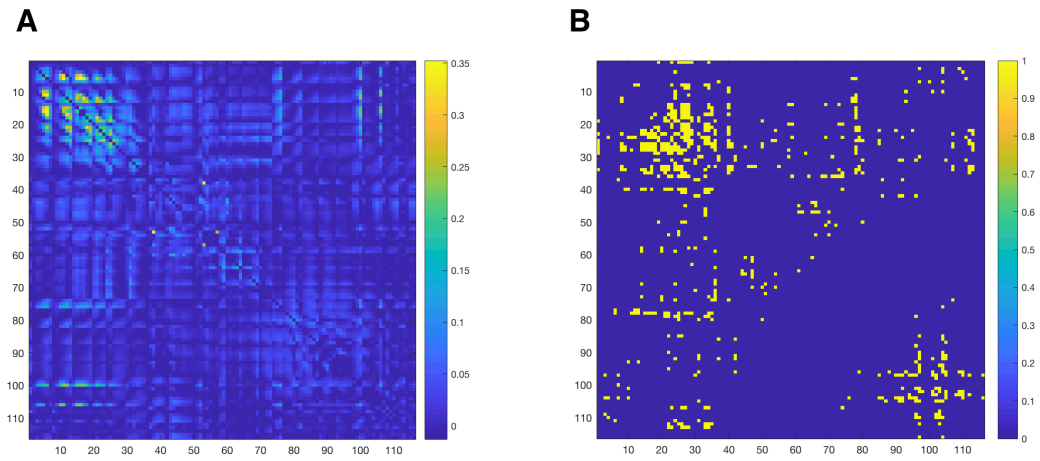

Figure 2.12. Global connectivity analyses

Global values can be calculated across all pairs below the diagonal (A), or for selected connections (yellow, B).

2.4.2. Network Based Statistics

In contrast to global analyses reflecting overall connectivity, network analyses help to identify differences between groups or experimental conditions at each possible connection in the connectivity matrix. The Network Based Statistics program (NBS) is used to identify significant differences in the connectivity strength of networks between different groups or experimental conditions(Andrew Zalesky, Fornito, & Bullmore, 2010) (Fig. 2.13A). The program adopts a non-parametric statistical method that utilizes permutation testing to infer *p*-values. The advantage of permutation testing is that it avoids the multiple comparisons problem. The multiple comparisons problem arises when values for each connection pair are tested in large networks and the probability of a false positive or Type I error increases with the increasing amount of tests that are being done.

Permutation testing works in 4 steps: 1) the statistical test of the null-hypothesis is tested for every connection in the connectivity matrix A; 2) a chosen test-statistic threshold defines supra-threshold connections; 3) clusters are identified from the supra-threshold connections that are close in the topological space, these clusters are called components; 4) a FWER (family wise error rate)-corrected p-value is calculated for each component with permutation testing.

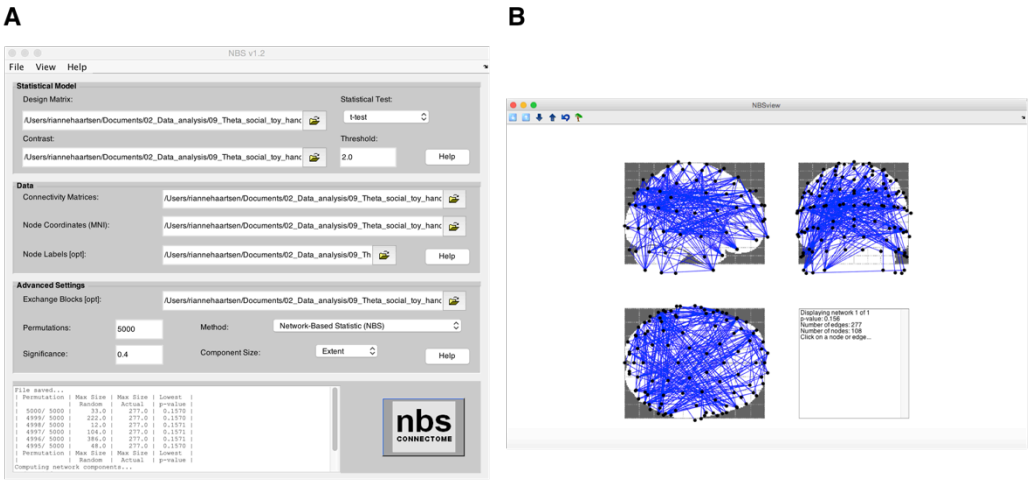

Figure 2.13. Network based analyses

Network Based Statistics (NBS) can be used to identify differences between conditions or groups at each connection (A). Significant networks are displayed in NBS view (B).

Permutation testing assumes that if there is no difference between groups or conditions, the data belonging to each group or condition can be randomly assigned to a different group or condition without changing the test-statistic (Maris & Oostenveld, 2007). If there would be a difference between the groups or conditions, the test-statistic would be different when the data are randomly assigned to a different group or condition. With each permutation, the data are randomly assigned to different groups or conditions. Then, steps 1 through 3 from the NBS are repeated and the size of the largest component is saved for each permutation. Repeating this permutation process thousand times creates a null

distribution of sizes for the largest component if the null hypothesis was true. Finally, the size of the component for the actual data is compared with the null distribution obtained during the permutation testing. The FWER-corrected p-value for the actual data is calculated as the percentage of permutations for which the largest component was the same or greater than the size of the component in the actual data (Zalesky, 2012).

The NBS is implemented with several different statistical tests and options that can be defined by the researcher. For example, t-test for independent samples for differences between groups of subjects, paired samples t-test for differences between conditions within the same subjects, analysis of variance (ANOVA) for mixed designs, and analysis of variance with covariates (ANCOVA) are examples of parametric tests. A non-parametric version using the Mann-Whitney U-test for differences between groups also exists. The tests further require a design matrix and a contrast variable that identify the hypotheses to be tested (increases or decreases between conditions). For within-subjects design, the analyses require an 'Exchange Blocks' variable to ensure that the data for conditions are exchanged within the subjects. The design matrix contains information about the conditions the connectivity matrices belong to. The threshold of the test statistic can be identified as well. A disadvantage of NBS is that no guidelines for the appropriate threshold exist, and this has to be defined by trial and error, or based thresholds used in previous studies. Users of NBS can further identify the number of permutations and the significance level.

If a network has been identified with connections that exhibit a significant difference between conditions or groups, the NBS view window displays the significant network (Fig. 2.13B). Further results, such as the connections included

in the network, can be derived from the NBS variable that contains all results. These results can be further used to calculate global connectivity across selected connections that show significant differences between groups or conditions as suggested in section 2.4.1. If no significant network has been identified, the NBS variable is empty.

2.4.3. Graph theory

Another method to further examine EEG connectivity is to focus on the functional organisation of the brain network. Global connectivity reflects the overall amount of synchronisation across the whole brain. Graph theory metrics can inform on the efficiency of the information processing, and the amount of segregation and integration of the EEG connectivity pattern (Bullmore & Sporns, 2009; Rubinov & Sporns, 2010). Networks consist of nodes (here electrodes) and edges (connections reflected between nodes). The values of the edges represent the strength or presences/absence of the connections between the nodes (Fig. 2.14).

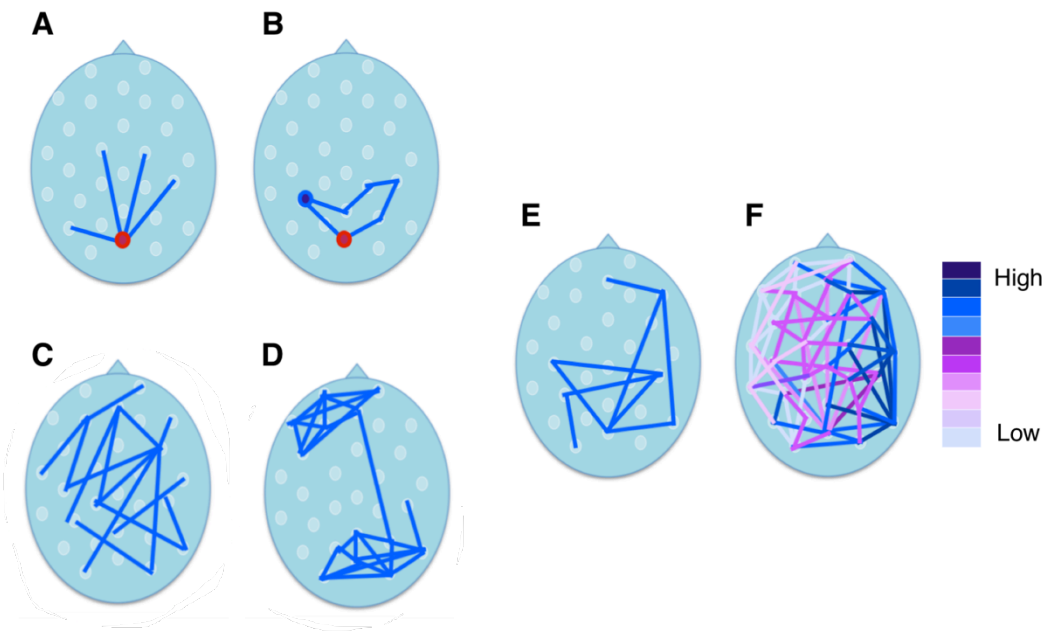

(previous page) Figure 2.14. Graph theory metrics

Graph metrics calculate the number of connections for each node (degree, A), shortest path length (shortest route between red and blue node is one, as opposed to 5 for the other route, B), the amount of segregation (average shortest path length, higher in C than D), the amount of integration (clustering coefficient, higher in D than C). Binary networks can be obtained by applying a threshold where connections are present or absent (E). Weighted networks represent the strength of each connection (darker colours represent high connectivity, lighter colours represent low connectivity strengths in F).

The degree of a node k_i reflects the number of other nodes it is connected to:

$$k_i = \sum_{j \in N} a_{ij}$$

where N is set of all nodes in the network, and a_{ij} is the connection between node *i* and *j*, which would be 0 for absence, and 1 for presence of connection in a binary network (Fig. 2.14A). Path lengths are sequences of connections between nodes reflect different routes for information flow. Short path lengths suggest stronger potential for neural integration than long path lengths (Fig. 2.14B). Shortest path lengths d_{ij} are calculated with:

$$d_{ij} = \sum_{a_{uv} \in gi \leftrightarrow j} a_{uv}$$

where d_{ij} is the shortest path length or distance between nodes *i* and *j*, and $gi \leftrightarrow j$ is the shortest path between nodes *i* and *j*. Characteristic path length is defined as the average shortest path length across the network:

$$L = \frac{1}{n} \sum_{i \in N} L_i = \frac{1}{n} \sum_{i \in N} \frac{\sum_{j \in N\ j \neq i} d_{ij}}{n-1}$$

where L is the characteristic path length of the network, L_i is the average distance between node i and all other nodes (Fig. 2.14C and D).

The clustering coefficient C is the amount of clustering in a network defined as the average of clustering across all nodes:

$$C = \frac{1}{n}\sum_{i \in N} C_i = \frac{1}{n}\sum_{i \in N} \frac{2t_i}{k_i(k_i - 1)}$$

where C is the clustering coefficient of the network, C_i is the clustering coefficient of the node i ($C_i = 0$ if the degree of the node is smaller than 2). Higher values of C indicate a higher segregation of neural processing in the network (Fig. 2.14C and D).

The above formulas are applied to binary networks that reflect the presence or absence of a connection link between 2 nodes. Binary networks can be obtained by applying a threshold to weighted networks. However, the thresholds used are often arbitrary (van Diessen et al., 2015; van Wijk, Stam, & Daffertshofer, 2010). Calculations for graph theory metrics in weighted matrices have therefore also been suggested (Fig. 2.14E and F). The links in the weighted matrices are signified by w_{ij} that are normalized such that w_{ij} ranges between 0 and 1 for each connection pair. To calculate the metrics for a weighted connectivity matrix, the following definitions are used:

For the weighted nodal degree, k_i^w:

$$k_i^w = \sum_{j \in N} w_{ij}$$

For the weighted shortest path length between nodes i and j, d_{ij}^w:

$$d_{ij}^w = \sum\nolimits_{f_g^w\, i \leftrightarrow i} f(w_{uv})$$

where $f(w_{uv})$ is an inversing of the weights to length. Then, the weighted characteristic path length L^w is defined as:

$$L^w = \frac{1}{n}\sum_{i \in N} \frac{\sum_{j \in N\ j \neq i} d_{ij}^w}{n-1}$$

The weighted clustering coefficient of the network C^w becomes:

$$C^w = \frac{1}{n}\sum_{i \in N} \frac{2t_{ij}^w}{k_i(k_i-1)}$$

A network with optimal efficiency would require a balanced combination of both high clustering and integration; also known as 'small-world' network (Watts & Strogatz, 1998). Small-worldness of a network can be calculated by comparing the cluster coefficients of the observed network C and a randomized network C_{rand}, and the characteristic path lengths of the observed network L and randomized networks L_{rand}. Then these values are combined to reflect a clustering to path length ratio, also defined small-worldness S for binary networks, and as S^w for weighted networks:

$$S = \frac{C/C_{rand}}{L/L_{rand}}$$

$$S^w = \frac{C^w/C_{rand}^w}{L^w/L_{rand}^w}$$

If the values of S or S^w are higher than 1, the observed network is characterized by small-worldness, and displays an efficient network organization (Humphries & Gurney, 2008).

Graph theory metrics could be applied to functional, structural, and effective connectivity matrices, and binary and weighted matrices. The metrics thus inform on the organization and efficiency of the network, which inform on a different aspect of connectivity compared to global connectivity analyses, and

network statistics. The metrics of graph theory can be calculated using the Brain Connectivity Toolbox (BCT) (Rubinov & Sporns, 2010).

2.5. Description of datasets and statement of contribution

The current thesis is based on several pre-existing datasets. Table 2.1 provides an overview of the data included in each experiment and the source of these data. The first dataset analysed in the test-retest reliability chapter was shared with me by Utrecht University. Data were collected by a team of research assistants, and EEG data were cleaned by a PhD candidate from Utrecht University. Matlab scripts to cut the data into epochs were created by myself, but dbWPLI and PLI values were calculated using Matlab scripts created and used by E.V. Orekhova (Orekhova et al., 2014). Connectivity values for each channel pair for each frequency were calculated with the scripts written for the previous study by E. Orekhova, and scripts adapted by Cosmin Stamate that decreased computation times. Further scripts to calculate spectral power, visualize the data and calculate reliability measures were created by me using FieldTrip and Matlab functions.

Table 2.1. **Overview of data included in each of the chapters and experiments**

			Source of EEG data		
Chapter	*Experiment*	*N*	*UU dataset*	*BASIS Ph 1*	*BASIS Ph 2*
3	Frequency band	73	73	-	-
	Long epochs [1]	19	19	-	-
	Short epochs	22	22	-	-
	Constant	41	41	-	-

4	Frequency band	101	-	-	101
	Group analyses (replication) [2]	101	-	-	101
	Dimensional traits (replication) [3]	79	-	-	79
	Subtypes of RRBs [3]	103	-	27	76
5	Frequency band	155	-	54	101
	Hand vs. Toy:				
	- Group analyses [2]	64	-	14	50
	Social vs. Non-social:				
	- Group analyses [2]	68	-	13	55
	- Dimensional traits [3]	66	-	13	53
6	Alpha band:				
	- Group analyses [2]	155	-	54	101
	- Dimensional traits [3]	151	-	54	97
	Theta band:				
	- Group analyses [2]	68	-	13	55
	- Dimensional traits [3]	66	-	13	53
7	Childhood outcomes:				
	- Alpha [4]	56	-	35	21
	- Theta [4]	19	-	8	11
	Change in traits:				
	- Alpha [5]	53	-	35	18
	- Theta [5]	16	-	8	8

Total of infants available in datasets: $N_{\text{Utrecht Univerisity}} = 73$, $N_{\text{BASIS Phase 1}} = 104$, and $N_{\text{BASIS Phase 2}} = 143$.

[1] These numbers are for subsets of data cut into different epoch lengths and numbers (see Chapter 3, section 3.2.3.2.2.).

[2] EEG data during the 14-month-old visit, and clinical assessment during the 36-month-old visit.

[3] EEG data during the 14-month-old visit, and traits of ASD assessed during the 36-month-old visit.

[4] EEG data during the 14-month-old visit, and traits of ASD assessed during the

childhood follow-up studies BASIS7 and gBASIS (at 5 to 10 years of age).
[5] EEG data during the 14-month-old visit, and traits of ASD assessed during the 36-month-old visit, and the childhood follow-up studies BASIS7 and gBASIS (at 5 to 10 years of age).
Abbreviations used: UU – Utrecht University; BASIS Ph 1 – BASIS study cohort Phase 1; and BASIS Ph2 – BASIS study cohort Phase 2.

The second dataset was derived from the BASIS study, and was used in each of the other chapters (Fig. 2.15). The BASIS study is a longitudinal prospective study with a high-risk infant sibling design. The study includes multiple infant and toddler visits, and follow-up during childhood. In total, data for two cohorts have been collected so far: Phase 1, and Phase 2; and for one cohort data collection is still in progress: Phase 3. EEG data analysed in these thesis were collected during the Phase 1 12-15-month-old visit, and the Phase 2 14-15-month-old visit. Data from Phase 1 have all been preprocessed, cleaned, and analysed by E. Orekhova, with results published in (Orekhova et al., 2014). I preprocessed, cleaned, and analysed the data from Phase 2.

As for the EEG data, videos were coded by myself and a research assistant. I myself created a coding manual for looking and interference in the Mangold Interact system, as the previous study used a different coding program. The looking and interference coding categories were based on the previous study, but slightly adapted to improve efficiency. EEG preprocessing and cleaning were done using the Matlab scripts that had been written by E. Orekhova for the previous study. However, the EEG data files, and video coding files were in different formats compared to the previous study, thus the scripts had to be adapted to the current formats by myself. No other changes were made to the preprocessing scripts.

Connectivity values for each channel pair for each frequency were calculated with the scripts that were also used in the Utrecht University datasets. Scripts used to create topoplots were also written by E. Orekhova. Further scripts to visualize data, calculate spectral power, average across frequencies and infants, preparing connectivity matrices for NBS analyses, implementing graph theory functions were created by myself using FieldTrip, BCT, and Matlab functions.

Measures of behaviours and clinical assessments were collected during the infant visits, the 36-month-old visit, and the follow-up assessments at childhood. Two follow-up assessments were performed: BASIS7 aimed to follow-up participants from Phase 1 at 7 years of age, and gBASIS focussed on the childhood follow up from both Phase 1 and 2, where participants were between 5 and 10 years at the time of assessment. BASIS data had all been collected by the BASIS team (infant data by the team based at Birkbeck College, toddler data by the team based at King's College, and childhood data by team members from both locations). The BASIS team also performed data processing and the calculation of scores on the different questionnaires, parental interviews, and behavioural assessments.

Finally, I was actively involved in data collection for the infant visit in Phase 3 as a second tester; checking questionnaire responses, eye-tracking, assessment and scoring of different behaviour measures (Labtab, Mullen Scales for Early Learning (MSEL), and Autism Observation Scale for Infants assessment and scoring, (AOSI) (Bryson, Zwaigenbaum, McDermott, Rombough, & Brian, 2008; Mullen, 1995)), and neural measures (fNIRS and EEG tasks), and parent-child interaction. I assisted in 31 5-month-old visits, 36 10-month-old visits, and 18 14-month-old visits. Data collection for this cohort is currently still on going. As

outcome data are not yet available for the whole group, only data from the previous cohorts were included in the analyses of this thesis.

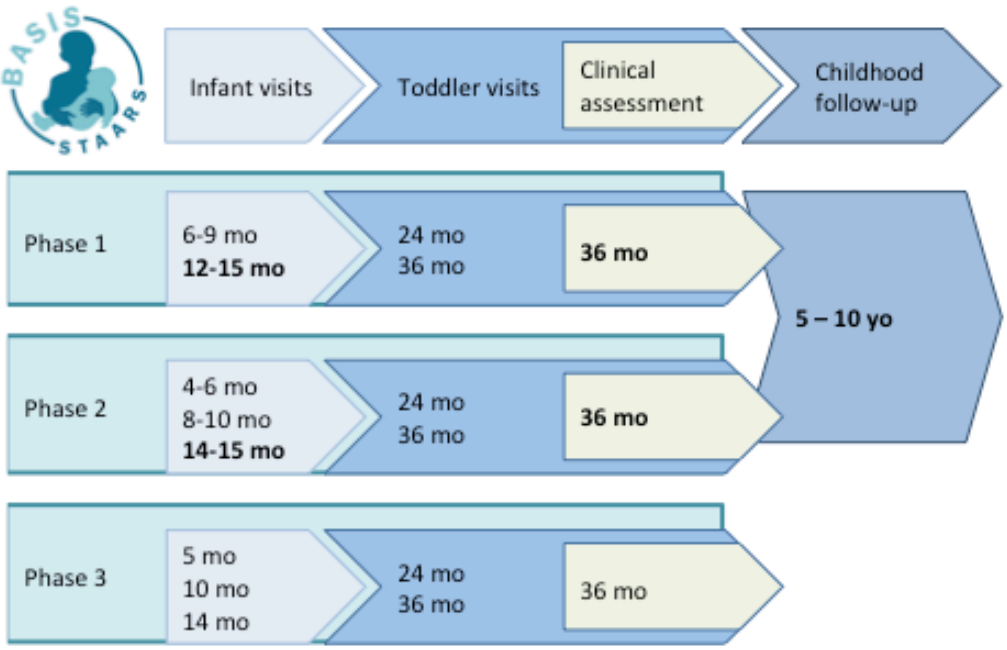

Figure 2.15. The BASIS study

The BASIS study includes a battery of behavioural and neural assessments at multiple time points during infancy and toddlerhood (visits from which data were used in this thesis are printed in bold). Datasets exist for different cohorts.

2.6. Summary of Chapter 2

EEG measures changes in electric potentials across the scalp that arise from synchronized populations of pyramidal neurons. EEG is characterized by a high temporal resolution that allows for careful investigation of temporal events. Although many measures of EEG connectivity exist, they differ among each other with regard to sensitivity to effects of volume conduction, noise, and the amount of epochs analysed. The functional connectivity matrices that result from these

analyses can be further analysed using global or whole brain connectivity measures, network based statistics, and graph theory metrics.

The use of the different methods in measuring connectivity during the early development of ASD may have contributed to the inconsistency in findings in the infant EEG connectivity literature in ASD. It has been suggested that infant EEG connectivity may be an early marker for ASD, but markers require high reliability and reproducibility. Test-retest reliability of EEG connectivity measures as the PLI and dbWPLI in infants with typical development remains unknown. The next chapter therefore aimed to define the parameters for EEG connectivity calculations with high tests-retest reliability with in typically developing infants.

Chapter 3: Reliability of EEG alpha band connectivity measures in typically developing 10-month-old infants

3.1. Introduction

This thesis aims to examine how EEG connectivity during infancy is related to later ASD diagnosis and dimensional traits. EEG connectivity might be used as an early infant marker for ASD, which could facilitate early detection and intervention. Criteria for an early marker that predicts later outcome at an individual level include high accuracy, reproducibility, and reliability (Singh & Rose, 2009; Strimbu & Tavel, 2011). Research investigating EEG/MEG connectivity in infants with a later diagnosis ASD has shown mixed findings, possibly arising from differences in methods to calculate EEG connectivity (Boersma et al., 2013; O'Reilly et al., 2017; Orekhova et al., 2014; Righi et al., 2014) (see also Chapter 2 for different methods to calculate EEG connectivity, and Appendix A3.1 for overview of methods used in previous studies). Replication studies might help clarify these findings, but are currently scarce. Furthermore, reliability studies examining the test-retest reliability of EEG connectivity in infants are limited.

Only recently researchers have started to systematically investigate the parameters of EEG connectivity methods that provide the most reliable results in adults for measurements taken with intervals of several days to years (Deuker et al., 2009; Fraschini et al., 2016; Hardmeier et al., 2014; Höller, Butz, et al., 2017; Höller, Uhl, et al., 2017; Jin, Seol, Kim, & Chung, 2011). These studies have revealed that test-retest reliability of functional connectivity measures depends on several factors, including the number and duration of trials, the connectivity measure itself, the metric derived from the functional connectivity measures, and the frequency band under investigation, among others. Furthermore, findings in typically developing adults do not necessarily apply to other populations. Test-retest reliability differed between frequency ranges and pathological groups in a

recent study comparing individuals with mild cognitive impairment, temporal lobe epilepsy, subjective cognitive complaints, and typically developing controls (Höller, Butz, et al., 2017). Similarly, it is likely that parameters for optimal reliability defined in adult studies are different, and more importantly, not feasible in young infants, for example due to data availability, and noise levels.

3.1.1. Duration and number of epochs

The amount of artefact free segments is different between adult and infant data. While adults are able to sit still with eyes closed or open for several minutes, infants are more likely to move around during EEG recordings. There is a trade-off between the duration and number of epochs: high numbers of short epochs, or low numbers of long epochs. Higher numbers of epochs might decrease inter-subject variability resulting in higher reliability values as has been suggested for spectral power findings (Levy, 1987). However, short epochs might not be sensitive enough in picking up functional connectivity, while longer epochs might be more influenced by fluctuations in the EEG signal, also referred to as non-stationary signals (M. X. Cohen, 2014; Kuntzelman & Miskovic, 2017).

This trade-off plays an even greater role in infant data characterized by shorter segments of artefact-free data. It has been suggested that more reliable global connectivity results are achieved for 6 epochs of at least 10 seconds compared to 6 shorter epochs for adult data (Fraschini et al., 2016). If this criterion would be used in infant studies, analyses would be performed with small sample sizes meanwhile decreasing statistical power. In contrast, it has been suggested cutting data into a higher number of shorter epochs increases reliability of global connectivity, although reliability decreases again with too many epochs (Höller, Uhl, et al., 2017; Kuntzelman & Miskovic, 2017). Other reliability studies use 1

epoch with a duration of 2.25 or 9 minutes (Deuker et al., 2009), 4 4-second epochs (Hatz et al., 2016), 12 4-second epochs (Hardmeier et al., 2014), 123 1-second epochs and 147 0.5-second epochs (Höller, Uhl, et al., 2017), 120 2-second epochs (Kuntzelman & Miskovic, 2017), or at least 20 4.76-second epochs (Miskovic & Keil, 2015). Meanwhile, reliability of connectivity measures in infants remains relatively unknown.

3.1.2. Measures of functional connectivity

The numbers and durations of epochs optimal for reliable connectivity measures also depend on the measure used. As discussed in the previous chapter on methods, many different measures of functional connectivity exist that also show differences in sensitivity to noise, volume conduction, number of trials, and length of trials (van Diessen et al., 2015). Undirected connectivity measures are overall more reliable when calculated across higher numbers of short epochs, whereas directed connectivity measures are largely unaffected by epoch length (Höller, Uhl, et al., 2017). The phase lag index measures, such as the PLI and dbWPLI, are often used due to their robustness against volume conduction effects. The dbWPLI is furthermore less sensitive to noise, and small and variable numbers of epochs as a result of the weighting and debiasing components when compared to the PLI measure (see chapter 2, and (Stam et al., 2007; van Diessen et al., 2015; Vinck et al., 2011). Consequently, these measures are more often used on infant data characterized by high levels of noise (Boersma et al., 2013; Orekhova et al., 2014).

The optimal parameters for calculating connectivity with dbWPLI and PLI on infant data remains unclear, and uses vary. For example, Orekhova and colleagues suggest that at least 120 1-second epochs are needed to calculate reliable dbWPLI values in 14-month-old infants (Orekhova et al., 2014). In

contrast, Vinck and colleagues suggested that at least 30 epochs are needed required for reliable dbWPLI values (Vinck et al., 2011). Studies using the PLI as measure have used as few as 12 4-second epochs (Hardmeier et al., 2014), 6 12-second epochs (Fraschini et al., 2016) in adults, or 4 16-second epochs in children (Boersma et al., 2011), or on average 30 1-second epochs in toddlers (Boersma et al., 2013). It seems that a higher number of shorter epochs are used for dbWPLI calculations, whereas a lower number of longer epochs are used for PLI calculations. Together, these data suggest that optimal parameters for high reliability differ between these measures, but direct comparisons are needed to further examine this.

Functional connectivity has typically been investigated using different metrics, such as global connectivity, and graph metrics. Global connectivity informs on whole brain connectivity, whereas graph metrics inform on the functional organisation of the brain networks (Rubinov & Sporns, 2010). The characteristic path length has been interpreted as measure of functional integration, reflecting the average shortest path that connects two nodes. The clustering coefficient informs on functional segregation, and reflects the cliquishness of the network by measuring how often 2 neighbours of 1 node are also neighbours of each other. Small-worldness reflects the efficiency of the network, where more efficient networks display higher normalized local clustering than normalized path lengths (Rubinov & Sporns, 2010). Previous work has shown than test-retest reliability for global connectivity is higher than for the (normalised) clustering coefficient and characteristic path length, which in turn are higher than small-worldness (Deuker et al., 2009; Hardmeier et al., 2014). How

the test-retest reliability measures for global and graph theory metrics relate to the amount of data used is still unclear.

3.1.3. Frequency band of interest

The test-retest reliability also differs between frequency bands. Adult studies using the resting state paradigm showed that alpha frequencies show highest values of test-retest reliability. Theta and beta frequencies show overall lower reliabilities than alpha, whereas lowest values are found for the gamma frequency range (Hardmeier et al., 2014; Hatz et al., 2016; Höller, Uhl, et al., 2017; Jin et al., 2011; Kuntzelman & Miskovic, 2017).

In infants, the alpha frequency band might have the largest potential for high test-retest reliability values also, and is therefore selected as the focus of this study. Indeed, previous results suggest that theta and alpha band frequencies provide higher reliability values than the other frequency bands (Van der Velde, Haartsen, & Kemner, n.d.). As mentioned in the previous chapter, the alpha band has a higher signal-to-noise ratio than other frequency bands. Infant alpha band activations are related to attentional control while watching videos of women singing nursery rhymes and spinning toys. Another practical consideration for selecting alpha frequencies is that alpha is less modulated by social content as opposed to theta frequencies that also have a high signal-to-noise ratio. This allows collapsing data across conditions while increasing the amount of artefact-free data for test-retest reliability analyses. Finally, test-retest reliability of alpha frequency band is relevant here as the study that will be replicated in the next chapter focussed on alpha band also (Orekhova et al., 2014).

As discussed in the previous chapter, frequency bands for power in adults and infants are known to occupy different ranges. In adults, the alpha band is

typically defined as 8 to 12 Hz. Peaks in the alpha band at younger ages occur at lower frequencies (Saby & Marshall, 2012). I therefore first inspected the power spectrum of the infant data averaged across infants as to define the appropriate frequency range for this sample (Orekhova et al., 2014; Shackman et al., 2010), after which analyses were continued to test test-retest reliability of alpha frequency band connectivity.

3.1.4. Aim of this chapter

The goal of this study is to examine how epoch numbers and duration affect the test-retest reliability of alpha frequency band connectivity metrics measured with the dbWPLI and PLI, in particular global connectivity, the normalized path length, the normalized clustering coefficient, and the small-worldness index. This study will help guide future studies looking into functional connectivity in young infants. Further, high test-retest reliability is considered necessary for markers as early predictive individual marker.

To this end, I used EEG data recorded from 10-month-old infants while the infants watched videos of women singing nursery rhymes, and spinning toys (Jones et al., 2015). The measurements were repeated after approximately 1 week. Different numbers and durations of epochs were randomly selected in order to systematically compare test-retest reliabilities between different levels of these parameters. Test-retest reliability was investigated using the intraclass correlation (Hardmeier et al., 2014; Hatz et al., 2016).

3.2. Methods

3.2.1. Participants

In total, 79 typically infants participated in the study performed at Utrecht University, The Netherlands. Families were recruited upon written invitations where addresses were obtained via the communal register of the cities within the Utrecht province. Parents / caregivers were informed about the study and experimental procedure, and gave written informed consent before the start of the session. This study has been approved by the medical ethical committee of the University Medical Center Utrecht (Protocol ID: 14-221, General Assessment and Registration form number: 49099).

After the each testing day, families received a 30-euro incentive, and a toy for the infant. Infants were 10 months old at the time of the first session. Data were available for 73 infants for the first session, and 64 infants for the second session as the other families did not want to return for a second visit.

3.2.2. Experimental procedure

The EEG experiment was part of a study that investigated the reliability of behavioural, eye tracking, and EEG measures across 2 sessions separated by 1 to 2 weeks. Data were collected by a team of trained and experienced researchers and research assistants at the Kinder Kennis Centrum at Utrecht University, the Netherlands.

3.2.2.1. EEG experiment

The EEG session consisted of the presentation of social and non-social videos: the social video displayed women singing Dutch nursery rhymes (recorded in the Netherlands after (Jones et al., 2015)), whereas the non-social video showed

moving toys (Jones et al., 2015). Durations for both videos were 60 seconds. The order of presentation of the social and non-social videos was counterbalanced, and repeated 2 times. Infants were seated in a high chair in front of the stimulus screen, with their parents sitting behind them. A curtain separated the participants and stimulus screen from the experimenter and recording screen to avoid the infants being distracted by the experimenter.

During the presentation of the social and non-social videos, the EEG signal was recorded with a 32 electrode Biosemi ActiveTwo system at a sampling rate of 2048 Hz. The Common Mode Sense (CMS) and Driven Right Leg (DRL) were used as active ground signal. Furthermore, two external electrodes on the left and right mastoid and one electrode under the eye were recorded. Finally, the EEG session was recorded with a video camera for later coding of looking behaviour.

3.2.3. EEG preprocessing

3.2.3.1. Preprocessing by Utrecht University

The EEG data and video recordings were pre-processed by Bauke van der Velde, PhD candidate at the Utrecht University. This was done to a) ensure anonymity of the participating infants and families, and b) allow for later comparison between connectivity results using different lab-specific analyses methods while using the same artefact-free data (Van der Velde et al., n.d.). For the preprocessing of the data, van der Velde used Fieldtrip functions (Oostenveld et al., 2011) in Matlab. First, he down sampled the data from 2048 Hz to 512 Hz. A band pass filter from 0.1 to 70 Hz and a Notch filter at 50 Hz were applied to the data to filter out high-frequency noise, slow wave drift, and line noise from the equipment in the EEG recording room. Videos recorded during the EEG sessions were coded for attention (from the first frame the child was not looking at the screen to the last frame the

child was not looking) using the Aegisub program for frame-by-frame inspection, and Microsoft Excel to mark the frames. Segments during which the infant was not looking at the screen were removed from further analyses. Next, the researcher used ICA to identify and remove blinks and eye movements in the data. Artefacts caused by flat lines, jumps in the signal, muscles, clipping, or excessive noise were manually removed from the data. Channels were removed from the data if artefacts affected more than 50% of the signal. After data cleaning, the data were re-referenced to the average reference. The remaining segments of artefact-free data were shared with me, in addition to data on demographics.

3.2.3.2. Preprocessing by myself

3.2.3.2.1. Selection of the alpha frequency band

First, I wanted to define the alpha frequency band. The specific borders of the alpha and theta frequency bands depend on the age of the participants. The previous study in high-risk autism siblings investigated 14-month-olds and defined the alpha band as 7-8 Hz by inspecting the power spectrum (Orekhova et al., 2014). It is possible that the alpha frequency band has lower borders in 10-month-old infants than in 14-month-old infants. Furthermore, it has been suggested that spectral power depends on the epoch length as well. In order to investigate this, all available data for session 1 were cut into 1, 2, 3, 4, 5, and 6 second epochs using my own scripts to cut the data (see Fig. 3.1 for an overview of the methods). Data for each of the 73 infants were included.

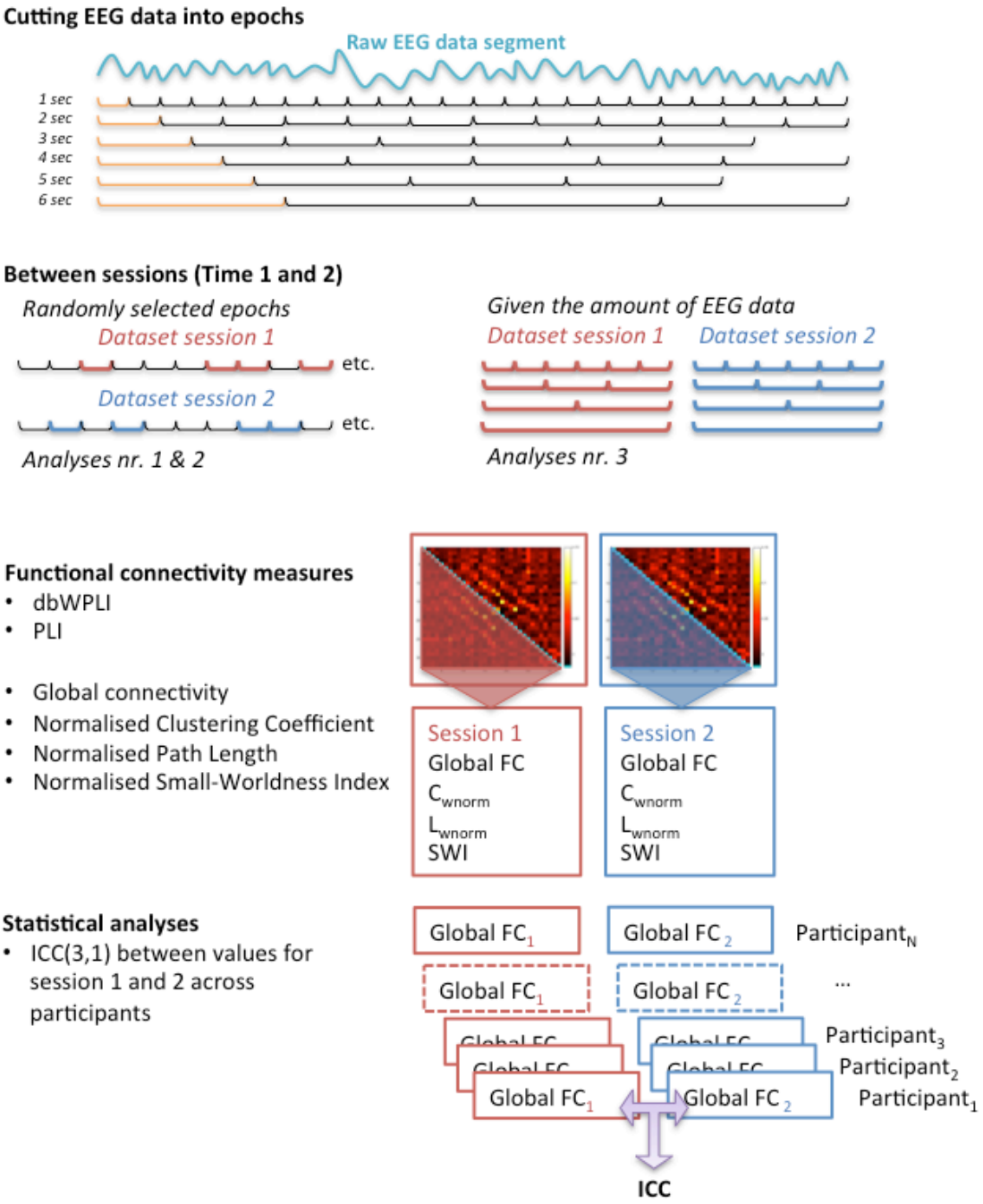

Figure 3.1. Preprocessing steps for reliability analyses

Visualization of the preprocessing steps: cutting data into different epoch lengths, calculation of connectivity metrics, and statistical analyses.

Abbreviations: phase lag index (PLI), debiased weighted phase lag index (dbWPLI), functional connectivity (FC), normalised clustering coefficient (C_{wnorm}), normalised path length (L_{wnorm}), small-worldness index (SWI), and intraclass correlation (ICC).

Spectral power was calculated for each epoch from the Fast Fourier Transform (FFT) after applying a Hanning taper to the epoch data using FieldTrip functions, in accordance with the previous study on functional connectivity in high-risk infants (Orekhova et al., 2014). The absolute values of the complex Fourier values were first squared, and then averaged across epochs. A natural log transform (MATLAB function *log* which returns the natural logarithm *ln(x)*) was applied to the data. Thereafter the log- transformed values were averaged across all channels. Finally, data for 0 to 30 Hz were plotted and visually inspected to identify the frequency boundaries of the alpha peak. These values of the alpha peaks are used as frequencies of interest for the subsequent functional connectivity analyses. Matlab scripts to calculate spectral power from the complex Fourier values and to visualize the data were written by myself.

3.2.3.2.2. Functional connectivity measures

To investigate the effect of different epoch lengths and numbers on the reliability of functional connectivity measures in young infants, functional connectivity measures were calculated across different sets of epochs from both session 1 and 2. Only infants with data from all 32 electrodes were included in these analyses since the number of electrodes might influence the results of the graph theory metrics and I wanted to keep the datasets consistent across analyses. Epoch lengths and numbers were chosen to ensure that parameters used in previous studies were included, while maintaining reasonable group sizes. This resulted in 3 different datasets with different epoch lengths and numbers to be compared within separate groups of individuals (see table 3.1).

For the first 2 sets of analyses, epoch lengths ranged between 1 and 5 seconds, and epoch numbers ranged from 20 to 150. For analysis 1, I chose length

between 1 and 5 seconds since these lengths are most often used. I expected that for the PLI longer epochs would be required for reliable values, whereas for the dbWPLI reliable values would be possible with short epochs. Furthermore, Vinck suggested that at least 30 epochs are needed for reliable dbWPLI calculations (Vinck et al., 2011). Thus here I chose epoch numbers between 20 and 60 to examine whether reliability would low for 20 epochs and higher for more than 30 epochs.

The choice of epoch lengths and numbers for the second analysis was based on findings from Orekhova and colleagues suggesting that more than 120 1-second epochs are required for dbWPLI calculations. Thus here I chose for epoch numbers ranging from 30 to 150, with epoch lengths of 1 and 2 seconds. Datasets for these analyses were created by randomly selecting epochs from those that were already cut from session 1 and 2.

Next, I wanted to investigate whether cutting data into many short epochs or few long epochs would benefit reliability. It is important that the amount of data remains constant for these analyses as results might become more reliable when calculated across larger amounts of data. This analysis is a pragmatic assessment of the optimal parameters to use given a certain amount of data. To further investigate this, I focussed on shorter epochs, by randomly selecting 20 6-second epochs for each infant, and cutting this data into 40 3-second epochs, 60 2-second epochs, and 120 1-second epochs (nr. 3).

Table 3.1. **Overview of planned test-retest reliability analyses**

Length and amount of epochs (different amounts of data)

Analyses nr.	*Epoch length (sec)*	*N epochs (for each length)*	*N infants*
1	1-2-3-4-5	20-30-40-50-60	19
2	1-2	30-60-90-120-150	22

Constant amount of data

Analyses nr.	*Epoch length (sec)*	*N epochs*	*N infants*
3	1-2-3-6	120-60-40-20 resp.	41

Note the previous study using the dbWPLI used 1-second epochs with 50% overlap to calculate functional connectivity across at least 120 epochs. I decided here to cut epochs without overlap allowing investigating different numbers and durations in a systematic way. Defining and varying the amount of overlap would add an extra variable, and additional complexity to the test-retest reliability analyses. Furthermore, other test-retest studies or toddler studies using the PLI did not use overlapping data. Using non-overlapping data here facilitates comparison across studies (Boersma et al., 2013; Hardmeier et al., 2014; Van der Velde et al., n.d.).

After selecting the epochs for the different analyses, the PLI and dbWPLI were calculated from the complex Fourier values from these epochs using Matlab scripts created by E. Orekhova (Orekhova et al., 2014). These scripts calculate the dbWPLI and PLI in accordance with the formulas described in Chapter 2. Functional connectivity matrices for each of the frequencies were averaged across

the frequencies within the alpha band resulting in 1 alpha band connectivity matrix for each infant.

Next, the metrics were calculated from the functional connectivity matrices: a) global connectivity, defined as the average connectivity values across all electrode pairs (section 2.4.1), b) normalized clustering coefficient C_{wnorm}, c) normalized characteristic path length L_{wnorm}, and d) small-worldness index (SWI). These metrics were calculated for both the dbWPLI and PLI, using Matlab functions and the Brain Connectivity Toolbox (BCT) (Rubinov & Sporns, 2010), separately for data from session 1 and 2. Since the BCT toolbox assumes that the connectivity values range between 0 and 1, and the dbWPLI values also involve negative values, the absolute dbWPLI values were used to calculate the graph theory metrics. PLI values range between 0 and 1, and were thus not transformed for graph metrics calculations. The graph theory metrics were calculated based on weighted connectivity matrices as opposed to binary matrices, since thresholds for binary matrices are often arbitrarily chosen, and weak connections also provide information on the network (van Diessen et al., 2015).

The normalised clustering coefficient or C_{wnorm} was calculated by dividing the observed clustering coefficient C_w from the weighted connectivity matrix by the average clustering coefficient C_{wrand} from 1000 randomized matrices (Boersma et al., 2013). The weighted clustering coefficient reflects the amount of triangles around a node. Here, C_w was calculated as the average weighted clustering coefficient across all 32 nodes using the BCT function `clustering_coef_wu` after rescaling the connection weights using the BCT function `weight_conversion(W, 'normalize')`. Then, the surrogate matrices are calculated by randomizing the weights from the observed network (Boersma et al.,

2013; Hardmeier et al., 2014). The $C_{w\ surrogate}$ is calculated for each surrogate matrix as for the observed matrix. The average C_{wrand} across 1000 surrogate networks is finally used to calculate C_{wnorm}. Small-world networks typically show much larger values for C_w compared to C_{wrand}, displaying a C_{wnorm} much larger than 1 (Onnela, Saramäki, Kertész, & Kaski, 2005; Watts & Strogatz, 1998).

The normalised path length or L_{wnorm} was calculated as the observed characteristic path length for the weighted connectivity matrix divided by the average characteristic path length L_{wrand} across 1000 surrogate connectivity matrices. Characteristic path length is defined as the sum of the weight of the edges. In accordance to the graph theory, shorter path lengths are more beneficial, and in the functional connectivity measures used here higher values or weights are considered to reflect 'better' connections. Therefore, the weighted connectivity matrix *W* is first inversed using the following code: `W(W>0) = 1./W(W>0)`, after which the weighted distance between the nodes is calculated with the BCT function `distance_wei`. This distance matrix holds the lengths of the shortest paths between nodes. L_w is then calculated as the mean of the weighted distances. Finally, L_w is divided by the average $L_{w\ surrogate}$ from 1000 surrogate networks to obtain L_{wnorm}. A network is typically defined as small-world when L_w is larger or similar to L_{wrand}, resulting in an L_{wnorm} which is higher than 1 (Watts & Strogatz, 1998).

Finally, the small-worldness can also be calculated using the small-world index (SWI) (Humphries & Gurney, 2008). The SWI was calculated as the ratio between the normalized clustering coefficient and normalized path length (section 2.4.3): SWI = C_{wnorm}/L_{wnorm}. Values above 1 indicate that the network displays small-worldness characteristics where it is beneficial to have a high clustering

coefficient, and similar characteristic path length compared to randomized networks. In short, after preprocessing each infant had a value for global connectivity, normalized characteristic path length, normalized clustering coefficient, and small-worldness index based on the PLI and the dbWPLI for session 1 and session 2.

3.2.4. Statistical analyses

Test-retest reliability was measured using the intraclass correlation for each of the 3 planned analyses with different epoch lengths and numbers, for global connectivity, and the 3 graph theory metrics. Test-retest reliability between session 1 and 2 was calculated across participants using the ICC(3,1) (also called ICC(C-1)) with the following formula

$$ICC(3,1) = \frac{MS_R - MS_E}{MS_R + (k-1)MS_E}$$

where MS_R is between object variance (participant here), MS_E is the error variability or mean squared error, and *k* is the number of measurements per participant. The ICC (3,1) is a two-way model ICC for single scores measuring consistency (Field, 2005; Shrout & Fleiss, 1979; Weir, 2005). This measure has also been used in other reliability studies looking into functional connectivity (Hardmeier et al., 2014; Hatz et al., 2016; Kuntzelman & Miskovic, 2017). ICC values typically range between -1 and 1. Values close to 1 reflect good reliability, whereas those close to 0 reflect poor reliability. Both significance values (testing whether the ICC values are significantly different from 0) and 95% confidence interval levels are given with the ICC values to facilitate interpretation. Overall, reliability studies adhere to the following convention: values below .40 indicate poor reliability, between .40 and .60 reflects fair reliability, whereas values

between .60 and .75 are considered good, and values above .75 as excellent reliability (Deuker et al., 2009; Hardmeier et al., 2014; Hatz et al., 2016; Kuntzelman & Miskovic, 2017).

3.3. Results

3.3.1. Participants

For the analyses focusing on the selection of the alpha frequency band, only data from the first session were considered. 73 infants were included in these analyses (35 males, M_{Age} = 302 days, sd_{Age} = 13, range 272 – 344 days).

Final samples for the 3 analyses focusing on test-retest reliability differed depending on data availability. Numbers of total participants, number of males, ages (mean, standard deviation, and ranges) during the first visit, and interval between the first and second visit (mean, standard deviation, and ranges) are displayed in table 3.2.

Table 3.2. **Demographics for the different analyses**

Analysis nr.	N_{total} (males)	Age [a]	Test-retest interval [a]
1	19 (7)	302 (15), 279 – 342	7 (2), 7 – 14
2	22 (7)	304 (15), 279 – 342	8 (2), 5 – 15
3	41 (16)	302 (12), 279 – 342	8 (3), 2 – 20

[a] Mean (sd), and range, in days

3.3.2. Selection of alpha frequency band

Figure 3.2 displays power values for epoch lengths ranging from 1 to 6 seconds recorded during the first session. The graphs display the typical shape of a power spectrum where power is higher for lower frequencies than higher frequencies

(also see Chapter 2, section 2.3.1). Two clear peaks could be observed in each graph: around 3 – 5 Hz, and around 6 – 8 Hz. The first peak is the theta frequency band, whereas the second is the alpha band. Further, power values differed across different epochs lengths (see Appendix A3.2 for more details). After visual inspection of these graphs, I decided to use 6-8 Hz as the alpha band for this 10-month-old infant dataset.

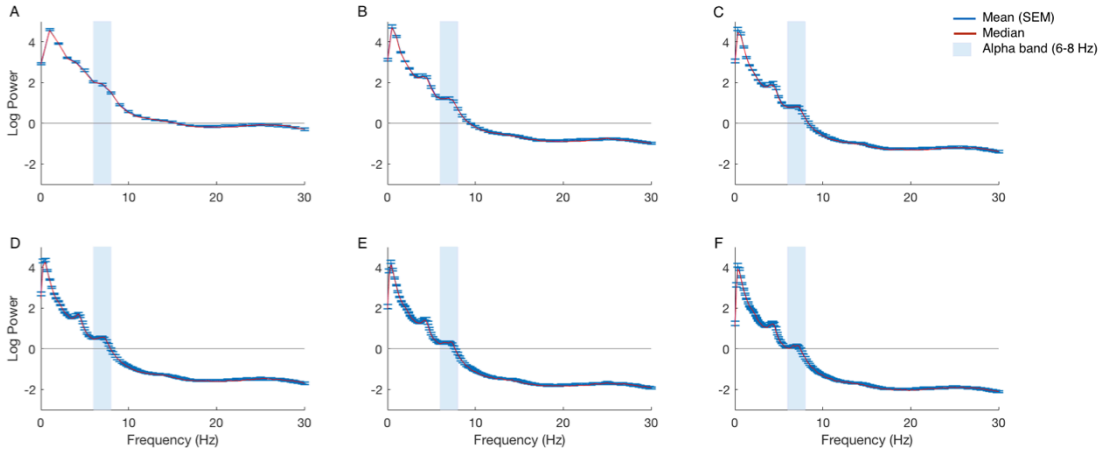

Figure 3.2. Spectral power for 10-month-olds across different frequencies and epoch lengths

Log transformed power values (mean and standard error of mean in blue, and median in red) averaged across all available epochs for different lengths: 1, 2, 3, 4, 5, and 6 seconds in graphs A-F, resp. Frequencies range from 0 to 30 Hz. Light blue box marks the alpha frequency band from 6 to 8 Hz.

3.3.3. Reliability of global connectivity

After defining the alpha frequency band as running from 6 to 8 Hz in this sample of 10-month-old infants, test-retest reliability was calculated for global connectivity measured with the dbWPLI and PLI for each of the 3 proposed analyses.

Figure 3.3 shows mean, and SEM values for global connectivity for the different analyses. The graphs showed that overall global connectivity values were lower for shorter than longer epochs. Furthermore, global connectivity estimates were higher for the PLI than the dbWPLI. The global PLI was more influenced by the number of epochs than the global dbWPLI. For the global PLI values were higher across smaller numbers of epochs and lower across larger numbers of epochs. In contrast, for the global dbWPLI values were more consistent across different numbers of epochs and thus less dependent on the number of epochs. When the total amount of data was kept consistent (Fig. 3.3E & F), global dbWPLI values were more consistent across different epoch durations and numbers than global PLI values, which showed increased values for lower numbers of longer epochs as opposed to higher numbers of short epochs.

For test-retest reliability, the ICC values ranged from -.08 to .85 for the global dbWPLI, and from -.34 to .87 for the global PLI across all analyses (tables 3.3 – 3.5). For both measures, ICC values increased with increasing epoch numbers and duration. For very small numbers of short epochs ICC values were poor for both the dbWPLI and PLI, in particular for values based on less than 40 1 or 2-second epochs. Good and excellent values were reached for more than 30 4-sec epochs, and 20 5-sec epochs for global dbWPLI (.62 < ICC < .85), and for more than 50 4-sec epochs, and more than 40 5-sec epochs for global PLI (.60 < ICC < .87, table 3.3). Similar values were obtained when more than 60 short epochs are included. With more than 90 epochs, 1-second epochs show better reliability values than 2-second epochs while being in the 'good' range, and ICC values are higher for the dbWPLI (.76 < $ICC_{dbWPLI,\ 1\text{-}sec}$ < .82, and .63 < $ICC_{dbWPLI,\ 2\text{-}sec}$ < .70) than the PLI (.67 < $ICC_{PLI,\ 1\text{-}sec}$ < .79, and .51 < $ICC_{PLI,\ 2\text{-}sec}$ < .62, table 3.4), reaching even

excellent values of test-retest reliability. These data suggest that highest test-retest reliabilities are obtained for more than 90 1-second epochs.

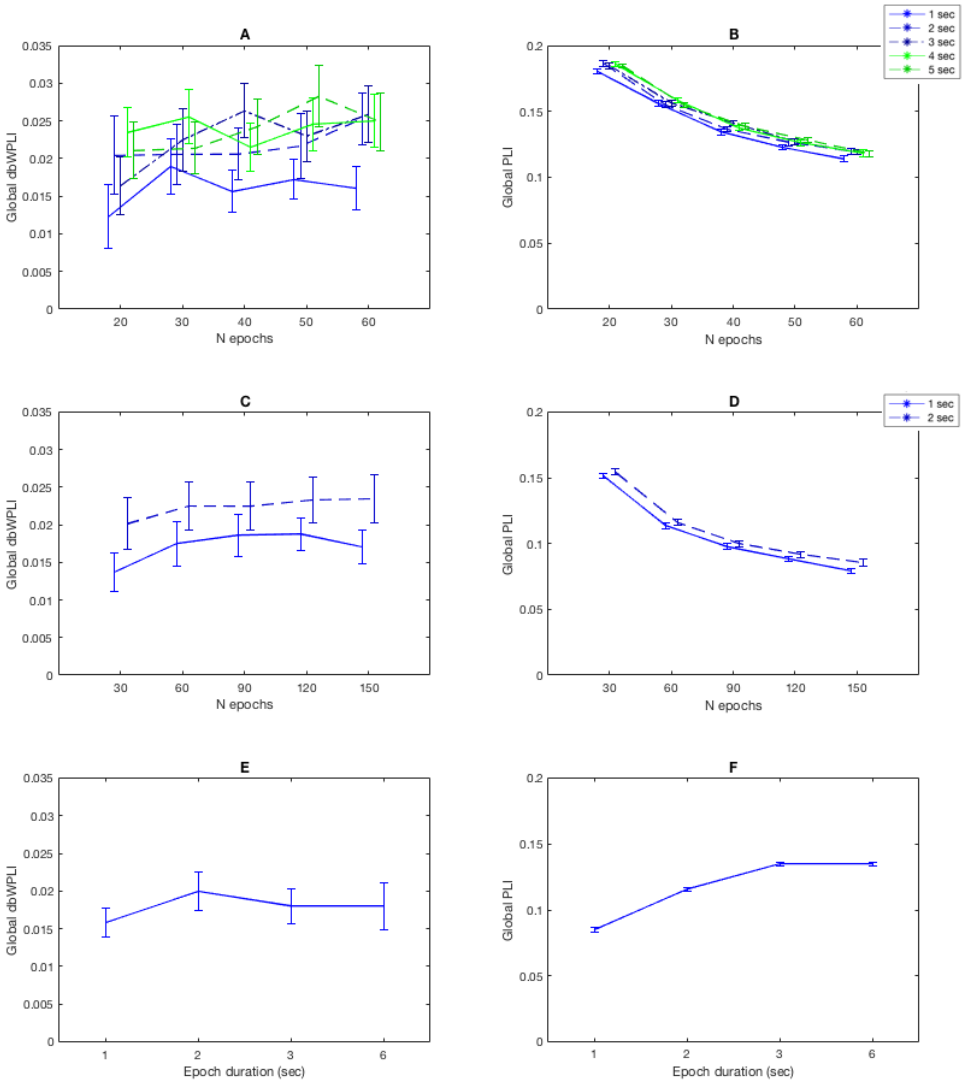

Figure 3.3. Global connectivity values

Mean and SEM (error bars) values for global connectivity measured with the dbWPLI (left column), and the PLI (right column), for the different analyses (different rows). Different colours represent different epochs lengths, with the numbers of epochs reflected on the x-axis (A-D). Graphs E-F display values for when a given amount of data is cut into different epochs lengths.

Table 3.3. **Test-retest reliability of *global dbWPLI and PLI* for 20 to 60 1-5 second epochs**

	Epoch duration	Number of epochs				
		20	30	40	50	60
dbWPLI	1 sec	**-.08** [-.51, .38]	**.21** [-.25, .60]	**.33** [-.14, .67]	**.24** [-.23, .62]	**.67***** [.32, .86]
	2 sec	**.24** [-.23, .62]	**.13** [-.34, .54]	**.51*** [.09, .78]	**.46*** [.02, .75]	**.59**** [.19, .82]
	3 sec	**.59**** [.21, .82]	**.53**** [.12, .79]	**.64**** [.27, .84]	**.51*** [.09, .78]	**.50*** [.07, .77]
	4 sec	**.05** [-.40, .49]	**.64**** [.28, .85]	**.63** ** [.26, .84]	**.78***** [.52, .91]	**.85***** [.66 - .94]
	5 sec	**.62**** [.24, .83]	**.70***** [.37, .87]	**.71***** [.39, .88]	**.62**** [.24, .83]	**.77***** [.50, .90]
PLI	1 sec	**-.34** [-.68, .12]	**.02** [-.43, .46]	**.33** [-.13, .67]	**.45*** [.01, .74]	**.50*** [.08, .77]
	2 sec	**.14** [-.32, .55]	**-.06** [-.49, .39]	**.27** [-.20, .64]	**.45*** [.00, .74]	**.56**** [.15, .80]
	3 sec	**.31** [-.16, .66]	**.37** [-.08, .70]	**.57**** [.17, .81]	**.44*** [.00, .74]	**.49*** [.06, .77]
	4 sec	**.06** [-.39, .49]	**.53**** [.12, .79]	**.56**** [.15, .80]	**.78***** [.52, .91]	**.87***** [.69, .95]
	5 sec	**.41*** [-.04, .72]	**.55**** [.14, .80]	**.64**** [.28, .84]	**.60**** [.21, .82]	**.77***** [.50, .91]

Intraclass correlation in bold, and lower and upper bound of the 95% confidence interval in square brackets below, * p < .05, ** p < .01, *** p < 0.001.

Table 3.4. **Test-retest reliability of *global dbWPLI and PLI* for 30 to 150 1- and 2-second epochs**

	Epoch duration	Number of epochs				
		30	60	90	120	150
dbWPLI	1 sec	**-.03**	**.38***	**.76*****	**.82*****	**.71*****
		[-.44, .39]	[-.04, .69]	[.50, .89]	[.62, .92]	[.42, .87]
	2 sec	**.10**	**.55****	**.63*****	**.65*****	**.70*****
		[-.33, .49]	[.18, .79]	[.30, .83]	[.32, .84]	[.41, .86]
PLI	1 sec	**-.21**	**.23**	**.70*****	**.79*****	**.67*****
		[-.57, .22]	[-.20, .59]	[.40, .86]	[.56, .91]	[.35, .85]
	2 sec	**0**	**.50****	**.53****	**.51****	**.62*****
		[-.42, .41]	[.11, .76]	[.15, .78]	[.12, .76]	[.28, .82]

Intraclass correlation in bold, and lower and upper bound of the 95% confidence interval in square brackets below, * p < .05, ** p < .01, *** p < 0.001.

Table 3.5. **Test-retest reliability of *global dbWPLI and PLI* for a constant amount of EEG data cut into 1, 2, 3, and 6-second epochs**

	Number and length of epochs			
	120 x 1 sec	60 x 2 sec	40 x 3 sec	20 x 6 sec
dbWPLI	**.53*****	**.68*****	**.50*****	**.58*****
	[.27, .72]	[.47, .81]	[.23, .70]	[.33, .75]
PLI	**.57*****	**.58*****	**.43****	**.51*****
	[.32, .74]	[.34, .75]	[.14, .65]	[.25, .71]

Intraclass correlation in bold, and lower and upper bound of the 95% confidence interval in square brackets below, * p < .05, ** p < .01, *** p < 0.001.

However, it is possible that global connectivity estimates are more reliable with larger amounts of data included in the analyses. When the total amount of data was held constant, while being cut into different lengths of epochs, ICC values varied from .50 to .68 for the dbWPLI, and from .43 to .58 for the PLI. For the dbWPLI, reliability was slightly higher for 2-second epochs than 1-second epochs, whereas this difference was minimal for PLI values (table 3.5).

3.3.4. Reliability of normalized clustering coefficient

The normalized clustering coefficient informs on functional segregation observed in a network. The values for normalized clustering coefficients for different epoch durations and numbers are displayed in Figure 3.4. For the dbWPLI, values increased with increasing numbers of epochs, while differences in duration had minimal effect on the values. For the PLI, values increased with increasing numbers, and with shorter epoch durations. With consistent amounts of data across comparisons, normalized clustering coefficients were higher for a higher number of shorter epochs than lower numbers of longer epochs. This pattern is the same for both the dbWPLI and PLI. Finally, normalised clustering coefficients are overall above 1 suggesting that the observed clustering coefficient was higher than the clustering coefficients from randomized networks. This implies that the networks display a more organised graph configuration than random graphs, and are thus characterised by small-worldness.

Turning to the test-retest reliability of the normalized clustering coefficient, overall test-retest reliabilities were higher and reached significance more frequently for the dbWPLI than the PLI based measure ($-.08 < ICC_{dbWPLI} < .72$, and $-.26 < ICC_{PLI} < .54$, tables 3.6 through 3.8). For 20-60 1-5-second epochs, dbWPLI reliability is fair for 50 and 60 2-second epochs, 20 and 30 3-second epochs, and

20, 40 and 50 5-second epochs (.41 < ICC < .57). Good reliability was observed for 60 1-second epochs, 50 and 60 4-second epochs, and 30 5-second epochs (.65 < ICC < .72). Reliability for the other combinations was poor. For the PLI, reliability was fair for 60 3-second epochs, 50 4- and 5-second epochs (.43 < ICC < .54), while the other reliabilities were poor (table 3.6).

For the comparisons across shorter epochs (1-2 seconds), test-retest reliabilities were fair for only a few combinations using the dbWPLI, while reliabilities were poor for the PLI. Test-retest reliability was fair for more than 90 1-second epochs for the dbWPLI (.48 < ICC < .59, table 3.7), and also higher than 90 and 120 2-second epochs for the same epoch numbers (ICC_{90} = .42, and ICC_{120} = .49). ICC values for the PLI however for 1- and 2-second epochs were all poor. The analyses where the total amount of data is held constant showed that reliability was higher for the dbWPLI than the PLI, with similar fair values for 1 and 2-second epochs (ICC_{1s} = .59, and ICC_{2s} = .57). In contrast, for the PLI, only the 1-second epochs reached fair reliability values (ICC_{1s} = .44), whereas the other values were poor.

In short, these data suggest that the normalized clustering coefficient can be reliably calculated by the dbWPLI across more than 90 1-second epochs, as opposed to the PLI or across a lower number or longer duration of epochs. Reliability for normalized clustering coefficients is overall lower than test-retest reliability for global connectivity.

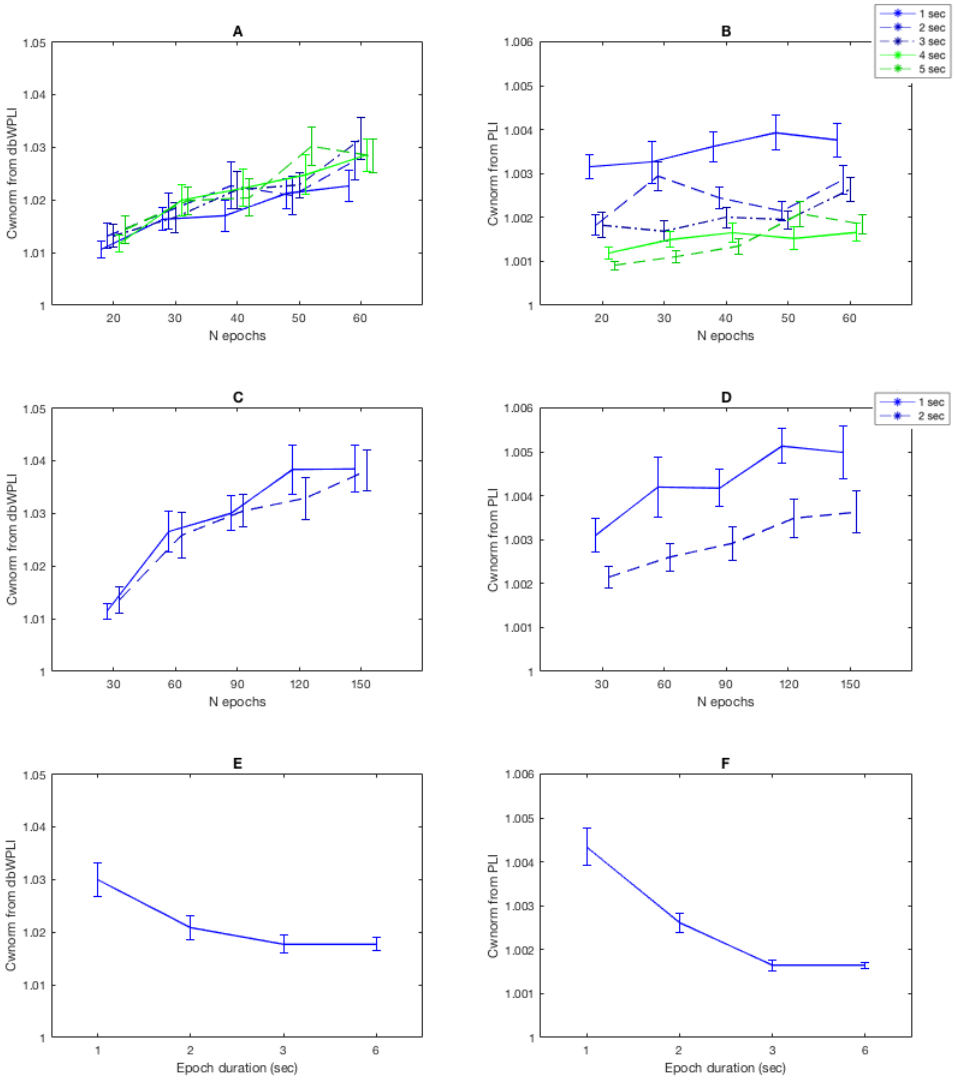

Figure 3.4. Normalised clustering coefficient values

Mean and SEM (error bars) values for normalised clustering coefficient measured with the dbWPLI (left column), and the PLI (right column), for the different analyses (different rows). Different colours represent different epochs lengths, with the numbers of epochs reflected on the x-axis (A-D). Graphs E-F display values for when a given amount of data is cut into different epochs lengths. Note that graphs for the dbWPLI and PLI have different y-axis limits.

Table 3.6. **Test-retest reliability of *normalized clustering coefficient* for 20 to 60 1-5 second epochs**

	Epoch duration	Number of epochs				
		20	30	40	50	60
dbWPLI	1 sec	**.09** [-.36, .51]	**.17** [-.29, .57]	**.15** [-.32, .56]	**-.08** [-.51, .37]	**.72***** [.40, .88]
	2 sec	**-.01** [-.57, .43]	**.24** [-.23, .62]	**.16** [-.31, .56]	**.43*** [-.01, .74]	**.46*** [.02, .75]
	3 sec	**.58**** [.18, .81]	**.43*** [-.02, .73]	**.26** [-.20, .63]	**.38*** [-.07, .71]	**.25** [-.21, .63]
	4 sec	**.22** [-.24, .61]	**.36** [-.10, .70]	**.31** [-.16, .66]	**.65**** [.29, .85]	**.67***** [.32, .86]
	5 sec	**.57**** [.17, .81]	**.69***** [.35, .86]	**.41*** [-.05, .72]	**.52**** [.10, .78]	**.36** [-.10, .70]
PLI	1 sec	**.12** [-.35, .53]	**.27** [-.20, .64]	**.38*** [-.07, .71]	**-.12** [-.54, .34]	**.14** [-.32, .55]
	2 sec	**.30** [-.17, .65]	**-.16** [-.57, .30]	**-.10** [-.51, .36]	**.31** [-.16, .67]	**-.11** [-.53, .35]
	3 sec	**.10** [-.36, .52]	**.19** [-.28, .58]	**.15** [-.32, .55]	**-.14** [-.55, .32]	**.46*** [.02, .75]
	4 sec	**.13** [-.33, .54]	**.28** [-.19, .64]	**.39*** [-.07, .71]	**.54**** [.13, .79]	**.38** [-.08, .70]
	5 sec	**-.26** [-.63, .21]	**.22** [-.25, .60]	**.26** [-.20, .63]	**.43*** [-.02, .73]	**.38** [-.08, .70

Intraclass correlation in bold, and lower and upper bound of the 95% confidence interval in square brackets below, * p < .05, ** p < .01, *** p < 0.001.

Table 3.7. **Test-retest reliability of *normalized clustering coefficient* for 30 to 150 1- and 2-second epochs**

	Epoch duration	Number of epochs				
		30	60	90	120	150
dbWPLI	1 sec	**.22** [-.22, .58]	**.30** [-.13, .63]	**.59**** [.24, .80]	**.53**** [.15, .78]	**.48*** [.08, .74]
	2 sec	**.37*** [-.05, .68]	**.32** [-.10, .65]	**.42*** [.01, .71]	**.49**** [.10, .75]	**.27** [-.16, .61]
PLI	1 sec	**.20** [-.23, .57]	**.08** [-.34, .48]	**.20** [-.23, .56]	**.27** [-.16, .62]	**.32** [-.11, .65]
	2 sec	**.21** [-.22, .58]	**.14** [-.29, .52]	**-.05** [-.46, .37]	**.29** [-.14, .63]	**-.03** [-.44, .39]

Intraclass correlation in bold, and lower and upper bound of the 95% confidence interval in square brackets below, * p < .05, ** p < .01, *** p < 0.001.

Table 3.8. **Test-retest reliability of *normalized clustering coefficient* for a constant amount of EEG data cut into 1, 2, 3, and 6-second epochs**

	Number and length of epochs			
	120 x 1 sec	60 x 2 sec	40 x 3 sec	20 x 6 sec
dbWPLI	**.59***** [.35, .76]	**.57***** [.32, .76]	**.38**** [.08, .61]	**.51***** [.24, .70]
PLI	**.44**** [.16, .66]	**.35*** [.05, .59]	**.23** [-.08, .50]	**.24** [-.07, .50]

Intraclass correlation in bold, and lower and upper bound of the 95% confidence interval in square brackets below, * p < .05, ** p < .01, *** p < 0.001.

3.3.5. Reliability of normalized characteristic path length

While the normalized clustering coefficient informs on functional segregation observed in a network, the normalized path length is a measure of functional integration of the network. The normalized path length values display a similar pattern as the normalized clustering coefficients: normalized path length measured with the dbWPLI increased with increasing number of epochs, while the duration seemed to have smaller effects (Figure 3.5). For the PLI, normalized path length was lower for longer epochs, but largely consistent across different numbers of epochs. When the amount of data was held constant, normalized path lengths were higher for higher numbers of short epochs than lower numbers of long epochs for both the dbWPLI and PLI. Furthermore, most values exceeded 1 suggesting that the observed path length was higher than the path length of randomized networks.

For most combinations of different epoch durations and numbers, test-retest reliability of normalized path length was poor and was not reaching significance (table 3.9 – 3.11). Few values reached the fair range, and a spurious correlation reached good reliability (e.g. ICC = .64 for 40 3-s epochs). However, there was no clear pattern of increasing or decreasing ICC values with varying durations or numbers of epochs, even when more than 60 epochs were included in the analyses. ICC values for the normalized path length did again seem higher for the dbWPLI (-.34 < ICC < .64) than PLI (-.34 < ICC < .47). Lastly, test-retest reliability was higher for 1-second cut epochs as opposed to other epoch lengths when the total amount of data was held constant, and when based on the dbWPLI (ICC = .44). Other combinations resulted in ICC values in the poor range without reaching significance.

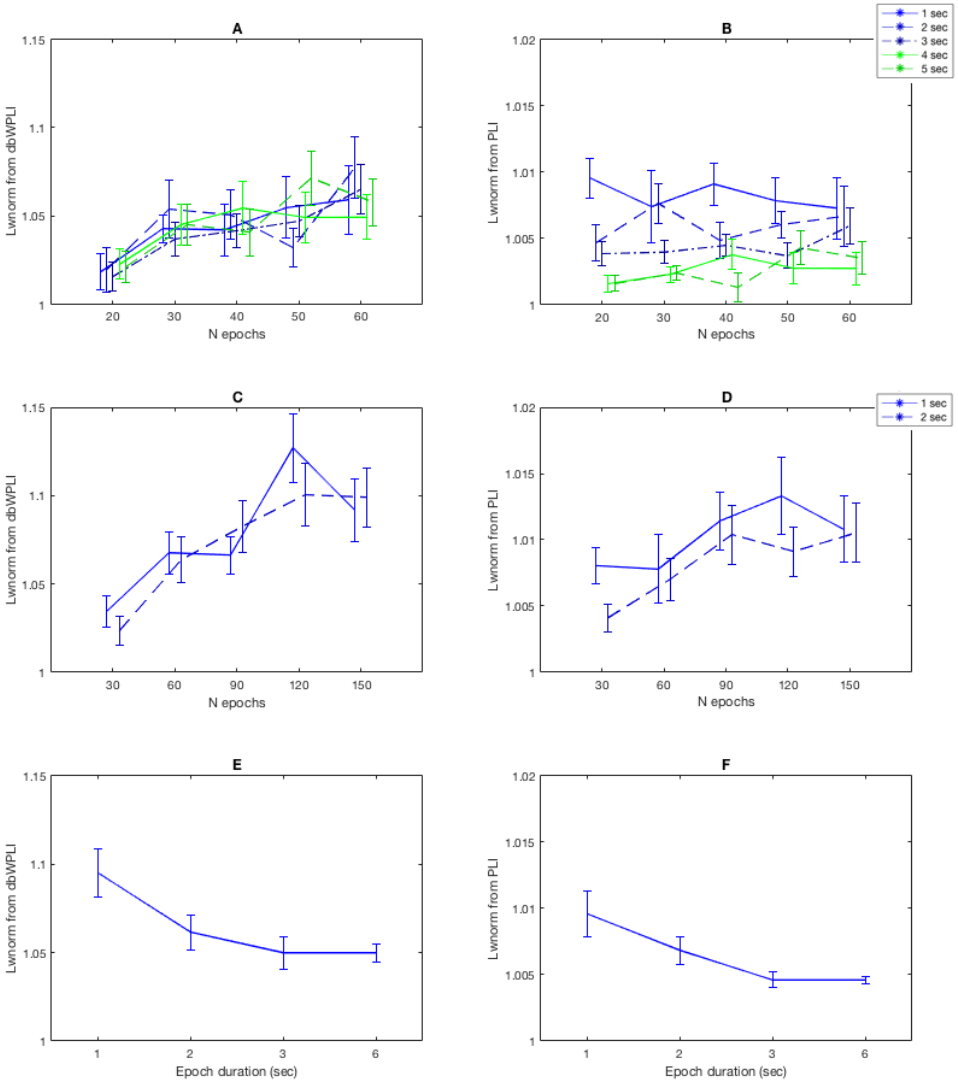

Figure 3.5. Normalised path length values

Mean and SEM (error bars) values for normalised path length measured with the dbWPLI (left column), and the PLI (right column), for the different analyses (different rows). Different colours represent different epochs lengths, with the numbers of epochs reflected on the x-axis (A-D). Graphs E-F display values for when a given amount of data is cut into different epochs lengths.

Table 3.9. **Test-retest reliability of *normalized path length* for 20 to 60 1-5 second epochs**

	Epoch duration	Number of epochs				
		20	30	40	50	60
dbWPLI	1 sec	**-.09** [-.51, .37]	**-.08** [-.51, .38]	**-.02** [-.46, .43]	**.32** [-.14, .67]	**.08** [-.38, .51]
	2 sec	**.41*** [-.05, .72]	**-.19** [-.58, .28]	**-.08** [-.50, .38]	**.43*** [-.02, .73]	**.15** [-.31, .56]
	3 sec	**-.34** [-.68, .12]	**-.19** [-.58, .28]	**.64**** [.27, .84]	**-.14** [-.55, .32]	**-.20** [-.59, .27]
	4 sec	**.10** [-.36, .52]	**.13** [-.34, .54]	**.41*** [-.04, .72]	**.19** [-.28, .59]	**.55**** [.14, .80]
	5 sec	**.42*** [-.02, .73]	**.33** [-.13, .68]	**-.21** [-.60, .26]	**.35** [-.11, .69]	**.19** [-.28, .58]
PLI	1 sec	**.02** [-.43, .46]	**-.04** [-.48, .41]	**-.11** [-.53, .35]	**-.34** [-.68, .12]	**-.05** [-.48, .40]
	2 sec	**-.09** [-.51, .37]	**-.01** [-.45, .44]	**-.31** [-.66, .16]	**.20** [-.27, .59]	**.17** [-.30, .57]
	3 sec	**-.27** [-.64, .20]	**-.14** [-.55, .32]	**.18** [-.29, .58]	**-.24** [-.62, .23]	**-.09** [-.52, .37]
	4 sec	**.40*** [-.06, .72]	**.40*** [-.05, .72]	**.17** [-.30, .57]	**.47*** [.04, .76]	**.30** [-.16, .66]
	5 sec	**-.04** [-.48, .41]	**-.23** [-.61, .24]	**-.15** [-.56, .31]	**.38** [-.08, .70]	**.18** [-.28, .58]

Intraclass correlation in bold, and lower and upper bound of the 95% confidence interval in square brackets below, * p < .05, ** p < .01, *** p < 0.001.

***Table 3.10*. Test-retest reliability of *normalized path length* for 30 to 150 1- and 2-second epochs**

	Epoch duration	Number of epochs				
		30	60	90	120	150
dbWPLI	1 sec	**-.08** [-.48, .35]	**.38*** [-.04, .68]	**-.18** [-.55, .25]	**.30** [-.13, .63]	**.34** [-.09, .66]
	2 sec	**-.13** [-.52, .30]	**.09** [-.34, .48]	**.46*** [.06, .73]	**.41*** [-.01, .70]	**.35*** [-.07, .67]
PLI	1 sec	**.01** [-.40, .42]	**.04** [-.38, .44]	**.01** [-.41, .42]	**.26** [-.17, .61]	**-.04** [-.44, .38]
	2 sec	**-.21** [-.57, .22]	**.30** [-.13, .63]	**.10** [-.33, .49]	**.37*** [-.04, .68]	**.20** [-.23, .57]

Intraclass correlation in bold, and lower and upper bound of the 95% confidence interval in square brackets below, * p < .05, ** p < .01, *** p < 0.001.

***Table 3.11*. Test-retest reliability of *normalized path length* for a constant amount of EEG data cut into 1, 2, 3, and 6-second epochs**

	Number and length of epochs			
	120 x 1 sec	60 x 2 sec	40 x 3 sec	20 x 6 sec
dbWPLI	**.44**** [.16, .66]	**.12** [-.19, .41]	**.29*** [-.01, .55]	**.34*** [.04, .58]
PLI	**-.24** [-.51, .06]	**.20** [-.11, .48]	**.07** [-.24, .36]	**.19** [-.12, .47]

Intraclass correlation in bold, and lower and upper bound of the 95% confidence interval in square brackets below, * p < .05, ** p < .01, *** p < 0.001.

In sum, these results suggest that normalized path length based on the dbWPLI calculated over a high number of 1-second epochs is more reliable than based on the PLI or calculated over a low number of long epochs. Test-retest

reliability for normalized path lengths is lower than for both global connectivity, and normalized clustering coefficients.

3.3.6. Reliability of the small-worldness index

The small-worldness index (SWI) is the ratio between the normalized clustering coefficient and normalized path length. It is a measure of efficiency of the network where values above 1 are considered beneficial to the network organization. Overall, the results displayed a decrease in small-worldness index values with increasing epoch numbers for the dbWPLI, whereas epoch length had minimal effect (Figure 3.6). For the PLI, small-worldness index remained largely consistent across different epoch numbers and durations.

Test-retest reliabilities for the small-worldness index were slightly higher for the dbWPLI (-.39 < ICC < .64) than the PLI (-.36 < ICC < .57, in tables 3.12 – 3.14), consistent with the patterns observed for the other connectivity metrics. Across 20-60 1-5 second epochs, test-retest reliability for the dbWPLI is mostly poor, with the exception of a few combinations for more than 40 epochs in the 3, 4, and 5-second epochs reaching fair values (.40 < ICC < .64). For the PLI, the same pattern was evident, with a few fair values for 50 or more 4-5-second epochs (.42 < ICC < .57). Even when a larger number of epochs were included, ICC values did not reach good test-retest reliability values, although values were again higher for the dbWPLI than the PLI. When the total amount of data was held constant, ICC values were highest across 120 1-sec epochs (ICC = .40). Overall higher values were observed for the dbWPLI than the PLI, except when cut into 6-sec epochs where the PLI based value was slightly higher the dbWPLI based small-worldness index (ICC_{PLI} = .25 and ICC_{dbWPLI} = .22). Still test-retest reliabilities were rather poor.

In sum, small-worldness index measures are more reliable when measured with the dbWPLI across larger amounts of data, in particular across a higher number of shorter epochs. This implies that larger amounts of data are needed to obtain reliable results for graph metrics as compared to global connectivity. Furthermore, dbWPLI based metrics are more reliable than PLI based metrics across a higher number of short epochs for infant data.

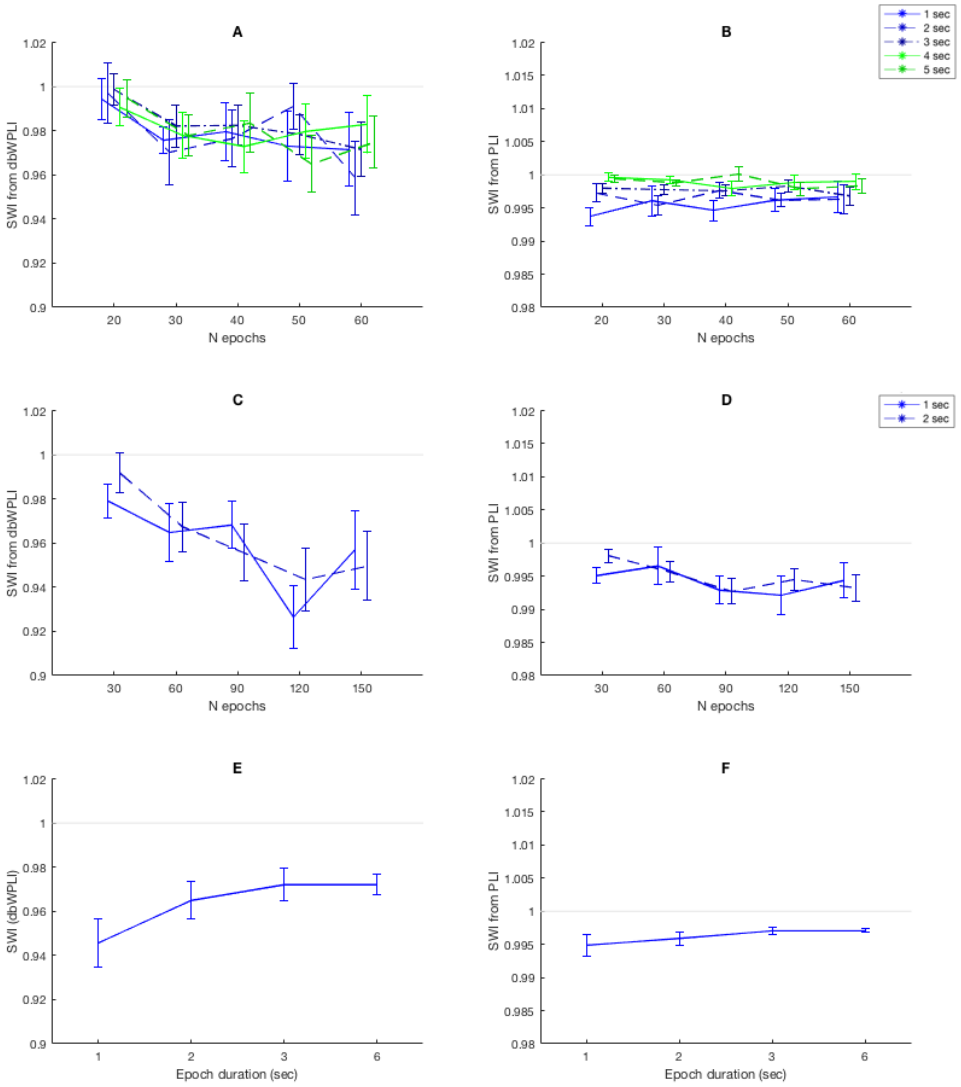

Figure 3.6. Small-worldness index values

Mean and SEM (error bars) values for small-worldness index measured with the dbWPLI (left column), and the PLI (right column), for the different analyses (different rows). Different colours represent different epochs lengths, with the numbers of epochs reflected on the x-axis (A-D). Graphs E-F display values for when a given amount of data is cut into different epochs lengths.

Table 3.12. **Test-retest reliability of *small-worldness index* for 20 to 60 1-5 second epochs**

	Epoch duration	Number of epochs				
		20	30	40	50	60
dbWPLI	1 sec	**-.07** [-.50, .39]	**-.11** [-.53, .35]	**-.19** [-.58, .28]	**.26** [-.21, .63]	**.07** [-.39, .50]
	2 sec	**.25** [-.22, .62]	**-.04** [-.47, .41]	**.01** [-.44, .45]	**.54**** [.12, .79]	**.25** [-.22, .62]
	3 sec	**-.39** [-.71, .06]	**-.09** [-.51, .37]	**.64**** [.27, .84]	**-.03** [-.46, .42]	**-.32** [-.67, .14]
	4 sec	**.19** [-.27, .59]	**.22** [-.24, .61]	**.39*** [-.07, .71]	**.30** [-.16, .66]	**.60**** [.21, .82]
	5 sec	**.34** [-.12, .68]	**.32** [-.14, .67]	**-.10** [-.52, .36]	**.40*** [-.05, .72]	**.35** [-.11, .69]
PLI	1 sec	**-.00** [-.44, .44]	**-.02** [-.46, .43]	**-.10** [-.52, .36]	**-.36** [-.70, .10]	**-.11** [-.53, .35]
	2 sec	**-.20** [-.60, .27]	**.04** [-.41, .48]	**-.29** [-.65, .17]	**.27** [-.20, .64]	**.10** [-.36, .52]
	3 sec	**-.24** [-.62, .23]	**-.08** [-.51, .36]	**.21** [-.26, .60]	**-.31** [-.66, .15]	**-.20** [-.59, .27]
	4 sec	**.35** [-.11, .69]	**.36** [-.10, .69]	**.15** [-.31, .56]	**.57**** [.17, .81]	**.42*** [-.02, .73]
	5 sec	**.06** [-.40, .49]	**-.19** [-.58, .28]	**-.07** [-.50, .38]	**.45*** [.01, .75]	**.33** [-.14, .67]

Intraclass correlation in bold, and lower and upper bound of the 95% confidence interval below, * p < .05, ** p < .01, *** p < 0.001.

Table 3.13. **Test-retest reliability of *small-worldness index* for 30 to 150 1- and 2-second epochs**

	Epoch duration	Number of epochs				
		30	60	90	120	150
dbWPLI	1 sec	**-.06**	**.46***	**-.07**	**.31**	**.41***
		[-.46, .36]	[.05, .73]	[-.47, .35]	[-.10, .65]	[0, .71]
	2 sec	**-.05**	**.13**	**.40***	**.37***	**.36***
		[-.45, .37]	[-.30, .51]	[-.02, .70]	[-.05, .68]	[-.07, .67]
PLI	1 sec	**-.02**	**.08**	**-.16**	**.33**	**.07**
		[-.43, .39]	[-.34, .48]	[-.53, .27]	[-.09, .66]	[-.35, .47]
	2 sec	**-.20**	**.31**	**.10**	**.34**	**.20**
		[-.57, .23]	[-.12, .64]	[-.32, .49]	[-.08, .66]	[-.23, .57]

Intraclass correlation in bold, and lower and upper bound of the 95% confidence interval below, * p < .05, ** p < .01, *** p < 0.001.

Table 3.14. **Test-retest reliability of *small-worldness index* for a constant amount of EEG data cut into 1, 2, 3, and 6-second epochs**

	Number and length of epochs			
	120 x 1 sec	60 x 2 sec	40 x 3 sec	20 x 6 sec
dbWPLI	**.40****	**.14**	**.33***	**.22**
	[.10, .62]	[-.17, .42]	[.03, .58]	[-.09, .49]
PLI	**-.22**	**.06**	**.02**	**.25**
	[-.49, .09]	[-.25, .36]	[-.29, .32]	[-.06, .51]

Intraclass correlation (ICC) in bold, and lower and upper bound of the 95% confidence interval CI, * $p < .05$, ** $p < .01$, *** $p < .001$.

3.4. Discussion

The current chapter set out to examine how epoch number and length relate to test-retest reliability of functional connectivity in the alpha frequency band in 10-month-old infants. In this sample, the alpha frequency band was defined as running from 6 to 8 Hz. The current results suggest that test-retest reliability generally increases with increasing epoch numbers and durations. However, when given the option to cut the data into shorter or longer epochs, cutting the data into a high number of shorter epochs yields overall more reliable results than cutting the data into a low number of longer epochs.

Test-retest reliabilities are higher for dbWPLI-based measures than PLI-based connectivity metrics. Global connectivity measures are more reliable than graph theory measures, where global connectivity ICC values were more frequently within the good range than ICC values for graph theory metrics. Furthermore, the normalized clustering coefficient exhibited higher reliability values than the normalized path length and the small-worldness index. These findings and their implications will be discussed in more detail below.

3.4.1. Alpha frequency band

The frequencies from 6 to 8 Hz were selected as alpha frequency band for the 10-month-old sample. This range is lower than the typical band of 8-12 Hz used in adults, while similar to ranges used in other infant studies; 6-8 Hz in 8- and 11-month-olds (Stroganova et al., 1999), 6-9 Hz in 6- and 12-month-olds (Orekhova et al., 2001), 7-8 Hz in 10-month-olds (Marshall et al., 2002), 6-9 Hz in 12-month-olds (Jones et al., 2015), 6-7 Hz in 12-month-olds (Marshall et al., 2002), 7-8 Hz in 14-month-olds (Orekhova et al., 2014), and 8 Hz in 14 -to 24-month-olds (Marshall et al., 2002).

While the peaks in the power spectra were constant across different epoch lengths, frequency resolution and power estimates were not (see also Appendix A3.2). These results support the use of epochs with identical data lengths across participants, as it is difficult to disentangle data length effects from experimental effects within studies when varying data lengths are used. Since the connectivity measures used here are derived from the FFT values, this likely also holds for connectivity analyses. Indeed, van Diessen and colleagues suggested that data length and sampling frequency should be equal across participants (van Diessen et al., 2015). They further recommend performing spectral power analyses along connectivity analyses as to distinguish power from connectivity effects. Thus, epoch length should be equal across participants, and chosen in accordance with the functional connectivity measure used.

3.4.2. The influence of epoch number and length on reliability of connectivity measures

In the current study, functional connectivity metrics showed overall higher test-retest reliability for 1-second epochs than longer epochs, and reliability increased with increasing number of epochs in 10-month-old infants for recordings with a 1 week interval. In particular, 1-second epochs provided more reliable functional connectivity measures for most metrics than longer epochs when the total amount of data was kept consistent. These effects also depended on the functional connectivity measure used (dbWPLI or PLI), and the connectivity metric of interest (global connectivity, normalized path length, normalized clustering coefficient, or small-worldness index).

3.4.2.1. The dbWPLI and PLI

Test-retest reliability was overall higher for dbWPLI than PLI based connectivity measures for the epoch numbers and lengths investigated here. Both measures reflect the consistency of the phase lag. In contrast to the PLI, the dbWPLI has an added debiasing method to avoid the overestimation bias when calculated across a small number of epochs, and a weighting component to decrease sensitivity to noise. This debiasing effect is clearly visible in the graphs displaying global connectivity values for the first session: global PLI values exhibit a larger decrease with increasing numbers of epochs than global dbWPLI. For both measures, global connectivity is lower across shorter epochs than longer epochs; even the amount of data is held constant.

One possibility is that phase lags calculated over shorter epochs display less consistency than those calculated over longer epochs as a result of the use of Hanning windows: this tapering leads to a data loss that has more impact on short epochs than long epochs. Fraschini and colleagues observed that global PLI decreased for 6 epochs with increasing epoch length (1 to 12 seconds) (Fraschini et al., 2016), while I observed increasing global PLI values with increasing epoch lengths. The differences in methods to calculate the PLI (Hilbert transform vs. FFT with Hanning windows here), or the populations (adults vs. infants with more noisy data here) might be the reason for these differences in epoch length effects for global PLI. Nonetheless, the global connectivity values for different methods do not necessarily inform on their test-retest reliability. The current results suggested that high test-retest reliability could be obtained for higher numbers of shorter epochs, even with lower global connectivity values.

No previous studies have directly compared test-retest reliability for dbWPLI and PLI based measures in adults, nor infants. One study however compared adult test-retest reliability between the PLI and weighted PLI (WPLI) across 12 4-second epochs with a 2-year interval between recordings. Global connectivity calculated with the PLI and WPLI showed comparable reliability values within the excellent range (ICC_{PLI} = .79, and ICC_{dbWPLI} = .80). Graph theory measures showed reliability values within the poor to good ranges where PLI based measures (.57 < ICC < .64) showed slightly higher reliability than WPLI based measures (.12 < ICC < .50)(Hardmeier et al., 2014). The current results also reached excellent reliability values for global PLI and dbWPLI connectivity for 4-second epochs, even though it was across 60 epochs rather than 12 (ICC_{dbWPLI} = .85, and ICC_{PLI} = .87). When metrics were calculated for 20 4-second epochs, normalized path length and small-worldness were more reliable for the PLI than dbWPLI, while the opposite was observed for normalized clustering coefficient. For the other combinations of epoch numbers and durations investigated here, the infant data however showed slightly higher reliability for graph measures derived from the dbWPLI than from the PLI. Thus, in adults the basic PLI provides more reliable results than the adjusted PLI (WPLI), while in infants the adjusted PLI (dbWPLI) provides more reliable results than the PLI. This result probably arises from the fact that longer epochs are available in adult studies (12 4-second epochs (Hardmeier et al., 2014), 6 10-second epochs (Fraschini et al., 2016), or 5 10-second epochs (Jin et al., 2011). In infant studies, shorter episodes of artefact-free data are available, thus reliability is investigated for shorter epochs lengths (1, 2, or 3 seconds). Consequently, dbWPLI values are more reliable than PLI values for infant data.

Another possible explanation for the differences in dbWPLI and PLI reliability findings between adults and infants might be the overall noisiness of the data. It is well known that infant data contains more noise than adult data, for example due to movement artefacts (Goncharova et al., 2003; Orekhova et al., 2014). The dbWPLI is less sensitive to noise than the PLI as small phase lags from noise are assigned smaller weights than larger phase lags unlikely to result from noise (Vinck et al., 2011). If infant data is noisier than adult data, the use of noise robust measures should result in more reliable measures of functional connectivity than measures that are less robust to noise effects. Indeed, the reliability values for the PLI in infants found here are much lower than in adults, while reliability values for the dbWPLI in infants are within similar ranges as in adults.

Test-retest reliability of other measures of functional connectivity than phase lag indices has also been investigated. In adults, global dbWPLI connectivity showed higher reliability than global coherence connectivity in the alpha band for 120 2-second epochs, while coherence was more reliable for the delta and theta frequency band (Kuntzelman & Miskovic, 2017). Higher reliability values for coherence compared to other measures of connectivity have also been found in other studies (Höller, Butz, et al., 2017). Reliability for connectivity measures overall increases with increasing number of epochs, likely due to the increasing amount of data included in the analyses. More epochs are needed for phase-based measures (phase synchrony) than coherence measures to achieve good reliability values (Miskovic & Keil, 2015). However, it is important to note that coherence is more sensitive to volume conduction, as discussed in Chapter 2. Reliability values might be inflated due to consistency in volume conduction effects, rather than consistency of functional connectivity over time. The use of phase lag index

measures avoids this problem. Moreover, phase lag indices are more likely to measure 'true' brain connectivity than measures that are more sensitive to volume conduction (van Diessen et al., 2015; Vinck et al., 2011).

3.4.2.3. Global connectivity and graph theory metrics

Test-retest reliability was not only modulated by the functional connectivity measure used, but also by the metric calculated from the functional connectivity matrices. Global connectivity values showed higher reliability values than graph metrics. Normalized clustering coefficients were more consistent across the 1-week interval than normalized path length and small-worldness index, where the latter two showed similar reliability values. Previous reliability studies have found similar patterns of results where global connectivity values are more reliable than graph metrics, and normalized clustering coefficients are more reliable than normalized path lengths (Deuker et al., 2009; Fraschini et al., 2016; Hardmeier et al., 2014; Hatz et al., 2016; Van der Velde et al., n.d.).

Global connectivity values are probably more reliable since this measures is less influenced by extreme connectivity values for electrode pairs than the graph theory measures. A slight change in connectivity values between specific electrode pairs over time will have a smaller effect on global overall connectivity, while the topology on which the graph theory metrics are based would be more severely affected. These extreme connectivity values might result from increased measurement noise when connectivity is calculated across a smaller amount of data. Indeed, the pattern of topology of the network becomes clearer, and fewer electrode pairs display extreme values when calculated across a larger number of epochs for individual participants (Fig. 3.7, and 3.8, resp.) (Fraschini et al., 2016; Hardmeier et al., 2014).

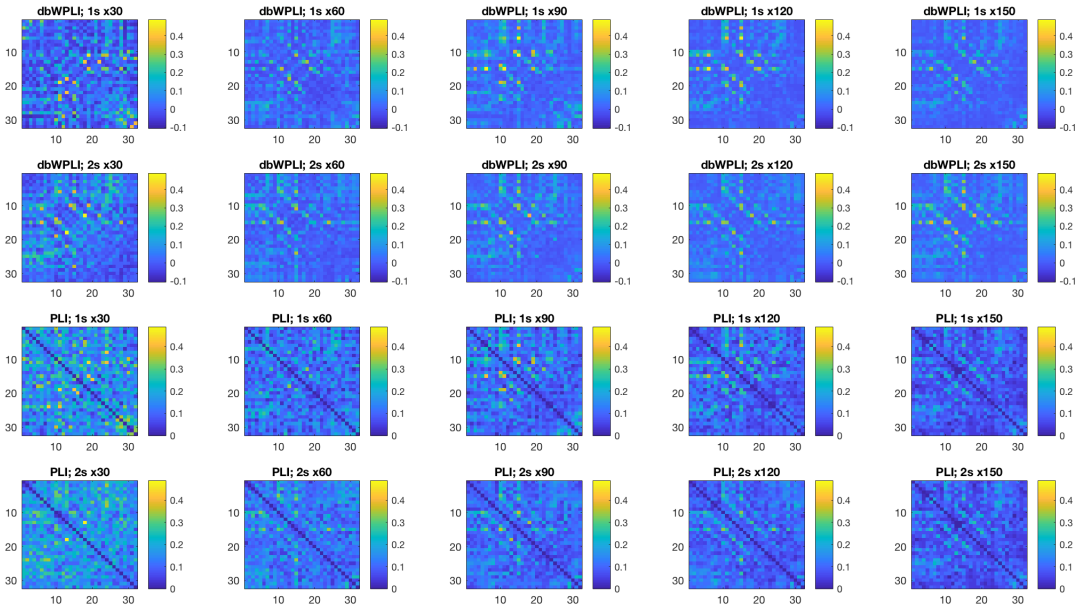

Figure 3.7. Functional connectivity matrices for 1 individual

The topology within functional connectivity matrices becomes clearer when averaged across a larger number of epochs, and/or longer epochs, i.e. the diagonal lines in the matrix become clearer.

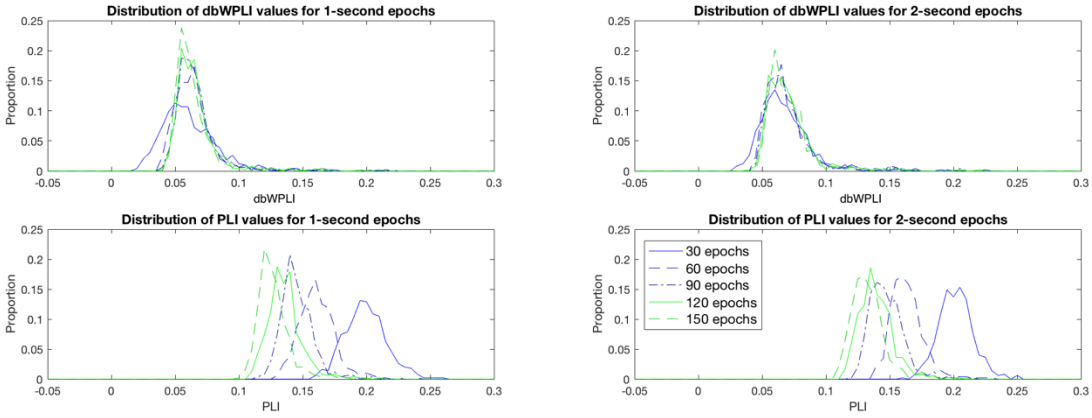

Figure 3.8. Distribution of connectivity vales within functional connectivity matrices for 1 individual

The distributions for dbWPLI values become higher and narrower with increasing numbers of epochs, whereas the distribution for the PLI shifts leftwards, and become higher and narrower with increasing numbers of epochs. This suggests that topography of the networks becomes clearer when computed across higher amounts of data (data are for same individual as in Figure 3.7).

Differences in test-retest reliability are also evident between graph theory metrics. Normalized clustering coefficients display higher reliability values than normalized path lengths. In their original paper introducing the clustering coefficient and path length, Watts and Strogatz demonstrated that a small change in the network by increasing randomness has nonlinear effects on path lengths, while linear effects were observed for the clustering coefficient (Watts & Strogatz, 1998). If this were true for the neural connectivity measures here as well, the clustering coefficient as a local property would be more robust to connectivity changes and thus show higher test-retest reliability values compared to the path length as a global property of the network. Furthermore, the clustering coefficient is based on connectivity values that are rescaled before calculating the graph metrics. In contrast, the path length is based on the values of the connectivity weights making them more susceptible to changes in connection weights than the clustering coefficient. Variability in the connectivity weights over time might thus have a larger effect of path length than on clustering coefficient, with as result the latter being more reliable over time than the former.

Although the test-retest reliability of the graph metrics did not show considerable changes with increasing numbers or durations of epochs, the graph metrics themselves did show differences with different parameters. Both normalized path length and normalized clustering coefficient increased with increasing numbers of epochs. There are several factors that may account for this effect. First, the topography of the network becomes clearer with increasing number of epochs as measurement noise decreases and weight differences between connections increase (Hardmeier et al., 2014). Randomizing the weights in clearly patterned networks will lead to a larger change in typology compared to

randomizing weights in blurry networks. Indeed, the difference between the graph metrics for the observed matrix and the randomized matrices increases with increasing numbers of epochs (Fig. 3.9). We can observe that the clustering coefficient decreases, and characteristic path length increases with clearer topography. The measure used (dbWPLI of PLI) might also play a role here. Due to the weighting of the imaginary component in the dbWPLI calculations, estimates are less influenced by noise, while connectivity between short-range connections is underestimated. This would facilitate a clearer topology pattern. In comparison, the clearness or blurriness of the topology for the PLI would only depend on epoch numbers and length.

Second, graph metrics depend on the average degree or strength of the networks (van Wijk et al., 2010). This holds for the path length in particular, since weights (connectivity values) are inversely related to path lengths, and higher weights lead to shorter path lengths. Thus the observations of lower global connectivity with increasing epoch numbers could theoretically lead to higher characteristic path lengths. For the clustering coefficients, smaller weights would however lead to lower clustering coefficients. For example, in Figure 3.9 weights for the dbWPLI were overall lower than for the PLI, with clustering coefficient having lower values for the dbWPLI (0.05 – 0.13) than for the PLI (0.26 – 0.42), and characteristic path lengths having values in higher ranges for the dbWPLI (10 – 45) than for the PLI (6 – 13).

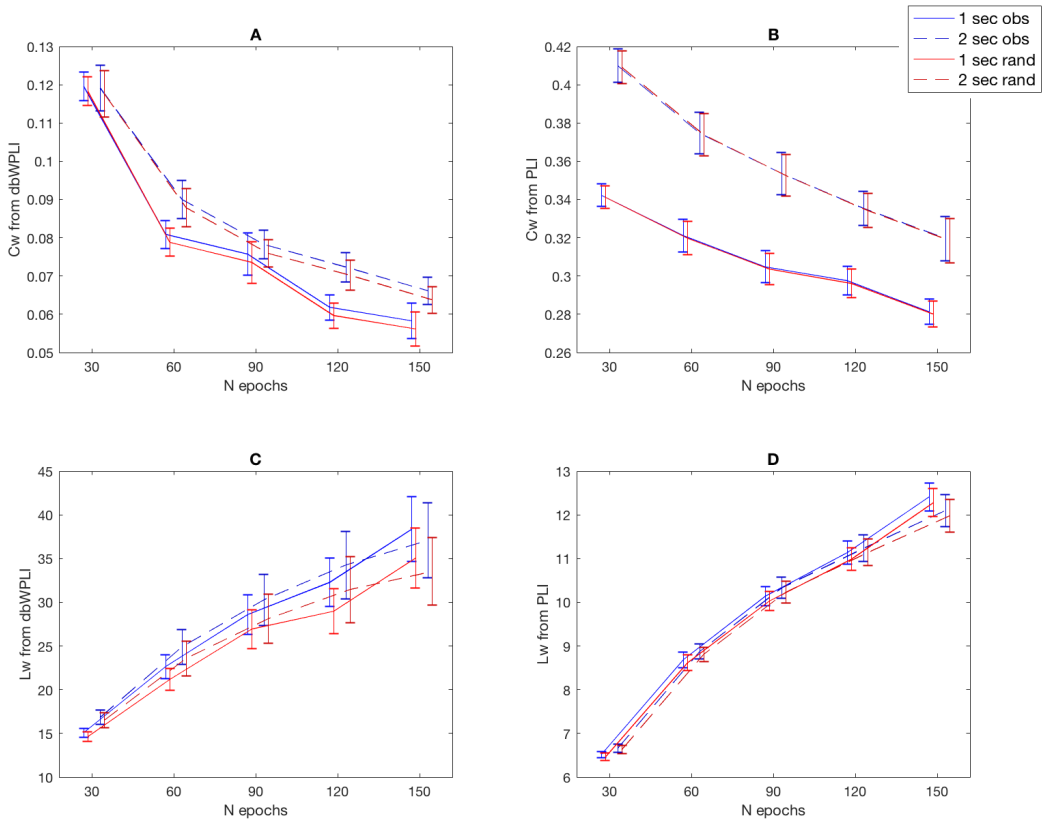

Figure 3.9. Exploration of graph theory measures for observed and randomized data
Each panel displays the mean (standard error of measurement) values for characteristic path length L_w for the dbWPLI (A), and PLI (B), and for the clustering coefficient C_w for the dbWPLI (C), and the PLI (D). Values based on 1-second epochs are connected by a solid line, while those based on 2-second epochs are connected by the dashed lines. Values for the observed network are displayed in blue, while values in red reflect the values averaged across 50 randomizations of the observed network.

The small-worldness index depends on both the normalized clustering coefficient and normalized path length. It is therefore not surprising that test-retest reliability for the small-worldness index is lower than those for the normalized clustering coefficient. The values of the small-worldness index overall decrease with increasing numbers of epochs. This can be explained by a larger increase of normalized path length compared to the normalized clustering coefficient due to the formers increased sensitivity to changes in connections

weights as values are being averaged across a higher number of epochs (Watts & Strogatz, 1998).

It was suggested that networks display small-worldness if the values for the small-worldness index exceeds 1 (Humphries & Gurney, 2008). These networks are characterised by higher clustering than in a random network, and path lengths similar to a random network. However, the current results show that most values are below 1, suggesting that the connectivity patterns observed here do not exhibit as the same quantity of small-worldness as other real world networks, for example social networks, information networks, or technical networks. However, real world networks with values below 1 have also been observed. Small-worldness might not be feasible due to physical constraints such as limitations for the numbers of edges or nodes, or functional constraints for example where a small-world configuration is not optimal for efficiently alternating between synchronized and desynchronized oscillations in neural networks (Humphries & Gurney, 2008). Another possible explanation for small-worldness values below 1 is that the network size is too low. Real world networks with a small number of nodes are less likely to display small-worldness than networks with a larger number of electrodes. Is it possible that the network including 32 nodes here is less likely to show a small-worldness index above 1 than networks with a higher number of nodes (Humphries & Gurney, 2008; van Wijk et al., 2010).

In summary, graph theory metrics and their reliability depend on several interdependent factors including the connection weights, epoch numbers and lengths, connectivity measure used, and network size. Local metrics as the normalized clustering coefficient show higher reliability values than global metrics

as the normalized path length, and derivatives of other metrics as the small-worldness index.

3.4.3. Implication for future studies

The findings in this study suggest that the use of more than 120 1-sec epochs with calculations for the dbWPLI is an appropriate measure for measuring functional connectivity with infant EEG data recorded while infants were watching singing women, and spinning toys. This is consistent with methods used in the previous high-risk infant sibling study (Orekhova et al., 2014). In contrast, the PLI seems a less appropriate measure for infants, as longer epochs are needed to achieve data with high test-retest reliability.

Each of the connectivity metrics is furthermore appropriate for group level analyses. Global connectivity and the normalized clustering coefficient however are more appropriate for individual level analyses and correlational research than normalized path length and small-worldness index (e.g. for dbWPLI across 120 1-second epochs; $ICC_{Global\ connectivity}$ = .53 and ICC_{Cwnorm} = .59 are higher than ICC_{Lwnorm} = .44, and ICC_{SWI} = .40, see tables 3.5, 3.8, 3.11, and 3.14).

. The reason for this is because the latter two metrics exhibit lower test-retest reliability compared to the former two metrics. This is important to consider as the additional value of inter-subject variability measures, and brain-behaviour correlations to traditional comparisons of group means are more often acknowledged (Seghier & Price, 2018), and high reliability for these measures is essential. In particular in clinical research, the call for a dimensional approach looking a individual variability rather than a categorical approach is gaining increasing support (Insel et al., 2010; Singh & Rose, 2009).

3.4.4. Limitations

The study reported in this chapter has a few limitations. First, only gaze behaviour was coded here. Behaviours that might have interfered with the EEG recordings, such as excessive movement or parents or experimenters talking to the infant, have not been coded and excluded from further data analyses (Orekhova et al., 2014). It is possible that artefacts from muscles have inflated the connectivity values, and influenced the test-retest reliability values.

Second, different groups of infants were used for different analyses with different combinations of epoch numbers and lengths. This was done to ensure that extreme epoch numbers and lengths could be investigated, while maintaining reasonable group sizes. This however hinders comparisons of test-retest reliability across analyses: test-retest reliability values for connectivity calculated across 60 1-second epochs are different between the first 2 analyses, as are the comparisons for 120 1-second epochs between analysis numbers 2 and 3. Also, there are likely differences in attentiveness during the EEG recording between the groups. Infants with high attentiveness are more often included as they have more data available than infants with low attentiveness. Infants in the analyses focusing combinations requiring more data (60 5-second epochs in Analyses 1) have been more attentive overall than infants in the analyses requiring less data (120 1-second epochs in Analyses 3). Given the assumption that alpha frequency connectivity is related to sustained attention, stability in attentiveness and mood over time could have played a factor in test-retest reliability as well.

2.5. Summary of Chapter 3

This chapter has shown than EEG connectivity can be reliably measured in infants when calculated across a large number of epochs with short durations with the

dbWPLI. The PLI is more reliable across epochs with longer durations, making this measure less appropriate for infant data. Different connectivity metrics can be used to describe connectivity patterns in groups, such as global connectivity, normalized clustering coefficient, normalized path length, and small-worldness index. The former two are also suitable for investigating individual differences and brain-behaviour correlations.

This suggests that the method of calculating the dbWPLI across at least 120 1-second epochs as done in the study by Orekhova and colleagues is reliable and appropriate for infant data ($ICC_{Global\ dbWPLI}$ = .82 (Orekhova et al., 2014)). In addition, in the analyses where the amount data is kept constant ICC values are generally higher for the dbWPLI metrics across 120 1-second epochs ($ICC_{Global\ connectivity}$ = .53, ICC_{Cwnorm} = .59, ICC_{Lwnorm} = .44, and ICC_{SWI} = .40) and are within the ranges of fair reliability values. In contrast, for the other numbers and lengths of epochs ICC values display more variability, for example across 60 2-second epochs ICCs are within the good range ($ICC_{Global\ connectivity}$ = .68, ICC_{Cwnorm} = .57) and within the poor reliability range (ICC_{Lwnorm} = .12, and ICC_{SWI} = .14, see tables 3.5, 3.8, 3.11, and 3.14). This provides a strong background for using the same method in the next chapter that focuses on a replication study of the study by Orekhova and colleagues.

Chapter 4: The association between alpha EEG connectivity at 14 months and restricted and repetitive behaviours at 36 months of age in high-risk infants

4.1. Introduction

Previous studies have suggested that ASD might be characterised by atypical connectivity from an early age. Findings however are mixed, and depend on a range of methodological factors, including the choice of EEG connectivity measure (O'Reilly et al., 2017; Schwartz et al., 2016). While the previous chapter showed that the dbWPLI is a reliable measure of EEG connectivity over time, this chapter is focusing on the replication of a previous study using the dbWPLI in infants who received a later diagnosis of ASD.

Replication of previous findings in ASD is crucial at this time. In psychology, only a small amount of the previous findings is replicated in independent cohorts. This discovery gave rise to the currently on going replication crisis (Button et al., 2013; Open Science Collaboration, 2015). More importantly, findings in ASD research tend to vary due to the heterogeneity of the samples. Differences in samples composed of different subgroups of ASD, small sample sizes in the cohorts, different age ranges of interest, and differences in inclusion criteria for ASD diagnosis all contribute to the inconsistencies in findings (Schwartz et al., 2016). Thus the importance of replication studies is increasing.

4.1.1. The original study

The study by Orekhova and colleagues (2014) in particular deserves further attention, and will be the study to be replicated in this chapter. This original study aimed to investigate differences in EEG connectivity in the alpha frequency band (7 – 8 Hz) between infants at 14 months of age who did and did not develop ASD at a later age, and how this associated with the severity of ASD symptoms at later age. Infants watched videos of spinning toys, a hand spinning toys, and women singing

nursery rhymes while their EEG signal was being recorded. EEG alpha connectivity was measured with the dbWPLI (also see Chapter 2 and 3). These data were collected as part of the British Autism Study in Infant Siblings (BASIS). The BASIS study is a longitudinal study with a prospective design that examines early precursors and diagnostic markers of ASD. Each infant had an older sibling who was typically developing or had a community diagnosis of ASD, making the infant participating in the study a high-risk for ASD infant, or a low-risk infant, respectively. At 36 months of age, the infants received a clinical assessment to assess whether the infants were meeting criteria for ASD (HR-ASD infants) or not (HR-no ASD infants).

The results showed that the HR-ASD group displayed higher EEG connectivity in the alpha frequency band than the LR group and HR-no ASD groups at 14 months of age. The connections that displayed increased dbWPLI values in the HR-ASD group compared to both the LR and HR-no ASD groups were located across frontal and central areas. The authors note that this is in line with findings of structural overconnectivity in the frontal cortex in young individuals with ASD that might arise from an excitation/ inhibition imbalance in the frontal cortex. This suggests that EEG alpha connectivity might be a marker for ASD outcome.

Furthermore, Orekhova and colleagues examined the associations between alpha connectivity and symptom severity of social communication difficulties, and restricted and repetitive behaviours. In the complete HR group (HR-ASD and HR-no ASD infants collapsed), alpha connectivity averaged across all connections showed trends for a positive association with more social communication difficulties, and restricted and repetitive behaviours measured by a parental interview (Autism Diagnostic Interview – Revised, ADI-R (Rutter, Le Couteur, &

Lord, 2003)), but not when measured by behavioural observations (Autism Diagnostic Observation Schedule – Generic, ADOS-G (Lord et al., 2000)).

For the HR-ASD group, alpha connectivity across the fronto-central connections that showed increases in the HR-ASD group compared to both the LR and HR-no ASD group was significantly related to more severe restricted and repetitive behaviours measured with the ADI-R. The association between connectivity across the selected fronto-central connections and social difficulties based on ADI-R however did not reach significance in this group, nor did those associations with the social communication difficulties, and restricted and repetitive behaviours measured with the ADOS. Lastly, no significant correlations were observed in the HR-no ASD group. These findings suggest that alpha connectivity in fronto-central connections is related to restricted and repetitive behaviours in infants who develop ASD at a later age (Orekhova et al., 2014).

4.1.2. Further EEG connectivity studies during infancy

Few other studies have looked into how EEG connectivity relates to later categorical outcome or dimensional traits. In one study, infants listened to speech sounds at 6 and at 12 months of age while watching a research assistant blowing bubbles. Connectivity (coherence) for the gamma frequency band between frontal and temporo-parietal areas was lower for the HR group at 12 months than for the LR group, whereas there were no differences between groups at 6 months of age. Outcome analyses showed that the HR-ASD group displayed lower connectivity than the HR-no ASD group who in turn displayed lower connectivity than the LR group (Righi et al., 2014).

This study thus shows underconnectivity rather than hyper connectivity in infants around 1 year of age. One possibility is that EEG connectivity patterns are

different for different frequencies bands, for example hyperconnectivity across the lower alpha band and hypoconnectivity across the higher gamma band in a the HR-ASD group than the LR or HR-no ASD groups. Another possibility is that the differences in paradigms led to different findings (videos or live stimuli). However, Righi and colleagues only examined associations between connectivity and categorical ASD outcome, and did not analyse dimensional ASD traits. Finally, the use of different connectivity measures might account for the difference in findings. Coherence used by Righi and colleagues is more sensitive to volume conduction than the dbWPLI used by Orekhova and colleagues (van Diessen et al., 2015). Findings might thus arise from differences in volume conduction between groups rather than differences in connectivity between populations of neurons. Finally, the gamma frequency band is more susceptible to muscle artefacts, and displays a smaller signal to noise ratio than the alpha band (Muthukumaraswamy, 2013) (also see Chapter 2). It is possible that these differences are also related to the different results.

The other study using a high-risk infant sibling design was conducted by Keehn and colleagues. They found no differences at 6 months of age in gamma phase coherence between LR and HR groups when infants were presented with pictures of their mother. At 12 months of age, the HR group showed higher connectivity within the left hemisphere compared to the right hemisphere. This leftward lateralization was larger in the HR-ASD group than in the LR and HR-no ASD groups. There were no differences between groups in whole brain connectivity at either age. The amount of leftward lateralization in the HR-ASD group was furthermore related to increased symptom severity at both 24 and 36

months measured by the ADOS (Keehn, Vogel-Farley, Tager-Flusberg, & Nelson, 2015).

The study by Keehn and colleagues did not reveal any differences in whole brain gamma connectivity between groups, in contrast to the study Righi and colleagues that displayed decreases in gamma connectivity. This difference in findings might arise from the difference in tasks. Still, this study used coherence to calculate connectivity values, which is less robust to volume conduction effects than the dbWPLI used by Orekhova and colleagues. Both differences in methods and frequency bands of interest might account for the variability in results.

Interestingly, studies by Keehn and Orekhova both investigated associations with categorical ASD diagnosis, and ASD dimensional traits. Both studies showed that larger differences in the direction of the observed connectivity differences were related to more severe symptoms (higher alpha connectivity when hyperconnectivity was observed, and more leftward lateralization gamma connectivity where higher leftward lateralization was found in the HR-ASD group compared to the other groups). There are two further considerations here. Righi and colleagues investigated only total severity of symptoms. It is possible that associations between with different frequency bands exhibit different strengths with different symptom domains (social difficulties, or restricted and repetitive behaviours).

Also, the severity of symptoms was measured with clinical observations via the ADOS. The advantage of this method is that the severity of ASD behaviours is directly assessed by an experienced researcher. The disadvantage however that behaviours are only seen during a short period of time. Behaviours that are expressed in other contexts or less frequently are less likely to be picked up with

the ADOS than with the ADI-R. The study by Orekhova and colleagues examined symptom severity or ASD traits in the 2 core domains (social interaction, and restricted and repetitive behaviours), and with both clinical observations and parental interviews (ADOS, and ADI-R, resp.).

4.1.3. Rationale for the current replication study

In the current study, the aim was to test whether EEG alpha connectivity relates to later ASD outcome and dimensional traits. To this end, I attempted to replicate the previous study by Orekhova and colleagues. There were several reasons for selecting this study in particular; a) the previous study focussed on both categorical outcomes and dimensions of traits in different ASD domains; social and communication difficulties, and restricted and repetitive behaviours. In contrast, other infant studies investigating functional connectivity as potential marker for ASD have focussed on categorical outcomes only, or dimensions of ASD symptoms overall rather than specific domains (Keehn et al., 2015; Righi et al., 2014); b) the alpha frequency band is characterized by a high signal-to-noise ratio and is less susceptible to myogenic artefacts than other frequency bands e.g. beta or gamma band (Goncharova et al., 2003; Muthukumaraswamy, 2013); c) the use of the dbWPLI as a measure of functional connectivity, since the dbWPLI is less sensitive to noise as a result of the weighting, and reliable when calculated over a small number of epochs (see Chapter 2, and (Vinck et al., 2011)). This is especially relevant for infant data as these contain more noise, and commonly fewer artefact-free epochs than adult data; d) the videos used in this paradigm have been proven to be suitable for infants as infants have shown sustained attention while watching these videos in previous studies (Elsabbagh, Volein, Csibra, et al., 2009; Jones et al., 2015; Orekhova et al., 2014); and e) the final reason for replication of this study

was pragmatic, as data from an independent cohort with this particular design were readily available, and would allow for direct comparisons with the original study. Using the same paradigm and methods would also allow me to combine the previous and current dataset as to increase statistical power for further analyses.

Although the same paradigm and methods were used in the current study, the current study used different outcome groups than the original study. While the original study compared 3 groups: LR, HR-no ASD, and HR-ASD groups, the current study compared 4 groups: LR, HR-TD, HR-Atyp, and HR-ASD groups. These four groups allow for investigation of typical development in a high-risk group, and of the broader autism phenotype. Comparison between the HR-ASD and HR-TD groups reflects differences between typical development and development of ASD, possibly revealing protective factors for later development. The HR-Atyp group consists of individuals with other developmental atypicalities. Thus comparison between the HR-Atyp and HR-ASD groups might reveal underlying mechanisms of ASD diagnosis specifically, and potential risk factors for later development of ASD. I therefore expect a graded effect in the HR-TD, HR-Atyp, and HR-ASD groups.

Finally, I tested whether there might have been any confounding factors influencing the categorical results, such as gender, age, cognitive skills, and amount of epochs included. Furthermore, to disentangle connectivity and spectral power effects, differences in overall, posterior, and central (mu) alpha power between groups were analysed as well. These additional analyses were performed because previous results suggest that connectivity measures or ASD outcomes and dimensional traits might be modulated by gender (Bedford et al., 2016), age (Boersma et al., 2011; Smit et al., 2012), cognitive abilities (Orekhova et al., 2014),

number of epochs (Vinck et al., 2011), and spectral power (Orekhova et al., 2014; van Diessen et al., 2015).

Based on the findings in the original study, I predict that functional connectivity in the alpha range will be increased in the frontal and central areas for HR-ASD infants compared to the other groups, whereas there will be no differences between groups for spectral power in the same frequency band. Furthermore, I hypothesize that the amount of over-connectivity in the selected connections is positively related to the severity of repetitive and restrictive behaviours in the HR-ASD group, while there is no such association between overconnectivity and severity of social communication symptoms in this group.

4.2. Methods

4.2.1. Participants

143 infants participated in this cohort of the BASIS study (Phase 2), from which 101 infants were included for further analyses. 42 infants were excluded due to missing outcome data at the visit at 3 years of age (3 infants), no data recorded (8 infants: no visit for 1 infant, equipment failure for 2 infants, and 5 infants were indisposed; too tired, unwell, or too upset at the start so the assessment was terminated), too many artefacts in the data in such a way that no artefact-free epochs could be defined (5 infants), data affected by a heart rate signal (13 infants), and insufficient amount of artefact-free data (13 infants with less than 120 artefact-free epochs, see also section 4.2.3). Infants were between 13 and 18 months old during EEG data collection.

Participants were recruited via the BASIS study website, and the Centre for Brain and Cognitive Development at Birkbeck, University of London, United

Kingdom. The protocol of this study has been approved by the UK National Health Service National Research Ethics Service London code 08/H0718/76; 06/MRE02/73. Each of the assessments and experiments during the visits were performed in accordance with the relevant guidelines and regulations. Parents/ caregivers gave informed consent before the start of the study.

4.2.2. Procedure and clinical assessment

Participants participating in the BASIS study came into the Babylab for multiple visits during the first years of life. Each visit consists of a battery of eye tracking, behavioural, and neuroimaging tasks, which are assessed by the BASIS team.

4.2.2.1. Infants with and without risk for ASD

At the start of the participation in the BASIS study, infants were recruited into low risk (LR) and high risk (HR) for ASD group. Participating infants had at least one older sibling who was older than 3 years of age at the time of study entry. Each of 81 HR infants participating in the study had an older sibling (proband) with a community clinical diagnosis of ASD. Each of 20 LR infants had an older siblings showing typical development, and had no family history of ASD within first-degree relatives (for methods, see Appendix A4.1).

4.2.2.2. The 14-month-old visit

The tasks from the 14-month-old visit relevant for this study are the EEG task, and the Mullen Scales of Early Learning. Data during this visit were collected by members of the BASIS team located at the Centre for Brain and Cognitive Development, Birkbeck College, University of London.

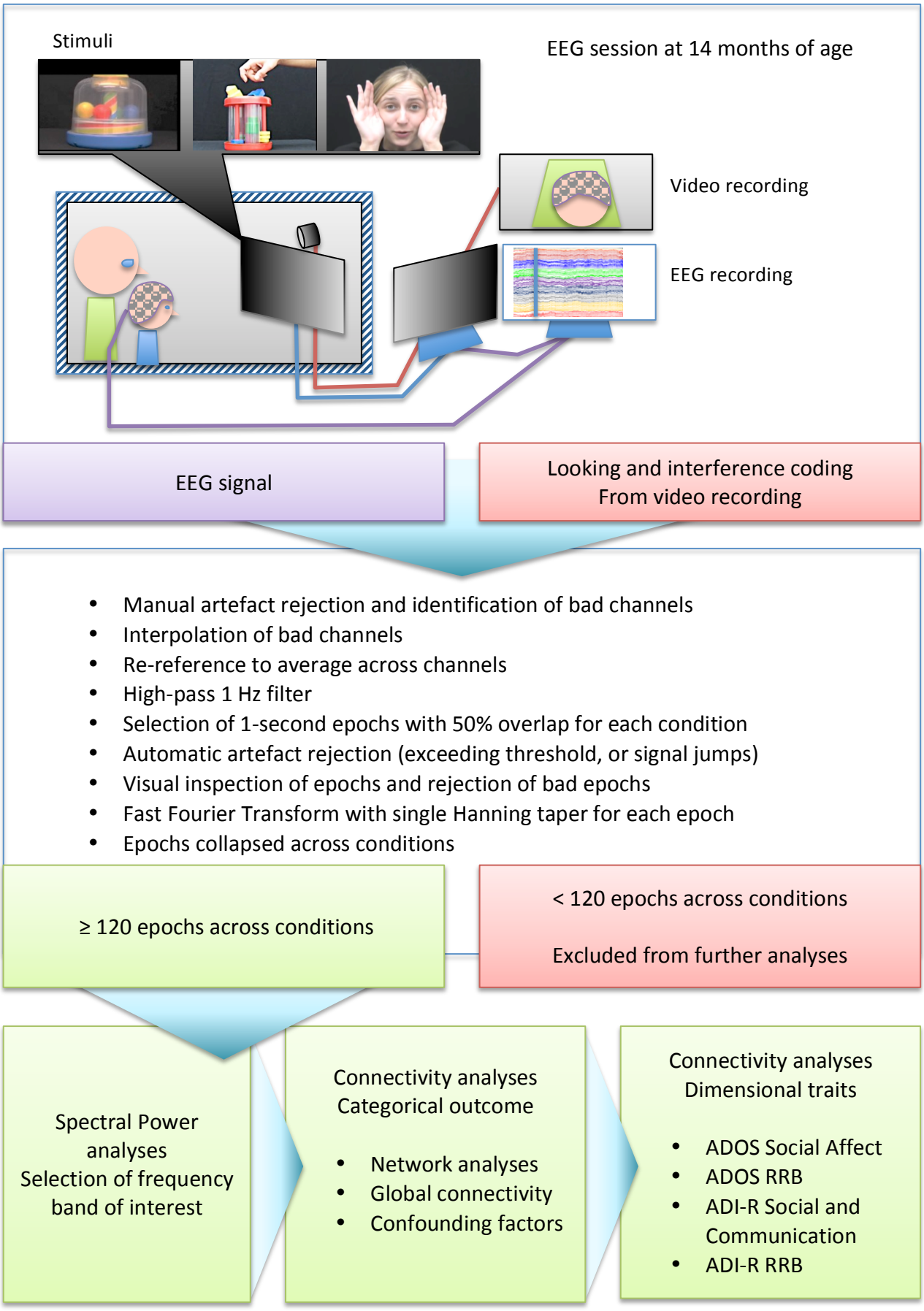
Stimuli
EEG session at 14 months of age
Video recording
EEG recording
EEG signal
Looking and interference coding
From video recording
• Manual artefact rejection and identification of bad channels
• Interpolation of bad channels
• Re-reference to average across channels
• High-pass 1 Hz filter
• Selection of 1-second epochs with 50% overlap for each condition
• Automatic artefact rejection (exceeding threshold, or signal jumps)
• Visual inspection of epochs and rejection of bad epochs
• Fast Fourier Transform with single Hanning taper for each epoch
• Epochs collapsed across conditions
≥ 120 epochs across conditions
< 120 epochs across conditions
Excluded from further analyses
Spectral Power analyses
Selection of frequency band of interest
Connectivity analyses
Categorical outcome
• Network analyses
• Global connectivity
• Confounding factors
Connectivity analyses
Dimensional traits
• ADOS Social Affect
• ADOS RRB
• ADI-R Social and Communication
• ADI-R RRB

(Previous page)

Figure 4.1. Overview of methods

The upper part of the figure represents EEG procedure, the middle part displays the preprocessing steps, and the lower part displays the analyses steps.
Abbreviations: Autism Diagnostic Interview – Revised (ADI-R), and Autism Diagnostic Observational Schedule (ADOS).

EEG task: Infants were presented with 3 different videos. A video of spinning toys was presented for 44 seconds in the toy condition. The hand condition consisted of a video showing a hand spinning toys for 41 seconds. The social condition showed women singing nursery rhymes for 32 seconds (see Fig. 4.1). The 3 videos were presented in a random order, and subsequently repeated 2 times, resulting in 3 presentations for each condition in total. Infants sat on their parent's lap in an electrically shielded room while looking at the videos being presented at computer screen. Simultaneously, infants' EEG signals were recorded with a 128 channels EGI electrode system and Netstation EGI software at a sampling rate of 500 Hz. The infants' behaviour during this EEG session was recorded with a video camera for later behavioural coding. Previous studies showed that these stimuli are suitable for infants since infants pay attention to the stimuli and remain calm that allows for the collection of artefact-free EEG data (Elsabbagh, Volein, Csibra, et al., 2009). However, the EEG session was terminated if the infant became too fussy to continue as judged by the BASIS researcher.

Mullen Scales for Early Learning (MSEL): The Mullen Scales for Early Learning (Mullen, 1995) are a behavioural assessment measuring developmental levels from birth to 68 months of age across five domain scales. Each scale consists of different items with increasing difficulty attempting to find the infant's basal and upper level of abilities for visual processing, fine and gross motor skills, and

receptive and expressive language (see Appendix A4.2 for more details on the scales). The scores on these domains can be combined into one Early Learning Composite standard score that reflects the infant's current level of cognitive development. Higher scores reflect better levels of cognitive skills.

4.2.2.3. The 36-month-old visit: clinical assessment

At the visit at 36 months of age, the MSEL assessment was repeated. All HR toddlers were assessed with the Autism Diagnostic Observation Schedule, while parents participated in the Autism Diagnostic Interview – Revised. Parents also filled in several questionnaires, including the Vineland Adaptive Behavior Scale-II, and the Social Communication Questionnaire. Data collection and the clinical assessment were performed by the BASIS research team located at King's College London, Institute of Psychiatry, Psychology & Neuroscience.

Autism Diagnostic Observation Schedule – 2 (ADOS-2): The Autism Diagnostic Observation Schedule – 2 (Lord, DiLavore, & Gotham, 2012) is a standardized observational assessment that evaluates the current level of ASD symptom severity in the target individual. In the Toddler Module, each of items is assessed in a playful manner by an experienced clinician. Different versions exist for younger toddlers or older toddlers who use few or no words, and for older toddlers who use some words. Item scores range from 0 to 3 or 4. Also scores of 7, 8, or 9 are possible if an item is not applicable.

The frequency, quality, and appropriateness of toddlers' responses to the items during this session are rated. Examples of relevant behaviours are joint attention, eye contact, focused attention, motor behaviour, expression of emotions, sharing of interest, anticipation to routines, social smiling, use of verbal and non-verbal language, repetitive behaviours during play, unusual sensory interests,

repetitive motor behaviours, and others. Scores on each of the items are combined into algorithm scores for 2 domains: 1) Social Affect Algorithm, as measure of communication and reciprocal social interaction, and 2) Restricted and Repetitive Behaviour Algorithm, as a measure of restricted and repetitive behaviours. The scores on these two algorithms can be combined into one overall Total score that reflects the severity of the overall ASD symptoms in the toddler. The ADOS-2 Social Affect score used in the analyses in the previous study and here is derived from the ADOS-2 Social Affect Algorithm, while the ADOS-2 Restricted and Repetitive Behaviour score is derived from the ADOS-2 Restricted and Repetitive Behaviour Algorithm. Higher scores on the items and scales indicate more severe symptoms.

Autism Diagnostic Interview – Revised (ADI-R): In addition to the ADOS-2, the Autism Diagnostic Interview – Revised (ADI-R (Lord, Rutter, & Le Couteur, 1994; Rutter, Le Couteur, et al., 2003)) was used to assess symptom severity. The ADI-R is a standardized, semi-structured interview that is conducted with the parent or caregiver of the target individual. The ADI-R can be used for target individuals from 2 years of age, including adults. The interview includes 93 items that investigate the history and current severity of ASD symptoms. The first questions gather information on the onset of the symptoms, followed by questions on the acquisition and loss of language and other skills, language and communication functioning, social development and play, interests and behaviours, and other general behaviours such as gait, aggression or special skills.

In general, 2 scores are given for each item: the current severity giving a 'current score', and whether this was ever a problem in the past or the severity around 4-5 years of age when most abnormalities would be expected giving an 'ever score'. Possible scores are 0, 1, 2, 3, 8 (Not applicable), or 9 (not known or not

asked). In the case of our 36-month-old toddlers, current and ever scores are likely to be similar as they have not yet reached the age symptoms are expected to be most severe. It should also be kept in mind that some items are not as applicable to toddlers as older children, for instance play with peers or friendships. Similarly, items asking about make-believe and social imitative play are not appropriate for children older 10 years.

The raw scores for the items are converted into algorithm scores by summing recoded raw scores from specific items with use of the pre-specified scoring form at the end of the ADI-R questionnaire booklet. The scores are combined into three domains: 1) Qualitative Abnormalities in Reciprocal Social Interaction (Social domain), 2) Qualitative Abnormalities in Communication (Communication domain), and 3) Restrictive, Repetitive and Stereotyped Patterns of Behaviour (Restricted and Repetitive Behaviours domain). The ADI-R Social and Communication measure used in the analyses in the previous study by Orekhova and colleagues and in the current study is calculated by summing the scores of the Social domain and the Communication domain. The ADI-R Restricted and Repetitive Behaviours measure used is the ADI-R Restricted, Repetitive and Stereotyped Patterns of Behaviour Algorithm score.

Questionnaires: Parents also filled in two questionnaires with regard to their child's behaviours: 1) the Social Communication Questionnaire (SCQ (Rutter, Bailey, & Lord, 2003)) assessing ASD symptomatology, and 2) the Vineland Adaptive Behaviours Scale-II (VABS-II, (Sparrow, Balla, & Cicchetti, 2005; Sparrow, Bella, & Cicchetti, 1984)), which measures adaptive behaviours during daily life (see Appendix A4.1 for the SCQ, and A4.3 for VABS-II).

Categorical outcome: Outcomes for the HR toddlers (TD, Atyp, or ASD) were based on consensus of clinical judgement after reviewing on all relevant information after the 36-month-old visit, including results from the ADI-R, ADOS-2, and SCQ measuring ASD symptoms; from the VABS-II measuring adaptive behaviour; and from the MSEL measuring developmental levels of cognitive skills. The clinical judgement was made by a team of experienced clinical researchers led by a licensed clinical psychologist Tony Charman (see Appendix A4.4 for clinical outcomes for the complete cohort).

4.2.3. EEG preprocessing

Before starting EEG preprocessing, video recordings from the EEG session were coded for looking and interference. Looking was coded from the first frame the child was looking at the screen to the last frame the child was looking at the screen. This coding category was identical to the one used in the previous study.

Interference was defined as any behaviour that is distracting the infant from looking at the screen that would not show up in the EEG signal, such as a parent or the experimenter talking to the infant, pointing to the screen to redirect the infant's attention, or stroking the infant. Interference was coded from the first to the last frame the behaviour was present if persisting for longer than 1 second. This category was adapted from the previous study as to improve coding efficiency (see Appendix A4.5).

A research volunteer and myself coded behaviour during each of the videos. Inter-rater reliability was high for looking (Spearman's rho = .90) and moderate for interference (Spearman's rho = .73) for the double-coded videos of 12 infants that were randomly chosen from the complete sample. The researcher coded videos of EEG sessions for 38 infants, while I coded sessions for 84 infants (38 + 84

+ 12 double coded for interference + 9 infants without data = 143). Percentages of looking and interference across the EEG session were also calculated as to test whether there were differences in these behaviours between groups that might confound the connectivity analyses.

The EEG data were preprocessed using Fieldtrip (Oostenveld et al., 2011) and MATLAB_R2015a by myself. First, both separate EEG and behavioural data files for each presented video were imported into Matlab for manual artefact rejection. The continuous raw EEG data were filtered for visual inspection with a high-pass 1 Hz filter and a 48-52 Hz band stop filter. The segments where the child was not looking at the screen and those where there was interference present were marked for exclusion from further analyses. The data were then first visually inspected (automatic artefact detection was performed later also), and segments containing artefacts were manually selected and marked for exclusion as well. Blink artefacts were defined as a positive deflection of EEG signal frontal electrodes and a simultaneous negative deflection at occipital electrodes. Muscle artefacts were characterized by high frequency signal in frontal, central and occipital channels. General movement was characterized by a jump that was evident in all electrodes simultaneously.

In addition, events of small jumps in more than 2 channels, very large jumps in 1 to 2 channels, or more than 3 channels with a flat signal were also marked as artefacts. Channels for individual participants were marked as bad when behaving differently from other channels throughout the session: losing signal very often, showing many jumps in the signal, showing a lot of high frequency noise, and/or showing a flat signal. Specific electrodes on the outer side of the net were bad in most infants and discarded from further analyses (E17, E48, E49, E73, E81, E88,

E113, E119, E125, E126, E127, and E128) (see Fig. 4.2). The raw data for these individual bad channels were interpolated before using the average reference. The data were then filtered with a high-pass 1 Hz filter.

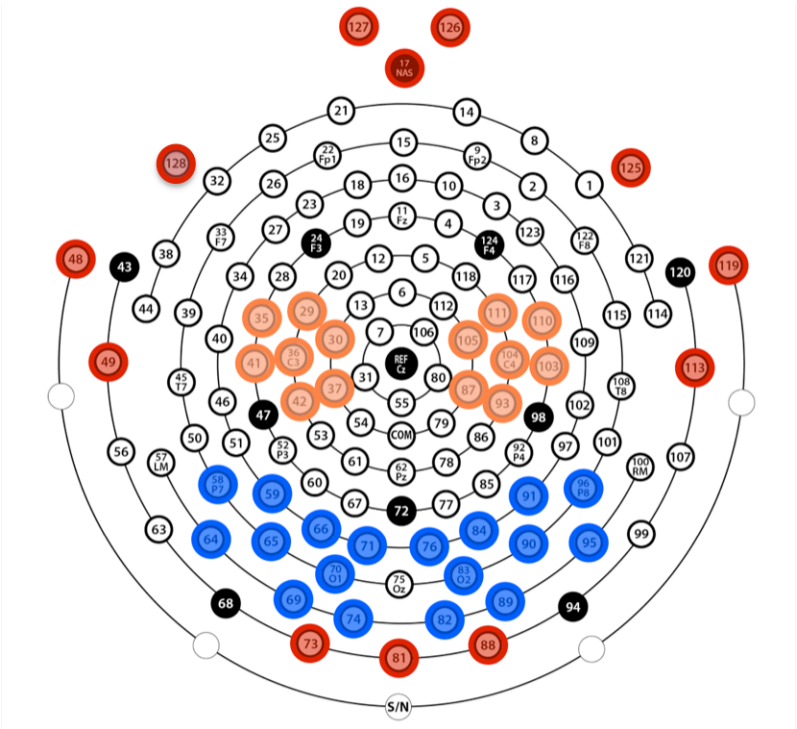

Figure 4.2. Layout of the EEG net for alpha analyses

Layout of the net used in the current study. Electrodes that were discarded because of bad signal in most participants are marked in red. For spectral power analyses for posterior areas, values were averaged across electrodes marked in blue, and for analyses for central areas, averages were calculated across electrodes marked in orange.

The remaining data, e.g. data segments that had not been marked as bad, were cut into 1-second epochs with 50% overlap. Epochs selected from different video presentations but from the same condition were concatenated (e.g. all toy epochs into 1 variable). Another round of automatic data cleaning followed for each of the epochs. Line noise was removed using a dft filter, filtering out noise at

50, 100, and 150 Hz. The EEG signals for individual channels were interpolated if the signal exceeded a threshold of 150 mkV or showed a jump of more than 100 mkV in 4 ms. Epochs were only interpolated when these events occurred in less than 15% of the channels. If interpolation failed, these epochs were rejected from further analyses. A second round of visual artefact rejection followed to ensure the 1-second epochs contained no bad data.

Fast Fourier Transform (FFT) with a single Hanning taper was applied to the clean epochs for each of the three conditions (hand, toy, and social). The complex Fourier values were obtained for each epoch, for each channel, and for each frequency between 0 and 250 Hz (N epochs x 116 channels x 251 frequencies). Finally, frequency data were concatenated across all conditions. Epochs across conditions were collapsed as this would result in a higher inclusion rate of infants with this cut-off. Infants with more than 120 clean epochs across conditions were included for further analyses. I chose 120 epochs as cut-off based on the cut-off of the original study, and the results of Chapter 3. The authors in the original study chose this cut-off, as the bias to overestimate connectivity with a low number of epochs would be minimal when 120 or more epochs would be used for the dbWPLI. Furthermore, the results from Chapter 3 suggested that 120 epochs or more can give rise to reliable dbWPLI values ($ICC_{Global\ dbWPLI}$ = .82, which is considered as excellent reliability, also see table 3.4).

4.2.4. Spectral power analyses

Connectivity analyses are typically accompanied by spectral power analyses for 2 reasons: a) selecting the appropriate frequency band of interest for the connectivity analyses with this paradigm, and b) disentangling spectral power differences from connectivity differences between the HR-ASD and comparison

groups (Orekhova et al., 2014; van Diessen et al., 2015). To this end, I calculated the spectral power by squaring the absolute values of the complex Fourier values for each epoch before calculating the average over trials. Finally, the values were log transformed using the log function in Matlab (ln(x)) and averaged across all channels. The frequency band of interest for alpha was chosen based on visual inspection of the spectral power spectrum for 0 to 30 Hz. I expected to see a peak for the alpha rhythm between 7 and 8 Hz as in the original study.

In additional analyses, I tested whether there were any differences between groups in occipital alpha or central alpha (also mu) oscillations. Occipital alpha power was defined as the average power values for 7 to 8 Hz over posterior electrodes over the left and right hemisphere (E58, E59, E64, E65, E66, E69, E70, E71, and E74 for left, and E76, E82, E83, E84, E89, E90, E91, E95, and E96 for right hemisphere electrodes). Central mu power values were calculated by averaging power values for 7 to 8 Hz across central left and right electrodes (E29, E30, E35, E36, E37, E41, and E42 for left, and E87, E93, E103, E104, E105, E110, and E111 for right hemisphere electrodes) (see Fig. 4.2).

4.2.5. Functional connectivity measure

Functional connectivity was measured with the debiased weighted phase lag index (dbWPLI). The methods for calculating the dbWPLI have been described in Chapter 2 of this thesis. This measure was chosen because this method was also used in the original study I am aiming to replicate here. The robustness to volume conduction and noise effects, and lower and varying numbers of epochs are other strengths that make the dbWPLI appropriate for this study, as mentioned previously.

The dbWPLI values were calculated from the FFT values for each epoch, and then averaged over all available epochs per individual as described in Chapter 2 of this thesis. The connectivity matrix for the alpha band was obtained by averaging the connectivity matrices for 7 and 8 Hz. One connectivity matrix was calculated for each infant. These connectivity matrices were used for further network analyses. Further, global connectivity across all connections (averaging all values below the diagonal), and global connectivity across selected connections (averaging connectivity across selected connections based on current network results, or previous results if no significant network is found here) were calculated to be used in further analyses on categorical outcome and dimensional traits (see Fig. 4.3).

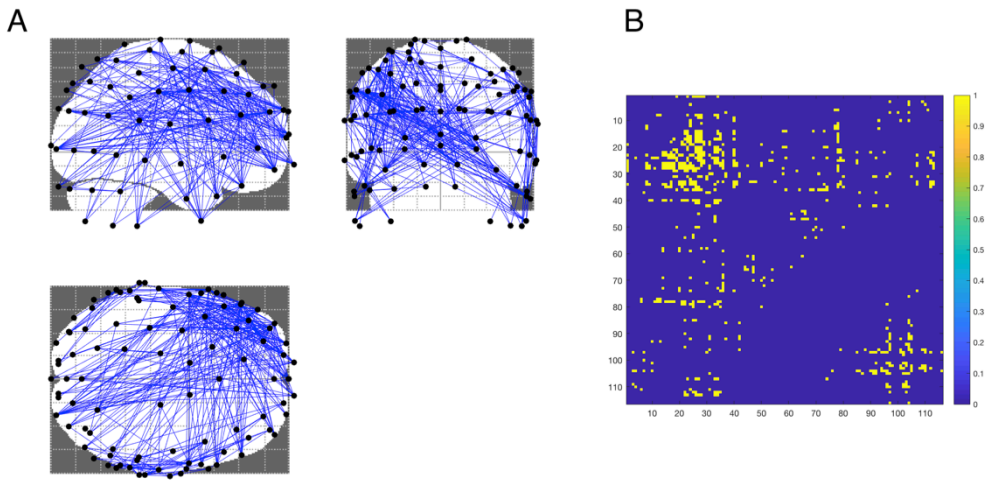

Figure 4.3. Selected fronto-central connections based on the original study
A) Network of connections that showed higher connectivity in the HR-ASD group compared to both the LR and HR-no ASD groups in the original study by Orekhova and colleagues (2014). B) Mask used for selecting the fronto-central connections in A.

4.2.6. Statistical analyses

4.2.6.1. Participants

The statistical analyses aimed to test for differences in demographic data between the HR-ASD group and the comparison groups: HR-ASD versus LR infants; HR-ASD versus HR-TD infants; and HR-ASD versus HR-Atyp infants. All analyses were performed with the Statistical Package for Social Sciences (IBM SPSS Statistics, version 22). To test for differences in gender between groups, I used a Chi-square test for independence since both group and gender are categorical variables.

Next, I tested for differences in ages, MSEL scores, and scores on the ADI-R and ADOS-2 between the HR-ASD and comparison groups. The first step of the statistical analyses was exploring by visualizing the data for the different groups. Parametric tests such as analyses of variance (ANOVA) and t-tests assume that data are normally distributed within groups, and that the variance is equal across groups. If these assumptions are violated, a non-parametric test such as a Mann Whitney U-test that does not assume normality and homogeneity of variance is more appropriate. Normality and homogeneity of variance were tested with a Shapiro-Wilk test and a Levene's test, respectively. If the resulting p-values are above .05, the assumptions tested for have been met.

If both assumptions were met, a parametric independent samples t-test for means was used to compare data between the HR-ASD group and the other comparison groups (LR, HR-TD, and HR-Atyp group). Means and standard deviations were reported. If one of the assumptions for a parametric test were not met, the non-parametric Mann-Whitney U-test was used to test whether there was a significant difference between the HR-ASD and the comparison groups. Medians and interquartile ranges were reported instead of means and standard deviations.

Separate independent samples t-tests or Mann-Whitney U-tests were performed on the demographic factors to test for differences in these factors between groups: age at EEG assessment during the 14-month-old visit, age at clinical assessment at the 36-month-old visit, MSEL composite score at the 14-month-old visit, MSEL composite score at the 36-month-old visit, domain scores for the ADI-R Social Total, ADI-R Communication Total, ADI-R Restricted and Repetitive Behaviours Total, ADOS-2 Social Affect Total, and ADOS-2 Restricted and Repetitive Behaviours Total. This procedure of analyses was also applied in the previous study (Orekhova et al., 2014).

4.2.6.2. Alpha connectivity and categorical outcome

To test whether HR-ASD infants show higher connectivity than LR, HR-TD, and HR-Atyp infants, 3 sets of analyses were performed.

4.2.6.2.1. Network analyses

Network analyses identify networks that are significantly different between groups or conditions. For these analyses, I used Network Based Statistics (NBS) (Andrew Zalesky et al., 2010). These analyses use permutation based testing to identify p-values, and thereby circumvents the multiple comparisons problem (see Chapter 2). The same version and settings as used in the previous study were used in the current study: the Mann-Whitney U test as test-statistic, with a one-tailed test and alpha significance level .05. The number of permutations was set to 5000. The Z-score threshold used was 1.96, since 95% of the area under the normal distribution lies below this value, only values above this score are considered significant. This test was used to test for networks with increased connectivity strengths for the HR-ASD group compared to the other groups. If no significant group differences would be found, additional analyses would be performed to test

for group differences across the fronto-central connections found in the original study ((Orekhova et al., 2014) and Fig. 4.3). To this end, masked connectivity matrices would be used, where only connections showing higher connectivity in the HR-ASD group compared to both the LR and HR-no ASD groups in the original study would be tested for group differences.

4.2.6.2.2. Global connectivity analyses

The second step of the connectivity analyses involved testing for any significant differences between groups for global connectivity (global dbWPLI), that is connectivity values averaged across all connectivity values below the diagonal. A Shapiro-Wilk test and a Levene's test for normality and equality of variances were used to establish whether an independent samples t-test or Mann-Whitney U-test would be appropriate to use. The same analyses were repeated for global connectivity across selected connections resulting from the NBS analyses, or across fronto-central connections from the original study if no differences were found in the current cohort.

4.2.6.2.3. Global connectivity analyses and confounding factors

Connectivity results have been influenced methodological factors, such as amount of epochs and spectral power, and demographic factors such as gender, age, and cognitive abilities, among others. I therefore conducted additional analyses to investigate whether any factors could have confounded the connectivity results. If there were differences between groups in means or in correlations between the potential confounding factor and global connectivity, this factor would be included in a General Linear Model (GLM) testing for the effect of Group (LR, HR-TD, HR-Atyp, HR-ASD infants). Separate General Linear Models were performed for each factor showing differences between groups. This was done for several potential

confounding factors: a) methodological factors included percentage looking and interference during EEG assessment, numbers of epochs included (across all conditions, from each separate condition, proportion of social epochs, and proportion of overlapping epochs), spectral power (across all electrodes, and electrodes in left/right posterior/central regions), and 2) demographic factors included gender, age at EEG assessment, and MSEL Early Learning Composite scores at EEG assessment (also see Appendix A4.6)

In case any of the potential confounding factors showed differences between groups, an addition GLM would be performed to test for group differences in connectivity while taking into account the confounding factor. Separate GLMs were performed for each confounding factor for the sake of clear interpretation of the results. General Linear Models were applied to the global connectivity data with Group as factor and separate confounding factors as additional factor (Gender), or covariate (other variables).

4.2.6.3. Alpha connectivity and dimensional traits

The previous study investigated associations between alpha connectivity and dimensional traits of autism, in addition to the associations with categorical outcome. The same was done in the current study. For these analyses, I chose to use Spearman's rank correlation, rather than Pearson's correlation. Pearson's correlation assumes that the 2 variables are 2 continuous variables, whereas Spearman's correlation can also be used with variables that are ordinal and are part of a scale (Field, 2014). The severity of ASD symptoms in the ADI-R and ADOS-2 are rated on scales, making Spearman's correlations more appropriate for these analyses than Pearson's correlations. Moreover, Spearman's correlation does not

assume normality and is less sensitive to outliers (Field, 2014; Rousselet & Pernet, 2012). Finally, Spearman's correlations were also used in the previous study.

Social communication and restricted and repetitive behaviours domains: Correlations were calculated between global dbWPLI across all connections and 4 measures of ASD symptoms severity at the 36-month-old visit separately: a) the ADI-R, Social and Communication Algorithm Total (sum of the scores on the Social Total and Communication Total), b) the ADI-R, Behaviours/Repetitive Interests Algorithm Total (Restricted and Repetitive Behaviours scale), c) the ADOS-2, Social Affect Total, and d) the ADOS-2 Restrictive and Repetitive Behaviors Total. Another series of correlational analyses were performed with global dbWPLI across selected connections from the previous study and the 4 measures of ASD symptom severity. Analyses were first performed for the group of HR infants (HR-TD, HR-Atyp, and HR-ASD combined), and then for HR-ASD infants as was done in the previous study. In order to give a bigger perspective on the data, separate analyses in the HR-TD and HR-Atyp groups were done as well.

A False Discovery Rate correction (FDR) was finally applied to the results within the groups for which there was no a priori hypothesis (HR-TD and HR-Atyp groups). The FDR method has been shown to a less conservative method to control for multiple comparisons than the Bonferroni method. Furthermore, correlation values below .30 were considered as small, above .50 as large, and between .30 and .50 as medium effects. 95% confidence intervals (CIs) based on bias corrected and accelerated bootstrap analyses with 1000 samples are reported also (J. Cohen, 1988; Field, 2014).

4.3. Results

4.3.1. Participants

The final sample of participants consisted of 101 infants: 20 low risk (LR) infants, 47 infants with a high risk who were typically developing at 3 years of age (HR-TD infants), 21 infants with a high risk who were atypically developing at 3 years of age (HR-Atyp infants), and 13 infants with a high risk who were diagnosed with ASD at 3 years of age (HR-ASD infants). The demographics and clinical scores for the final current sample are displayed in table 4.1.

The HR-ASD group contained more males than females. This ratio was similar in the HR-Atyp group (p = .249), but different in the HR-TD group (p = .015), whereas the differences in ratios between the LR and HR-ASD group reached a trend (p = .078). MSEL scores at both 14 and 36 months were higher for the LR and HR-TD groups than the HR-ASD group (p's ≤ .004), whereas the HR-Atyp and HR-ASD groups showed no significant difference (p's ≥ .270). No differences were observed between the HR-ASD and comparison groups in age at EEG or diagnostic assessment (p's ≥ .158).

As for the clinical data, HR-ASD infants displayed higher scores on ADI-R scales when compared to the LR, HR-TD, and HR-Atyp group. This was the case for each of the scales: Social Total, Communication Total, and Behaviours / Repetitive Interests (p's < .001). The HR-ASD group also displayed higher scores on the ADOS Social Affect scale when compared to the HR-TD group (p = .001), whereas the difference with the LR group reached a trend (p = .095), and the difference with the HR-Atyp group did not reach significance (p = .542). Lastly, the HR-ASD group displayed higher scores on the ADOS Restricted and Repetitive Behaviours scale

when compared to the LR and HR-TD groups (*p*'s ≤ .031). There were no significant differences on this scale between the HR-ASD and HR-Atyp groups.

Table 4.1. **Demographics of the current sample**

	LR	*HR-TD*	*HR-Atyp*	*HR-ASD*
Number of participants (male)	20 (11) $\chi^2(1)$ = 3.11, p =.078 [1]	47 (22) $\chi^2(1)$ = 5.88, p =.015	21 (14) $\chi^2(1)$ = 1.33, p =.249	13 (11)
Age at EEG assessment, in days	473 (49)[2] *U* = 91.5, *p* =.158 [4]	470 (41) *U* = 234.5, *p* =.203 [5]	465 (46) *U* = 113, *p* =.420 [4]	446 (57)
Age at diagnostic assessment, in months	38.0 (1.0)[2] *U* = 106, *p* =.950 [4]	39.0(1.3) *U* = 230.5, *p* =.369 [5]	38.0 (2.0) *U* = 118.5, *p* =.782 [4]	38.5 (1.0)
MSEL [a] Composite Standard Score at visit at 14 months	102 (14)[3] 81 – 133[6] *t*(31) = 3.10, *p* =.004	98 (12) 71 – 121 *t*(58) = 2.96, *p* =.004	93 (16) 67 – 123 *t*(32) = 1.12, *p* =.270	87 (13) 65 – 113
MSEL [a] Composite Standard Score at visit at 36 months [7]	123 (15)[2] 69 – 137[6] *U* = 37, *p* =.002 [4]	115 (20) 79 – 142 *U* = 103.5, *p* =.001 [5]	83 (26) 54 – 145 *U* = 107, *p* =.494 [4]	78 (40) 49 – 142
ADI-R Social Total [b,7]	1 (2) [2] 0 – 6 [f] *U* = 6, *p* <.001 [4]	1 (2) 0 – 11 *U* = 16.5, *p* <.001 [5]	2 (3) 0 – 10 *U* = 13, *p* <.001 [4]	13 (5) 2 – 25
ADI-R, Communication Total [c, 7]	0 (1) [2] 0 – 4 *U* = 0.5, *p* <.001 [4]	1 (3) 0 – 11 *U* = 17, *p* <.001 [5]	3 (6) 0 – 14 *U* = 25, *p* <.001 [4]	12 (5) 4 – 19

ADI-R	0 (0) [2]	0 (1)	1 (2)	6 (4)
BRI Total [d, 7]	0 – 1 [f]	0 – 3	0 – 9	0 – 10
	U = 10,	*U* = 35.5,	*U* = 32,	
	p < .001 [4]	*p* <.001 [5]	*p* <.001 [4]	
ADOS-2,	2.5 (5) [2]	1 (1)	6 (7)	5 (6)
SA Total [e, 7]	0 – 9 [f]	0 – 5	0 – 13	1 – 12
	U = 68,	*U* = 111.5,	*U* = 109,	
	p = .095 [4]	*p* =.001 [5]	*p* =.542 [4]	
ADOS-2	1 (1) [2]	1(1)	2 (2)	1 (3)
RRB Total [f, 7]	0 – 3 [f]	0 – 3	0 – 6	1 – 6
	U = 57,	*U* = 141,	*U* = 124.5,	
	p = .031 [4]	*p* = .006 [5]	*p* = .956 [4]	

[1] Pearson Chi-Square with asymptotic significance values (2-sided).

[2] Medians and interquartile range in parentheses, with results for the Mann-Whitney U-test when compared with the HR-ASD group.

[3] Means and standard deviations in parentheses, with results for the t-test for independent samples when compared with the HR-ASD group.

[4] Exact 2-tailed.

[5] Asymptotic 2-tailed.

[6] Range with minimum and maximum score.

[7] Data for the 36-month-old visit was only available for 18 LR infants, 46 HR-TD infants, 21 HR-Atyp infants, and 12 HR-ASD infants.

[a] Mullen Scale for Early Learning (MSEL).

[b] Autism Diagnostic Interview – Revised, Social Algorithm Total at 36 months.

[c] Autism Diagnostic Interview – Revised, Communication Algorithm Total at 36 months.

[d] Autism Diagnostic Interview – Revised, Behaviours/ Repetitive Interests Algorithm Total 36 months.

[e] Autism Diagnostic Observation Scale – 2, Social Affect Total 36 months.

[f] Autism Diagnostic Observation Scale – 2, Restricted and Repetitive Behaviours Total 36 months.

4.3.2. Selection of the alpha frequency band

Visual inspection of the spectral power across the each group from 0 to 30 Hz confirmed the peak for 7 to 8 Hz, similar to the original study (Orekhova et al., 2014) (see Fig. 4.4A). Power spectra from individual infants showed considerable variation, with some infants showing a clear alpha peak, whereas others showed no distinct alpha peak (5/20 LR, 10/47 HR-TD, 4/21 HR-Atyp, and 2/13 HR-ASD infants). However, the aim of this chapter was to investigate alpha band connectivity in groups with different outcomes, rather than individual alpha peaks, and to replicate previous results by applying identical methods to the data. The alpha frequency band in this dataset that would be used in further spectral power and connectivity analyses was therefore defined as 7 to 8 Hz.

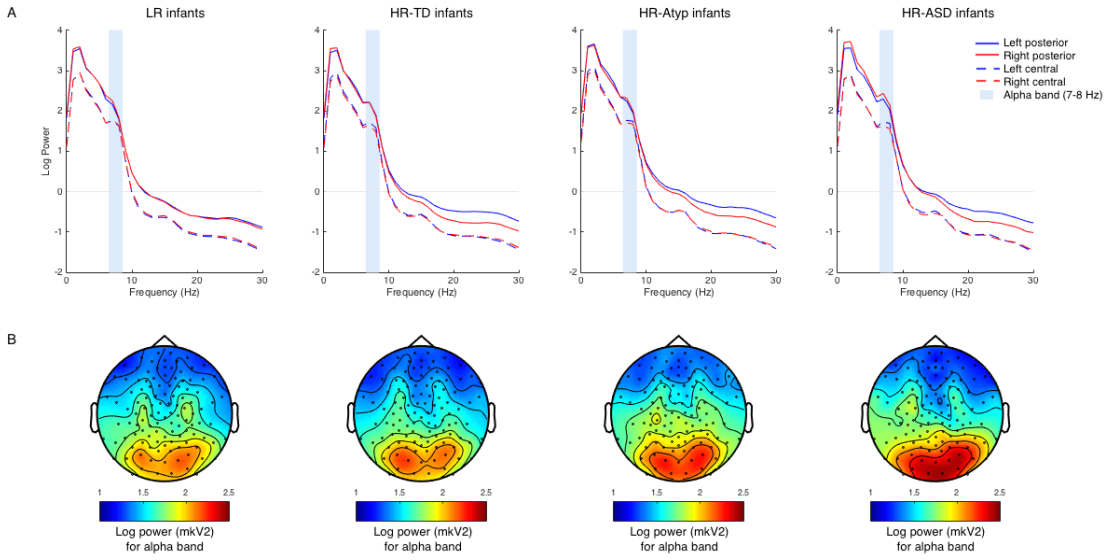

Figure 4.4. Spectral power for each group across all conditions

A) Spectral log power averaged across left posterior (solid blue line), right posterior (solid red line), left central (dashed blue line), and right central (dashed red line) electrodes for 0 to 30 Hz for each group. The alpha band (7-8 Hz) is highlighted in cyan. B) Topoplots for spectral log power for the 7-8 Hz alpha band for each group.

4.3.2. Alpha connectivity and categorical outcome

Graphs for connectivity values across each group for 0 to 30 Hz (Fig. 4.5) showed a clear peak for 7-8 Hz in accordance with the graphs for spectral power. This demonstrates the high signal to noise ratio for this frequency band, and further shows that the data cleaning was successful.

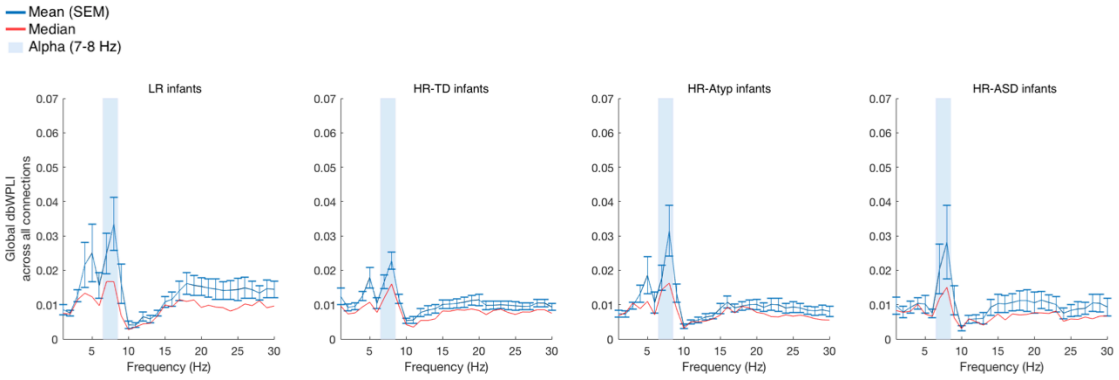

Figure 4.5. Connectivity spectra for each group across all conditions

Mean (standard error of the mean, in blue) and median (red) global dbWPLI averaged across all electrodes for each group for 0 to 30 Hz. The alpha band (7-8 Hz) is marked in light blue.

4.3.3.1. Network analyses

Next, I tested whether there were any increased connections in the HR-ASD infants when compared with the other groups with the NBS program. No significant increases in the networks in the alpha range were found for HR-ASD versus LR infants, HR-ASD versus HR-TD infants, or HR-ASD versus HR-Atyp infants (see Figure 4.6A). The analyses were repeated with the selected connections that had been identified as increased in the HR-ASD group in the previous study (Orekhova et al., 2014) (see Figure 4.6B). These revealed a similar pattern: there were no increased connections for the HR-ASD group compared to the other groups among the fronto-central connections identified previously.

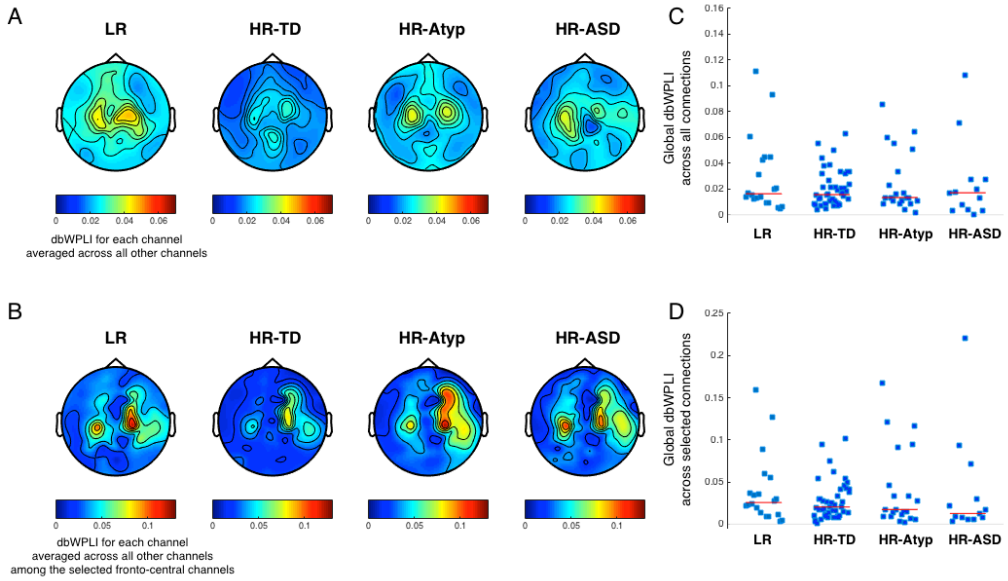

Figure 4.6. Topoplots and global alpha connectivity for each group

A) Topoplots for global dbWPLI for the alpha frequency range for each group. B) Topoplots for dbWPLI across selected fronto-central channels based on the previous study for each group. C) Individual global dbWPLI values across all connections. Red bars reflect medians for each group. D) Individual global dbWPLI values across fronto-central connections with median values for each group (red bars).

4.3.3.2. Global connectivity analyses

Second, analyses on the global dbWPLI values were performed with SPSS. A Mann-Whitney U-test was used to test whether there were any differences between the HR-ASD group and the comparison groups, as the assumptions for normality (p's ≤ .001) and homogeneity of variance were not met (p = .007). The comparisons between the HR-ASD groups and the other groups yielded no significant differences between the groups: LR vs. HR-ASD: U = 104, z = -0.958, exact 2-tailed p = .353, r = -.17; HR-TD vs. HR-ASD: U = 275, z = -0.547, asymptotic 2-tailed p = .580, r = -.07; HR-Atyp vs. HR-ASD: U = 125, z = -0.408, exact 2-tailed p = .701, r = -

.07; Mdn_{LR} = 0.0162, IQR_{LR} = 0.03; $Mdn_{HR\text{-}TD}$ = 0.0156, $IQR_{HR\text{-}TD}$ = 0.02; $Mdn_{HR\text{-}Atyp}$ = 0.0133, $IQR_{HR\text{-}Atyp}$ = 0.03; and $Mdn_{HR\text{-}ASD}$ = 0.0170, $IQR_{HR\text{-}ASD}$ = 0.02 (see Figure 4.6C).

The same analyses were repeated for the alpha connectivity for the selected fronto-central connections found in the previous study (Fig. 4.3). Again, the assumptions for normality (p's < 0.001) and equal variances among groups were not met (p = 0.003). No differences were found in global connectivity for selected connections between the HR-ASD and comparison groups: LR vs. HR-ASD: U = 97, z = -1.216, exact 2-tailed p = .235, r = -.21; HR-TD vs. HR-ASD: U = 254, z = 0.924, asymptotic 2-tailed p = .355, r = -.12; HR-Atyp vs. HR-ASD: U = 115, z = -0.762, exact 2-tailed p = .462, r = -.13; Mdn_{LR} = 0.0257, IQR_{LR} = 0.04; $Mdn_{HR\text{-}TD}$ = 0.0203, $IQR_{HR\text{-}TD}$ = 0.03; $Mdn_{HR\text{-}Atyp}$ = 0.0173, $IQR_{HR\text{-}Atyp}$ = 0.06; and $Mdn_{HR\text{-}ASD}$ = 0.0126, $IQR_{HR\text{-}ASD}$ = 0.04 (see Figure 4.6D).

In brief, both global connectivity and network based connectivity analyses revealed no differences between the HR-ASD and LR, HR-TD, or HR-Atyp group.

4.3.2. Potential confounding factors for connectivity analyses

The findings described in the previous section may be influenced by the number of epochs included, spectral power, gender, age, or cognitive skills. If any of these variables revealed differences between groups, these would be included in additional General Linear Model analyses to test for an effect of group on global alpha connectivity while taking into account the potentially confounding variable. The GLM without taking into account additional variables revealed no effect for Group, $F(3,97) = 0.91$, p = .438, η_p^2 = .027.

4.3.2.1. Methodological factors

The analyses focusing on behaviours during the EEG recording revealed no differences between the HR-ASD and comparison groups in percentage of looking

or interference (*p*'s ≥ .128, see Appendix A4.7). There were differences between groups for the amount of epochs included from the social condition: fewer epochs from the social condition were included in the combined dataset for the HR-ASD group than for the HR-Atyp group (p = .042, see Table 4.2). There were no differences between numbers of social epochs for the LR and HR-ASD groups (p = .128), whereas the difference between the HR-TD and HR-ASD group reached a trend (p = .097).

To further investigate this, I calculated the proportion of social trials in the combined dataset. The proportion of social trials in the combined dataset was significantly smaller for the HR-ASD group than for the other groups (LR vs. HR-ASD: U = 56, z = -2.69, exact 2-tailed p = .006; HR-TD vs. HR-ASD: U = 177, z = -2.306, asymptotic 2-tailed p = .021; HR-Atyp vs. HR-ASD: U = 70, z = -2.357, exact 2-tailed p = .018; Mdn_{LR} = 38, IQR_{LR} = 18; $Mdn_{\text{HR-TD}}$ = 35, $IQR_{\text{HR-TD}}$ = 12; $Mdn_{\text{HR-Atyp}}$ = 36, $IQR_{\text{HR-Atyp}}$ = 10; and $Mdn_{\text{HR-ASD}}$ = 30, $IQR_{\text{HR-ASD}}$ = 29). This implies that the comparison groups were more attentive and showed less interference during the social condition than the HR-ASD group. This effect seems specific to the social condition, since there were no differences between the HR-ASD and comparisons groups in epochs across all conditions.

No differences between the HR-ASD and comparison groups were observed for the amount of epochs included from the hand or toy condition, total amount of epochs from the combined dataset, or proportion of overlapping epochs (*p*'s ≥ .128). Together these findings suggest that there were no differences between the HR-ASD and other groups in looking or interference during the EEG session, or in the amount of epochs across conditions. However, the proportion of social epochs in the combined set across conditions was smaller in the HR-ASD group than the

other groups and might thus be a confounding factor. The proportion of social epochs will therefore be included as covariate in the third set of analyses.

Table 4.2. **Amount of epochs in the current sample**

	LR	*HR-TD*	*HR-Atyp*	*HR-ASD*
Number of trials for combined dataset [b]	311 (114) $t(31) = -0.378$, $p = .708$	351 (125) $t(58) = 0.560$, $p = .578$	351 (113) $t(32) =$ 0.496, $p = .623$	329 (147)
Number of trials from toy condition [a]	65 (109) $U = 88.0$, $p = .128$ [c]	85 (95) $U = 245.5$, $p = .282$ [d]	94 (61) $U = 106.0$, $p = .292$ [c]	124 (72)
Number of trials from hand condition [b]	112 (44) $t (31) = -0.011$ $p = .991$	128 (46) $t (58) = 1.021$, $p = .312$	124 (45) $t (32) =$ 0.642, $p = .526$	112 (64)
Number of trials from social condition [a]	125 (40) $U = 88.5$, $p = .128$ [c]	124(64) $U = 213.0$, $p = .097$ [d]	141 (41) $U = 79.5$, $p = .042$ [c]	98 (73)
Proportion of trials from the social condition in the combined dataset (%)[a]	38 (18) $U = 57$, $p = .006$ [c]	35 (12) $U = 177$, $p = .021$ [d]	36 (10) $U = 70$, $p = .018$ [c]	30(29)
Proportion of trials with 2 other overlapping trials in the combined dataset (%)	78 (10) $U = 107$, $p = .413$ [c]	78 (13) $U = 290$, $p = .781$ [d]	76 (9) $U = 129$, $p = .807$ [c]	75(16)

[a] Medians and interquartile range in parentheses, with results for the Mann-Whitney U-test when compared with the HR-ASD group.

[b] Means and standard deviations in parentheses, with results for the t-test for independent samples when compared with the HR-ASD group.

[c] Exact 2-tailed.

[d] Asymptotic 2-tailed.

Note: Only the distributions for Number of trials from the toy condition in the LR group, Number of trials in the social condition in the HR-Atyp group, Proportion of social trials in the combined dataset for the HR-TD and HR-ASD groups, and Proportion of overlapping trials for the HR-TD and HR-Atyp group were non-Gaussian (p's ≤ .046). Variances were equal across groups for each of the six dependent variables displayed in this table (p's ≥ .060).

The GLM including Group as between-subject factor and the proportion of social epochs in the combined dataset as covariate revealed no significant effect of Group, p = .262, η_p^2 = .041. Further analyses suggest the assumption for homogeneity across slopes were met, since the interaction between Group and Proportion of Social trials did not reach significance, p = .206, η_p^2 = .048. Taking into account proportion of social epochs did thus not significantly change the primary result of Group.

In addition to the amount of data, spectral power may also influence connectivity results. However, no differences were found between the LR and HR-ASD group, HR-TD and HR-ASD group, or HR-Atyp and HR-ASD group for alpha band spectral power averaged across all channels, posterior or central channels, or left or right posterior or central channels (p's ≥ .254, see Appendix A4.8). Together these data suggest that spectral power and the proportion of social epochs did not influence the current alpha connectivity findings.

4.3.2.2. Demographic factors

Gender, age, or developmental levels are other potentially confounding factors that may have influenced the alpha connectivity group results.

Gender: The analyses on demographics in section 4.3.1 revealed differences between the HR-ASD and other groups in gender, where the HR-ASD group contained more males than females. Gender might thus be one confounding factor that could influence the connectivity results. Global alpha connectivity however did not differ between males and females, $U = 1068$, $z = -1.229$, asymptotic 2-tailed $p = .219$, $r = -.12$ ($Mdn_{Males} = 0.0163$, $IQR_{Males} = 0.02$, and $Mdn_{Females} = 0.0142$, $IQR_{Females} = 0.02$, see also Appendix A4.9 for figure). Results of the GLM including Gender as factor showed no significant effect for Group, $p = .512$, $\eta_p^2 = .024$, as was found in the initial GLM including Group only.

Age at EEG assessment: Although there were no group differences in age at EEG assessment, there might be differences between groups in associations between connectivity and age. Age showed a Gaussian distribution for the LR group only, not for the whole sample, HR-TD, HR-Atyp, or HR-ASD group (p's ≤ .049). In the HR-TD group, functional connectivity decreased with increasing age (Spearman's *rho* = -.33, $p = .023$). The opposite correlation was found in the HR-Atyp group where functional connectivity increased with age (Spearman's *rho* = .52, $p = .015$; even after removal of the HR-Atyp infant with an age of 578 days at the age of assessment, the correlation remained significant, Spearman's *rho* = .45, $p = .047$) (see Fig. 4.7A). Global dbWPLI was not related to age in the whole sample (Spearman's *rho* = -.04, $p = .69$), the LR group (Pearson's *rho* = .02, $p = .92$), or the HR-ASD group (Spearman's *rho* = -.47, $p = .109$).

The GLM including age as covariate revealed no significant effect of group after controlling for age, $F(3,96) = 0.89$, $p = .449$, $\eta_p^2 = .027$. Further analyses however did show a significant interaction effect between Age and Group, $F(3,93) = 3.68$, $p = .012$, $\eta_p^2 = .111$. The slopes between global dbWPLI and age are

different between groups, matching the results from the correlational analyses. This suggests that the current group connectivity findings have not been confounded by age at the 14-month-old visit, but caution is warranted, since the data do not meet the assumption of homogeneity across slopes.

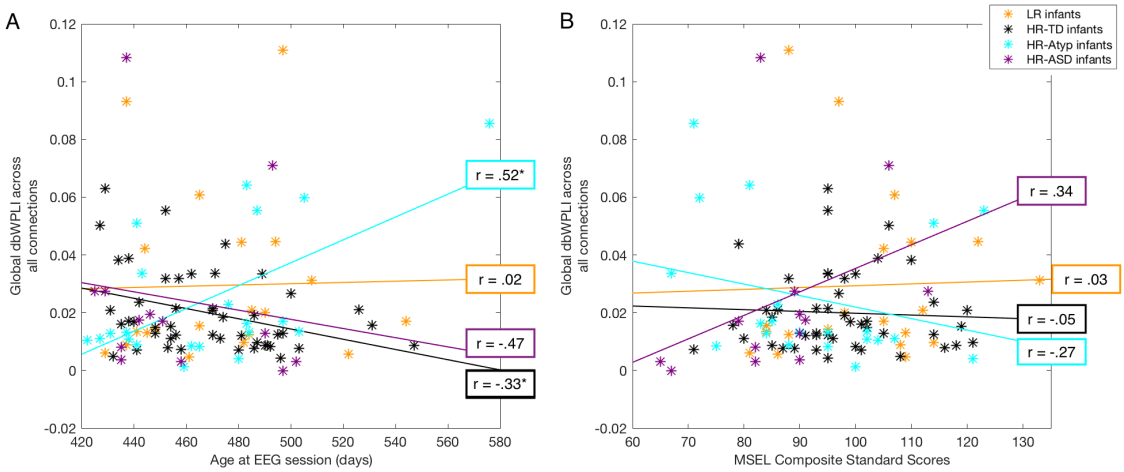

Figure 4.7. Global alpha connectivity with age and MSEL scores at the EEG session Scatterplot for global connectivity across all connections with age (in days) (A) and with MSEL Composite Standard Scores (B) at the time of the EEG assessment. Each asterisk represents an infant; different colours represent different outcome groups. Lines with r values represent Spearman's rho in each group, which are marked by * if p < .05.

Cognitive levels at 14-month-old visit: The analyses on demographics further showed that the HR-Atyp and HR-ASD groups had similar scores on the MSEL at the 14-month-old visit, whereas the LR and HR-TD group both had higher scores than the HR-ASD group. The composite standard Scores for the MSEL at the 14-month-old visit showed a normal distribution for each of the 4 groups (p's ≥ .282). None of the correlations between global alpha connectivity and MSEL scores in the separate groups reached significance (p's ≥ .241, Fig. 4.7B). The GLM analysis showed no significant effect of Group after controlling for the MSEL scores at 14 months, $F(3,96) = 0.91$, $p = .440$, $\eta_p^2 = .028$. The interaction term between MSEL

scores and group did not reach significance either, $F(3,96) = 1.48$, $p = .220$, $\eta_p^2 = .046$, confirming that the assumption for homogeneity of slopes have been met. The MSEL scores did thus not influence the current group connectivity findings either.

In summary, the alpha connectivity analyses examining categorical ASD outcome revealed no differences between the HR-ASD group and the LR, HR-TD, or HR-Atyp group. These results were similar for network based, and global connectivity based analyses. Additional analyses taking into account possible confounding factors did not change the initial results.

4.3.4. Alpha connectivity and dimensional traits

4.3.4.1. Social communication and restricted and repetitive behaviours domains

The previous study by Orekhova and colleagues found correlations between global connectivity across all connections and the ADI-R Restricted and Repetitive Behaviours domain scores, and the ADI-R Social and Communication domain scores composite in the whole HR group (HR-TD, HR-Atyp, and HR-ASD groups collapsed). No correlations were observed with the ADOS domains. Furthermore, in the HR-ASD group, a significant association was found between global connectivity across selected connections and ADI-R Restricted and Repetitive Behaviours. These selected connections showed higher connectivity in the HR-ASD group compared to both the LR and HR-no ASD group. No correlations were found with the ADI-R Social and Communication composite score, or the ADOS domains. The HR-no ASD group displayed no significant correlations.

I attempted to replicate these findings in the current cohort by first focusing on the whole HR group, and then the HR-ASD group only. Spearman's correlations were used to test whether there were any correlations between functional

connectivity and ASD symptom severity at 36 months of age in the complete HR sample and the HR-ASD sample. Finally, correlations were also analysed in the HR-TD and HR-Atyp groups separately as to provide a broader perspective on the dataset. Both ADI-R and ADOS-2 data were missing for 1 HR-TD and 1 HR-ASD infant. The final sample for the brain behaviour correlations consisted of 46 HR-TD infants, 21 HR-Atyp infants, and 12 HR-ASD infants. Further, the selected connections found in the previous study were used for analyses using selected connections for 2 reasons: a) the current findings did not reveal a significant network that can be used as mask for selected connections, and b) replicating previous findings using the connections of the previous study would strengthen the previous finding as correlations with the same selected connections would be replicated in an independent cohort. In the original study, the selected connections were obtained from the group comparisons based on the ADI-R scores. It is possible that the associations between the connectivity in these selected connections and the behaviours measured by the ADI-R have been induced by this procedure. By using the connections from the original study, we can investigate whether associations have been induced.

For the complete sample, there were no significant correlations between global connectivity across all connections and ADI-R Social and Communication composite score (see Figure 4.8A), or ADI-R Restricted and Repetitive Behaviours (see Figure 4.8B and Table 4.3). Associations between global connectivity across all connections and the ADOS-2 Restricted and Repetitive Behaviours total, and the ADOS-2 Social Affect total did not reach significance either (p's ≥ .254). No significant correlations were found between global connectivity among selected connections and the measures of ASD symptom severity (p's ≥ .259).

For the HR-ASD group, a trend correlation was found between global connectivity and the ADI-R Behaviours/ Repetitive Interests total (r = .52, p = .086). The correlation between global connectivity and the other symptom severity scales were not significant (p's ≥ .776). Turning to the global connectivity among selected connections, the correlation between connectivity and ADI-R Behaviours/ Repetitive Interests total was significant (r = .60, p = .037, see Figure 4.8C). The correlations between connectivity and the other symptom severity scales were not significant (p's ≥ .752) (Table 4.3).

(Next page)

Figure 4.8. Global alpha connectivity and ASD symptom severity

Scatterplots for global dbWPLI across all connections with ADI-R Social and Communication composite scores (A), and with ADI-R Restricted and Repetitive Behaviours (RRB) scores (B), and for global connectivity across selected fronto-central connections and ADI-R Restricted and Repetitive Behaviours in the HR-ASD group (C). Each asterisk represents one infant: black for HR-TD infants, cyan for HR-Atyp infants, and purple for HR-ASD infants. Black dotted lines represent correlations across all HR infants that are not reaching significance. Purple line represents the correlation reaching significance in the HR-ASD group. Spearman's rho values are reflected by *r*, with significant values flagged by *.

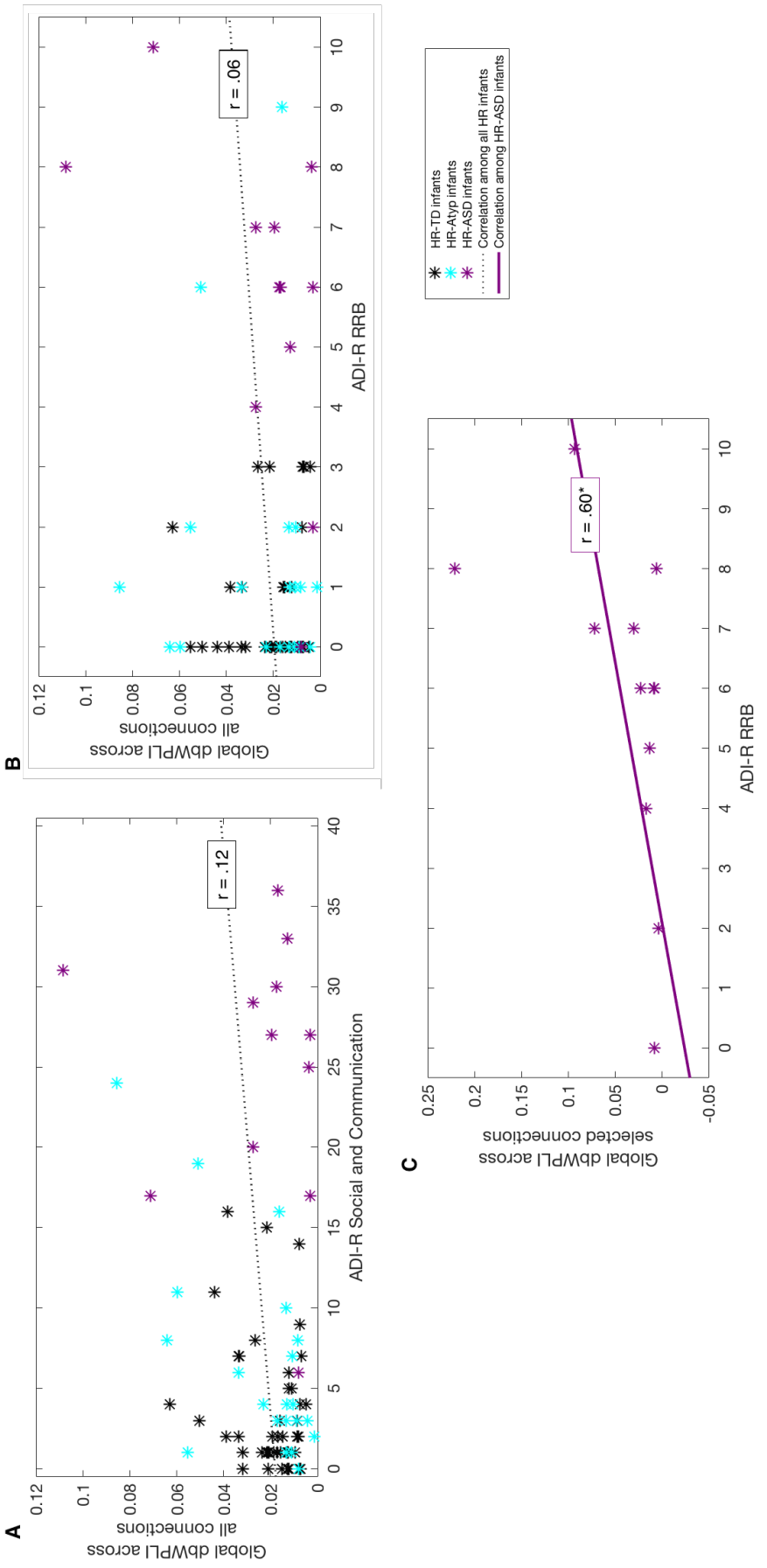
A
Global dbWPLI across all connections
ADI-R Social and Communication
r = .12
B
Global dbWPLI across all connections
ADI-R RRB
r = .06
C
Global dbWPLI across selected connections
ADI-R RRB
r = .60*
HR-TD infants
HR-Atyp infants
HR-ASD infants
Correlation among all HR infants
Correlation among HR-ASD infants

Table 4.3. **Associations between alpha connectivity and dimensional traits in the whole HR group and HR-ASD group**

	Global dbWPLI across all connections	*Global dbWPLI across selected connections*
HR group (N = 79)		
ADI-R Social and Communication [a]	r = .12[+], p = .300, [-.10, .31]	r = .03, p = .788, [-.19, .25]
ADI-R RRB [b]	r = .06[+], p = .584, [-.17, .32]	r = -.02, p = .890, [-.25, .23]
ADOS SA [c]	r = -.07, p = .584, [-.30, .17]	r = -.05, p = .664, [-.28, .20]
ADOS RRB [d]	r = .13, p = .254, [-.09, .34]	r = .13, p = .259, [-.09, .34]
HR-ASD group (N = 12)		
ADI-R Social and Communication [a]	r = .20, p = .526, [-.60, .80]	r = .39, p = .211, [-.38, .89]
ADI-R RRB [b]	r = .52, p = .086, [-.24, .95]	**r = .60[+], p = .037, [-.14, .96]**
ADOS SA [c]	r = -.09, p = .776, [-.71, .59]	r = -.01, p = .983, [-.70, .77]
ADOS RRB [d]	r = -.06, p = .847, [-.70, .72]	r = .08, p = .797, [-.68, .79]

Spearman's rho values are represented by r. P-values are 2-tailed. The correlation reaching significance at 0.05 significance level is printed in bold.

[a] Autism Diagnostic Interview – Revised, sum of the Social Algorithm Total and Communication Algorithm Total at 36 months.

[b] Autism Diagnostic Interview – Revised, Behaviours/ Repetitive Interests Algorithm Total 36 months.

[c] Autism Diagnostic Observation Scale – 2, Social Affect Total 36 months.

[d] Autism Diagnostic Observation Scale – 2, Restrictive and Repetitive Behaviours Total 36 months.

[+] Correlations expected to reach significance based on the previous study.

Table 4.4. **Associations between alpha connectivity and dimensional traits in the HR-TD group, and HR-Atyp group**

	Global dbWPLI across all connections	*Global dbWPLI across selected connections*
HR-TD group (N = 46)		
ADI-R Social and Communication [a]	*r* = .01, *p* = .926, [-.28, .32]	*r* = .11, *p* = .460, [-.36, .16]
ADI-R RRB [b]	*r* = -.04, *p* = .806, [-.38, .31]	*r* = -.13, *p* = .407, [-.44, .19]
ADOS SA [c]	*r* = .02, *p* = .872, [-.28, .31]	*r* = .10, *p* = .525, [-.20, .37]
ADOS RRB [d]	*r* = .20, *p* = .173, [-.14, .48]	*r* = .24, *p* = .105, [-.11, .52]
HR-Atyp group (N = 21)		
ADI-R Social and Communication [a]	*r* = .51, *p* = .019, [.00, .82]	*r* = .52, *p* = .019, [.11, .81]
ADI-R RRB [b]	*r* = .13, *p* = .580, [-.32, .52]	*r* = .10, *p* = .680, [-.33, .51]
ADOS SA [c]	*r* = -.17, *p* = .453, [-.56, .31]	*r* = -.22, *p* = .348, [-.61, .31]
ADOS RRB [d]	*r* = .01, *p* = .966, [-.38, .40]	*r* = -.01, *p* = .957, [-.41, .35]

Spearman's rho values are represented by r. P-values are 2-tailed.

[a] Autism Diagnostic Interview – Revised, sum of the Social Algorithm Total and Communication Algorithm Total at 36 months.

[b] Autism Diagnostic Interview – Revised, Behaviours/ Repetitive Interests Algorithm Total 36 months.

[c] Autism Diagnostic Observation Scale – 2, Social Affect Total 36 months.

[d] Autism Diagnostic Observation Scale – 2, Restrictive and Repetitive Behaviours Total 36 months.

After investigating the correlations between functional connectivity and symptom severity in the complete HR sample and HR-ASD group separately, the next question is whether there were any other significant correlations within the HR-TD and HR-Atyp groups (Table 4.4). Only 2 significant correlations were found, both in the HR-Atyp group: the correlation between global connectivity and ADI-R Social and Communication composite (Spearman's *rho* = .51, *p* = .019), and between global connectivity among selected connections and ADI-R Social and Communication composite (Spearman's *rho* = .52, *p* = .019). However, these correlations did not survive after the FDR correction.

In short, the current findings did not replicate the original findings of trend associations between connectivity across all connections and ADI-R Social and Communication scores, or Restricted and Repetitive Behaviour scores in the whole HR group. I did replicate the previous association between connectivity across selected connections and Restricted and Repetitive Behaviour scores from the ADI-R. Both here and in the original study, associations with the ADOS-2 domain scores did not reach significance.

4.3.4.2. Exploratory analyses: Subtypes of restricted and repetitive behaviours

The results in the previous sections show that higher alpha connectivity in the selected connections was related to more severe restricted and repetitive behaviours at later age. The Restricted and Repetitive Behaviours domain consists of different behaviours that can be further divided into three subtypes: repetitive motor behaviours, insistence on sameness, and circumscribed interests (Lam, Bodfish, & Piven, 2008; Langen, Durston, Kas, van Engeland, & Staal, 2011). In further exploratory analyses I therefore investigated whether the replicated

association between alpha connectivity and restricted and repetitive behaviours might be driven by a strong association with a subtype of these behaviours.

Specifically, I tested for associations between alpha connectivity and repetitive motor behaviours, insistence on sameness, or circumscribed interests. These subtypes of behaviours were measured with the ADI-R by summing up unconverted raw ever and current scores of specific items of the ADI-R related to the subtypes of restricted and repetitive behaviours (see Appendix A4.10 for more details and a summary of scores). With the data from the previous study available, I collapsed the data from the current and previous cohort (BASIS Phase 1 and Phase 2) into one combined cohort. (The protocol for the BASIS Phase 1 cohort has been approved by the UK National Health Service National Research Ethics Service London code 08/H0718/76; 06/MRE02/73 (see (Orekhova et al., 2014)). Informed consent was taken from the parents/ caregivers before the start of the study.) This increases the statistical power for the analyses, in particular for analyses in the HR-ASD group ($N_{Current\ cohort}$ = 12, and $N_{Combined\ cohorts}$ = 21, see Appendix A4.11 for results in separate cohorts). Spearman's correlations were performed separately for both ever and current scores, with global dbWPLI across all connections, and global dbWPLI across selected fronto-central connections found in the previous study. Analyses were performed in the overall HR group, HR-no ASD group (HR-TD and HR-Atyp infants), and the HR-ASD group separately, and FDR corrections were applied to each group separately.

When based on ever scores, higher alpha connectivity across all connections was related to more severe circumscribed interests in the overall HR group, r = .26, p = .015 (see Table 4.5 and Appendix A4.12 for figures). The association between alpha connectivity across selected fronto-central connections

and circumscribed interests also reached significance in the HR group, r = .30, p = .004. Correlations with the repetitive motor behaviours, or insistence on sameness in this group did not reach significance. None of the investigated associations continued to reach significance after FDR correction in the HR-no ASD or HR-ASD group, although the association between connectivity and circumscribed interests in the HR-ASD group displayed medium effect sizes. When based on current scores, the association between connectivity across selected fronto-central connections and the severity of circumscribed interests reached significance in the overall HR group, r = .29, p = .005. No other correlations reaching significance were observed. However, medium effect sizes were again observed for the association between global connectivity and circumscribed interests in the HR-ASD group.

Table 4.5. **Associations between functional connectivity and subtypes of RRBs in the combined sample**

Ever scores	*Subtype*	*N*	*Global dbWPLI across all connections*	*Global dbWPLI across selected connections*
All HR infants	RMB	103	r = .15, p = .126, [-.06, .34]	r = .15, p = .126, [-.08, .35]
	IS	102	r = .14, p = .153, [-.06, .33]	r = .07, p = .500, [-.16, .27]
	CI	90	**r = .26, p = .015, [.04, .45]**	**r = .30, p = .004, [.10, .48]**
HR-no ASD	RMB	82	r = .01, p = .948, [-.18, .20]	r = .01, p = .946, [-.21, .23]
	IS	81	r = -.06, p = .574, [-.29, .16]	r = -.18, p = .103, [-.38, .03]
	CI	69	r = .05, p = .686, [-.21, .32]	r = .07, p = .558, [-.18, .32]
HR-ASD	RMB	21	r = .12, p = .605, [-.47, .67]	r = .06, p = .797, [-.57, .60]

	IS	21	r = .12, p = .617, [-.40, .60]	r = .10, p = .677, [-.40, .56]
	CI	21	r = .35, p = .116, [-.12, .74]	r = .38, p = .086, [-.13, .79]

Current scores	*Subtype*	*N*	*Global dbWPLI across all connections*	*Global dbWPLI across selected connections*
All HR infants	RMB	103	r = .16, p = .105, [-.05, .36]	r = .17, p = .087, [-.04, .37]
	IS	103	r = .13, p = .180, [-.08, .34]	r = .05, p = .607, [-.16, .26]
	CI	92	r = .24, p = .021, [.01, .44]	**r = .29, p = .005, [.06, .50]**
HR-no ASD	RMB	82	r = .06, p = .602, [-.12, .24]	r = .09, p = .440, [-.12, .30]
	IS	82	r = -.03, p = .776, [-.27, .18]	r = -.16, p = .148, [-.39, .04]
	CI	71	r = -.03, p = .821, [-.28, .24]	r = .03, p = .809, [-.22, .27]
HR-ASD	RMB	21	r = .15, p = .531, [-.41, .68]	r = .07, p = .764, [-.52, .61]
	IS	21	r = .03, p = .883, [-.45, .55]	r = .001, p = .995, [-.48, .50]
	CI	21	r = .37, p = .095, [-.13, .74]	r = .37, p = .097, [-.18, .77]

Spearman's rho values are represented by r. P-values are 2-tailed. Correlations reaching significance and surviving FDR correction for the 6 comparisons made within each group are printed in bold.

Abbreviations used: Number of infants (N); Autism Diagnostic Interview – Revised, Restricted and Repetitive Behaviours Scale (ADI-R, RRB); repetitive motor behaviours (RMB); insistence on sameness (IS); and circumscribed interests (CI).

Spearman's rho values are represented by *r*. P-values are 2-tailed.

All together, these findings suggest that the observed association between alpha connectivity and the restricted and repetitive behaviours domain is driven by an association between alpha connectivity and circumscribed interests. These associations are overall stronger for the ever scores than the current scores.

4.4. Discussion

The current study aimed to investigate functional connectivity in 14-month-old infants who developed ASD at a later age and its relations with severity of symptoms in 2 main domains: social and communication difficulties, and restricted and repetitive behaviours. The results of the current study showed no significant differences for global alpha connectivity across all connections or fronto-central connections identified in the previous study between the HR-ASD group and the comparison groups. The current study did thus not replicate the previously found associations between infant global alpha connectivity and later categorical outcome.

As for the analyses on dimensional outcomes, the association between functional connectivity among selected fronto-central connections and the severity of restrictive and repetitive behaviours measured by the ADI-R in the HR-ASD group reached significance. This finding is consistent with the previous findings and thus replicates the previous study. There were no other significant correlations between functional connectivity and behavioural symptoms. Further exploratory analyses showed that global alpha connectivity displayed the strongest associations with circumscribed interests out of the 3 subtypes of RRBs.

4.4.1. Alpha connectivity and categorical outcome

In contrast to my hypothesis, there were no differences in alpha connectivity between the HR-ASD and other comparison groups in the current sample. This finding was consistent for connectivity across all connections, and across the fronto-central connections. I did not replicate the findings of the previous study that found hyper connectivity in HR-ASD infants compared to LR, and HR-no ASD infants (Orekhova et al., 2014). Overall, these data suggest that alpha connectivity at 14 months of age is similar across groups with different later outcomes (even for combined cohorts in Appendix A4.13). Other studies have found no differences between infants, toddlers, and children with ASD or typical development in whole brain alpha EEG connectivity either (Boersma et al., 2013; Buckley et al., 2015; Peters et al., 2013). Studies using different neuroimaging techniques suggest a similar pattern of conflicting findings: the HR group displayed lower fNIRS connectivity at 12 months of age than the LR group (Keehn, Wagner, Tager-Flusberg, & Nelson, 2013). Structural MRI findings in individuals around 12 months report *no* differences in connectivity between HR-ASD and HR-no ASD groups at 12 months of age (Wolff et al., 2012), or in posterior white matter tracts in groups of infants with and without ASD (Solso et al., 2016). *Increases* in structural connectivity however have also been reported in frontal and fronto-temporal connections in toddlers with ASD compared to toddlers with TD or developmental disorders (Conti et al., 2017; Solso et al., 2016). Overall, this suggests that whole brain alpha EEG connectivity is not strongly related to categorical outcome of ASD.

One possible explanation for lack of group differences in whole brain connectivity in the current cohort is intra-individual variability across time.

Fluctuations in connectivity across small periods of time might influence the reliability of connectivity findings across long periods of time. Microstates are short periods of quasi-stable activation with a certain topology lasting for 80 to 120 ms, and likely play a role in the rapid organisation and adaptation of brain networks (Koenig et al., 2002; Van De Ville, Britz, & Michel, 2010). EEG connectivity calculated for these microstates has been shown to be more reliable than EEG connectivity calculated over several seconds of data (Hatz et al., 2016). This is probably due to the higher stationarity of the EEG signal during microstates compared several seconds. Topologies and durations of EEG microstates change across development, and might be atypical in individuals with psychiatric disorders (Koenig et al., 2002). A recent MRI study found that functional connectivity in individuals with autism is more variable across time when compared to typically developing individuals (Falahpour et al., 2016). Together, this suggests that higher intra-individual variability during the EEG recording in the HR-ASD group could have led to the failure to replicate the previously found differences between the HR-ASD and other groups.

Alternatively, inter-individual variability between the individuals with ASD may explain the current findings. Heterogeneity in ASD is present in developmental trajectories of cognitive abilities, and severity of ASD symptoms experienced during early development (Landa, Gross, Stuart, & Bauman, 2012; Lord, Bishop, & Anderson, 2015; Lord, Luyster, Guthrie, & Pickles, 2012). The same holds for brain development: a group of children with ASD (7 – 16 year old) followed a different developmental trajectory of whole brain MEG connectivity (WPLI) than their typically developing peers, and displayed greater inter-individual variability in developmental trajectories within the group. There were

no differences however between the groups in whole brain connectivity across the whole age range (Vakorin et al., 2016). Furthermore, fMRI research has shown higher intra-individual variability in topologies of functional network activation within the ASD group than within the TD group (Hahamy, Behrmann, & Malach, 2015; Uddin, 2015).

Inter-individual variability in the HR-ASD group in the current and previous cohort might also explain the null findings here. The current sample contained 2 infants with high connectivity values out of 13 infants in the HR-ASD group, whereas the previous sample contained 6 infants with high connectivity values out of the 10 HR-ASD infants (Orekhova et al., 2014). This heterogeneity in EEG connectivity might arise from the heterogeneity of genetic and environmental factors that play a role in the development of ASD (Geschwind, 2009; Grayson & Guidotti, 2016; Mandy & Lai, 2016). Indeed, it has been suggested that different subgroups of individuals with ASD might experience symptoms and structural and functional brain characteristics caused by different underlying mechanisms (Loth et al., 2016). Gender might play a role in different causal pathways also by moderating the relation between early ASD markers and later categorical outcome (Bedford et al., 2016). In the current cohort, males tended to display higher global connectivity than females. Further analyses suggested that this was not different between groups, thus gender might not play a larger role in relations between early connectivity and later ASD outcome. Another possibility is that variability in age has played a role, since infants in the previous sample were younger than those in the current sample (see Appendix A4.14).

In addition to demographical factors, visual preferences and atypical attention towards social or non-social stimuli may play role in the current findings

and relate to a specific subgroup of ASD. Previous studies suggest that a subgroup of toddlers with ASD display a visual preference for dynamic geometric images compared to dynamic social images (Pierce et al., 2016, 2011), which are comparable to the non-social and social videos displayed here. The toddlers with ASD showing a strong preference for the geometric stimuli furthermore displayed fewer saccades and longer periods of sustained attention when looking at their preferred stimuli compared to the toddlers with ASD who displayed a stronger preference to dynamic social images and the groups showing typical development, developmental delay, other developmental atypicalities, but not compared to toddlers with elevated levels of ASD traits without meeting criteria for a diagnosis. When the toddlers with ASD and the geometric preference fixated on their non-preferred stimuli (social images), they displayed more saccades than each of the other groups. Considering that saccades and eye-movements cause artefacts in the EEG data and visual preference may influence the amounts of clean EEG data, it is possible that a subset of HR-ASD infants with a visual preference for geometric images, or toys, would provide more clean EEG epochs for a geometric/toy condition than for a social condition.

Indeed, the findings from the current study showed that the clean EEG data of HR-ASD group consisted of a smaller percentage of epochs from the social condition than the LR, HR-TD, and HR-Atyp groups. It is possible that this arises from a visual preference for the non-social stimuli rather than the social stimuli in a subset of the HR-ASD infants. Further analyses however did not suggest that this might have affected the current connectivity findings. First, there were no differences between groups in the total amount of social, toy, or hand trials. If visual preference had played a role, one would have expected to find significant

differences in the number of trials of each condition between the diagnostic groups. Second, the pattern of results did not change when the percentage of social epochs was included in the analyses. Third, there were no differences between the HR-ASD group and comparison groups in the amounts of overlapping trials, or gaze during the session. This suggests that there were no differences in duration of bouts of sustained attention resulting in clean EEG data. Finally, results from a recent study with eye-tracking data from the same group of participants (BASIS Phase 2) showed that HR-ASD toddlers at 27 months of age displayed the same looking behaviours towards social and toy stimuli as the LR and HR-no ASD toddlers (Vernetti et al., 2018). Together these findings suggest that visual preference towards the non-social stimuli compared to the social stimuli in the HR-ASD group is unlikely to have played a large role in the current finding of EEG alpha connectivity. Still, EEG alpha connectivity in 14-month-old infants might be used for stratification to define different subtypes of ASD, thereby creating more homogeneous groups.

Finally, other frequency bands than alpha might be a more fruitful marker for ASD. For example, theta EEG connectivity might be a more accurate marker for later categorical outcome of ASD. Activity in the theta frequency band is sensitive to social processing (Jones et al., 2015). Furthermore, previous research has found atypicalities in social processing in HR-ASD infants (Lloyd-Fox et al., 2013, 2017), and atypical theta activity in response to social and non-social stimuli in toddlers with ASD (Dawson et al., 2012; Jones, Dawson, et al., 2017). The current results also showed that the datasets of the HR-ASD group contained a smaller percentage of epochs from the social stimuli than the other comparison groups, suggesting that social processing might be atypical in these infants. It is possible that theta

band EEG connectivity in response to social and non-social stimuli is a more sensitive marker for categorical outcome than alpha band connectivity across all conditions. The next chapter will further examine this possibility.

4.4.1.2. Alpha connectivity and age

Previous research has shown that global EEG connectivity decreases with age during childhood (Boersma et al., 2011). Further, the largest changes in functional connectivity seem to occur during the first year of life, with further changes and refinements occurring in the second year of life (Gao et al., 2011). Here, global alpha connectivity was related to age at EEG assessment in the HR-Atyp and HR-TD groups, but not the LR and HR-ASD groups. In the HR-Atyp group, global alpha connectivity increased with ages, whereas connectivity decreased with age in the HR-TD group. Although age was not related to the group effect, the relations with age were significantly different across groups. In the original study, age was not related to global connectivity in the LR or HR-ASD group either. Also, no significant association was found in the HR-no ASD group, probably because this group combined the HR-TD and HR-Atyp groups that show opposite relationships in the current sample.

Possibly, different groups are characterised by different developmental trajectories. While minimal connectivity changes occur in LR and HR-ASD groups, connectivity does change in the HR-Atyp and HR-TD group during the few months around the 14-months-old visit. The HR-TD group may be characterised by a compensatory mechanism that allows them to 'catch up' with the LR group by showing decreases in functional connectivity with increasing age. In contrast, the HR-Atyp group shows an increase in functional connectivity with increasing age,

which might be related to atypical development. This however can only be further investigated in longitudinal studies.

4.4.2. Alpha connectivity and dimensional outcomes

The second aim of the current study was to investigate the association between global alpha connectivity and later dimensional outcomes of ASD. The current results showed a significant association between alpha connectivity in fronto-central connections and severity of restricted and repetitive behaviours measured by the ADI-R in the HR-ASD group. This finding is a replication of the previous result found by Orekhova and colleagues (Orekhova et al., 2014). As research suggests that different subtypes of restricted and repetitive behaviours might arise from different underlying mechanisms (Langen et al., 2011), I further examined whether different subtypes of these behaviours might show different associations to alpha connectivity measures. Analyses on the collapsed cohorts suggested that the association with global alpha connectivity was strongest for circumscribed interests in the overall HR group. In the HR-ASD group, medium effect sizes for the same association were found, although these probably did not reach significance due to sample sizes. These data suggest that alpha connectivity is related to restricted and repetitive behaviours in the HR-ASD group, and that this relationship might be driven by an association with circumscribed interests. These findings furthermore demonstrate that a dimensional approach should be taken in addition to a categorical approach when examining potential markers for ASD.

Structural connectivity studies have found associations with restricted and repetitive behaviours also. The corpus callosum connecting the two hemispheres shows relations with restricted and repetitive behaviours. Specifically, increases in surface area at 6 months of age and thickness of the cortex in the corpus callosum

at 6 and 12 month of age were related to restricted and repetitive behaviours measured by the parental survey Repetitive Behaviour Scale – Revised at 24 months of age in the HR-ASD group (Wolff et al., 2015). Further, higher connectivity in the genu of the corpus callosum that is connected with frontal circuits at 6 months of age was related to more severe restricted and repetitive behaviours at 24 months of age in the HR-ASD group. This association was stronger for higher order behaviours such as rituals, insistence on sameness, and compulsive behaviours, than for lower order behaviours such as stereotypical motor behaviours (Wolff et al., 2017). It is possible that the replicated association between increased alpha connectivity in fronto-central regions at 14 months and restricted and repetitive behaviours at 36 months is related to structural overconnectivity in the corpus callosum in the current HR-ASD group.

Another possibility is that alterations in alpha connectivity are related to atypicalities in sustained attention. A recent study showed that alpha connectivity was reduced across central and parietal areas during periods of sustained attention compared to periods of inattention in 6 to 12-month-olds (Xie, Mallin, & Richards, 2018). Source level analyses revealed that alpha band connectivity between regions within the dorsal attention network and default mode network was attenuated during sustained attention also. Possibly increases in connectivity across fronto-central areas in the current result are related to atypical attentional control which may result in an over-focused attentional style leading to restricted and repetitive behaviours and interests at later age. The results of the exploratory findings are in line with this.

4.4.2.1 Alpha connectivity and circumscribed interests

The exploratory analyses suggested that the association between fronto-central alpha connectivity and restricted and repetitive behaviours might arise from a strong association with circumscribed interests. In the whole HR group and HR-ASD groups, alpha hyperconnectivity displayed a medium-sized positive relationship with more severe circumscribed interests. As suggested earlier, altered alpha band connectivity may be related to atypicalities in the dorsal attention network (Xie et al., 2018), and thus possibly attentional control. It is possible that alterations in alpha connectivity relate to a focal attention style leading to strong circumscribed interests. This focal attentional style may be part of an adaptive response to cope with the quantity of information processing (Johnson, 2017; Johnson et al., 2015).

Furthermore, atypicalities in limbic circuits may explain the current result. It has been suggested that different subtypes arise from different underlying mechanisms. The limbic circuit for example plays a role in circumscribed interests and obsessive behaviours observed in ASD and obsessive-compulsive disorder (Fuccillo, 2016; Langen et al., 2011). This circuitry innervates the anterior cingulate cortex (ACC) and orbitofrontal cortex (OFC), and is important for behavioural control (Langen et al., 2011). Previous studies have revealed fMRI overconnectivity in the limbic circuit in children with ASD (Abbott et al., 2017), and increased levels of glutamate in the ACC in children with ASD compared to peers with OCD, which were also related to increases in compulsive behaviours (Naaijen et al., 2017). These findings are consistent with the suggestion that atypicalities in the limbic loop, which also includes the frontal cortex, may be related to circumscribed interests.

In addition to atypicalities in the limbic circuit, atypical activation and connectivity in reward and salience networks may also account for the observed association. The ACC, and OFC, in addition to the striatum, are furthermore part of the salience and reward networks, which mediate reward expectancy, salience attribution, and cognitive control (Traynor & Hall, 2015). An adult study revealed hyper-activation in the reward network in participants with ASD while viewing images related to their circumscribed interests (Dichter et al., 2012). Children with ASD exhibited increased activation in regions included in the salience network when viewing pictures of their own interests compared pictures of others' interests (Cascio et al., 2014). Another study revealed that hyperconnectivity in the salience network was associated with more severe restricted and repetitive behaviours in older children with ASD (Uddin, Supekar, Lynch, et al., 2013), although associations with circumscribed interests remain unclear as subtypes of RRBs were not investigated. It is possible that these hyper-activations and connectivity within the reward and salience network relate to higher EEG connectivity over fronto-central areas, because parts of these networks such as ACC and insular cortex are located in the frontal and central parts of the brain. Further research combining both EEG and MRI methods that allows for source location of EEG signals, and looking into different subtypes of RRBs would further understanding of the relationship between EEG connectivity and specific brain networks.

4.4.2.2. Associations for specific behavioural measures in specific groups

The associations between brain and behaviour only reached significance when measured with the ADI-R, not with the ADOS-2; only in the HR-ASD group, not in the HR-no ASD or overall HR groups; and only in the restricted and repetitive

behaviours domain, not the social and communication domain. Several factors might have played a role in these findings. First, the ADI-R is a parental interview, whereas the ADOS-2 is a clinical observation measure. Restricted and repetitive behaviours are not frequently displayed, and therefore more likely to be picked up with the ADI-R covering longer periods of time than with the ADOS-2 covering 1 or 2 hours. The exploratory findings also indicate that associations between alpha connectivity and restricted and repetitive behaviours are stronger for ever scores than current scores. This suggests that alpha connectivity is related to the highest severity of restricted and repetitive behaviour symptoms, rather than current severity that is also measured with the ADOS-2.

Second, the ADI-R has been designed to pick up on ASD symptomatology. The interview is less sensitive to typical variation in the complete HR group and the HR-no ASD group, resulting in smaller ranges and reduced variability in scores for these groups than the HR-ASD group. Indeed, the group of HR-ASD infants displays higher median and interquartile range values than the groups of HR-no ASD and overall HR infants. Due to the higher variation in the HR-ASD group, associations are more likely to reach significance than in the HR group and HR-no ASD group.

Then the question remains why the associations with subtypes of RRBs did not reach significance in the HR-ASD group as this groups showed higher median and interquartile range values than the other groups also. One possible explanation is that the associations with subtypes of RRBs are overall relatively weak, where a large samples size is required to reach significance. Indeed, the significant association with the overall RRBs domain in the HR-ASD group had a Spearman's correlation value of .60, whereas the significant associations with the

RRB subtypes in the overall HR group had values ranging between .26 and .30. Careful inspection of the tables shows that for the HR-ASD group correlation values with circumscribed interests showed similar values between .35 and .37, and p-values reaching trends. However, these weak correlations might not have reached significance due to the smaller sample size of 21 infants, whereas the weak associations with circumscribed interest did reach significant in the HR group with a sample size almost 5 times the HR-ASD sample size.

Third, social and communication difficulties and restricted and repetitive behaviours might arise from different underlying mechanisms. The current results suggest that alpha connectivity is related to the severity of restricted and repetitive behaviours. It is possible that social and communication difficulties are related to atypical connectivity in a different frequency band, for example the theta frequency band, as mentioned previously. This band has been related to social and emotional processing (Jones et al., 2015; Saby & Marshall, 2012). Atypicalities in theta connectivity in response to social and non-social stimuli might be a more suitable marker for dimensional traits for later social and communication difficulties than atypicalities in alpha connectivity (Dawson et al., 2012; Jones et al., 2015). Further research comparing theta band connectivity in response to social and non-social stimuli between LR, HR-TD, HR-Atyp, and HR-ASD infants is needed to clarify this.

4.4.3. Limitations

The current study has a few limitations. First, although the current study includes more participants than the previous study, the sample sizes remain small, in particular for the HR-ASD group: 10 HR-ASD infants in the previous cohort, and 13 HR-ASD infants in the current cohort. It has been suggested that a replication study

that used the same sample sizes has decreased statistical power for finding a true effect (Button et al., 2013). It is possible that the lack of power has influenced the results. Studies with larger cohorts might be able to stratify HR-ASD infants in different groups with different subtypes of ASD. It is possible that alpha connectivity can help to clarify different causal pathways in these different subgroups.

Second, the weighting method of the dbWPLI used here to measure EEG connectivity minimized the effect of noise, but also minimizes the effect of 0° and 180° phase lags. This means that short-range connections with small phase lags are underestimated. The dbWPLI thus reflects 'true' brain connectivity that is otherwise masked by volume conduction effects, but underestimates short-range connectivity. Thus the results might give a better estimate of connectivity across long-range connections, suggesting that there are no differences in long-range connectivity between the HR-ASD and other groups in this sample. In contrast, connectivity across short-range connections is underestimated, making it difficult to interpret short-range connectivity differences between groups. The original study showed that the increases in connectivity did not depend on electrode distances. However, it is possible that connectivity is increased for short-range connections, since the dbWPLI underestimates short-range connectivity.

4.5. Summary of Chapter 4

The current study aimed to replicate and extend previous findings that showed hyperconnectivity in the alpha band in the HR-ASD group at compared to LR and HR-no ASD groups at 14 months of age. The current results revealed no differences in alpha connectivity between HR-ASD infants, and LR, HR-TD, or HR-Atyp infants. Previous findings also suggested that fronto-central alpha hyperconnectivity was

related to more severe restricted and repetitive behaviours in the HR-ASD infants. In the current study, the current findings replicated this result, and further suggested that a strong association between alpha connectivity and circumscribed interests might underlie this replicated association.

Altogether the findings suggest that alpha connectivity is not related to categorical ASD outcome, but rather to dimensional outcome, in particular severity of symptoms in the restricted and repetitive behaviours domain. Possibly, connectivity in the theta frequency band might show a stronger relation to categorical outcomes, and dimensional outcomes for the social and communication domain. I will examine this possibility in the next chapter.

Chapter 5: The association between theta EEG connectivity at 14 months and later social communication abilities at 36 months in high-risk infants?

5.1. Introduction

In the previous chapter, alpha EEG connectivity measured at infancy was found to be an individual predictor of restricted and repetitive behaviours during toddlerhood in the HR-ASD group. However, I did not find an individual predictor of social communication and interaction difficulties, even though these behaviours represent a core domain of ASD. The next question that arises is which neural processes may be considered as an early predictor for this set of ASD traits. It has been suggested that atypicalities in social processing during early development have cascading effects on the interactive specialization of the social brain and development of social skills (Chevallier, Kohls, Troiani, Brodkin, & Schultz, 2012; Johnson, 2011). According to the Interactive Specialization hypothesis, neural activation patterns in the social brain become more specialized and fine-tuned towards the processing of social stimuli (Johnson, 2011). It is possible that the social difficulties in ASD are associated with the atypical specialization of the neural processing towards social stimuli. Investigating neural activation patterns during social and non-social stimuli in infants with a later diagnosis of ASD may identify indices of interactive specialisation, and help to reveal underlying mechanisms of ASD (Jones, Venema, Lowy, Earl, & Webb, 2015).

One suitable candidate to examine neural processing in response to social and non-social processing is theta frequency oscillations. Activity in the theta frequency band is associated with social engagement, processing of emotional information, executive control of attention, and memory (Saby & Marshall, 2012). It has been suggested that the processing of social information is atypical in individuals with ASD (Chevallier et al., 2012). Recent studies have shown evidence of atypical neural processing of socially relevant stimuli from as early as 6 months

in infants at risk for ASD (Braukmann et al., 2017; Lloyd-Fox et al., 2013, 2017). Examining theta frequency activity during social processing during the early development of ASD may help towards understanding the underlying neural processing of social information in the development of ASD (Jones et al., 2015).

5.1.1. Theta frequency oscillations in typical development

Theta frequencies oscillations range from 3 to 6 Hz in young typically developing infants (Saby & Marshall, 2012). Spectral power in the theta band increased during the presentation of social stimuli when compared to non-social stimuli in 6- and 12-month-olds (Jones et al., 2015). During social stimulation, for example, an individual is speaking to the infant, or playing peek-a-boo in a socially engaging way. Examples of non-social stimulation are spinning toys, or an experimenter blowing bubbles in front of the infant. Increases in power furthermore occurred when infants were playing with toys or listening to an socially engaging adult when compared to a condition when infants were watching an adult blowing bubbles (Orekhova, Stroganova, Posikera, & Elam, 2006).

Another study found that theta power was higher during the anticipation of reappearance during a peek-a-boo game than during the reappearance itself in the game or while watching someone blowing bubbles. The authors suggest that theta oscillations are related to the internal control of attention (Orekhova, Stroganova, & Posikera, 1999). Thus theta frequency oscillations are also related to attentional processes and the internal control of attention, in addition to social processing.

The increases in theta power related to social processing and attentional control change over development. These changes over development occur in activation as well as topology. One study showed that differences in theta power between social and non-social stimuli were minimal at 6 months of age. At 12

months of age, theta changes were stronger than at 6 months of age, and more prominent at frontal and occipital areas (Jones et al., 2015). During a peek-a-boo game, frontal theta power increases in 8-9-month-old infants were larger than the increases in 10-11-month-old infants. Theta increases in the older infants were more prominent at posterior-temporal areas instead of at frontal areas (Orekhova et al., 1999). A similar pattern was found when responses in infants were compared to those in pre-schoolers: theta increases with social stimuli were larger and more widespread in infants than in preschool children. These responses were most pronounced in frontal areas in infants, whereas in pre-schoolers the responses were most pronounced in parieto-occipital areas (Orekhova et al., 2006).

Together these findings demonstrate that the increased theta responses to social stimuli when compared to non-social stimuli decrease from infancy to preschool ages in typical development. The areas showing the most prominent theta changes shift from anterior to posterior regions with increasing age. Lastly, these findings illustrate that differences in theta activation between social and non-social stimuli could be used to investigate social processing during early typical development, and also atypical development for example in ASD (Jones et al., 2015).

5.1.2. Theta frequency oscillations in ASD

Few studies have focused on theta frequency responses to social and non-social stimuli as a method to examine atypical social processing in early ASD. One study examined the results of different interventions in children with ASD (Dawson et al., 2012). Typically developing children showed increased theta power responses when looking at pictures of faces compared to pictures of objects. Children with

ASD who had received an intensive intervention called the Early Start Denver Model showed the same response pattern to the stimuli as the TD children. In contrast, children with ASD who had received typical community intervention showed increased theta power responses to the object stimuli than the face stimuli. Higher theta power to faces than objects was furthermore related to better communication abilities measured with a parent-report questionnaire.

Previous findings from studies using event-related potentials, eye-tracking, and fNIRS techniques suggest that atypical social processing occurs from an early age in HR infants (Jones et al., 2016; Lloyd-Fox et al., 2017). Possibly, differences in theta power in response to social versus non-social stimuli are different in young infants with high risk for ASD compared to those with low risk at 14 months of age. These differences in theta power might be related to later social and communication difficulties. In addition, theta EEG connectivity may also be modulated by the processing of social information. It is possible that infants with high and low risk show differences in global theta connectivity and topology in response to social and non-social stimuli. However, far less is known about theta EEG connectivity during the processing of social information.

5.1.3. Theta connectivity in infants at risk for ASD

The previous study by Orekhova and colleagues (2014) reported findings for the theta frequencies in the supplementary information. There were no differences between the HR-ASD group and LR or HR-no ASD group in theta power across all channels in the social, non-social (hand and toy condition), or combined conditions. Nor where there any differences between the groups for connectivity in either condition. This result was consistent for analyses focusing on global dbWPLI averaged across all connections, and connectivity networks compared

using NBS. The authors note that the lack of group difference may arise from a lower signal-to-noise ratio for theta than for alpha frequencies, or high inter-individual variability due to differences in emotional states. Theta power was also strongly affected by condition, which is consistent with findings of theta power in social and non-social conditions. This means that collapsing data across conditions would be problematic for theta investigations. However, sample sizes for theta comparisons would be small and statistical power would have been low in this previous study if data had not been collapsed across conditions.

Another possibility is that risk or outcome group differences exist for differences between conditions rather than on group averages for connectivity in the social or non-social condition. In previous studies looking at spectral power, comparisons with repeated measures contrasts for condition were used, not contrasts between groups as in the study by Orekhova and colleagues. It is possible that different networks become active when processing social information when compared to processing non-social information. These networks might also differ between groups with respect to activation and topology. For example, infants in the LR group might show stronger condition differences in a given network than the combined or separate HR groups, or the LR groups might show a network with a different topology when compared to the other groups. To investigate this, connectivity would have to be compared between conditions within groups rather than comparing between groups within conditions. In addition, a larger dataset is needed to compare connectivity between conditions within groups.

5.1.4. Aims of this chapter

The current study aims to examine differences in theta spectral power and connectivity in response to social and non-social stimuli in infants with different

risks and outcomes. If there is atypical social processing in infants at risk for ASD who also later develop ASD, I hypothesized reduced connectivity and power differences between the social and non-social condition in the HR-ASD group than in the LR group. Specifically, I predicted to find a graded effect where condition effects for power and connectivity diminish with increasing ASD risk: strongest condition effects for LR, then HR-TD, the HR-Atyp, and smallest condition effects for HR-ASD infants.

I further aimed to examine whether differences in theta power and connectivity between conditions were related to later social and communication abilities. If theta oscillations are related to social processing, atypicalities in these oscillations in response to social stimuli might be related to difficulties with social interactions and receptive and expressive communication. I hypothesized that larger differences in power and connectivity between social and non-social conditions were related to better social and communication abilities.

5.2. Methods

5.2.1. Participants

Participants in this chapter are the same participants as included in the previous chapter on alpha connectivity. Infants from the previous cohort and the current cohort were collapsed in order to increase statistical power for analyses in separate conditions on theta connectivity. All infants were recruited via the BASIS study (see Chapter 4 for a more detailed description). The complete combined sample of infants contained 46 LR infants, 56 HR-TD infants, 30 HR-Atyp infants, and 23 HR-ASD infants (comparisons for age and cognitive skills between cohort were reported in Appendix A4.14). Different subsets of these infants were used for

different comparisons between conditions since not all infants had a sufficient amount of data available in each condition.

First, an initial exploratory analysis to define the frequency band of interest for theta included the complete combined sample. Next, I aimed to compare spectral power and connectivity between hand and toy stimuli. Collapsing data across the two non-social conditions would increase sample sizes for these comparisons. Infants with 90 or more epochs for both the hand and toy condition were included in the analyses testing for differences between these conditions. The cut-off of 90 was chosen here, as this would allow for the inclusion of more infants compared to a cut-off of 120 epochs. Findings from Chapter 3 suggest that 90 epochs is an acceptable cut-off as well. Data for the hand and toy condition were collapsed into one non-social condition to increase sample sizes and statistical power (see Appendix A5.1 for more details on sample sizes for different cut-offs).

Finally, the comparisons comparing neural measures between the social and non-social condition were based on a subset of infants with 120 or more epochs in the social and non-social condition. The threshold of 120 epochs was chosen, as this was also the threshold chosen in the study by Orekhova and colleagues (2014) and the previous chapter, and was found to result in reliable connectivity estimates in Chapter 3.

5.2.2. Procedure and measures

The procedure and measures are identical to the ones described in the previous chapter: for the 14-month-old visit, these include the EEG task and MSEL. Measures included from the 36-month-old visit are ADOS-2 scores for the Social Affect domain, and the Restricted and Repetitive Behaviours domain (Lord et al., 2000); and ADI-R scores for the Social domain, the Communication domain, and

the Behaviour / Repetitive Interests domain (Lord, Rutter, & Le Couteur, 1994a).

In addition, the standard scores for the Communication domain, and the Socialization domain of the Vineland Adaptive Behaviour Scales-II (VABS-II) (Sparrow et al., 1984) were included to examine how social communication skills are associated with theta power and connectivity measures. Items included in the Communication domain assess skills for receptive, expressive, and written communication. Items in the Socialization domain measure social interaction skills, use of play and leisure time, and coping skills (see also Appendix A4.3).

Descriptions for the measures at the 14 and 36-month-old visits can be found in sections 4.2.2.2 and 4.2.2.3, respectively. Procedures for assessment of familial risk and diagnostic categorical outcome are reported in sections 4.2.2.1, and 4.2.2.3.

5.2.3. Data processing and analyses

5.2.3.1. Selection of theta frequencies

First, I aimed to explore whether the dbWPLI spectra for separate conditions showed the same 2 distinctive peaks as in the previous study. In the previous study by Orekhova and colleagues (2014), the dbWPLI spectrum showed 2 peaks. The first peak was in the theta range from 4 to 5 Hz, and the second in the alpha range from 7 to 8 Hz. Here, the log power and dbWPLI values were calculated from the complex Fourier values for 0 to 29 Hz across epochs from the social, toy, and hand condition, separately. All epochs for each condition were included in the calculations for each infant in the complete combined dataset. The frequencies for the theta band would be selected based on visual inspection of the graphs.

5.2.3.2. Comparisons between the hand and toy condition

5.2.3.2.1. EEG preprocessing

In the second set of analyses, I wanted to investigate whether it would be possible to collapse the hand and toy condition data into one non-social condition. Collapsing data across conditions would increase the samples sizes considerably (also see section *5.*2.1). This however would only be justified if there were no differences in connectivity between the hand and toy condition. Differences between these conditions in theta connectivity might exist if the videos would elicit differences in executive control, or learning or memory, as these cognitive skills have been associated with theta frequency band oscillations (Saby & Marshall, 2012). Therefore these analyses focused on comparing the hand and toy condition.

Clean epochs from both the hand and toy condition were selected for these analyses. The amount of epochs for both conditions was kept constant within participants. For example, if for the toy condition 120 epochs were available, whereas for the hand condition 150 epochs were available, then the dbWPLI would be calculated across the 120 toy epochs, and 120 hand epochs that were randomly selected from the 150 available hand epochs. I ensured the numbers of epochs were equal across conditions since the amount of debiasing for the calculation of the dbWPLI depends on the number of epochs and would then be the same for both conditions for each individual infant.

Spectral power was calculated for the theta frequencies of interest based on the visual inspection of the frequency spectra. The procedure was identical to the one described in section 4.2.4, with the only difference of averaged across different frequencies, and across different groups of channels (here based on the study by

Jones and colleagues (2015) focusing on theta power rather than the study by Orekhova and colleagues (2014) focusing on alpha power). Spectral power across all channels was defined as the average power across all 116 channels (see Fig. 5.1). Spectral power for specific regions was defined as the average power across different sets of electrodes: E27, E23, E28, E24, E19, and E20 for frontal left; E4, E3, E118, E124, E123, and E117 for frontal right; E44, E39, E40, and E45 for temporal left; E109, E115, E114, and E108 for temporal right; E41, E36, E30, E47, E42, and E37 for parietal left; E105, E104, E103, E87, E93, and E98 for parietal right; E60, E67, E66, E65, and E70 for occipital left; and E77, E85, E84, E83, and E90 for occipital right (Jones et al., 2015).

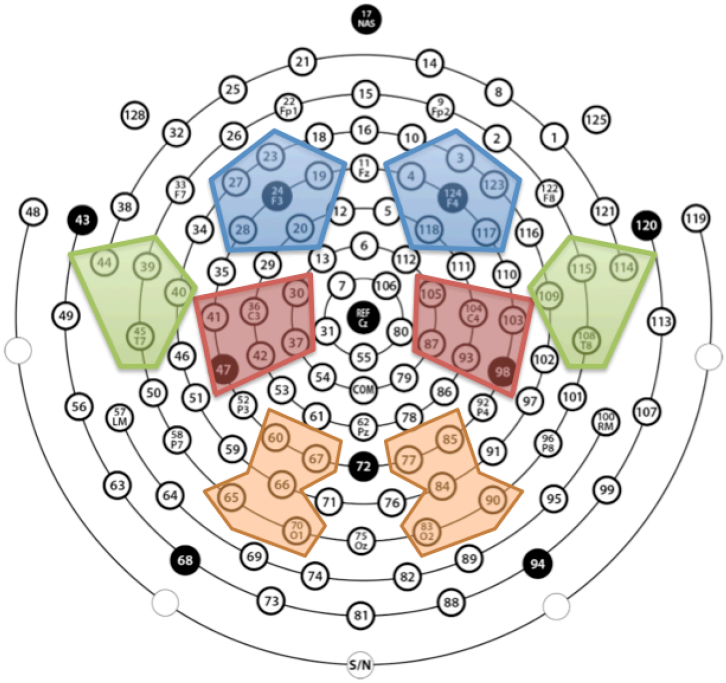

Figure 5.1. Layout of EEG net for theta analyses

For theta spectral power analyses, power for specific regions was averaged across different sets of electrodes: frontal (blue), temporal (green), parietal (red), and occipital (orange).

After spectral power calculations, dbWPLI for the theta frequencies was calculated for the selected epochs from the hand and toy condition separately, using identical methods as described in section 4.2.3 and 4.2.5. The dbWPLI was first calculated for each frequency within the theta band, and then averaged across frequencies. Infants with 90 or more epochs for each condition were included in further analyses. This value was chosen based on the results from Chapter 3 revealing that 90 1-second epochs is the lowest amount of 1-second epochs the global dbWPLI can be calculated across while still providing a reliable measure: $ICC_{60\ 1\text{-s epochs}}$ = .38 which is considered as poor reliability, and $ICC_{90\ 1\text{-s epochs}}$ = .76 which is in the range of excellent reliability (see table 3.4). Finally, this threshold was chosen due to the higher number of infants that could be included into the hand-toy analyses with the use of 90 epochs (N = 64) as threshold compared to 120 epochs as threshold (N = 36, also see Appendix A5.1).

5.2.3.2.2. Statistical analyses

First, I compared spectral power between the hand and toy condition. A 2x2 mixed model analysis of variance (ANOVA) was used with Condition (Hand, Toy) as within-subject factor, and Risk Group (LR, HR) as between-subject factor was applied to the data for power averaged across all channels. If the Risk group effect was significant, further follow-up analyses were performed to test for an effect of Outcome Group (LR, HR-TD, HR-Atyp, HR-ASD). In the previous chapter, the analyses focused on Outcome group, since hypotheses for outcome groups were specifically defined based on the study that I aimed to replicate. As the current research question has not been investigated before, the effect of Risk group was tested prior to testing the effect of Outcome group. To test whether there were any differences in regions or hemispheres in theta power, a 2x4x2x2 mixed model

ANOVA was used with Condition (Hand, Toy), Region (Frontal, Temporal, Parietal, Occipital), and Hemisphere (Left, Right) as within-subject factors, and Risk Group (LR, HR) as between-subject factor was used. The IBM SPSS Statistics Version 22 was used to run these analyses.

Second, I investigated whether functional connectivity in the theta frequencies differed between the hand and toy condition. Connectivity between conditions was compared on global level and network level. For global level analyses, I compared global dbWPLI between conditions using a non-parametric related samples Wilcoxon Signed Rank test with SPSS. This test was chosen, since the assumptions for normality and homogeneity of variance between the groups were not met. The Wilcoxon Signed Rank test was used to compare differences between conditions in the complete sample, in the LR group, HR combined group, HR-TD group, HR-Atyp group, and HR-ASD group.

For network level analyses, the Network-based Statistic (NBS) program was used. This method uses permutation testing and cluster-based methods to identify connections that are related to differences between conditions or groups (also described in Chapter 4). I tested whether there were any connections showing significant differences between conditions using a paired samples t-test with significance level 0.05, Extent, and different thresholds. This test differs from the Mann Whitney U-test used in the previous chapter. In the current chapter, the factor of interest is the within-subject factor Condition (Hand vs. Toy), whereas in the previous chapter the factor of interest was the between-subject Group (HR-ASD vs. LR, HR-TD, and HR-Atyp). Permutation testing is based on the random permutation of labels to data, and the subsequent testing of the null hypothesis for that permutation. In between subject designs, data labels are randomly exchanged

between individuals. In a repeated measures design, data labels for conditions are exchanged within the individual. Since the current analyses are based on a repeated measures design, I chose to perform a paired samples t-test instead of a Mann Whitney U-test for a between subjects design. Two contrasts were tested: higher connectivity for hand than toy, and lower connectivity for hand than toy.

Finally, additional analyses were performed to test for possible influences from spectral power and the number of epochs as these are know to be related to the dbWPLI connectivity measures. Since the non-parametric tests and NBS analyses do not allow for the option to include covariates, separate General Linear Models were used here with Condition (Toy, Hand) as within-subject factor, and Risk Group (LR, HR) as between-subject factor, with the difference in spectral theta power between conditions or the number of epochs as covariate.

5.2.3.3. Comparisons between the social and non-social condition

5.2.3.3.1. EEG preprocessing

After confirming that connectivity is the same across the hand and toy condition, data were preprocessed for comparisons between the social and non-social condition in a third set of analyses. As before, epochs were selected from different conditions to make sure that the amount of epochs in the social and non-social condition were matched within each participant. Data for the non-social condition consisted of equal amounts of epochs the toy and hand condition where possible. This was done to ensure that epochs were selected from different sections across the EEG session rather than selecting epochs from the beginning of the session only.

After the selection of the appropriate epochs and creating datasets containing equal amounts of epochs for the social and non-social condition,

spectral power and the dbWPLI were calculated for each condition separately as described before in section 5.2.3.2.1. The measures resulting from the preprocessing step were: spectral power across all channels, spectral power across specific regions, connectivity matrices, and global connectivity values for both the social and non-social condition, for each infant. Only infants with 120 or more epochs for the social and non-social condition were included in further analyses. This threshold was chosen based on the findings from Chapter 3 that showed global dbWPLI calculated across 120 epochs provides a measure with excellent reliability ($ICC_{Global\ dbWPLI}$ = .82, see table 3.4). Further, this threshold was chosen in order to maintain consistency with Chapter 4 and the original study by Orekhova and colleagues (Orekhova et al., 2014).

5.2.3.3.2. Statistical analyses

Statistical analyses for the social versus non-social comparisons were similar to the analyses used for the hand versus toy comparisons. For spectral power across all channels, I used a 2x2 mixed model analysis of variance (ANOVA) was used with Condition (Social, Non-Social) as within-subject factor, and Risk Group (LR, HR) as between-subject factor. To test whether there were any differences in regions or hemispheres in theta power, a 2x4x2x2 mixed model ANOVA was used with Condition (Social, Non-Social), Region (Frontal, Temporal, Parietal, Occipital), and Hemisphere (Left, Right) as within-subject factors, and Risk Group (LR, HR) as between-subject factor was performed. If main effects for Risk Group reached significance, follow-up analyses examining the effect of Outcome Group (LR, HR-TD, HR-Atyp, HR-ASD) were performed.

For global connectivity, a related-samples Wilcoxon Signed Rank test was used to test whether there were any differences in global connectivity between the

social and non-social condition. This difference was tested across all groups, in the LR group, in the HR combined group, in the HR-TD group, in the HR-Atyp group, and in the HR-ASD group. Asymptotic significant levels for 2-sided test are reported unless otherwise specified. Further analyses to test whether the effects of condition differed between groups involved pairwise comparisons of the LR group with the other groups, and the HR-ASD group with the other groups. To this end, I used Independent Samples Mann-Whitney U test for group comparisons with the differences in global dbWPLI between the social and non-social condition as dependent variable.

For network connectivity, the NBS program was used to test whether any connections were significantly different between the social and non-social condition. I used the same methods as for the hand-toy comparisons: a paired-samples t-test, significance level 0.05, with Extent as NBS options. Analyses were performed for 2 different contrasts: higher connectivity in the social than non-social condition, and higher connectivity in the non-social than social condition. Conditions were compared across all infants, in the HR combined group, in the HR-TD group, in the HR-Atyp group, and in the HR-ASD group separately.

Again, it is possible that spectral power or the number of epochs influenced the theta connectivity results. Additional GLMs were performed which included Condition (Social, Non-Social) as within-subject factor, and Risk Group (LR, HR) as between-subject factor, and the difference in spectral theta power between conditions or the number of epochs as covariate.

5.2.3.3.3. Analyses with dimensional traits

Finally, I examined whether there were any associations between theta responses and dimensional ASD traits. I expected that connectivity and power differences

between the conditions would be related to later social and communication difficulties. The experimental measures for these correlations were: 1) difference for power between social and non-social conditions averaged across all channels, 2) difference for power between social and non-social conditions averaged across connections in the HR 3.1 network identified in the NBS analyses, 3) difference for dbWPLI between social and non-social conditions averaged across all connections, and 4) difference for dbWPLI between social and non-social conditions averaged across connections in the HR 3.1 network. Domain scores for the ADOS-2, ADI-R, and VABS were used as measures of behaviour in these brain-behaviour correlations: 1) ADOS-2 Social Affect domain scores, 2) ADOS-2 Restricted and Repetitive Behaviour domain scores, 3) ADI-R Social and Communication domain score (sum of the scores for the ADI-R Social domain and the Communication domain), 4) ADI-R Behaviour / Repetitive Interests domain score, 5) VABS Communication domain standard score, and 6) VABS Socialization standard score.

Each of the correlations were performed using Spearman's correlation because this measure is less susceptible to extreme values, provides a better estimation with non-Gaussian distributed data, and can be used with ordinal data. Bootstrap methods were used to acquire robust bias corrected and accelerated bootstrap 95% confidence intervals for the correlation coefficients. Correlations were considered significant and reported if the p-value was below 0.05. A correction for multiple comparisons using the False Discovery rate was applied to the comparisons made for each of the measures of behaviour (ADOS-2, ADI-R, and VABS) (Benjamini & Hochberg, 1995). If correlations in the whole group were significant, I tested for effects within the LR and HR group. If the correlation in the

HR group reached significance as well, I further tested for significant correlations in the HR-TD, HR-Atyp, and HR-ASD group separately.

5.3. Results

5.3.1. Selection of theta frequencies

The first step in this study was to identify the theta frequency band by visually inspecting the frequency spectra for both power and the dbWPLI. All infants who were included in the alpha connectivity analyses in the previous chapter were included in these graphs for visual inspection (N_{LR} = 46 for social condition, and 45 for toy and hand condition, $N_{HR\text{-}TD}$ = 56, $N_{HR\text{-}TD}$ = 30, and $N_{HR\text{-}TD}$ = 23). Figures 5.2 and 5.3 contain the frequency spectra for log power and dbWPLI, respectively, for each condition and group separately.

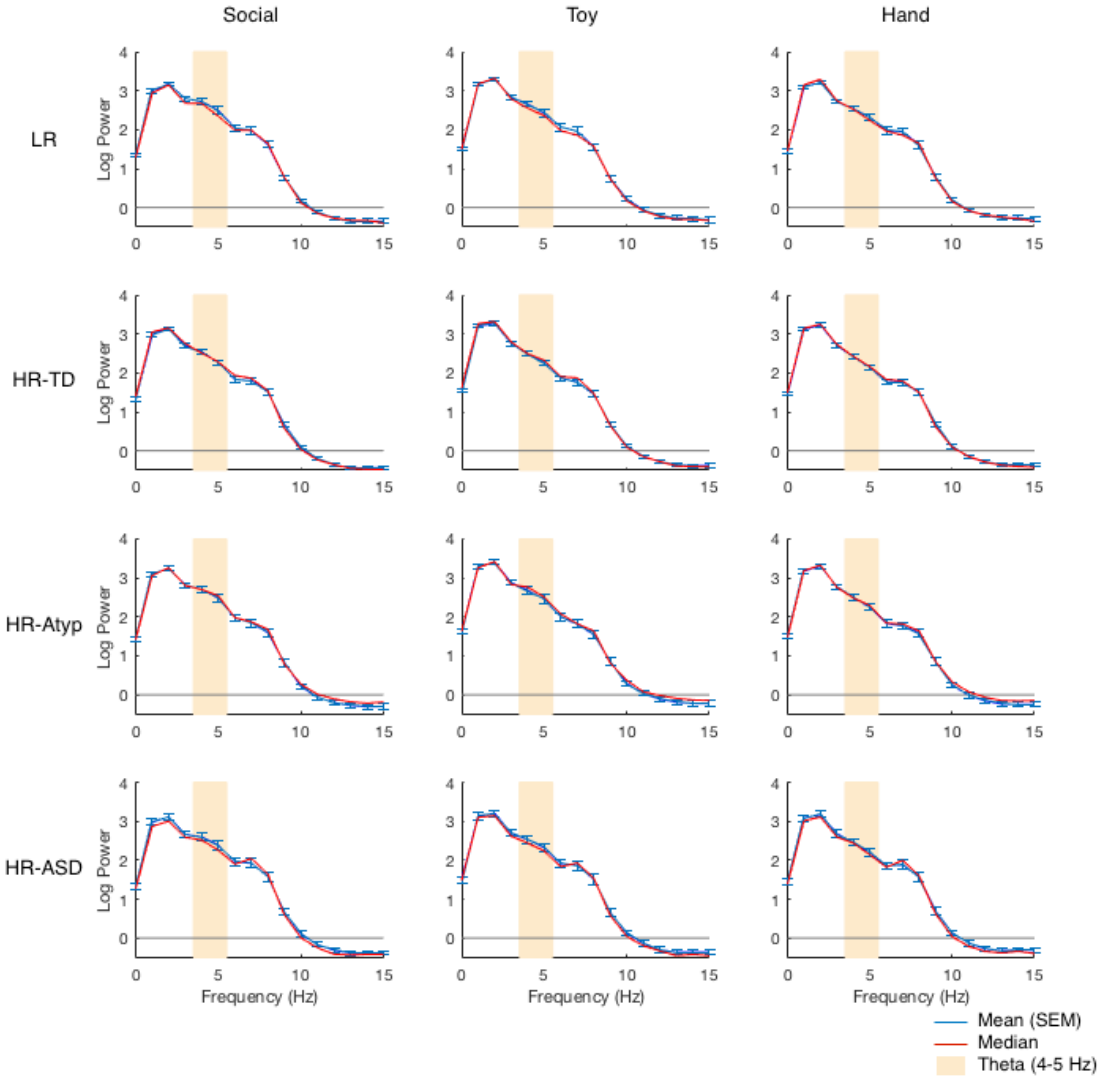

Figure 5.2. Log power values for 0 to 15 Hz for different conditions and groups

Graphs for different conditions are displayed in different columns: social condition (left), toy condition (middle), and hand condition (right). Graphs for different groups are displayed in different rows. The orange rectangle marks the 4 to 5 Hz frequency band.

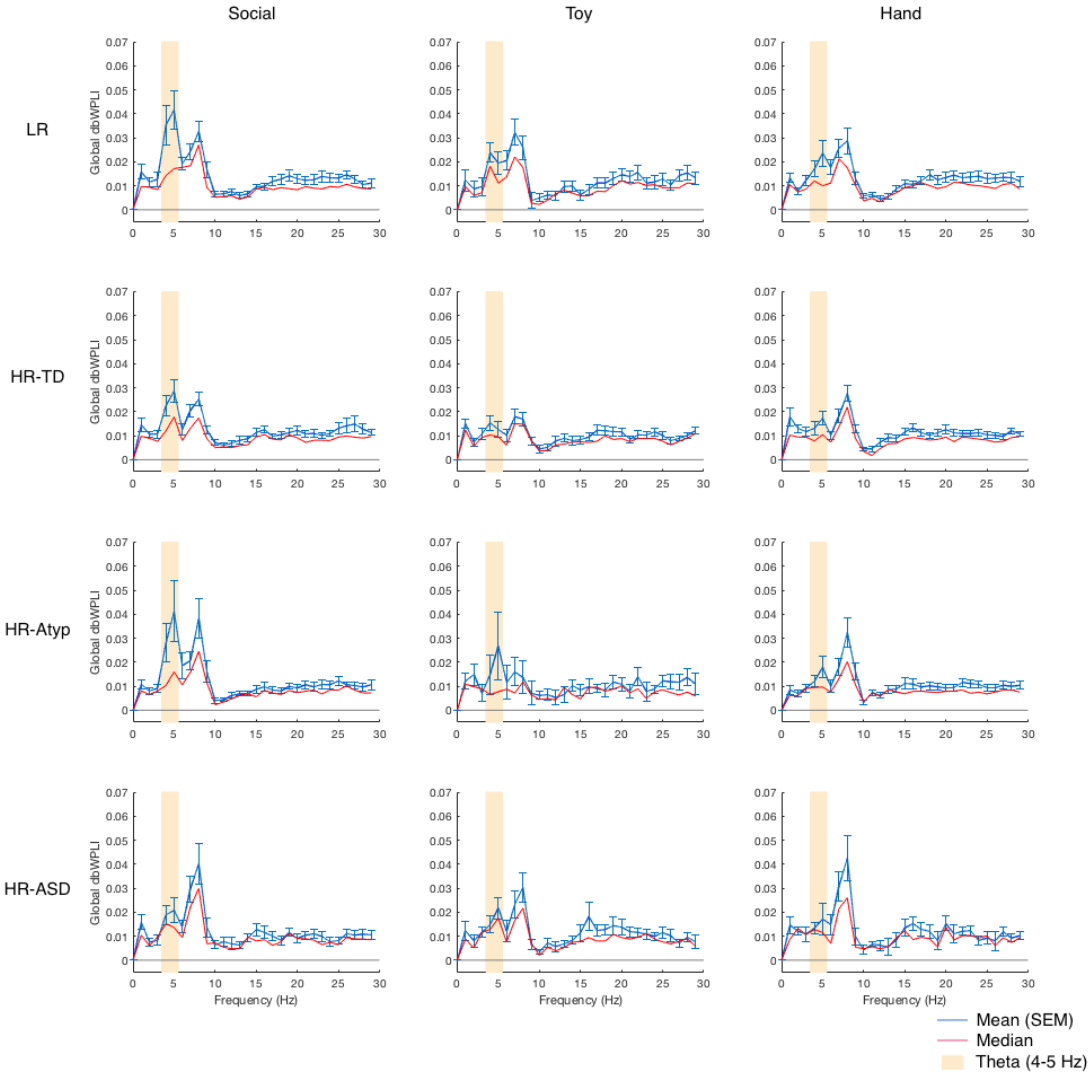

Figure 5.3. Global dbWPLI values for 0 to 29 Hz for different conditions and groups
Graphs for different conditions are displayed in different columns: social condition (left), toy condition (middle), and hand condition (right). Graphs for different groups are displayed in different rows. The orange rectangle marks the 4 to 5 Hz frequency band.

Peaks in the power spectrum are less clear from the graphs. In contrast, the global dbWPLI graphs show two clearly visible peaks: one for theta in the lower frequency bands around 4 to 5 Hz, and one for alpha in the higher frequency bands around 7 to 8 Hz. I decided to select 4 to 5 Hz as my frequency band of interest for theta band in the rest of the analyses.

5.3.2. Comparisons between the hand and toy condition

5.3.2.1. Participants

Next, I investigated whether it was justified to collapse data from the hand and toy condition into 1 non-social condition to compare with data from the social condition. If this would be the case, samples for social versus non-social comparisons would be considerably increased. The sample for comparisons between the hand and toy condition consisted of 17 LR, 25 HR-TD, 13 HR-Atyp, and 9 HR-ASD infants.

5.3.2.2. Spectral power

Graphs with global power for the hand and toy conditions, topoplots, and plots for differences between conditions are displayed in Figure 5.4. For power across all channels, a 2x2 mixed model ANOVA was used with Condition (Hand, Toy) as within-subject factor, and Risk Group (LR, HR) as between-subject factor was used. The assumptions of normality across groups were met for each variable, while the assumption for equality of variance was only met for power across all channels in the hand condition (p's ≥ .058).

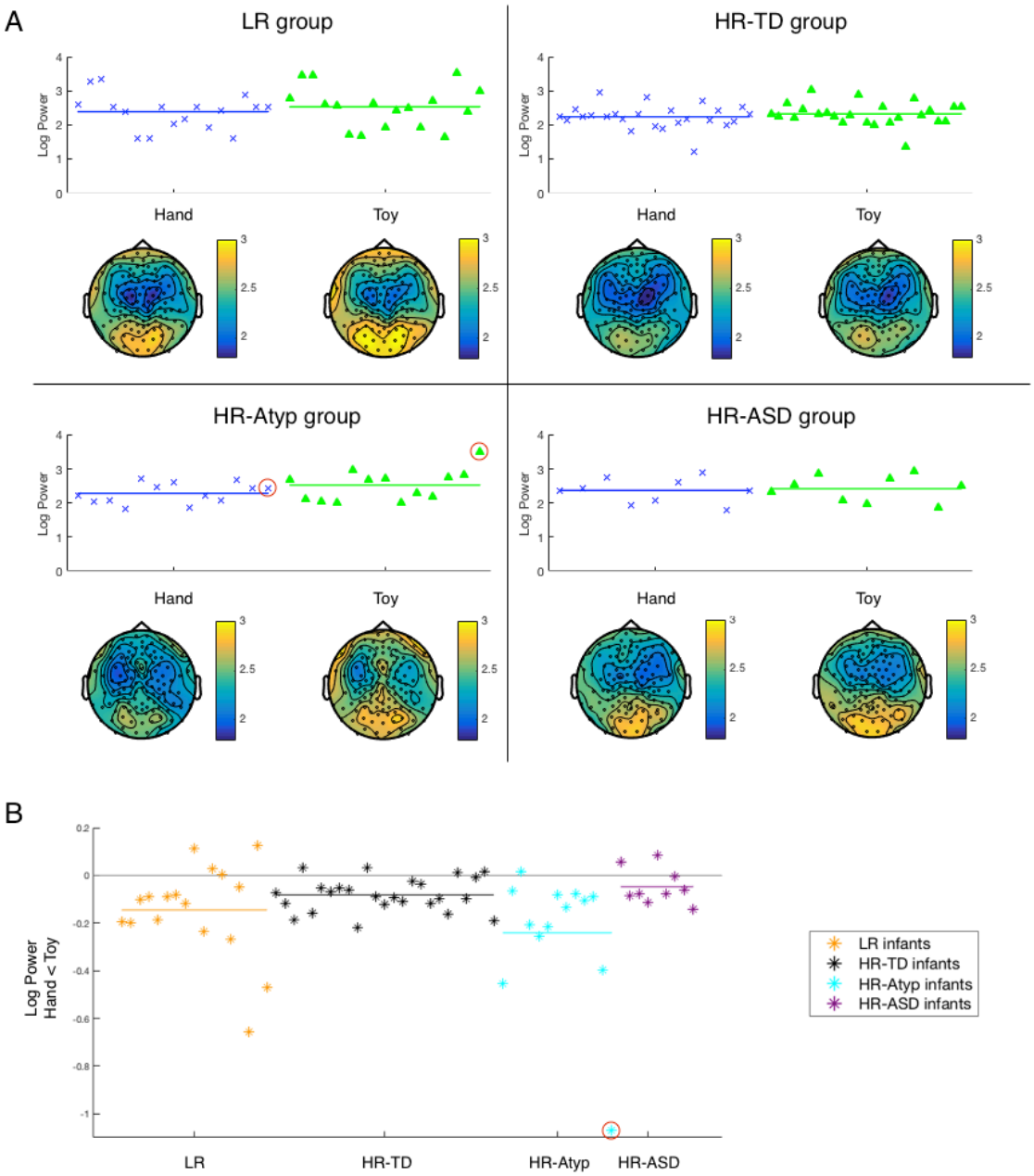

Figure 5.4. Global theta power in the hand and toy condition

A) Global power across all channels for individual infants for the hand and toy condition (blue crosses, and green triangles, resp.), with topoplots averaged across infants in the outcome groups (LR group in top left panel, HR-TD group in top right, HR-Atyp group in bottom left, and HR-ASD group in bottom right panel). B) Differences in global power between the hand and toy condition for individual infants in the different outcome groups. Horizontal lines represent group means. Note red circle marks an outlier in the HR-Atyp group.

The results revealed a main effect of Condition, $F(1,62) = 26.91$, $p < .001$, $\eta_p^2 = .303$, where theta power across all channels was higher for the toy than the hand condition, ($M_{Toy} = 2.43$, $sd_{Toy} = 0.45$; and $M_{Hand} = 2.30$, $sd_{Hand} = 0.39$). The main effect of Risk Group, and interaction effect between Condition and Risk Group did not reach significance (p's ≥ .320, η_p^2's ≤ .016).

To test whether there were any differences in regions or hemispheres in theta power, a 2x4x2x2 mixed model ANOVA was used with Condition (Hand, Toy), Region (Frontal, Temporal, Parietal, Occipital, and Hemisphere (Left, Right) as within-subject factors, and Risk Group (LR, HR) as between-subject factor was used. Assumptions for normality were met for most variables (p's ≥ .121), except in the HR group for left and right parietal areas during both conditions (p's ≤ .036). Assumptions for homogeneity of variance were met for most variables (p's ≥ .050), except for left occipital and right temporal areas during both conditions, left parietal region during the hand condition, and left frontal region during the toy condition (p's ≤ .046). For factors for which the assumption of sphericity was not met, Huynh-Feldt corrected degree of freedom values are reported, as the estimates were larger than .75.

The main effects for Condition, and Region both reached significance. Theta power was higher during the toy than hand condition in the selected channels, $F(1,62) = 26.05$, $p \leq .001$, $\eta_p^2 = .296$ ($M_{Toy} = 2.42$, $SE_{Toy} = 0.05$; and $M_{Hand} = 2.30$, $SE_{Hand} = 0.06$). Power was different between regions, $F(2.75,170.26) = 94.75$, $p \leq .001$, $\eta_p^2 = .604$, showing highest values for occipital ($M_O = 2.69$, $SE_O = 0.06$), then temporal ($M_T = 2.37$, $SE_T = 0.05$), then frontal regions ($M_F = 2.25$, $SE_F = 0.06$), and lowest values for parietal regions ($M_P = 2.14$, $SE_P = 0.06$). There were trends for Hemisphere, $F(1,62) = 3.39$, $p = .071$, $\eta_p^2 = .052$, and for the interaction between

Region, Hemisphere, and Risk Group, $F(3,186) = 2.21$, $p = .088$, $\eta_p^2 = .034$. No other main or interaction effects reached significance (p's ≥ .117, η_p^2's ≤ .031), including Risk Group, $F(1,62) = 1.06$, $p = .308$, $\eta_p^2 = .017$ (see Appendix A5.2 for additional graphs).

The graphs indicate that there might be an outlier in the HR-Atyp group. Analyses were therefore repeated while excluding this outlier. The pattern of results did not change compared to the results from the analyses including the outlier (see Appendix A5.3).

In summary, theta spectral power is higher for the toy than the hand condition, and differs between regions. There were no differences between risk groups however, and no further significant effects were observed. Possibly, similar effects occur for theta connectivity measures.

5.3.2.3. Functional theta connectivity

To investigate whether there were any differences between the hand and toy condition in global dbWPLI, I tested for differences between these conditions using related-samples Wilcoxon Signed Rank tests in SPSS. I chose this test because assumptions for normality and homogeneity of variance were not met for each of the variables in the groups (p's < .001). No significant differences in global dbWPLI between the hand and toy condition were found across all participants, or when tested within the LR, or HR groups separately (p's ≥ .303, r's ≤ .11) (see Fig. 5.5). Excluding the outlier from the analyses did not change these findings (Appendix A5.4).

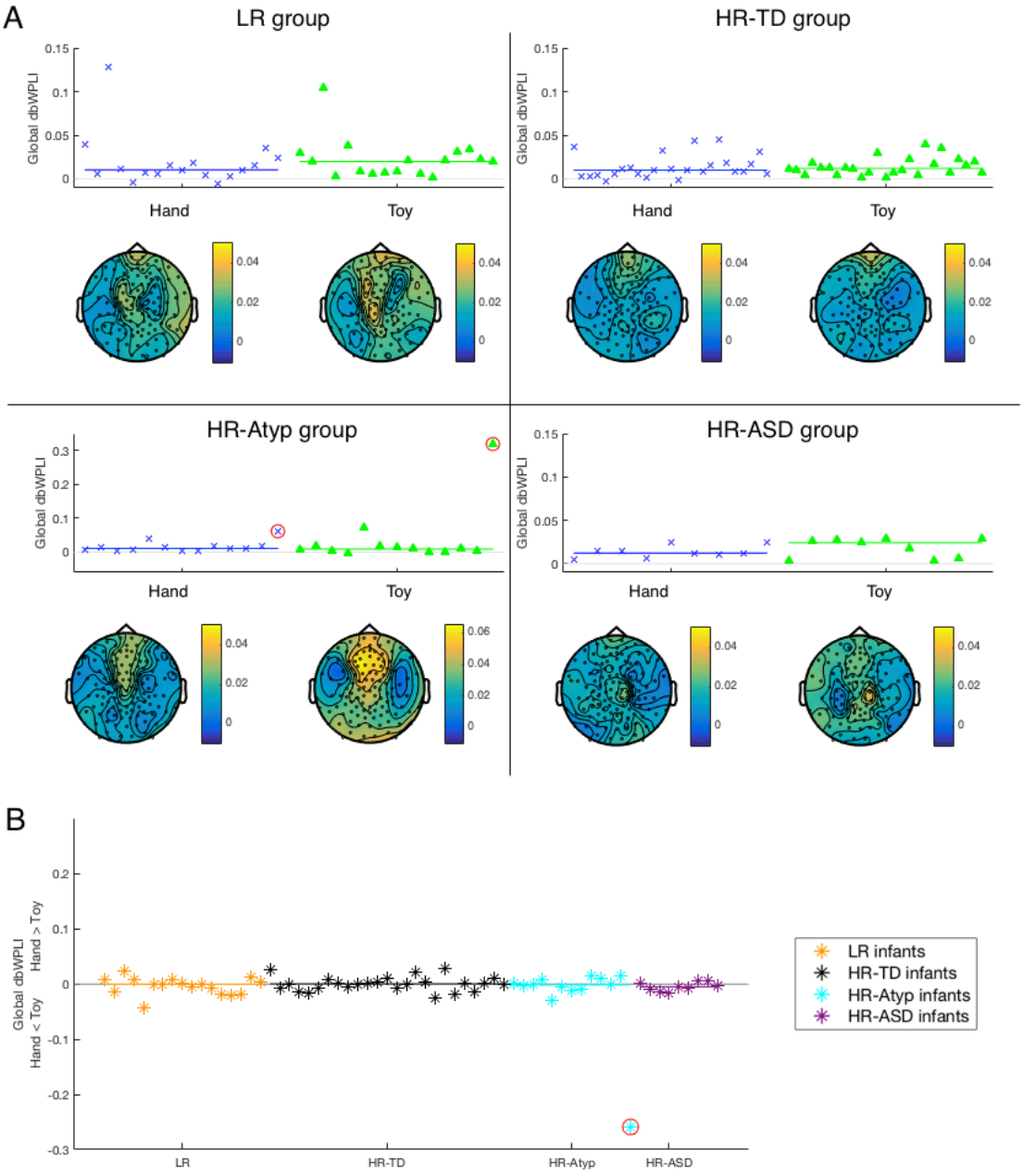

Figure 5.5. Global theta dbWPLI in the hand and toy condition

A) Global dbWPLI across all channels for individual infants for the hand and toy condition (blue crosses, and green triangles, resp.), with topoplots averaged across infants in the outcome groups (LR group in top left panel, HR-TD group in top right, HR-Atyp group in bottom left, and HR-ASD group in bottom right panel). B) Differences in global dbWPLI between the hand and toy condition for individual infants in the different outcome groups. Horizontal lines represent group medians. Note red circle marks an outlier in the HR-Atyp group.

Table 5.1. **Overview NBS results for comparisons between connectivity in the toy and hand condition**

Contrast Toy > Hand

Group	*N subjects*	*Min. N epochs*	*Threshold 3.5*	*Threshold 3.1*
All	64	90	NS	NS
	36	120	NS	NS
LR	17	90	NS	NS
HR	47	90	NS	1 network: 10 edges, 11 nodes, p = .045
	27	120	NS	NS
HR-TD	25	90	NS	NS
HR-Atyp	13	90	NS	NS
HR-ASD	9	90	NS	NS

Contrast Hand > Toy

Group	*N subjects*	*Min. N epochs*	*Threshold 3.5*	*Threshold 3.1*
All	64	90	NS	NS
	36	120	NS	NS
LR	17	90	NS	NS
HR	47	90	NS	NS

NS: no significant network observed by NBS analyses.

Results for the analyses with the NBS testing whether there are significant differences between conditions for each connection are displayed in table 5.1. In the HR group, a network with 10 edges and 11 nodes exhibited significantly increased theta connectivity values during the toy condition compared to the hand condition for threshold of 3.1 (p = .045). However, this effect did not survive correction for multiple comparisons, nor when infants with 120 or more epochs

were included in the analyses, nor when the effect in separate HR groups was tested (HR-TD, HR-Atyp, and HR-ASD), or when the outlier was excluded from these analyses (Appendix A5.4). Analyses using the opposite contrast showed that there were no networks where connectivity was consistently higher in the hand than in the toy condition, for any of the groups.

The observed effects in connectivity may be influenced by other measures, such spectral power or the number of epochs. The first GLM analysis performed included the factors Condition, and Risk Group only. None of the effects reached significance: for Condition, $p = .321$, $\eta_p^2 = .016$; for Risk Group, $p = .709$, $\eta_p^2 = .002$; and for the interaction, $p = .754$, $\eta_p^2 = .002$. When adding the difference in spectral theta power between the toy and hand condition across all channels as covariate, Condition showed a main effect, $F(3,61) = 8.49$, $p = .005$, $\eta_p^2 = .122$: theta connectivity was higher for the toy than the hand condition ($M_{\text{Toy}} = 0.021$, $SE_{\text{Toy}} = 0.004$; and $M_{\text{Hand}} = 0.017$, $SE_{\text{Hand}} = 0.003$). No other effects reached significance (p's ≥ .392, η_p^2's ≤ .012). The analysis including the number of epochs as a covariate did not alter the initial main results found in the non-parametric tests and NBS analyses (p's ≥ .317, η_p^2's ≤ .016). However, effect for Condition, Risk Group, or interactions did not reach significance when the outlier was excluded and spectral power or number of epochs were included as covariates (Appendix A5.4). This suggests that this single outlier is likely driving any observed effects of condition in connectivity.

In brief, theta spectral power was higher for the toy than hand condition, while no differences between conditions were observed for theta connectivity at global or network level. Any observed effects between conditions in connectivity were mostly driven by a single participant. Furthermore, risk groups did not show

any differences in spectral power and connectivity between the toy and hand condition. Since there were no differences between the hand and toy condition in theta connectivity, I decided to collapse data from these conditions into one non-social condition for comparisons between social and non-social stimuli. In order to provide a whole picture of the data, I also examined theta power differences between the social and non-social conditions. It is furthermore recommended to do spectral power analyses along connectivity analyses, since the former may influence the results of the latter (van Diessen et al., 2015).

5.3.3. Comparisons between the social and non-social condition

5.3.3.1. Participants

The final sample for the theta connectivity analyses comparing social and non-social conditions consisted of 17 LR, 27 HR-TD, 16 HR-Atyp, and 8 HR-ASD infants (Table 5.2). Only participants with 120 or more epochs in the social and non-social condition were included here. The ratio between males and females differed between the outcome groups, $\chi^2(3) = 12.09$, $p = .007$. At both 14 and 36 months of age, MSEL scores differed between groups, $F(3,64)=3.92$, $p = .012$. For MSEL scores at 14 months, there were no significant differences between the HR-ASD, HR-Atyp and HR-TD groups, or between the HR-Atyp, HR-TD, and LR groups in age. The former subset of three groups also displayed lower MSEL scores than the latter subset of three groups. At 36 months, the LR and HR-TD groups displayed similar MSEL scores, as did the HR-Atyp and HR-ASD groups. Scores in the LR and HR-TD groups were higher than the scores in the HR-Atyp and HR-ASD groups. There were no differences between groups for age of the EEG assessment, amount of epochs included for analyses, or age of the clinical assessment (p's ≥ .391).

Clinical data from the assessment at 36 months for each group are displayed in Table 5.3. The groups differed on each of the clinical assessment measures, *p*'s < .001: 1) For ADI-R Social Total algorithm, the HR-ASD group displayed higher scores than the other groups, with no significant differences between the LR and HR-TD groups, or between the LR and HR-Atyp groups. 2) For the ADI-R Communication Total algorithm, the HR-ASD group displayed the highest scores, while the LR group showed the lowest scores. The HR-Atyp and HR-TD did not significantly differ in scores and showed values intermediate of the HR-ASD and LR groups. 3) For the ADI-R Behaviour/ Repetitive Interests algorithm, values were higher in the HR-ASD group than the HR-Atyp group. The HR-Atyp group showed higher values than both the HR-TD and LR group, with no significant difference between the latter two groups. 4) For the ADOS-2 Social Affect algorithm, scores in the HR-ASD and HR-Atyp group did not significantly differ. These groups exhibited higher scores than the HR-TD group that in turn exhibited higher values than the LR group. 5) For the ADOS-2 Restricted and Repetitive Behaviour algorithm, the HR-ASD and HR-Atyp group, and the LR and HR-TD group displayed similar scores. The scores in the HR-ASD and HR-Atyp groups were higher than the scores in the LR and HR-TD groups.

Table 5.2. **Demographics of the sample for comparisons between the social and non-social condition**

	LR	*HR-TD*	*HR-Atyp*	*HR-ASD*	*Test statistics*
Number of participants (male)	17 (5)	27 (8)	16 (10)	8 (7)	$\chi^2(3) = 12.09$, $p = .007$
Age at EEG assessment, in days[3]	471 (34)	474 (35)	466 (28)	466(28)	$F(3,64) = 0.17$, $p = .917$
N epochs included in EEG [2]	143 (28) 123 – 177	145 (44) 121 – 233	148 (22) 130 – 161	139 (26) 130 – 161	$H(3) = 1.25$, $p = .741$[5]
Age at diagnostic assessment, in months [2]	38.0 (2.0)	39.0(2.0)	38.0 (3.0)	38.0 (3.0)	$H(3) = 3.01$, $p = .391$[5]
MSEL [a] Composite Standard Score at visit at 14 months	108 (16)[3] 86 – 133[6]	98 (14) 71 – 121	96 (15) 72 – 123	89 (12) 78 – 113	$F(3,64) = 3.92$, $p = .012$ (HR-ASD = HR-Atyp = HR-TD) > (HR-Atyp = HR-TD = LR)
MSEL [a] Composite Standard Score at visit at 36 months [b]	121 (8)[2] 95 – 137[6]	120 (26) 81 – 138	84 (25) 56 – 145	86 (42) 49 – 142	$H(3) = 22.27$, $p < .001$[5] (LR = HR-TD) > (HR-Atyp

					= HR-ASD)

[1] Pearson Chi-Square with asymptotic significance values (2-sided).

[2] Medians and interquartile range in parentheses, with results for the Independent-Samples Kruskal-Wallis test, and stepwise step-down follow-up analyses if significant p-value.

[3] Means and standard deviations in parentheses, with results for the analysis of variance with Group as factor (LR, HR-TD, HR-Atyp, HR-ASD).

[4] Exact 2-tailed.

[5] Asymptotic 2-tailed.

[6] Range with minimum and maximum score.

[a] Mullen Scale for Early Learning (MSEL).

[b] For the 36-month-old visit data for MSEL were missing for 2 LR infants.

Table 5.3. **Clinical information of the sample for comparisons between the social and non-social condition**

	LR	*HR-TD*	*HR-Atyp*	*HR-ASD*	*Test statistic*
ADI-R Social Total [1, a]	1.5 (3) [2] 0 – 3 [6]	1 (1) 0 – 5	2 (3) 0 – 8	12 (12) 7 – 25	$H(3) = 24.03$, $p < .001$[5] HR-ASD > (LR = HR-TD), and HR-ASD > (HR-Atyp = LR)

ADI-R, Communication Total [1, b]	0 (0) [2] 0 – 3 [6]	1 (3) 0 – 5	2.5 (5) 0 – 11	11 (3) 5 – 19	$H(3) = 24.79$, $p < .001$[5] HR-ASD > (HR-Atyp = HR-TD) > LR
ADI-R BRI Total [1, c]	0 (0) [2] 0 – 0 [6]	0 (0) 0 – 3	0.5 (2) 0 – 9	4 (3) 2 – 8	$H(3) = 26.58$, $p < .001$[5] HR-ASD > HR-Atyp > (HR-TD = LR)
ADOS-2, SA Total [2, d]	3 (4) [2] 0 – 12 [6]	1 (1) 0 – 4	7.5 (8) 0 – 13	9 (13) 2 – 20	$H(3) = 30.68$, $p < .001$[5] (HR-ASD = HR-Atyp) > LR > HR-TD
ADOS-2 RRB Total [2, e]	1 (1) [2] 0 – 4 [6]	0(1) 0 – 3	2 (2) 0 – 6	3.5 (4) 1 – 6	$H(3) = 20.62$, $p < .001$[5] (HR-ASD = HR-Atyp) > (LR = HR-TD)

Medians and interquartile range in parentheses, and range with minimum and maximum score below. The last column represents results for the Independent-Samples Kruskal-Wallis test with asymptotic 2-tailed p-values,

and stepwise step-down follow-up analyses if p-value is below 0.05.

[1] Data for ADOS-2 were missing for 2 LR infants.

[2] Data for ADI-R were missing for 9 LR infants, and 1 HR-ASD infant.

[a] Autism Diagnostic Interview – Revised, Social Algorithm Total at 36 months.

[b] Autism Diagnostic Interview – Revised, Communication Algorithm Total at 36 months.

[c] Autism Diagnostic Interview – Revised, Behaviours/ Repetitive Interests Algorithm Total 36 months.

[d] Autism Diagnostic Observation Scale – 2, Social Affect Total 36 months.

[e] Autism Diagnostic Observation Scale – 2, Restricted and Repetitive Behaviours Total 36 months.

5.3.3.2. Spectral power

As in the series of analyses for the toy versus hand condition, I started with comparing spectral power values for the social and non-social conditions (global power values and topoplots in Fig. 5.6). For power across all channels, a 2x2 mixed model ANOVA was used with Condition (Social, Non-Social) as within-subject factor, and Risk Group (LR, HR) as between-subject factor. The assumptions of normality were met for each variable (p's ≥ .273). The assumption for homogeneity of variance across groups was met for the non-social condition (p = .183), but not for the social condition (p = .015).

There was a significant main effect of Condition: theta power across all channels was higher for the social than the non-social condition, $F(1,66) = 13.04$, p = .001, η_p^2 = .165 (M_{Soc} = 2.54, SE_{Soc} = 0.07; and $M_{N\text{-}Soc}$ = 2.45, $SE_{N\text{-}Soc}$ = 0.06). No other main or interaction effects were observed (p's ≥ .130, η_p^2's ≤ .034).

To test whether there were any differences in regions or hemispheres in theta power, a 2x4x2x2 mixed model ANOVA was used with Condition (Social, Non-

Social), Region (Frontal, Temporal, Parietal, Occipital), and Hemisphere (Left, Right) as within-subject factors, and Risk Group (LR, HR) as between-subject factor. Assumptions for normality were met for most variables (p's ≥ .069), except in the HR group for right parietal during the social condition, and both left and right parietal areas for the non-social condition, and right temporal during the non-social condition (p's ≤ .047). Assumptions for homogeneity of variance were met for most variables (p's ≥ .051), except for left and right frontal and occipital regions, and right temporal region during the social condition, and left occipital during the non-social condition (p's ≤ .050). For factors for which the assumption of sphericity was not met, Huynh-Feldt corrected degree of freedom values are reported, as the estimates were larger than .75.

Main effects for Condition, Region, and Hemisphere each reached significance. Theta power was higher for the social than the non-social condition, $F(1,66) = 12.64$, $p = .001$, $\eta_p^2 = .161$ ($M_{Soc} = 2.51$, $SE_{Soc} = 0.07$; and $M_{N\text{-}Soc} = 2.42$, $SE_{N\text{-}Soc} = 0.06$). Overall power differed between regions, $F(2.65,174.89) = 110.72$, $p < .001$, $\eta_p^2 = .627$, showing highest values for occipital ($M_O = 2.84$, $SE_O = 0.07$), then temporal ($M_T = 2.44$, $SE_T = 0.06$), and frontal regions ($M_F = 2.35$, $SE_F = 0.07$), and lowest values for parietal regions ($M_P = 2.22$, $SE_P = 0.07$). Theta power was higher in the left than right hemisphere, $F(1,66) = 8.97$, $p = .004$, $\eta_p^2 = .120$ ($M_{LH} = 2.50$, $SE_{LH} = 0.07$, and $M_{RH} = 2.43$, $SE_{RH} = 0.07$). There was no main effect of Group ($p = .136$, $\eta_p^2 = .033$).

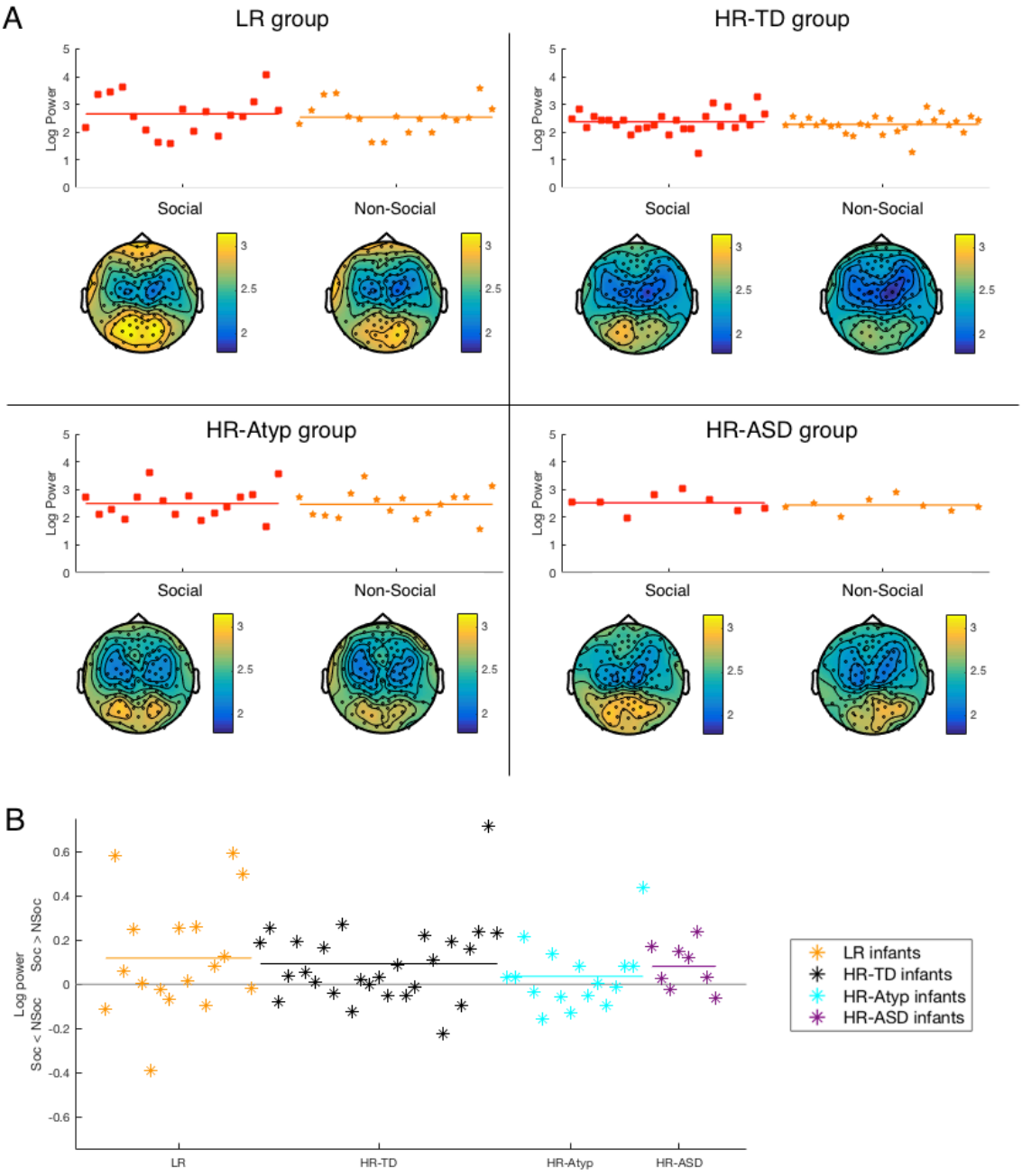

Figure 5.6. Global theta power in the social and non-social condition

A) Global power across all channels for individual infants for the social and non-social conditions (red squares, and orange pentagrams, resp.), with topoplots averaged across infants in the outcome groups (LR group in top left panel, HR-TD group in top right, HR-Atyp group in bottom left, and HR-ASD group in bottom right panel). B) Differences in global power between the social and non-social conditions for individual infants in the different outcome groups. Horizontal lines represent group means.

The interaction effects between Condition and Region, and Condition and Hemisphere also reached significance: $F(2.50,162.27) = 24.56$, $p < 0.001$, $\eta_p^2 = .271$; and $F(1,66) = 5.36$, $p = .024$, $\eta_p^2 = .075$, resp. Among different regions, the difference between conditions was strongest in the occipital area ($t(67) = 5.85$, $p < .001$, $d = .348$). The effects were weaker in the frontal and parietal areas ($t(67) = 4.61$, $p < .001$, $d = .270$, and $t(67) = 2.70$, $p = .009$, $d = .112$, resp.), whereas the effect was not significant in the temporal area ($p = .830$, , $d = .014$). Furthermore, the difference between conditions was stronger in the left hemisphere than in the right hemisphere ($t(67) = 4.06$, $p < .001$, $d = .237$, and $t(67) = 3.10$, $p = .003$, $d = .155$, resp.). No other main or interaction effects were observed (p's ≥ .094, η_p^2's ≤ .033, see Appendix A5.5 for additional graphs).

In summary, theta power was overall higher for the social than the non-social condition. Theta increases for the social condition were higher in occipital areas than in frontal and parietal areas, and higher across the left than the right hemisphere. No differences in overall theta spectral power or increases with the social condition were observed between the risk groups.

5.3.3.3. Functional theta connectivity

To investigate whether there were any differences between the social and non-social condition in global dbWPLI, I tested for differences between these conditions using related-samples Wilcoxon Signed Rank tests. I chose this test because assumptions for normality and homogeneity of variance were not met for each of the variables in the groups (p's ≤ .002). Data for dbWPLI across the social and non-social contained are displayed in Figure 5.7.

The difference between conditions for global dbWPLI reached significance when compared across all groups, showing increased connectivity during social

than non-social stimuli (Mdn_{Soc} = 0.0160, and $Mdn_{N\text{-}Soc}$ = 0.0114; T = 1779, p < 0.001, r = .32). In the LR group, the difference between conditions reached significance (Mdn_{Soc} = 0.0207, and $Mdn_{N\text{-}Soc}$ = 0.0100; T = 137, p = .004, r = .49). In the HR combined group, the difference between the social and non-social condition did reach significance as well (Mdn_{Soc} = 0.0160, and $Mdn_{N\text{-}Soc}$ = 0.0118; T = 939, p = .010, r = .26). The difference between conditions reached a trend in the HR-TD group (Mdn_{Soc} = 0.0167, and $Mdn_{N\text{-}Soc}$ = 0.0118; T = 268, p = .058, r = .26). There were no significant differences between conditions in the HR-Atyp, or HR-ASD groups (T = 91, p = .234, r = .21, and T = 27, p = .208, r = .32, resp.).

To further examine differences between risk and outcome groups, I used an Independent Samples Mann-Whitney U test for group comparisons on the differences in global dbWPLI for the social and non-social condition. The effect for Risk Group reached a trend, where differences in connectivity between conditions were lower for HR group than the LR group (U = 311, z = -1.74, p = .083, r = -.21; Mdn_{LR} = 0.0093, and Mdn_{HR} = 0.0042). The comparisons between the LR and separate HR groups revealed similar small effect sizes; for the LR versus HR-TD group (U = 162, z = -1.63, p = .104, r = -.25; Mdn_{LR} = 0.0093, and $Mdn_{HR\text{-}TD}$ = 0.0045;), for the LR versus HR-Atyp group (U = 100, z = -1.63, *exact* p = .204, r = -.23; Mdn_{LR} = 0.0093, and $Mdn_{HR\text{-}Atyp}$ = 0.0031), and for the LR versus HR-ASD group (U = 49, z = -1.11, *exact* p = .288, r = -.22; Mdn_{LR} = 0.0093, and $Mdn_{HR\text{-}ASD}$ = 0.0068). Comparisons between the separate HR groups exhibited even smaller effect sizes: for the HR-TD versus HR-Atyp group (U = 209, z = -.18, p = .860, r = -.03; $Mdn_{HR\text{-}TD}$ = 0.0045, and $Mdn_{HR\text{-}Atyp}$ = 0.0031;), for the HR-TD versus HR-ASD group (U = 116, z = .314, *exact* p = .773, r = .05; $Mdn_{HR\text{-}TD}$ = 0.0045, and $Mdn_{HR\text{-}ASD}$ = 0.0068), and for

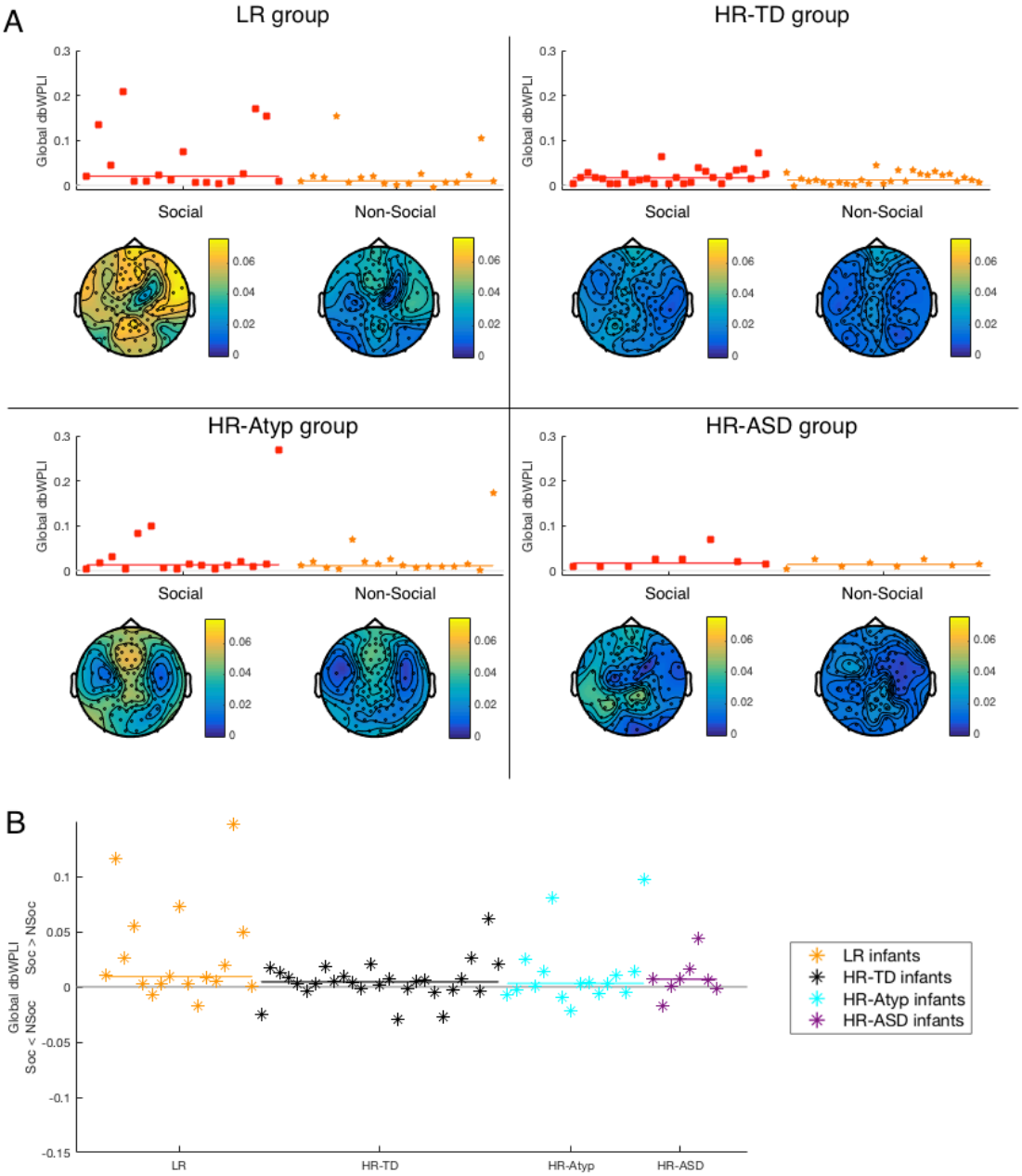

Figure 5.7. Global theta dbWPLI in the social and non-social condition

A) Global dbWPLI across all channels for individual infants for the social and non-social conditions (red squares, and orange pentagrams, resp.), with topoplots averaged across infants in the outcome groups (LR group in top left panel, HR-TD group in top right, HR-Atyp group in bottom left, and HR-ASD group in bottom right panel). B) Differences in global dbWPLI between the social and non-social conditions for individual infants in the different outcome groups. Horizontal lines represent group medians.

the HR-Atyp versus HR-ASD group (U = 71, z = .429, *exact* p = .697, r = .09; $Mdn_{HR\text{-}Atyp}$ = 0.0031, and $Mdn_{HR\text{-}ASD}$ = 0.0068). Together, these findings suggest that global theta connectivity is higher for the social than non-social condition. This difference is marginally stronger in the LR group than the HR group, and similar across the HR-TD, HR-Atyp, and HR-ASD group.

In addition to differences in global theta connectivity, differences between the social and non-social condition may be stronger at specific regions or connections. To test for differences between conditions at the level of individual connections, I used the NBS program with the t-test with a repeated measures design matrix in NBS program. The results for the NBS analyses testing for higher connectivity in the social than non-social condition, and the opposite contrast are presented in Table 5.4. Graphs of the network are displayed in Figure 5.8.

Table 5.4. **Overview of NBS results for comparisons between the social and non-social condition**

Contrast Social > Non-Social

Group	*N*	*Threshold 3.5*	*Threshold 3.1*	*Threshold 2.5*
Across all groups	68	2 networks: 1) 44 edges, 31 nodes, p = .001 2) 4 edges, 5 nodes, p = .043	1 network: 186 edges, 83 nodes, p < .001	1 network: 843 edges, 115 nodes, p < .001
LR	17	1 network: 6 edges, 6 nodes, p = .032	1 network: 30 edges, 26 nodes, p = .023	1 network: 305 edges, 104 nodes, p = .009
HR	51	1 network: 6 edges, 6 nodes, p = .036	1 network: 19 edges, 18 nodes, p = .047	1 network: 255 edges, 100 nodes, p = .008

HR-TD	27	NS	NS	NS
HR-Atyp	16	NS	NS	NS
HR-ASD	8	NS	NS	NS

Contrast Non-Social > Social

Group	*N*	*Threshold 3.5*	*Threshold 3.1*
All	68	NS	NS
LR	17	NS	NS
HR	51	NS	NS
HR-TD	27	NS	NS
HR-Atyp	16	NS	NS
HR-ASD	8	NS	NS

NS: no significant network observed by NBS analyses.

The NBS results revealed significant networks that showed higher activation during the social than the non-social condition when compared across all groups, the LR group, and the HR combined group. The networks observed in the LR and HR groups showed different topologies. The LR network displayed more pronounced connections between parietal and occipital areas, whereas the HR network contained more pronounced connections between frontal and parietal areas. No significant networks were observed in the HR-TD, HR-Atyp, or HR-ASD group that showed higher activation in the social than the non-social condition. There were no significant networks showing higher connectivity for the non-social than social condition in any of the groups tested: across all groups, LR group, HR combined group, HR-TD group, HR-Atyp group, or HR-ASD group.

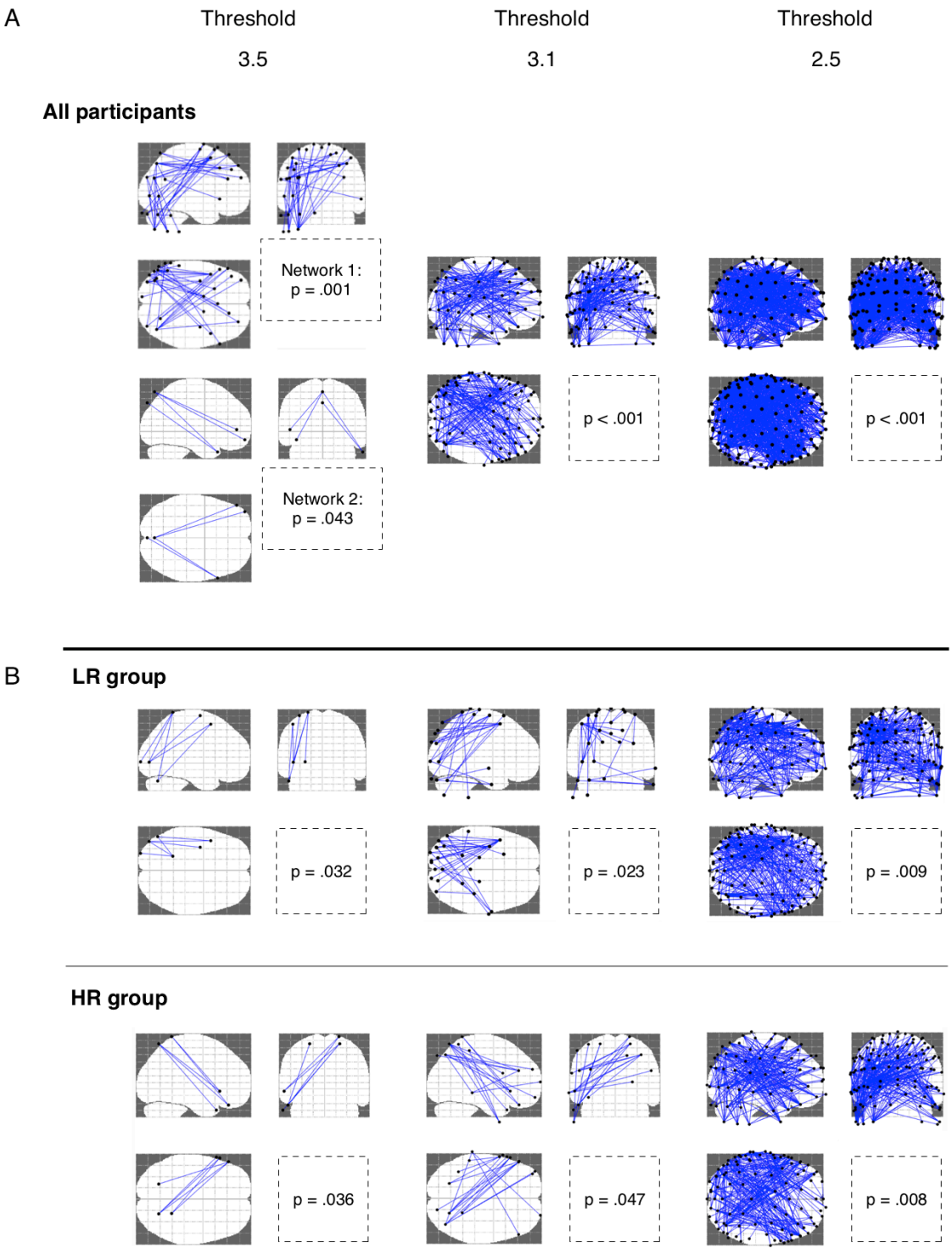

Figure 5.8. Significant networks showing higher connectivity for the social than the non-social condition

Networks reaching significance for across all participants (A), and in separate risk groups (B: LR group upper row, and HR in lower row), for different thresholds in different columns (Threshold 3.5 left, 3.1 middle, and 2.5 right column). Specific numbers of edges and nodes in the networks are reported in table 5.4.

Finally, I examined whether the connectivity results may have been affected by theta band spectral power, or the number of epochs connectivity was calculated across. Without taking into account any covariates into the GLM with Condition and Risk Group, there was a significant main effect of Condition, $F(1,66) = 20.04$, $p < .0001$, $\eta_p^2 = .233$, and for the interaction between Condition and Risk Group, $F(1,66) = 6.80$, $p = .011$, $\eta_p^2 = .098$, suggesting that theta connectivity was higher in the social than non-social condition, and that this difference was stronger in the LR group than the HR group. The main effect of Risk Group reached a trend, $F(1,66) = 2.81$, $p = .098$, $\eta_p^2 = .041$. Including the difference in spectral power decreased the effect size for the effect for Condition, $F(1,65) = 6.20$, $p = .015$, $\eta_p^2 = .087$, and increased the effect size for the interaction between Condition and Risk group, $F(1,65) = 7.53$, $p = .008$, $\eta_p^2 = .104$, while both still reached significance. The effect of Risk Group became weaker and did no longer reach significance, $p = .159$, $\eta_p^2 = .03$. Including the number of epochs did not change the observed interaction effect between Condition and Risk group, $F(1,65) = 6.66$, $p = .012$, $\eta_p^2 = .093$, but the effect for Condition again was decreased, $p = .560$, $\eta_p^2 = .005$, as was the effect of Risk Group, $p = .117$, $\eta_p^2 = .037$. Together these findings suggest that theta spectral power and the number of epochs play a large role in the effects of Condition and Risk Group in theta connectivity, but a smaller role in the differences between the risk groups in the connectivity differences between the social and non-social condition.

In sum, both the LR and the HR groups displayed higher connectivity for the social than the non-social stimuli. The topology of the connections showing condition differences was different between the LR and HR combined groups. The HR-Atyp and HR-ASD group displayed no differences in connectivity between

conditions. These results were consistent across the global connectivity and network analyses. For the HR-TD group, global connectivity differences between conditions reached a trend. The network analyses however did not reveal any specific connections showing differences between conditions in the HR-TD group.

5.3.2.3.1. Exploratory analyses: risk or compensatory networks?

The analyses above identified different networks showing increased activation during social stimulation in the LR and HR combined groups. The next question is how this finding might arise. One possibility is that the HR network reflects the configuration of risk topology. Alternatively, the HR network might represent a protective factor, as the difference between conditions was strongest in the HR-TD group amongst the HR groups in the global connectivity analyses. To this end, I explored network topologies in HR-TD, HR-Atyp, and HR-ASD groups. If the HR network represents a risk network, the topology of the network in the HR-ASD group would display a closer resemblance to the topology of the HR network than the topology of the network in the HR-TD group. If the HR network arises from a protective factor, the topology of the HR-TD network would display more similarities with the HR network than the topology of the network in the HR-ASD group. In order to examine the network topology in the separate HR groups, NBS analyses were repeated while changing the threshold and the p-value for the HR-TD group, HR-Atyp group, and HR-ASD group separately. Tables reporting results and the different thresholds and p-values used are reported in the Appendix A5.6. Figure 5.9 gives a comprehensive overview of the findings.

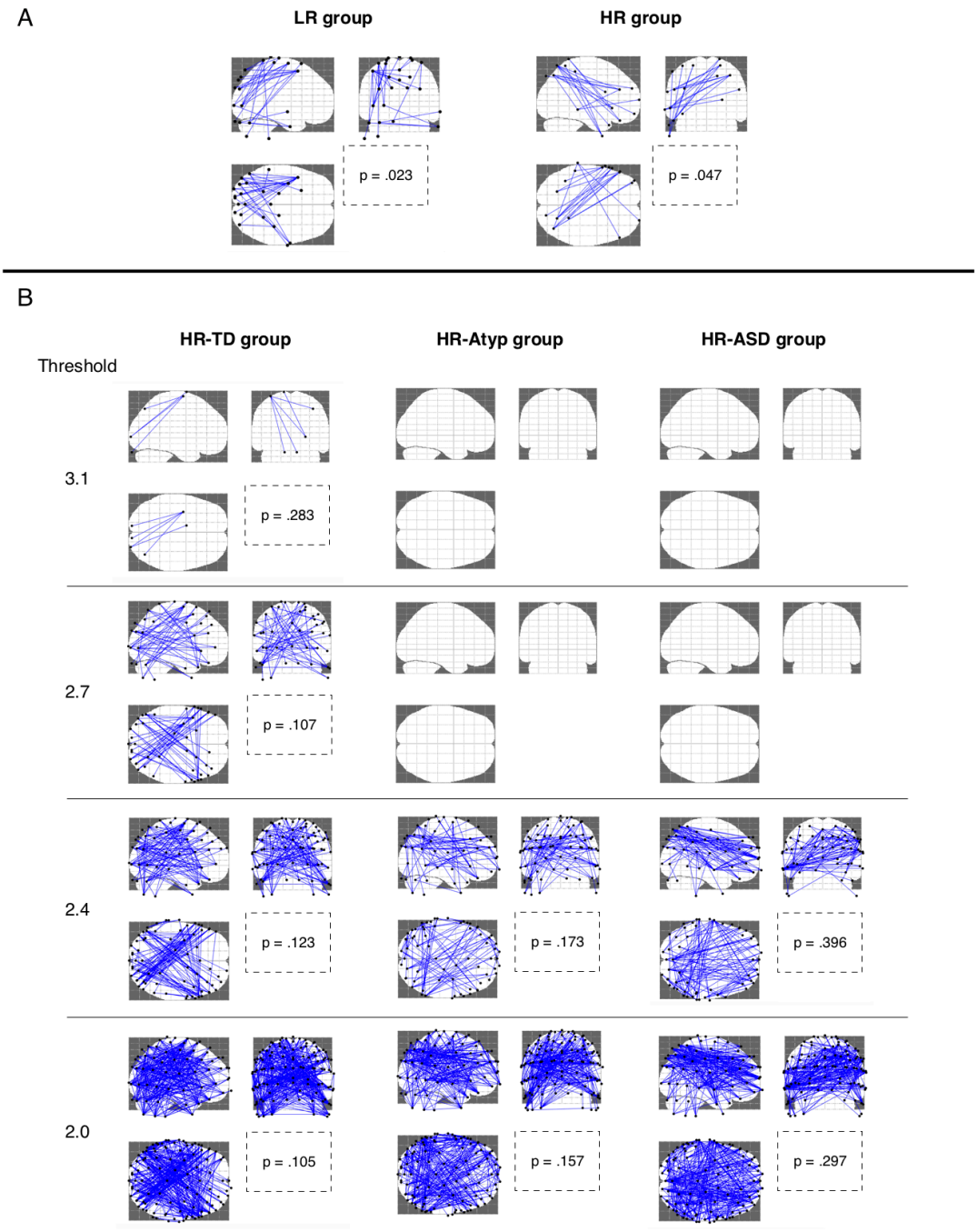

Figure 5.9. Results for exploratory analyses for risk or compensatory networks

A) Previous findings from the NBS analyses in the LR and HR group for threshold 3.1. B) Significant networks for the HR-TD (left), HR-Atyp (middle), and HR-ASD group (right) are displayed in left, middle, and right columns, respectively. If no significant network was found, the network graph is empty. Each row reflects a different threshold used with p-value 0.4 set as NBS criteria.

The effect of significant networks seems stronger for the HR-TD group than the HR-Atyp, which in turn shows stronger effects than HR-ASD groups, since significant networks emerge with higher thresholds and lower p-values compared to the other groups. This is in line with the SPSS findings in the previous section, and likely arises from differences in sample sizes in these groups. The network in the HR-ASD group seems to involve more frontal, temporal, and parietal connections, whereas the network in the HR-TD group shows significant condition differences in temporal, parietal, and occipital regions. Overall the topology of the HR group at threshold 3.1 displays more resemblance to the HR-ASD group than the HR-TD group, which is consistent with the HR network being a risk topology. This suggests that the HR network may be related to risk rather than compensatory factors.

5.3.4. Functional connectivity and dimensional traits

Finally, I examined whether differences between conditions in theta power and connectivity measures were related to social and communication difficulties using Spearman's correlations. The results for analyses with log power, and theta connectivity are displayed in table 5.5 and 5.6, respectively (and Appendix A5.7 for scatterplots).

Table 5.5. **Associations between differences in log power for the social and non-social condition, and measures of ASD traits across the whole group**

Measure	*N*	*Domain*	*Power averaged across all channels*	*Power averaged across channels from HR mask*
ADOS-2	*66*	*SA* [a]	r = .13, p = .291, [-.11, .36]	**r = .24, p = .048, [.01, .46]**
		RRB [b]	r = .09, p = .491,	r = .10, p = .405,

			[-.16, .34]	[-.14, .35]
ADI-R	*58*	*SaC* [c]	*r* = .02, *p* = .899,	*r* = .08, *p* = .539,
			[-.22, .28]	[-.18, .33]
		RRB [d]	*r* = -.10, *p* = .436,	*r* = -.02, *p* = .871,
			[-.33, .15]	[-.28, .23]
VABS	*66*	*Com* [e]	*r* = -.08, *p* = .548,	*r* =- .10, *p* = .414,
			[-.32, .19]	[-.34, .16]
		Soc [f]	*r* = .13, *p* = .292,	*r* = .14, *p* = .262,
			[-.13, .37]	[-.13, .38]

Spearman's rho values (*r*), with p-values, and bias corrected and accelerated bootstrap 95% confidence intervals in square brackets. Correlations in bold reached significance (uncorrected for multiple comparisons).

[a] Autism Diagnostic Observation Scale – 2, Social Affect Total 36 months.

[b] Autism Diagnostic Observation Scale – 2, Restricted and Repetitive Behaviours Total 36 months.

[c] Autism Diagnostic Interview – Revised; Social and communication score: sum of the scores of the social domain and communication domain in the ADI-R.

[d] Autism Diagnostic Interview – Revised; Restricted and Repetitive Behaviours.

[e] VABS Communication domain Standard Score.

[f] VABS Socialization Standard Score.

Table 5.6. **Associations between differences in connectivity for the social and non-social condition, and measures of ASD traits across the whole group**

Measure	*N*	*Domain*	*dbWPLI averaged across all connections*	*dbWPLI averaged across connections from HR mask*
ADOS-2	*66*	*SA* [a]	*r* = .19, *p* = .138,	*r* = .20, *p* = .108,
			[-.10, .44]	[-.07, .44]
		RRB [b]	*r* = -.05, *p* = .679,	*r* = -.03, *p* = .796,
			[-.31, .21]	[-.28, .23]
ADI-R	*58*	*SaC* [c]	*r* = -.10, *p* = .440,	*r* = .06, *p* = .660,
			[-.35, .15]	[-.25, .33]
		RRB [d]	*r* = -.03, *p* = .840,	*r* = .14, *p* = .290,

			[-.27, .21]	[-.12, .38]
VABS	*66*	*Com* [e]	r = .15, p = .236, [-.35, .34]	r = .02, p = .852, [-.21, .23]
		Soc [f]	r = .06, p = .620, [-.16, .28]	r = -.08, p = .540, [-.34, .16]

Spearman's rho values (*r)*, with p-values, and bias corrected and accelerated bootstrap 95% confidence intervals in square brackets.

[a] Autism Diagnostic Observation Scale – 2, Social Affect Total 36 months.

[b] Autism Diagnostic Observation Scale – 2, Restricted and Repetitive Behaviours Total 36 months.

[c] Autism Diagnostic Interview – Revised; Social and communication score: sum of the scores of the social domain and communication domain in the ADI-R.

[d] Autism Diagnostic Interview – Revised; Restricted and Repetitive Behaviours.

[e] VABS Communication domain Standard Score.

[f] VABS Socialization Standard Score.

For log power, one association reached significance: larger average power differences between conditions across the selected channels from the HR3.1 network were related to higher ADOS-2 Social Affect scores (r = .24, p = .048). This association did not reach significance in the LR group (p = .280), nor the HR group (p = .106). Further, the results across all infants would not survive correction for multiple comparisons. For theta connectivity, no significant associations with the scores in domains of the ADOS-2, ADI-R, or VABS were observed.

The results of correlations between neural responses and behaviours do not show a clear consistent pattern. Although it seemed that larger power differences between conditions across selected channels were related to higher scores on the ADOS-2 Social Affect domain, this effect was weak and not observed in separate risk groups. No significant associations were observed for connectivity measures.

5.4. Discussion

The current study aimed to investigate social processing in infants at high risk for ASD by focusing on differences in theta frequency responses to social and non-social stimuli. The results showed that theta spectral power was higher during the social than the non-social condition. The theta power increases with condition were more pronounced in occipital areas than in frontal and parietal areas, and in the left than in the right hemisphere. No differences between the risk or outcome groups in overall power or effects of condition were found.

Global theta connectivity was higher during social than non-social stimulation across all infants, and in the LR and HR groups. This effect was stronger in the LR group than the HR group, but similar between the HR-TD, HR-Atyp, and HR-ASD groups. The network analyses revealed specific networks that showed higher connectivity in the social than the non-social condition across all infants. The network showing increased theta connectivity with social stimuli in the LR group showed a different topology from the network found in the HR group. Exploratory analyses suggested that the HR network might be related to risk factors.

Finally, there were no strong associations between theta increases in power or connectivity and any of the behavioural measures (ADOS-2 Social Affect, ADOS-2 Restricted and Repetitive Behaviours, ADI-R Social and Communication, ADI-R Behaviours/ Repetitive Interests, VABS-II Communication, and VABS Socialization).

5.4.1. Theta power increases for social stimuli

Theta power was overall increased for social stimuli compared to non-social stimuli. This is consistent with the previous study by Jones and colleagues (2015) that showed increased activation for social stimuli compared to spinning toys in typically developing infants at 12 months. In these 12-month-old infants, the differences between conditions were stronger in both occipital and frontal regions, and absent in temporal and parietal regions. The 14-month-olds in this study show stronger condition effects in occipital regions as well, but the effect is less pronounced in frontal regions and parietal regions, while absent in temporal regions. One possible explanation for the differences in these findings is that magnitudes and topology of theta responses to social stimuli change with age. At younger ages, changes in theta are more prominent in frontal areas, whereas in older children changes are more prominent in parieto-occipital areas (Orekhova et al., 2006; Orekhova et al., 1999).

The increase in frontal activation in younger infants during social stimulation could be explained by the greater need for allocation or internal control of attention while watching socially engaging videos, whereas older infants do not need this additional control. The prefrontal cortex is known to be involved in executive functioning and attentional control, and might play a role in the coordination of activation in sensory and motor regions (Grossmann, 2015; Johnson, Jones, & Gliga, 2015). According to the Interactive Specialization (IS) view (Johnson et al., 2005; Johnson, 2011; Johnson, Grossmann, & Cohen Kadosh, 2009), neural activation patterns and interactions between brain areas in response to specific stimuli become more specialized and fine-tuned toward a specific set of stimuli. It has been suggested that regions involved in the social brain network

such as the prefrontal cortex, and superior temporal sulcus (STS) become more specialized to the processing of social stimuli compared to non-social stimuli. As a result, activations in response to stimuli should become more localized, and decrease in amplitude. Less additional activations from the prefrontal cortex to allocate resources are needed with increasing specialization of the brain toward social stimuli. This would explain why the theta increases with social processing are strongest frontally in the 12-month-olds, and weaker in frontal areas in the 14-month-olds investigated here.

Since infants who later develop ASD show atypical social processing, it was hypothesized that HR-ASD infants might show differences in theta increases towards social stimuli compared to LR, HR-TD, or HR-Atyp infants. This study however found no differences in theta power increases between risk groups. This suggests that infants at high risk for ASD show similar social processing as infants at low risk at 14 months of age. These results are in line with other studies showing typical social processing in HR-ASD infants around their first birthday. For example, one study found neural processing differences between HR-ASD infants and HR-no ASD infants in social processing at 6 months of age, but not at 12 months of age (Jones et al., 2016). Another study showed that there were no differences between LR, HR-TD, HR-Atyp, or HR-ASD infants in gaze following at 7 or 13 months of age (Bedford et al., 2012). Toddlers in the HR-ASD group furthermore displayed identical looking behaviours (initial and second looks, looking duration) to social and toy stimuli as their peers in the LR and HR-no ASD groups (Vernetti et al., 2018). Note, the current findings cannot be attributed to differences in visual preferences for social or non-social stimuli expressed by differences in looking behaviours (Pierce et al., 2016, 2011), since only EEG epochs

where the infant was looking at the stimuli was included, and the amount of included epochs for the social and non-social conditions was identical. Possibly, differences between HR groups in theta responses to social stimuli arise at other ages than investigated here. It is also possible that differences exist in the connections between regions rather than in the amplitude of the oscillations as will be discussed in the next section.

5.4.2. Theta connectivity differences between social and non-social stimuli

Connectivity across the brain was higher during the viewing of social stimuli than during the non-social stimuli. This effect was found for whole brain connectivity and across specific connections. The network graphs revealed that the connections that showed the most consistent differences across all participants were between frontal central regions and occipital parietal regions. These findings extend the power results that also showed higher activation for the social than the non-social condition, with strongest differences in the occipital region.

Further analyses showed that this difference between conditions was also significant within the LR group and within the HR group, and is stronger in the LR group than the separate HR groups. The differences between conditions were stronger in the HR-TD group than the HR-Atyp group, which in turns were stronger than the HR-ASD group. However, these differences in strengths of condition effects between groups are probably related to the different group sample sizes, where smaller groups showed smaller effects. The topologies of the networks differ also. The LR group exhibited stronger connectivity across central, parietal, and occipital regions during the social condition than during the non-social condition. The HR group displayed stronger connectivity across prefrontal and parietal regions during the social condition than during the non-social

condition. These results cannot be related spectral power, since those analyses did not show group differences, and taking into account spectral power did not strongly change the interaction effect between condition and risk group. One possible account for this finding is that HR infants need extra attentional resources to integrate the social information across sensory cortices due to atypical or delayed specialization of the brain towards social stimuli (Johnson, 2011; Johnson et al., 2009). LR infants would not require this extra frontal activation for the allocation of attention, as their brain responses are more fine-tuned to social processing compared to the HR infants. Furthermore, altered connectivity patterns in the HR group may be part of the adaptive response. It is possible that these alterations are related to network reorganisation in response to atypical neural processing (Johnson, 2017; Johnson et al., 2015).

Further exploratory analyses suggest that the network found in the HR group may be associated with risk rather than compensatory (or adaptive) processes. The topologies of the networks in de different HR-TD, HR-Atyp and HR-ASD groups looked different. The network in the HR-ASD infants showed a weaker effect of condition and involved more prefrontal, temporal, and parietal areas, whereas the HR-TD network showed a stronger effect and involved more temporal, parietal, and occipital areas. Overall the HR network seemed more similar to the HR-ASD network, which would provide evidence for a risk network. This is however a tentative conclusion, and further research is needed to examine the risk and compensatory mechanisms in EEG connectivity. It thus remains unknown whether the network found in the HR group is related to risk or compensatory processes.

The current findings suggest that there are no differences in connectivity in response to social stimuli between the HR groups. It is possible that differences between the HR groups emerge at a different ages than 14 months, for example later in life when behavioural differences start to emerge. Prospective longitudinal behavioural studies have shown that the frequency of social behaviours such as gaze to faces and smiling are similar LR and HR-ASD infants at 6 months, but start to become less frequent in HR-ASD infants than in LR infants between 12 and 18 months (Ozonoff et al., 2010). Differences between HR-TD, HR-Atyp, and HR-ASD groups in the social and communication domains start to unfold during the second year of life (Estes et al., 2015; Hudry et al., 2014). Network differences between the LR and HR groups in response to social stimuli might be evident during the beginning of the second year of life, whereas differences between the HR-TD, HR-Atyp, and HR-ASD group become apparent during the end of the second year of life. This is in line with a recent review that found mixed support for atypical functioning in the social brain during the first year of life. Atypical development of brain networks supporting integration of multisensory information becomes evident when required for more complex behaviours at older ages. These atypicalities are furthermore related to the broader ASD phenotype rather than ASD outcome (Elsabbagh & Johnson, 2016). Future research with longitudinal designs will be needed to further investigate this.

Another possibility is that differences are evident in the organisation of connectivity patterns, rather than whole brain connectivity or brain connectivity averaged across specific regions or connections. Future research can examine this possibility by using graph theory metrics such as small-worldness, clustering and

path length which reflect levels of segregation and integration of a brain network (Bullmore & Sporns, 2009).

5.4.4. Associations between theta oscillations and social and communication behaviours

The current study also aimed to explore associations between theta increases in response to social stimuli, and social and communication skills. The results did not show a clear pattern of associations for spectral power or connectivity measures. One possibility is that the directions of associations within groups are different. If specialization towards social stimuli is atypical or delayed, associations between neural responses and social and communication behaviours might be different between groups. For example, typically developing infants (LR and HR-TD) with smaller differences between conditions in neural responses to social stimuli might experience better communication skills. Atypically developing infants (HR-Atyp and HR-ASD) with larger differences between conditions in neural responses might show better communication skills. If the groups were taken together, the resulting correlation would not reach significance. Naturally, sample size and strength of the associations also might have played a role. For only 7 HR-ASD infants, and 8 LR infants ADI-R data were available.

Another possibility is that differences in measures across the HR network are not as informative of atypical social processing as differences in connections across LR network or the network found across all participants. If strong differences between conditions in the LR network are related to better communication skills, smaller differences may be related to difficulties in communication. Finally, associations between neural responses and behaviours are small, which makes them more difficult to pick up in small samples.

Associations may furthermore be stronger with measures at other ages when behavioural differences clearly emerge.

5.4.5. Theta power differences between toy and hand stimuli

The comparisons for power between the toy and hand conditions revealed increased theta power for the toy condition compared to the hand condition, which was similar across groups. One way of explaining these results is by considering previous experience with these events. By the age of 14 months, infants will have had many experiences observing caregivers spinning toys using their hands. It is possible that the hand stimuli display more familiar events and therefore require less control of attention, whereas the toy stimuli display unfamiliar events that require more control of attention. Alternatively, theta oscillations have been related to emotional processing. The unfamiliarity of the toy stimuli could elicit a positive state related to the increase in theta power (Saby & Marshall, 2012).

5.4.6. Limitations

There are a few limitations to this study. First, analyses for comparisons between the toy and hand conditions and between the social and non-social conditions were performed with different subsets of infants, since not all infants had enough epochs available to be included in the toy versus hand condition comparisons. It is possible that responses to the different conditions differ between the different subsets of infants and may have affected the results.

Second, sample size for the HR-ASD group is very small (N = 8), and differed from the other HR groups. This may have affected the results in the connectivity analyses comparing the condition effects between groups. These small samples size also hindered further analyses looking into whether the HR network would be

a compensatory or risk network, and possible gender effects (7 boys and 1 girl in the HR-ASD group). It is possible that effects are different in boys when compared to girls (Bedford et al., 2016).

Third, here I used the parametric related samples t-test in the NBS program. The previous study looking into alpha connectivity used the non-parametric Mann Whitney U-test. Unfortunately, no non-parametric test for repeated measures was available in NBS, and thus I chose for a parametric version instead. It is possible that results might have differed with the use of a non-parametric version.

Fourth, the dbWPLI is a measure of undirected connectivity. It is not possible to infer into which direction the connections act in the LR and HR networks, and how the direction of information flow between frontal areas and other brain regions may differ between the risk groups. Future research can further investigate the connectivity in the LR and HR network by using other measures of effective connectivity, such as the phase slope index that is less susceptible to volume conduction effects than Granger causality (van Diessen et al., 2015).

5.5. Summary of Chapter 5

To summarize, the findings in this chapter showed that the brain displays increased theta log power and connectivity at specific connections during the viewing of social stimuli compared to non-social stimuli in 14-month-old infants. There were no differences observed between risk groups for these condition effects in log power.

For connectivity, there were topological differences between the networks showing higher connectivity in the social conditions in the LR group compared to the HR group. This effect seemed to be graded across the HR-TD, HR-Atyp, and HR-

ASD groups, with the first showing strongest differences between conditions, and the last showing weakest differences between the social and non-social condition. This is consistent with previous work suggesting that early atypicalities in brain connectivity are related to the broader autism phenotype rather than outcome. The topologies of the network for the HR infants displayed more connections involving frontal areas than LR infants. One possibility is that HR infants require additional allocations of resources by frontal areas during social processing due to atypical specialization towards social stimuli. The allocation of resources might facilitate the integration of the multisensory information during social processing. Exploratory analyses suggested that the network in the HR group might be associated with risk. It is possible that in addition to global connectivity, LR and HR infants also exhibit differences in organization of connectivity patterns. Previous studies have shown evidence of atypical integration and segregation in toddlers with ASD using graph theory measures (Boersma et al., 2013), but it remains unknown whether differences in functional organisation exist at earlier ages in LR and HR infants. Therefore, I will focus on graph theory measures in LR and HR infants in the next chapter.

Chapter 6: Alpha and theta band graph organisation at 14 months of age in high-risk infants

6.1 Introduction

For optimal information processing, a network should be optimally organised with small segregated clusters performing local processing, and a few long-range connections connecting these clusters to integrate the information processing on a larger global level. Networks with this configuration are termed small-world networks (Watts & Strogatz, 1998). It has been suggested that brain networks also contain these features (Humphries & Gurney, 2008). To measure the amount of segregation and integration in a network, graph theory metrics can be used (Rubinov & Sporns, 2010). Whereas global connectivity measures inform on the overall amount of communication across the whole brain, graph theory can inform on the topographic organisation of the brain network. Previous research has suggested that the organisation of brain networks might be atypical in ASD, in addition to overall global connectivity (Belmonte et al., 2004).

In Chapter 4 and 5, I have examined whole brain alpha and theta band connectivity, where the former showed associations with dimensional traits, and the latter with risk group. The focus of this chapter is graph organisation in the alpha and theta band frequencies, where I will be examining whether functional segregation, integration, and balance between these are different between infants with and without risk for ASD, and between infants with typical, atypical, or ASD outcomes. Chapter 3 showed that these graph measures have moderate test-retest reliability in young infants and within the range of fair reliability values (based on 120 1-second epochs and dbWPLI measures: $ICC_{\text{Normalised clustering coefficient}} = .59$, $ICC_{\text{Normalised path length}} = .44$, and $ICC_{\text{Small Worldness Index}} = .40$, see tables 3.8, 3.11, and 3.14), which makes them suitable for categorical analyses. The normalised clustering coefficient in particular proved to be more reliable than the other graph

metrics, and will therefore also be used to examine associations with dimensional traits in this chapter.

6.1.1. Network organisation in ASD during resting state

Previous research has suggested that not only whole brain connectivity, but also the functional organisation of brain networks might be atypical in individuals with ASD. It has been hypothesized that short-range connections in ASD are increased, whereas long-range connections are decreased in ASD compared to TD (Belmonte et al., 2004; Courchesne et al., 2007; Just, Keller, Malave, Kana, & Varma, 2012). One could argue that this would result in an altered network organisation with differences in segregation, and integration compared to typically developing individuals. Indeed, individuals with ASD have displayed increases in local connectivity/ short-range connections/ connectivity within clusters or modules, and decreases in global connectivity/ long-range connections/ connectivity between clusters or modules in fMRI studies. These differences are also associated with severity of ASD symptoms (Ecker et al., 2015; Rudie et al., 2013).

Research examining organisation of EEG graphs has only recently started to emerge. Due to the high temporal resolution of the method, EEG is able to measure dynamic coupling between high frequency neural oscillations. The weakness of EEG however is its low spatial resolution. The nodes in the EEG graphs are typically assigned to the sensors, or source-reconstructed sources (Rubinov & Sporns, 2010). Sensor-level measures are more likely affected by volume conduction effects, and are less robust to variation in preprocessing methods than source-level measures (Fraschini et al., 2016; van Diessen et al., 2015). Source-level methods however are not always suitable for infant data. The use of phase lag indices at sensor-level for graph theory metrics is more appropriate for infant

data, as it minimizes volume conduction influences (Stam et al., 2007; Vinck et al., 2011), and provides reliable measures when calculated across more than 120 short epochs (Chapter 3). Indeed, previous studies have used this method also (Boersma et al., 2013; J. Han et al., 2017).

Findings of graph theory metrics in ASD vary depending on the graph theory measures applied, and the age range of interest, similarly to global connectivity findings. During an eyes-open resting state paradigm, children with ASD between 3 and 11 years old displayed increases in the normalised clustering coefficient and the normalised path length for theta and alpha frequency bands in a resting state EEG paradigm, whereas small-worldness for these bands was decreased in those children compared to children with typical development (J. Han et al., 2017). In other words, the EEG graphs in children with ASD were characterised by increased segregation of local information processing, and increased integration with global information processing, but this processing ratio is less optimal than in children with typical development.

The graph metrics were also dependent on the age of the subjects. In the younger participants, the normalised clustering coefficient was increased for both theta and alpha bands, while the normalised path length only showed differences in the theta band, with increases in those with ASD compared to the TD children. The small-worldness index was similar in both groups of 3 to 6-year-olds, but showed decreases for the 6-11 year olds with ASD compared to those with typical development for the theta and alpha band. The older group also showed increases in normalised clustering coefficient and path length for children with ASD in these bands. These findings demonstrate that the organisation of brain resting state

networks in children with ASD is atypical, with group differences becoming evident across a higher number of graph metrics with increasing age.

The organisation of EEG graphs has been shown to be atypical in toddlers with ASD. In the study by Boersma and colleagues, 3.5-year-old toddlers were shown pictures of faces and cars while their EEG was being recorded (Boersma et al., 2013). Toddlers with ASD displayed a decrease for the normalised clustering coefficient and small-worldness index compared to typically developing toddlers in the theta-alpha broad band (4-10 Hz) for the data collapsed across conditions. Meanwhile, the normalised characteristic path length was similar across groups for the theta-alpha band, but increased for the toddlers with ASD across the broad band (.1 – 30 Hz). No significant correlations were found with age or IQ. Thus younger individuals with ASD might show reductions in local processing or segregation compared to peers with typical development, while there are no differences between groups in global processing.

The organisation of EEG graphs before toddlerhood in individuals with a risk for ASD or later ASD outcome is mostly unknown, and has not been investigated previously to the best of my knowledge. Work from MRI studies demonstrates that the organisational structure of structural and functional brain networks is already present at birth, and continues to develop during postnatal life (Cao, Huang, & He, 2017; Huang et al., 2015). The most dramatic changes in network organisation occur during the first postnatal year, while less drastic changes and further refinements occur during the second postnatal year (Gao, Alcauter, Smith, et al., 2015). Normalised clustering of functional networks increases, while normalised path length decreases, and small-worldness increases with development during the 1st two years of postnatal life (Gao et al., 2011). A

recent EEG connectivity study revealed a similar pattern: normalised clustering increased, while normalised path length increased in the theta and alpha frequency bands with age between 6 and 12 months of age. The small-worldness index exceeded 1 at 6 and 8 months, but not 10 and 12 months of age (Xie et al., 2018). If development in HR or HR-ASD infants is atypical or delayed compared development in LR, HR-TD, and HR-Atyp infants, differences in network organisation might already be evident before toddlerhood, for instance during 14 months of age, when measured with EEG (Johnson, 2011; Johnson et al., 2015).

Further, atypicalities in network organisation might also relate to dimensional traits, or severity of symptoms. Most studies focussed on differences between groups of individuals with ASD and with TD only, while research on associations between graph theory metrics and severity of clinical symptoms is scarce. One study found a trend association between small-worldness in the alpha range and social interaction difficulties measured with the ADOS (Takahashi et al., 2017). In other studies this was not investigated due to lack of data on clinical measures (Boersma et al., 2013). Thus, associations between graph metrics and dimensional traits deserve more attention also.

6.1.2. Network organisation in ASD during social and non-social processing

Activity in the theta frequency band has been associated with social processing. In Chapter 5, global theta connectivity showed increases while 14-month-old infants watched social videos compared to non-social videos. Other studies using fMRI have also found that functional connectivity increases and organisational structure changes during sustained attention, or while viewing socio-affective stimuli, compared to resting-states or more neural emotional stimuli (Göttlich, Ye, Rodriguez-Fornells, Münte, & Krämer, 2017; You et al., 2013). It is possible that the

organisation of the graphs is also different between social and non-social conditions. One could speculate that networks would show increased efficient organisation to facilitate processing of social stimuli compared to non-social stimuli due to interactive specialisation towards social stimuli (Johnson, 2011). An efficient organisation would be characterised by increased segregation to process information from different modalities, and increased integration to combine information from different processing streams. Simultaneously, small-worldness would be increased to ensure optimal processing capacity (Rubinov & Sporns, 2010).

The results of the previous chapter suggested that topography of the networks showing increased connectivity in the social condition differed between the LR and HR group. The effect of condition reached a trend in the HR-TD group, while not reaching significance in the HR-Atyp or HR-ASD group. Perhaps the efficiency of the organisation of the networks is also different between the risk and outcome groups. The study by Boersma and colleagues compared graph metrics between groups with ASD and TD within the cars and face condition (Boersma et al., 2013). In the car condition, normalised clustering coefficient was reduced in the theta-alpha band in the ASD group compared to the TD group. No group differences were observed for the normalised path length in this condition. In the face condition, values were similar between groups for each of the three graph metrics. The difference in normalised clustering between groups for the cars condition was present, even though global connectivity was similar across the ASD and TD group. These results suggest that the functional organisation of brain networks in ASD might be abnormal, and might be related to the cognitive or emotional state of the toddler.

It remains however unclear whether there are differences between the groups within the social and non-social condition. Also, activity in different frequency bands has been related to different cognitive functions. It is possible that connectivity in the theta band which is sensitive to social processing, shows a different pattern of differences between conditions than the broader theta-alpha band, or broad band that were investigated by Boersma and colleagues. Indeed, previous studies have found different results for graph metrics depending on the frequency band of interest (Boersma et al., 2013; J. Han et al., 2017; Kitzbichler et al., 2015; Takahashi et al., 2017). Functional integration and segregation in the theta band might show bigger differences between a social condition and non-social condition in infants with low familial risk or without later diagnosis of ASD compared to those with high familial risk or with later diagnosis of ASD. Similarly, associations between theta band connectivity graph metrics and dimensional traits remain unexplored.

6.1.2 Aim of this chapter

This chapter aims to investigate 1) whether network organisation in young infants at risk for ASD is different from those at low risk, 2) if there are differences between LR and HR groups, whether there are differences in network organisation between high-risk groups with different outcomes, and 3) whether there are any associations between network organisation measures and dimensional traits. To this end, I further analysed the data in the alpha frequency band from Chapter 4, and data in the theta frequency band for the social and non-social conditions from Chapter 5.

If the functional organisation of brain networks is different between infants with low and high familial risk for ASD, and with different outcomes, I expect to

find similar patterns as the study by Boersma and colleagues: reduced normalised clustering, increased normalised path length, and decreased small-worldness in the HR group compared to LR group, and in the HR-ASD group compared to HR-TD and HR-Atyp groups in the alpha frequency band. This pattern would be consistent with a delay in network development in ASD since clustering increases, path length decreases, and small-worldness increases with age during early development.

In addition to differences between groups with different categorical outcomes, I was interested in associations between graph metrics and dimensional traits. In Chapter 3, I found that the normalised clustering coefficient is more reliable than other graph metrics, which is important when looking at individual variability. Therefore, I tested whether the normalised clustering coefficient in the alpha band was related to behaviours from the social communication and interactions domain, and the restricted and repetitive behaviour domain measured with the ADI-R, and ADOS-2, or with the socialisation and communication domains from the VABS-II. I hypothesized that the alpha normalised clustering coefficient would be related to restricted and repetitive behaviour domains. This hypothesis was based on the findings from the previous study by Orekhova and colleagues (Orekhova et al., 2014), and those in Chapter 4 showing an association between global connectivity in this frequency band and restricted and repetitive behaviours.

For the theta frequency band, graph metrics have not previously been compared between social and non-social conditions, but only within condition, where differences were found between toddlers with ASD and TD in the non-social condition, but not the social condition. If graph organisation for the social condition is more efficient than for the non-social condition, I predict increased

normalised clustering, decreased normalised path lengths, and increased small-worldness during the social condition (woman singing nursery rhymes) compared to the non-social condition (spinning toys with and without hand).

Turning to the different risk and outcome groups, it is furthermore important to investigate whether differences in graph metrics between conditions might be related to autism familial risk and is therefore part of the broader autism phenotype, and if so, whether graph metric differences are also related to diagnosis of ASD. Thus differences were tested between the risk groups, and between outcome groups if the former reached significance. If there is atypical specialization towards social stimuli, I expect to find smaller differences between conditions in the HR and HR-ASD groups, compared to the LR, and HR-TD, and HR-Atyp groups.

I further calculated the difference in the normalised clustering coefficient between the social and non-social condition, and tested whether this was associated with traits in the domains of the ADI-R, ADOS-2, and VABS-II. I expected that the differences between conditions for the theta normalised clustering coefficient would be related to social interactions and communication domains, since theta oscillations have previously been associated with social processing (Jones, Venema, Lowy, Earl, & Webb, 2015; Orekhova, Stroganova, Posikera, & Elam, 2006). Also, a recent study found that increased theta connectivity in adults with social anxiety disorder was related to increased anxiety levels, supporting the relevance of theta connectivity in socially related processing (Xing et al., 2017).

Finally, confounding factors such as global connectivity, age, cognitive ability levels, or gender might influence group effects on graph metrics. I therefore

performed additional analyses to test for group differences while taking into account these confounding factors, similarly to the analyses in Chapters 4 and 5.

6.2. Methods

6.2.1. Participants

Participants in this chapter are identical to the ones included in the previous chapters. For alpha connectivity analyses, infants included in the analyses reported on by Orekhova and colleagues (Orekhova et al., 2014), and those included in Chapter 4 were collapsed into one sample. For theta connectivity analyses, infants included in Chapter 5 were included here.

6.2.2. Procedure and materials

For this chapter the dataset is identical to the ones in the previous Chapters 4 and 5, and the procedure and materials are identical to previous Chapters 3 through 5. The data used in this chapter were derived from the EEG task and recording, ADI-R, ADOS-2, MSEL, and VABS-II described in Chapter 4 (Lord, DiLavore, & Gotham, 2012; Mullen, 1995; Orekhova et al., 2014; Rutter, Le Couteur, & Lord, 2003; Sparrow, Balla, & Cicchetti, 2005). Furthermore, clinical outcome data at 36 months were used to investigate differences between outcomes of the HR infants: typically developing, atypically developing, or meeting criteria for ASD.

6.2.3. Graph theory metrics

The graph metrics of interest in this chapter are the normalised clustering coefficient C_{wnorm} or gamma, the normalised path length L_{wnorm} or lambda, and the small-worldness index SWI (also see Table 6.1). I selected these metrics to focus on since a) these measures have received most attention in previous studies, b) a

previous study found differences between toddlers with ASD and TD in these metrics (Boersma et al., 2013), and c) these metrics were also the focus in Chapter 3 that focused on the reliability of these measures.

Table 6.1. **Overview of the graph theory measures**

Measure	*Definition*	*Application*
Clustering coefficient (C) for segregation	The extent to which two neighbours of one node are also neighbours of each other, or cliquiness (Onnela et al., 2005; Watts & Strogatz, 1998)	Calculated for each node and then averaged across all nodes, possible to normalise when divided by the average clustering coefficients of randomised networks (C_{wnorm} or gamma)
Characteristic path length (L) for integration	Shortest sequence of edges between 2 nodes (Watts & Strogatz, 1998)	Calculated for each node and then averaged across all nodes, possible to normalise when divided by the average clustering coefficients of randomised networks (L_{wnorm} or lambda)
Small-Worldness Index (SWI) for the balance between segregation and integration	A small-world network is characterised by a high normalised clustering coefficient and a low normalised path length (Watts & Strogatz, 1998), also indicated by a value above 1 for SWI (Humphries & Gurney, 2008).	SWI is calculated by dividing the normalised clustering coefficient by the normalised path length.

For a description of the formulas and use of BCT scripts, see section 2.4.3 in Chapter 2, and section 3.2.3.2.2 in Chapter 3.

The results from Chapter 3 showed that both global connectivity and graph theory metrics showed reliability values in the fair to excellent ranges when calculated across 120 1-second epochs with the dbWPLI ($ICC_{Global\ connecitivty}$ = .82 for analyses examining 1 and 2-second epochs, and $ICC_{Global\ connectivity}$ = .53, ICC_{Cwnorm} = .59, ICC_{Lwnorm} = .44, and ICC_{SWI} = .40 when keeping the total amount of data constant, see tables 3.5, 3.8, 3.11, and 3.14). I therefore decided to examine graph theory metrics based on dbWPLI calculations across 120 or more 1-second epochs. Furthermore, as in previous chapters I was interested in effects at both group and individual level. Analyses at individual level such as correlational analyses focusing on dimensional traits require measures with higher test-retest reliability compared to analyses at group level. The previous results in Chapter 3 showed that ICCs for normalised path length (ICC = .44) and small-worldness index (ICC = .40) are lower than for global connectivity (ICC = .53) and normalised clustering coefficient (ICC = .59). Based on these results I examined associations with different risk and outcome groups for each of the 3 graph theory metrics, whereas I only focused on the normalised clustering coefficient for associations with dimensional traits.

The graph theory metrics were derived from the functional connectivity matrices based on the dbWPLI values, which were used in the previous Chapters 4 and 5 to calculate global connectivity values. Absolute values of the dbWPLI values were taken from the functional connectivity matrices with 116 nodes before the graph metrics were calculated using the BCT functions from Chapter 3 (Rubinov & Sporns, 2010). Then, I obtained normalised metrics by dividing the observed value (C_w and L_w) by the same value averaged across 1000 randomized surrogate networks (C_{wrand} and L_{wrand}, resp.), similar to the 1000 randomized networks used

by Boersma and colleagues (Boersma et al., 2013). Finally, dividing the normalised clustering coefficients by the normalized characteristic path length resulted in the small-worldness index SWI (also see section 2.4.3 in Chapter 2, and section 3.2.3.2.2 in Chapter 3.).

For the alpha analyses, graph metrics were derived for each infant from the alpha frequency band connectivity matrices across all conditions. For the theta analyses, graph metrics were derived from the theta frequency band connectivity matrices for the social condition, and for the non-social condition. This resulted in graph metric values for each infant for the social and the non-social condition.

6.2.4. Statistical analyses

6.2.4.1. Alpha frequency band

6.2.4.1.1. Categorical analyses: familial risk and clinical outcome

All statistical analyses were performed using SPSS. First, distributions within groups and variances between groups were explored for each of the graph metrics to determine which test would be appropriate. Normality of the distributions, and homogeneity of variances across groups (LR and HR; LR, HR-TD, HR-Atyp, and HR-ASD infants) were tested with the Shapiro-Wilk test, and Levene's test, respectively, as in Chapter 4. If assumptions for normality and homogeneity of variances were met, parametric tests were used to compare the effect of group: independent samples t-test for 2 groups, and analysis of variance (ANOVA) for more than two groups. If assumptions were not met, non-parametric tests were used: Mann-Whitney U-test for 2 groups, and independent Kruskal-Wallis test for more than two groups. As it was expected that the meeting of these assumptions would differ among the graph metrics, separate tests were performed for each of the 3 dependent variables, rather than using multivariate analyses.

Second, group differences were tested between the LR and HR infants using the parametric or non-parametric tests described above depending on the assumptions. If this difference reached significance (p-value below .05), further follow-up analyses were performed to test differences between the LR, HR-TD, HR-Atyp, and HR-ASD group.

Third, I tested group differences using general linear models (GLM) while taking into account potentially confounding factors, such as global connectivity, age at the EEG recording, MSEL ELC scores, and gender. Spearman's correlations were first performed for the former 4 confounding factors to examine the associations between graph metrics and these factors. Next, a GLM was performed with group (LR, HR), and the covariate (global connectivity, age, or MSEL) in the full factorial model to test for a difference between groups while controlling for the covariate. A second GLM was performed with the addition of the interaction between the group and covariate to the model to test whether the assumption for homogeneity of slopes in the groups was met. Not meeting this assumption (interaction effect with p-value < .05) would suggest that results of the first GLM should be interpreted with caution. If a significant effect was found for outcome in the first GLM, follow-up GLM analyses were performed with 4 levels of the group factor (LR, HR-TD, HR-Atyp, and HR-ASD). Separate analyses were performed for each covariate. Finally, the effect of gender was tested by performing a GLM including gender (male, female) as factor in the full factorial model.

Each of these 3 steps was performed for each of the 3 graph metrics: the normalised clustering coefficient, normalised path length, and small-worldness index.

6.2.4.1.2. Dimensional traits

As in the previous Chapters 4 and 5, I examined associations between connectivity measures and dimensional traits. In Chapter 3, I found that the clustering coefficient is more reliable than characteristic path length or the small-worldness index. I therefore examined associations between ASD trait measures and the normalised clustering coefficient. The ASD traits were measured with the following scales: 1) ADOS-2 Social Affect domain scores, 2) ADOS-2 Restricted and Repetitive Behaviour domain scores, 3) ADI-R Social and Communication domain score (sum of the scores for the ADI-R Social domain and the Communication domain), 4) ADI-R Behaviour / Repetitive Interests domain score, 5) VABS-II Communication domain standard score, and 6) VABS-II Socialization standard score. Again, Spearman's correlation coefficients were used to examine these associations, due to its robustness to extreme values and non-Gaussian distributed data, and suitability for ordinal data. Associations were tested in the whole group, before testing in the separate LR and HR groups, with possibly further testing in the separate HR-TD, HR-Atyp, and HR-ASD groups.

6.2.4.2. Theta frequency band

6.2.4.2.1. Differences between the social and non-social condition

For the theta frequency band, I aimed to examine differences between the social and non-social conditions for different graph metrics. First, assumptions of normality and homogeneity of variance were tested for graph metrics in the social and non-social condition across the whole group, in the LR and HR group, and in the HR-TD, HR-Atyp, and HR-ASD group, using the same method as described in the previous section. In contrast to the alpha analyses which focused on group differences in independent samples, here analyses for a repeated measures design

were used to test the differences between social and non-social conditions: related-samples Wilcoxon signed rank test if data did not meet assumptions, or paired-samples t-test when data did meet assumptions.

Second, the graph metric values were compared between conditions across the whole sample using the appropriate tests based on meeting the assumptions. Further analyses were performed to test whether these differences were different between the LR and HR group. Specifically, a difference score for the conditions was calculated by subtracting the value for the social condition from the value of the non-social condition. If the difference between conditions was different between the LR and HR infants, further follow-up analyses were performed to examine whether these differences also differed between the LR, HR-TD, HR-Atyp, and HR-ASD group.

Third, as for the alpha analyses, additional GLMs were performed to examine the effect of group on the differences between conditions when taking into account the global connectivity difference between conditions, age at EEG recording, MSEL ELC scores, and gender. Dependent variables were difference values between conditions for normalised clustering coefficient, normalised path length, and small-worldness index, risk group (LR, HR) as factor, and global connectivity differences, age, and MSEL scores as covariate, and gender as factor (male, female), in separate GLM analyses. I chose here to use the difference score between conditions rather than using the values for the social and non-social condition, as adding another repeated measures factor would increase the complexity of the model, and using fewer factors facilitates interpretation of the results. If the effect of group (LR, HR) reached significance, further GLMs were performed by investigating the effect of outcome (LR, HR-TD, HR-Atyp, HR-ASD).

6.2.4.2.2. Dimensional traits

In the last set of analyses, I tested whether differences in the normalised clustering coefficients between the social and non-social conditions were associated with ASD traits. Difference scores were obtained by subtracting the normalised clustering coefficient during social stimuli from the coefficient during the non-social stimuli. The same measures of ASD traits, and statistical methods were used as for the associations with alpha band normalised clustering coefficient described in section 6.2.4.1.2.

6.3. Results

6.3.1. Alpha frequency band: Participants

The final combined sample for the alpha frequency analyses consisted of 155 infants: 46 LR infants, 56 HR-Atyp infants, 30 HR-TD infants, and 23 HR-ASD infants. This sample is different from the sample used in Chapter 4, as it combines the original cohort from Phase 1 and the new independent cohort from Phase 2. Demographics and clinical data for this combined sample are presented in Table 6.2.

During the 14-month-old visit, MSEL ELC scores were lower in the HR-ASD group compared to the LR, HR-TD, and HR-Atyp groups that showed no differences among them ($p < .001$). This pattern was slightly different at the 36-month-old visit, where scores were similar for the LR and HR-TD groups, but lower for the HR-Atyp and HR-ASD groups that showed no differences between them ($p < .001$).

The groups also showed differences for the severity of symptoms measured with different scales on the ADI-R, and ADOS-2 ($p's < .001$). The HR-ASD group displayed higher scores on the ADI-R Social Total, and ADI-R Behaviour/

Repetitive Interests Total compared to the HR-Atyp group, which in turn scored higher than the LR and HR-TD group. For the ADI-R Communication Total, each group was significantly different from the others where the HR-ASD group showed the highest scores, then the HR-Atyp group, followed by the HR-TD group, and the LR group showing the lowest scores.

Table 6.2. **Demographics of the sample for alpha analyses (combined cohorts)**

	LR	*HR-TD*	*HR-Atyp*	*HR-ASD*	*Test statistic*
Number of participants (male)	46 (23)	56 (24)	30 (15)	23 (18)	
Age at EEG assessment (days)[1]	458 (35) [1]	463 (37)	457 (41)	449(34)	$F(3,151) = 0.92$, $p = .435$
MSEL [a] Composite Standard Score at visit at 14 months [5]	103 (16) [1] 73 – 154 [4]	98 (12) 71 – 121	96 (15) 67 – 123	86 (14) 56 – 113	$F(3,150) = 7.338$, $p < .001$ (LR = HR-TD = HR-Atyp) > HR-ASD
Age at diagnostic assessment (months)	38.0 (2.0) [2]	39.0(2.0)	38.0 (2.0)	38.0 (2.0)	$H(3) = 2.62$, $p = .454$
MSEL [a] Composite Standard Score at visit at 36 months [b, 6]	120 (15) [2] 69 – 137 [4]	114 (21) 79 – 142	95 (39) 54 – 145	90 (46) 49 – 147	$H(3) = 28.29$, $p < .001$ (LR = HR-TD) > (HR-Atyp = HR-ASD)
ADI-R Social Total [b, 6]	1 (2) [2] 0 – 6 [4]	1 (3) 0 – 11	2.5 (3) 0 – 18	11 (7) 1 – 25	$H(3) = 46.69$, $p < .001$ (LR = HR-TD) < HR-Atyp < HR-ASD
ADI-R, Communication Total [c, 6]	0 (1) [2] 0 – 4 [4]	1 (3) 0 – 11	3 (5) 0 – 20	11 (7) 2 – 19	$H(3) = 51.07$, $p < .001$ LR < HR-TD < HR-Atyp < HR-ASD

ADI-R BRI Total [d, 6]	0 (0) [2] 0 – 1 [4]	0 (1) 0 – 3	1(2) 0 – 9	5 (4) 0 – 10	$H(3) = 54.54$, $p < .001$ (LR = HR-TD) < HR-Atyp < HR-ASD
ADOS-2, SA Total [e, 6]	4 (5) [2] 0 – 12 [4]	2 (2) 0 – 5	7.5 (7) 0 – 15	8 (8) 1 – 20	$H(3) = 48.86$, $p < .001$ HR-TD < LR < (HR-Atyp = HR-ASD)
ADOS-2 RRB Total [f, 6]	1 (1) [2] 0 – 5 [4]	1 (1) 0 – 3	1.5 (2) 0 – 6	3 (4) 1 – 6	$H(3) = 30.51$, $p < .001$ (LR = HR-TD) < (HR-Atyp = HR-ASD)

[1] Means and standard deviations in parentheses, with results for the analysis of variance with Group as factor (LR, HR-TD, HR-Atyp, HR-ASD).

[2] Medians and interquartile range in parentheses, with results for the Independent-Samples Kruskal-Wallis test, and stepwise step-down follow-up analyses if significant asymptotic 2-tailed p-value.

[4] Range with minimum and maximum score.

[5] MSEL data for the 14-month-old visit were missing for 1 LR infant.

[6] Data for the 36-month-old visit were only available for 44 LR infants, 55 HR-TD infants, 30 HR-Atyp infants, and 22 HR-ASD infants.

[a] Mullen Scale for Early Learning (MSEL).

[b] Autism Diagnostic Interview – Revised, Social Algorithm Total at 36 months.

[c] Autism Diagnostic Interview – Revised, Communication Algorithm Total at 36 months.

[d] Autism Diagnostic Interview – Revised, Behaviours/ Repetitive Interests Algorithm Total 36 months.

[e] Autism Diagnostic Observation Schedule – 2, Social Affect Total 36 months.

[f] Autism Diagnostic Observation Schedule – 2, Restricted and Repetitive Behaviours Total 36 months.

On both the ADOS-2 Social Affect domain, and Restricted/ Repetitive Behaviours domain, the HR-ASD and HR-Atyp groups showed similar scores. The Social Affect scores for the HR-ASD and HR-Atyp groups were higher than for the LR group, which in turn were higher than those in the HR-TD group. The scores on the Restricted/ Repetitive Behaviour scale were higher for the HR-ASD and HR-Atyp group compared to the LR and HR-TD group.

6.3.1.1. Alpha frequency band: Group level

Figure 6.1 displays the data for the normalised clustering coefficient (A), the normalised path length (B), and small-worldness index (C). The assumption for normality was violated for the normalised clustering coefficient in the HR group (p = .002), and the normalised path length in both the LR and HR groups (p's ≤ .025). Assumptions of normality and homogeneity of variance between groups were met for all other graph metrics in the LR and HR group (p's ≥ .480).

Independent-Samples Mann-Whitney U-tests revealed no differences between the LR and HR group for the normalised clustering coefficient (p = .536, r = -.05), or the normalised path length (p = .820, r = -.02) in the alpha frequency band. For the small-worldness index, the difference between the LR and HR group did not reach significance either (independent samples t-test, p = .760, d = -.05).

Next, I tested whether the comparisons between the LR and HR group might have been affected by confounding factors such as global connectivity, age at the EEG assessment, cognitive abilities, or gender. The normalised clustering coefficient was positively related to global connectivity in both groups (r_{LR} = .75, p_{LR} < .0001, and r_{HR} = .65, p_{HR} < .0001, resp., Figure 6.2A), but not to age (p's ≥ .794), or cognitive abilities (p's ≥ .581) in the LR or HR group. The association with global connectivity also reached significance in the separate HR groups ($r_{HR\text{-}TD}$ =

.73, $p_{HR\text{-}TD} < .0001$; $r_{HR\text{-}Atyp} = .65$, $p_{HR\text{-}Atyp} < .0001$; and $r_{HR\text{-}ASD} = .55$, $p_{HR\text{-}ASD} = .007$). The GLM with Risk Group only revealed no significant effect for Risk Group, $p = .790$, $\eta_p^2 = 0$. Further GLM analyses revealed the same pattern of a non-significant effect for Risk Group while including global connectivity ($p = .695$, $\eta_p^2 = .001$), age ($p = .790$, $\eta_p^2 = 0$), or cognitive abilities ($p = .737$, $\eta_p^2 = .001$). The homogeneity of slopes between the LR and HR group were met for all three covariates, as the interaction effects between Risk Group and the covariate did not reach significance ($p_{\text{Group * GlobFC}} = .939$, $p_{\text{Group * Age}} = .932$, or $p_{\text{Group * MSEL}} = .650$). Finally, including Gender in the GLM did not change the effect of Risk group ($p = .796$, $\eta_p^2 = 0$).

The normalised path length showed a positive correlation with global connectivity in the HR group ($r = .32$, $p < .0001$), whereas this association did not reach significance in the LR group ($r = .15$, $p = .326$, Figure 6.2B). This association was also significant in the HR-TD and HR-ASD groups ($r_{HR\text{-}TD} = .27$, $p_{HR\text{-}TD} = .046$, and $r_{HR\text{-}ASD} = .62$, $p_{HR\text{-}ASD} = .002$), but not the HR-Atyp group ($r = .22$, $p = .234$). No other significant correlations were observed between the normalised path length and age (p's ≥ .545), or cognitive abilities (p's ≥ .876) in the LR or HR group. The GLMs for the normalised path length showed the same pattern of results as those for the normalised clustering coefficient: the effect of Risk Group did not reach significance when no other variables were included, $p = .756$, $\eta_p^2 = .001$. This effect of Risk Group did not change when including any of the covariates (with global connectivity: $p = .905$ $\eta_p^2 = 0$; with age: $p = .761$, $\eta_p^2 = .001$, or with MSEL: $p = .556$, $\eta_p^2 = .002$). Again, the assumption of homogeneity of slopes in the risk groups was met for each of the covariates ($p_{\text{Group * GlobFC}} = .200$, $p_{\text{Group * Age}} = .998$, or $p_{\text{Group * MSEL}} = .735$). When taking into account Gender as a factor, the effect of Risk Group remained small, $p = .748$ $\eta_p^2 = .001$.

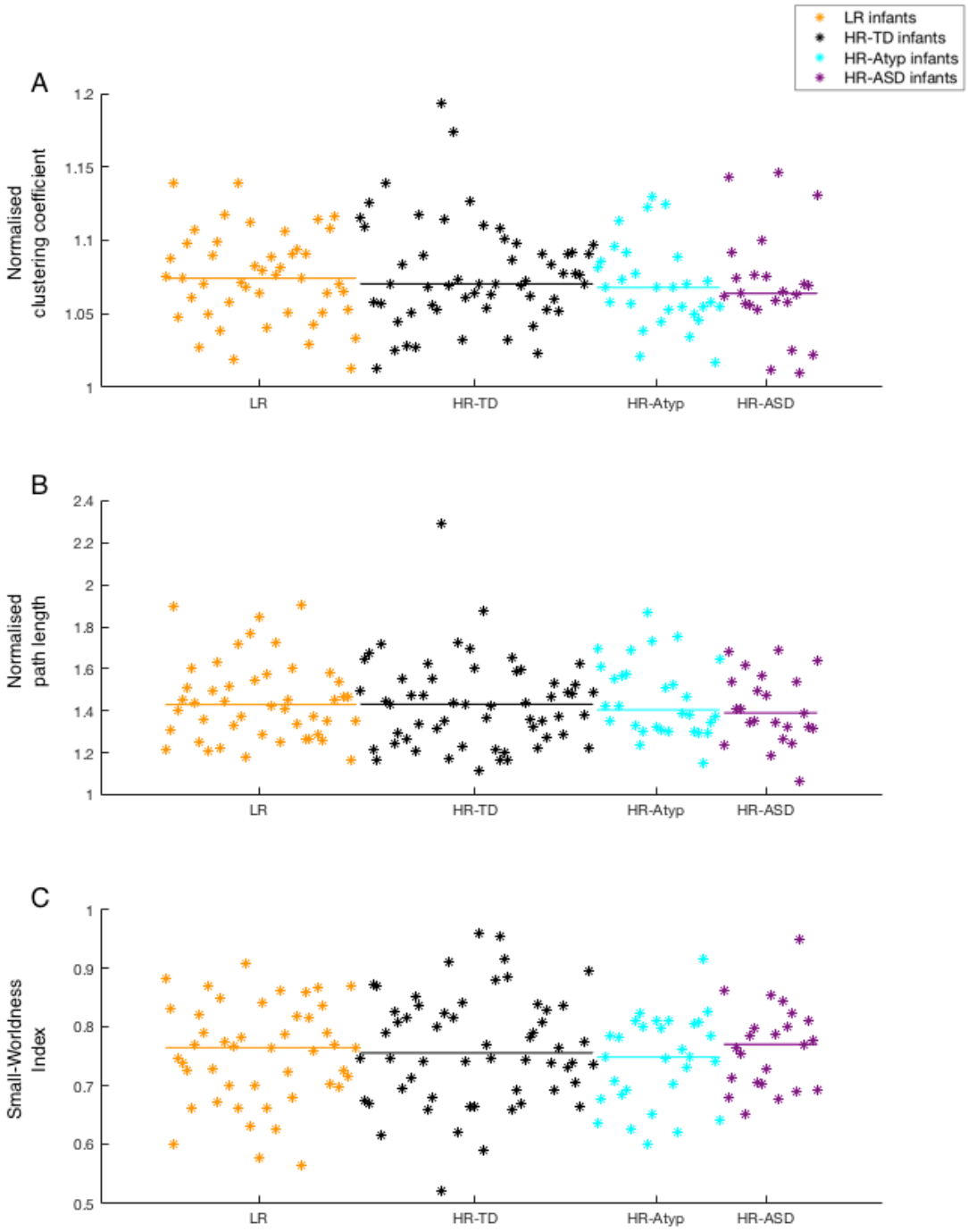

Figure 6.1. Graph metrics for alpha frequency band

The normalised clustering coefficient (A), the normalised path length (B), and small-worldness index (C). Each asterisk reflects an infant for different groups, with the horizontal lines displaying the median for each group.

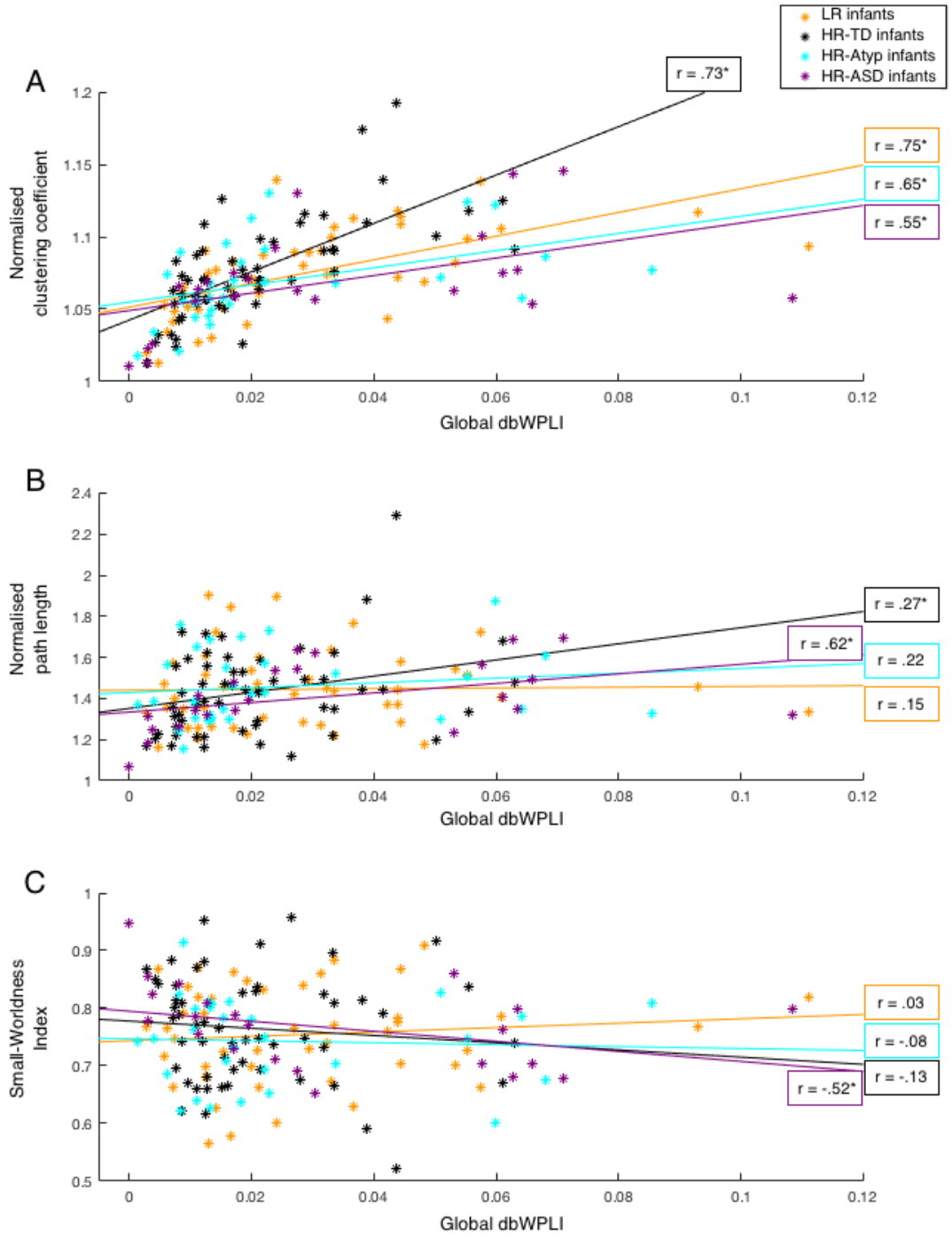

Figure 6.2. Associations between global connectivity and graph metrics for alpha frequency band

The normalised clustering coefficient (A), the normalised path length (B), and small-worldness index (C). Each asterisk reflects an infant for different groups, with the lines displaying the correlation in each group (r values represent Spearman's rho and are flagged if reaching significance, $p < .05$).

For the small-worldness index, a negative significant correlation was observed with global connectivity in the HR group (r = -.21, p = .026), but not in the LR group (r = .03, p = .856, Figure 6.2C). The association in the HR combined group seemed to be driven by the HR-ASD group (r = -.52, p = .011), in contrast to the other HR groups that showed no significant association between small-worldness index and global connectivity ($r_{HR\text{-}TD}$ = -.13, $p_{HR\text{-}TD}$ = .328, and $r_{HR\text{-}Atyp}$ = -.08, $p_{HR\text{-}Atyp}$ = .682). This suggests that lower connectivity is associated with increased small-worldness in the HR-ASD group. Again, correlations with age did not reach significance (p's ≥ .619), nor with cognitive abilities in either group (p's ≥ .294). The GLMs revealed no differences between risk groups when taking into account none of the other variables, p = .760, η_p^2 = .001, nor when taking into account any of the covariates (for global connectivity, p = .814, η_p^2 = 0; for age, p = .767, η_p^2 = .001; or for MSEL, p = .614, η_p^2 = .002), even though the assumption of homogeneity between groups was met for each covariate ($p_{\text{Group * GlobFC}}$ = .179, $p_{\text{Group * Age}}$ = .962, or $p_{\text{Group * MSEL}}$ = .969). Including Gender into the model did not change the effect of Risk Group either, p = .751, η_p^2 = .002.

These results suggest that there are no differences between the LR and HR group for the normalised clustering coefficient, the normalised path length, or the small-worldness index in the alpha frequency band. Global connectivity was associated with the normalised clustering coefficient in both risk groups, and in the HR group with the normalised path length and the small-worldness index, whereas these latter two associations were not observed in the LR group. In the HR-ASD group, increased global connectivity was associated with decreased small-worldness. Taking into account global connectivity, age, cognitive abilities, or gender did not change the effect of risk group.

6.3.1.2. Alpha frequency band: Dimensional traits

The results for the analyses on associations between the alpha band normalised clustering coefficient and dimensional ASD traits are displayed in Table 6.3. None of the investigated associations in the whole group reached significance (*p*'s ≥ .120). This suggests that the normalised clustering coefficient in the alpha band is not associated with ASD traits.

Considering that the association between alpha connectivity and circumscribed interests seemed to underlie the association between alpha connectivity and restricted and repetitive behaviours (Chapter 4), it possible that circumscribed interests might be associated with normalised clustering and the small worldness index, because global alpha connectivity was related with these graph theory metrics also. Exploratory analyses did not reveal any significant findings, but the effects approaching medium sizes suggest that higher normalised clustering coefficients and decreased small-worldness indices are related to more severe circumscribed interests in the HR-ASD group. The failure of reaching significance may be due to small sample sizes (see Appendix A6.1).

Table 6.3. **Associations between alpha band clustering coefficient, and measures of ASD traits across the whole group**

Measure	*N*	*Domain*	*Normalised clustering coefficient for theta band*
ADOS-2	*151*	*SA* [a]	*r* = -.01, *p* = .877, [-.18, .15]
	151	*RRB* [b]	*r* = -.03, *p* = .729, [-.19, .14]
ADI-R	*124*	*SaC* [c]	*r* = .01, *p* = .905, [-.17, .19]
	124	*RRB* [d]	*r* = -.13, *p* = .164, [-.31, .05]
VABS	*150*	*Com* [e]	*r* = .13, *p* = .120, [-.03, .28]
	149	*Soc* [f]	*r* = .11, *p* = .202, [-.05, .26]

Spearman's rho values (*r)*, with p-values, and bias corrected and accelerated

bootstrap 95% confidence intervals in square brackets.

[a] Autism Diagnostic Observation Schedule – 2, Social Affect Total 36 months.

[b] Autism Diagnostic Observation Schedule – 2, Restricted and Repetitive Behaviours Total 36 months.

[c] Autism Diagnostic Interview – Revised; Social and Communication score: sum of the scores of the Social domain and Communication domain in the ADI-R.

[d] Autism Diagnostic Interview – Revised; Restricted and Repetitive Behaviours.

[e] VABS Communication domain Standard Score.

[f] VABS Socialization Standard Score.

6.3.2. Theta frequency band: Participants

For the theta band comparisons, the sample was identical to the one described in Chapter 5 containing 68 infants in total: 17 LR infants, 27 HR-TD infants, 16 HR-Atyp infants, and 8 HR-ASD infants. Demographics and clinical information of this sample are displayed in Table 5.3 and 5.4 in the previous chapter.

6.3.2.1. Theta frequency band: Differences between social and non-social condition

Graph metric values for the social and non-social condition for different groups are displayed in Figure 6.3. Data across the whole group for the normalised clustering and the normalised path length in both the social and non-social condition showed non-Gaussian distributions (p's ≤ .013), whereas small-worldness index values in both conditions did show a Gaussian distribution (p's ≥ .199). Values for differences between the conditions (Social – Non-Social) are displayed in Figure 6.4. Differences between the conditions for the normalised clustering coefficient and path length were normally distributed in both the LR and HR group, and variances between groups were equal (p's ≥ .190). For the small-worldness index, differences between conditions were normally distributed in both groups (p's ≥ .424), but variances between the LR and HR group were unequal (p = .042).

In the whole sample, the normalised clustering coefficient was increased in the social compared to the non-social condition (Mdn_{Social} = 1.0458, $Mdn_{Non\text{-}Social}$ = 1.0417, T = 1554, p = .020, r = .10). Further analyses on the normalised clustering coefficient revealed no differences reaching significance between conditions in the LR group (p = .136, r = .26), while there was a trend for the HR combined group (Mdn_{Social} = 1.0458, $Mdn_{Non\text{-}Social}$ = 1.0446, T = 863, p = .061, r = .19). There were no differences in any of the HR-TD (p = .230, r = .16), HR-Atyp (p = .501, r = .12), or HR-ASD groups (p = .263, r = .28). The significance levels may be affected by samples sizes, as effect sizes suggest there is an effect. Analyses on the difference scores between conditions yielded no significant differences between the LR and HR group (p = .680, d = .11, and Fig. 6.4A).

Turning to the normalised path length, comparisons between values for the social and non-social condition did not reach significance in the whole sample (p = .138, r = -.13). Also, the LR and HR group showed the same absence of difference between conditions when focusing on the Social – Non-Social difference scores (p = .692, d = .12, and Fig. 6.4B).

Findings for the small-worldness index revealed a similar pattern as those for the normalised path length; no significant difference was observed between conditions for the small-worldness index (p = .246, d = -.18), or between the LR and HR group for conditional difference scores (p = .602, d = -.16, and Fig. 6.4C).

(Next page)

Figure 6.3. Graph metrics for the social and non-social condition in the theta frequency band

The normalised clustering coefficient (A), the normalised path length (B), and small-worldness index (C), for the different groups in the different columns, with individual data (red square for social, orange pentagram for non-social condition), and medians (red line for social, orange line for non-social condition).

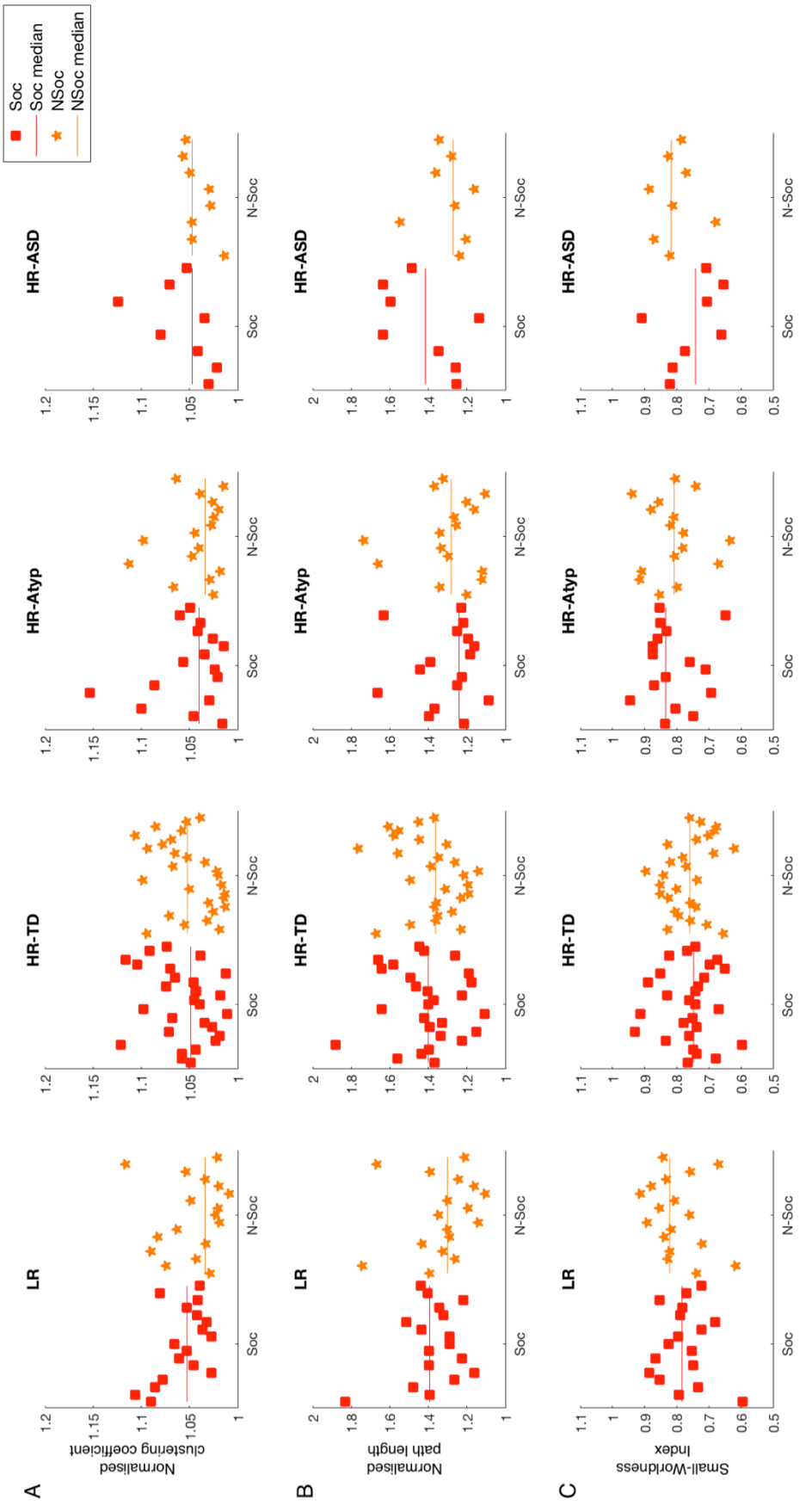
Soc
Soc median
NSoc
NSoc median
A
B
C
LR
HR-TD
HR-Atyp
HR-ASD
Normalised clustering coefficient
Normalised path length
Small-Worldness index
Soc
N-Soc

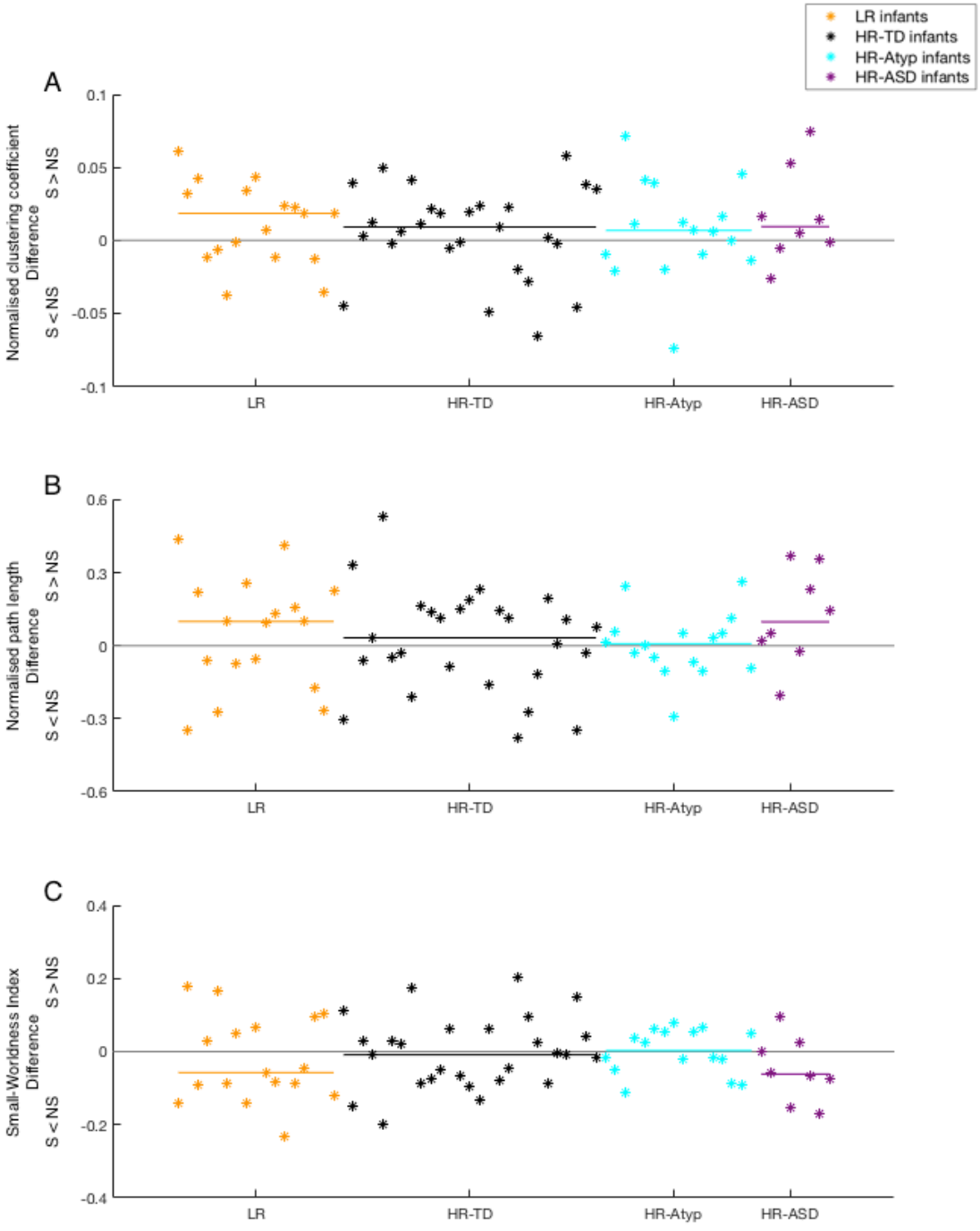

Figure 6.4. Differences between social and non-social condition for each of the graph metrics in the theta frequency band

Differences between the social (S) and non-social (NS) conditions for the normalised clustering coefficient (A), the normalised path length (B), and small-worldness index (C). Horizontal lines reflect the median difference between conditions for each outcome group.

Next, I examined whether other variables could have influenced the results, such as global connectivity, age, cognitive abilities, and gender. The normalised clustering coefficient difference between conditions was overall positively related to global connectivity differences between conditions (r = .62, p < .0001); while this association did not reach significance in the LR group (r = .29, p = .264), it did in the HR group (r = .74, p < .0001). Further analyses showed that this pattern was also evident in the separate HR groups: the HR-TD group (r = .73, p < .0001), the HR-Atyp group (r = .70, p = .003), and the HR-ASD group (r = .83, p = .010, and Figure 6.5A). For the GLM including Risk Group only, the effect of Risk Group did not reach significance, p = .680, η_p^2 = .003. Including global connectivity differences as a covariate in the GLM analyses yielded no significance differences between the LR and HR group (p = .651, η_p^2 = .003). The assumption of homogeneity of slopes however was violated for this covariate as indicated by a significant interaction effect (F(1,64) = 11.15, p = .001, η_p^2 = .148), and the correlations reported earlier. Associations of the normalised clustering coefficient differences with age did not reach significance (p's ≥ .416), nor with the MSEL ELC scores (p's ≥ .390). Again, including age or MSEL ELC scores in GLM analyses, did not change the effect of Risk Group ($p_{\text{with Age}}$ = .673, η_p^2 = .003 or $p_{\text{with MSEL}}$ = .801, η_p^2 = .001), even though the assumption of homogeneity between groups was met for each covariate ($p_{\text{Group * Age}}$ = .837, or $p_{\text{Group * MSEL}}$ = .926). The effect of Risk Group was unchanged when adding Gender into the model, p = .577, η_p^2 = .005.

The potential effect of confounding factors was also tested for the normalised path length difference between conditions. The association with global connectivity differences between conditions reached significance in the HR group (r = .35, p = .013), but not the LR group (r = -.34, p = .181), or the separate HR

groups (r's ≤ .34, p's ≥ .103). No difference was found between the LR and HR group in for the normalised path length difference between conditions when including global connectivity differences as covariate in the GLM (p = .444, η_p^2 = .009). Again, this result should be interpreted with caution as the interaction effect between Group and the covariate reached significance (F(1,64) = 7.46, p = .008, η_p^2 = .104). Further analyses revealed no significant associations between the normalised path length difference and age, or MSEL ELC scores (p's ≥ .287). The GLMs revealed no significant effect of Risk Group when adding age or MSEL scores as covariates (p's ≥ .639, η_p^2's = .003), even though assumptions for homogeneity of slopes were met (p's ≥ .288, η_p^2's ≤ .018 for interaction effects between Risk Group and the covariates). Finally, including Gender did not change the effect of Risk Group compared to excluding Gender, p = .550, η_p^2 = .006.

Small-worldness differences between conditions were not associated with global connectivity differences between conditions, age, or MSEL ELC scores in either group (p's ≥ .130). When only including Risk Group, no differences between groups were revealed, p = .602, η_p^2 = .004. Further GLMs did not reveal any significant differences between the LR and HR group for small-worldness differences when including any of the covariates (p's ≥ .237, η_p^2's ≤ .021 for main effects of Risk Group, and p's ≥ .222, η_p^2's ≤ .023 for interaction effects between Risk Group and the covariates age and MSEL, but p = .029, η_p^2 = .072 for the interaction effect between risk group and global connectivity differences. This suggests that the associations are different between the LR and HR groups.). Lastly, including gender in the GLM did not change the Risk Group effect (p = .475, η_p^2 = .008).

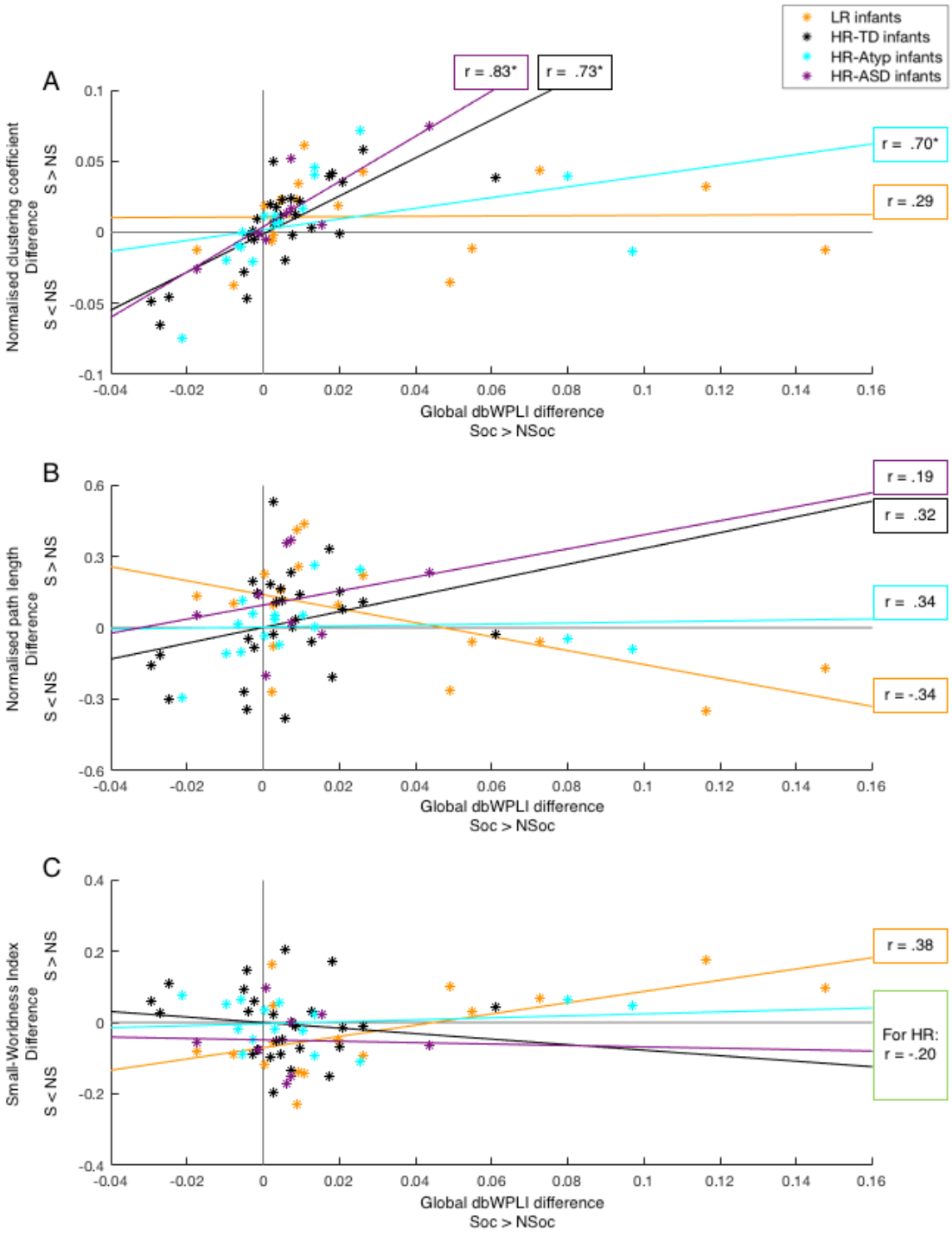

Figure 6.5. Associations between differences between conditions for global connectivity and graph metrics for theta frequency band

The normalised clustering coefficient (A), the normalised path length (B), and small-worldness index (C). Each asterisk reflects an infant for different groups, with the lines displaying the correlation in each group (r values represent Spearman's rho and are flagged if reaching significance, $p < .05$).

In sum, the theta band normalised clustering coefficient was overall higher in the social condition than in the non-social condition. This difference between conditions was not observed within the separate LR and HR combined groups, nor were differences between the risk groups observed for difference scores between conditions. The normalised path length and small-worldness index were similar for the social and non-social condition, and for the LR and HR combined group. Additional analyses taking into account global connectivity differences between conditions, age, cognitive level, and gender showed the same pattern of results as the primary analyses. Interestingly, the differences between conditions in the normalised clustering coefficient were related to global connectivity differences in the combined HR group, and the HR-TD, HR-Atyp, and HR-ASD groups, but not the LR group.

6.3.2.3. Dimensional traits analyses for difference scores

Analyses focusing on dimensional traits showed no strong significant associations between condition differences in the normalised clustering coefficient and the ADOS-2, ADI-R, or VABS-II domain scores (Table 6.4). The association with the ADOS-2 Social Affect domain reached a trend (r = .24, p = .056), suggesting that increased normalised clustering during social conditions compared to non-social conditions relates to more severe problems with social affect. Further analyses suggested that this association was not driven by the LR group (p = .543), but rather the HR group (r = .23, p = .104), which in turn seemed to be driven by the HR-TD group (r = .54, p = .004), not the HR-Atyp or HR-ASD group (p's ≥ .346, see Figure 6.6).

Table 6.4. **Associations between theta band clustering coefficient differences between social and non-social conditions, and measures of ASD traits across the whole group**

Measure	*N*	*Domain*	*Normalised clustering coefficient for theta band*
ADOS-2	*66*	*SA* [a]	***r* = .24, *p* = .056, [-.02, .45]**
		RRB [b]	*r* = -.03, *p* = .823, [-.29, .23]
ADI-R	*58*	*SaC* [c]	*r* = -.05, *p* = .703, [-.28, .19]
		RRB [d]	*r* = .02, *p* = .859, [-.24, .30]
VABS	*66*	*Com* [e]	*r* = .13, *p* = .297. [-.16, .39]
		Soc [f]	*r* = .04, *p* = .727. [-.23, .32]

Spearman's rho values (*r)*, with p-values, and bias corrected and accelerated bootstrap 95% confidence intervals in square brackets. Correlations in bold reached a trend (uncorrected for multiple comparisons).

[a] Autism Diagnostic Observation Schedule – 2, Social Affect Total 36 months.

[b] Autism Diagnostic Observation Schedule – 2, Restricted and Repetitive Behaviours Total 36 months.

[c] Autism Diagnostic Interview – Revised; Social and Communication score: sum of the scores of the Social domain and Communication domain in the ADI-R.

[d] Autism Diagnostic Interview – Revised; Restricted and Repetitive Behaviours.

[e] VABS Communication domain Standard Score.

[f] VABS Socialization Standard Score.

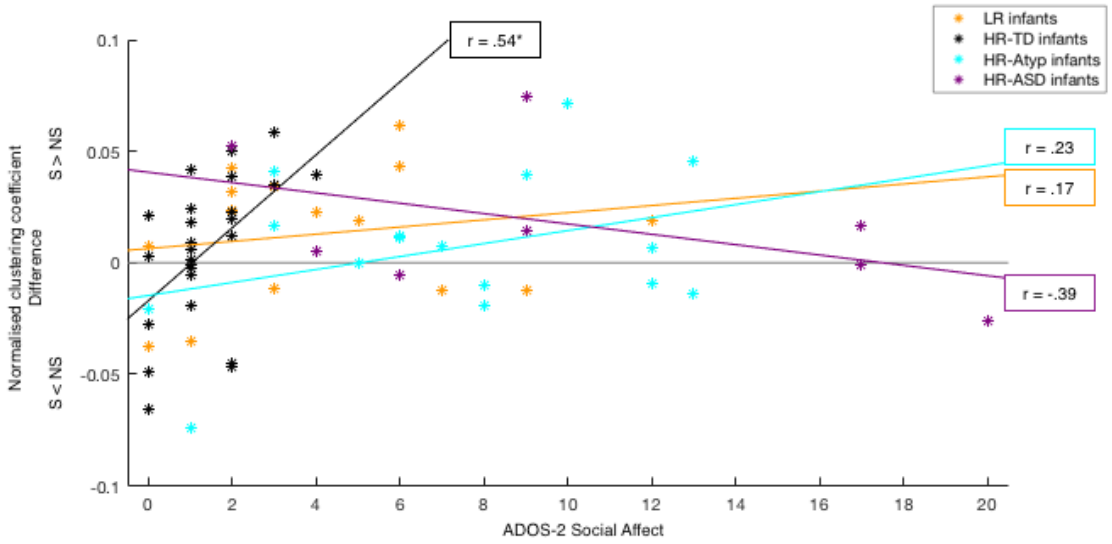

Figure 6.6. Associations between differences between conditions for the normalised clustering coefficient for theta frequency band and ADOS-2 Social Affect score
Each circle reflects an infant for different groups, with the lines displaying the correlation in each group (r values represent Spearman's rho and are flagged if reaching significance, $p < .05$).

6.4 Discussion

The current chapter set out to investigate whether graph organisation in the alpha and theta bands might be atypical during the early development of ASD. The results revealed no significant differences between risk or outcome groups in the alpha band for normalised clustering coefficient, normalised path length, or small-worldness index. Similar patterns were observed when global connectivity, age, cognitive level scores, and gender were included in the analyses. None of the associations between normalised clustering in the alpha band and dimensional traits reached significance.

For graph organisation in the theta band, normalised clustering was higher during the social than the non-social condition, suggesting an increase in local information processing during the processing of social stimuli compared to non-

social stimuli. The direction of this effect was consistent in the separate risk and outcome groups, but the effects did not reach significance probably because statistical power was too low. Neither normalised path length nor small-worldness in the theta band showed differences between conditions, or risk or outcome groups. Although graph metrics were related to global connectivity values, including global connectivity as covariate in further analyses did not change any of the results. The same pattern was observed when including age, cognitive ability levels, or gender.

The above results suggest that 14-month-old infants at high risk for ASD show similar network organisation when compared to those with low risk, in both alpha and theta band frequencies when measured with the normalised clustering coefficient, normalised path length, and small-worldness index.

6.4.1. Typical alpha network organisation in HR infants

The current study found no differences in alpha band network organisation between infants with high and low risk for later ASD diagnosis at the age of 14 months. This suggests that there is no altered network segregation, integration, or balance between segregation and integration in the HR or HR-ASD group compared to the other LR and HR-no ASD groups in the current sample using the current methods. At very young ages differences between those with increased risk and later ASD diagnosis in EEG graph organisation might be absent or very minimal, while aberrant EEG graph organisation might become more pronounced with increasing age during toddlerhood and childhood. In typical development, global alpha connectivity increases with age between 6 and 12 months (Xie et al., 2018), decreases during mid-childhood (Boersma et al., 2011), and increases from childhood to middle-adulthood before continuing to decline during later life (Smit

et al., 2012). Path lengths decrease, while clustering increases with increasing age in infancy and early childhood, suggesting that integration of networks increases, while nodes become more connected (Bathelt, O'Reilly, Clayden, Cross, & De Haan, 2013; Boersma et al., 2011; Xie et al., 2018). During childhood and adolescence, both path length and clustering show increases over time. Thus brain networks become more organised and display less randomness with increasing age (Smit et al., 2012).

Observed differences in EEG graph organisation between individuals with ASD and with typical development in other studies were mostly evident after infancy. By focusing on infancy here, the current findings extend previous results from MEG/EEG studies in older children. The current data revealed no differences in alpha graph metrics between infants with and without risk for ASD. During toddlerhood, however, normalized clustering and small-worldness are reduced in the theta-alpha band in the ASD group (Boersma et al., 2013). During early childhood (3-6 years), normalised clustering in the alpha band is increased in children with ASD. Then, both normalised clustering and path length are increased in ASD during later childhood (6-11 years), and small-worldness is decreased in ASD compared to TD children (J. Han et al., 2017). Together, these data suggest that alterations in graph organisation related to ASD emerge after infancy, and the direction of the alteration may depend on the developmental period. Although the current study further extends previous findings, only future longitudinal studies focusing on individuals across a wide range of ages from infancy to adulthood can inform on the developmental trajectories of whole brain connectivity and graph organisation. It is possible that these different aspects of brain connectivity and their interactions are related to early development of ASD.

A lack of differences in alpha band clustering and path length between children with ASD and typical development nonetheless have also been found (6-year-olds, 6 – 21-year-olds, 0.7 – 25.2-year-olds in (Kitzbichler et al., 2015; Peters et al., 2013; Takahashi et al., 2017)). However, it is important to note that these studies used non-normalised clustering coefficient and path length values. Non-normalised graph metrics are strongly influenced by connectivity values in the network. Graphs with higher global connectivity also show higher clustering coefficients and lower path lengths. It is possible that results are related to overall connectivity rather than graph or network organisation when comparing different groups or experimental conditions. Normalising the graph metrics by comparing the values to those of randomised networks is one method to correct for this dependency, and therefore an important step in the graph theory analyses (van Wijk et al., 2010).

6.4.1.1. Associations between alpha graph metrics and other variables

Overall, increases in global alpha connectivity were related to increases in normalised clustering coefficient and normalised path length, and decreases in small-worldness index. This effect seemed to be present for all graph metrics in the HR group, and only for the normalised clustering coefficient in the LR group. Further analyses however indicated that the relations were not significantly different between groups. This suggests that the alpha band graph theory metrics depend on the overall connectivity levels in the whole sample. The fact that this association occurs with normalised values rather than non-normalised suggests that this association arises from topological factors rather than the amount of overall connectivity. In this sample presumably clearer topologies with lower and higher connections are related to overall higher global connectivity that will result

is a larger difference compared to randomized networks, and thus higher normalised values.

If the topology of graphs becomes more pronounced with increasing age, graph metrics measuring this topology might also become less dependent on the global connectivity levels. The current results did not reveal a significant association with age however, but it is possible that the combination of unclear graph topology and the relatively small age range at EEG assessment led to weak non-significant associations (364 – 576 days here compared to several years in other studies (Boersma et al., 2011; J. Han et al., 2017; Peters et al., 2013; Takahashi et al., 2017)). In contrast, global alpha connectivity across all connections did reveal associations with age, in particular in the HR-TD and HR-Atyp group, but not the LR and HR-ASD group (Chapter 4). The main finding of similar graph metrics in the LR and HR groups however did not change when taking into account global alpha connectivity, age at EEG assessment, cognitive abilities, or gender. If the connectivity graphs contain weak topologies, confounding factors and covariates only would have minimal effects on relatively small graph metric values.

6.4.1.2. Associations between alpha graph metrics and later dimensional traits

In addition to categorical levels, I also examined how the alpha normalised clustering coefficient related to dimensional traits. The results revealed no associations between the alpha normalised clustering coefficients and any of later dimensional traits, including severities of social difficulties, communication difficulties, or restricted, and repetitive behaviours measured by parental interview, clinical observations, or questionnaires at the 36-month-old visit (ADI-R, ADOS-2, and VABS-II, resp.). Again, this finding may arise from weak graph

topologies during infancy that are not sensitive enough to predict or explain later individual variability during toddlerhood.

Exploratory analyses focusing on associations with circumscribed interests based on previous findings suggested that the normalised clustering coefficient and small-worldness index might be associated with circumscribed interests in the HR-ASD group. Possibly both global alpha connectivity and graph metrics may be able to explain or predict later individual variability in dimensional traits, but the specific associations between connectivity parameters and dimensional traits are complex (see also Chapter 4).

6.4.2. Theta band graph segregation increases during social processing

In the previous chapter, global theta connectivity was increased for social compared to non-social videos. I further examined here whether theta band graph metrics are different for social and non-social stimuli also. The normalised clustering coefficient was increased during social videos compared to non-social videos. This suggests that functional segregation, or the amount of local processing, is increased during social processing. This is in line with the hypothesis that network organisation becomes more efficient during social processing. The increased clustering coefficient possibly reflects increased localised processing of social information from different modalities in more segregated clusters (Johnson, 2011). If cortical regions become more specialized towards the processing of social information, the cortical response will become more fine tuned, and less widespread across the brain, while processing in more localised clusters increases. It is possible that the observed increases in segregation during the social condition are related to increases in fine-tuning towards social information processing.

It should however be noted that the effect for condition on the normalised clustering coefficient was small sized (r = .10), even though reaching significance in this large group. One possibility is that a small increase in segregated information processing reflects a small degree of fine-tuning towards social processing. If interactive specialisation increases with development, more distinct modulations of graph organisation by social processing may emerge at later age (Johnson, 2011; Jones et al., 2015). The current results further revealed that the amount of integration of information (normalised path length), and small-worldness were similar for social and non-social processing. Possibly, differences in graph organisation between conditions emerge earlier for clustering than for path length and small-worldness during the interactive specialisation of the network. If the modulation of cortical processing by social content becomes more pronounced at later ages (Jones et al., 2015), the modulation of graph organisation by social content may be become more distinct across different measures of graph organisation at later age as well.

Together, the current findings suggest that graph segregation is modulated by the processing of information with social content in infants as young as 14 months. No such modulations were observed for graph integration or small-worldness. Possibly, these modulations in graph organisation become more pronounced and widespread across different graph metrics with age. Longitudinal studies with larger cohorts would be needed to further examine this.

6.4.2.1. Theta graph organisation similar between LR and HR infants

When comparing across all groups, normalised clustering coefficients were increased during the social compared to the non-social condition. This effect however did not reach significance in the separate LR and HR groups. Comparisons

of difference scores revealed no differences in any of the graph metrics between groups either. This suggests that graph integration and segregation, and the balance between these two is similar in LR and HR infants.

It seems that global theta connectivity is differently related to social and non-social processing in the risk groups at the age of 14 months (see Chapter 5), while graph organisation is not. The explanation for this finding might be similar to the one presented in the previous section: if differences in graph organisation in response to social and non-social stimuli may become more pronounced at older ages, alterations in graph metrics associated with familial risk with ASD may become more distinct also. Previous studies in toddlers and children indeed found more altered graph metrics in individuals with ASD at later ages than at younger ages (Boersma et al., 2013; J. Han et al., 2017). Thus the modulation of graph organisation by social information processing is similar across infants at low and high familial risk for ASD at 14 months of age.

6.4.2.2. Theta network organisation differences associate with global connectivity differences in HR groups, not LR group

Although there were no differences between groups for graph metrics in the theta frequency band, there were differences between groups for associations between the graph metrics and global connectivity differences. In the HR group, more positive differences between the social and non-social condition for normalised clustering and normalised path length were associated with more positive differences between conditions in global theta connectivity. These associations did not reach significance in the LR group. The additional analyses even confirmed that these associations were different between groups.

These data suggest that graph organisation is more dependent on global connectivity in the HR group, whereas this is not the case in the LR group. As discussed in section 6.4.1.1, graph organisation might be clearer and less dependent on global connectivity in the LR group with typical development, whereas the variables are still interdepend in the HR groups with an atypical developmental trajectory.

6.4.2.3. Theta normalised clustering differences and social affect difficulties

The analyses looking into associations between theta graph metrics and dimensional traits revealed a trend where a larger positive difference in normalised clustering between the social and non-social videos was associated with more severe social affect difficulties. Further analyses showed that this association seemed to be driven by a strong correlation in the HR-TD group. This finding likely arises from the low values and small range of values on the ADOS-2 Social Affect domain in this group. Comparison between the groups indeed showed that this group had lower values than the LR group (see Table 6.1), and this is also clearly visible in Figure 6.6. Thus differences in theta graph metrics between conditions are not strongly associated with social difficulties.

6.4.4. Methodological considerations and limitations

The lack of significant group differences in this study might point towards typical graph organisation in young infants with high risk and with a later diagnosis of ASD. Another possibility however is that at this age connectivity patterns or their topology are not strong enough to reveal significant group differences using scalp EEG techniques. First, the scalp EEG method might not be sensitive enough to pick up on graph differences between infants with high and low risk for autism, and only be sensitive to strong graph differences in older toddlers and children. The

neural signals recorded by the scalp EEG system are more attenuated than the signal extracted from source localisation or MEG methods, therefore any significant network organisation differences at this young age might be lost when analysed with scalp EEG methods. For example, a recent study examining both source and sensor-level connectivity during states of attention found effects for graph metrics in the source-level analyses, that were not evident in the sensor-level analyses (Xie et al., 2018). MEG/EEG source localisation methods that are more robust to volume conduction and field spread might be more sensitive to network differences in young infants.

Second, the use of dbWPLI might explain the differences in findings with other studies as they used the PLI or synchronisation likelihood (Barttfeld et al., 2013; Boersma et al., 2013; J. Han et al., 2017; Takahashi et al., 2017). The main advantage of the dbWPLI is the weighting of the phase lag by the imaginary component that makes the measure more robust to noise. Simultaneously, connectivity for short-range connections or more local connections is underestimated. It is possible that the clustering coefficient, which is a local measure of the EEG graph, is underestimated by the dbWPLI. This might also explain why small-worldness values are below instead of above 1 in these datasets (and in the infant study using WPLI (Xie et al., 2018)). If the amount of clustering is underestimated, normalised clustering will be closer to randomness, i.e. closer to 1, while the normalised path length is less affected by the weighting. Small-worldness being calculated as the ratio between normalised clustering and normalised path length will then be less likely to exceed the value of 1, as we observe both here, and in Chapter 3. The unweighted versions of the PLI such as

the PLI and ubPLI do not have this underestimation, but are also more likely to be influenced by noise with small phase lags.

Third, it is possible that other graph theory metrics are more sensitive to differences between risk and outcome groups. I chose to use the normalised clustering coefficient, normalised path length, and small-worldness index as these metrics were used in the study focusing on toddlers with ASD and typical development by Boersma and colleagues (Boersma et al., 2013), but also in others (Boersma et al., 2011; J. Han et al., 2017; Peters et al., 2013; Smit et al., 2012; Takahashi et al., 2017). Further, these graph metrics are the basic graph theory measures, and therefore seemed a reasonable choice to start. However, other graph metrics reflecting integration and segregation exist also (Rubinov & Sporns, 2010): such as modularity, and local and global efficiency (Alaerts et al., 2015; Kitzbichler et al., 2015; Lewis, Theilmann, Townsend, & Evans, 2013; Peters et al., 2013). Possibly these measures are more sensitive to differences in EEG graph organisation between risk and outcome groups at young ages than the graph metrics used here.

Fourth, other neuroimaging methods than electrophysiology may be able pick up on differences in network organisation between risk groups. Studies examining structural connectivity using DTI have found reduced efficiency in small sub-networks, and whole brain networks in 24-month-old HR-ASD infants, in comparison to both LR and HR-no ASD infants (Lewis et al., 2014). Studies focusing on young children or infants are however still scarce, since most graph theory fMRI or DTI studies focus on children, adolescents, and adults (Alaerts et al., 2015; Redcay et al., 2013; Rudie et al., 2013).

6.5. Summary of Chapter 6

In sum, this chapter showed that infants with low and high familial risk for ASD display similar graph organisation in the theta and alpha frequency band. The theta band normalised clustering coefficient suggested that the segregation of the graph was modulated by social information processing, which had not been revealed before. This effect was similar across risk groups. Interestingly, graph theory metrics showed stronger associations with global connectivity values in the HR group, than the LR group. One possibility is that there are no atypicalities in EEG graph organisations at 14 months of age in HR infants. Another possibility is that the methodology applied here is not a sensitive measure of graph organisation during infancy.

Further, none of these graph metrics in either the theta or alpha frequency band were related to dimensional traits at 3 years of age. First, it is possible that these individual variables only show very weak associations with later outcomes. Combining the measures into one statistical model might have more explanatory value than each of these measures on its own. This also holds for the global connectivity measures. Second, ASD related behaviours and symptoms only start to emerge during toddlerhood, while becoming more prominent during childhood. It is possible that associations between early EEG connectivity measures and later dimensional traits depend on developmental periods. The next chapter aims to further investigate these questions by combining connectivity parameters from the previous chapters and examining associations with later ASD traits.

Chapter 7: The association between EEG connectivity metrics at 14 months and later traits of ASD during childhood

7.1. Introduction

In the previous chapters, the associations between EEG connectivity parameters and ASD traits measured during toddlerhood were examined. I found that EEG alpha connectivity was related to later restricted and repetitive behaviours, while EEG theta connectivity in response social and non-social stimuli was different in HR and LR infants, and not related to ASD symptomatology at 3 years of age (Chapter 4 and 5). Graph organisation parameters in both the alpha and theta band were not different between HR and LR, or outcome groups, and were not related to ASD symptoms during toddlerhood (Chapter 6). While in some individuals ASD symptoms have already emerged during toddlerhood, in other individuals these do not emerge until childhood. According to the DSM-V definition, ASD traits might not appear until the demands of the environment exceed the individuals' abilities (American Psychological Association, 2013). ASD traits are typically most severe or prototypical around 4 and 5 years (Rutter, Le Couteur, et al., 2003). This stresses the importance of continued monitoring and follow-up studies of HR siblings throughout childhood. It is possible that associations between early EEG connectivity and outcomes during toddlerhood are different from those with outcomes at later ages, such as childhood. The current chapter aimed to further examine this.

7.1.1. Developmental trajectories in individuals with ASD

Longitudinal studies examining ASD diagnosis and symptomatology during childhood have revealed changes over time. For example, Charman and colleagues examined children with an ASD diagnosis at 2 years, and found that fewer children tend to meet ASD criteria with each investigated time point: 3, 4-5, and 7 years.

Symptoms in the different core domains showed different developmental trajectories; difficulties in reciprocal social interactions showed considerable decreases between 4-5 and 7 years time points, difficulties in the non-verbal communication domain decreased with each time point, and the severity of restricted and repetitive behaviours showed an increase between 3 and 4-5 years of age with a subsequent decrease to the 7 year time point. However, not all children showed this developmental trajectory, which suggests that ASD is also characterised by heterogeneity of developmental trajectories (Charman et al., 2005).

Indeed, other studies including larger sample sizes, which allows for latent class analyses, have shown that in children with an ASD diagnosis developmental trajectories are heterogeneous. About 80% of the children display a trajectory with persistent high or persistent moderate symptom severity between the ages of 2 and 15 years, whereas a further 15% shows a trajectory characterised by worsening or improvement of symptom severity. The remaining children show a stable trajectory with mild symptom severity (Gotham, Pickles, & Lord, 2012). Patterns of development are largely similar across the three ASD symptom domains, although the social and communication domain tend to show overall improvement over time while the restricted and repetitive behaviour domain shows little change (Fountain, Winter, & Bearman, 2012). Furthermore, most developmental changes occurred during younger ages (before 6 or 8 years of age), with largely stable symptomatology across older ages (Fountain et al., 2012; Gotham et al., 2012). This is consistent with the study by Charman that also showed that developmental changes occur before the age of 7 years.

Similar patterns of stable high or moderate symptoms, worsening, and improving trajectories have been found in other studies from toddlerhood to adolescence (between 13 and 18 months – 36 months old (Lord, Luyster, et al., 2012), 2.5 – 5.5 years old (Venker, Ray-Subramanian, Bolt, & Weismer, 2014), age of diagnosis - 14 years old (Fountain et al., 2012), 2 – 19 years old (Lord et al., 2015)).

The different observed developmental trajectories across childhood and adolescence have been associated with differences in cognitive skills. Verbal skills were associated with outcomes in the severe, worsening, and improving developmental trajectories. The persistent high severity developmental trajectory was associated with lower verbal skills, and lower adaptive functioning skills (Gotham et al., 2012). Children with higher verbal IQ scores tend to show improvements of cognitive skills, adaptive functioning, and multiple domains of ASD symptoms, whereas children with lower verbal IQ scores displayed no change or decreases on cognitive and adaptive skills, and increases in scores for the symptom domains (Lord et al., 2015).

These associations of developmental trajectories with cognitive abilities are also observed at younger ages across toddlerhood and childhood: differences between groups with different developmental trajectories are minimal for expressive and receptive language at 2.5 years of age, but are lower for the high and moderate persistent group compared to the improving and worsening groups at 5.5 years of age. In contrast, scores for non-verbal cognition and adaptive behaviour showed consistent differences across the whole age range. Specifically, scores on these skills are lower for the high persistent group than other groups throughout the investigated age range (Venker et al., 2014). Turning to

dimensional measures, non-verbal abilities, language skills, and symptom severity at 3 years were related to those same measures at 7 year of age (Charman et al., 2005). The variability in symptom severity and cognitive skills furthermore increases with age, showing larger differences between individual children at older ages compared to younger ages (Charman et al., 2005; Lord et al., 2015). In contrast, gender seems not to be related to the developmental trajectory class (Gotham et al., 2012; Venker et al., 2014).

In sum, previous findings suggest that there is heterogeneity in developmental trajectories between individuals with ASD across infancy and adolescence. The different developmental trajectories have also been associated with differences in cognitive skills and adaptive behaviours. This suggests ASD diagnosis and symptom severity may change after the 3 years of age when most clinical assessments in infant sibling studies are collected. HR infants with an ASD diagnosis at 3 years of age may not meet criteria at later ages while displaying less severe symptoms, also termed 'lost diagnosis'. Similarly, about 30% of the HR toddlers who do not meet criteria for ASD at age 3 years still show elevated levels of ASD symptoms compared to LR children (Charman et al., 2017). These HR-no ASD toddlers may meet ASD criteria at later age, also termed children with a 'late diagnosis'. Continued monitoring of ASD symptoms after the 3-year-old time point might further reveal different developmental trajectories, and underlying developmental mechanisms of ASD in these HR infants.

7.1.2. Developmental trajectories in HR siblings

Findings from HR sibling studies show that ASD diagnosis given at 3 years of age is largely stable. In a group of 67 HR siblings, 18 received a diagnosis at 3 years of age. At 5 years of age, 17 toddlers had retained their diagnosis, while 1 did no

longer meet criteria, and 6 toddlers received a late diagnosis. At 9 years of age, 8 children had retained their diagnosis, while 3 additional children received a diagnosis of ASD. Each of the children with a late diagnosis experienced social, language, or behavioural difficulties at 3 or 5 years of age. These children also exhibited lower severity of ASD symptoms, and higher receptive language skills compared to those with an early diagnosis at 3 years of age (Brian et al., 2016).

The follow-up study from the BASIS study (Phase 1) revealed a similar pattern. At 7 years of age, 10 children had retained their ASD diagnosis received at 3 years of age, 3 children lost their diagnosis, whereas 5 children received a late diagnosis. Differences in symptomatology and cognitive skills between the HR-ASD-7 and other groups were more frequently observed than differences between the HR-no ASD-7 and LR groups, which provides little support for the BAP at 7 years of age. Further, males displayed higher ADOS scores and lower communication scores than females. This pattern was similar across all outcome groups (Shephard et al., 2017). Further investigations into cognitive and adaptive skills from 7 months to 7 years of age show little support for the BAP also. Both HR groups (ASD-7 and no ASD-7) displayed lower cognitive and adaptive skills than the LR group. Overall, levels on cognitive skills (global, verbal, and non-verbal IQ) increased over time for all groups. For adaptive functioning, variability increased over time and group differences became more apparent, with the HR-ASD-7 group displaying increasing difficulties over time, whereas the LR and HR-no ASD-7 groups displayed similar levels of adaptive functioning over time (Salomone et al., 2018).

In short, diagnosis and severity of ASD symptoms may change from toddlerhood to childhood. The change in scores may arise from an increase in

symptom severity, where symptoms are not detected at 3 years of age, but emerge during childhood, resulting in a better measurement of symptom severity during childhood. It is likely that there are dynamic developmental processes at play that differ across developmental stages. The investigation of how infant markers relate to ASD traits expressed at different developmental stages may help understand these dynamic processes by revealing associations with earlier and later emerging symptoms, for example during toddlerhood and childhood. Previous high-risk sibling studies have shown that EEG measures were associated with later ASD diagnosis and traits measured at 3 years of age (Elsabbagh et al., 2012; Jones et al., 2014; Orekhova et al., 2014). The next question is whether EEG measures are also related to ASD diagnosis or symptom severity during mid-childhood.

One previous study suggests that neural responses in 7-month-olds are related to ASD outcome at 7 years (Bedford et al., 2017): the difference in neural amplitude in response to faces with directed and averted gaze was related to ASD diagnosis at 7 years of age, while disengagement measures using eye-tracking, and scores on the Autism Observation Scale for Infants did not show this association. This study however did not investigate whether responses were related to dimensional ASD traits, nor whether EEG connectivity was related to mid-childhood outcomes due to limited sample sizes for different categorical groups. Further, most published studies examining EEG connectivity in HR siblings report on outcomes during toddlerhood at age 2 or 3 years (Keehn et al., 2015; O'Reilly et al., 2017; Orekhova et al., 2014; Righi et al., 2014). Thus, the role of early EEG connectivity in the development of ASD traits during childhood remains largely unknown.

7.1.3. Aim of this chapter and hypotheses

Although the association between early connectivity and later ASD traits during childhood has not been investigated before, a series of different patterns could be expected. One possibility is that early EEG connectivity parameters are related to severity of ASD traits during mid-childhood. Associations between early EEG connectivity and mid-childhood outcomes might be clearer than associations with outcomes measured during toddlerhood since individual variability in ASD traits increases over time. Such a finding would suggest that EEG connectivity during infancy plays a role in behaviours expressed several years later. Another possibility is that infant EEG connectivity parameters are not related to later ASD traits during mid-childhood, which would suggest that EEG connectivity is not involved in development at longer term, but only at shorter term. It is also possible that different connectivity parameters show associations with ASD traits in different domains at toddlerhood and childhood. Different aspects of connectivity might play different roles at different developmental stages. The aim of the current study was to examine how EEG connectivity is associated with later ASD dimensional traits measured during mid-childhood, and with developmental changes in severity from toddlerhood to mid-childhood.

To this end, EEG connectivity data from the previous chapters will be used: a) global alpha connectivity, b) alpha connectivity across fronto-central connections, c) alpha normalised clustering coefficient, and differences between social and non-social conditions for d) global theta connectivity, e) across LR and HR masked connections, and f) theta normalised clustering coefficient. In addition, ASD traits during later childhood will be measured by the Social Responsiveness Scale – 2 (SRS-2), focusing on the subscales of Social Communication and

Interaction (SCI), and Restricted and Repetitive Behaviours (RRB) (Constantino & Gruber, 2012; Constantino et al., 2003). This questionnaire was chosen based on its practical subscales that match the social communication and restricted and repetitive behaviours domain investigated in the previous chapters in this thesis. Furthermore, it is a more sensitive measure of ASD traits in the general population than the ADOS-2 or ADI-R, and thus ensures enough variance on this scale in the whole group (LR and HR siblings). The other reason was practicality, as this measure was used in 2 separate childhood follow-up studies, which allows for an increased sample size, and increased statistical power. This measures was further used at the 3-year-old time point, and for the individuals with this data available, slopes of change in symptom severity could be calculated also.

If diagnosis and severity of traits remain largely stable, I expect to find associations between alpha connectivity parameters and severity of restricted and repetitive behaviours, while for theta connectivity I expect to find associations with the severity of social and communication symptoms. I hypothesized to find a similar pattern of associations between the EEG connectivity parameters and the slopes of change for the different symptom domains.

Finally, as in previous chapters, it is possible that EEG connectivity parameters and later ASD traits are related to other factors. For example, EEG connectivity measures are possibly influenced by the number of epochs, and spectral power (van Diessen et al., 2015). Other, less methodological, variables might also play a role. It is possible that familial risk or diagnostic outcome at 3 years is associated with early connectivity and childhood ASD traits (Orekhova et al., 2014). Gender seems to play a role in associations between early ASD markers and outcomes during toddlerhood (Bedford et al., 2016), although this might not

be the case for the childhood outcomes (Bedford et al., 2017; Salomone et al., 2018). Chapter 4 showed that gender and age at neural assessment were related to EEG connectivity. Age at follow-up assessment might be involved also, since severity of symptoms are expected to be highest between 4 and 5 years of age, and individual variability of symptoms increased with age (American Psychological Association, 2013; Charman et al., 2005). Finally, cognitive abilities might relate to EEG connectivity (Chapter 4), and later outcomes or developmental changes in ASD traits (Salomone et al., 2018; Shephard et al., 2017). To investigate the potential influences of these factors on associations between early EEG connectivity and childhood ASD traits, additional analyses including these factors were therefore performed to test whether any of these factors would change the results.

7.2. Methods

7.2.1. Participants

The participants in the current chapter are subsets of those analysed in the previous 3 chapters. Only infants with data for the SRS-2 at one of the follow-up studies were included in the analyses for alpha and theta connectivity. The follow-up studies were BASIS7 and gBASIS. BASIS7 involves a follow-up assessment at the lab with children who were participants of the BASIS Phase 1 study. These children were 6 to 7 years of age at the time of BASIS7. The other follow-up study, gBASIS, is a genetic study with children who participated in BASIS Phase 1 or 2 and their first-degree relatives (http://www.staars.org/gbasis). These children were between 5 and 10 years of age at the time of data collection. Both BASIS7 and gBASIS utilised the SRS-2 questionnaire. For the children who had participated in

both BASIS7 and gBASIS, data from the gBASIS study were included in the current analyses as this was the most recent assessment. Protocols for both the BASIS7 and gBASIS study were approved by the UK National Health Service National Research Ethics Service London: for BASIS7, code 08/H0718/76; 14/LO/0170; and for gBASIS, code 08/H0718/76; 15/LO/0468. Experimenters took the parents/ caregivers' written informed consent, and the child's written assent before the start of the study.

For a smaller set of infants, data from the SRS-2 were also available for the toddler time point at 3 years of age. Infants without these data were excluded from the analyses for the change in symptomatology across childhood.

7.2.2. Materials

7.2.2.1. Social Responsiveness Scale – 2

The Social Responsiveness Scale, Second Edition (SRS-2) is a 65-item questionnaire that measures ASD-related symptoms on a 4-point Likert scale (Constantino & Gruber, 2012). The questionnaire is appropriate for individuals from 2.5 years of age to adulthood, by the use of 3 different versions: Preschool (2.5 – 4.5 years), School-Age (4 – 18 years), and Adult (19 years and older). The adult form is a self-report questionnaire, while the other two versions are reports from the parents, caregiver, or teachers. The questionnaire can be completed in 15 to 20 minutes.

The 65 items concern ASD related behaviours exhibited by the target individual in the past 6 months. These are behaviours involving social awareness, social information processing, social responses, social motivation, social communication, and preoccupations and mannerisms. The responses to each item are scored on a scale from 1 to 4; 1 - 'not true', 2 - 'sometimes true', 3 - 'often true',

and 4 - 'almost always true'. The responses on each item are then recoded to 0, 1, 2, or 3, where some responses are mirrored. Missing responses are replaced by the median response on the item. Questionnaires with 7 or more missing responses are considered invalid.

The sum of all the recoded responses on the 65 items is the SRS-2 Total raw scores. Similarly sums of different items are the raw scores for 5 different subscales: a) Social Awareness, b) Social Cognition, c) Social Communication, d) Social Motivation, and e) Restricted Interests and Repetitive Behaviour. The sum of the scores on the first 4 subscales compromises the DSM-V compatible subscale Social Communication and Interaction (SCI). The raw score on the fifth subscale is identical to the raw score on the DSM-V compatible subscale Restricted Interests and Repetitive Behaviour (RRB). Higher raw scores on the subscales reflect higher severity of the measured traits.

The sums of raw scores on each subscale are converted to T-scores by identifying the T-score matched to the subscale sum score in the tables provided with the scoring sheet, and the manual. The T-scores have a mean of 50, and a standard deviation of 10, where higher scores indicate higher severity. These scores are based on standardization from a large representative American sample. Since differences in raw scores were found between males and females, and between parents and teachers at school age, separate tables for the different genders and raters were created for the School-Age version. In contrast, the Preschool and Adult version contain 1 version of each table as no score differences between genders or raters were found.

For this chapter, the focus was on severity of social communication difficulties and restricted and repetitive behaviours during childhood, and the

change in severity between toddlerhood and childhood. To this end, T-scores for the SCI and RRB DSM-V compatible subscales were derived from the SRS-2 School-Age version collected by the research teams from the BASIS7 and gBASIS study during childhood. T-scores for the same subscales were derived from the SRS-2 Preschool version collected by the research team from the BASIS Phase 1 and 2 studies during toddlerhood. All questionnaires were filled in by the child's parent or caregiver.

Item responses on the SRS-2 had been entered by the research teams into a database, and were subsequently shared with me. T-scores were then calculated from the responses using SPSS syntax. The script automatically recodes the responses, sums scores for the different scales, and identifies T-scores. This syntax was originally created for the Preschool version by a researcher from the BASIS team (Greg Pasco), but was then adjusted by me. Using this script as a basis, I created a script for the School-Age version that also takes into account the child's gender when calculating the T-scores from the raw summed scores.

For the childhood outcome analyses, T-scores on the SCI and RRB subscale measured at the follow up were used. For the developmental change analyses, slopes of change in symptoms were used. The slopes were calculated by dividing the differences between childhood and toddlerhood SRS-2 T-scores ($T_{childhood} - T_{toddlerhood}$) by the differences in ages at assessments in months ($Age_{childhood} - Age_{toddlerhood}$). For children whose age was missing in the SRS-2 dataset, age was calculated from the dates of birth and assessment of the other questionnaires in the same study (BASIS7), or date recorded on the consent form (gBASIS). This resulted in a slope of change in symptom severity for both the SCI and RRB subscales.

7.2.2.2. EEG connectivity measures during infancy

The EEG connectivity measures included in this chapter are taken from the previous chapters. These measures have been derived from EEG recordings in 14-month-olds as part of the BASIS study (see Chapters 4 through 6 for descriptions of the EEG assessment and calculations of EEG connectivity measures). The following parameters were included in this chapter. For connectivity in the alpha frequency band: 1) global connectivity across all channels (Chapter 4), 2) global connectivity across frontal-central channels that showed higher connectivity in the HR-ASD group compared to both the LR and HR-no ASD group in the original study (Chapter 4, (Orekhova et al., 2014)), and 3) normalised clustering coefficient (Chapter 6). For connectivity in the theta band, measures were based on differences between the social and non-social condition for 1) global connectivity across all channels (Chapter 5), 2) global connectivity across channels that showed significant differences between conditions for the matching group, i.e. connections in the LR mask for LR individuals and connections in the HR mask for HR individuals (Chapter 5), and 3) normalised clustering coefficient (Chapter 6). The normalised clustering coefficient was included as measure of graph organisation since this measure was more reliable than other graph theory metrics (Chapter 3).

In this chapter, I chose to focus on global connectivity across all and selected connections, and on the normalised clustering coefficient based on the findings from Chapter 3. The results from this chapter revealed that global connectivity (ICC = .53) and the normalised clustering coefficient measures (ICC = .59) are more reliable than the normalised path length (ICC = .44) and the small-worldness index (ICC = .40, see tables 3.8, 3.11, and 3.14). The focus of this chapter is individual variability in dimensional traits at later age that requires higher

reliability than analyses focusing categorical groups. Thus, I used global connectivity and normalised clustering coefficient as connectivity measures of interest.

7.2.2.3. Potentially confounding variables

As in previous chapters, the possible effects of confounding factors were considered here also. Calculation of EEG connectivity for example might be influenced by the number of epochs values were calculated over, or the amount of spectral power (here power averaged across all channels). Clinical variables such as familial risk, and diagnostic outcome at 3 years of age (and severity of ASD traits at toddlerhood for developmental changes), or demographic variables such as gender, ages at EEG and follow-up assessment might have influenced results as well. Lastly, cognitive abilities might be related to associations between early connectivity and childhood ASD traits or changes. These were measured with the MSEL ELC at 14 months of age. It is possible that each of these variables changes any observed associations between early EEG connectivity and later ASD traits and their developmental changes.

7.2.3. Statistical analyses

All statistical analyses were performed using SPSS. Due to differences in sample sizes for participants with alpha and theta connectivity data, statistical approaches to these datasets were different. For the alpha connectivity, multivariate general linear models (GLMs) were performed with the 3 alpha connectivity measures as independent variables. The T-scores for the SCI and RRB subscales during childhood were the dependent variables in the multivariate model. A separate GLM included slopes of change for the two subscales as dependent variables. The focus was on effect sizes while interpreting the results since these were considered more

informative than levels of significance in the context of small sample sizes. Effect sizes were assessed with partial eta squared: values < .01 as minimal, values from .01 through < .06 as small, values from .06 through < .14 as medium, and values ≥ .14 as large effect sizes (J. Cohen, 1988; Field, 2014). If the multivariate model reached a medium or larger effect size, follow-up analyses were performed with separate univariate GLMs for the SCI and RRB subscales. I used Pillai's trace as test statistic, since this statistic is more robust to violations of the assumption of homogeneity of variance across groups, and is appropriate for uneven and small sample sizes (see also Appendix A7.1 for the rationale of using GLM as opposed the hierarchical linear modelling).

For the theta analyses, a different approach was taken. This dataset included approximately a third of the participants of the alpha dataset. Therefore I decided to conduct Spearman's correlations to examine the associations between theta connectivity parameters and childhood ASD traits, and change of severity of traits during childhood. This approach was selected as it was also used in the previous chapters, and it was expected that the measures were not normally distributed. Again, correlation values above .30 were considered medium effects, while values above .50 were considered large (J. Cohen, 1988; Field, 2014).

Finally, additional analyses were performed to test whether results would be different if possibly confounding variables were included in the models. Separate GLMs and correlational analyses were performed for each variable to test its effect. For the GLMs with alpha connectivity, variables were added as covariate (number of epochs, power, age at EEG, age at follow-up assessment, and MSEL at 14 months), or factor (risk group (HR, LR), outcome group at 3 years of age (LR, HR-TD, HR-Atyp, HR-ASD), and gender (male, female)). Also, the SRS-2 T-scores at

3 years of age were included as extra covariate in the analyses with slope of change, as initial scores might be associated with the rates of change. For the correlations with theta connectivity, partial correlations were performed with each of the possibly confounding variables that were also tested for the alpha analyses. Only results of the connectivity variables are reported since I was interested how these changed with the inclusion of other variables, not the effects of these variables on later ASD traits or developmental changes. Again, the focus was on effect sizes while interpreting the results rather than p-values.

7.3. Results

7.3.1. Participants

The final sample used for the alpha analyses with childhood outcomes consisted of 56 participants. Characteristics of the participants for the alpha analyses are displayed in table 7.1. The sample further consisted of 24 males, and 32 females, and 20 LR, 19 HR-TD, 8 HR-Atyp, and 9 HR-ASD participants based on the clinical assessments at 3 years of age. Cognitive skills measured by the MSEL at infancy were similar between the LR, HR-TD, and HR-Atyp groups, and between the HR-TD and HR-ASD groups, where the latter 2 groups displayed lower scores than the former 3 groups, p = .003.

During toddlerhood, differences between groups were observed for both the SRS-2 scales: 1) for the SCI subscale, scores did not differ between the LR, and HR-Atyp group, or between the HR-TD, HR-Atyp, and HR-ASD group, but scores were lower for the former set of groups than the latter set, p = .009. 2) For the RRB subscale, scores did not differ between the LR, HR-TD, and HR-Atyp group, or between the HR-TD, HR-Atyp, and HR-ASD group. Again, scores were lower for the

former set of groups than the latter set, $p < .001$. The HR-ASD group also showed higher ASD symptoms compared to the other groups, which showed no differences among each other for the each of the 3 ADI-R subscales, and the ADOS RRB subscale, p's ≤ .002. For the ADOS SA subscale, the HR-TD group showed higher values than the HR-ASD and LR group, which showed similar scores, and were higher than the HR-Atyp group scores. The HR-Atyp group scores were not different from the HR-ASD scores, $p < .001$.

For the follow-up assessment, there were no significant differences in age between the LR, HR-TD, and HR-Atyp group, or between the LR, HR-Atyp, and HR-ASD group, where the former set of groups showed lower scores than the latter, $p = .042$. SRS-2 scores on both SCI and RRB subscales were lower for the LR group than the other groups, which showed no differences among each other (HR-TD, HR-Atyp, and HR-ASD group), p's = .001.

For 23 out of 56 participants, no diagnostic data were available at follow-up. In the group of participants with follow-up diagnostic data from BASIS7, 17 were LR participants, 11 HR participants did not meet criteria at either 3 years or the follow-up, and 3 HR participants met criteria for ASD at both 3 years and the follow-up. Two participants had a change of diagnosis at the follow-up; 1 participant lost the ASD diagnosis, whereas the other participant received a late diagnosis (see (Shephard et al., 2017) for a description of diagnostic stability in the complete BASIS7 sample). Since I was interested in dimensional traits and their developmental changes, rather than categorical diagnosis, the two participants with change in diagnosis between time points were not excluded from the analyses.

Table 7.1. **Demographics of the sample for alpha analyses according to diagnostic group at 3 years of age**

	LR	*HR-TD*	*HR-Atyp*	*HR-ASD*	*Total*
N (male)	20 (8)	19 (7)	8 (2)	9 (7)	56 (24)
Infancy	*LR*	*HR-TD*	*HR-Atyp*	*HR-ASD*	*Test statistic*
Age at EEG assessment, in days [1]	450 (41) [1] 374 – 544	464 (52) 364 – 547	441 (44) 366 – 512	450 (22) 429 – 487	$F(1,52) = 0.70$, $p = .558$
MSEL Composite Standard Score at visit at 14 months [3]	107 (17) [1] 85 – 154	96 (15) 71 – 121	102 (11) 90 – 118	85 (7) 74 – 95	$F(3,51) = 5.22$, $p = .003$ (LR = HR-TD = HR-Atyp) > (HR-TD = HR-ASD
Toddlerhood	*LR*	*HR-TD*	*HR-Atyp*	*HR-ASD*	*Test statistic*
Age at lab assessment, in months	37 (1) [2] 36 – 50	38 (3) 33 – 53	38 (2) 32 – 38	39 (2) 37 – 41	$H(3) = 5.834$, $p = .120$
SRS-2 SCI T-scores [4]	42 (7) [2] 35 – 48	47 (10) 40 – 81	44 (3) 37 – 88	54 (31) 40 – 89	$H(3) = 13.72$, $p = .003$, (LR = HR-Atyp) < (HR-Atyp = HR-TD = HR-ASD)

SRS-2 RRB T-scores [4]	40 (6) [2] 40 – 58	44 (6) 40 – 66	42 (6) 40– 104	48 (34) 42 – 102	$H(3)$ = 11.51, p = .009, (LR = HR-Atyp = HR-TD) < (HR-Atyp = HR-TD = HR-ASD)
ADI-R Social Total [5]	0 [2] 0 – 1	2 (4) 0 – 11	3.5 (3) 0 – 18	11 (10) 7 – 25	$H(3)$ = 19.31, p < .001, (LR = HR-TD = HR-Atyp) < HR-ASD
ADI-R, Communication Total [5]	0 [2] 0 – 1	2 (5) 0 – 7	3 (6) 0 – 20	11 (5) 2 – 19	$H(3)$ = 15.51, p = .001, (LR = HR-TD = HR-Atyp) < HR-ASD
ADI-R BRI Total [5]	0 (0) [2] 0	0 (1) 0 – 3	0.5 (3) 0 – 4	5.5 (4) 0 – 8	$H(3)$ = 19.86, p < .001, (LR = HR-TD = HR-Atyp) < HR-ASD

ADOS-2, SA Total [5]	5 (7) [2] 1 – 12	2 (2) 0 – 5	11.5 (5) 6 – 15	9 (11) 1 – 17	*H*(3) = 23.68, *p* < .001, HR-TD < (LR = HR-ASD) < (HR-ASD = HR-Atyp)
ADOS-2 RRB Total [5]	1 (2) [2] 0 – 5	0 (1) 0 – 3	1 (3) 0 – 3	3 (4) 1 – 5	*H*(3) = 15.12, *p* = .002, (LR = HR-TD = HR-Atyp) < HR-ASD

Childhood	*LR*	*HR-TD*	*HR-Atyp*	*HR-ASD*	*Test statistic*
Age at follow-up assessment, in months	92 (18) [2] 79 – 125	85 (24) 64 – 120	98 (31) 81 – 121	89 (42) 71 – 125	*H*(3) = 8.22, *p* = .042, (LR = HR-TD = HR-Atyp) < (LR = HR-Atyp = HR-ASD)
SRS-2 SCI T-scores	44 (7) [2] 37 – 66	49 (9) 38 – 81	56 (11) 49 – 85	70 (40) 39 – 88	*H*(3) = 15.70, *p* = .001, LR < (HR-TD = HR-Atyp = HR-ASD)

SRS-2 RRB T-scores	42 (3) [2] 41 – 52	46 (7) 41 – 76	49 (17) 42 – 90	54 (45) 41 – 94	$H(3) = 17.04$, $p = .001$, LR < (HR-TD = HR-Atyp = HR-ASD)

[1] Means and standard deviations in parentheses, with minimum and maximum scores, and results for the analysis of variance with Group as factor (LR, HR-TD, HR-Atyp, HR-ASD).

[2] Medians and interquartile range in parentheses, with minimum and maximum scores, and results for the Independent-Samples Kruskal-Wallis test, and stepwise step-down follow-up analyses if significant asymptotic 2-tailed p-value.

[3] MSEL data for the 14-month-old visit were missing for 1 LR infant.

[4] SRS-2 data were missing for 2 HR-TD infants, and 1 HR-Atyp infants in this dataset.

[5] ADI-R data were only available for 3 LR infants, 19 HR-TD infants, 8 HR-Atyp infants, and 8 HR-ASD infants.

Table 7.2. **Demographics of the sample for theta analyses according to diagnostic group at 3 years of age**

	LR	*HR-TD*	*HR-Atyp*	*HR-ASD*	*Total*
N (male)	4 (0)	8 (3)	2 (2)	5 (4)	19 (9)
Infancy	*LR*	*HR-TD*	*HR-Atyp*	*HR-ASD*	
Age at EEG assessment, in days[1]	445 (43) [1] 387 – 481	479 (49) 392 – 547	437, 484	462 (23) 437 – 487	
MSEL Composite Standard Score at visit at 14 months [3]	117 (13) [1] 105 – 130	97 (20) 71 – 121	90, 95	86 (8) 78 – 95	
Toddlerhood	*LR*	*HR-TD*	*HR-Atyp*	*HR-ASD*	
Age at lab assessment, in months	38 (2) [2] 36 – 38	39 (2) 37 – 53	37, 38	39 (3) 37 – 41	
SRS-2 SCI T-scores [4]	39 (3) [2] 38 – 42	46 (11) 41 – 53	37	54 (35) 47 – 89	
SRS-2 RRB T-scores [4]	41 (4) [2] 40 – 44	46 (8) 40 – 52	42	48 (47) 44 – 102	
ADI-R Social Total [5]	0	1 (4) [2] 0 – 5	1, 4	14 (17) 7 – 25	
ADI-R, Communication Total [5]	0	2 (5) [2] 0 – 7	0, 6	11 (2) 9 – 19	
ADI-R BRI Total [5]	0	0 (2) [2] 0 – 3	0	5 (4) 3 – 8	
ADOS-2, SA Total [5]	7 (8) [2] 3 – 12	1 (2) 0 – 3	6, 12	9 (10) 6 – 17	
ADOS-2 RRB Total [5]	0.5 (1) [2] 0 – 1	0 (1) 0 – 2	1, 3	4 (3) 1 – 5	

Childhood	*LR*	*HR-TD*	*HR-Atyp*	*HR-ASD*
Age at follow-up assessment, in months	100 (31) [2] 80 – 116	77 (22) 64 – 96	104 81, 119	101 (40) 72 – 125
SRS-2 SCI T-scores	43 (11) [2] 37 – 50	49 (7) 39 – 52	55, 61	70 (39) 39 – 88
SRS-2 RRB T-scores	42 (6) [2] 42 – 50	47 (7) 43 – 54	52, 62	54 (47) 41 – 94

[1] Means and standard deviations in parentheses, with minimum and maximum (or individual scores if N ≤ 2, or the score is identical for all participants).
[2] Medians and interquartile range in parentheses, with minimum and maximum (or individual scores if N ≤ 2, or the score is identical for all participants).
[3] MSEL data for the 14-month-old visit were missing for 1 LR infant.
[4] SRS-2 data were missing for 2 HR-TD infants, and 1 HR-Atyp infants in this dataset. Raw data for the 1 HR-Atyp infant are reported in the table.
[5] ADI-R data were only available for 1 LR infant, 8 HR-TD infants, 2 HR-Atyp infants, and 4 HR-ASD infants. Raw data for the 1 LR infant are reported in the table.

For the theta analyses, a subset of the sample again was used. Out of the 56 participants included in the alpha analyses with follow-up data, 19 participants had theta data available. Characteristics for the sample included in the theta analyses are presented in table 7.2 (no statistical tests were done due to limited group sample sizes). This sample consisted of 4 LR participants, 8 HR-TD participants, 2 HR-Atyp participants, and 5 HR-ASD participants. The participants with lost and late ASD diagnosis were not included in these analyses, as they did not have sufficient theta data (number of epochs for the social and non-social conditions was below 120).

7.3.2. Developmental trajectories of ASD traits

ASD is characterised by heterogeneity in ASD traits, and in developmental trajectories. Some participants may show increases in severity of traits, while others display decreases, or no change across early ages. Figure 7.1 illustrates ASD traits at the different ages of assessment. This figure shows that some participants experienced less severe ASD traits as a toddler than as a school-age child. Developmental trajectories in the opposite direction, or minimal changes in ASD trait severity are also present. On another note, higher levels of severity of ASD traits seem to occur during early childhood, which would be consistent with the notion that most severe ASD symptoms are observed around 4 and 5 years of age. This figure demonstrates the heterogeneity of developmental traits in HR-ASD participants. In the next section, I examined whether alpha connectivity parameters are associated ASD traits during mid-childhood, and rate of changes of these traits between toddlerhood and childhood.

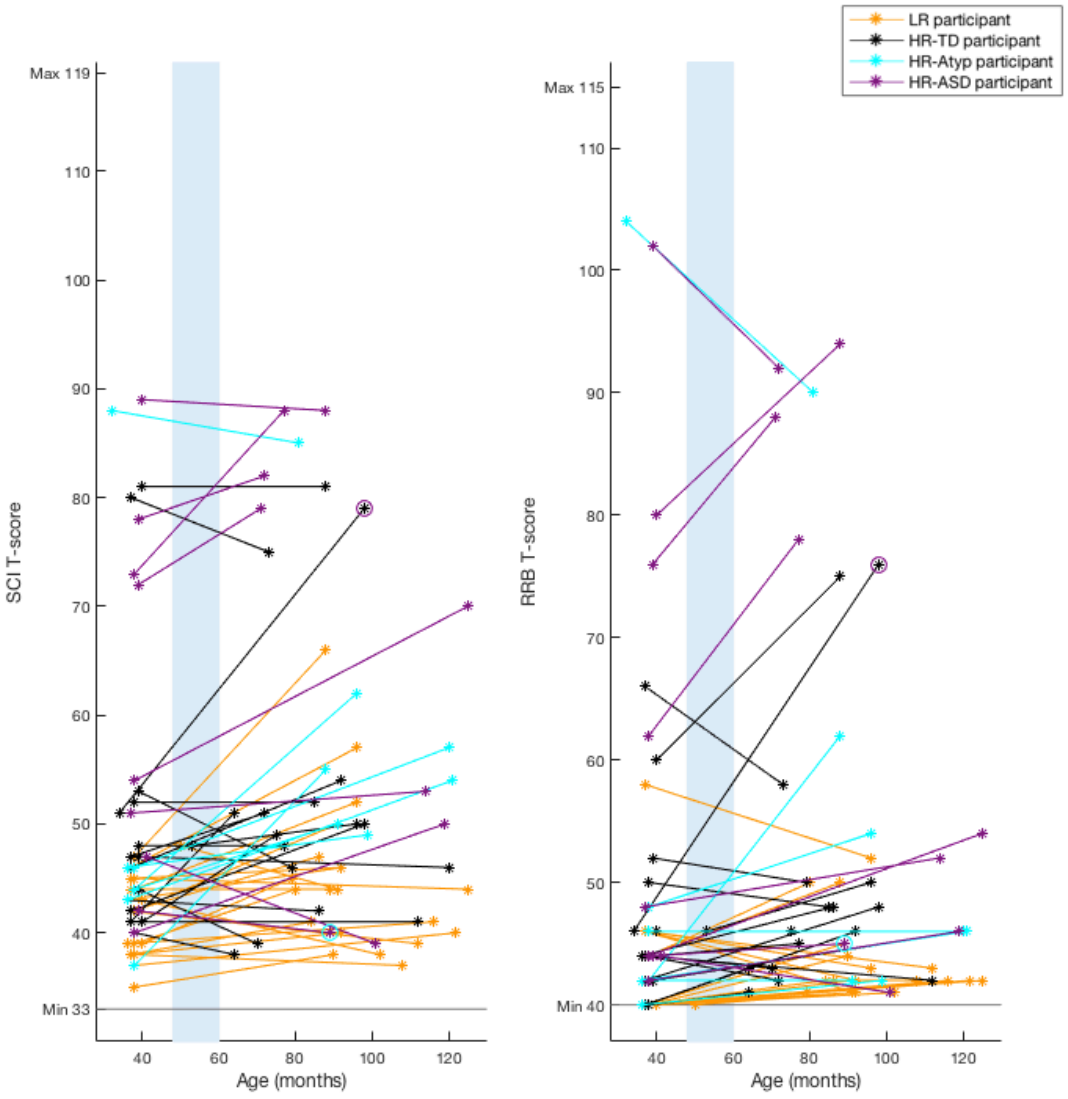

Figure 7.1. Trajectories of ASD traits measured with the SRS-2 across toddlerhood and childhood

T-scores for the SCI SRS-2 subscale (left), and RRB SRS-2 subscale (right) at different ages of assessment during toddlerhood (32 to 53 months of age), and childhood (64 to 125 months of age). Different colours reflect different outcome groups at 3 years of age. For 2 participants with a change in diagnosis, an outer circle in the colour of the childhood diagnostic outcome marks the diagnostic change (purple for late diagnosis, and cyan for lost diagnosis). Note diagnosis at the childhood assessment was unknown for a number of participants. Light blue marked ages represent 4 to 5 years.

7.3.3. Alpha EEG connectivity

7.3.3.1. Alpha EEG connectivity and childhood ASD traits

First, I tested whether the 3 alpha connectivity parameters were related to both SCI and RRB SRS-2 outcome measures at childhood using a multivariate GLM. Scatterplots are displayed in Figure 7.2. Using Pillai's trace, the results revealed a medium effect of the normalised clustering coefficients on the combined ASD trait measures at childhood, $V = .17$, $F(2,51) = 5.84$, $p = .005$, $\eta_p^2 = .186$. The other connectivity parameters showed a small effect: for global alpha connectivity, $V = .03$, $F(2,51) = 0.90$, $p = .413$, $\eta_p^2 = .034$, and for global fronto-central alpha connectivity, $V = .03$, $F(2,51) = 0.66$, $p = .521$, $\eta_p^2 = .025$.

Follow-up analyses with separate GLMs for the SRS-2 subscales including the normalised clustering coefficient as only connectivity parameter showed that the normalised clustering coefficient had a small effect on the SCI subscale, $F(1,54) = 0.65$, $p = .424$, $\eta_p^2 = .012$. For the RRB subscale, the normalised clustering coefficient had a medium effect: $F(1,54) = 5.84$, $p = .070$, $\eta_p^2 = .060$. Smaller normalised clustering coefficients at early age were thus related with higher severity of restricted and repetitive behaviours during childhood (Fig. 7.2).

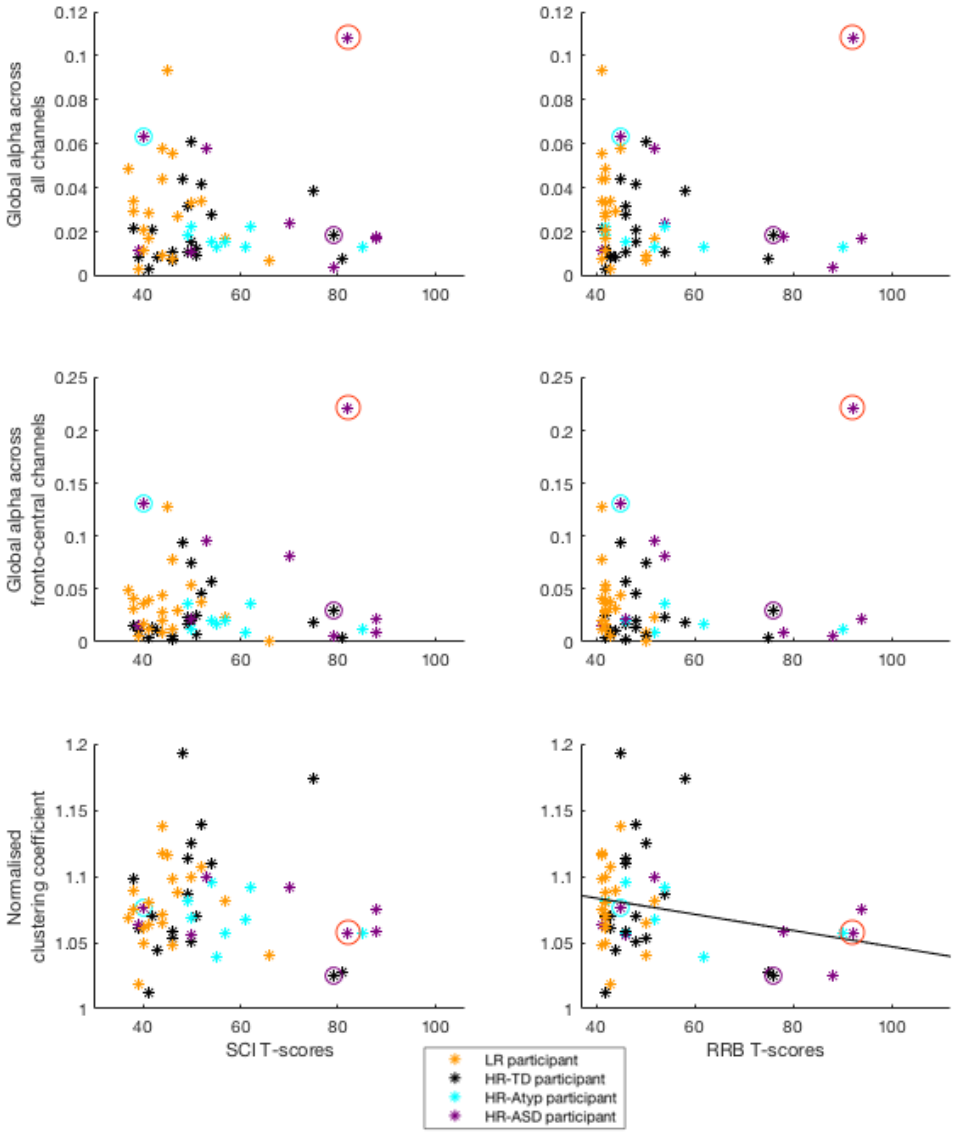

Figure 7.2. Scatterplots for the alpha connectivity data and ASD traits measured during childhood

Rows represent the different connectivity parameters: global connectivity across all channels (top), global connectivity across fronto-central channels (middle), and normalised clustering coefficients (bottom). Columns reflect the SRS-2 subscales: SCI on the left, and RRB on the right. Different colours signify the diagnostic group at 3 years of age, and circled values signify a diagnostic change (purple for late diagnosis in HR-TD participant, and cyan for lost diagnosis in HR-ASD participant) or outlier (in red). Only normalised clustering coefficient was associated with RRB T-scores (black line).

When inspecting the scatterplots, one participant in the HR-ASD group could be marked as an outlier (marked with a red circle in Fig. 7.2). The outlier was excluded from both global connectivity and normalised clustering analyses for consistency across analyses, and because abnormally high global connectivity likely affects normalised clustering coefficients also. These analyses revealed a similar pattern compared to the primary analyses, although effect sizes were overall smaller: the normalised clustering coefficient showed a medium effect size, $V = .12$, $F(2,50) = 3.34$, $p = .044$, $\eta_p^2 = .118$, global alpha connectivity a small effect size, $V = .04$, $F(2,50) = 0.93$, $p = .402$, $\eta_p^2 = .036$, and fronto-central alpha connectivity a minimal effect size, $V = .004$, $F(2,50) = 0.09$, $p = .918$, $\eta_p^2 = .004$. The association for the normalised clustering coefficient was stronger with the SRS-2 RRB subscale, $F(1,53) = 3.07$, $p = .085$, $\eta_p^2 = .055$, than the SCI subscale, $F(1,53) = 0.45$, $p = .505$, $\eta_p^2 = .008$. Since the results with and without including the outlier were fairly similar, the outlier was included in the further analyses examining the effects of possible confounding variables.

The additional analyses taking into account confounding variables did not change the pattern of results found in the primary analyses: smaller normalised clustering coefficients during infancy are related to more severe restricted and repetitive behaviours during childhood. This held for each of the variables included: methodological variables (number of epochs, power), clinical variables (risk group, outcome group at 3 years of age), demographic variables (gender, age at EEG assessment and follow-up assessment), and cognitive variables (developmental levels at EEG assessment) (see Appendix A7.2). The observed association was stronger than for global connectivity across all channels and

across fronto-central channels, and social communication and interaction difficulties during childhood.

In short, these results suggest that the organisation of brain graphs in the alpha frequency during infancy is related to later ASD traits during childhood, with a stronger effect for the severity of restricted and repetitive behaviours than for social communication and interaction difficulties. In contrast, global connectivity across all channels, and across fronto-central channels showed weaker associations with the ASD traits at childhood.

7.3.3.2. Alpha EEG connectivity and change in ASD traits

The results from the previous section suggest that alpha connectivity parameters are strongly related to dimensional ASD traits during childhood. Possibly, EEG connectivity parameters are related to developmental trajectories of ASD behaviours, in addition to outcomes. Using a multivariate GLM, I first tested how alpha connectivity parameters measured during infancy were related to the slopes of change in ASD traits across toddlerhood and childhood (Fig. 7.3). The results revealed only small effect sizes: for global alpha connectivity across all connections, $V = .02$, $F(2,48) = 0.76$, $p = .689$, $\eta_p^2 = .015$; for global alpha across fronto-central connections, $V = .05$, $F(2,48) = 1.32$, $p = .301$, $\eta_p^2 = .049$; and for the normalised clustering coefficient, $V = .03$, $F(2,48) = 0.75$, $p = .479$, $\eta_p^2 = .030$.

The scatterplots in Figure 7.3 again reveal an outlier in the dataset, which was also identified as outlier in the Figure 7.2. Analyses excluding this outlier, revealed a strong effect of the normalised clustering coefficient in the GLM multivariate, $V = .09$, $F(2,47) = 2.29$, $p = .113$, $\eta_p^2 = .089$; but small effects for the other connectivity measures: for global alpha connectivity, $V = .02$, $F(2,47) = 0.48$,

p = .625, η_p^2 = .020; and for fronto-central connectivity, V = .02, $F(2,47)$ = 0.41, p = .665, η_p^2 = .017.

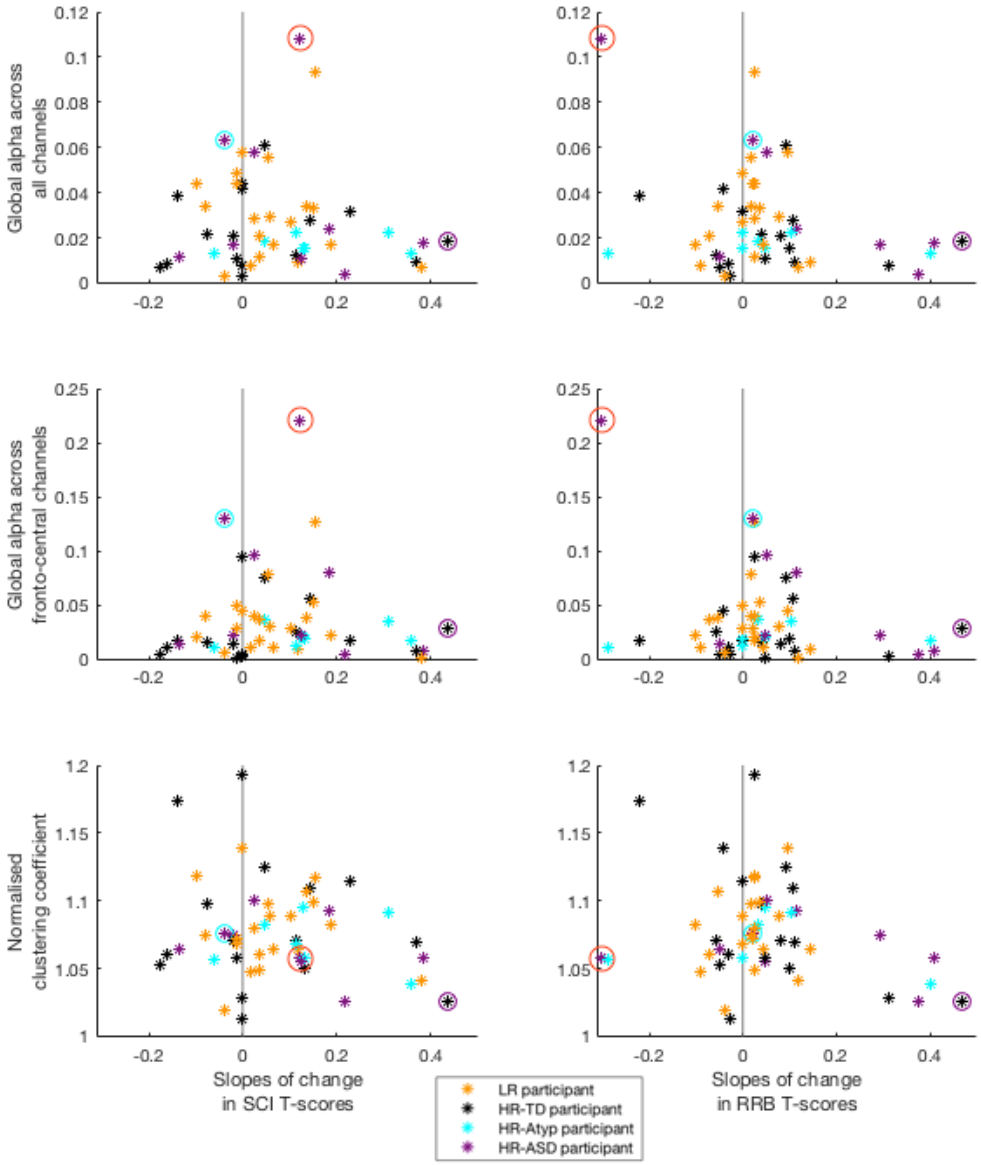

Figure 7.3. Scatterplots for the alpha connectivity data and rate of change for ASD traits between toddlerhood and childhood

Rows represent the different connectivity parameters: global connectivity across all channels (top), global connectivity across fronto-central channels (middle), and normalised clustering coefficients (bottom). Columns reflect the SRS-2 subscales: SCI on the left, and RRB on the right. Different colours signify the diagnostic group at 3 years of age, and circled values signify a diagnostic change (purple for late diagnosis in HR-TD participant, and cyan for lost diagnosis in HR-ASD participant) or outlier (in red).

Follow-up analyses showed that the effect size with the normalised clustering coefficient was larger for the RRB subscale, $F(1,50) = 5.37$, $p = .025$, $\eta_p^2 = .097$, than the SCI subscale of the SRS-2, $F(1,50) = 2.11$, $p = .152$, $\eta_p^2 = .041$. These analyses revealed a stronger pattern of results than the primary analyses. The data suggest that a lower normalised clustering coefficient during infancy is related to a stronger increase in severity of restricted and repetitive behaviours between toddlerhood and childhood. Only small effect sized effects were observed for global connectivity across all and fronto-central connections, and for the SCI subscale of the SRS-2.

Additional analyses taking into account confounding variables are reported in the appendix, while both in- and excluding the outlier (see Appendix A7.3). Results for slopes of change showed a less convergent pattern than for the analyses focusing on ASD traits at childhood when including the outlier reported in the previous section. When including number of epochs, familial risk, diagnostic outcome at 3 years of age, gender, and cognitive levels, results suggested that fronto-central connectivity is negatively associated with the slopes of change in restricted and repetitive behaviours. The associations remained small when including other confounding factors. When excluding the outlier, the primary results remained unchanged for inclusion of each of the technical, clinical, demographical, or cognitive variables: lower normalised clustering coefficients are related to stronger increases in RRB traits, while higher normalised clustering coefficients are related to stronger decreases in RRB traits.

In sum, the current results suggest that alpha connectivity parameters during infancy in general are related to ASD traits at childhood, and slopes of change during toddlerhood and childhood, where effects sizes are larger for

severities of restricted and repetitive behaviours, than difficulties with social communication and interaction difficulties. The specific patterns of associations between connectivity parameters and ASD traits seem to differ across different subsamples of the dataset. Possibly, different subgroups of individuals show different associations between connectivity parameters and ASD traits, for example with theta connectivity parameters. Theta connectivity parameters might be related to social communication and interaction difficulties during childhood rather than restricted and repetitive behaviours.

7.3.4. Theta EEG connectivity

7.3.4.1. Theta EEG connectivity and childhood ASD traits

After looking at alpha connectivity in relation to dimensional childhood outcomes, I focused on the associations with theta connectivity parameters. None of the investigated correlations revealed a medium or large effect size, nor reached significance, $-.23 \leq r\text{'s} \leq .12$, and $p\text{'s} \geq .347$ (see Figure 7.4, and Table 7.3). Excluding the HR-ASD outlier from the analyses that was also excluded in the alpha analyses did not yield any associations with medium or larger effect sizes, $-.24 \leq r\text{'s} \leq .21$, and $p\text{'s} \geq .349$. Inspection of Figure 7.4 also shows an LR outlier. Excluding this participant from the analyses did not change the results either, $-.24 \leq r\text{'s} \leq .11$, and $p\text{'s} \geq .332$. This suggests that differences in theta connectivity parameters between the social and non-social condition are not associated with social communication and interaction difficulties, or restricted and repetitive behaviours expressed during childhood.

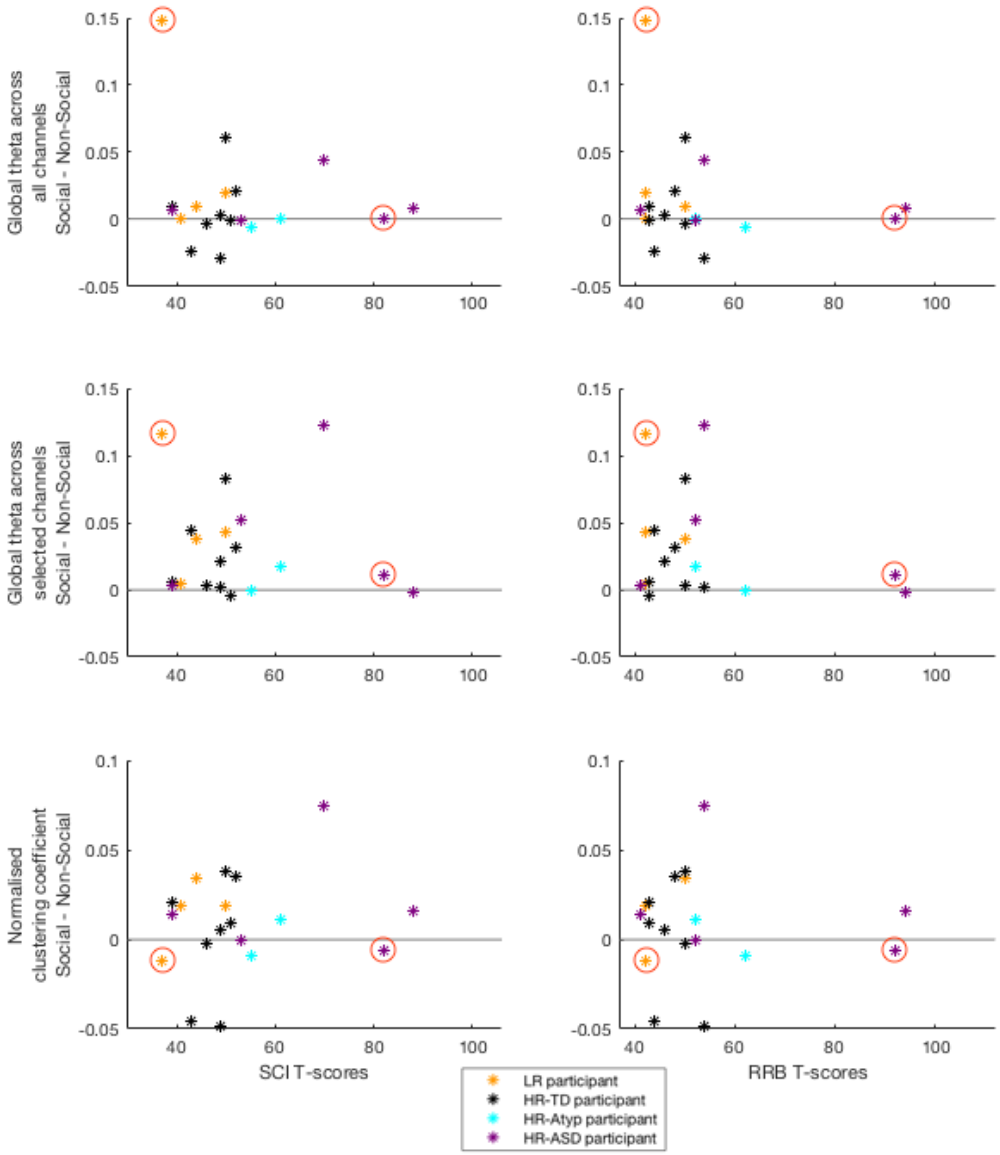

Figure 7.4. Scatterplots for the theta connectivity data and ASD traits measured during childhood

Rows represent the different connectivity parameters: global connectivity across all channels (top), global connectivity across fronto-central channels (middle), and normalised clustering coefficients (bottom). Columns reflect the SRS-2 subscales: SCI on the left, and RRB on the right. Different colours signify the diagnostic group at 3 years of age, and the outliers are circled in red. None of the investigated associations reached a medium or larger effect size.

Table 7.3. **Associations for theta band connectivity differences between the social and non-social condition with ASD traits during childhood**

	SRS-2 Subscale	
	SCI [a] T-scores	*RRB [b] T-scores*
Global connectivity across all channels	r = -.05, p = .828, [-.50, .42]	r = -.23, p = .347, [-.65, .26]
Connectivity across selected channels [c]	r = -.10, p = .678, [-.57, .40]	r = -.15, p = .550, [-.65, .40]
Normalised clustering coefficient	r = .12, p = .624, [-.38, .54]	r = -.12, p = .612, [-.56, .44]

Spearman's rho values (*r)*, with p-values, and bias corrected and accelerated bootstrap 95% confidence intervals in square brackets.

[a] Social Communication and Interaction DSM-V compatible subscale on the SRS-2.

[b] Restricted and Repetitive Behaviours DSM-V compatible subscale on the SRS-2.

[c] Selected channels that show differences between conditions revealed by NBS analyses, specifically across the LR masked connections for LR participants, and across HR masked connections for HR participants (see Chapter 5).

Other variables may have masked any associations between theta connectivity parameters and later childhood outcomes. Separate partial correlations were therefore performed while taking into account possible confounding variables: number of epochs, differences between conditions in theta power, familial risk for ASD, diagnostic outcome at 3 years of age, gender, age at EEG assessment, age at follow-up assessment, and MSEL scores at 14 months old. When including MSEL scores at 14 months of age, a medium effect size was found: differences in theta connectivity across selected channels were negatively related to RRB T-scores on the SRS-2, r = -.32, p = .203, [-.64, .20]. None of the other accounted for variables reached medium effect sizes of .30 or higher: -.22 ≤ r's ≤ .26, and .306 ≤ p's ≤ .984 (see Appendix A7.4).

This suggests that differences between the social and non-social condition in theta connectivity parameters are not strongly related to later ASD traits during childhood. When cognitive abilities are taken into account, lower connectivity differences for the social than non-social condition across selected channels is related to more severe restricted and repetitive behaviours during childhood.

7.3.4.2. Theta EEG connectivity and change in ASD traits

After examining alpha connectivity parameters, I turned to the investigation of associations between theta connectivity parameters and the slopes of change in ASD traits between toddlerhood and childhood (Fig. 7.5). None of the correlations examined reached medium or larger effect sizes, $-.17 \leq r\text{'s} \leq .21$, and $p\text{'s} \geq .434$. Again, similar results were obtained when the HR-ASD outlier was excluded, $-.15 \leq r\text{'s} \leq .11$, and $p\text{'s} \geq .603$, or the LR outlier was excluded, $-.13 \leq r\text{'s} \leq .18$, and $p\text{'s} \geq .524$. This suggests that differences between conditions in theta global connectivity across all channels, across selected channels, or normalised clustering coefficients are not related to the rate of change in ASD traits between toddlerhood and childhood, neither for social communication and interaction difficulties, nor for restricted and repetitive behaviours.

Taking into account any other variables did not change the main result where theta connectivity parameters are minimally associated with the change of ASD traits between toddlerhood and childhood (see Appendix A7.5). This held for each of the confounding variables investigated: number of epochs, power across all channels, familial risk, diagnostic outcome at 3 years of age, ASD traits at 3 years indicated by the SCI and RRB T-scores, gender, age at EEG and follow-up assessment, or cognitive abilities during infancy measured with the MSEL, with $-.21 \leq r\text{'s} \leq .27$, and $p\text{'s} \geq .335$.

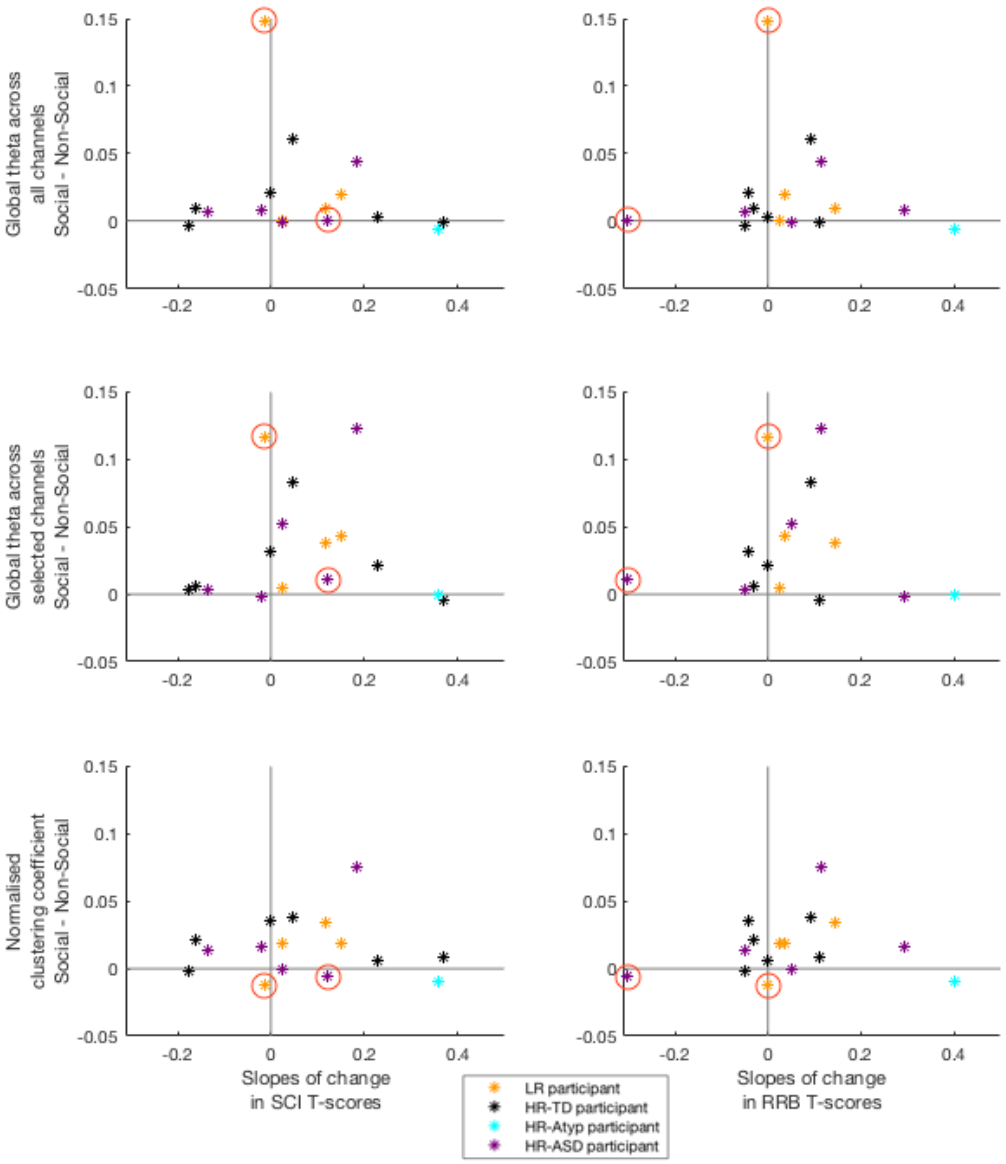

Figure 7.5. Scatterplots for the theta connectivity data and rate of change for ASD traits between toddlerhood and childhood

Rows represent the different connectivity parameters: global connectivity across all channels (top), global connectivity across fronto-central channels (middle), and normalised clustering coefficients (bottom). Columns reflect the SRS-2 subscales: SCI on the left, and RRB on the right. Different colours signify the diagnostic group at 3 years of age, and the outliers are circled in red. Positive rates signify increases, while negative rates of change signify decreases.

Table 7.4. **Associations for theta band connectivity differences between the social and non-social condition with the slope of change in ASD traits between toddlerhood and childhood**

	SRS-2 Subscale	
	Slope for SCI [a] T-scores	*Slope for RRB [b] T-scores*
Global connectivity across all channels	r = -.17, p = .520, [-.67, .41]	r = -.03, p = .918, [-.52, .42]
Connectivity across selected channels [c]	r = .09, p = .753, [-.55, .69]	r = -.01, p = .974, [-.51, .60]
Normalised clustering coefficient	r = -.02, p = .957, [-.52, .56]	r = .21, p = .434, [-.33, .69]

Spearman's rho values (*r)*, with p-values, and bias corrected and accelerated bootstrap 95% confidence intervals in square brackets.

[a] Social Communication and Interaction DSM-V compatible subscale on the SRS-2.

[b] Restricted and Repetitive Behaviours DSM-V compatible subscale on the SRS-2.

[c] Selected channels that show differences between conditions revealed by NBS analyses, specifically across the LR masked connections for LR participants, and across HR masked connections for HR participants (see Chapter 5).

7.4. Discussion

The severity of ASD traits may change from early toddlerhood to mid-childhood in HR infants. In this chapter, I aimed to investigate whether infant EEG connectivity parameters are related to the severity of ASD traits during childhood rather than toddlerhood as was examined in the previous chapters. The other aim was to examine whether developmental changes in ASD traits were related to infant EEG connectivity parameters. Indeed, the results displayed different developmental trajectories for the severity of ASD traits across childhood. Overall, alpha connectivity parameters showed stronger associations with restricted and

repetitive behaviours during childhood, than with social and communication difficulties, although the specific patterns differed between analyses. For theta connectivity parameters, however, no strong associations were observed with ASD traits during childhood, or change in ASD traits between toddlerhood and childhood. The current findings extend previous high-risk infant siblings studies investigating EEG connectivity parameters by examining associations between these parameters with ASD-related behaviours after the typical 2 or 3-year-old visit reported in most studies.

7.4.1. Heterogeneous developmental trajectories in ASD traits between toddlerhood and childhood

As expected, the results showed variability in developmental trajectories in ASD traits between toddlerhood and childhood, and across core domains. Differences in ASD traits between diagnostic outcome groups were also more apparent at childhood assessment, than at toddlerhood assessment. This is in line with previous reports suggesting that variability between individuals and severity of ASD traits increase during childhood (Charman et al., 2005). Further, the finding of higher levels of severity of ASD traits in the HR groups than the LR group supports the BAP (Bolton et al., 1994). Similar findings have been reported in 3-year-old toddlers using ADI-R and ADOS measures (Charman et al., 2017), and in 7-year-olds for adaptive behaviours in the BASIS7 follow-up study (Salomone et al., 2018). Furthermore, variability in trajectories of severity of traits have been found in other studies also (Gotham et al., 2012; Lord, Luyster, et al., 2012; Venker et al., 2014). The heterogeneity in the group also poses a challenge as this makes it more difficult to draw overall conclusions about ASD. The stratification of participants

into more homogeneous subgroups could help solve this matter (Loth et al., 2017, 2016).

7.4.2. Alpha connectivity parameters and ASD traits during childhood

One possibility would be to stratify participants into subgroups based on neural phenotypes. The advantage of neural measures is that these are objective rather than subjective, such as parent report using a questionnaire (SRS-2) or interview (ADI-R). In both a previous study and Chapter 4, *higher* global alpha connectivity across fronto-central connections was related to *more severe* restricted and repetitive behaviours measured by the ADI-R at toddlerhood. Normalised alpha clustering coefficients were not related to later ASD traits measured by the ADI-R or ADOS-2 at toddlerhood, though exploratory analyses suggested that higher normalised clustering coefficients were related to more severe circumscribed interests at toddlerhood. The findings of the current analyses examining ASD traits at mid-childhood showed completely different patterns: *lower* connectivity parameters were related to *more severe* ASD traits at childhood, and more positive rates of change between toddlerhood and childhood. As hypothesized, associations were stronger with traits in the restricted and repetitive behaviours domain than the social communication and interaction domain, but were also stronger for the normalised clustering coefficient than global connectivity measures across all or fronto-central connections.

Together, these findings suggest that associations between connectivity parameters and ASD trait severity are more nuanced, where atypical alpha connectivity is related to more severe ASD traits during childhood. One possibility is that the extent of deviations from typical connectivity is related to severity of traits. Individuals showing larger deviations, either in a positive or negative

direction, might also show more severe ASD traits, and higher increases in severity of these traits during childhood. A previous MEG study showed that children and adolescents with ASD exhibiting larger deviations in connectivity from the patterns observed in their typically developing peers experienced more severe ASD traits (Vakorin et al., 2016). Similarly, very high or very low alpha connectivity during infancy could be associated with more severe traits during toddlerhood and childhood. This is also compatible with the previous finding of the relation between increased alpha connectivity across fronto-central connections during infancy and increased restricted and repetitive behaviours during toddlerhood (see (Orekhova et al., 2014) and Chapter 4).

The deviations in connectivity patterns possibly arise from an adaptive response aiming to restore the excitation/ inhibition imbalance by altering the connectivity patterns (Johnson et al., 2015). Subgroups characterised by different patterns of connectivity atypicalities may constitute different adaptive mechanisms attempting to restore neural homeostasis in the brain from E/I imbalance. Another possibility is that different subgroups arise from different excitation/ inhibition imbalances, for example by different directions of the imbalance (increased excitation compared to inhibition, or increased inhibition compared to excitation), or occurring at different regions in the brain (widespread, prefrontal cortex, subcortical regions, or others) (Nelson & Valakh, 2015).

A failure to restore neural homeostasis early in development may further lead to accumulating alterations in brain connectivity patterns. With the increasing deviations, severity of ASD traits may increase as well (Nelson & Valakh, 2015). This would be compatible with the observation of increased severities in ASD traits in some individuals in the current data. If connectivity patterns would

deviate more from typical connectivity patterns with increasing age, differences in connectivity parameters between different outcome groups and subgroups would become clearer at later ages. Longitudinal follow-up studies focusing on both connectivity parameters and ASD traits are needed to further examine this.

Another finding worth considering here is that associations observed with connectivity parameters for toddlerhood data in the previous chapters are different from those observed in the current chapter: first, *increased* global connectivity across fronto-central connections was associated with increased restricted and repetitive behaviours during toddlerhood (Chapter 4), whereas *decreased* global connectivity was associated with increased restricted and repetitive behaviours during childhood. Second, normalised clustering coefficients were *not* related to ASD traits during toddlerhood (Chapter 6), whereas *decreased* normalised clustering coefficients were related to increased restricted and repetitive behaviours during childhood. The associations for alpha connectivity parameters are consistently stronger for restricted and repetitive behaviours domain than the social communication and interaction domain, consistent with associations with ASD traits at toddlerhood (see Chapter 4). Several factors may explain the findings with regard to different connectivity parameters.

First, different aspects of connectivity may be more significant at different developmental stages. It is possible that neural synchronisation and also global whole brain connectivity play a larger role in the early establishment of cortical networks that relate to early behaviours. The functional organisation of brain graphs increases with age (Boersma et al., 2011; Fair et al., 2007; Smit et al., 2012; Uhlhaas et al., 2009, 2010). Possibly the neural synchronisation and functional organisation measured at infancy provide a foundation for brain networks that

will become more important later in development. Previous results showed that at infancy global connectivity was related to ASD traits (see Chapter 4 and (Orekhova et al., 2014)), but normalised clustering coefficients were not (Chapter 6). At toddlerhood, normalised alpha clustering coefficients were related to ASD diagnostic outcome, but global connectivity was not (Boersma et al., 2013). Longitudinal studies examining both global connectivity and graph theory parameters could further clarify the relevance of different connectivity parameters at different developmental periods.

Second, different subgroups of participants could display different associations between connectivity parameters and ASD traits during childhood. The different analyses performed throughout this thesis included different subsets of participants. For some of the HR-ASD infants with high global connectivity values during infancy follow-up data were not available. It is possible that those infants follow a different developmental trajectory, and provide a different pattern of results if included here (also see Appendix A7.6 for an example of a cluster analysis, although not further included here due to small sample numbers).

Third, differences in measurement tools of the severity of ASD traits across chapters may have led to different findings. In the previous chapters, the severity of ASD traits was measured with the ADI-R. The ADI-R was designed to facilitate categorical diagnosis, and is thereby less sensitive to small variations in ASD traits than the SRS-2 questionnaire used in the current chapter. The SRS-2 measures symptom severity over the past 6 months, whereas the ADI-R focuses on the past 3 months. Also, possible ranges for ADI-R algorithm are smaller than those of the SRS-2 subscales which would inherently result in less inter-individual variability. Finally, the ADI-R is a parental interview where responses are interpreted and

rated by an experienced clinical researcher. It is possible that behaviours are differently rated from a parental perspective in the SRS-2 than from a clinical perspective in the ADI-R. While the domain scores for the measures collected at toddlerhood were highly correlated (.7 and .8, see Appendix A7.7), alpha connectivity parameters did not exhibit any strong associations with the SRS-2 measures, not even for global connectivity across fronto-central connections and restricted and repetitive behaviours (see Appendix A7.8). The use of ADI-R scores at childhood may reveal different results than found here.

Finally, a more technical explanation for that the primary finding of differences in associations between ASD traits and alpha connectivity parameters is the difference in distributions of the variables. Data for the normalised clustering coefficients were more normally distributed than data for global connectivity across all connections or fronto-central connections. As the normalised clustering coefficient does not violate the assumption of normality, this variable is more likely to have a stronger effect size compared to variables that did violate this assumption, i.e. the other alpha connectivity parameters (Field, 2014). Further, ranges and interquartile ranges for the SRS-2 measures are larger at childhood than toddlerhood, making it more difficult to pick up on associations with toddlerhood measures than childhood measures (see Table 7.1).

To summarize, the current results suggest that lower alpha clustering coefficients are associated with more severe ASD traits during childhood. Larger deviations from typical alpha connectivity patterns likely associate with more severe ASD traits, and possibly arise from failure to restore and stabilise into a state of optimal E/I balance. Further research into different subgroups via larger

cohorts and longitudinal studies is needed to further examine underlying mechanisms of atypical connectivity and ASD traits.

7.4.3. Theta connectivity parameters not associated with ASD traits during childhood

In contrast to alpha connectivity parameters, the theta frequency band connectivity parameters did not strongly associate with ASD traits during childhood, or change in the severity of ASD traits between toddlerhood and childhood. This is consistent with findings from previous chapters that did not show any strong associations between theta connectivity parameters and ASD traits during toddlerhood either.

One possible explanation for the lack of strong associations is the limited statistical power due to the small sample size. The sample size for the theta analyses was approximately a third of the alpha analyses, which significantly reduces the power to pick up on a medium association between theta connectivity parameters and later ASD traits during childhood, or define subgroups. The limited sample size is likely due to the small amounts of participants with sufficient epochs from both social and non-social conditions. Larger cohort and a paradigm with more equal video durations for both conditions would enable the inclusion of a larger number of infants.

Another possible explanation is that theta frequency band connectivity parameters are less informative for early and later development in ASD traits than alpha frequency band parameters. Previous studies suggested that spectral power peaks in the alpha frequency band relate to brain development, and might therefore be more relevant when examining developmental disorders (Bazanova & Vernon, 2014; Dickinson, DiStefano, Senturk, & Jeste, 2018; Marshall et al., 2002).

Differences in connectivity between groups of young individuals with and without ASD are more consistently reported for the alpha band (Bathelt et al., 2013; Boersma et al., 2013; Dickinson, DiStefano, Lin, et al., 2018; J. Han et al., 2017; Kitzbichler et al., 2015; Orekhova et al., 2014). It is possible that atypical alpha connectivity parameters reflect general atypical brain development, and are more informative than theta connectivity parameters when studying the early development of ASD.

7.4.4. Considerations and limitations

There are a few things we should take into consideration while interpreting the findings above. First, it is possible that different diagnostic outcome groups at mid-childhood change the pattern of results as diagnostic outcome at 3 years of age changed the pattern in Chapter 4. Diagnostic outcome at childhood however was unknown for 23 out of 56 participants. It is possible that diagnostic outcome changed during childhood for some of these children, as it did for 2 of the other 33 children (Shephard et al., 2017), and this may have played a role in the current findings.

Second, treatment or intervention between infancy and childhood may have influenced later ASD traits. This information was not available either for all the participants, and therefore not examined in here. It is likely that interventions are associated with developmental change in ASD traits (Green et al., 2015; Jones, Dawson, et al., 2017; Pickles et al., 2016; Venker et al., 2014).

Third, the participants included in this study may not be a representative sample of the population. Although this holds for all samples in longitudinal high-risk sibling studies, this might be even more the case in the follow-up studies. It is possible that families with younger siblings with more severe ASD behaviours are

more intrinsically motivated and likely to consent to participation in follow-up assessments taking place several years after the first assessment. In addition, families with higher social economic status or educational degrees might be more likely to further participate as well.

7.5. Summary of Chapter 7

This chapter aimed to examine how infant EEG connectivity parameters are associated with later ASD traits during childhood, and changes in these traits between toddlerhood and childhood. The results revealed that atypical values for alpha connectivity parameters were related to more severe ASD traits during childhood. Larger deviations in connectivity from connectivity patterns observed in typically developing participants may arise from insufficient homeostasis sustaining optimal E/I balance in neural networks. Connectivity parameters in the alpha frequency band seem more informative for atypical development than in the theta frequency band. Studies including larger cohorts and multiple longitudinal assessments are necessary for 1) examining the relevance of different connectivity parameters across early typical and atypical development, and 2) stratification of participants into subgroups based on behavioural and neural phenotypes that will help forward research into markers of ASD.

The next chapter will discuss the theoretical and clinical implications, and contribution of the current findings reported in this thesis to previous studies.

Chapter 8: Discussion

8.1. Introduction

This PhD thesis set out to investigate how EEG connectivity during infancy is related to familial risk, later categorical diagnosis and dimensional traits of ASD. It has been suggested that brain connectivity may be altered in ASD, possibly as a result of an adaptive response to atypical neural processing during the first years of life (Belmonte et al., 2004; Johnson, 2017; Johnson et al., 2015; Just et al., 2004; Uddin, Supekar, & Menon, 2013). If this is true, alterations in EEG connectivity may be evident from an early age in individuals who receive a diagnosis at later age, and may be used as an early marker for ASD (Jeste, Frohlich, & Loo, 2015; Orekhova et al., 2014).

Early markers measured during infancy would facilitate early identification before the onset of behavioural symptoms, and could help predict later individual outcomes. Early identification could lead to early intervention resulting in better outcomes for the individual at later age (Webb et al., 2014). Early markers may further help in the selection of appropriate intervention and monitor intervention effects, since not all individuals with ASD may respond to treatments in the same way. Research into ASD markers can also inform on the underlying mechanisms of the disorder by examining brain-behaviour relationships. For example, if specific aspects of altered connectivity are found to be related to familial risk for ASD, later diagnostic outcome, or dimensional traits, this may point towards certain underlying mechanisms of ASD (Insel et al., 2010; Singh & Rose, 2009; Walsh et al., 2011). Finally, markers may be used for stratification: creating more homogeneous subgroups of individuals with ASD. Stratification helps coping with the heterogeneity present in ASD. Different subgroups may consist of different

subtypes of ASD displaying different neural and behavioural phenotypes (Loth et al., 2016).

The ultimate objective is to use these early markers as biomarkers in clinical research and practise, but reaching the required high accuracy, specificity, sensitivity, and reproducibility for these objective measures has proven to be difficult (Waterhouse, London, & Gillberg, 2016). The first step in the search for early connectivity markers of ASD includes characterising the reliability of these connectivity measures, and establishing associations between later ASD outcomes and early connectivity measures that are potential candidates for ASD markers, by replicating and extending previous results.

To summarise the current results in this thesis: findings confirmed that the previously used paradigm and methods provide a reliable estimate of EEG alpha connectivity in infants: the debiased weighted phase lag index estimated across more than 120 1-second EEG epochs recorded while infants watch social and non-social videos of women singing nursery rhymes, and spinning toys (Chapter 3). Next, I used these methods aiming to replicate previous findings showing alpha hyper-connectivity in a group of HR-ASD infants (Orekhova et al., 2014). In the new independent cohort, there were no group differences in alpha connectivity between the HR-ASD group and the LR, HR-TD, or HR-Atyp group. The amount of alpha connectivity in fronto-central areas however was positively related to the severity of restricted and repetitive behaviours during toddlerhood in the HR-ASD group, as was found in the original study. Furthermore, this finding seemed to be driven by an association between alpha connectivity and circumscribed interests (Chapter 4).

Further studies focused on extending these findings examining whether other parameters of EEG connectivity, such as theta band connectivity, might relate to social communication and interaction difficulties. Global theta connectivity was higher during social than during non-social videos. Theta connectivity differences between conditions revealed different network topologies between the LR and HR groups, whereas no strong differences in connectivity patterns were observed between the HR-TD, HR-Atyp, and HR-ASD groups (Chapter 5). In addition to global connectivity, graph organisation was examined while focussing on: normalised clustering coefficient, normalised path length, and small-worldness. No differences were found between different risk and outcome groups for any of the graph theory metrics in either the theta or alpha frequency band (Chapter 6). No significant associations between the EEG connectivity measures of theta band or graph organisation, and ASD symptom severity in the social communication and interaction domain, or restricted and repetitive behaviours domain during toddlerhood were found (Chapter 5 and 6).

Finally, I examined whether infant EEG connectivity was related to ASD traits measured during childhood, since diagnosis and severity of traits might change over time. Indeed, different developmental trajectories of ASD traits were found. Lower alpha normalised clustering coefficients during infancy related to more severe and higher increases of ASD traits during childhood (Chapter 7).

The results of these studies have contributed to previous studies in several ways, and have implications for research EEG connectivity as candidate early marker for ASD: for the methodology, early detection of ASD, and underlying mechanisms of ASD. Limitations and directions for future research are discussed also.

8.2. EEG connectivity methodology in infancy

A marker of ASD requires high reproducibility. When considering EEG connectivity as early candidate marker for ASD, test-retest reliability should be examined in infants also. EEG connectivity measures with high test-retest reliability are suitable for predictions of ASD at both the individual and group level, whereas those with lower test-retest reliability are not suitable for prediction at individual level. Examining how EEG connectivity relates to cognitive functioning may furthermore help revealing underlying mechanisms if atypicalities emerge. Before applying the EEG connectivity methods to atypical developing populations, test-retest reliability of EEG connectivity and associations with cognitive functions need to be examined in typically developing infants.

8.2.1. Reliability of EEG connectivity measures in typically developing infants

Systematic research into the test-retest reliability of EEG connectivity measures over time had mostly been conducted in adults. Optimal EEG connectivity parameters in adult studies however may not always be feasible for infants, due to limited availability of artefact-free data, robust methods for infant source analyses, and increased levels of noise for infants compared to adults. Methods to calculate EEG connectivity measures in adults can thus not be easily applied to infant EEG data. The findings of the current research contributed to the adult findings by focusing on the test-retest reliability of infant data, and examining the influence of different epoch lengths and numbers on the test-retest reliability of EEG connectivity metrics.

The results revealed that overall using more than 90 or 120 short 1-second epochs with the dbWPLI results in EEG connectivity metrics with good test-retest reliability in infants. For the PLI, longer rather than shorter epochs resulted in more reliable results in infants. This is consistent with the adult literature for this measure. The disadvantage of the PLI though is that it is more sensitive to noise with small phase lags. Considering that infant EEG is characterised by noise, the dbWPLI would be a more appropriate measure of true EEG connectivity than the PLI.

Different metrics calculated from the EEG connectivity measures showed differences in reliability also. Global connectivity calculated across all connections showed more reliable results than graph theory metrics. The measure of local graph organisation was also more reliable than the measure of global graph organisation: specifically, normalised clustering coefficients showed higher test-retest reliability than normalised path length, and small-worldness index. This is consistent with findings from the adult literature, and extends previous findings by showing similar patterns in infant data.

The test-retest reliability results had implications for the further studies conducted in this thesis. The findings confirmed that the methods adapted by Orekhova and colleagues in the original study provided reliable measures in a systematic investigation of epoch parameters (Orekhova et al., 2014). Thus the use of more than 120 1-second epochs for the calculation of EEG connectivity with the dbWPLI in infants is reinforced by the current findings. Furthermore, global EEG connectivity and normalised clustering coefficients are suitable to both individual and group-level analysis, while normalised path length and the small-worldness index are more suitable group-level analysis rather than individual-level analysis.

These results guided the decisions made in the following studies reported in this thesis: a) for dbWPLI calculations, only infants with more than 120 artefact-free 1-second epochs across all conditions, or for the social and non-social conditions were included in the analyses, b) group-level analyses focused on global connectivity measures and graph theory metrics, whereas individual-level analyses focused on global connectivity measures and the normalised clustering coefficient.

Similarly, the current test-retest reliability results may function as a guideline for future research. This reliability study was by my knowledge the first to examine the influence of epoch length and duration on EEG connectivity measures in infants. The number of studies looking into EEG connectivity in younger populations is rising. While the use of graph theory metrics in infants was still limited a few years ago, the method is now being applied more often to infant EEG data. The current findings may help future researchers selecting the appropriate EEG connectivity measure, and epoch length and numbers in line with the age group investigated and the research questions. Furthermore, this systematic investigation provides a more robust foundation for methodological choices compared to the argument that similar methods were used in previous studies and are therefore likely an appropriate choice.

In addition, the systematic approach and the findings strengthen the current approach taken, and may facilitate use of the phase lag indexes as opposed to coherence-based measures. Several studies are mostly using coherence-based measures. The use of similar measures could enable comparisons of findings across studies of EEG connectivity in ASD. Furthermore, the phase lag index measures are less susceptible to influences from volume conduction. Thus

interpretation of the findings of phase lag based measures are not confounded by possible volume conduction effects, but are more likely to measure underlying brain connectivity than coherence-based measures.

In short, the current results provide a strong background for methodological decisions in infant EEG connectivity research: deriving EEG connectivity values from many short epochs provides more reliable results than deriving values from few long epochs, in particular when using the dbWPLI. The dbWPLI has the advantage that values are less influenced by noise, or a small number of epochs. These findings suggest that these measures are suitable for analyses on individual levels, rather than just group levels, which is particularly important in ASD research.

8.2.2. EEG connectivity and cognitive functions

In addition to test-retest reliability, the results also provide new insights into how functional connectivity might be associated with cognition, and emphasize the importance of considering context. The current infant resting state paradigm can be used in multiple ways, to examine 1) overall resting state connectivity across all conditions, and 2) connectivity modulated by social stimulation using comparisons of connectivity patterns during social and non-social videos. Previous infant connectivity studies have mainly been examining EEG connectivity during one condition or across several conditions, in particular when comparing groups with typical and atypical development in ASD. For example, alpha connectivity across social and non-social videos, theta connectivity during social videos, theta connectivity during non-social videos (Orekhova et al., 2014), theta-alpha connectivity while watching pictures of cars and/or faces (Boersma et al., 2013), gamma connectivity while watching pictures of their mothers' faces (Keehn et al.,

2015), or alpha connectivity while watching videos of moving bubbles (Dickinson, DiStefano, Lin, et al., 2018). How connectivity changes are related to the processing of different stimuli or cognitive processing however remains largely unknown.

Findings from spectral power research suggest that decreases in oscillatory power in the alpha frequency band are related to sustained attention (Jones, Venema, Lowy, Earl, & Webb, 2015; Orekhova, Stroganova, & Posikera, 2001; Stroganova, Orekhova, & Posikera, 1999; Xie, Mallin, & Richards, 2017), whereas increases in spectral power in the theta band are related attentional control, and emotional and social processing (Jones et al., 2015; Orekhova, Stroganova, Posikera, & Elam, 2006; Orekhova, Stroganova, & Posikera, 1999; Xie et al., 2017). It is possible EEG connectivity shows similar modulations to spectral power. A recent study exhibited decreases in EEG connectivity in the alpha band across central and parietal areas during periods of sustained attention in infants (Xie et al., 2018). In addition, theta connectivity was increased during the social condition compared to non-social conditions (Chapter 5), consistent with previous spectral power results in this band (Jones et al., 2015). This suggests that connectivity may indeed show similar modulations as spectral power.

Moreover, the nature of the stimuli may also play a role. One previous study further found that both theta and alpha power differences between social and non-social conditions were more prominent during live stimulation compared to videos. Possibly connectivity in both the theta and alpha frequency band are similarly modulated by the social content of live stimuli, while only theta connectivity is modulated by social content of videos.

Overall, these findings suggest that global EEG connectivity is modulated by different contexts in similar ways as spectral power. Connectivity measures can

however inform on communication between brain areas, whereas spectral power informs on activation in brain regions. Further research is however needed to further clarify how global connectivity and topology of networks are associated with cognitive processing. Examining how brain connectivity is modulated by different stimuli and cognitive tasks may help further our understanding of underlying mechanisms of atypical brain connectivity in ASD (Vasa, Mostofsky, & Ewen, 2016), or help towards early detection of ASD.

8.3. Early detection of ASD: Categorical and dimensional outcomes

Associations between EEG connectivity and ASD outcomes vary across studies, possibly due to differences in methods, paradigms, and age groups. The studies in this thesis suggest that individual variability in atypical development may also play a role here. The study in Chapter 4 aimed to replicate previous results showing that alpha connectivity was related to both categorical and dimensional outcomes of ASD. The identical paradigm, methods, and age group were used in this replication study in a new, independent cohort. The results indicated that alpha connectivity was not associated with later categorical diagnosis. This difference in findings may be explained by increased variability between individuals in atypical developmental samples. Variability in methods is less likely to explain these results, since methods were identical across the two studies. The first contribution to ASD research is thus the focus on replication of previous results.

Second, these findings emphasize the need to consider both categorical and dimensional outcomes when examining markers for ASD. While the relation with categorical outcome was not replicated, the relation with dimensional outcomes at toddlerhood in the HR-ASD group was replicated, in particular for global fronto-

central alpha connectivity and the severity of traits in the restricted and repetitive behaviours domain. These findings suggest that individual variability in brain connectivity is related to variability in severity of traits, and that examining associations with dimensional traits is important too. Predicting categorical outcomes will inform on which group an individual will belong to, whereas predicting dimensional outcomes will inform on individual differences in ASD traits. Several high-risk infant sibling studies and studies examining connectivity in toddlers have been focusing on group differences between those with and without ASD diagnosis at toddlerhood (Boersma et al., 2013; Dickinson et al., 2018; Keehn et al., 2015; Orekhova et al., 2014; Righi, Tierney, Tager-Flusberg, & Nelson, 2014). In order to establish individual predictive markers of ASD, one would have to examine associations between dimensions of different variables however rather than categories.

Recent studies have indeed shifted their focus and are also examining individual differences now, for example how individual differences in EEG connectivity associate with differences in total severity scores on the ADOS or ADI-R (Dickinson, DiStefano, Lin, et al., 2018). However, studies mostly examine total symptom severity including symptoms from all core domains. Considering the heterogeneity and complexity of underlying mechanisms in ASD, it is likely that these infants and toddlers with a later diagnosis experience different levels of symptom severity in the different core domains: social and communication difficulties, and restricted and repetitive behaviours. Associations between markers of ASD and different domains of later symptoms may also vary. For example, the current studies suggest that alpha connectivity parameters show stronger associations with the restricted and repetitive behaviours domain than

the social and communication difficulties domain. Predicting individual variability in later dimensional traits is important as it may help select appropriate treatment for each individual. Thus establishing how individual differences in connectivity markers relate to individual differences in different domains of traits could help develop individual markers of ASD. This thesis contributed to this line of research by focusing on individual differences of ASD traits in separate core domains in addition to group differences.

Third, the studies in this thesis contributed to the previous findings by examining how altered connectivity relates to later outcomes at different periods during development. Most high-risk infant sibling and toddler studies examined associations between connectivity and ASD outcomes during toddlerhood (Boersma et al., 2013; Dickinson, DiStefano, Lin, et al., 2018; Keehn et al., 2015; Orekhova et al., 2014; Righi et al., 2014). The severity of ASD traits and diagnosis measured at age 2 or 3 years however may change during childhood, when social environments get more demanding, and difficulties might be more clearly visible. Severities of traits could increase and worsen or decrease and improve, resulting in a late or loss of ASD diagnosis given during toddlerhood, respectively (Charman et al., 2005; Shephard et al., 2017). Associations between early connectivity parameters and severity of later ASD traits may further depend on the developmental period during which measures are collected (infancy, toddlerhood, or childhood (Johnson, 2017)).

The current results revealed that early connectivity parameters during infancy are related to ASD outcomes at later age. The associations between EEG connectivity during infancy and ASD traits during childhood seemed to differ from those observed with ASD traits during toddlerhood, in particular for the alpha

band normalised clustering coefficient and global alpha fronto-central connectivity. Normalised clustering showed a stronger association with traits measured during mid-childhood than toddlerhood, while global fronto-central connectivity showed the opposite pattern of results. These findings suggest that associations between neural and behavioural measures are not static, but dynamic during development (Karmiloff-Smith, 1998). Furthermore, these results demonstrate the complexity of ASD and the heterogeneity of developmental trajectories, and emphasize the importance of follow-up assessments of participants in the high-risk infant sibling studies.

Together the results in this thesis suggest that there is increased variability in developmental trajectories in samples with atypical development. It is likely that different samples of individuals with atypical development included in different studies led to varying findings in the ASD literature. It has been suggested that creating more homogeneous subgroups with similar behavioural or neural phenotypes may help managing this heterogeneity and complexity of ASD (Loth et al., 2016). Participants included in the research samples may thus be part of different subgroups of ASD, which are for example associated with very high or very low connectivity parameters.

This also likely applies to the studies in this thesis. Different subsamples from the Phase 1 and Phase 2 cohort were used in the analyses in different chapters. The original connectivity study by Orekhova and colleagues contained several HR-ASD infants with very high connectivity, whereas the replication sample contained only a few infants with very high connectivity (Orekhova et al., 2014). This may have played a role in the failure to replicate the findings with regard to categorical diagnosis, while previous findings with regard to dimensional

traits were successfully replicated. The original and new independent cohort were collapsed for the further analyses, but only a subset of the sample was included into the chapter focusing on theta connectivity, and an even smaller subset was included in the childhood follow-up analyses. Thus, different subsets examined in the analyses likely consist of different combinations of participants from different subgroups. The presence of subgroups with different connectivity patterns may account for the varying results in the studies of this thesis, and previous studies of EEG connectivity in ASD.

In sum, the studies reported in this thesis contributed to previous findings by 1) replication of previous findings in an independent cohort, 2) focusing on both categorical and dimensional outcomes across separate core domains, and 3) examining outcomes at both toddlerhood and childhood. Overall, the results suggest that increased variability in atypical development may account for variability in findings across studies. These findings emphasize the need for investigating both categorical and dimensional outcomes. It is possible that associations between alterations in EEG connectivity and categorical and dimensional outcomes of ASD vary between different subgroups of individuals with ASD. These different subgroups may be related to different underlying mechanisms of ASD.

8.4. Underlying mechanisms

In addition to the potential early detection of ASD, research into markers can help reveal underlying mechanisms of the disorder. This can give rise to changes in theoretical accounts, or newly proposed theories of ASD aetiology.

8.4.1. ASD as a disorder characterised by altered connectivity

Over a decade ago, Just and colleagues suggested that brain connectivity in individuals with ASD might be decreased compared to individuals without a diagnosis (Just et al., 2004). This has led to an increase in the amount of studies focusing on brain connectivity in ASD. However, underconnectivity was not found across all brain connections: short-range distance connections displayed increased connectivity, whereas long-range connections showed decreased connectivity (Belmonte et al., 2004). Developmental research examining children and adolescents with ASD revealed increases in connectivity, leading to the hypothesis of overconnectivity at early ages, and underconnectivity at later ages in life (Conti et al., 2017; Hoppenbrouwers et al., 2014; Nomi & Uddin, 2015; Supekar et al., 2013; Uddin, Supekar, & Menon, 2013).

More recent studies suggest that increased variability or idiosyncrasy in individuals with ASD is associated with increased ASD symptomatology. Increases in intra-individual variability were found for spatial patterns of functional fMRI connectivity (Hahamy et al., 2015; Holiga et al., 2018; Nunes, Peatfield, Vakorin, & Doesburg, 2018) and functional MEG connectivity (Vakorin et al., 2016), and also in dynamic fluctuations of fMRI connectivity within individuals with ASD (Chen, Nomi, Uddin, Duan, & Chen, 2017; Falahpour et al., 2016). It is possible that larger atypicalities in brain connectivity rather than over- or under-connectivity per se are associated with ASD diagnosis and symptoms.

The findings in the current thesis suggest that increases in atypical connectivity during infancy are related to ASD risk and later ASD-like behaviours. For example, higher fronto-central alpha band connectivity in the group of HR-ASD infants was related to later restricted and repetitive behaviours during

toddlerhood. Atypical theta connectivity patterns were observed in response to social stimuli in the HR group compared to the LR group. Atypical functional organisation of alpha connectivity patterns was related to more severe ASD traits during childhood. Atypicalities in global connectivity across all and fronto-central connections, and functional organisation seemed to be associated with more severe ASD traits during childhood. Together these findings indicate that increased variability in EEG alpha connectivity during infancy is associated with increased risk or dimensional traits of ASD at later ages. The variability in connectivity is apparent across a range of different connectivity parameters. The atypicalities in brain connectivity associated with ASD are thus much more complex than initially anticipated.

The next challenge is to unravel the complex relationship between alterations in connectivity and ASD outcomes. One possibility is that atypicalities in different connectivity parameters have small additive affects leading to increased severity of ASD traits. It has been suggested that small genetic variations have additive effects that may lead to more severe ASD traits and simultaneously reaching criteria for diagnosis (De La Torre-Ubieta et al., 2016; Geschwind, 2009). Research from high-risk infant sibling studies show that atypicalities in behavioural and neurocognitive measures (gaze following, disengagement of attention, AOSI, EEG measures) had additive effects when predicting later diagnosis at toddlerhood and childhood (Bedford et al., 2014, 2017). Similarly, atypicalities in brain connectivity may have additive effects where more widespread atypicalities across different measures of brain connectivity and network organisation lead to increased severities of ASD traits.

Another possibility is that atypicalities in different connectivity parameters are related to different subtypes of ASD. ASD is defined as a behavioural phenotype, which likely arises from a collection of distinct pathophysiological mechanisms with bidirectional influences on genetics, neurotransmitters and synaptic receptors, brain microstructure and anatomy, brain circuits and connectivity, and cognition and environmental influences (Geschwind, 2009). Different subtypes of ASD may be associated with different abnormalities of brain connectivity. For example, global connectivity in different brain regions, circuits, or resting state networks; atypical organisation and efficiency of the brain networks; or atypicalities in connectivity at different time scales (fMRI versus M/EEG frequency bands). Animal models for example suggest that atypicalities in different networks or circuits are related to different domains of ASD-like behaviours (Kim et al., 2016). These different subtypes of ASD with variability in connectivity abnormalities may also be related to variability in cognition.

8.4.2. Cognitive theories

The current results provided further insights into multiple possible underlying cognitive mechanisms. Associations between over-connectivity in the alpha band in fronto-central regions and restricted and repetitive behaviours were replicated in the replication study. Further analyses into the subtypes of different restricted and repetitive behaviours showed stronger associations with circumscribed interests than the other subtypes of behaviours. Overall, alpha connectivity parameters showed stronger associations with later restricted and repetitive behaviours. It has been suggested that alpha oscillations may play a role in attentional processes (Xie et al., 2018), and the mediation of top-down control

(Fries, 2015). There are multiple cognitive theories that may account for these findings.

First, the theory of Executive Dysfunction hypothesizes that severity of ASD symptoms arises from difficulties in executive functions such as attentional control (Hill, 2004b, 2004a; Rajendran & Mitchell, 2007). Possibly, variability in alpha connectivity is related to variability in attentional systems. Atypical alpha connectivity in fronto-central regions or decreased normalised clustering may for example relate to atypicalities in the attention networks. Indeed, one previous study reported decreases in alpha connectivity in the dorsal attention and default mode networks during periods of sustained attention (Xie et al., 2018). The increased alpha connectivity observed here may be related to atypical sustained attention, and reduced flexibility of control of attention. This atypical sustained attention could relate to an over-focused attentional style, leading to increased severity of restricted and repetitive behaviours including increased circumscribed interests. Reduced flexibility of attentional control and difficulties with disengaging attention may also lead to 'locking' onto a specific aspect of the stimulus or topic (Elsabbagh, Volein, Holmboe, et al., 2009). Previous high-risk infant sibling studies have reported associations between difficulties in attentional disengagement and risk and later categorical outcome of ASD (Bedford et al., 2017; Elsabbagh et al., 2013; Elsabbagh, Volein, Holmboe, et al., 2009). In contrast, strong executive function skills, including efficient control of attention, may act as a protective mechanism: increases in flexibility of attentional control may be related to less severe restricted and repetitive behaviours, in particular circumscribed interests (Johnson, 2012). Thus, altered alpha connectivity may relate to difficulties in attentional control such as the sustainment and disengagement of

attention, which in turn may relate to restricted and repetitive behaviours such as circumscribed interests.

Second, as mentioned above, atypical sustained attention may relate to a local information processing style. According to the Weak Central Coherence theory, individuals with ASD have a bias towards local information processing rather than global information processing. It is possible that a detailed, local information processing style is related to over-focussed spatial attention and difficulties in shifting between narrow and broadened attention (Elsabbagh, Volein, Holmboe, et al., 2009; Frith & Happé, 1994; Happé & Frith, 2006). Similarly, an over-focussed and narrow attentional style may relate to a narrow range of interests. On another note, this theory also proposes a decrease in integration in connectivity patterns, or underconnectivity in ASD. The current findings in contrast revealed that early overconnectivity was related to later dimensional traits of ASD. Furthermore, no differences in normalised path length (or other graph metrics) were found between risk or outcome groups, suggesting that integration was similar between infants with and without risk and later ASD diagnosis. Thus, the current results could be explained from the Weak Central Coherence perspective to some extent, but the direction of altered connectivity patterns in the current results are not consistent with the predictions of this theory. Possibly, associations between altered connectivity patterns and attentional styles depend on developmental periods, and are part of an adaptive response (see later).

Third, atypical alpha connectivity may relate to atypical top-down control and atypical predictive processing. The predictive coding theory of ASD suggests that individuals with ASD experience difficulties integrating prior information and

forming predictions for future events based on this previous information (Lawson et al., 2014; Pellicano & Burr, 2012). It has been suggested that high frequency oscillations such as gamma are related to bottom-up influences and play a role in the coding of a mismatch between the predictions and sensory events, whereas low frequency oscillations such as alpha are related to top-down influences and play a role in the top-down signalling of the predictions (Fries, 2015; Kessler, Seymour, & Rippon, 2016). Considering that the prefrontal cortex is related to top-down control, altered alpha connectivity between this and other regions may be associated with aberrant top-down influences and difficulties in predictive coding (Kessler et al., 2016). If individuals with ASD have more difficulties with predictive coding, creating more predictable environments with predictable events would minimize prediction errors from mismatches between perception and prediction. Restricted and repetitive behaviours may similarly minimize prediction errors (Lawson et al., 2014; Pellicano & Burr, 2012). One might argue that by focusing on similar specific topics of interests, information processing is more predictable and can be more easily integrated with prior information and matching prior predictions.

In addition to restricted and repetitive behaviours, the studies in this thesis also aimed to examine possible underlying mechanisms of difficulties with social interaction and communication. Analyses focusing on social and non-social context suggested that there are differences in social processing between individuals with high and low risk for ASD, and these differences are possibly related to increased risk for ASD in infants with high risk for ASD (Chapter 5). Furthermore, the group of HR-ASD infants seemed to be less attentive and more distracted during the presentation of social stimuli compared to LR, HR-TD, and HR-Atyp groups

(Chapter 4). These results seem in line with the social motivation hypothesis that suggests that diminished social motivation leads to cascading effects for social cognition such as social orienting, which in turn lead to social communication and interaction related difficulties in ASD (Chevallier et al., 2012). Although the results are in line with the hypothesis of an early onset of diminished social motivation, no clear cascading effects for traits of ASD were observed: the dimensional trait analyses revealed no strong associations between altered connectivity metrics at infancy and social difficulties at toddlerhood or childhood (Chapters 4, 5, 6, and 7). As mentioned earlier, it is possible that associations between EEG connectivity and later traits of ASD become clearer at later ages than 14 months, since brain connectivity continues to develop during the second year of postnatal life. The same may be true for associations between EEG connectivity and later categorical outcomes of ASD.

An alternative explanation to the social motivation theory is that there is delayed or atypical interactive specialization towards social stimuli in social brain regions in infants at high familial risk for ASD compared to infants at low risk for ASD. According to Johnson, the brain gets more specialised and fine-tuned towards processing of specific stimuli such as social stimuli (Johnson, 2011). This increased specialisation occurs via re-organisation of inter-regional interactions, or connectivity, with less widespread and more localised neural responses. A stronger difference between connectivity in the social and non-social conditions may reflect a more selective response to social stimuli. The stronger difference in the LR group compared to the HR group may reflect delayed or atypical specialisation in the HR group (Chapter 5). Graph theory findings however are not completely consistent with this hypothesis. The Interactive Specialisation theory

also suggests that segregation and integration in brain networks increase with increased specialisation. Although there was an increase in segregated processing during the social compared to the non-social condition as indicated by the normalised clustering coefficient, this increase was similar across risk groups. Possibly, alterations in global connectivity and graph organisation do not occur simultaneously but become clearer at different periods during development.

Finally, the differences in network topologies for social and non-social stimuli in the risk groups suggest a difference in re-organisation in connectivity patterns and are more consistent with the theory of atypical interactive specialisation. Topologies did especially differ with respect to the frontal areas, which showed stronger increases in connectivity in the LR group than the HR group. If there is atypical or delayed specialisation in the HR or HR-ASD group, social processing may require more involvement of frontal areas to orchestrate the processing in different brain regions in these groups compared to the LR or HR-no ASD groups (Johnson, 2011; Johnson et al., 2015; Jones, Venema, Earl, Lowy, & Webb, 2017).

To summarise, cognitive theories such as Executive Dysfunction, Weak Central Coherence, and predictive processing may account for associations between alpha connectivity and restricted and repetitive behaviours found in this thesis. Findings with regard to theta connectivity during social and non-social processing may relate to the social motivation hypothesis, and interactive specialisation theory. The latter theory also stresses the importance of developmental trajectories. Another possibility is that these alterations in global and network EEG connectivity are related to early adaptive responses, as will be discussed next.

8.4.3. ASD as an adaptive response during early development

While emphasizing developmental trajectories, Johnson and colleagues suggested that ASD is characterised as an adaptive process during early development in response to atypical neural processing. The atypicalities in neural processing may arise from pre- and perinatal factors, genetic influences, and an atypical balance between excitatory and inhibitory neural processes, which may lead to insufficient signal-to-noise ratios. Optimal signal-to-noise ratios are however essential for brain development and cortical specialisation, including interactive specialisation. ASD may be the result of an adaptive pathway in response to atypical neural processing via several whole brain adaptation processes (Johnson, 2017; Johnson et al., 2015).

One form of this adaptation is redundancy, which assumes that multiple processing pathways for a particular function exist and thereby allows for compensation if one of the pathways fails. One may suggest that the increased alpha connectivity related to more severe restricted and repetitive behaviours is related to increased redundancy in ASD. In addition, the finding of less strong consistent differences between social and non-social conditions in the HR groups than the LR group may indicate that activations in the HR groups are more variable across different connections than in the LR group. It is possible that connections in the HR groups are less consistently activated due to increased redundancy compared to the LR group.

Second, another whole brain adaptation process is prolonged plasticity and a delayed developmental trajectory. As previously suggested, the differences in activation in response to social and non-social stimuli between risk groups may reflect atypical or delayed interactive specialization in groups with high familial

risk for ASD. Connectivity was only examined at 14 months however, thus the current results do not allow for any conclusions on developmental trajectories.

Third, re-organization of brain connectivity has been proposed as another adaptive mechanism. The prefrontal cortex may also play a role in this process, while shaping and orchestrating synchronised activation across different brain networks (Johnson, 2012; Johnson et al., 2015). It is possible that the observed atypicalities in brain connectivity in the current studies are associated with this re-organisation. Indeed, alpha connectivity in fronto-central areas was related to increased ASD traits during toddlerhood in the HR-ASD group. Theta connectivity patterns in response to social stimuli suggested differential connectivity between the prefrontal cortex and other cortical areas between HR and LR groups. It is possible that atypical connectivity patterns across frontal areas are related to adaptive processes in ASD.

A fourth form of adaptation is niche construction, which would entail selecting and construction the appropriate environment that matches the individuals' atypical neural processing. Variability in cognition could arise from this form of adaptation as well. The authors suggest that a focal attention style could help limiting inputs to prevent parallel processing in an altered neural system with inappropriate signal-to-noise ratios. This focal, or over-focussed, attentional style may result in increased restricted and repetitive behaviours, such as circumscribed interests. Selecting temporally predictable sensory stimulation patterns may result in repetitive behaviours also. In contrast, social situations would be avoided since the complex dynamic processing and low predictability of these situations would provide a mismatch with the neural processing capacity.

Finally, this theory emphasizes the importance of developmental periods. Assuming ASD is characterised as an adaptive response during early development, early predictive markers of ASD may not be consistent over time. This is consistent with the findings in this thesis revealing that associations between infant EEG connectivity and later dimensional traits of ASD were different with traits measured at toddlerhood compared to mid-childhood.

In short, it is possible that the observed results are part of adaptive responses such as redundancy, altered developmental trajectories, re-organisation of connectivity, and niche construction. Further longitudinal studies measuring EEG connectivity at multiple time points, and directed connectivity may help clarify the role of how EEG connectivity is involved in adaptive responses during early development in ASD. The next sections will focus on limitations of the current studies.

8.5. Limitations

There are a few limitations to the studies in this thesis that require more discussion. The first limitation is the use of relatively small sample sizes for group level analyses. Small sample sizes have decreased statistical power to detect significant results. This may account for the lack of group differences reaching significant p-levels (Field, 2014). Although collapsing data across the Phase 1 and 2 BASIS cohorts increased overall sample sizes, missing data for behavioural measures (e.g. ADI-R and ADOS for LR participants at toddlerhood in Phase 1, SRS-2 at toddlerhood or childhood assessments) or insufficient amounts of artefact-free EEG data hindered inclusion of some participants in the analyses, in particular for comparisons between conditions. The latter might arise from strict behavioural

coding and EEG cleaning, or the EEG resting state paradigm, which involved fewer opportunities for social than non-social stimulation. As a result, the amount of data included in social versus non-social comparisons was limited. One way to handle this was to report effect sizes of the results as well. Another way is to study larger cohorts, which will also allow for more careful investigation of subgroups of ASDs.

It should also be noted that the same infants were used throughout the 4 studies examining EEG connectivity in ASD. It is possible that certain outliers included across studies have influenced the results, for example the consistent finding where alpha EEG connectivity parameters associated most strongly with traits in the restricted and repetitive behaviours domain may be caused by a few HR-ASD infants with high ADI-R scores for this domain at toddlerhood.

Second, the EEG connectivity calculated at sensor-level with the dbWPLI has some limitations as well. Effects of common pick-up from a single source by multiple electrodes and volume conduction cannot be excluded. The use of the phase lag index measures reduces the effects of volume conduction to a better extent than coherence-based measures, but does not eliminate them. Further, the common pick-up could have inflated connectivity estimates at shorter distances. The weighting component copes with this by assigning smaller weights to small phase lags often occurring between short-distance electrodes. The result is that short-range connectivity is under-estimated. Still, the dbWPLI is likely to be a more accurate estimate of 'true' connectivity than unbiased phase lag indices (van Diessen et al., 2015; Vinck et al., 2011).

The use of the sensor-level dbWPLI has also consequences for the interpretation of graph theory measures. The nodes in the graphs are assigned to the EEG channels, and the edges or connectivity values between them may be

influenced by the volume conduction and common pick-up effects (De Vico Fallani, Richiardi, Chavez, & Achard, 2014; Rubinov & Sporns, 2010; van Diessen et al., 2015). Local graph metrics may be more influenced by these artefacts than global graph metrics. Graph theory also adds another level of abstraction to neural analyses. While spectral power examines activity, connectivity patterns measure similarity in activity, and graph theory measures organisation and efficiency of the connectivity patterns. Interpretation of increases or decreases in path length, clustering coefficients or small-worldness should be carefully explained to avoid confusion or misinterpretation (De Vico Fallani et al., 2014). Further, graph theory metrics are modulated by a number of methodological aspects, such as using weighted or binary values for the edges, and the number of nodes included in the graph (van Wijk et al., 2010). The analyses here used weighted graphs because the selection of a threshold is often arbitrary, and connections with low connectivity values are informative too. It is possible that results differ when examined across a range of different thresholds for the edges, or range of different numbers of edges or nodes included in the analyses. For example, differences in graph metrics between groups are more distinct for networks with lower intensities compared to those where there is a weighted edge present between each of the nodes (Alaerts et al., 2015; Xie et al., 2018).

A final methodological limitation to the dbWPLI is that this measure reflects undirected EEG connectivity. Measures of directed connectivity can inform on the direction of information flow, while undirected connectivity measures only suggest that there is a flow of information across different brain regions. Directed connectivity may reveal more abnormalities in brain connectivity in individuals with ASD, or whether there may be compensatory mechanisms. A recent study

using a directed EEG connectivity measure suggested that frontal and cingulate regions provide a stronger drive to other regions in toddlers with ASD compared to TD toddlers while viewing social stimuli (Sperdin et al., 2018). Thus directed measures of connectivity may reveal the direction of relations in brain networks.

A third general limitation is the use of frequency bands rather than individual peaks. Previous studies have reported that there is variability between individuals in the frequency at which the alpha peak occurs (Bazanova & Vernon, 2014). Another recent study suggested that the alpha peak for spectral power in children with ASD occurs at a lower frequency than in children with TD (Dickinson, DiStefano, Senturk, et al., 2018). It is possible that the alpha connectivity peak also occurs at lower frequencies in the HR-ASD infants than the other comparison groups. The initial rationale for using frequency bands here was that previous EEG connectivity studies have been using frequency bands (Boersma et al., 2013; Keehn et al., 2015; Orekhova et al., 2014; Righi et al., 2014; Xie et al., 2018). Second, I aimed to examine reliability of previous methods and to replicate previous results from a study that focussed on the 4-5 Hz and 7-8 Hz frequency bands. Third, in some infants no clear peaks were visible in the power and connectivity spectra, thus selecting a peak frequency would have been difficult for these cases.

The use of frequency bands rather than individual peaks may have influenced the results, including the replication results. It is possible that differences between risk and outcome groups are clearer at individualized peaks, if these peak frequencies did not all fall into the frequency bands. The frequency bands were based on spectra averaged across all participants, thus it is possible that some infants had a peak outside the specified bands. Then, HR-ASD infants

may show increased connectivity at individual peaks compared to connectivity at individualized peaks of HR-no ASD and LR infants rather than across the broader frequency bands. Averaging across frequencies may also result in a decreased connectivity value compared to selecting 1 individual frequency for each participant. Alternatively, connectivity may be similar across individuals at individual peak frequencies. One might suggest that then findings in the narrow group frequency band could inform on variability in neural responses. If peaks do not occur in the expected frequency band, this may point towards atypical development, whereas peak occurring at the expected frequency may point towards typical development. This may hold for both the alpha connectivity measured across all conditions, and theta connectivity measured during social and non-social stimuli. Nonetheless, it remains unknown whether variability in individual peak frequencies for theta and alpha connectivity are related to variability in development as individual peak frequencies for spectral power. The individual peak frequency and connectivity metrics at that peak frequency may even be a more suitable marker for individual prediction than connectivity metrics for frequency bands based on group averages.

Finally, a fourth limitation to these studies is that EEG connectivity was only analysed for one time point during infancy here. As a consequence, we can only speculate on early developmental trajectories for connectivity in the different risk groups, and the underlying mechanisms of critical windows of brain development and specialization. Differences between groups may differ depending on the age of the participants. This thesis only reports on findings in participants at 14 months of age. Unfortunately, this paradigm was not included in the 4-6 month visit in Phase 2. Only the toy condition was presented during the 6-9 month visit in Phase

1, and 8-10 month visit in Phase 2. Sample sizes for these age groups were too small for further analysis, as only few participants had more than 120 artefact-free epochs of data available for connectivity analysis.

In short, the main limitations of this research are limited sample sizes for group level analyses, calculations of EEG connectivity are based on sensor-level data using the undirected dbWPLI, the use of frequency bands, and limited number of time-points analysed. These limitations also lead to more outstanding questions that can be examined in future research.

8.6. Future research directions

The studies conducted in this PhD project contributed to both lines of infant EEG connectivity research, and research on the early development of ASD. The limitations and contributions of these studies also provide new directions for these fields of research.

8.6.1. Measures of EEG connectivity during infancy

The current findings provide a good foundation for methodological choices when calculating EEG connectivity in infants; selection of number and length of epochs, appropriate EEG connectivity measure, and selection of an EEG paradigm suitable for young infants. Typical development of brain networks during infancy however still remains unknown. Longitudinal studies throughout infancy and childhood examining a range of parameters could establish how efficient brain networks emerge during early development. To this end, future research could focus on effective connectivity measures (Sperdin et al., 2018), interactions between structural and functional connectivity during early development for example in

well-known resting state networks (Honey et al., 2009; Xie et al., 2018), and other graph theory metrics examining global and local efficiency or network resilience (Rubinov & Sporns, 2010).

More studies are also needed to examine how EEG connectivity is related to cognitive processes. The current studies suggest that theta band connectivity is modulated by social context, and a recent study suggests that alpha EEG connectivity is modulated by attentional state (Xie et al., 2018). Replication studies will be needed to further examine these novel findings. Similarly, EEG connectivity in other frequency bands may also be associated with cognitive processes, as spectral power in different frequencies is known to associate with different cognitive functions (Saby & Marshall, 2012).

8.6.2. Subtypes of ASD in larger cohorts

Research into biomarkers of ASD has proposed that different subtypes of ASD exist with different behavioural, neural, and clinical phenotypes, arising from distinct underlying mechanisms (Geschwind, 2009; Loth et al., 2016). Different subgroups may be characterised by different associations between connectivity parameters and categorical ASD diagnosis, or combinations of severity of traits for social communication and interaction difficulties, restricted and repetitive behaviours, or sensory hyper- and hyposensitivity. Limited sample sizes unfortunately hindered further examination of homogeneous subtypes of ASD (also see Appendix A7.6). Future research including larger cohorts could help disentangle the complex association between connectivity and ASD outcomes across different subtypes of ASD (Loth et al., 2017).

Furthermore, larger cohorts will allow for more complex analyses examining individual and additive effects of multiple candidate markers for ASD.

Most research has examined the associations of a single candidate marker with ASD outcomes. One possibility is that one connectivity parameter provides more information than another parameter with regard to later outcomes, for example fronto-central alpha connectivity may be more informative than whole brain alpha connectivity. Another possibility is that the combined markers have additive effects. Previous studies using modelling or machine learning techniques have shown that diagnostic outcome and individual differences during toddlerhood could be predicted based on individual and combined markers: eye-tracking measures of attentional control (Bedford et al., 2014), event-related potentials (Bedford et al., 2017), and observational measures of autism traits at infancy, and developmental levels (Bussu et al., 2018). Techniques like these require large sample sizes in order to create, and test the fit of an algorithm or model to the data. Collecting data in larger cohorts, or combining data from cohorts collected across different research sites in collaborative consortia would also allow for examination of predictions on both group and individual levels (e.g. in (Loth et al., 2017)). The combination of markers of behavioural and neural phenotypes may increase the accuracy of early predictive markers of later outcomes of ASD, and could provide a more coherent understanding of the complex underlying mechanisms of ASD.

8.6.3. Universality and specificity of atypicalities in connectivity in ASD

Another question that could be pursued in future research is whether atypicalities in brain connectivity are present in all individuals with a diagnosis of ASD. In other words, whether early brain connectivity abnormalities are universal in ASD (Rajendran & Mitchell, 2007). The underlying genetic mechanisms of ASD in the HR-ASD participants in this high-risk infant sibling study may differ from those of individuals without a first-degree relative with ASD, and in whom small additive

effects of de novo mutations may result in ASD (De La Torre-Ubieta et al., 2016). Further, connectivity abnormalities may vary between individuals with different comorbidities, such as anxiety or attention deficit/ hyperactivity disorder (ADHD).

In addition to the question of universality, one could also focus on the specificity of connectivity abnormalities in ASD. Abnormal brain connectivity is likely present in multiple psychiatric disorders, and developmental disorders (Menon, 2013). Indeed previous research has revealed altered brain connectivity in ADHD, (Di Martino et al., 2013; Gargaro, Rinehart, Bradshaw, Tonge, & Sheppard, 2011; Konrad & Eickhoff, 2010), and Tuberous Sclerosis (Peters et al., 2013). This leads to the question what aspects of brain connectivity are specific for ASD during early development. Alternatively, cross syndrome comparisons between ASD and other disorders could reveal common pathways of underlying aetiology.

8.6.4. Early interventions

Markers for ASD could inform on later categorical and dimensional outcomes, underlying mechanisms, but may also help selecting the appropriate early intervention and monitoring the response to the intervention (Singh & Rose, 2009). Different early interventions exist focusing on improving social interaction skills, regulating negative affect, and increasing the caregiver's sensitivity via parent training, or via more intense sessions with therapists (Webb et al., 2014). Young children may however benefit differently from different early interventions. Recent studies furthermore suggest that early interventions affect both behavioural and neurocognitive phenotypes (Dawson et al., 2012; Green et al., 2017; Jones, Dawson, et al., 2017; Pickles et al., 2016). It is currently unknown whether connectivity patterns are affected by early interventions as well. Further,

evaluation of different ASD treatment models is still scarce. Future research may further clarify the potential of EEG connectivity as marker for treatment selection and monitoring.

8.7. EEG connectivity as biomarker for ASD

The final question that arises from the studies presented in this thesis is whether EEG connectivity is a suitable biomarker for ASD. A biomarker or biological marker is 'a characteristic that is objectively measured and evaluated as an indicator of a normal biological process, pathogenic process, or pharmacologic response to a therapeutic intervention' (Strimbu & Tavel, 2011). Such a marker can be any biological process, including EEG connectivity. Important requirements for measurements of a biomarker are high accuracy and reproducibility. The test-retest reliability study presented in Chapter 3 of this thesis demonstrated that global EEG connectivity could indeed be reliably measured across more than 120 1-second epochs with the dbWPLI (ICC = .82). This measure also is more robust to noise and biases when calculated across a small number of epochs, which suggests that this is a more accurate estimate of the underlying connectivity patterns than other measures of EEG connectivity. In addition, the replication study in Chapter 4 showed that the association between fronto-central hyperconnectivity and later severity of restricted and repetitive behaviours is reproducible. These novel findings of high accuracy and moderate reproducibility support the suitability of EEG connectivity as a biomarker.

Biomarkers should additionally provide clinically relevant information for the public and clinical professionals (Strimbu & Tavel, 2011). To this end, biomarkers for ASD can have different functions. One example is predicting later

outcome, in particular the severity of symptoms of ASD. The results of the replication study in Chapter 4 showed that the association between early fronto-central alpha connectivity and later restricted and repetitive behaviours replicated in a new, independent sample. This finding provides strong support for the use of EEG alpha connectivity as a biomarker for later symptom severity. However, further evaluation of this biomarker function is needed. An outstanding question is whether this association also is applicable to individuals in other developmental stages (Karmiloff-Smith, 1998). The current studies focussed on EEG connectivity in infants. The brain structure and function change rapidly during early life (Haartsen et al., 2016). It is possible that this association between fronto-central alpha connectivity and restricted and repetitive behaviours is specific to early development, and is altered when EEG connectivity is measured during childhood, adolescence, or adulthood (Walsh et al., 2011).

In addition to diagnosis and prediction of later symptom severity, a biomarker could help further the understanding of underlying mechanism and causal developmental pathways (Walsh et al., 2011). The results of the current studies suggest that EEG connectivity is a suitable biomarker for this function. The dbWPLI EEG connectivity measure provides information on the functional communication between brain regions at a high temporal resolution, and is a reliable measure of brain connectivity. As discussed in section 8.4 of this chapter, we can make inferences about underlying mechanisms of ASD and atypical development based on the results of the current studies, and relate these to theories of ASD aetiology. For example, connectivity atypicalities rather than overall hyper or hypoconnectivity are related to ASD symptom severities. Associations between different measures of EEG connectivity and severity of

symptom domains could relate to cognitive theories of ASDs. In particular, atypicalities in alpha fronto-central connectivity associated with restricted and repetitive behaviours, which could be explained by atypical attentional control. The current results further suggest that atypical connectivity may be related to an adaptive response to atypical neural processing. Atypicalities in neural processing may arise from an excitation/inhibition imbalance leading to a decreased signal to noise ratio. Alterations in functional connectivity patterns have been suggested as adaptive or compensatory mechanism for this atypical processing. Thus, EEG connectivity is a suitable biomarker to examine underlying mechanisms of ASD.

There are some functions of a biomarker EEG connectivity might not be suitable for. First, a biomarker could further provide relevant information by diagnosing an individual with ASD. The studies in the current thesis do not suggest that EEG connectivity is a suitable biomarker for the detection of ASD: neither alpha nor theta connectivity measures were associated with ASD diagnosis during toddlerhood (chapters 4, 5, and 6). On another note, such a biomarker would require a threshold that provides high sensitivity (correct identification of those with a diagnosis, true positive) and specificity (correct identification of those without a diagnosis, true negatives) (Pierce et al., 2016, 2011), which was not examined here due to limited sample sizes. Studies with larger samples sizes would be needed to examine sensitivity and specificity of EEG connectivity.

Second, some potential functions for a biomarker were not investigated here, and thus remain unclear. For example, a biomarker could provide relevant information for interventions: for selecting the appropriate intervention, or monitoring the effectiveness of the treatment. One possibility is that the EEG alpha and theta connectivity might be relevant for treatments targeting attentional

control (Wass, Porayska-Pomsta, & Johnson, 2011), or targeting social skills (Dawson et al., 2012; Jones, Dawson, et al., 2017; Webb et al., 2014). Another example of a biomarker function is the stratification of individuals with ASD into more homogeneous subgroups. It is possible that the ASD behavioural phenotype arises from different underlying mechanisms. Stratifying individual with ASD into homogeneous subgroups will help further research into biomarkers for ASD (Holiga et al., 2018; Loth et al., 2017). Again, a larger sample will be needed as subgroups need to be of sufficient size for further analyses.

To conclude, EEG connectivity is a promising biomarker with high accuracy and reliability when measured with the dbWPLI. The results in the studies presented here suggest that EEG connectivity is suitable as biomarker for the prediction of later severity of symptoms and for unravelling underlying causal mechanisms of the developmental disorder. However, EEG connectivity is not a suitable biomarker for clinical diagnosis of ASD. Further studies are needed to re-evaluate the use of EEG connectivity as biomarker for symptom prediction and underlying mechanisms, and other functions not investigated here, i.e. the selection and monitoring of effects or treatment, and the stratification into homogeneous subgroups.

8.8. Conclusions of this PhD thesis

The overall aim of this PhD project was to examine associations between early EEG connectivity and later ASD categorical diagnosis and dimensional traits during toddlerhood and childhood. The results suggest that there is a complex relation between early EEG connectivity and later ASD outcomes, where different

connectivity parameters show complex associations with ASD categorical outcomes and dimensional outcomes at different time points during development.

The current studies contributed to research into EEG connectivity as an early marker for ASD by focusing on the reproducibility of EEG connectivity candidate markers, examining optimal parameters and test-retest reliability for EEG connectivity measures, and exploring how EEG connectivity is modulated by social context. Further contributions to ASD research involve replication of previous results, focus on both categorical and dimensional ASD outcomes at toddlerhood and childhood, and exploring underlying mechanisms of ASD by focusing on different EEG connectivity parameters (global connectivity across all and selected connections, graph theory metrics, both alpha and theta frequency band connectivity), and separate symptom domains (social communication and interaction core domain, restricted and repetitive behaviours core domain, and subtypes of the latter domain).

Future directions for research include examining additional measures of EEG connectivity in infants, and establishing associations between EEG connectivity modulations and potential underlying cognitive processes. Further ASD studies involving longitudinal designs and larger cohorts may reveal EEG connectivity markers of developmental processes and subgroups of ASD. Research into early markers for ASD could lead to early detection and intervention, and better outcomes during later life.

List of References

Abbott, A. E., Linke, A. C., Nair, A., Jahedi, A., Alba, L. A., Keown, C. L., … Müller, R.-A. (2017). Repetitive behaviors in autism are linked to imbalance of corticostriatal connectivity: a functional connectivity MRI study. *Social Cognitive and Affective Neuroscience*, *13*(1), 32–42. http://doi.org/10.1093/scan/nsx129

Alaerts, K., Geerlings, F., Herremans, L., Swinnen, S. P., Verhoeven, J. S., Sunaert, S., & Wenderoth, N. (2015). Functional organization of the action observation network in autism: A graph theory approach. *PLoS ONE*, *10*(8), 1–21. http://doi.org/10.1371/journal.pone.0137020

Alcauter, S., Lin, W., Smith, J. K., Short, S. J., Goldman, B. D., Reznick, J. S., … Gao, W. (2014). Development of Thalamocortical Connectivity during Infancy and Its Cognitive Correlations. *The Journal of Neuroscience : The Official Journal of the Society for Neuroscience*, *34*(27), 9067–75. http://doi.org/10.1523/JNEUROSCI.0796-14.2014

American Psychological Association. (2013). *Diagnostic and statistical manual of mental disorders* (5th editio). Arlington, VA: American Psychiatric Publishing.

Aslin, R. N., Shukla, M., & Emberson, L. L. (2015). Hemodynamic Correlates of Cognition in Human infants. *Annual Review of Psychology*, *3*(66), 349–379. http://doi.org/10.1146/annurev-psych-010213-115108.Hemodynamic

Asperger, H. (1944). Die 'Autistisehen Psychopathen' im Kindesalter. *Archiv Für Psychiatrie Und Nervenkrankheiten*, *117*(1), 76–136. http://doi.org/10.1007/BF01837709

Baillet, S., Mosher, J. C., & Leahy, R. M. (2001). Electromagnetic brain mapping. *IEEE Signal Processing Magazine*, *18*(6), 14–30. http://doi.org/10.1109/79.962275

Ball, G., Aljabar, P., Zebari, S., Tusor, N., Arichi, T., Merchant, N., … Counsell, S. J. (2014). Rich-club organization of the newborn human brain. *Proceedings of the National Academy of Sciences of the United States of America*, *111*(20), 7456–61. http://doi.org/10.1073/pnas.1324118111

Ball, G., Srinivasan, L., Aljabar, P., Counsell, S. J., Durighel, G., Hajnal, J. V, … Edwards, A. D. (2013). Development of cortical microstructure in the preterm human brain. *Proceedings of the National Academy of Sciences of the United States of America*, *110*(23), 9541–6. http://doi.org/10.1073/pnas.1301652110

Baron-Cohen, S. (1989). The Autistic Child's Theory of Mind: a Case of Specific Developmental Delay. *Journal of Child Psychology and Psychiatry*, *30*(2), 285–297.

Baron-Cohen, S., Leslie, A. M., & Frith, U. (1985). Does the autistic child have a 'theory of mind' ? *Cognition*, *21*(1), 37–46. http://doi.org/10.1016/0010-0277(85)90022-8

Barttfeld, P., Amoruso, L., Ais, J., Cukier, S., Bavassi, L., Tomio, A., … Sigman, M. (2013). Organization of brain networks governed by long-range connections index autistic traits in the general population. *Journal of Neurodevelopmental Disorders*, *5*(1), 16. http://doi.org/10.1186/1866-1955-5-16

Barttfeld, P., Wicker, B., Cukier, S., Navarta, S., Lew, S., & Sigman, M. (2011). A big-world network in ASD: Dynamical connectivity analysis reflects a deficit in long-range connections and an excess of short-range connections. *Neuropsychologia*, *49*(2), 254–263. http://doi.org/10.1016/j.neuropsychologia.2010.11.024

Bastos, A. M., & Schoffelen, J.-M. (2016). A Tutorial Review of Functional

Connectivity Analysis Methods and Their Interpretational Pitfalls. *Frontiers in Systems Neuroscience*, *9*(January), 1–23. http://doi.org/10.3389/fnsys.2015.00175

Bathelt, J., O'Reilly, H., Clayden, J. D., Cross, J. H., & De Haan, M. (2013). Functional brain network organisation of children between 2 and 5years derived from reconstructed activity of cortical sources of high-density EEG recordings. *NeuroImage*, *82*, 595–604. http://doi.org/10.1016/j.neuroimage.2013.06.003

Bathelt, J., O'Reilly, H., & de Haan, M. (2014). Cortical source analysis of high-density EEG recordings in children. *Journal of Visualized Experiments : JoVE*, *c*(88), e51705. http://doi.org/10.3791/51705

Bazanova, O. M., & Vernon, D. (2014). Interpreting EEG alpha activity. *Neuroscience and Biobehavioral Reviews*, *44*, 94–110. http://doi.org/10.1016/j.neubiorev.2013.05.007

Bedford, R., Elsabbagh, M., Gliga, T., Pickles, A., Senju, A., Charman, T., & Johnson, M. H. (2012). Precursors to social and communication difficulties in infants at-risk for autism: Gaze following and attentional engagement. *Journal of Autism and Developmental Disorders*, *42*(10), 2208–2218. http://doi.org/10.1007/s10803-012-1450-y

Bedford, R., Gliga, T., Shephard, E., Elsabbagh, M., Pickles, A., Charman, T., & Johnson, M. H. (2017). Neurocognitive and observational markers: Prediction of autism spectrum disorder from infancy to mid-childhood. *Molecular Autism*, *8*(49), 1–34. http://doi.org/10.1186/s13229-017-0167-3

Bedford, R., Jones, E. J. H., Johnson, M. H., Pickles, A., Charman, T., & Gliga, T. (2016). Sex differences in the association between infant markers and later autistic traits. *Molecular Autism*, *7*(1). http://doi.org/10.1186/s13229-016-0094-8

Bedford, R., Pickles, A., Gliga, T., Elsabbagh, M., Charman, T., Johnson, M. H., … Volein, A. (2014). Additive effects of social and non-social attention during infancy relate to later autism spectrum disorder. *Developmental Science*, *17*(4), 612–620. http://doi.org/10.1111/desc.12139

Bejjani, A., O'Neill, J., Kim, J. A., Frew, A. J., Yee, V. W., Ly, R., … Levitt, J. G. (2012). Elevated glutamatergic compounds in pregenual anterior cingulate in pediatric autism spectrum disorder demonstrated by1H MRS and1H MRSI. *PLoS ONE*, *7*(7), 1–12. http://doi.org/10.1371/journal.pone.0038786

Belmonte, M. K., Allen, G., Beckel-Mitchener, A., Boulanger, L. M., Carper, R. A., & Webb, S. J. (2004). Autism and Abnormal Development of Brain Connectivity. *The Journal of Neuroscience*, *24*(42), 9228–9231. http://doi.org/10.1523/JNEUROSCI.3340-04.2004

Benders, M. J. N. L., Palmu, K., Menache, C., Borradori-Tolsa, C., Lazeyras, F., Sizonenko, S., … Hüppi, P. S. (2015). Early Brain Activity Relates to Subsequent Brain Growth in Premature Infants. *Cerebral Cortex (New York, N.Y. : 1991)*, *25*(September), 3014–3024. http://doi.org/10.1093/cercor/bhu097

Benjamini, Y., & Hochberg, Y. (1995). Controlling the False Discovery Rate: A Practical and Powerful Approach to Multiple Testing. *Journal of the Royal Statistical Society. Series B*, *57*(1), 289–300.

Bhat, A. N., Galloway, J. C., & Landa, R. J. (2012). Relation between early motor delay and later communication delay in infants at risk for autism. *Infant Behavior and Development*, *35*(4), 838–846. http://doi.org/10.1016/j.infbeh.2012.07.019

Boersma, M., Kemner, C., De Reus, M. a, Collin, G., Snijders, T. M., Hofman, D., … van den Heuvel, M. P. (2013). Disrupted functional brain networks in autistic

toddlers. *Brain Connectivity*, *3*(1), 41–9. http://doi.org/10.1089/brain.2012.0127

Boersma, M., Smit, D. J. A., De Bie, H. M. A., Van Baal, G. C. M., Boomsma, D. I., De Geus, E. J. C., … Stam, C. J. (2011). Network analysis of resting state EEG in the developing young brain: Structure comes with maturation. *Human Brain Mapping*, *32*(3), 413–425. http://doi.org/10.1002/hbm.21030

Bolton, P., Macdonald, H., Pickles, A., Rios, P., Goode, S., Crowson, M., … Rutter, M. (1994). A Case-Control Family History Study of Autism. *Journal of Child Psychology and Psychiatry*, *35*(5), 877–900. http://doi.org/10.1111/j.1469-7610.1994.tb02300.x

Braukmann, R., Lloyd-Fox, S., Blasi, A., Johnson, M. H., Bekkering, H., Buitelaar, J. K., & Hunnius, S. (2017). Diminished socially selective neural processing in 5-month-old infants at high familial risk of autism. *European Journal of Neuroscience*, 1–9. http://doi.org/10.1111/ejn.13751

Brian, J., Bryson, S. E., Smith, I. M., Roberts, W., Roncadin, C., Szatmari, P., & Zwaigenbaum, L. (2016). Stability and change in autism spectrum disorder diagnosis from age 3 to middle childhood in a high-risk sibling cohort. *Autism*, *20*(7), 888–892. http://doi.org/10.1177/1362361315614979

Brown, C. J., Miller, S. P., Booth, B. G., Andrews, S., Chau, V., Poskitt, K. J., & Hamarneh, G. (2014). Structural network analysis of brain development in young preterm neonates. *NeuroImage*, *101*, 667–680. http://doi.org/10.1016/j.neuroimage.2014.07.030

Bryson, S. E., Zwaigenbaum, L., McDermott, C., Rombough, V., & Brian, J. (2008). The autism observation scale for infants: Scale development and reliability data. *Journal of Autism and Developmental Disorders*, *38*(4), 731–738. http://doi.org/10.1007/s10803-007-0440-y

Buckley, A. W., Scott, R., Tyler, A., Mahoney, J. M., Thurm, A., Farmer, C., … Holmes, G. L. (2015). State-Dependent Differences in Functional Connectivity in Young Children With Autism Spectrum Disorder. *EBioMedicine*, *2*(12), 1905–1915. http://doi.org/10.1016/j.ebiom.2015.11.004

Bullmore, E., & Sporns, O. (2009). Complex brain networks: graph theoretical analysis of structural and functional systems. *Nat Rev Neurosci.*, *10*(3), 186–198. http://doi.org/10.1038/nrn2575

Bussu, G., Jones, E. J. H., Charman, T., Johnson, M. H., Buitelaar, J. K., & Team, B. (2018). Prediction of Autism at 3 Years from Behavioural and Developmental Measures in High-Risk Infants: A Longitudinal Cross-Domain Classifier Analysis. *Journal of Autism and Developmental Disorders*, *0*(0), 0. http://doi.org/10.1007/s10803-018-3509-x

Button, K. S., Ioannidis, J. P. a, Mokrysz, C., Nosek, B. a, Flint, J., Robinson, E. S. J., & Munafò, M. R. (2013). Power failure: why small sample size undermines the reliability of neuroscience. *Nature Reviews. Neuroscience*, *14*(5), 365–376. http://doi.org/10.1038/nrn3475

Buzsáki, G., Anastassiou, C. A., & Koch, C. (2012). The origin of extracellular fields and currents-EEG, ECoG, LFP and spikes. *Nature Reviews Neuroscience*, *13*(6), 407–420. http://doi.org/10.1038/nrn3241

Cao, M., Huang, H., & He, Y. (2017). Developmental Connectomics from Infancy through Early Childhood. *Trends in Neurosciences*, (July). http://doi.org/10.1016/j.tins.2017.06.003

Cascio, C. J., Foss-Feig, J. H., Heacock, J., Schauder, K. B., Loring, W. A., Rogers, B. P., … Bolton, S. (2014). Affective neural response to restricted interests in autism

spectrum disorders. *Journal of Child Psychology and Psychiatry and Allied Disciplines*, *55*(2), 162–171. http://doi.org/10.1111/jcpp.12147

Catarino, A., Andrade, A., Churches, O., Wagner, A. P., Baron-Cohen, S., & Ring, H. (2013). Task-related functional connectivity in autism spectrum conditions: an EEG study using wavelet transform coherence. *Molecular Autism*, *4*(1), 1. http://doi.org/10.1186/2040-2392-4-1

Charman, T., & Baird, G. (2002). Practitioner Review: Diagnosis of autism spectrum disorder in 2-and 3-year-old children. *Journal of Child Psychology and Psychiatry*, *43*(3), 289–305. http://doi.org/10.1111/1469-7610.00022

Charman, T., Taylor, E., Drew, A., Cockerill, H., Brown, J. A., & Baird, G. (2005). Outcome at 7 years of children diagnosed with autism at age 2: Predictive validity of assessments conducted at 2 and 3 years of age and pattern of symptom change over time. *Journal of Child Psychology and Psychiatry and Allied Disciplines*, *46*(5), 500–513. http://doi.org/10.1111/j.1469-7610.2004.00377.x

Charman, T., Young, G. S., Brian, J., Carter, A., Carver, L. J., Chawarska, K., … Zwaigenbaum, L. (2017). Non-ASD outcomes at 36 months in siblings at familial risk for autism spectrum disorder (ASD): A baby siblings research consortium (BSRC) study. *Autism Research*, *10*(1), 169–178. http://doi.org/10.1002/aur.1669

Chaste, P., & Leboyer, M. (2012). Autism risk factors: Genes, environment, and gene-environment interactions. *Dialogues in Clinical Neuroscience*, *14*(3), 281–292. http://doi.org/10.2217/epi.11.19

Chen, H., Nomi, J. S., Uddin, L. Q., Duan, X., & Chen, H. (2017). Intrinsic functional connectivity variance and state-specific under-connectivity in autism. *Human Brain Mapping*, *38*(11), 5740–5755. http://doi.org/https://doi.org/10.1002/hbm.23764

Cheung, C. H. M., Bedford, R., Johnson, M. H., Charman, T., & Gliga, T. (2016). Visual search performance in infants associates with later ASD diagnosis. *Developmental Cognitive Neuroscience*. http://doi.org/10.1016/j.dcn.2016.09.003

Chevallier, C., Kohls, G., Troiani, V., Brodkin, E. S., & Schultz, R. T. (2012). The social motivation theory of autism. *Trends in Cognitive Sciences*, *16*(4), 231–238. http://doi.org/10.1016/j.tics.2012.02.007

Christensen, D. L., Baio, J., Braun, K. V. N., Bilder, D., Charles, J., Constantino, J. N., … Yeargin-Allsopp, M. (2016). Prevalence and Characteristics of Autism Spectrum Disorder Among Children Aged 8 Years - Autism and Developmental Disabilities Monitoring Network, 11 Sites, United States, 2012. *MMWR Surveillance Summaries*, *65*(3), 1–23. http://doi.org/10.15585/mmwr.ss6503a1

Chu, C. J., Tanaka, N., Diaz, J., Edlow, B. L., Wu, O., Hämäläinen, M., … Kramer, M. A. (2015). EEG functional connectivity is partially predicted by underlying white matter connectivity. *NeuroImage*, *108*, 23–33. http://doi.org/10.1016/j.neuroimage.2014.12.033

Coben, R., Clarke, A. R., Hudspeth, W., & Barry, R. J. (2008). EEG power and coherence in autistic spectrum disorder. *Clinical Neurophysiology*, *119*(5), 1002–1009. http://doi.org/10.1016/j.clinph.2008.01.013

Cohen, J. (1988). *Statistical power analysis for the behavioral sciences (2nd ed.).* (2nd ed.). Hillsdale, NJ: Erlbaum.

Cohen, M. X. (2014). *Analizing Neural Time Series Data: Theory and Practise*.

Cambridge, Massachusetts: MIT Press.
Constantino, J. N., Davis, S. A., Todd, R. D., Schindler, M. K., Gross, M. M., Brophy, S. L., … Reich, W. (2003). Validation of a brief quantitative measure of autistic traits: Comparison of the social responsiveness scale with the Autism Diagnostic Interview-Revised. *Journal of Autism and Developmental Disorders*, *33*(4), 427–433. http://doi.org/10.1023/A:1025014929212
Constantino, J. N., & Gruber, C. P. (2012). *Social Responsiveness Scale, Second Edition (SRS-2).* Torrance, CA: Western Psychological Services.
Conti, E., Mitra, J., Calderoni, S., Pannek, K., Shen, K. K., Pagnozzi, A., … Guzzetta, A. (2017). Network Over-Connectivity Differentiates Autism Spectrum Disorder from Other Developmental Disorders in Toddlers : A Diffusion MRI Study. *Human Brain Mapping*, *00*, 1–12. http://doi.org/10.1002/hbm.23520
Courchesne, E., Campbell, K., & Solso, S. (2011). Brain growth across the life span in autism: Age-specific changes in anatomical pathology. *Brain Research*, *1380*, 138–145. http://doi.org/10.1016/j.brainres.2010.09.101
Courchesne, E., Pierce, K., Schumann, C. M., Redcay, E., Buckwalter, J. a, Kennedy, D. P., & Morgan, J. (2007). Mapping early brain development in autism. *Neuron*, *56*(2), 399–413. http://doi.org/10.1016/j.neuron.2007.10.016
Dawson, G., Jones, E. J. H., Merkle, K., Venema, K., Lowy, R., Faja, S., … Webb, S. J. (2012). Early Behavioral Intervention Is Associated With Normalized Brain Activity in Young Children With Autism. *Journal of the American Academy of Child & Adolescent Psychiatry*, *51*(11), 1150–1159. http://doi.org/10.1016/j.jaac.2012.08.018
De La Torre-Ubieta, L., Won, H., Stein, J. L., & Geschwind, D. H. (2016). Advancing the understanding of autism disease mechanisms through genetics. *Nature Medicine*, *22*(4), 345–361. http://doi.org/10.1038/nm.4071
De Vico Fallani, F., Richiardi, J., Chavez, M., & Achard, S. (2014). Graph analysis of functional brain networks: practical issues in translational neuroscience. *Philosophical Transactions. Biological Sciences*, *369*, 20130521. http://doi.org/10.1098/rstb.2013.0521
Delorme, A., & Makeig, S. (2004). EEGLAB: an open source toolbox for analysis of single-trial EEG dynamics including independent component analysis. *Journal of Neuroscience Methods*, *134*, 9–21. http://doi.org/10.1007/3-540-35375-5
Deuker, L., Bullmore, E. T., Smith, M., Christensen, S., Nathan, P. J., Rockstroh, B., & Bassett, D. S. (2009). Reproducibility of graph metrics of human brain functional networks. *NeuroImage*, *47*(4), 1460–1468. http://doi.org/10.1016/j.neuroimage.2009.05.035
Di Martino, A., Zuo, X.-N. X., Kelly, C., Grzadzinski, R., Mennes, M., Schvarcz, A., … Milham, M. P. (2013). Shared and distinct intrinsic functional network centrality in autism and attention-deficit/hyperactivity disorder. *Biological Psychiatry*, *74*(8), 623–632. http://doi.org/10.1016/j.biopsych.2013.02.011
Diamond, A. (2013). Executive Functions. *Annual Review of Psychology*, *64*, 135–168. http://doi.org/10.1016/j.biotechadv.2011.08.021.Secreted
Dichter, G. S., Felder, J. N., Green, S. R., Rittenberg, A. M., Sasson, N. J., & Bodfish, J. W. (2012). Reward circuitry function in autism spectrum disorders. *Social Cognitive and Affective Neuroscience*, *7*(2), 160–172. http://doi.org/10.1093/scan/nsq095
Dickinson, A., DiStefano, C., Lin, Y.-Y., Scheffler, A. W., Senturk, D., & Jeste, S. S. (2018). Interhemispheric alpha-band hypoconnectivity in children with autism spectrum disorder. *Behavioural Brain Research*, *348*(January), 227–

234. http://doi.org/10.1016/j.bbr.2018.04.026
Dickinson, A., DiStefano, C., Senturk, D., & Jeste, S. S. (2018). Peak alpha frequency is a neural marker of cognitive function across the autism spectrum. *European Journal of Neuroscience*, *47*(6), 643–651. http://doi.org/10.1111/ejn.13645
Dolnicar, S. (2002). A Review of Unquestioned Standards in Using Cluster Analysis for Data-Driven Market Segmentation. In *CD Conference Proceedings of the Australian and New Zealand Marketing Academy Conference*. http://doi.org/10.1084/jem.20030437
Dubois, J., Kostovic, I., & Judas, M. (2015). Development of structural and functional connectivity. *Brain Mapping: An Encyclopedic Reference*, *2*, 423–437.
Duffy, F. H., & Als, H. (2012). A stable pattern of EEG spectral coherence distinguishes children with autism from neuro-typical controls - a large case control study. *BMC Medicine*, *10*(1), 64. http://doi.org/10.1186/1741-7015-10-64
Ecker, C., Bookheimer, S. Y., & Murphy, D. G. M. (2015). Neuroimaging in autism spectrum disorder: Brain structure and function across the lifespan. *The Lancet Neurology*, *14*(11), 1121–1134. http://doi.org/10.1016/S1474-4422(15)00050-2
Elhabashy, H., Raafat, O., Afifi, L., Raafat, H., & Abdullah, K. (2015). Quantitative EEG in autistic children. *The Egyptian Journal of Neurology, Psychiatry and Neurosurgery*, *52*(3), 176–182. http://doi.org/10.4103/1110-1083.162031
Elison, J. T., Paterson, S. J., Wolff, J. J., Reznick, J. S., Sasson, N. J., Gu, H., … Piven, J. (2013). White matter microstructure and atypical visual orienting in 7-month-olds at risk for autism. *American Journal of Psychiatry*, *170*(August), 899–908. http://doi.org/10.1176/appi.ajp.2012.12091150
Elsabbagh, M., Fernandes, J., Jane Webb, S., Dawson, G., Charman, T., & Johnson, M. H. (2013). Disengagement of visual attention in infancy is associated with emerging autism in toddlerhood. *Biological Psychiatry*, *74*(3), 189–194. http://doi.org/10.1016/j.biopsych.2012.11.030
Elsabbagh, M., & Johnson, M. H. (2016). Autism and the social brain: The first year puzzle. *Biological Psychiatry*. http://doi.org/10.1016/j.biopsych.2016.02.019
Elsabbagh, M., Mercure, E., Hudry, K., Chandler, S., Pasco, G., Charman, T., … Johnson, M. H. (2012). Infant Neural Sensitivity to Dynamic Eye Gaze Is Associated with Later Emerging Autism. *Current Biology*, *22*(4), 338–342. http://doi.org/10.1016/j.cub.2011.12.056
Elsabbagh, M., Volein, A., Csibra, G., Holmboe, K., Garwood, H., Tucker, L. A., … Johnson, M. H. (2009). Neural Correlates of Eye Gaze Processing in the Infant Broader Autism Phenotype. *Biological Psychiatry*, *65*(1), 31–38. http://doi.org/10.1016/j.biopsych.2008.09.034
Elsabbagh, M., Volein, A., Holmboe, K., Tucker, L. A., Csibra, G., Baron-Cohen, S., … Johnson, M. H. (2009). Visual orienting in the early broader autism phenotype: Disengagement and facilitation. *Journal of Child Psychology and Psychiatry and Allied Disciplines*, *50*(5), 637–642. http://doi.org/10.1111/j.1469-7610.2008.02051.x
Emerson, R. W., Adams, C. M., Nishino, T., Hazlett, H. C., Wolff, J. J., Zwaigenbaum, L., … Piven, J. (2017). Functional neuroimaging of high-risk 6-month-old infants predicts a diagnosis of autism at 24 months of age, *9*(393), 1–8. http://doi.org/10.1126/scitranslmed.aag2882
Estes, A., Zwaigenbaum, L., Gu, H., St. John, T., Paterson, S. J., Elison, J. T., … Piven, J. (2015). Behavioral, cognitive, and adaptive development in infants with

autism spectrum disorder in the first 2 years of life. *Journal of Neurodevelopmental Disorders*, *7*(1), 24. http://doi.org/10.1186/s11689-015-9117-6

Fair, D. A., Dosenbach, N. U. F., Church, J. A., Cohen, A. L., Brahmbhatt, S., Miezin, F. M., … Schlaggar, B. L. (2007). Development of distinct control networks through segregation and integration. *Proceedings of the National Academy of Sciences*, *104*(33), 13507–13512. http://doi.org/10.1073/pnas.0705843104

Falahpour, M., Thompson, W. K., Abbott, A. E., Jahedi, A., Mulvey, M. E., Datko, M., … Müller, R.-A. (2016). Underconnected, But Not Broken? Dynamic Functional Connectivity MRI Shows Underconnectivity in Autism Is Linked to Increased Intra-Individual Variability Across Time. *Brain Connectivity*, *6*(5), 403–414. http://doi.org/10.1089/brain.2015.0389

Field, A. P. (2005). Intraclass Correlation. In B. S. Everitt & D. C. Howell (Eds.), *Encyclopedia of Statistics in Behavioral Science* (Vol. 2, pp. 948–954). Chichester: John Wiley & Sons, Ltd.

Field, A. P. (2014). *Discovering statistics using IBM SPSS Statistics*. (M. Carmichael, Ed.) (4th ed.). London: SAGE Publications Ltd.

Flanagan, J. E., Landa, R. J., Bhat, A. N., & Bauman, M. (2012). Head lag in infants at risk for autism: A preliminary study. *American Journal of Occupational Therapy*, *66*(5), 577–585. http://doi.org/10.5014/ajot.2012.004192

Fountain, C., Winter, a. S., & Bearman, P. S. (2012). Six Developmental Trajectories Characterize Children With Autism. *Pediatrics*, *129*(5), e1112–e1120. http://doi.org/10.1542/peds.2011-1601

Fraschini, M., Demuru, M., Crobe, A., Marrosu, F., Stam, C. J., & Hillebrand, A. (2016). The effect of epoch length on estimated EEG functional connectivity and brain network organization. *Journal of Neural Engineering*, *13*(3), 036015. http://doi.org/10.1017/CBO9781107415324.004

Fries, P. (2005). A mechanism for cognitive dynamics: Neuronal communication through neuronal coherence. *Trends in Cognitive Sciences*, *9*(10), 474–480. http://doi.org/10.1016/j.tics.2005.08.011

Fries, P. (2015). Rhythms for Cognition: Communication through Coherence. *Neuron*, *88*(1), 220–235. http://doi.org/10.1016/j.neuron.2015.09.034

Frith, U., & Happé, F. (1994). Autism: beyond 'theory of mind'. *Cognition*, *50*(1–3), 115–132. http://doi.org/10.1016/0010-0277(94)90024-8

Fuccillo, M. V. (2016). Striatal circuits as a common node for autism pathophysiology. *Frontiers in Neuroscience*, *10*(FEB). http://doi.org/10.3389/fnins.2016.00027

Gao, W., Alcauter, S., Elton, A., Hernandez-Castillo, C. R., Smith, J. K., Ramirez, J., & Lin, W. (2015). Functional Network Development During the First Year: Relative Sequence and Socioeconomic Correlations. *Cerebral Cortex*, *25*(9), 2919–2928. http://doi.org/10.1093/cercor/bhu088

Gao, W., Alcauter, S., Smith, J. K., Gilmore, J., & Lin, W. (2015). Development of human brain cortical network architecture during infancy. *Brain Structural Function*, *220*(2), 1173–1186. http://doi.org/10.1002/aur.1474.Replication

Gao, W., Gilmore, J. H., Giovanello, K. S., Smith, J. K., Shen, D., Zhu, H., & Lin, W. (2011). Temporal and spatial evolution of brain network topology during the first two years of life. *PLoS ONE*, *6*(9). http://doi.org/10.1371/journal.pone.0025278

García Domínguez, L., Stieben, J., Pérez Velázquez, J. L., & Shanker, S. (2013). The Imaginary Part of Coherency in Autism: Differences in Cortical Functional

Connectivity in Preschool Children. *PLoS ONE*, *8*(10), e75941. http://doi.org/10.1371/journal.pone.0075941

Gargaro, B. a., Rinehart, N. J., Bradshaw, J. L., Tonge, B. J., & Sheppard, D. M. (2011). Autism and ADHD: How far have we come in the comorbidity debate? *Neuroscience and Biobehavioral Reviews*, *35*(5), 1081–1088. http://doi.org/10.1016/j.neubiorev.2010.11.002

Geschwind, D. H. (2009). Advances in Autism. *Annual Review of Medicine*, *60*, 367–380. http://doi.org/10.1146/annurev.med.60.053107.121225.Advances

Goncharova, I. I., McFarland, D. J., Vaughan, T. M., & Wolpaw, J. R. (2003). EMG contamination of EEG: Spectral and topographical characteristics. *Clinical Neurophysiology*, *114*(9), 1580–1593. http://doi.org/10.1016/S1388-2457(03)00093-2

Goodman, R., Ford, T., Richards, H., Gatward, R., & Meltzer, H. (2000). The Development and Well-Being Assessment: Description and Initial Validation of an Integrated Assessment of Child and Adolescent Psychopathology. *Journal of Child Psychology and Psychiatry*, *41*(5), 645–655. http://doi.org/10.1111/j.1469-7610.2000.tb02345.x

Gotham, K., Pickles, A., & Lord, C. (2012). Trajectories of Autism Severity in Children Using Standardized ADOS Scores. *Pediatrics*, *130*(5), e1278–e1284. http://doi.org/10.1542/peds.2011-3668

Göttlich, M., Ye, Z., Rodriguez-Fornells, A., Münte, T. F., & Krämer, U. M. (2017). Viewing socio-affective stimuli increases connectivity within an extended default mode network. *NeuroImage*, *148*(December 2016), 8–19. http://doi.org/10.1016/j.neuroimage.2016.12.044

Grayson, D. R., & Guidotti, A. (2016). Merging data from genetic and epigenetic approaches to better understand autistic spectrum disorder. *Epigenomics*, *8*(1), 85–104. http://doi.org/10.2217/epi.15.92

Green, J., Charman, T., Pickles, A., Wan, M. W., Elsabbagh, M., Slonims, V., … Johnson, M. H. (2015). Parent-mediated intervention versus no intervention for infants at high risk of autism: A parallel, single-blind, randomised trial. *The Lancet Psychiatry*, *2*(2), 133–140. http://doi.org/10.1016/S2215-0366(14)00091-1

Green, J., Pickles, A., Pasco, G., Bedford, R., Wan, M. W., Elsabbagh, M., … Johnson, M. H. (2017). Randomised trial of a parent-mediated intervention for infants at high risk for autism: Longitudinal outcomes to age 3 years. *Journal of Child Psychology and Psychiatry and Allied Disciplines*, (April). http://doi.org/10.1111/jcpp.12728

Grossmann, T. (2015). The development of social brain functions in infancy. *Psychological Bulletin*, *141*(6), 1266–1287. http://doi.org/10.1037/bul0000002

Guan, J., & Li, G. (2017). Injury Mortality in Individuals With Autism. *American Journal of Public Health*, *107*(5), 791–793. http://doi.org/10.2105/AJPH.2017.303696

Haartsen, R., Jones, E. J. H., & Johnson, M. H. (2016). Human Brain Development over the Early Years. *Current Opinion in Behavioral Sciences*.

Hahamy, A., Behrmann, M., & Malach, R. (2015). The idiosyncratic brain: distortion of spontaneous connectivity patterns in autism spectrum disorder. *Nature Neuroscience*, *18*(January), 302–309. http://doi.org/10.1038/nn.3919

Hallmayer, J., Cleveland, S., Torres, A., Phillips, J., Cohen, B., Torigoe, T., … Risch, N. (2011). Genetic heritability and shared environmental factors among twin pairs with autism. *Archives of General Psychiatry*, *68*(11), 1095–1102.

http://doi.org/10.1001/archgenpsychiatry.2011.76
Han, J., Zeng, K., Kang, J., Tong, Z., Cai, E., Chen, H., … Li, X. (2017). Development of Brain Network in Children with Autism from Early Childhood to Late Childhood. *Neuroscience*, *367*, 134–146. http://doi.org/10.1016/j.neuroscience.2017.10.015
Han, Y. M. Y., Chan, A. S., Sze, S. L., Cheung, M.-C., Wong, C., Lam, J. M. K., & Poon, P. M. K. (2013). Altered immune function associated with disordered neural connectivity and executive dysfunctions: A neurophysiological study on children with autism spectrum disorders. *Research in Autism Spectrum Disorders*, *7*(6), 662–674. http://doi.org/10.1016/j.rasd.2013.02.011
Happé, F., & Frith, U. (2006). The weak coherence account: Detail-focused cognitive style in autism spectrum disorders. *Journal of Autism and Developmental Disorders*, *36*(1), 5–25. http://doi.org/10.1007/s10803-005-0039-0
Hardmeier, M., Hatz, F., Bousleiman, H., Schindler, C., Stam, C. J., & Fuhr, P. (2014). Reproducibility of functional connectivity and graph measures based on the phase lag index (PLI) and weighted phase lag index (wPLI) derived from high resolution EEG. *PLoS ONE*, *9*(10). http://doi.org/10.1371/journal.pone.0108648
Harris, J. J., Reynell, C., & Attwell, D. (2011). The physiology of developmental changes in BOLD functional imaging signals. *Developmental Cognitive Neuroscience*, *1*(3), 199–216. http://doi.org/10.1016/j.dcn.2011.04.001
Hatz, F., Hardmeier, M., Bousleiman, H., Rüegg, S., Schindler, C., & Fuhr, P. (2016). Reliability of Functional Connectivity of Electroencephalography Applying Microstate-Segmented Versus Classical Calculation of Phase Lag Index. *Brain Connectivity*, *6*(6), 461–469. http://doi.org/10.1089/brain.2015.0368
Hazlett, H. C., Gu, H., Munsell, B. C., Kim, S. H., Styner, M. A., Wolff, J. J., … Piven, J. (2017). Early brain development in infants at high risk for autism spectrum disorder. *Nature Publishing Group*, *542*. http://doi.org/10.1038/nature21369
Hill, E. L. (2004a). Evaluating the theory of executive dysfunction in autism. *Developmental Review*, *24*(2), 189–233. http://doi.org/10.1016/j.dr.2004.01.001
Hill, E. L. (2004b). Executive dysfunction in autism. *Trends in Cognitive Sciences*, *8*(1), 26–32. http://doi.org/10.1016/j.tics.2003.11.003
Hillebrand, A., Tewarie, P., van Dellen, E., Yu, P., Carbo, E., Douw, L., … Stam, C. J. (2016). Direction of information flow in large-scale resting-state networks is frequency dependent. *Neuron*, *113*(14), 3867–3872. http://doi.org/10.1073/pnas.1515657113
Hoff, G. E. A.-J., Van den Heuvel, M. P., Benders, M. J. N. L., Kersbergen, K. J., & De Vries, L. S. (2013). On development of functional brain connectivity in the young brain. *Frontiers in Human Neuroscience*, *7*(October), 650. http://doi.org/10.3389/fnhum.2013.00650
Holiga, Š., Hipp, J. F., Chatham, C. H., Garces, P., Spooren, W., Ardhuy, L. D., … Albis, M.-A. (2018). Reproducible functional connectivity alterations are associated with autism spectrum disorder, (April). http://doi.org/10.1101/303115
Höller, Y., Butz, K., Thomschewski, A., Schmid, E., Uhl, A., Bathke, A. C., … Trinka, E. (2017). Reliability of EEG Interactions Differs between Measures and Is Specific for Neurological Diseases. *Frontiers in Human Neuroscience*, *11*(July), 1–18. http://doi.org/10.3389/fnhum.2017.00350
Höller, Y., Uhl, A., Bathke, A. C., Thomschewski, A., Butz, K., Nardone, R., … Trinka, E. (2017). Reliability of EEG Measures of Interaction: A Paradigm Shift Is Needed

to Fight the Reproducibility Crisis. *Frontiers in Human Neuroscience*, *11*(August), 1–15. http://doi.org/10.3389/fnhum.2017.00441

Honey, C. J., Sporns, O., Cammoun, L., Gigandet, X., Thiran, J.-P., Meuli, R., & Hagmann, P. (2009). Predicting human resting-state functional connectivity. *Proc. Natl. Acad. Sci. USA*, *106*(6), 2035–2040.

Hoppenbrouwers, M., Vandermosten, M., & Boets, B. (2014). Autism as a disconnection syndrome: A qualitative and quantitative review of diffusion tensor imaging studies. *Research in Autism Spectrum Disorders*, *8*(4), 387–412. http://doi.org/10.1016/j.rasd.2013.12.018

Huang, H., Shu, N., Mishra, V., Jeon, T., Chalak, L., Wang, Z. J., … He, Y. (2015). Development of Human Brain Structural Networks Through Infancy and Childhood. *Cerebral Cortex*, *25*(5), 1389–1404. http://doi.org/10.1093/cercor/bht335

Hudry, K., Chandler, S., Bedford, R., Pasco, G., Gliga, T., Elsabbagh, M., … Charman, T. (2014). Early language profiles in infants at high-risk for autism spectrum disorders. *Journal of Autism and Developmental Disorders*, *44*(1), 154–167. http://doi.org/10.1007/s10803-013-1861-4

Humphries, M. D., & Gurney, K. (2008). Network 'small-world-ness': A quantitative method for determining canonical network equivalence. *PLoS ONE*, *3*(4). http://doi.org/10.1371/journal.pone.0002051

Hutsler, J. J., & Casanova, M. F. (2015). Review: Cortical construction in autism spectrum disorder: Columns, connectivity and the subplate. *Neuropathology and Applied Neurobiology*, *42*(2), 115–134. http://doi.org/10.1111/nan.12227

Insel, T., Cuthbert, B., Garvey, M., Heinssen, R., Pine, D. S., Quinn, K., … Wang, P. (2010). Research Domain Criteria (RDoC): Toward a new classification framework for research on mental disorders. *American Journal of Psychiatry*, *167*(7), 748–751. http://doi.org/10.1176/appi.ajp.2010.09091379

Isler, J. R., Martien, K. M., Grieve, P. G., Stark, R. I., & Herbert, M. R. (2010). Reduced functional connectivity in visual evoked potentials in children with autism spectrum disorder. *Clinical Neurophysiology*, *121*(12), 2035–2043. http://doi.org/10.1016/j.clinph.2010.05.004

Jeste, S. S., Frohlich, J., & Loo, S. K. (2015). Electrophysiological Biomarkers of Diagnosis and Outcome in Neurodevelopmental Disorders. *Current Opinion in Neurology*, *28*, 110–116. http://doi.org/10.1007/3-540-35375-5

Jin, S.-H., Seol, J., Kim, J. S., & Chung, C. K. (2011). How reliable are the functional connectivity networks of MEG in resting states? *Journal of Neurophysiology*, *106*(6), 2888–2895. http://doi.org/10.1152/jn.00335.2011

Johnson, M. H. (2011). Interactive Specialization: A domain-general framework for human functional brain development? *Developmental Cognitive Neuroscience*, *1*(1), 7–21. http://doi.org/10.1016/j.dcn.2010.07.003

Johnson, M. H. (2012). Executive function and developmental disorders: The flip side of the coin. *Trends in Cognitive Sciences*, *16*(9), 454–457. http://doi.org/10.1016/j.tics.2012.07.001

Johnson, M. H. (2017). Autism as an adaptive common variant pathway for human brain development. *Developmental Cognitive Neuroscience*. http://doi.org/10.1016/j.dcn.2017.02.004

Johnson, M. H., De Haan, M., Oliver, A., Smith, W., Hatzakis, H., Tucker, L. A., & Csibra, G. (2001). Recording and analyzing high-density event-related potentials with infants. Using the Geodesic sensor net. *Developmental*

Neuropsychology, *19*(3), 295–323. http://doi.org/10.1207/S15326942DN1903_4

Johnson, M. H., Griffin, R., Csibra, G., Halit, H., Farroni, T., De Haan, M., … Richards, J. E. (2005). The emergence of the social brain network: evidence from typical and atypical development. *Dev.Psychopathol.*, *17*(0954–5794 (Print)), 599–619.

Johnson, M. H., Grossmann, T., & Cohen Kadosh, K. (2009). Mapping functional brain development: Building a social brain through interactive specialization. *Developmental Psychology*, *45*(1), 151–159. http://doi.org/10.1037/a0014548

Johnson, M. H., Jones, E. J. H., & Gliga, T. (2015). Brain adaptation and alternative developmental trajectories. *Development and Psychopathology*, *27*(2), 425–444. http://doi.org/10.1128/AEM.01604-07

Jones, E. J. H., Dawson, G., Kelly, J., Estes, A., & Jane Webb, S. (2017). Parent-delivered early intervention in infants at risk for ASD: Effects on electrophysiological and habituation measures of social attention. *Autism Research*, *10*(5), 961–972. http://doi.org/10.1002/aur.1754

Jones, E. J. H., Gliga, T., Bedford, R., Charman, T., & Johnson, M. H. (2014). Developmental pathways to autism: A review of prospective studies of infants at risk. *Neuroscience and Biobehavioral Reviews*, *39*, 1–33. http://doi.org/10.1016/j.neubiorev.2013.12.001

Jones, E. J. H., Venema, K., Earl, R. K., Lowy, R., & Webb, S. J. (2017). Infant social attention: an endophenotype of ASD-related traits? *Journal of Child Psychology and Psychiatry and Allied Disciplines*, *58*(3), 270–281. http://doi.org/10.1111/jcpp.12650

Jones, E. J. H., Venema, K., Earl, R., Lowy, R., Barnes, K., Estes, A., … Webb, S. J. (2016). Reduced engagement with social stimuli in 6-month-old infants with later autism spectrum disorder: A longitudinal prospective study of infants at high familial risk. *Journal of Neurodevelopmental Disorders*, *8*, 7. http://doi.org/10.1186/s11689-016-9139-8

Jones, E. J. H., Venema, K., Lowy, R., Earl, R. K., & Webb, S. J. (2015). Developmental changes in infant brain activity during naturalistic social experiences. *Developmental Psychobiology*, n/a-n/a. http://doi.org/10.1002/dev.21336

Joshi, G., Biederman, J., Wozniak, J., Goldin, R. L., Crowley, D., Furtak, S., … Gönenç, A. (2013). Magnetic resonance spectroscopy study of the glutamatergic system in adolescent males with high-functioning autistic disorder: A pilot study at 4T. *European Archives of Psychiatry and Clinical Neuroscience*, *263*(5), 379–384. http://doi.org/10.1007/s00406-012-0369-9

Just, M. A., Cherkassky, V. L., Keller, T. A., & Minshew, N. J. (2004). Cortical activation and synchronization during sentence comprehension in high-functioning autism: Evidence of underconnectivity. *Brain*, *127*(8), 1811–1821. http://doi.org/10.1093/brain/awh199

Just, M. A., Keller, T. a., Malave, V. L., Kana, R. K., & Varma, S. (2012). Autism as a neural systems disorder: A theory of frontal-posterior underconnectivity. *Neuroscience and Biobehavioral Reviews*, *36*(4), 1292–1313. http://doi.org/10.1016/j.neubiorev.2012.02.007

Kanner, L. (1943). Autistic Disturbances of Affective Contact. *Nervous Child*.

Karmiloff-Smith, A. (1998). Development itself is the key to understanding developmental disorders. *Trends in Cognitive Sciences*, *2*(10), 389–398.

Keehn, B., Vogel-Farley, V., Tager-Flusberg, H. B., & Nelson, C. A. (2015). Atypical

hemispheric specialization for faces in infants at-risk for Autism Spectrum Disorder. *Autism Research*, *8*(2), 187–198. http://doi.org/10.1002/aur.1438.

Keehn, B., Wagner, J. B., Tager-Flusberg, H. B., & Nelson, C. A. (2013). Functional connectivity in the first year of life in infants at-risk for autism: a preliminary near-infrared spectroscopy study. *Frontiers in Human Neuroscience*, *7*(August), 444. http://doi.org/10.3389/fnhum.2013.00444

Kenet, T., Orekhova, E. V., Bharadwaj, H., Shetty, N. R., Israeli, E., Lee, A. K. C., … Manoach, D. S. (2012). Disconnectivity of the cortical ocular motor control network in autism spectrum disorders. *NeuroImage*, *61*(4), 1226–1234. http://doi.org/10.1016/j.neuroimage.2012.03.010

Kessler, K., Seymour, R. Al, & Rippon, G. (2016). Brain oscillations and connectivity in autism spectrum disorders (ASD): new approaches to methodology, measurement and modelling. *Neuroscience and Biobehavioral Reviews*. http://doi.org/10.1016/j.neubiorev.2016.10.002

Khan, S., Gramfort, A., Shetty, N. R., Kitzbichler, M. G., Ganesan, S., Moran, J. M., … Kenet, T. (2013). Local and long-range functional connectivity is reduced in concert in autism spectrum disorders. *Proceedings of the National Academy of Sciences*, *110*(8), 3107–3112. http://doi.org/10.1073/pnas.1214533110

Kim, H., Lim, C.-S., & Kaang, B.-K. (2016). Neuronal mechanisms and circuits underlying repetitive behaviors in mouse models of autism spectrum disorder. *Behavioral and Brain Functions*, *12*(3), 1–13. http://doi.org/10.1186/s12993-016-0087-y

Kitzbichler, M. G., Khan, S., Ganesan, S., Vangel, M. G., Herbert, M. R., H??m??l??inen, M. S., & Kenet, T. (2015). Altered development and multifaceted band-specific abnormalities of resting state networks in autism. *Biological Psychiatry*, *77*(9), 794–804. http://doi.org/10.1016/j.biopsych.2014.05.012

Klimesch, W., Sauseng, P., & Hanslmayr, S. (2007). EEG alpha oscillations: The inhibition-timing hypothesis. *Brain Research Reviews*, *53*(1), 63–88. http://doi.org/10.1016/j.brainresrev.2006.06.003

Koenig, T., Prichep, L., Lehmann, D., Sosa, P. V., Braeker, E., Kleinlogel, H., … John, E. R. (2002). Millisecond by Millisecond, Year by Year: Normative EEG Microstates and Developmental Stages. *NeuroImage*, *16*(1), 41–48. http://doi.org/10.1006/nimg.2002.1070

Konrad, K., & Eickhoff, S. B. (2010). Is the ADHD brain wired differently? A review on structural and functional connectivity in attention deficit hyperactivity disorder. *Human Brain Mapping*, *31*(May), 904–916. http://doi.org/10.1002/hbm.21058

Kuntzelman, K., & Miskovic, V. (2017). Reliability of graph metrics derived from resting-state human EEG. *Psychophysiology*, *54*, 51–61. http://doi.org/10.1111/psyp.12600

Lam, K. S. L., Bodfish, J. W., & Piven, J. (2008). Evidence for three subtypes of repetitive behavior in autism that differ in familiarity and association with other symptoms. *Journal of Child Psychology and Psychiatry*, *49*(11), 1193–1200. http://doi.org/10.1016/j.immuni.2010.12.017.Two-stage

Landa, R. J., Gross, A. L., Stuart, E. A., & Bauman, M. (2012). Latent class analysis of early developmental trajectory in baby siblings of children with autism. *Journal of Child Psychology and Psychiatry and Allied Disciplines*, *53*(9), 986–996. http://doi.org/10.1111/j.1469-7610.2012.02558.x

Landa, R. J., Holman, K. C., & Garrett-Mayer, E. (2007). Social and Communication Development in Toddlers With Early and Later Diagnosis of Autism Spectrum

Disorders. *Archives of General Psychiatry*, *64*(7), 853. http://doi.org/10.1001/archpsyc.64.7.853

Langen, M., Durston, S., Kas, M. J. H., van Engeland, H., & Staal, W. G. (2011). The neurobiology of repetitive behavior: ...and men. *Neuroscience and Biobehavioral Reviews*, *35*(3), 356–365. http://doi.org/10.1016/j.neubiorev.2010.02.005

Lawson, R. P., Rees, G., & Friston, K. J. (2014). An aberrant precision account of autism. *Frontiers in Human Neuroscience*, *8*(May), 302. http://doi.org/10.3389/fnhum.2014.00302

Lazarev, V. V., Pontes, A., Mitrofanov, A. A., & deAzevedo, L. C. (2010). Interhemispheric asymmetry in EEG photic driving coherence in childhood autism. *Clinical Neurophysiology*, *121*(2), 145–152. http://doi.org/10.1016/j.clinph.2009.10.010

Leonard, H. C., Elsabbagh, M., Hill, E. L., & Team, B. (2014). Early and persistent motor difficulties in infants at-risk of developing autism spectrum disorder: A prospective study. *European Journal of Developmental Psychology*, *11*(1), 18–35. http://doi.org/10.1080/17405629.2013.801626

Levy, W. J. (1987). Effect of Epoch Length on Power Spectrum of the EEG. *Anesthesiology*, *66*, 489–495. http://doi.org/10.1167/8.5.1.

Lew, S., Sliva, D. D., Choe, M. S., Grant, P. E., Okada, Y., Wolters, C. H., & Hämäläinen, M. S. (2013). Effects of sutures and fontanels on MEG and EEG source analysis in a realistic infant head model. *NeuroImage*, *76*, 282–293. http://doi.org/10.1016/j.neuroimage.2013.03.017

Lewis, J. D., Evans, A. C., Pruett, J. R., Botteron, K., Zwaigenbaum, L., Estes, A., … Piven, J. (2014). Network inefficiencies in autism spectrum disorder at 24 months. *Transl Psychiatry*, *4*(5), e388. http://doi.org/10.1038/tp.2014.24

Lewis, J. D., Theilmann, R. J., Townsend, J., & Evans, A. C. (2013). Network efficiency in autism spectrum disorder and its relation to brain overgrowth. *Frontiers in Human Neuroscience*, *7*(December), 1–12. http://doi.org/10.3389/fnhum.2013.00845

Libertus, K., Sheperd, K. a., Ross, S. W., & Landa, R. J. (2014). Limited fine motor and grasping skills in 6-month-old infants at high risk for autism. *Child Development*, *85*(6), 2218–2231. http://doi.org/10.1111/cdev.12262

Lloyd-Fox, S., Blasi, A., Elwell, C. E., Charman, T., Murphy, D. G. M., & Johnson, M. H. (2013). Reduced neural sensitivity to social stimuli in infants at risk for autism. *Proceedings. Biological Sciences / The Royal Society*, *280*(1758), 20123026. http://doi.org/10.1098/rspb.2012.3026

Lloyd-Fox, S., Blasi, A., Pasco, G., Gliga, T., Jones, E. J. H., Murphy, D. G. M., … Johnson, M. H. (2017). Cortical responses before 6 months of life associate with later autism. *European Journal of Neuroscience*, 1–14. http://doi.org/10.1111/ejn.13757

Loh, A., Soman, T., Brian, J., Bryson, S. E., Roberts, W., Szatmari, P., … Zwaigenbaum, L. (2007). Stereotyped motor behaviors associated with autism in high-risk infants: A pilot videotape analysis of a sibling sample. *Journal of Autism and Developmental Disorders*, *37*(1), 25–36. http://doi.org/10.1007/s10803-006-0333-5

Lopes da Silva, F. (2013). EEG and MEG: Relevance to neuroscience. *Neuron*, *80*(5), 1112–1128. http://doi.org/10.1016/j.neuron.2013.10.017

Lord, C., Bishop, S., & Anderson, D. (2015). Developmental Trajectories as Autism Phenotypes. *American Journal of Medical Genetics Part C: Seminars in Medical*

Genetics, *169*(2), 198–208. http://doi.org/10.1002/ajmg.c.31440.Developmental

Lord, C., Luyster, R., Guthrie, W., & Pickles, A. (2012). Patterns of Developmental Trajectories in Toddlers With Autism Spectrum Disorder. *Journal of Consulting and Clinical Psychology*, *80*(3), 477–489. http://doi.org/10.1037/a0027214

Lord, C., Risi, S., Lambrecht, L., Cook Jr., E. H., Leventhal, B. L., DiLavore, P. C., … Rutter, M. (2000). The Autism Diagnostic Observation Schedule – Generic: A standard measures of social and communication deficits associated with the spectrum of autism. *Journal of Autism and Developmental Disorders*, *30*(3), 205–223. http://doi.org/10.1023/A:1005592401947

Lord, C., Rutter, M., DiLavore, P., Risi, S., Gotham, K., & Bishop, S. (2012). *Autism Diagnostic Observation Schedule Second Edition (ADOS-2) Manual (Part 1): Modules 1-4*. Torrance, CA: Western Psychological Services.

Lord, C., Rutter, M., & Le Couteur, A. (1994a). Autism Diagnostic Interview-Revised: a revised version of a diagnostic interview for caregivers of individuals with possible pervasive developmental disorders. *Journal of Autism and Developmental Disorders*, *24*(5), 659–85. Retrieved from http://www.ncbi.nlm.nih.gov/pubmed/7814313

Lord, C., Rutter, M., & Le Couteur, A. (1994b). Autism diagnostic interview-revised: A revised version of a diagnostic interview for caregivers of individuals with possible pervasive developmental disorders. *Journal of Autism and Developmental Disorders1*, (24), 659–685.

Loth, E., Charman, T., Collier, D. A., & Williams, S. C. R. (2016). Identification and validation of biomarkers for autism spectrum disorders. *Nature Reviews Drug Discovery*, (February 2016). http://doi.org/10.1093/nrd.2015.7

Loth, E., Charman, T., Mason, L., Tillmann, J., Jones, E. J. H., Wooldridge, C., … K., B. J. (2017). The EU-AIMS Longitudinal European Autism Project (LEAP): design and methodologies to identify and validate stratification biomarkers for autism spectrum disorders. *Molecular Autism*, *8*(24), 27. http://doi.org/10.1186/s13229-017-0146-8

Luck, S. J. (2014). *An introduction to the event-related potential technique*.

Mandy, W., & Lai, M.-C. (2016). Annual Research Review: The role of the environment in the developmental psychopathology of autism spectrum condition. *Journal of Child Psychology and Psychiatry*, *57*(3), 271–292. http://doi.org/10.1111/jcpp.12501

Maris, E., Fries, P., & van Ede, F. (2016). Diverse Phase Relations among Neuronal Rhythms and Their Potential Function. *Trends in Neurosciences*, *39*(2), 86–99. http://doi.org/10.1016/j.tins.2015.12.004

Maris, E., & Oostenveld, R. (2007). Nonparametric statistical testing of EEG- and MEG-data. *Journal of Neuroscience Methods*, *164*(1), 177–190. http://doi.org/10.1016/j.jneumeth.2007.03.024

Marshall, P. J., Bar-Haim, Y., & Fox, N. A. (2002). Development of the EEG from 5 months to 4 years of age. *Clinical Neurophysiology*, *113*(8), 1199–1208. http://doi.org/10.1016/S1388-2457(02)00163-3

Marshall, P. J., & Meltzoff, A. N. (2011). Neural mirroring systems: Exploring the EEG mu rhythm in human infancy. *Developmental Cognitive Neuroscience*, *1*(2), 110–123. http://doi.org/10.1016/j.dcn.2010.09.001

Marshall, P. J., Young, T., & Meltzoff, A. N. (2011). Neural correlates of action observation and execution in 14-month-old infants: An event-related EEG desynchronization study. *Developmental Science*, *14*, 474–480.

http://doi.org/10.1111/j.1467-7687.2010.00991.x
Mathewson, K. J., Jetha, M. K., Drmic, I. E., Bryson, S. E., Goldberg, J. O., & Schmidt, L. A. (2012). Regional EEG alpha power, coherence, and behavioral symptomatology in autism spectrum disorder. *Clinical Neurophysiology*, *123*(9), 1798–1809. http://doi.org/10.1016/j.clinph.2012.02.061
Menon, V. (2013). Developmental pathways to functional brain networks: Emerging principles. *Trends in Cognitive Sciences*, *17*(12), 627–640. http://doi.org/10.1016/j.tics.2013.09.015
Messinger, D. S., Young, G. S., Webb, S. J., Ozonoff, S. J., Bryson, S. E., Carter, A., … Zwaigenbaum, L. (2015). Early sex differences are not autism-specific: A Baby Siblings Research Consortium (BSRC) study. *Molecular Autism*, *6*(1), 1–12. http://doi.org/10.1186/s13229-015-0027-y
Miskovic, V., & Keil, A. (2015). Reliability of event-related EEG functional connectivity during visual entrainment : Magnitude squared coherence and phase synchrony estimates. *Psychophysiology*, *52*, 81–89. http://doi.org/10.1111/psyp.12287
Mitchell, C., Schneper, L. M., & Notterman, D. A. (2016). DNA methylation, early life environment, and health outcomes. *Pediatric Research*, *79*, 212–219. http://doi.org/10.1038/pr.2015.193.DNA
Mohammad-Rezazadeh, I., Frohlich, J., Loo, S. K., & Jeste, S. S. (2016). Brain Connectivity in Autism Spectrum Disorder. *Current Opinion in Neurology*, *29*(2), 137–147. http://doi.org/10.1097/WCO.0000000000000301.
Mullen, E. M. (1995). *Mullen Scales of Early Learning manual, AGS edition.* Circle Pines, MN: American Guidance Service.
Muthukumaraswamy, S. D. (2013). High-frequency brain activity and muscle artifacts in MEG/EEG: a review and recommendations. *Frontiers in Human Neuroscience*, *7*(April), 1–11. http://doi.org/10.3389/fnhum.2013.00138
Naaijen, J., Zwiers, M. P., Amiri, H., Williams, S. C. R., Durston, S., Oranje, B., … Lythgoe, D. J. (2017). Fronto-striatal glutamate in autism spectrum disorder and obsessive compulsive disorder. *Neuropsychopharmacology*, *42*(12), 2456–2465. http://doi.org/10.1038/npp.2016.260
Nelson, S. B., & Valakh, V. (2015). Excitatory/Inhibitory Balance and Circuit Homeostasis in Autism Spectrum Disorders. *Neuron*, *87*(4), 684–698. http://doi.org/10.1016/j.neuron.2015.07.033
Nolte, G., Bai, O., Wheaton, L., Mari, Z., Vorbach, S., & Hallett, M. (2004). Identifying true brain interaction from EEG data using the imaginary part of coherency. *Clinical Neurophysiology*, *115*(10), 2292–2307. http://doi.org/10.1016/j.clinph.2004.04.029
Nomi, J. S., & Uddin, L. Q. (2015). Developmental changes in large-scale network connectivity in autism. *NeuroImage: Clinical*, *7*, 732–741. http://doi.org/10.1016/j.nicl.2015.02.024
Nunes, A. S., Peatfield, N., Vakorin, V. A., & Doesburg, S. M. (2018). Idiosyncratic organization of cortical networks in autism spectrum disorder. *NeuroImage*. http://doi.org/10.1016/j.neuroimage.2018.01.022
Nunez, P. L., Srinivasan, R., Westdorp, A. F., Wijesinghe, R. S., Tucker, D. M., Silberstein, R. B., & Cadusch, P. J. (1997). EEG coherency I: Statistics, reference electrode, volume conduction, Laplacians, cortical imaging, and interpretation at multiple scales. *Electroencephalography and Clinical Neurophysiology*, *103*(5), 499–515. http://doi.org/10.1016/S0013-4694(97)00066-7
O'Reilly, C., Lewis, J. D., & Elsabbagh, M. (2017). Is functional brain connectivity

atypical in autism? A systematic review of EEG and MEG studies. *Plos One*, *12*(5), e0175870. http://doi.org/10.1371/journal.pone.0175870

Onnela, J. P., Saramäki, J., Kertész, J., & Kaski, K. (2005). Intensity and coherence of motifs in weighted complex networks. *Physical Review E - Statistical, Nonlinear, and Soft Matter Physics*, *71*(6). http://doi.org/10.1103/PhysRevE.71.065103

Oostenveld, R., Fries, P., Maris, E., & Schoffelen, J.-M. (2011). FieldTrip: Open source software for advanced analysis of MEG, EEG, and invasive electrophysiological data. *Computational Intelligence and Neuroscience*, 1–9. http://doi.org/10.1155/2011/156869

Open Science Collaboration, . (2015). Estimating the reproducibility of psychological science. *Science*, *349*(6251). http://doi.org/10.1126/science.aac4716

Orekhova, E. V., Elsabbagh, M., Jones, E. J. H., Dawson, G., Charman, T., Johnson, M. H., & Team, B. (2014). EEG hyper-connectivity in high-risk infants is associated with later autism. *Journal of Neurodevelopmental Disorders*, *6*(40), 1–11.

Orekhova, E. V., Stroganova, T. A., & Posikera, I. N. (1999). Theta synchronization during sustained anticipatory attention in infants over the second half of the first year of life. *International Journal of Psychophysiology*, *32*(2), 151–172. http://doi.org/10.1016/S0167-8760(99)00011-2

Orekhova, E. V., Stroganova, T. A., & Posikera, I. N. (2001). Alpha activity as an index of cortical inhibition during sustained internally controlled attention in infants. *Clinical Neurophysiology*, *112*(5), 740–749. http://doi.org/10.1016/S1388-2457(01)00502-8

Orekhova, E. V., Stroganova, T. A., Posikera, I. N., & Elam, M. (2006). EEG theta rhythm in infants and preschool children. *Clinical Neurophysiology*, *117*(5), 1047–1062. http://doi.org/10.1016/j.clinph.2005.12.027

Ozonoff, S. J., Iosif, A., Baguio, F., Cook, I. C., Moore Hill, M., Hutman, T., … Young, G. S. (2010). A prospective study of the emergence of early behavioral signs of autism. *Journal of the American Academy of Child & Adolescent Psychiatry*, *48*(3), 256–266. http://doi.org/10.1038/jid.2014.371

Ozonoff, S. J., Macari, S. L., Young, G. S., Goldring, S., & Thompson, M. (2008). Atypical object exploration at 12 months of age is associated with autism in a prospective sample. *Autism*, *12*(5), 457–472. http://doi.org/10.1016/j.biotechadv.2011.08.021.Secreted

Ozonoff, S. J., Pennington, B. F., & Rogers, S. J. (1991). Executive function deficits in high functioning autistic individuals: relationship to theory of mind. *Journal of Child Psychology & Psychiatry\r*, *32*(7), 1081–1105.

Ozonoff, S. J., Young, G. S., Landa, R. J., Brian, J., Bryson, S., Charman, T., … Iosif, A. (2015). Diagnostic stability in young children at risk for autism spectrum disorder : a baby siblings research consortium study. *Journal of Child Psychology and Psychiatry*, *56*(9), 988–998. http://doi.org/10.1111/jcpp.12421.Diagnostic

Park, H.-J., & Friston, K. J. (2013). Structural and functional brain networks: from connections to cognition. *Science (New York, N.Y.)*, *342*(6158), 1238411. http://doi.org/10.1126/science.1238411

Pasco, G. (2011). The diagnosis and epidemiology of autism. *Tizard Learning Disability Review*, *16*(4), 5–19.

Paul, R., Fuerst, Y., Ramsay, G., Chawarska, K., & Klin, A. (2011). Out of the mouths

of babes: Vocal production in infant siblings of children with ASD. *Journal of Child Psychology and Psychiatry and Allied Disciplines*, *52*(5), 588–598. http://doi.org/10.1111/j.1469-7610.2010.02332.x

Pellicano, E., & Burr, D. (2012). When the world becomes 'too real': A Bayesian explanation of autistic perception. *Trends in Cognitive Sciences*, *16*(10), 504–510. http://doi.org/10.1016/j.tics.2012.08.009

Perez Velazquez, J. L., Barcelo, F., Hung, Y., Leshchenko, Y., Nenadovic, V., Belkas, J., … Garcia Dominguez, L. (2009). Decreased brain coordinated activity in autism spectrum disorders during executive tasks: Reduced long-range synchronization in the fronto-parietal networks. *International Journal of Psychophysiology*, *73*(3), 341–349. http://doi.org/10.1016/j.ijpsycho.2009.05.009

Peters, J. M., Taquet, M., Vega, C., Jeste, S. S., Fernández, I. S., Tan, J., … Warfield, S. K. (2013). Brain functional networks in syndromic and non-syndromic autism: a graph theoretical study of EEG connectivity. *BMC Medicine*, *11*(1), 54. http://doi.org/10.1186/1741-7015-11-54

Peterson, E. J., & Voytek, B. (2015). Balanced Oscillatory Coupling Improves Information Flow. *BioRxiv*, (September), 030304. http://doi.org/10.1101/030304

Pfurtscheller, G., & Lopes Da Silva, F. (1999). Event-related EEG / MEG synchronization and desynchronization : basic principles. *Clinical Neurophysiology*, *110*, 1842–1857. http://doi.org/10.1016/S1388-2457(99)00141-8

Pickles, A., Le Couteur, A., Leadbitter, K., Salomone, E., Cole-Fletcher, R., Tobin, H., … Green, J. (2016). Parent-mediated social communication therapy for young children with autism (PACT): long-term follow-up of a randomised controlled trial. *The Lancet*, *388*(10059), 2501–2509. http://doi.org/10.1016/S0140-6736(16)31229-6

Pierce, K., Conant, D., Hazin, R., Stoner, R., & Desmond, J. (2011). Preference for geometric patterns early in life as a risk factor for autism. *Archives of General Psychiatry*, *68*(1), 101–109. http://doi.org/10.1001/archgenpsychiatry.2010.113

Pierce, K., Marinero, S., Hazin, R., McKenna, B., Barnes, C. C., & Malige, A. (2016). Eye tracking reveals abnormal visual preference for geometric images as an early biomarker of an autism spectrum disorder subtype associated with increased symptom severity. *Biological Psychiatry*, *79*(8), 657–666. http://doi.org/10.1016/j.biopsych.2015.03.032

Rajendran, G., & Mitchell, P. (2007). Cognitive theories of autism. *Developmental Review*, *27*(2), 224–260. http://doi.org/10.1016/j.dr.2007.02.001

Redcay, E., Moran, J. M., Mavros, P. L., Tager-Flusberg, H. B., Gabrieli, J. D. E., & Whitfield-Gabrieli, S. (2013). Intrinsic functional network organization in high-functioning adolescents with autism spectrum disorder. *Frontiers in Human Neuroscience*, *7*(September), 1–11. http://doi.org/10.3389/fnhum.2013.00573

Reynolds, G. D., & Richards, J. E. (2009). Cortical source localization of infant cognition. *Developmental Neuropsychology*, *34*(3), 312–329. http://doi.org/10.1080/87565640902801890

Richards, J. E., Sanchez, C., Phillips-Meek, M., & Xie, W. (2016). A database of age-appropriate average MRI templates. *Neuroimage*, *124*, 1254–1259. http://doi.org/10.1126/science.1249098.Sleep

Righi, G., Tierney, A. L., Tager-Flusberg, H. B., & Nelson, C. A. (2014). Functional connectivity in the first year of life in infants at risk for autism spectrum disorder: An EEG study. *PLoS ONE*, *9*(8), 1–8. http://doi.org/10.1371/journal.pone.0105176

Risi, S., Lord, C., Gothan, K., Corsello, C., Chrysler, C., Szatmari, P., … Pickles, A. (2006). Combining Information From Multiple Sources in the Diagnosis of Autism Spectrum Disorders. *Journal of the American Academy of Child & Adolescent Psychiatry*, *45*(9), 1094–1103. http://doi.org/10.1097/01.chi.0000227880.42780.0e

Rousselet, G. A., & Pernet, C. R. (2012). Improving standards in brain-behavior correlation analyses. *Frontiers in Human Neuroscience*, *6*(May), 119. http://doi.org/10.3389/fnhum.2012.00119

Rubenstein, J. L. R., & Merzenich, M. M. (2003). Model of autism: increased ratio of excitation/inhibition in key neural systems. *Genes, Brain, and Behavior*, *2*(5), 255–267. http://doi.org/10.1046/j.1601-183X.2003.00037.x

Rubinov, M., & Sporns, O. (2010). Complex network measures of brain connectivity: Uses and interpretations. *NeuroImage*, *52*(3), 1059–1069. http://doi.org/10.1016/j.neuroimage.2009.10.003

Rudie, J. D., Brown, J. A., Beck-Pancer, D., Hernandez, L. M., Dennis, E. L., Thompson, P. M., … Dapretto, M. (2013). Altered functional and structural brain network organization in autism. *NeuroImage: Clinical*, *2*(1), 79–94. http://doi.org/10.1016/j.nicl.2012.11.006

Rutter, M., Bailey, A., & Lord, C. (2003). *The Social Communication Questionnaire*. Western Psychological Services. Retrieved from http://www.childhealthcare.org/ug/SCQ/SCQ_Manual-2.pdf

Rutter, M., Le Couteur, A., & Lord, C. (2003). Autism diagnostic interview-revised. *Los Angeles, CA: Western Psychological Servides.*, *29*(30).

Saby, J. N., & Marshall, P. J. (2012). The Utility of EEG Band Power Analysis in the Study of Infancy and Early Childhood. *Developmental Neuropsychology*, *37*(March 2014), 253–273. http://doi.org/10.1080/87565641.2011.614663

Salomone, E., Shephard, E., Milosavljevic, B., Johnson, M. H., Charman, T., Baron-Cohen, S., … Volein, A. (2018). Adaptive Behaviour and Cognitive Skills: Stability and Change from 7 Months to 7 Years in Siblings at High Familial Risk of Autism Spectrum Disorder. *Journal of Autism and Developmental Disorders*, *0*(0), 1–11. http://doi.org/10.1007/s10803-018-3554-5

Schwartz, S., Kessler, R., Gaughan, T., & Buckley, A. W. (2016). Electroencephalogram Coherence Patterns in Autism : An Updated Review. *Pediatric Neurology*. http://doi.org/10.1016/j.pediatrneurol.2016.10.018

Seghier, M. L., & Price, C. J. (2018). Interpreting and Utilising Intersubject Variability in Brain Function. *Trends in Cognitive Sciences*, *xx*, 1–14. http://doi.org/10.1016/j.tics.2018.03.003

Shackman, A. J., McMenamin, B. W., Maxwell, J. S., Greischar, L. L., & Davidson, R. J. (2010). Identifying robust and sensitive frequency bands for interrogating neural oscillations. *NeuroImage*, *51*(4), 1319–1333. http://doi.org/10.1016/j.neuroimage.2010.03.037

Shen, M. D., Nordahl, C. W., Young, G. S., Wootton-Gorges, S. L., Lee, A., Liston, S. E., … Amaral, D. G. (2013). Early brain enlargement and elevated extra-axial fluid in infants who develop autism spectrum disorder. *Brain*, *136*(9), 2825–2835. http://doi.org/10.1093/brain/awt166

Shephard, E., Milosavljevic, B., Pasco, G., Jones, E. J. H., Gliga, T., Happ?, F., …

Charman, T. (2017). Mid-childhood outcomes of infant siblings at familial high-risk of autism spectrum disorder. *Autism Research*, *10*(3), 546–557. http://doi.org/10.1002/aur.1733

Shrout, P. E., & Fleiss, J. L. (1979). Intraclass correlations: Uses in assessing rater reliability. *Psychological Bulletin*, *86*(2), 420–428. http://doi.org/10.1037/0033-2909.86.2.420

Singh, I., & Rose, N. (2009). Biomarkers in psychiatry. *Nature*, *460*(7252), 202–207. http://doi.org/10.1038/460202a

Smit, D. J. A., Boersma, M., Schnack, H. G., Micheloyannis, S., Boomsma, D. I., Hulshoff Pol, H. E., … de Geus, E. J. C. (2012). The Brain Matures with Stronger Functional Connectivity and Decreased Randomness of Its Network. *PLoS ONE*, *7*(5), e36896. http://doi.org/10.1371/journal.pone.0036896

Smith, S. W. (1999). *Digital Signal Processing* (Second Edi). San Diego: California Technical Publishing.

Smyser, C. D., & Neil, J. J. (2015). Use of resting-state functional MRI to study brain development and injury in neonates. *Seminars in Perinatology*, *39*(2), 130–140. http://doi.org/10.1053/j.semperi.2015.01.006

Solso, S., Xu, R., Proudfoot, J., Hagler, D. J., Campbell, K., Venkatraman, V., … Courchesne, E. (2016). Diffusion tensor imaging provides evidence of possible axonal overconnectivity in frontal lobes in autism spectrum disorder toddlers. *Biological Psychiatry*, *79*(8), 676–684. http://doi.org/10.1016/j.biopsych.2015.06.029

Southgate, V., Johnson, M. H., Osborne, T., & Csibra, G. (2009). Predictive motor activation during action observation in human infants. *Biology Letters*, *5*(June), 769–772. http://doi.org/10.1098/rsbl.2009.0474

Sparrow, S. S., Balla, D. A., & Cicchetti, D. V. (2005). Vineland adaptive behavior scales: Survey forms manual. *AGS Publ.*

Sparrow, S. S., Bella, D. A., & Cicchetti, D. (1984). *Vineland adaptive behavior scales*. Circle Pines, MN: AGS.

Sperdin, H. F., Coito, A., Kojovic, N., Rihs, T., Jan, R. K., Franchini, M., … Schaer, M. (2018). Early alterations of social brain networks in young children with autism. *ELife*, *7*, 1–18. http://doi.org/10.1101/180703

St. John, T., Estes, A. M., Dager, S. R., Kostopoulos, P., Wolff, J. J., Pandey, J., … Piven, J. (2016). Emerging executive functioning and motor development in infants at high and low risk for autism spectrum disorder. *Frontiers in Psychology*, *7*(JUL), 1–12. http://doi.org/10.3389/fpsyg.2016.01016

Stam, C. J., Nolte, G., & Daffertshofer, A. (2007). Phase lag index: Assessment of functional connectivity from multi channel EEG and MEG with diminished bias from common sources. *Human Brain Mapping*, *28*(11), 1178–1193. http://doi.org/10.1002/hbm.20346

Stinstra, J. G., & Peters, M. J. (1998). The volume conductor may act as a temporal filter on the ECG and EEG. *Medical \& Biological Engineering \& Computing*, *36*(November), 711–716. http://doi.org/10.1007/BF02518873

Strimbu, K., & Tavel, J. a. (2011). What are Biomarkers? *Curr Opin HIV AIDS*, *5*(6), 463–466. http://doi.org/10.1097/COH.0b013e32833ed177.What

Stroganova, T. A., Orekhova, E. V., & Posikera, I. N. (1999). EEG alpha rhythm in infants. *Clinical Neurophysiology*, *110*(6), 997–1012. http://doi.org/10.1016/S1388-2457(98)00009-1

Supekar, K., Uddin, L. Q., Khouzam, A., Phillips, J., Gaillard, W. D., Kenworthy, L. E., … Menon, V. (2013). Brain hyperconnectivity in children with autism and its

links to social deficits. *Cell Reports*, *5*(3), 738–47. http://doi.org/10.1016/j.celrep.2013.10.001

Szatmari, P., Chawarska, K., Dawson, G., Georgiades, S., Landa, R. J., Lord, C., … Halladay, A. (2016). Prospective Longitudinal Studies of Infant Siblings of Children with Autism: Lessons Learned and Future Directions. *Journal of the American Academy of Child and Adolescent Psychiatry*, *55*(3), 179–187. http://doi.org/10.1016/j.jaac.2015.12.014

Takagaki, K., Russell, J., Lippert, M. T., & Motamedi, G. K. (2015). Clinical Neurophysiology Development of the posterior basic rhythm in children with autism. *Clinical Neurophysiology*, *126*(2), 297–303. http://doi.org/10.1016/j.clinph.2014.04.022

Takahashi, T., Yamanishi, T., Nobukawa, S., Kasakawa, S., Yoshimura, Y., Hiraishi, H., … Kikuchi, M. (2017). Band-specific atypical functional connectivity pattern in childhood autism spectrum disorder. *Clinical Neurophysiology*, *128*(8), 1457–1465. http://doi.org/10.1016/j.clinph.2017.05.010

Thatcher, R. W., Biver, C. J., & North, D. M. (2004). EEG and brain connectivity: A tutorial. *Unpublished Manuscrips*.

Thatcher, R. W., North, D. M., & Biver, C. J. (2008). Development of cortical connections as measured by EEG coherence and phase delays. *Human Brain Mapping*, *29*(12), 1400–1415. http://doi.org/10.1002/hbm.20474

Toulmin, H., Beckmann, C. F., O'Muircheartaigh, J., Ball, G., Nongena, P., Makropoulos, A., … Edwards, A. D. (2015). Specialization and integration of functional thalamocortical connectivity in the human infant. *Proceedings of the National Academy of Sciences*, *112*(20), 201422638. http://doi.org/10.1073/pnas.1422638112

Traynor, J. M., & Hall, G. B. C. (2015). Structural and Functional Neuroimaging of Restricted Repetitive Behavior in Autism Spectrum Disorder. *Journal of Intellectual Disability-Diagnosis and Treatment*, *3*(1), 21–34.

Uddin, L. Q. (2015). Idiosyncratic connectivity in autism: Developmental and anatomical considerations. *Trends in Neurosciences*, *38*(5), 261–263. http://doi.org/10.1016/j.tins.2015.03.004

Uddin, L. Q., Supekar, K., Lynch, C. J., Khouzam, A., Phillips, J., Feinstein, C., … Menon, V. (2013). Salience network-based classification and prediction of symptom severity in children with autism. *JAMA Psychiatry*, *70*(8), 869–79. http://doi.org/10.1001/jamapsychiatry.2013.104

Uddin, L. Q., Supekar, K., & Menon, V. (2013). Reconceptualizing functional brain connectivity in autism from a developmental perspective. *Frontiers in Human Neuroscience*, *7*(August), 458. http://doi.org/10.3389/fnhum.2013.00458

Uhlhaas, P. J., Roux, F., Rodriguez, E., Rotarska-Jagiela, A., & Singer, W. (2010). Neural synchrony and the development of cortical networks. *Trends in Cognitive Sciences*, *14*(2), 72–80. http://doi.org/10.1016/j.tics.2009.12.002

Uhlhaas, P. J., Roux, F., Singer, W., Haenschel, C., Sireteanu, R., & Rodriguez, E. (2009). The development of neural synchrony reflects late maturation and restructuring of functional networks in humans. *Proceedings of the National Academy of Sciences*, *106*(24), 9866–9871. http://doi.org/10.1073/pnas.0900390106

Uzunova, G., Pallanti, S., & Hollander, E. (2016). Excitatory/inhibitory imbalance in autism spectrum disorders: Implications for interventions and therapeutics. *The World Journal of Biological Psychiatry*, *17*(3), 174–186. http://doi.org/10.3109/15622975.2015.1085597

Vakorin, V. A., Doesburg, S. M., Leung, R. C., Vogan, V. M., Anagnostou, E., & Taylor, M. J. (2016). Developmental changes in neuromagnetic rhythms and network synchrony in autism. *Annals of Neurology*, 1–13. http://doi.org/10.1002/ANA.24836

van Boxtel, J. J. a, & Lu, H. (2013). A predictive coding perspective on autism spectrum disorders. *Frontiers in Psychology*, *4*(January), 19. http://doi.org/10.3389/fpsyg.2013.00019

Van de Cruys, S., Evers, K., Van der Hallen, R., Van Eylen, L., Boets, B., De-Wit, L., & Wagemans, J. (2014). Precise minds in uncertain worlds: predictive coding in autism. *Psychological Review*, *121*(4), 649–75. http://doi.org/10.1037/a0037665

Van De Ville, D., Britz, J., & Michel, C. M. (2010). EEG microstate sequences in healthy humans at rest reveal scale-free dynamics. *PNAS*, *107*(42), 18179–18184. http://doi.org/10.1073/pnas.1007841107

Van der Velde, B., Haartsen, R., & Kemner, C. (n.d.). Test-retest Reliability of EEG Network Characteristics in Ten-Month-Old Infants. *Submitted Manuscript*.

van Diessen, E., Numan, T., van Dellen, E., van der Kooi, A. W., Boersma, M., Hofman, D., … Stam, C. J. (2015). Opportunities and methodological challenges in EEG and MEG resting state functional brain network research. *Clinical Neurophysiology*, *126*(8), 1468–1481. http://doi.org/10.1016/j.clinph.2014.11.018

van Wijk, B. C. M., Stam, C. J., & Daffertshofer, A. (2010). Comparing brain networks of different size and connectivity density using graph theory. *PLoS ONE*, *5*(10). http://doi.org/10.1371/journal.pone.0013701

Vasa, R. A., Mostofsky, S. H., & Ewen, J. B. (2016). The Disrupted Connectivity Hypothesis of Autism Spectrum Disorders: Time for the Next Phase in Research. *Biological Psychiatry: Cognitive Neuroscience and Neuroimaging*, *1*(3), 245–252. http://doi.org/10.1016/j.bpsc.2016.02.003

Venker, C. E., Ray-Subramanian, C. E., Bolt, D. M., & Weismer, S. E. (2014). Trajectories of autism severity in early childhood. *Journal of Autism and Developmental Disorders*, *44*(3), 546–563. http://doi.org/10.1007/s10803-013-1903-y

Vernetti, A., Senju, A., Charman, T., Johnson, M. H., Gliga, T., Baron-Cohen, S., … Yemane, F. (2018). Simulating interaction: Using gaze-contingent eye-tracking to measure the reward value of social signals in toddlers with and without autism. *Developmental Cognitive Neuroscience*, *29*(July 2017), 21–29. http://doi.org/10.1016/j.dcn.2017.08.004

Vértes, P. E., & Bullmore, E. T. (2015). Annual Research Review: Growth connectomics - the organization and reorganization of brain networks during normal and abnormal development. *Journal of Child Psychology and Psychiatry*, *56*(3), 299–320. http://doi.org/10.1111/jcpp.12365

Vinck, M., Oostenveld, R., Van Wingerden, M., Battaglia, F., & Pennartz, C. M. a. (2011). An improved index of phase-synchronization for electrophysiological data in the presence of volume-conduction, noise and sample-size bias. *NeuroImage*, *55*(4), 1548–1565. http://doi.org/10.1016/j.neuroimage.2011.01.055

Vissers, M. E., X Cohen, M., & Geurts, H. M. (2012). Brain connectivity and high functioning autism: A promising path of research that needs refined models, methodological convergence, and stronger behavioral links. *Neuroscience and Biobehavioral Reviews*, *36*(1), 604–625.

http://doi.org/10.1016/j.neubiorev.2011.09.003
Walsh, P., Elsabbagh, M., Bolton, P., & Singh, I. (2011). In search of biomarkers for autism: scientific, social and ethical challenges. *Nature Reviews. Neuroscience*, *12*(10), 603–612. http://doi.org/10.1038/nrn3113
Wang, Z., Dai, Z., Gong, G., Zhou, C., & He, Y. (2014). Understanding Structural-Functional Relationships in the Human Brain: A Large-Scale Network Perspective. *The Neuroscientist : A Review Journal Bringing Neurobiology, Neurology and Psychiatry*, (JUNE), 1073858414537560-. http://doi.org/10.1177/1073858414537560
Wass, S., Porayska-Pomsta, K., & Johnson, M. H. (2011). Training attentional control in infancy. *Current Biology*, *21*(18), 1543–1547. http://doi.org/10.1016/j.cub.2011.08.004
Waterhouse, L., London, E., & Gillberg, C. (2016). ASD Validity. *Review Journal of Autism and Developmental Disorders*, *3*(4), 302–329. http://doi.org/10.1007/s40489-016-0085-x
Watts, D. J., & Strogatz, S. H. H. (1998). Collective dynamics of 'small-world' networks. *Nature*, *393*(6684), 440–442. http://doi.org/10.1038/30918
Webb, S. J., Jones, E. J. H., Kelly, J., & Dawson, G. (2014). The motivation for very early intervention for infants at high risk for autism spectrum disorders. *International Journal of Speech-Language Pathology*, *16*(1), 36–42. http://doi.org/10.3109/17549507.2013.861018
Weir, J. P. (2005). Quantifying test-retest reliability using the intraclass correlation coefficient and the SEM. *Journal of Strength and Conditioning Research / National Strength & Conditioning Association*, *19*(1), 231–240. http://doi.org/10.1519/15184.1
Wilcox, T., & Biondi, M. (2015). fNIRS in the developmental sciences. *Wiley Interdisciplinary Reviews: Cognitive Science*, *6*(June), n/a-n/a. http://doi.org/10.1002/wcs.1343
Willsey, J. A., & State, M. W. (2015). Autism spectrum disorders: from genes to neurobiology. *Current Opinion in Neurobiology*, *30*, 92–99. http://doi.org/10.1016/j.conb.2014.10.015
Wolff, J. J., Botteron, K. N., Dager, S. R., Elison, J. T., Estes, A. M., Gu, H., … Piven, J. (2014). Longitudinal patterns of repetitive behavior in toddlers with autism. *Journal of Child Psychology and Psychiatry and Allied Disciplines*, *55*(8), 945–953. http://doi.org/10.1111/jcpp.12207
Wolff, J. J., Gerig, G., Lewis, J. D., Soda, T., Styner, M. A., Vachet, C., … Piven, J. (2015). Altered corpus callosum morphology associated with autism over the first 2 years of life. *Brain*, *138*, 2046–2058. http://doi.org/10.1093/brain/awv118
Wolff, J. J., Gu, H., Gerig, G., Elison, J. T., Styner, M. A., Botteron, K. N., … Piven, J. (2012). Differences in White Matter Fiber Tract Development Present From 6 to 24 Months in Infants With Autism. *American Journal of Psychiatry*, (169), 589–600wo.
Wolff, J. J., Swanson, M. R., Elison, J. T., Gerig, G., Pruett, J. R., Styner, M. A., … Piven, J. (2017). Neural circuitry at age 6 months associated with later repetitive behavior and sensory responsiveness in autism. *Molecular Autism*, 1–12. http://doi.org/10.1186/s13229-017-0126-z
Xie, W., Mallin, B. M., & Richards, J. E. (2017). Development of infant sustained attention and its relation to EEG oscillations: An EEG and cortical source analysis study. *Developmental Science*, (April). http://doi.org/10.1111/desc.12562

Xie, W., Mallin, B. M., & Richards, J. E. (2018). Development of brain functional connectivity and its relation to infant sustained attention in the first year of life. *Developmental Science*, 1–18. http://doi.org/10.1111/desc.12703

Xing, M., Tadayonnejad, R., MacNamara, A., Ajilore, O., DiGangi, J., Phan, K. L., … Klumpp, H. (2017). Resting-state theta band connectivity and graph analysis in generalized social anxiety disorder. *NeuroImage: Clinical*, *13*, 24–32. http://doi.org/10.1016/j.nicl.2016.11.009

You, X., Norr, M., Murphy, E., Kuschner, E. S., Bal, E., Gaillard, W. D., … Vaidya, C. J. (2013). Atypical modulation of distant functional connectivity by cognitive state in children with Autism Spectrum Disorders. *Frontiers in Human Neuroscience*, *7*(August), 1–13. http://doi.org/10.3389/fnhum.2013.00482

Zalesky, A. (2012). Reference Manual for NBS Connectome (v1.2).

Zalesky, A., Fornito, A., & Bullmore, E. T. (2010). Network-based statistic: Identifying differences in brain networks. *NeuroImage*, *53*(4), 1197–1207. http://doi.org/10.1016/j.neuroimage.2010.06.041

Zwaigenbaum, L., Bryson, S., & Garon, N. (2013). Early identification of autism spectrum disorders. *Behavioural Brain Research*, *251*, 133–146. http://doi.org/10.1016/j.bbr.2013.04.004

Zwaigenbaum, L., Bryson, S., Rogers, T., Roberts, W., Brian, J., & Szatmari, P. (2005). Behavioral manifestations of autism in the first year of life. *International Journal of Developmental Neuroscience*, *23*(2–3 SPEC. ISS.), 143–152. http://doi.org/10.1016/j.ijdevneu.2004.05.001

Appendix

Appendix to Chapter 2

A2.1. EEG connectivity measures in ASD research

Previous studies examining EEG connectivity in ASD have used a variety of methods, including the measure of EEG connectivity. Table A2.1 provides an overview of the specific measures previous studies used as an indication of EEG connectivity.

Table A2.1. Overview of M/EEG connectivity measures used in studies focusing on EEG connectivity in ASD

Authors	*Age*	*Method*	*Measure*
Orekhova et al., 2014	14 mo	EEG	dbWPLI (and ubPLI) (sensor level)
Righi et al., 2014	6 and 12 mo	EEG	Coherence (Morlet wavelet transform with 3 cycles, sensor level)
Keehn et al., 2013	6 and 12 mo	EEG	Phase coherence
Boersma et al., 2013	2-5 yo	EEG	PLI (sensor space)
Domínguez et al., 2013	2-5 yo	EEG	Imaginary part of coherence
Boersma et al., 2011	5 and 7 yo	EEG	Synchronization likelihood (sensor space)
Isler et al., 2010	5.5-8.5 yo	EEG	Coherence and phase synchrony
Duffy et al., 2012	2-12 yo	EEG	Spectral coherence (with Laplacian methods to minimize volume conduction effects)
Perez Velazquez et al., 2009	7-16 yo	MEG	Mean Phase Coherence (sensor level)

Thatcher et al., 2008	2mo - 16 yo	EEG	Cross-spectrum/coherence and EEG phase differences from FFT (sensor level)
Peters et al., 2013	.7-25.2 yo	EEG	Coherence weighted by segment length (sensor level)
Coben et al., 2008	6-11 yo	EEG	Coherence (Fourier, sensor level)
Han et al., 2013	8-17 yo	EEG	Coherence (FFT, sensor level)
Lazarev et al., 2010	6-17 yo	EEG	Coherence (normalized cross-power spectrum, sensor level)
Mathewson et al., 2012	Adults	EEG	Coherence (for pairs >5 cm apart, sensor level)
Barttfeld et al., 2011	Adults	EEG	Synchronization likelihood (sensor level)
Catarino et al., 2013	Adults	EEG	Wavelet transform coherence (sensor level)
Kenet et al., 2012	Adults	MEG	Coherence (from FFT, sensor and source level)
Khan et al., 2013	Adults	MEG	Z-coherence and PAC (source level)

Abbreviations: months old (mo), years old (yo), debiased weighted phase lag index (dbWPLI), unbiased phase lag index (ubPLI), phase lag index (PLI), Fast Fourier Transform (FFT), phase-amplitude coupling (PAC).

Appendix to Chapter 3

A3.1. Epoch length and numbers used in previous studies

Previous studies examining EEG connectivity in ASD across different age groups have used different lengths and numbers of epochs (see table A3.1, and Appendix A2.1). Numbers of epochs range from 1 to 518 per participants across different studies (Barttfeld et al., 2011; Orekhova et al., 2014), whereas the lengths of epochs used range from 400 ms to 7 minutes (Barttfeld et al., 2011; Catarino et al., 2013).

Table A3.1. Overview with different parameters in connectivity studies

Authors	*Age*	*Epoch length*	*Epoch numbers*
Orekhova et al., 2014	14 mo	1 second, 50% overlap	At least 120 trials per subject
Righi et al., 2014	6 and 12mo	800 ms	NA
Keehn et al., 2015	6 and 12mo	1200 ms	10 epochs
Dominguez et al., 2013	2-5 yo	NA (event related connectivity)	NA (event related connectivity)
Boersma et al., 2013	2-5 yo	1 second	M_{ASD} = 32.1 (sd=4.0), M_{TD} = 27.4 (sd=2.2)
Buckley et al., 2015	2-6 yo	NA	NA
Boersma et al., 2011	5 and 7 yo	16.384 seconds	4 artefact free epochs
Isler et al., 2010	5.5-8.5 yo	1 second	Minimum 18, M_{ASD} = 31, M_{TD} = 37
Duffy et al., 2012	2-12 yo	2 seconds	8-20 min EEG data per subject
Elhabashy et al., 2015	4-12 yo	4 seconds	More than 75 seconds clean data (19 epochs)
Perez Velazquez et al., 2009	7-16 yo	1 second	382
Thatcher et al., 2008	2mo - 16 yo	2 seconds	2-5 minutes EEG segments
Peters et al., 2013	.7-25.2 yo	Varies with each subject, M_{TSC} = 646 seconds, and $M_{non\text{-}TSC}$ = 439	NA
Coben et al., 2008	6-11 yo	2.56 seconds	24 trials (randomly selected)

Han et al., 2013	8-17 yo	1 minute	1 trial
Lazarev et al., 2010	6-14 yo	1 second	NA
Mathewson et al., 2012	adults	1 second, 50% overlap	Minimum 46 trials, on average 350 in each group
Barttfeld et al., 2011	adults	7 minutes	1 trial
Catarino et al., 2013	adults	400 milliseconds	NA
Kenet et al., 2012	adults	1 second	95 trials, randomly selected per subject per condition
Khan et al., 2013	adults	2 seconds	Minimum 40 trials

Abbreviations: months old (mo), years old (yo), not applicable/ not mentioned (NA), mean (M), standard deviation (sd).

A3.2. Spectral power and epoch length

Spectral power seemed to display different values across different epoch lengths for 1 to 6 second durations. To further examine this, data were also segmented in 8, 10, and 12-second epochs. Graphs for spectral power across all 9 different epoch lengths are displayed in Figure A3.1. The graphs show that peaks in the spectrum are more clearly distinguishable with longer epochs lengths, due to the increased frequency resolution of the power spectra with increasing length of the epochs: theta and alpha peaks are better distinguishable for 10 and 12 second epochs when compared to 1 and 2 second epochs. This likely arises from the increased frequency resolution inherent to a higher number of samples in longer epochs. The resolution of the power spectrum depends on the number of samples in the input signal so that N input samples give N/2+1 frequency samples in the frequency spectrum. When the epoch length increases with a factor 2, twice as many frequencies will be sampled in the frequency spectrum. To illustrate, the frequencies sampled for 1 second epochs here are 0 Hz, 1 Hz, 2 Hz, 3 Hz, etc., while for 2 second epochs the frequencies are 0 Hz, 0.5 Hz, 1 Hz, 1.5 Hz, 2 Hz, 2.5 Hz, 3 Hz, etc. Thus longer epochs contain a larger amount of samples, and will thus give higher a frequency resolution resulting in clearer peaks (Smith, 1999).

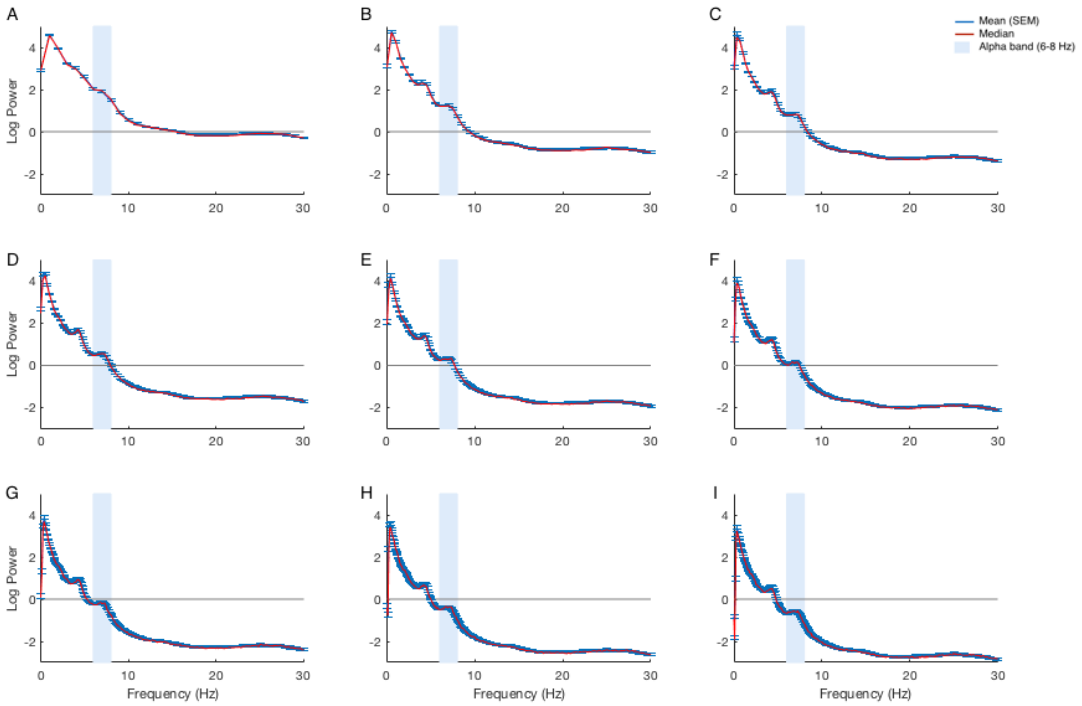

Figure A3.1. Spectral power for 10-month-olds across different frequencies and epoch lengths (1 to 12 seconds)

Log transformed power values (mean and standard error of mean in blue, and median in red) averaged across all available epochs for different lengths: 1, 2, 3, 4, 5, 6, 8, 10, and 12 seconds in graphs A-I, resp. Frequencies range from 0 to 30 Hz. Light blue box marks the alpha frequency band from 6 to 8 Hz.

Another observation for these graphs is that log power values for different frequencies decrease as epoch length increases. This finding is even more apparent in Figure A3.2 (left) showing average and median power values for 6-8 Hz decrease with increasing epoch length, while the standard error of the mean remains largely consistent. The decrease in power with increasing epoch length occurs in every subject (Figure A3.2, right).

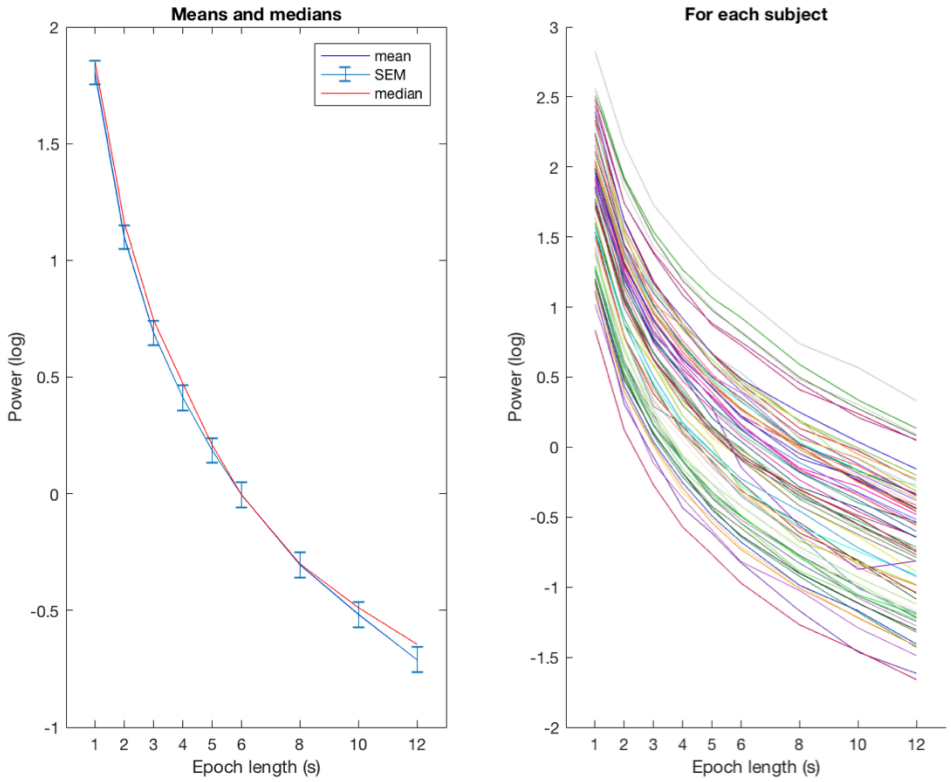

Figure A3.2. Power for 6-8 Hz across different epoch lengths

Log transformed power values across the alpha band (6-8 Hz) across different epoch lengths, averaged across the whole group (left) and for individual participants (right).

One possible explanation for this finding is the weak stationarity of the EEG signal (M. X. Cohen, 2014; Smith, 1999). The FFT assumes stationarity across the whole time series transformed (also discussed in Chapter 2). This assumption is more likely to be violated during longer epochs than during shorter epochs. It is more probable that episodes of non-stationarity occur during 10 or 12-second long epochs. This adds complexity to the signal resulting in the energy or power divided across a larger number of frequencies, which coincide with the higher frequency resolution of longer epochs. Consequently, spectral power across longer epochs is lower than across shorter epochs. These findings emphasize the use of consistent epoch length across participants when using the fast Fourier transform to calculate spectral power, or EEG connectivity.

Appendix to Chapter 4

A4.1. Assessment of risk of ASD in infant siblings

Recruitment of infants into the LR or HR group was based on symptomatology of ASD symptoms in an older sibling, or proband. For siblings in the HR group, probands had a community clinical diagnosis. This diagnosis was confirmed by parent-rated questionnaires measuring ASD symptomatology and child and adolescent psychopathology in the proband. Two questionnaires were used for this purpose: the Social Communication Questionnaire (SCQ) (Rutter, Bailey, et al., 2003), and the Development of Wellbeing Assessment (DAWBA) (Goodman, Ford, Richards, Gatward, & Meltzer, 2000).

The Social Communication Questionnaire (SCQ) (Rutter, Bailey, et al., 2003) is a parent-report survey consisting of 40 items that measure ASD symptomatology. Items are responded to with 'yes' or 'no'. The items are based on the items from the Autism Diagnostic Interview – Revised (ADI-R), with scores on subdomains parallel to the domains in the ADI-R: Qualitative Abnormalities in Reciprocal Social Interaction, Qualitative Abnormalities in Communication, and Restricted and Repetitive, and Stereotyped Patterns of Behaviour. The answers on the items also yield at Total Score reflecting the severity of ASD symptoms experienced by the target individual. The questionnaire is often used as a screening method for ASD and can be completed within 5 to 10 minutes rather than the 1.5 to 2.5 hours needed to complete the ADI-R. A total score of 15 of higher is considered as meeting the criteria for ASD.

The Development and Wellbeing Assessment (DAWBA) (Goodman et al., 2000) is an assessment that measures child and adolescent psychopathology. Here, the parent interview version was used to measure the symptoms and impact of psychiatric disorders. This questionnaire can take up to 50 minutes to complete. The survey is typically used as a screening for common behavioural disorders, such as separation anxiety, generalized anxiety, major depression, specific and social phobias, post-traumatic stress disorder, obsessive compulsive disorder, ADHD, and conduct-oppositional disorders. Items assess the presence of symptoms and their impact on the daily life of the child in present and the recent past (several months depending on the disorder).

After collecting the responses to the SCQ and DAWBA, a team of experienced clinical researchers within the BASIS team reviewed the results as to confirm the community diagnosis. Within the group of 81 HR infants included in the current analyses, the criteria for ASD were met on both the DAWBA and SQC for 66 probands. For 3 probands, criteria were met on the DAWBA but not the SQC, while criteria were met on the SCQ but not the DAWBA for 11 probands, and for 1 proband, criteria were met on the DAWBA whereas data for the SQC were missing. The experienced researchers however considered these younger infants at high risk for ASD, and thus these infants were included in the study.

For the 20 infant siblings in the LR group, each infant had at least one older sibling with typical development, and no family history of ASD within first-degree relatives. Parents of this group of infants also completed the SQC for the older sibling. None of the older siblings of these infants scored above the threshold for ASD on the SQC. This methods has also been descripted in a previous study that used the same dataset (Cheung et al., 2016).

A4.2. Domain scales of the MSEL

The Mullen Scales for Early Learning aim to measure developmental levels in individuals from birth to 68 months of age. The Scales of the Mullen Scales for Early Learning are divided into 5 domains: Visual Reception, Fine Motor, Receptive Language, Expressive Language, and Gross Motor scales. The Visual Reception scales test the infant's visual processing, such as visual discrimination and visual memory. Fine Motor items test the visuo-motor skills, such as picking up blocks, pincer grip, or holding a crayon. The Receptive Language scale provides a measure of the infant's comprehension of auditory language, and also involves auditory-visual integration. Expressive Language scales test the infant's abilities to produce language, such as babbling, the use of words, or short phrases. Finally, the Gross Motor scale assesses the infant's gross motor abilities, such at posture, mobility, and control of the limbs. Items are assessed in a performance-dependent order matching the individuals abilities as to characterise the floor and ceiling levels of these abilities (Mullen, 1995).

A4.3. Domain scales of the VABS

The Vineland Adaptive Behaviours Scale-II (VABS-II, (Sparrow et al., 2005, 1984)) measures different forms of adaptive behaviours in individuals from birth through 90 years of age. Forms are available as interview or caregiver/ parent survey. The latter version was used in this study. For assessment of behaviour in infants and children up to 6 years of age, items are clustered into 4 domains and 11 subdomains. The Communication domain entails receptive communication (listening, understanding), expressive communication (use of words and phrases), and written communication (reading and writing). The Daily Living Skills domain taps into personal skills (eating, dressing, personal hygiene), domestic skills (household tasks), and community (use of time, money, phone, computer, job skills). The Socialisation domain gathers information on interpersonal relationships (interacting with others), play and leisure time (kinds of play, use of leisure time), and coping skills (responsibilities, sensitivity to other people). Lastly, the Motor Skills domain assesses gross motor skills (movement and coordination of the limbs), and fine motor skills (use of hand and fingers to manipulate objects). There is an additional Maladaptive Behaviour domain, which is optional and measures the amount of internalizing and externalizing.

Each of the items is scored based on the typical performance of the individual, not their ability to perform the behaviour in question. Individuals might be able to perform the tasks, but the behaviour is not adaptive if not performed when required. Possible scores are 2 (usually), 1 (sometimes or partially), 0 (never), NO (no opportunity), or DK (do not know). The basal level is defined as a 2-score on 4 consecutive items, while the ceiling level is defined at a 0-score on 4 consecutive items. The basal item is the highest item in the 4 2-scores, and the ceiling item is the lowest item in the 4 0-scores. The scores of the items from the basal through ceiling item in the subdomains sum up to a domain composite score. These domain composite scores can be converted into standard scores, which sum up into the Adaptive Behaviour Composite. This composite score is a general measure of adaptive behaviours.

Scores on the separate domains and the Adaptive Behaviour Composite score are typically converted to standard scores with a mean of 100 and a standard deviation 15.

A4.4. Clinical outcomes for the complete cohort

The sample in the complete cohort consisted of 27 LR infants, and 116 HR infants. Out of the 116 HR infants, 17 toddlers who were considered to meet the criteria for ASD were identified as HR-ASD infants for further analyses. Toddlers who did not meet criteria for ASD but did not show typical development either were considered as HR-Atyp infants (N = 32). These toddlers received 1) scores above the threshold for the ADI-R and/or ADOS-2 cut-off, 2) scores of or below 77.5 on the MSEL composite score or the MSEL Expressive Language or Receptive Language subscales, or 3) scoring as defined by both point 1 and 2. Lastly, toddlers who did not meet criteria for ASD and showed scores within the normative range were categorised as HR-TD infants (N = 64). Finally, 3 infants had missing outcome data.

A4.5. Interference coding differences between the previous and current study

Gross body, head and arm movement, and chewing and sucking were coded in the previous study, but not here as this would show up in the EEG signal and can be efficiently removed during manual artefact rejection. Also, crying and smiling coded in the previous study were not coded here as to minimize bias toward data inclusion of infants with particular emotional states. The difference in interference coding between the original and current study did probably not influence the results since there were no differences between the current and previous cohort for percentages of interference across the different outcome groups (U = 2449, z = -1.044, asymptotic 2-tailed p = 0.296; Mdn_{Prev} = 15, IQR_{Prev} = 14, and Mdn_{Curr} = 15, IQR_{Curr} = 20). Nor were there any differences reaching significance within the LR, HR-no ASD, and HR-ASD groups (p's ≥ .451).

A4.6. Statistical analyses: confounding factors for global connectivity analyses

Confounding factors may have influenced functional connectivity measures. Additional analyses were therefore performed to examine whether any (lack of) differences between groups may be associated with methodological factors, or demographic data. Rationale and methods for these additional analyses are reported here.

A4.6.1. Methodological factors

Behaviour during the EEG recording: Differences between groups in behaviour during the EEG recording may influence the connectivity results for categorical outcome, such as looking, and interference. I therefore tested for differences in the percentage of looking, and interference between the HR-ASD and comparison groups in separate analyses with an independent samples t-test for normally distributed data, or a Mann-Whitney U-test for non-normally distributed data.

Furthermore, the amount of epochs, or the combination of epochs from different conditions included in the connectivity calculation might also play a role. Therefore, I also tested for differences between groups in the total amount of epochs included, the amount of epochs from the toy condition, the hand condition, the social condition, and the proportion of social epochs included in the total amount of epochs. I further calculated the amount of overlapping epochs as a measure of sustained attention. A higher proportion of overlapping epochs would suggest that the epochs were drawn from long periods where the infants was showing attention, rather than many short periods of fleeting attention without interference. Independent samples t-tests or Mann-Whitney U-tests were performed for normally and non-normally distributed data within groups, respectively.

If group differences were found between any of these measures, I further tested for differences between groups in associations between the measures and global connectivity using Spearman's correlation or Pearson's correlation analyses for data with a normal or non-normal distribution.

Spectral power: Studies looking into connectivity typically perform accompanying analyses for spectral power, as power might influence the connectivity results as well (van Diessen et al., 2015). I therefore tested for differences between the HR-ASD and comparison groups as done in the previous study for alpha power (7-8 Hz) across all electrodes, posterior electrodes, left posterior electrodes, right posterior electrodes, central electrodes (also called mu rhythm), left central electrodes, and right central electrodes (see Figure 4.2). Separate analyses were performed for each of the variables. Again, prior to analyses the distributions of the data were tested for normality and equality of variance across group to decide whether to perform independent samples t-tests or Mann-Whitney U-tests.

A4.6.2. Demographic factors

Gender: Gender was included as an additional factor in the General Linear Model, as this variable might modulate associations between early markers and later ASD symptoms (Bedford et al., 2016).

Age and MSEL composite scores at EEG assessment: Age or cognitive levels might influence connectivity as well. I therefore performed correlational analyses to test for group differences between the associations between connectivity and age or MSEL composite scores at the time of EEG assessment. A Shapiro-Wilk test and Levene's test were done to determine whether a parametric Pearson's correlation or a non-parametric Spearman's correlation should be performed. If there were differences between groups as a result from the analyses from the Participants section, or correlations where different between groups for age, age would be included as a covariate in the GLM. If this were the case for MSEL composite scores, MSEL composite scores would be included as covariate in a separate GLM analysis.

A4.7. Confounding factor: Behaviours during EEG recoding

In the following analyses I checked whether there were any differences between in behaviours during the EEG recording such at looking or interference or amount of epochs that might confound the connectivity analyses.

Looking behaviour showed non-Gaussian distributions in the LR, HR-Atyp and HR-ASD group (p's ≤ .028), and variances were equal across groups (p = .327). Mann Whitney U-tests comparing the comparison groups and the HR-ASD group showed no differences between groups for the percentage of looking behaviour during the EEG recording session (p's ≥ .355, see Table A4.1). Interference showed a non-Gaussian distribution for each group (p's ≤ .047), and variances were not equal across groups (p = .046). Mann Whitney U-tests comparing the comparison groups and the HR-ASD group showed no differences between groups for the percentage of interference during the EEG recording session (p's ≥ .128). These data suggest that there are no differences between groups in looking and interference during the EEG session. Thus looking and interference are not potential confounding factors for the connectivity analyses.

Table A4.1. Behaviour during EEG session

	LR	*HR-TD*	*HR-Atyp*	*HR-ASD*
Looking (%)[a]	89.9 (12.2) *U* = 127, *p* = .928 [b]	87.5 (9.3) *U* = 254, *p* = .355 [c]	89.6 (8.1) *U* = 124, *p* = .675 [b]	92.0 (13.3)
Interference (%)[a]	17.0 (34.1) *U* = 88, *p* = .128 [b]	11.0 (14.9) *U* = 254.5, *p* = .360 [c]	14.0 (22.7) *U* = 108.5, *p* = .326 [b]	6.5 (25.2)

[a] Medians and interquartile range in parentheses, with results for the Mann-Whitney U-test when compared with the HR-ASD group.

[b] Exact 2-tailed. [c] Asymptotic 2-tailed.

A4.8. Confounding factor: Spectral power across the alpha band

All power datasets showed Gaussian distributions (*p*'s ≥ 0.176), and variances across groups were equal (*p*'s ≥ 0.559). T-tests for independent samples were used to compare HR-ASD group with the comparison groups. There were no differences between the HR-ASD and comparison groups for grand average alpha power (7-8 Hz) (*p*'s ≥ 0.720, see Table A4.2 and Figure 4.2). No differences were observed between the HR-ASD and comparison groups for posterior alpha, posterior alpha left, posterior alpha right, central mu, central mu left, or central mu right (*p*'s ≥ .254).

Table A4.2. Spectral power for alpha and mu rhythms (7-8 Hz)

	LR	*HR-TD*	*HR-Atyp*	*HR-ASD*
Grand average alpha power	1.64 (0.15) [a] *t*(31) = -0.199, *p* = .844 [b]	1.61 (0.09) *t*(58) = -0.361, *p* = .720	1.70 (0.13) *t*(32) = 0.064, *p* = .949	1.69 (0.19)
Posterior alpha	2.02 (0.16) *t*(31) = -0.822,	2.05 (0.10) *t*(58) = -0.843,	2.13 (0.13) *t*(32) = -0.432,	2.23 (0.21)

	p = .418	p = .403	p = .669	
Posterior alpha left	1.98 (0.15) $t(31)$ = -0.697, p = .491	2.06 (0.09) t (58) = -0.506, p =.614	2.10 (0.13) $t(32)$ = -0.286, p = .776	2.16 (0.22)
Posterior alpha right	2.05 (0.16) $t(31)$ = -0.934, p = .358	2.04 (0.10) $t(58)$ = -1.151, p = .254	2.16 (0.14) $t(32)$ = -0.572, p = .571	2.29 (0.20)
Central mu	1.70 (0.20) $t(31)$ = 0.162, p = .873	1.61 (0.11) $t(58)$ = -0.175, p = .862	1.72 (0.18) $t(32)$ = 0.242, p = .810	1.65 (0.24)
Central mu left	1.69 (0.20) $t(31)$ = -0.052, p = .959	1.65 (0.12) $t(58)$ = -0.227, p = .822	1.76 (0.19) $t(32)$ = 0.151, p = .881	1.71 (0.26)
Central mu right	1.71 (0.21) $t(31)$ = 0.373, p = .712	1.57 (0.11) $t(58)$ = -0.112, p = .911	1.69 (0.17) $t(32)$ = 0.338, p = .738	1.60 (0.23)

[a] Mean (standard errors of the mean) values for spectral power.

[b] Significance level, 2-tailed

A4.9. Confounding factor: Gender

In the HR-ASD group, there were more males than females. The HR-Atyp group revealed a similar ratio, whereas the ratio between males and females in the HR-TD group and LR group were different from the HR-ASD group. Previous research suggests that global EEG connectivity is lower for males than females in the theta, alpha, and beta frequency band (Boersma et al., 2011).

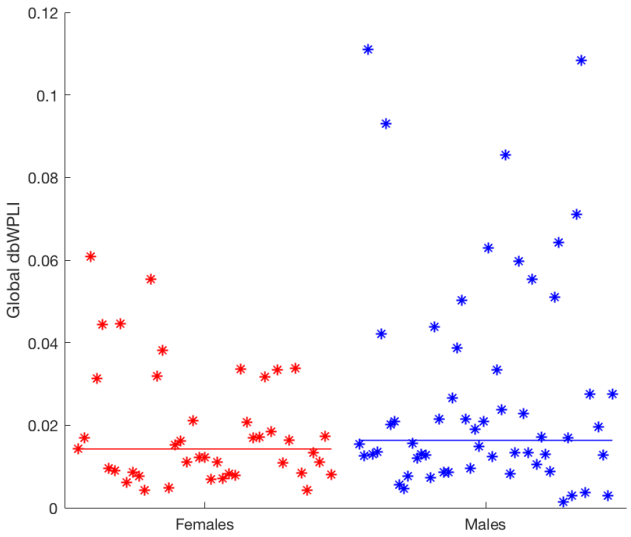

Figure A4.1. Global connectivity for females and males

Global connectivity values for females (red), and males (blue), and median values across groups represented by horizontal lines.

Then, I also tested whether alpha connectivity differs with gender as this may have influenced the results. Results of the Shapiro-Wilk test and Levene's test for homogeneity revealed that assumptions for normality and homogeneity of variance were not met (p's ≤ .003). Global alpha connectivity did not differ between females and males, U = 1068, z = -1.229, asymptotic 2-tailed p = .219, r = -.12, with Mdn_{Females}= 0.0142, IQR_{Females} = 0.02, and Mdn_{Males} = 0.0163, IQR_{Males} = 0.02.

A4.10. Calculations of scores for subtypes of restricted and repetitive behaviours

For Repetitive Motor Behaviours, scores of item 69 (Repetitive use of objects), item 77 (Hand and finger mannerisms), and item 78 (Other complex mannerisms and stereotyped body movements) were summed up to one score. Insistence on Sameness scores were the sum of scores on item 70 (Compulsions and rituals), item 74 (Difficulties with minor change in personal routine or environment), and item 75 (Resistance to trivial changes in the environment). Finally, Circumscribed Interests scores consisted of the sum of raw scores on item 67 (Unusual preoccupations), item 68 (Circumscribed Interests), and item 76 (Unusual attachment to objects) (based on results from factor analyses in (Lam et al., 2008)). If specific items were not asked or not applicable to some toddlers, that specific toddler was not included in the analyses for that subtype.

Table A4.3 presents descriptions of the scores across the whole HR group, the HR-no ASD group, and the HR-ASD group for the combined cohorts.

Table A4.3. Summary of scores for the groups of infants in the combined HR sample from our previous and current cohort

		N	*Median (IQR)*	*Minimum*	*Maximum*
All HR infants	ADI-R, RRB	103	0 (3)	0	10
	RMB $_{Ever}$	103	0 (1)	0	7
	RMB $_{Current}$	103	0 (1)	0	7
	IS $_{Ever}$	102	0 (1)	0	6
	IS $_{Current}$	103	0 (1)	0	6
	CI $_{Ever}$	90	0 (1)	0	5
	CI $_{Current}$	92	0 (1)	0	5
HR-no ASD	ADI-R, RRB	82	0 (1)	0	9
	RMB $_{Ever}$	82	0 (0)	0	5
	RMB $_{Current}$	82	0 (0)	0	5
	IS $_{Ever}$	81	0 (0)	0	4
	IS $_{Current}$	82	0 (0)	0	4
	CI $_{Ever}$	69	0 (0)	0	3
	CI $_{Current}$	71	0 (0)	0	3
HR-ASD	ADI-R, RRB	21	5 (4)	0	10
	RMB $_{Ever}$	21	2 (4)	0	7
	RMB $_{Current}$	21	2 (3)	0	7
	IS $_{Ever}$	21	3 (4)	0	6
	IS $_{Current}$	21	3 (5)	0	6
	CI $_{Ever}$	21	2 (2)	0	5
	CI $_{Current}$	21	2 (2)	0	5

Abbreviations used: Number of infants (N); Interquartile Range (IQR); Autism Diagnostic Interview – Revised, Restricted and Repetitive Behaviours Scale (ADI-R, RRB); repetitive motor behaviours (RMB); insistence on sameness (IS); and circumscribed interests (CI).

A4.11. Alpha connectivity and subtypes of restricted and repetitive behaviours in the previous and current cohort

Correlational analyses were also performed in the separate cohorts. In the previous cohort, the association between connectivity across all connections and insistence on sameness with ever scores reached significance, as did the associations for connectivity across selected connections and each of the 3 subtypes of restricted and repetitive behaviours in the whole HR group. In the HR-ASD group, associations between circumscribed interests and connectivity both across all and selected connections reached significance. For the analyses based on current scores, only the association with circumscribed interests in the HR group was significant and survived correction for multiple comparisons.

In the current, new cohort, none of the investigated associations reached significance.

A4.12. Scatterplots for scores on the different subtypes of restricted and repetitive behaviours and alpha connectivity

Figure A4.2 displays scatterplots based on ever scores in the ADI-R, while Figure A4.3 displays scatterplots based on current scores.

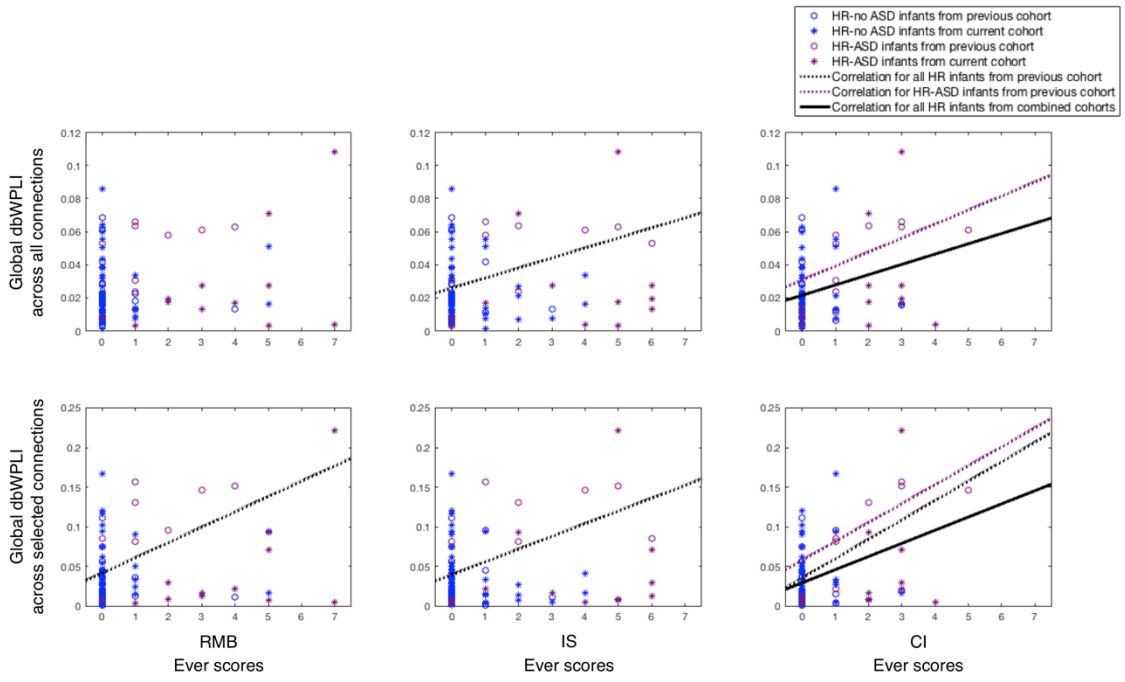

Figure A4.2. Scatterplots for alpha connectivity and subtypes of Restricted and Repetitive Behaviours based on ever scores

Plots of global dbWPLI across all connections (top), global dbWPLI across selected fronto-central connections (bottom) with ever scores for different subtypes of RRBs: repetitive motor behaviours (RMB, left), insistence on sameness (IS, middle), and circumscribed interests (CI, right). Open circles reflect data from the previous cohort, and asterisks signify data from the current cohort. Colours represent different outcome groups. Lines represent Spearman's correlations reaching significance.

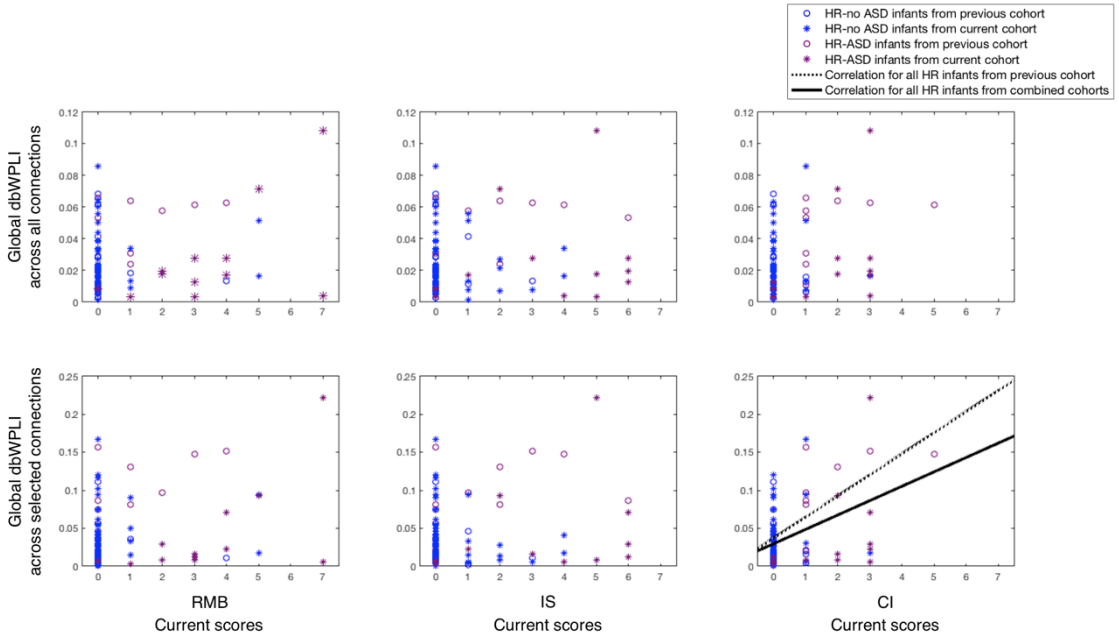

Figure A4.3. Scatterplots for alpha connectivity and subtypes of Restricted and Repetitive Behaviours based on current scores

Plots of global dbWPLI across all connections (top), global dbWPLI across selected fronto-central connections (bottom) with current scores for different subtypes of RRBs: repetitive motor behaviours (RMB, left), insistence on sameness (IS, middle), and circumscribed interests (CI, right). Open circles reflect data from the previous cohort, and asterisks signify data from the current cohort. Colours represent different outcome groups. Lines represent Spearman's correlations reaching significance.

A4.13. Global connectivity analyses for combined cohort

Cohorts were collapsed after investigating connectivity in the new cohort, for the purpose of increasing statistical power in further dimensional analyses. The question that remains unanswered is whether connectivity in the HR-ASD group is

increased compared to the other groups in this combined sample, and was examined here.

A Mann-Whitney U-test was used to test whether there were any differences between the HR-ASD group and the comparison groups in global alpha connectivity across all connections, as the assumptions for normality (p's ≤ .012) and homogeneity of variance were not met (p = .001). The comparisons between the HR-ASD groups and the other groups yielded no significant differences between the groups: LR vs. HR-ASD: U = 509, z = -0.255, asymptotic 2-tailed p = .799; HR-TD vs. HR-ASD: U = 526, z = -1.273, asymptotic 2-tailed p = .203; HR-Atyp vs. HR-ASD: U = 293, z = -0.933, asymptotic 2-tailed p = .351; Mdn_{LR} = 0.02, IQR_{LR} = 0.03; $Mdn_{HR\text{-}TD}$ = 0.02, $IQR_{HR\text{-}TD}$ = 0.02; $Mdn_{HR\text{-}Atyp}$ = 0.02, $IQR_{HR\text{-}Atyp}$ = 0.01; and $Mdn_{HR\text{-}ASD}$ = 0.02, $IQR_{HR\text{-}ASD}$ = 0.05.

The same analyses were repeated for global alpha connectivity across fronto-central connections identified in the previous study (Orekhova et al., 2014). Again, the assumptions for normality (p's < .003) and equal variances among groups were not met (p < .001). No differences were found in global connectivity for selected connections between the HR-ASD and comparison groups: LR vs. HR-ASD: U = 458, z = -0.904, asymptotic 2-tailed p = .366; HR-TD vs. HR-ASD: U = 491, z = -1.651, asymptotic 2-tailed p = .099; HR-Atyp vs. HR-ASD: U = 284, z = -1.095, asymptotic 2-tailed p = .274; Mdn_{LR} = 0.03, IQR_{LR} = 0.03; $Mdn_{HR\text{-}TD}$ = 0.02, $IQR_{HR\text{-}TD}$ = 0.03; $Mdn_{HR\text{-}Atyp}$ = 0.02, $IQR_{HR\text{-}Atyp}$ = 0.03; and $Mdn_{HR\text{-}ASD}$ = 0.03, $IQR_{HR\text{-}ASD}$ = 0.09.

Table A4.4. Comparisons between our previous and current cohort for age and cognitive skills

Group	*Measure*	*Previous cohort*	*Current cohort*	*Statistical values*
LR	*Age at EEG (in days)*	447 (35) [2] N = 26	471 (32) N = 20	**t(44) = -2.63, p = .012**
	MSEL[1] at 14 month visit	104 (17) [2] N = 25	102 (14) N = 20	t(43) = 0.49, p = .629
	Age at 36 month visit (months)	37 (3) [3] N = 26	38 (1) N = 18	**U = 153, p = .049[4]**

	MSEL at 36 month visit	118(20) [3] N = 26	123 (15) N = 18	U = 183, p = .218[4]
HR-no ASD	*Age at EEG (in days)*	422 (86) [2] N = 18	465 (46) N = 68	**U = 346.5, p = .005[4]**
	MSEL at 14 month visit	100 (12) [2] N = 18	96(13) N = 68	t(84) = 1.07, p = .287
	Age at 36 month visit (months)	37 (2) [2] N = 18	39 (2) N = 67	**U = 252.5, p < .001[4]**
	MSEL at 36 month visit	110 (18) [2] N = 18	106 (22) N = 67	t(83) = 0.72, p = .475
HR-ASD	*Age at EEG (in days)*	446 (49) [2] N = 10	444 (47) N = 13	U = 51, p = .410[5]
	MSEL at 14 month visit	86 (15) [2] N = 10	87 (13) N = 13	t(21) = -0.17, p = .869
	Age at 36 month visit (months)	38 (2) [3] N = 10	39 (2) N = 12	t(44) = -0.24, p = .809
	MSEL at 36 month visit	100 (27) [2] N = 9	84 (29) N = 12	t(19) = 1.29, p = .214

Comparisons reaching significance are printed in bold.

[1] Mullen Scale for Early Learning (MSEL).

[2] Means and standard deviations in parentheses, with results for the t-test for independent samples comparison between our prior and current cohort.

[3] Medians and interquartile range in parentheses, with results for the Mann-Whitney U-test comparison between our prior and current cohort.

[4] Asymptotic 2-tailed. [5] Exact 2-tailed.

Thus, no differences in global connectivity across all connections or selected fronto-central connections were observed between the HR-ASD group and LR, HR-TD, or HR-Atyp group in the combined sample.

A4.14. Comparisons of age and cognitive skills between cohorts

In order to examine whether differences in ages or developmental skills have influenced the failure to replicate, I compared the previous and new cohort on these measures (Table A4.4). The LR group in the previous cohort was younger than the LR group in the current cohort at both the 14 and 36-month-old visits (for 14 months: $t(44) = -2.63$, $p = .012$; and for 36 months: $U = 153$, $p = .049$). The HR-no ASD group in the previous cohort was also younger than the HR-no ASD group in the current cohort at both visits (for 14 months: $U = 346.5$, $p = .005$; and for 36 months: $U = 252.5$, $p < .001$). The HR-ASD groups in both cohorts did not show any differences in age at either visit (p's ≥ .410).

There were no differences between groups from the previous and current cohort in cognitive skills measured by the MSEL ELC at the 14- or 36-month-old visit (p's ≥ .214).

These findings suggest that differences in ages may have played a role in differences between findings in the current and previous cohort.

Appendix to Chapter 5

A5.1. Samples sizes for different thresholds

Sample sizes for the different thresholds used when comparing the toy and hand condition, and the social and non-social condition are presented in table A5.1.

Table A5.1. Sample sizes for different groups for the different comparisons and thresholds for numbers of epochs

Comparisons for	*Sizes for different groups*				
	LR	*HR-TD*	*HR-Atyp*	*HR-ASD*	*Total*
Social versus toy ≥120 epochs	10	15	4	6	35
Social versus hand ≥120 epochs	13	22	12	8	55
Toy versus hand ≥120 epochs	9	17	4	6	36

Toy versus hand ≥90 epochs	**17**	**25**	**13**	**9**	**64**
Social versus non-social ≥120 epochs	**17**	**27**	**16**	**8**	**68**

Thresholds selected for the analyses printed in bold.

A5.2. Comparisons of theta power between the hand and toy condition

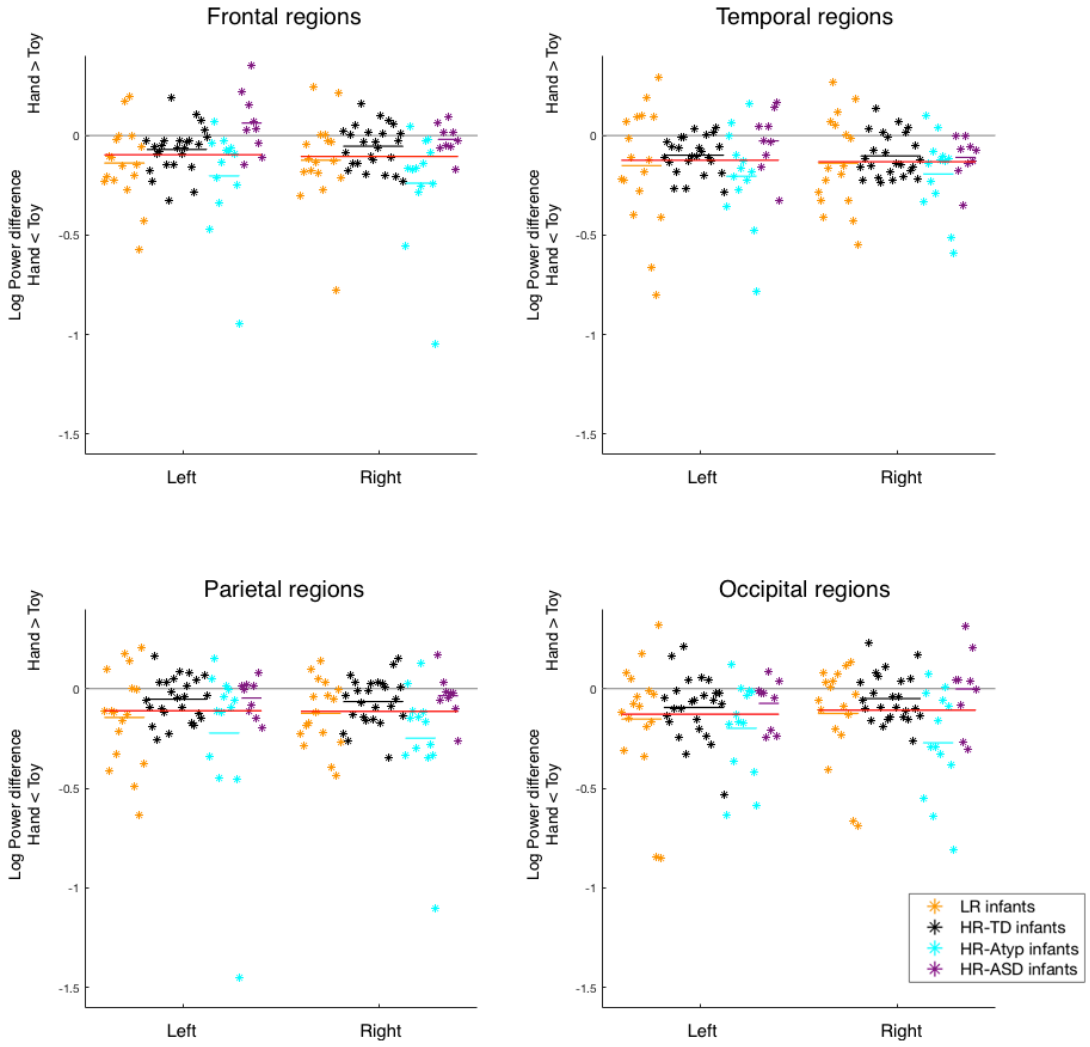

Figure A5.2. Global theta power for the hand and toy condition

Power differences for individual infants between the hand and toy conditions for selected regions based on fig. 5.1: frontal (upper left), temporal (upper right), parietal (lower left), and occipital regions (lower right), within the left and right hemisphere regions (left, right side of graphs). Each asterisk represents one infant; colours represent different outcome groups. Red horizontal bars represent mean power values

across groups, whereas shorter horizontal bars in the colours of the outcome groups represent mean power within that group.

A5.3. Comparisons of theta power between the hand and toy condition without the HR-Atyp outlier

The figure in the main text displayed one outlier in the HR-Atyp group. Possibly, this single participant is driving the effect of Condition. The analyses were repeated while excluding this HR-Atyp outlier as to examine this possibility (Figure A5.3). When excluding the outlier, there was a main effect of Condition for log power averaged across all channels, $F(1,61) = 41.21$, $p < .001$, $\eta_p^2 = .403$, where theta power across all channels was higher for the toy than the hand condition, ($M_{\text{Toy}} = 2.41$, $sd_{\text{Toy}} = 0.43$; and $M_{\text{Hand}} = 2.30$, $sd_{\text{Hand}} = 0.39$). The main effect of Risk Group, and interaction effect between Condition and Risk Group did not reach significance (p's ≥ .228, η_p^2's ≤ .024).

Next, I performed 2x4x2x2 mixed model ANOVA was used with Condition (Hand, Toy), Region (Frontal, Temporal, Parietal, Occipital, and Hemisphere (Left, Right) as within-subject factors, and Risk Group (LR, HR) as between-subject factor was used. Assumptions for normality were met for most variables (p's ≥ .130), except in the HR group for left and right parietal areas during both conditions (p's ≤ .037). Assumptions for homogeneity of variance were met for half of the variables (p's ≥ .054), and not for left occipital and right temporal areas during both conditions, and both frontal regions and left temporal and parietal regions during the toy condition (p's ≤ .049). For factors for which the assumption of sphericity was not met, Huynh-Feldt corrected degree of freedom values are reported, as the estimates were larger than .75.

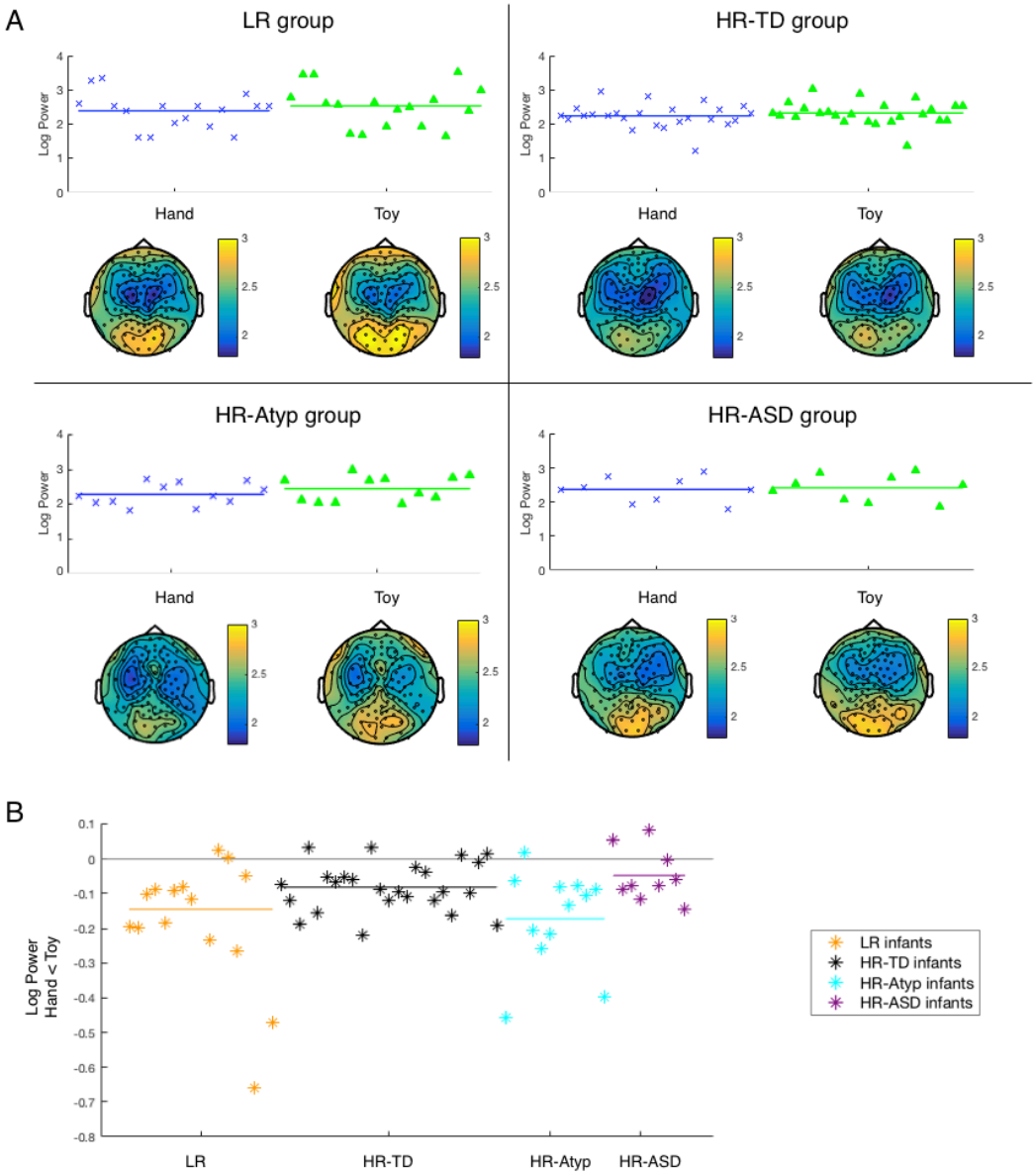

Figure A5.3. Global theta power in the hand and toy condition excluding the HR-Atyp outlier

A) Global power across all channels for individual infants for the hand and toy condition (blue crosses, and green triangles, resp.), with topoplots averaged across infants in the outcome groups (LR group in top left panel, HR-TD group in top right, HR-Atyp group in bottom left, and HR-ASD group in bottom right panel). B) Differences in global power between the hand and toy condition for individual infants in the different outcome groups. Horizontal lines represent group means.

The pattern of results for analyses excluding the outlier did not change compared to the pattern for analyses including the outlier. The main effects for Condition, and Region both reached significance. Theta power was higher during the toy than hand condition in the selected channels, $F(1,61) = 35.02$, $p \leq .001$, $\eta_p^2 = .365$ ($M_{Toy} = 2.41$, $SE_{Toy} = 0.06$; and $M_{Hand} = 2.30$, $SE_{Hand} = 0.06$). Power was different between regions, $F(2.78,169.77) = 98.98$, $p \leq .001$, $\eta_p^2 = .619$, showing highest values for occipital ($M_O = 2.68$, $SE_O = 0.06$), then temporal ($M_T = 2.36$, $SE_T = 0.05$), then frontal regions ($M_F = 2.24$, $SE_F = 0.06$), and lowest values for parietal regions ($M_P = 2.13$, $SE_P = 0.06$). There were trends with small effect sizes for Hemisphere, $F(1,61) = 3.64$, $p = .061$, $\eta_p^2 = .056$, and for the interaction between Region, Hemisphere, and Risk Group, $F(3,183) = 2.40$, $p = .069$, $\eta_p^2 = .038$. No other main or interaction effects reached significance (p's ≥ .164, η_p^2's ≤ .025), including Risk Group, $F(1,61) = 1.34$, $p = .252$, $\eta_p^2 = .021$.

These findings suggest that the pattern of results with differences in spectral power between the toy and hand condition is not strongly influenced by the data from the single HR-Atyp participant.

A5.4. Comparisons of functional theta connectivity between the hand and toy condition excluding the HR-Atyp outlier

As there was one outlier in the HR group, analyses were repeated without the outlier to examine whether this participant might have been influencing the results with regard to theta connectivity differences between the social and non-social condition (Figure A5.4). For global theta connectivity, normality assumptions were not met for the variables in each risk group (p's < .001), whereas the assumption for homogeneity of variance was only met for the toy condition ($p = .137$), not the social condition ($p = .035$). The results revealed similar patterns as those including the outlier, showing no differences between conditions across all subjects, or in the HR group (p's ≥ .404, r's ≤ .08).

The network analyses revealed no significant networks showing higher connectivity for either the toy or hand condition when the outlier was excluded (see table A5.2).

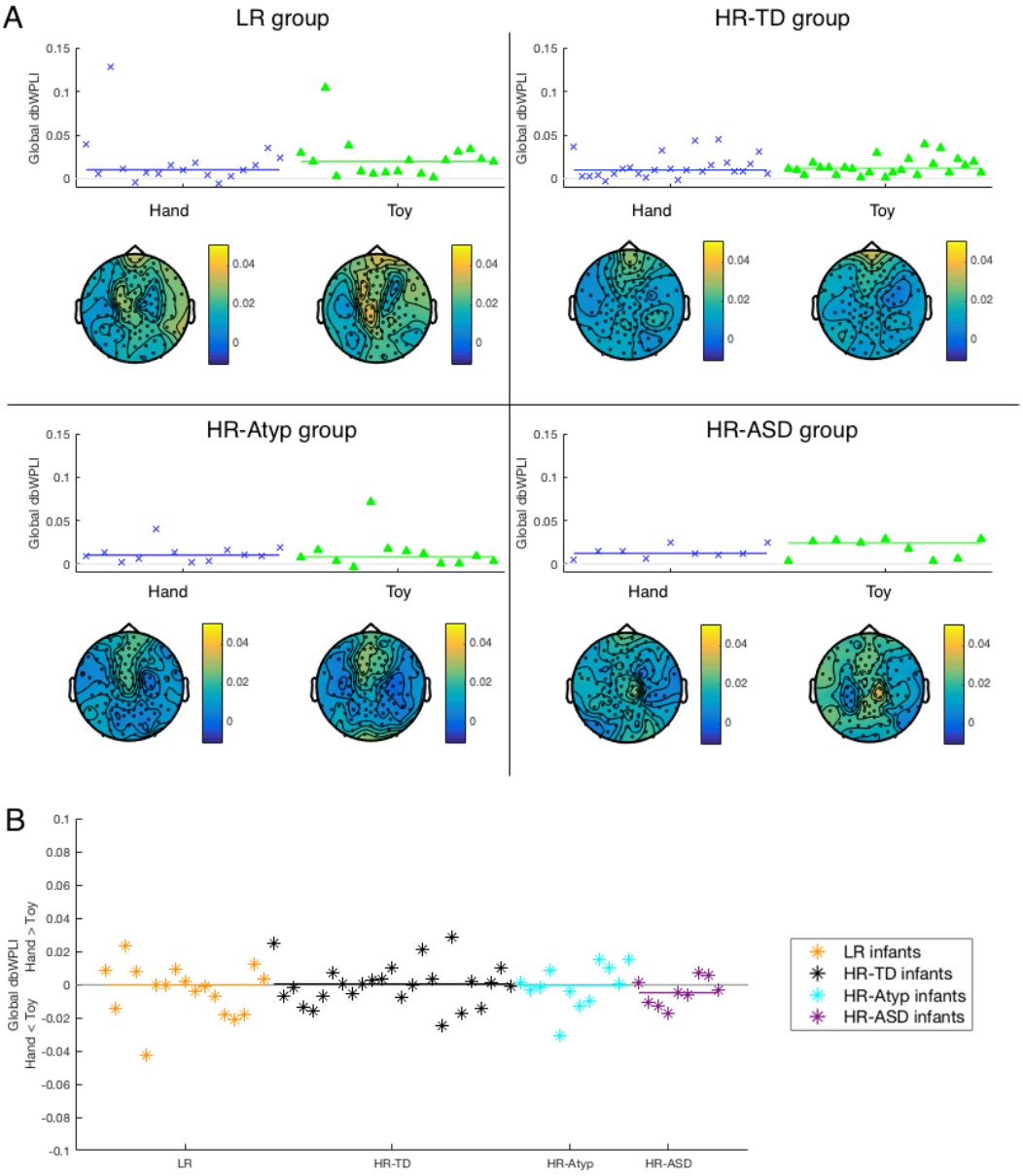

Figure A5.4. Global theta dbWPLI in the hand and toy condition excluding the outlier marked in Figure 5.5.

A) Global dbWPLI across all channels for individual infants for the hand and toy condition (blue crosses, and green triangles, resp.), with topoplots averaged across infants in the outcome groups (LR group in top left panel, HR-TD group in top right, HR-Atyp group in bottom left, and HR-ASD group in bottom right panel). B) Differences in global dbWPLI between the hand and toy condition for individual infants in the different outcome groups. Horizontal lines represent group medians.

Table A5.2. Overview NBS results for comparisons between connectivity in the toy and hand condition excluding the HR-Atyp outlier

Contrast Toy > Hand

Group	*N subjects*	*Min. N epochs*	*Threshold 3.5*	*Threshold 3.1*
All	64	90	NS	NS
	36	120	NS	NS
HR	46	90	NS	NS
	27	120	NS	NS
HR-Atyp	12	90	NS	NS

Contrast Hand > Toy

Group	*N subjects*	*Min. N epochs*	*Threshold 3.5*	*Threshold 3.1*
All	63	90	NS	NS
	36	120	NS	NS
HR	46	90	NS	NS

NS: no significant network observed by NBS analyses.

Finally, GLM analyses were performed to examine the potential influence of spectral power and the number of epochs. The GLM excluding any covariates revealed no effects reaching significance for Condition, $p = .241$, $\eta_p^2 = .022$, Risk Group, $p = .159$, $\eta_p^2 = .032$, or the interaction effect, $p = .526$, $\eta_p^2 = .007$. Adding the difference in spectral theta power between the toy and hand condition across all channels as covariate, did not change the pattern compared to analyses without the power variable, p's ≥ .189, η_p^2's ≤ .029. Adding the number of epochs, as covariate did not change the initial results either, p's ≥ .193, η_p^2's ≤ .028.

Together these findings suggest that there is no difference between the social and non-social condition in theta connectivity when excluding the outlier. This pattern occurs in the whole group, and HR group, and is not influenced by differences between conditions in spectral power, or numbers of epochs. This participant thus likely influences the results reported in the main text.

A5.5. Comparisons of theta power between the social and non-social condition

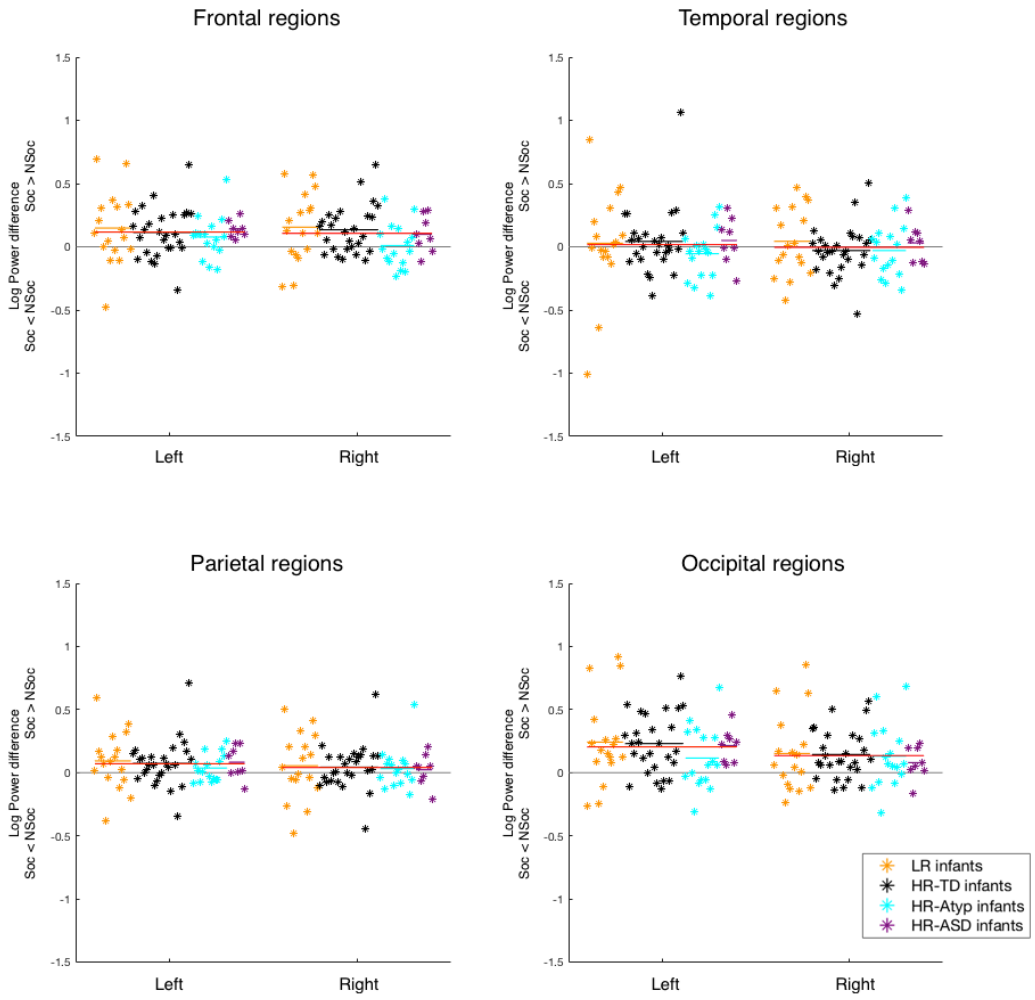

Figure A5.5. Global theta power for the social and non-social condition

Power differences for individual infants between the social and non-social conditions for selected regions based on fig. 5.1: frontal (upper left), temporal (upper right), parietal (lower left), and occipital regions (lower right), within the left and right hemisphere regions (left, right side of graphs). Each asterisk represents one infant; colours represent different outcome. Red horizontal bars represent mean power values across groups, whereas shorter horizontal bars in the colours of the outcome groups represent mean power within that group.

A5.6. Exploratory analyses of network topology in HR-TD, HR-Atyp, and HR-ASD groups

Tables below contain the results for exploratory analyses of networks showing higher activation during the social versus the non-social condition in the HR-TD group (table A5.3), HR-Atyp group (table A5.4), and HR-ASD group (table A5.5).

Table A5.3. **Overview NBS results when tested whether for Social > Non-Social contrast in the HR-TD group**

NBS settings		*Results*		
Threshold	*p-value*	*Number of edges*	*Number of nodes*	*p-value*
3.1	.06	NS network		
3.1	.1	NS network		
3.1	.2	NS network		
3.1	.5	5	6	.281
3.1	.3	5	6	.283
3.1	.26	6	7	.258
3.1	.25	NS network		
2.7	.26	55	45	.109
2.5	.26	95	60	.116
2.4	.26	120	70	.127
2.0	.26	338	105	.110

NS: non-significant

Table A5.4. **Overview NBS results when tested whether for Social > Non-Social contrast in the HR-Atyp group**

NBS settings		*Results*		
Threshold	*p-value*	*Number of edges*	*Number of nodes*	*p-value*
3.1	.06	NS network		
3.1	.1	NS network		
3.1	.2	NS network		
3.1	.5	NS network		
3.1	.3	NS network		
3.1	.6	NS network		
3.1	.7	NS network		
3.1	.8	NS network		
2	.05	NS network		
2	.1	NS network		
2	.2	277	108	.156
2	.3	277	108	.171
3.1	.2	NS network		
2.7	.2	NS network		
2.5	.2	NS network		
2.4	.2	85	69	.171
2.45	.2	70	61	.181
2.475	.2	NS network		
2.465	.2	64	56	.182
2.470	.2	NS network		

NS: non-significant

***Table A5.5*. Overview NBS results when tested whether for Social > Non-Social contrast in the HR-ASD group**

NBS settings		*Results*		
Threshold	*p-value*	*Number of edges*	*Number of nodes*	*p-value*
3.1	.06	NS network		
3.1	.1	NS network		
3.1	.2	NS network		
3.1	.5	NS network		
3.1	.3	NS network		
3.1	.6	NS network		
3.1	.7	NS network		
3.1	.8	NS network		
2	.05	NS network		
2	.1	NS network		
2	.2	NS network		
2	.3	284	95	.297
2	.4	284	95	.297
3.1	.3	NS network		
2.7	.3	NS network		
2.5	.3	NS network		
2.4	.3	NS network		
2.1	.3	NS network		
2.05	.3	NS network		
2.01	.3	NS network		
2.005	.3	NS network		
2.1	.4	221	89	.325
2.2	.4	174	83	.345
2.3	.4	137	75	.375
2.4	.4	105	59	.396
2.5	.4	87	55	.374
2.6	.4	NS network		

NS: non-significant

A5.7. Scatterplots for dimensional trait analyses in the main text

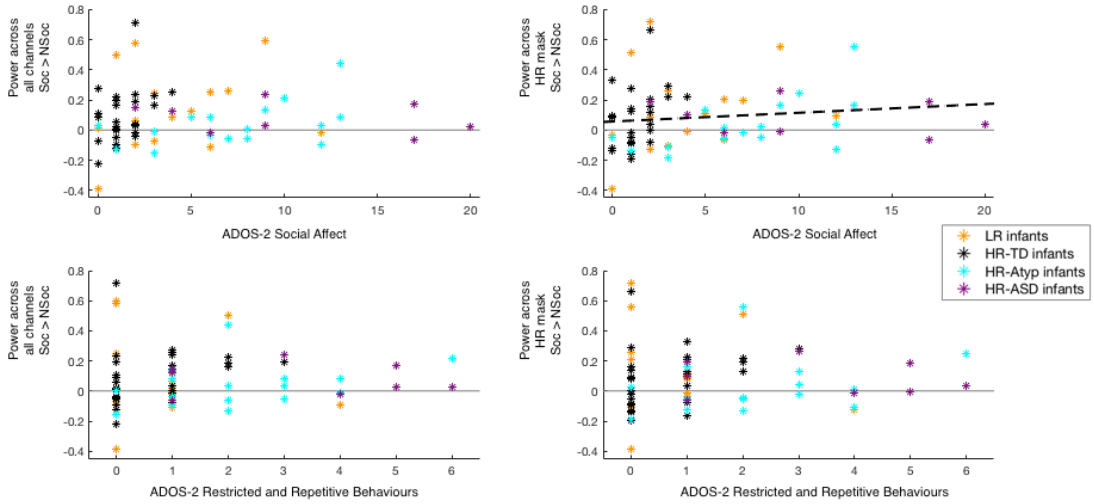

Figure A5.6. ADOS-2 domains and theta log power differences between conditions

The difference in theta log power between the social and non-social conditions averaged across all channels (left), and the channels from the HR 3.1 mask (right), with the ADOS-2 Social Affect domain scores (top) and the ADOS-2 Repetitive Behaviour domains scores (bottom). Dashed line represents the Spearman's correlation that reached significance but did not survive correction for multiple comparisons.

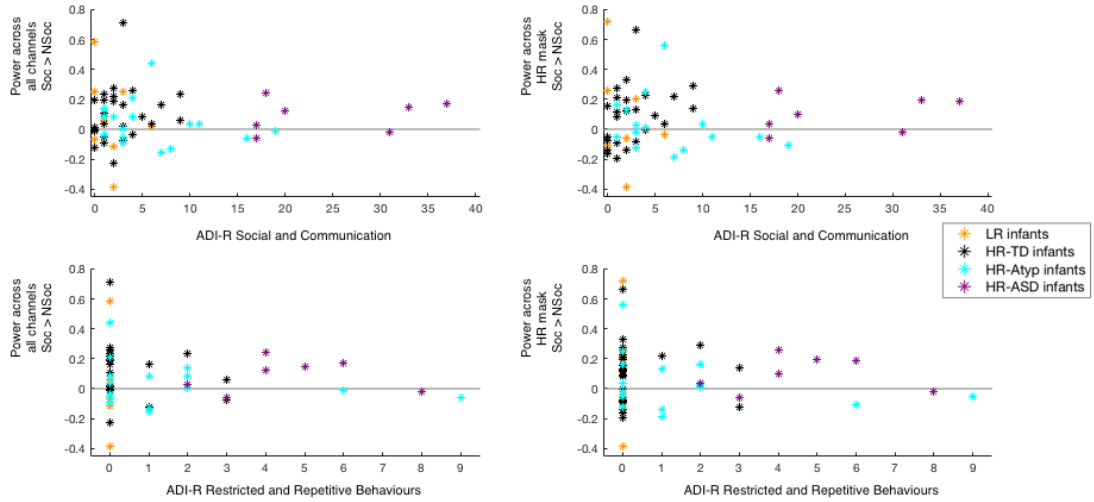

Figure A5.7. ADI-R domains and theta log power differences between conditions

The difference in theta log power between the social and non-social conditions averaged across all channels (left), and the channels from the HR 3.1 mask (right), with the ADI-R Social and Communication domain scores (top), and the ADI-R Behaviour/Repetitive Interests domain scores (bottom).

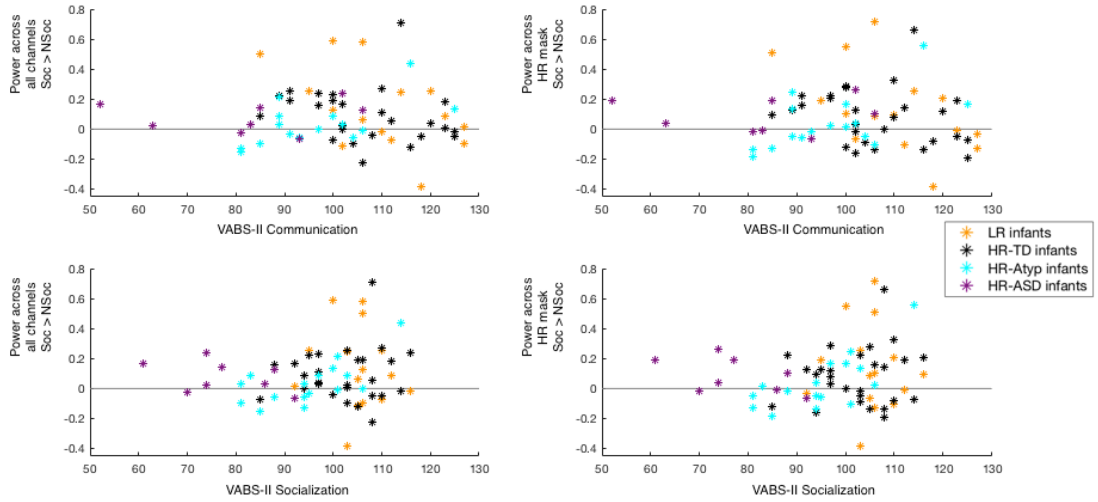

Figure A5.8. VABS domains and theta log power differences between conditions
The difference in theta log power between the social and non-social conditions averaged across all channels (left), and the channels from the HR 3.1 mask (right), with the VABS Communication domain standard scores (top), and the VABS Socialization domain standard scores (bottom).

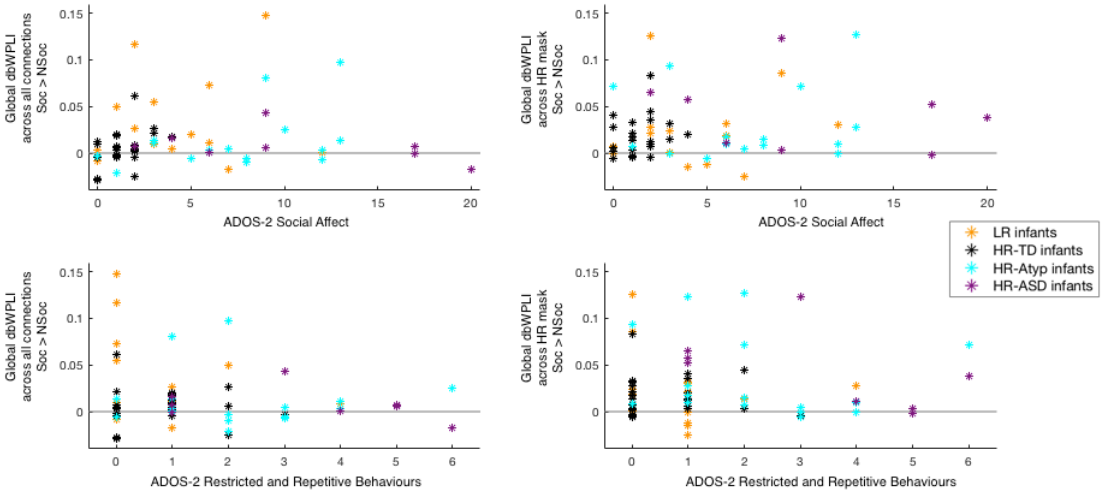

Figure A5.9. ADOS-2 domains and theta connectivity differences between conditions
The difference in global dbWPLI between the social and non-social conditions averaged across all connections (left), and the connections from the HR 3.1 mask (right), with the ADOS-2 Social Affect domain scores, (top), and the ADOS-2 Repetitive Behaviour domains scores (bottom).

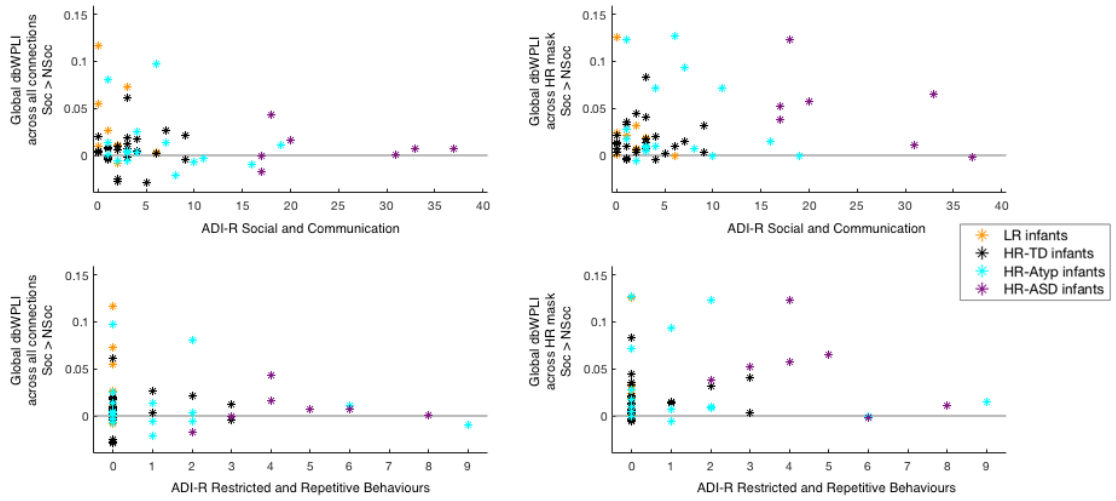

Figure A5.10. ADI-R domains and theta connectivity differences between conditions

The difference in global dbWPLI between the social and non-social conditions averaged across all connections (left), and the connections from the HR 3.1 mask (right), with the ADI-R Social and Communication domain scores (top), and the ADI-R Behaviour / Repetitive Interests domain scores (bottom).

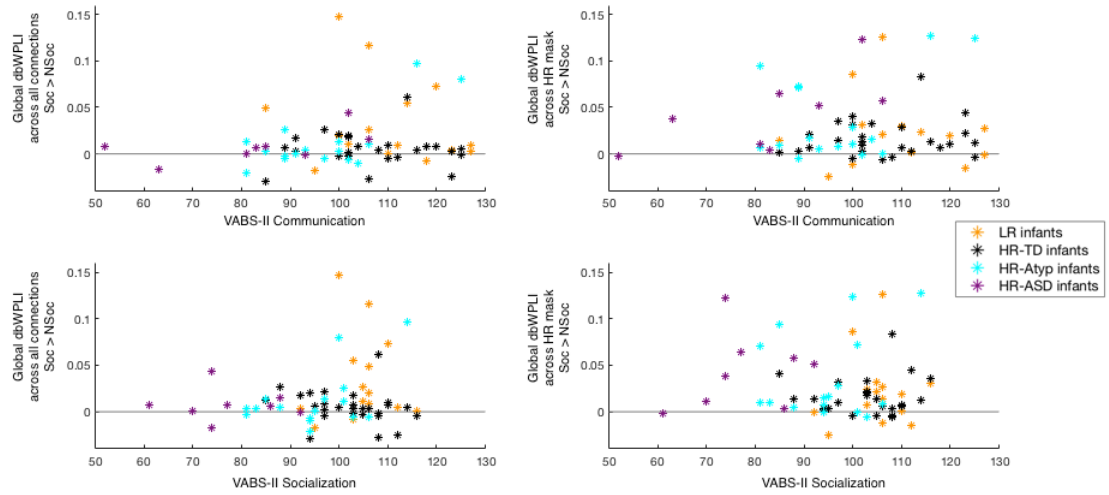

Figure A5.11. VABS domains and theta connectivity differences between conditions

The difference in global dbWPLI between the social and non-social conditions averaged across all connections (left column), and the connections from the HR 3.1 mask (right column), with the VABS Communication domain standard scores (top row), and the VABS Socialization domain standard scores (bottom row).

Appendix to Chapter 6

A6.1. Alpha frequency band: Circumscribed interests

In Chapter 4, alpha band connectivity across fronto-central connections showed a positive association with the severity of restricted and repetitive behaviours in the HR-ASD group. Further analyses suggested that this association might arise from the association between increased alpha band connectivity and the severity of circumscribed interests. The current chapter on graph metrics revealed that both the normalised clustering coefficient and small-worldness index are associated with global connectivity. Possibly, these metrics are also associated with circumscribed interests. None of the correlations reached significance, but in the HR-ASD group the correlations between small-worldness index the correlation with circumscribed interests scores were approaching medium effect sizes, as was the association between normalised clustering coefficient and current circumscribed interest scores.

Table A6.1. Spearman's correlations between graph metrics for the alpha band and circumscribed interests

Group	*N*	*Measures*	*Normalised clustering coefficient*	*Small-Worldness Index*
All HR infants	106	ADI-R, RRB	r = -.10, p = .283, [-.30, .10]	r = .08, p = .433, [-.12, .26]
	90	CI_{Ever}	r = -.04, p = .687, [-.24, .16]	r = -.03, p = .748, [-.23, .16]
	90	$CI_{Current}$	r = -.03, p = .783, [-.26, .20]	r = -.06, p = .582, [-.23, .11]
HR-ASD infants	21	ADI-R, RRB	r = .15, p = .513, [-.39, .59]	r = -.18, p = .415, [-.66, .38]
	21	CI_{Ever}	r = -.07, p = .750, [-.68, .19]	r = -.28*, p = .214, [-.68, .19]
	21	$CI_{Current}$	r = .29*, p = .197, [-.13, .65]	r = -.30*, p = .181, [-.66, .19]

Spearman's rho values (*r)*, with p-values, and bias corrected and accelerated

bootstrap 95% confidence intervals in square brackets. Correlations approaching medium effect sizes are marked with *.

Appendix to Chapter 7

A7.1. Rationale for the GLM approach

In addition to GLM, the current data might also have been analysed using hierarchical linear modelling (HLM). HLM involves the additive or combined predictive values of variables onto outcome variables. Under the current circumstances, the GLM approach was considered more appropriate than hierarchical linear modelling (HLM) approaches for the following reasons: a) HLM requires a large sample size when multiple variables are included as predictors, b) HLM in SPSS allows only 1 variable as dependent variable which increases the problem of multiple comparisons when one is interested in multiple measures such as here, and c) results are not generalizable if assumptions are violated, for example the assumption of no multicollinearity. This is problematic because preliminary analyses suggested that this assumption was violated here: a strong association was found for alpha connectivity across all channels and alpha connectivity across fronto-central connections, *Pearson's rho* = .88, $p < .001$. Further, variance loadings of these variables were highest on the same dimension, and the average variance inflation factor was above 1. This all suggests multicollinearity in the data, resulting in unreliable parameters, limited size of variance accounted for, and difficulty assessing the individual role of both predictors. Thus, GLM was considered a more appropriate approach than HLM (Field, 2014).

A7.2. Alpha EEG connectivity, childhood ASD traits, and confounding variables

It is possible that the results between alpha EEG connectivity and childhood ASD traits are influenced by other variables. Therefore additional GLMs were performed to test whether inclusion of other variables would change the pattern of results (including the outlier). When including the number of epochs into the model, large effect sizes were revealed for the normalised clustering coefficient, $V = .25$, $F(2,50) = 8.33$, $p = .001$, $\eta_p^2 = .250$, but small sizes were found for global

connectivity across all channels and fronto-central channels, *p*'s ≥ .295, *partial η²*'s ≤ .048. Further univariate GLM analyses showed a small effect size of normalised clustering coefficients on the SCI T-scores, $F(1,53) = 0.90$, $p = .348$, $\eta_p^2 = .017$, but a medium effect on the RRB T-scores, $F(1,53) = 5.07$, $p = .029$, $\eta_p^2 = .087$. The direction of the association between the normalised clustering coefficient and RRB T-scores remained unchanged.

Alpha power did not change the main results either. The multivariate GLM revealed a large effect size for the normalised clustering coefficient, $V = .19$, $F(2,50) = 5.74$, $p = .006$, $\eta_p^2 = .187$, but small sizes for the other connectivity measures, *p*'s ≥ .467, η_p^2's ≤ .039. Again, effect size for SCI T-scores of the normalised clustering coefficient with SCI T-scores was small, $F(1,53) = 1.00$, $p = .323$, $\eta_p^2 = .018$, but medium for the RRB T-scores of the normalised clustering coefficient, $F(1,53) = 4.27$, $p = .044$, $\eta_p^2 = .075$, with the same negative direction of the association as before. This suggests that the results were not related to differences in calculation of EEG connectivity, or strength of brain activity.

Clinical, demographic, and cognitive characteristics may also influence the results. When including familial risk (high or low) in to the multivariate GLM, the normalised clustering coefficients exhibited a larger effect size, $V = .21$, $F(2,50) = 6.83$, $p = .002$, $\eta_p^2 = .214$, than the other connectivity measures, *p*'s ≥ .396, η_p^2's ≤ .036. The effect sizes for the normalised clustering coefficient were larger for the RRB T-scores, $F(1,53) = 3.52$, $p = .066$, $\eta_p^2 = .062$, than the SCI T-scores, $F(1,53) = 0.57$, $p = .454$, $\eta_p^2 = .011$. In addition to using risk groups, one could also consider the outcomes at 3 years of age. Analyses including diagnostic group at 3 years of age revealed a similar pattern as those for risk group: a large effect for the normalised clustering coefficient, $V = .19$, $F(2,48) = 5.70$, $p = .006$, $\eta_p^2 = .192$, and minimal effect sizes for the other connectivity measures, *p*'s ≥ .312, η_p^2's ≤ .047. Effect sizes in for the separate subscales were small for the RRB T-score $F(1,51) = 2.35$, $p = .132$, $\eta_p^2 = .044$, and minimal for the SCI T-score, $F(1,51) = 0.11$, $p = .737$, $\eta_p^2 = .002$.

Turning to the demographic data, the multivariate model with gender again showed a large effect size for the normalised clustering coefficient, $V = .19$, $F(2,50) = 5.74$, $p = .006$, $\eta_p^2 = .183$, but not for the other connectivity measures, *p*'s ≥ .391, η_p^2's ≤ .037. Follow-up analyses revealed that effect sizes were in the small range

for both SCI T-scores, and RRB T-scores: $F_{SCI}(1,53) = 0.63$, $p_{SCI} = .431$, $\eta_{p^2\ SCI} = .012$, and $F_{RRB}(1,52) = 3.31$, $p_{RRB} = .074$, $\eta_{p^2\ RRB} = .059$. Including age at the EEG assessment showed a large effect size for the normalised clustering coefficient in the multivariate GLM, $V = .19$, $F(2,50) = 5.74$, $p = .006$, $\eta_{p^2} = .187$, but not for the other connectivity measures, p's ≥ .429, η_{p^2}'s ≤ .033. Effect sizes with the clustering coefficient for both SCI and RRB T-scores were small: SCI T-scores, $F(1,53) = 0.586$, $p = .447$, $\eta_{p^2} = .011$, and RRB T-scores, $F(1,53) = 5.74$, $p = .077$, $\eta_{p^2} = .058$. A similar pattern was found when age at the follow-up was included into the multivariate GLM: a large effect size for the normalised clustering coefficient, $V = .25$, $F(2,50) = 8.52$, $p = .006$, $\eta_{p^2} = .254$, but small effect sizes for the other connectivity measures, p's ≥ .410, η_{p^2}'s ≤ .035. Again, the effect size for the normalised clustering coefficient with RRB T-scores was larger, $F(1,53) = 5.78$, $p = .020$, $\eta_{p^2} = .098$, than with the SCI T-scores, $F(1,53) = 1.22$, $p = .247$, $\eta_{p^2} = .023$.

The same pattern of effect was revealed in the analyses that included cognitive abilities measured by the MSEL at 14 months into the model: the normalised clustering coefficient exhibited a large effect size, $V = .23$, $F(2,49) = 7.31$, $p = .002$, $\eta_{p^2} = .230$. This association was stronger for RRB T-scores, $F(1,52) = 6.23$, $p = .016$, $\eta_{p^2} = .107$, than SCI T-scores, $F(1, 52) = 1.42$, $p = .239$, $\eta_{p^2} = .027$. The multivariate GLM showed minimal effects of global connectivity across all channels or across fronto-central channels, p's ≥ .416, η_{p^2} 's ≤ .035.

In conclusion, the primary analyses revealing an association between lower normalised clustering coefficient and more severe restricted and repetitive behaviours at childhood reported in the main text were not influenced by the confounding variables.

A7.3. Alpha EEG connectivity, change in ASD traits, and confounding variables

A7.3.1. Including the outlier

The main text reports small effects between alpha connectivity parameters and the rate of change in ASD traits during early development when all participants were included. Methodological, clinical, demographical, or cognitive variables might have influenced the findings for associations between connectivity and rates of change in ASD traits. When the number of epochs was included into the multivariate GLM, the effect size for fronto-central connectivity became of medium

size, $V = .07$, $F(2,47) = 1.86$, $p = .167$, $\eta_p^2 = .073$, while the effect sizes for the other connectivity parameters remained small, p's ≥ .533, η_p^2's ≤ .026. Follow-up univariate analyses showed that fronto-central connectivity had a medium effect size on the slope for the RRB subscale, $F(1,50) = 3.25$, $p = .078$, $\eta_p^2 = .061$, suggesting that higher fronto-central alpha connectivity was related to a more negative slope, or a decrease in RRB traits ($B = -0.959$). The association with the slope for the SCI subscale only showed a small effect, $F(1,50) = 0.24$, $p = .623$, $\eta_p^2 = .005$. For analyses including the other methodological variable, power across all channels, all effect sizes remained small as in the primary analyses, p's ≥ .349, η_p^2's ≤ .044.

With regards to clinical characteristics, the multivariate GLM including familial risk revealed a medium effect size for fronto-central connectivity, $V = .07$, $F(2,47) = 1.75$, $p = .186$, $\eta_p^2 = .069$. A medium effect size was also observed for the negative association of fronto-central connectivity with the slope for RRBs, $F(1,50) = 3.96$, $p = .052$, $\eta_p^2 = .073$, but not with the slope of SCI traits, $F(1,50) = 0$, $p = .969$, *partial* $\eta^2 = 0$. The effect sizes in the multivariate GLM for the other connectivity parameters remained small, p's ≥ .533, η_p^2's ≤ .026. The analyses including diagnostic outcome at 3 years of age displayed the same findings: the association for fronto-central connectivity with slopes of ASD traits was of medium effect size, $V = .12$, $F(2,45) = 2.94$, $p = .068$, $\eta_p^2 = .115$, whereas effect sizes for global connectivity across all channels and the normalised clustering coefficient remained small, p's ≥ .440, η_p^2's ≤ .036. The former result occurred due to the larger effect size for the fronto-central connectivity with the RRB slope, $F(1,48) = 6.68$, $p = .013$, $\eta_p^2 = .122$, than the SCI slope, $F(1,48) = 0.01$, $p = .918$, $\eta_p^2 < .0001$.

Another possibility is that the severity of ASD traits during toddlerhood is related to the rate of change. When including both the SCI T-scores measured at 3 years of age into the multivariate, none of the effect sizes for the connectivity parameters reached medium levels, p's ≥ .267, η_p^2's ≤ .055. Including the RRB T-scores at toddlerhood resulted in the same pattern, p's ≥ .352, η_p^2's ≤ .043.

Demographic variables such as gender or age might also be related to the associations between early connectivity parameters and the slope of change in ASD traits. The multivariate GLM with gender revealed a medium effect size for fronto-central connectivity, $V = .09$, $F(2,47) = 2.38$, $p = .104$, $\eta_p^2 = .092$. The negative

association between fronto-central connectivity and the slope of change in RRB traits was stronger than with the slope of change in SCI traits: for the RRB slope, $F(1,50) = 4.50$, $p = .039$, $\eta_p^2 = .083$, and for the SCI slope, $F(1,50) = 0.07$, $p = .792$, $\eta_p^2 = .001$. Effect sizes for the other connectivity parameters in the multivariate GLM were small, p's ≥ .480, η_p^2's ≤ .031. Further multivariate GLM analyses including age at the EEG assessment and the follow-up assessment did not change the pattern of the primary results without the inclusion of these variables: for age at EEG, p's ≥ .300, η_p^2's ≤ .050, and for age at follow-up, p's ≥ .297, η_p^2's ≤ .050.

Finally, I examined whether cognitive abilities at 14 months of age might change the pattern of results when added into the multivariate model. Again, the association with fronto-central connectivity reached a medium effect size, $V = .08$, $F(2,46) = 1.86$, $p = .167$, $\eta_p^2 = .075$. Separate univariate GLMs showed a medium effect for a negative association of fronto-central connectivity with the slope for the change of RRB traits, $F(1,49) = 5.59$, $p = .022$, $\eta_p^2 = .102$, and a minimal effect for the association with the slope of change of SCI traits, $F(1,49) = 0.01$, $p = .917$, $\eta_p^2 < .0001$.

Overall, the results suggest that infant alpha connectivity parameters are not associated with the rate of change in ASD traits during toddlerhood and childhood. When different variables are accounted for however, lower alpha band fronto-central connectivity seems to be associated with a more positive slope of change in RRB traits, as indicated by medium effect sizes for this variable. This change of results occurred when the number of epochs, familial risk, diagnostic outcome at 3 years of age, gender, and cognitive abilities were included, but not when any of the other confounding variables were included.

A7.3.2. Excluding the outlier

As the outlier influenced the primary results, I investigated whether other variables may have influenced these results also in order to provide a more coherent picture of the data. Thus here the outlier was excluded. The results revealed similar patterns to the primary analyses excluding the outlier. When including the number of epochs, global connectivity across all and fronto-central connections showed a small effect, p's ≥ .429, η_p^2's ≤ .036, whereas the normalised clustering coefficient showed a medium effect size, $V = .12$, $F(2,46) = 3.02$, $p = .059$, $\eta_p^2 = .116$. The latter effect size was larger for the RRB subscale, $F(1,49) = 5.69$ p =

.021, η_p^2 = .104, than the SCI subscale, $F(1,49) = 0.99$, p = .326, η_p^2 = .020. The same pattern was observed when including spectral alpha power into the model: a medium effect size for the normalised clustering coefficient, V = .09, $F(2,46) = 2.29$, p = .113, η_p^2 = .090, but small effect sizes for the other alpha connectivity variables, p's ≥ .675, η_p^2's ≤ .017. The medium effect size for the normalised clustering coefficient was increased in size for the RRB subscale, $F(1,49) = 5.64$, p = .022, η_p^2 = .103, but was smaller for the SCI subscale, $F(1,49) = 1.73$, p = .194, η_p^2 = .034.

Turning to the clinical characteristics, including risk group did not change the main pattern of results. The normalised clustering coefficient had a medium sized effect on the change in ASD traits: V = .13, $F(2,46) = 3.33$, p = .045, η_p^2 = .126, whereas the other connectivity parameters had small effect sizes, p's ≥ .326, η_p^2's ≤ .022. The effect size of the normalised clustering coefficient was higher for the RRB subscale, $F(1,49) = 5.42$, p = .024, η_p^2 = .100, than the SCI subscale, $F(1,49) = 2.06$, p = .158, η_p^2 = .040. When including diagnostic outcome at 3 years, both global connectivity across all channels and the normalised clustering coefficient displayed a medium effect size, $V_{Glob\ FC}$ = .06, $F_{Glob\ FC}(2,44) = 1.51$, $p_{Glob\ FC}$ = .232, $\eta_{p\ Glob\ FC}^2$ = .064, and V_{Cnorm} = .10, $F_{Cnorm}(2,44) = 2.57$, p_{Cnorm} = .088, $\eta_{p\ Cnorm}^2$ = .104, while effect size for fronto-central connectivity remained small, V = .045, $F(2, 4) = 1.04$, p = .361, η_p^2 = .045. Follow-up analyses revealed a stronger effect size for the normalised clustering coefficient for the RRB subscale, $F(1,47) = 4.79$, p = .034, η_p^2 = .092, than the SCI subscale $F(1\ 47) = 1.51$, p = .225, η_p^2 = .031. However, effects for global connectivity across all channels were small in the univariate GLMs for both RRB and SCI subscales, p's ≥ .409, η_p^2's ≤ .015.

Next I examined the possibility that initial scores at toddlerhood may have played a role in the results. The pattern of results remained unchanged when including SCI T-scores or RRB T-scores measured at 3 years of age: multivariate GLM effect sizes were medium for the normalised clustering coefficient, $V_{SCI\ T\ included}$ = .11, $F_{SCI\ T\ included}(2,46) = 2.83$, $p_{SCI\ T\ included}$ = .069, $\eta_{p\ SCI\ T\ included}^2$ = .110, and $V_{RRB\ T\ included}$ = .09, $F_{RRB\ T\ included}(2,46) = 2.52$, $p_{RRB\ T\ included}$ = .119, $\eta_{p\ RRB\ T\ included}^2$ = .088, but small for the other connectivity variables, p's ≥ .533, η_p^2's ≤ .027. The univariate analyses showed stronger effects on the slopes for RRB subscale for both SCI and RRB T-scores at toddlerhood, $F_{SCI\ T\ included}(1,49) = 5.39$, $p_{SCI\ T\ included}$ = .024, $\eta_{p\ SCI\ T\ included}^2$ = .099, and $F_{RRB\ T\ included}(1,49) = 5.38$, $p_{RRB\ T\ included}$ = .025, $\eta_{p\ RRB\ T\ included}^2$ = .099,

compared to the effects on the slopes for SCI subscale, $F_{SCI\ T\ included}(1,49) = 2.10$, $p_{SCI\ T\ included} = .154$, $\eta_{p^2\ SCI\ T\ included} = .041$, and $F_{RRB\ T\ included}(1,49) = 2.29$, $p_{RRB\ T\ included} = .136$, $\eta_{p^2\ RRB\ T\ included} = .045$.

The primary results remained unchanged when including demographic data. When including gender, multivariate effect sizes for the normalised clustering coefficient were of medium size, $V = .09$, $F(2,46) = 2.14$, $p = .129$, $\eta_{p^2} = .085$, where the effect was stronger on the slopes of change for the RRB subscale, $F(1,49) = 5.27$, $p = .026$, $\eta_{p^2} = .097$, than the SCI subscale, $F(1,49) = 2.26$, $p = .139$, $\eta_{p^2} = .044$. Multivariate effect sizes for the other connectivity variables were small, p's $\geq .416$, η_{p^2}'s $\leq .037$.

For both ages at EEG and follow-up assessment, the pattern of results remained the same. While global connectivity across all and fronto-central connections revealed small effect sizes in the multivariate, p's $\geq .582$, η_{p^2}'s $\leq .023$, effect sizes for the normalised clustering coefficient were medium sizes for age at EEG, $V = .09$, $F(2,46) = 2.15$, $p = .128$, $\eta_{p^2} = .086$, and age at follow-up assessment, $V = .11$, $F(2,46) = 2.85$, $p = .068$, $\eta_{p^2} = .110$. Again, the effect sizes for the normalised clustering coefficient were stronger for the slope of change in RRB traits, $F_{AgeEEG}(1,49) = 5.07$, $p_{AgeEEG} = .029$, $\eta_{p^2\ AgeEEG} = .094$, and $F_{Age\ Follow\text{-}up}(1,49) = 6.15$, $p_{Age\ Follow\text{-}up} = .017$, $\eta_{p^2\ Age\ Follow\text{-}up} = .112$, than SCI traits, $F_{AgeEEG}(1,49) = 1.95$, $p_{AgeEEG} = .169$, $\eta_{p^2\ AgeEEG} = .038$, and $F_{Age\ Follow\text{-}up}(1,49) = 2.50$, $p_{Age\ Follow\text{-}up} = .121$, $\eta_{p^2\ Age\ Follow\text{-}up} = .048$.

Finally, the effect of including MSEL scores into the multivariate model was investigated. Similar to the other results, a medium effect size of the normalised clustering coefficient on the slopes of change in SRS-2 scales was found, $V = .11$, $F(2,45) = 2.81$, $p = .071$, $\eta_{p^2} = .111$. The effect sizes for the other connectivity variables remained small, p's $\geq .560$, η_{p^2}'s $\leq .025$. The follow-up analyses revealed stronger effect sizes of the normalised clustering coefficient for the slopes of change in RRB traits, $F(1,48) = 7.58$, $p = .008$, $\eta_{p^2} = .136$, than the slopes of change in SCI traits, $F(1,46) = 1.97$, $p = .167$, $\eta_{p^2} = .039$.

A7.4. Theta connectivity, childhood ASD traits, and confounding variables

Tables for theta connectivity parameters and later ASD traits during childhood while taking into account possible confounding variables are presented in below. Results without taking into account any other variables are reported in Table 7.3.

Table A7.1. Partial correlations for theta band connectivity differences between the social and non-social condition with ASD traits during childhood while taking into account the *number of epochs*

	SRS-2 Subscale	
	SCI T-scores	*RRB T-scores*
Global connectivity across all channels	r = -.14, p = .569, [-.50, .46]	r = -.14, p = .581, [-.38, .14]
Connectivity across selected channels	r = -.06, p = .828, [-.44, .41]	r = -.17, p = .489, [-.39, .06]
Normalised clustering coefficient	r = .21, p = .415, [-.25, .60]	r = -.02, p = .926, [-.38, .31]

Correlation values, with p-values, and bias corrected and accelerated bootstrap 95% confidence intervals in square brackets.

Table A7.2. Partial correlations for theta band connectivity differences between the social and non-social condition with ASD traits during childhood while taking into account *spectral power differences between conditions*

	SRS-2 Subscale	
	SCI T-scores	*RRB T-scores*
Global connectivity across all channels	r = -.06, p = .817, [-.52, .66]	r = -.10, p = .681, [-.43, .20]
Connectivity across selected channels	r = .04, p = .886, [-.55, .72]	r = -.19, p = .457, [-.56, .48]
Normalised clustering coefficient	r = .23, p = .362, [-.25, .62]	r = -.02, p = .930, [-.32, .20]

Correlation values, with p-values, and bias corrected and accelerated bootstrap 95% confidence intervals in square brackets.

Table A7.3. Partial correlations for theta band connectivity differences between the social and non-social condition with ASD traits during childhood while taking into account *familial risk*

	SRS-2 Subscale	
	SCI T-scores	*RRB T-scores*
Global connectivity across all channels	*r* = .01, *p* = .984, [-.32, .60]	*r* = -.05, *p* = .860, [-.26, .26]
Connectivity across selected channels	*r* = .03, *p* = .897, [-.36, .64]	*r* = -.16, *p* = .532, [-.41, .33]
Normalised clustering coefficient	*r* = .26, *p* = .305, [-.19, .66]	*r* = -.01, *p* = .963, [-.33, .28]

Correlation values, with p-values, and bias corrected and accelerated bootstrap 95% confidence intervals in square brackets.

Table A7.4. Partial correlations for theta band connectivity differences between the social and non-social condition with ASD traits during childhood while taking into account *diagnostic outcome at 3 years of age*

	SRS-2 Subscale	
	SCI T-scores	*RRB T-scores*
Global connectivity across all channels	*r* = .01, *p* = .975, [-.44, .55]	*r* = -.04, *p* = .888, [-.30, .16]
Connectivity across selected channels	*r* = -.02, *p* = .943, [-.38, .39]	*r* = -.22, *p* = .379, [-.58, .24]
Normalised clustering coefficient	*r* = .16, *p* = .520, [-.16, .59]	*r* = -.14, *p* = .576, [-.47, .23]

Correlation values, with p-values, and bias corrected and accelerated bootstrap 95% confidence intervals in square brackets.

Table A7.5. Partial correlations for theta band connectivity differences between the social and non-social condition with ASD traits during childhood while taking into account *gender*

	SRS-2 Subscale	
	SCI T-scores	*RRB T-scores*
Global connectivity across all channels	*r* = -.07, *p* = .779, [-.42, .47]	*r* = -.10, *p* = .699, [-.28, .07]
Connectivity across selected channels	*r* = .11, *p* = .674, [-.28, .62]	*r* = -.10, *p* = .698, [-.48, .57]
Normalised clustering coefficient	*r* = .13, *p* = .601, [-.21, .62]	*r* = -.01, *p* = .607, [-.43, .30]

Correlation values, with p-values, and bias corrected and accelerated bootstrap 95% confidence intervals in square brackets.

Table A7.6. Partial correlations for theta band connectivity differences between the social and non-social condition with ASD traits during childhood while taking into account *age at EEG assessment*

	SRS-2 Subscale	
	SCI T-scores	*RRB T-scores*
Global connectivity across all channels	*r* = -.14, *p* = .589, [-.50, .57]	*r* = -.15, *p* = .553, [-.44, .17]
Connectivity across selected channels	*r* = -.03, *p* = .916, [-.54, .75]	*r* = -.19, *p* = .463, [-.52, .53]
Normalised clustering coefficient	*r* = .18, *p* = .468, [-.32, .68]	*r* = -.07, *p* = .784, [-.41, .28]

Correlation values, with p-values, and bias corrected and accelerated bootstrap 95% confidence intervals in square brackets.

Table A7.7. Partial correlations for theta band connectivity differences between the social and non-social condition with ASD traits during childhood while taking into account *age at follow-up assessment*

	SRS-2 Subscale	
	SCI T-scores	*RRB T-scores*
Global connectivity across all channels	r = -.17, p = .501, [-.61, .45]	r = -.12, p = .648, [-.41, .19]
Connectivity across selected channels	r = -.10, p = .701, [-.54, .41]	r = -.16, p = .516, [-.51, .19]
Normalised clustering coefficient	r = .20, p = .420, [-.27, .55]	r = .02, p = .950, [-.43, .37]

Correlation values, with p-values, and bias corrected and accelerated bootstrap 95% confidence intervals in square brackets.

Table A7.8. Partial correlations for theta band connectivity differences between the social and non-social condition with ASD traits during childhood while taking into account *MSEL score at 14 months of age*

	SRS-2 Subscale	
	SCI T-scores	*RRB T-scores*
Global connectivity across all channels	r = -.17, p = .489, [-.51, .42]	r = -.20, p = .435, [-.42, .006]
Connectivity across selected channels	r = -.13, p = .615, [-.51, .46]	**r = -.32, p = .203, [-.64, .20]**
Normalised clustering coefficient	r = .20, p = .420, [-.17, .57]	r = -.08, p = .759, [-.43, .29]

Correlation values, with p-values, and bias corrected and accelerated bootstrap 95% confidence intervals in square brackets. The correlation reaching a medium effect size is printed in bold.

A7.5. Theta connectivity, change in ASD traits, and confounding variables

Tables for theta connectivity parameters and change of ASD traits during toddlerhood and childhood while taking into account possible confounding variables are presented in here. Results without taking into account any other variables are reported in Table 7.4.

Table A7.9. Associations for theta band connectivity differences between the social and non-social condition with the slope of change in ASD traits between toddlerhood and childhood while taking into account *number of epochs*

	SRS-2 Subscale	
	Slope for SCI T-scores	*Slope for RRB T-scores*
Global connectivity across all channels	r = -.15, p = .603, [-.45, .17]	r = -.05, p = .848, [-.37, .33]
Connectivity across selected channels	r = .02, p = .932, [-.43, .41]	r = .00, p = .994, [-.39, .45]
Normalised clustering coefficient	r = .01, p = .975, [-.43, .43]	r = .13, p = .638, [-.39, .60]

Spearman correlation values, with p-values, and bias corrected and accelerated bootstrap 95% confidence intervals in square brackets.

Table A7.10. Associations for theta band connectivity differences between the social and non-social condition with the slope of change in ASD traits between toddlerhood and childhood while taking into account *power across all channels*

	SRS-2 Subscale	
	Slope for SCI T-scores	*Slope for RRB T-scores*
Global connectivity across all channels	r = .13, p = .646, [-.34, .77]	r = -.13, p = .638, [-.58, .55]
Connectivity across selected channels	r = .27, p = .335, [-.47, .78]	r = -.04, p = .900, [-.43, .60]
Normalised clustering coefficient	r = -.08, p = .782, [-.42, .50]	r = .12, p = .658, [-.37, .63]

Spearman correlation values, with p-values, and bias corrected and accelerated bootstrap 95% confidence intervals in square brackets.

Table A7.11. Associations for theta band connectivity differences between the social and non-social condition with the slope of change in ASD traits between toddlerhood and childhood while taking into account *risk group*

	SRS-2 Subscale	
	Slope for SCI T-scores	*Slope for RRB T-scores*
Global connectivity across all channels	*r* = -.15, *p* = .586, [-.48, .42]	*r* = -.06, *p* = .820, [-.36, .52]
Connectivity across selected channels	*r* = .03, *p* = .922, [-.44, .57]	*r* = -.01, *p* = .964, [-.36, .56]
Normalised clustering coefficient	*r* = .01, *p* = .970, [-.55, .50]	*r* = .13, *p* = .651, [-.49, .74]

Spearman correlation values, with p-values, and bias corrected and accelerated bootstrap 95% confidence intervals in square brackets.

Table A7.12. Associations for theta band connectivity differences between the social and non-social condition with the slope of change in ASD traits between toddlerhood and childhood while taking into account *diagnostic group at 3 years of age*

	SRS-2 Subscale	
	Slope for SCI T-scores	*Slope for RRB T-scores*
Global connectivity across all channels	*r* = -.16, *p* = .582, [-.61, .40]	*r* = -.05, *p* = .852, [-.35, .42]
Connectivity across selected channels	*r* = .03, *p* = .929, [-.55, .58]	*r* = -.01, *p* = .975, [-.39, .61]
Normalised clustering coefficient	*r* = .01, *p* = .968, [-.65, .48]	*r* = .13, *p* = .653, [-.48, .75]

Spearman correlation values, with p-values, and bias corrected and accelerated bootstrap 95% confidence intervals in square brackets.

Table A7.13. Associations for theta band connectivity differences between the social and non-social condition with the slope of change in ASD traits between toddlerhood and childhood while taking into account *SCI T-scores during toddlerhood*

	SRS-2 Subscale	
	Slope for SCI T-scores	*Slope for RRB T-scores*
Global connectivity across all channels	r = -.19, p = .496, [-.62, .36]	r = -.08, p = .767, [-.50, .54]
Connectivity across selected channels	r = -.01, p = .966, [-.58, .63]	r = -.04, p = .903, [-.55, .92]
Normalised clustering coefficient	r = .02, p = .956, [-.60, .63]	r = .13, p = .641, [-.58, .83]

Spearman correlation values, with p-values, and bias corrected and accelerated bootstrap 95% confidence intervals in square brackets.

Table A7.14. Associations for theta band connectivity differences between the social and non-social condition with the slope of change in ASD traits between toddlerhood and childhood while taking into account *RRB T-scores during toddlerhood*

	SRS-2 Subscale	
	Slope for SCI T-scores	*Slope for RRB T-scores*
Global connectivity across all channels	r = -.17, p = .556, [-.61, .37]	r = -.13, p = .636, [-.49, .45]
Connectivity across selected channels	r = 0, p = .998, [-.61, .71]	r = -.11, p = .706, [-.51, .79]
Normalised clustering coefficient	r = -.01, p = .963, [-.54, .50]	r = .06, p = .844, [-.49, .68]

Spearman correlation values, with p-values, and bias corrected and accelerated bootstrap 95% confidence intervals in square brackets.

Table A7.15. Associations for theta band connectivity differences between the social and non-social condition with the slope of change in ASD traits between toddlerhood and childhood while taking into account *gender*

	SRS-2 Subscale	
	Slope for SCI T-scores	*Slope for RRB T-scores*
Global connectivity across all channels	*r* = -.16, *p* = .578, [-.40, .14]	*r* = -.03, *p* = .904, [-.29, .35]
Connectivity across selected channels	*r* = .02, *p* = .936, [-.32, .36]	*r* = .02, *p* = .945, [-.21, .32]
Normalised clustering coefficient	*r* = .01, *p* = .973, [-.40, .39]	*r* = .13, *p* = .640, [-.46, .76]

Spearman correlation values, with p-values, and bias corrected and accelerated bootstrap 95% confidence intervals in square brackets.

Table A7.16. Associations for theta band connectivity differences between the social and non-social condition with the slope of change in ASD traits between toddlerhood and childhood while taking into account *age at EEG assessment*

	SRS-2 Subscale	
	Slope for SCI T-scores	*Slope for RRB T-scores*
Global connectivity across all channels	*r* = -.21, *p* = .464, [-.56, .18]	*r* = -.15, *p* = .600, [-.44, .26]
Connectivity across selected channels	*r* = -.05, *p* = .862, [-.53, .51]	*r* = -.14, *p* = .632, [-.58, .44]
Normalised clustering coefficient	*r* = .00, *p* = .996, [-.54, .52]	*r* = .11, *p* = .686, [-.49, .68]

Spearman correlation values, with p-values, and bias corrected and accelerated bootstrap 95% confidence intervals in square brackets.

Table A7.17. Associations for theta band connectivity differences between the social and non-social condition with the slope of change in ASD traits between toddlerhood and childhood while taking into account *age at follow-up assessment*

	SRS-2 Subscale	
	Slope for SCI T-scores	*Slope for RRB T-scores*
Global connectivity across all channels	*r* = -.09, *p* = .739, [-.47, .41]	*r* = -.13, *p* = .649, [-.49, .39]
Connectivity across selected channels	*r* = .18, *p* = .599, [-.37, .63]	*r* = -.14, *p* = .629, [-.69, .52]
Normalised clustering coefficient	*r* = .06, *p* = .830, [-.43, .47]	*r* = .08, *p* = .770, [-.41, .62]

Spearman correlation values, with p-values, and bias corrected and accelerated bootstrap 95% confidence intervals in square brackets.

Table A7.18. Associations for theta band connectivity differences between the social and non-social condition with the slope of change in ASD traits between toddlerhood and childhood while taking into account *cognitive abilities measured by MSEL scores at 14 months of age*

	SRS-2 Subscale	
	Slope for SCI T-scores	*Slope for RRB T-scores*
Global connectivity across all channels	*r* = -.14, *p* = .617, [-.49, .30]	*r* = -.06, *p* = .841, [-.45, .46]
Connectivity across selected channels	*r* = .06, *p* = .842, [-.45, .55]	*r* = -.01, *p* = .969, [-.45, .56]
Normalised clustering coefficient	*r* = .02, *p* = .942, [-.45, .44]	*r* = .13, *p* = .652, [-.48, .69]

Spearman correlation values, with p-values, and bias corrected and accelerated bootstrap 95% confidence intervals in square brackets.

A7.6. Exploring subgroups with different behavioural and neural phenotypes

The results in Chapter 7 suggest that there might be different subgroups showing different patterns of behavioural and connectivity phenotypes. Stratification based on behavioural and neural phenotypes could help managing the heterogeneity in the disorder, as more homogeneous subgroups could reveal different underlying mechanisms (Loth et al., 2016). Here, I explored whether it would be possible to create subgroups with children showing similarities in developmental trajectories of ASD traits, or alpha connectivity parameters (analyses for theta parameters were not performed due to the small sample size of 19 participants).

For the exploratory subgroup analyses, I focussed on the 53 children included in the alpha analyses with data available for the SRS-2 at both toddlerhood and childhood. Subgroups for the behavioural phenotype were defined using hierarchical cluster analysis (Ward's method) with standardized values for the SRS-2 T-scores for the SCI and RRB subscales at toddlerhood and childhood, and the slopes of change for both subscales. This method was chosen based on its exploratory options, since it can be performed without pre-specifying the number of clusters. The number of clusters that would best fit the data was chosen based on the coefficients in the agglomeration schedule, and visualisation of the raw data, and dendograms. The number of clusters that would lead to the largest change in the coefficients, and be most informative, would be selected for the definition of subgroups. The same method was used to create subgroups for the neural phenotype using global alpha connectivity across all connections, global alpha connectivity across fronto-central connections, and the normalised clustering coefficient as variables. Finally, I explored whether the subgroups differed on multiple dimensions by cross-comparing differences in alpha connectivity parameters between behavioural phenotype subgroups, and differences in ASD traits and trajectories between neural phenotype subgroups.

A7.6.1. Defining subgroups

First, subgroups were defined based on behavioural data. Cluster analyses revealed that 4 clusters would best fit the data, hereafter referred to by cluster A, B, C, and D (see Fig. A7.1A). Overall, cluster A included children with high severity of ASD traits, and stable severity or increases in severity during childhood (N = 4). Cluster B was characterised by stable low severity of ASD traits (N = 40). Cluster C included children with overall high severity of traits, and stable severity or

decreases in severity during childhood (N = 3). Finally, cluster D involved children who showed low severity at toddlerhood, and higher severity of ASD traits during childhood (N = 6).

Second, subgroups were created based on the alpha connectivity parameters (see Fig. A7.1B). Four clusters were derived from the data: cluster 1) overall lower values for each connectivity parameter (N = 21), cluster 2) medium values for all connectivity parameters (N = 20), cluster 3) higher global connectivity across all and fronto-central connections, and medium normalised clustering coefficients (N = 6), and cluster 4) medium values for global connectivity across all and fronto-central connections, and higher normalised clustering coefficient (N = 6).

(Next page)

Figure A7.1. Subgroups based on behavioural and alpha EEG connectivity data
Clusters A, B, C, and D were based on SRS-2 data (left for SCI subscale, and right RRB scale in panel A). Clusters 1, 2, 3, and 4 were based on connectivity parameters (panel B, global connectivity across all connections on x-axis, global connectivity across fronto-central connection on the y-axis, and normalised clustering coefficient on the z-axis). Connectivity data marked by behavioural subgroups, and behavioural data marked by neural subgroups are displayed in panel C and D, respectively.
Bars denote means, and error bars 1 standard deviation. Note in panel C connectivity data for global measures are plotted against the left y-axis, and for normalised coefficient against the right y-axis, and the outlier marked in red was excluded from calculations of the mean and standard deviation for cluster C.

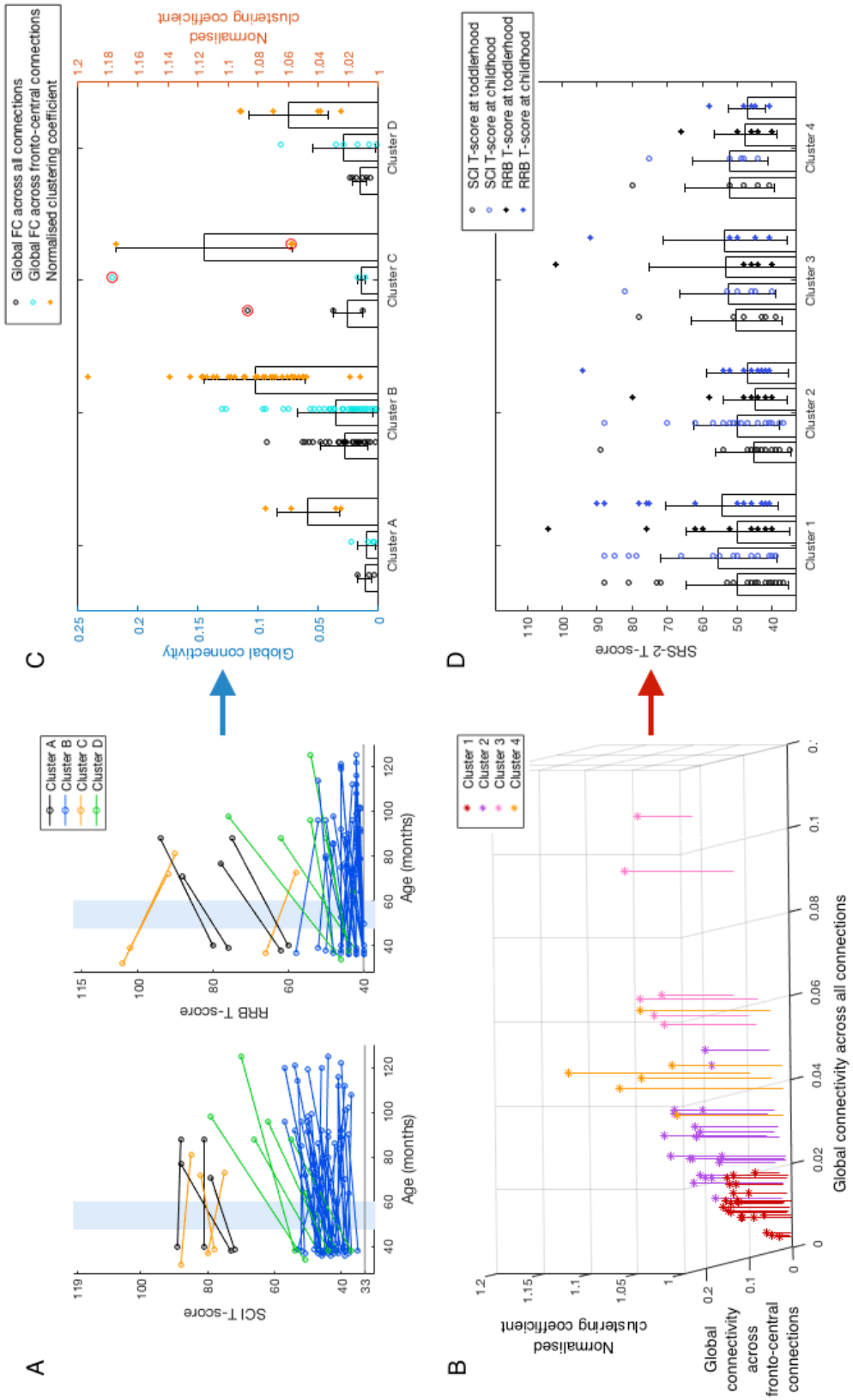
A
SCI T-score
RRB T-score
Age (months)
Cluster A
Cluster B
Cluster C
Cluster D
B
Normalised clustering coefficient
Global connectivity across fronto-central connections
Global connectivity across all connections
Cluster 1
Cluster 2
Cluster 3
Cluster 4
C
Global connectivity
Normalised clustering coefficient
Global FC across all connections
Global FC across fronto-central connections
Normalised clustering coefficient
D
SRS-2 T-score
SCI T-score at toddlerhood
SCI T-score at childhood
RRB T-score at toddlerhood
RRB T-score at childhood

The results of the cluster analyses suggest that it is possible to create subgroups with similar developmental trajectories of ASD traits, and similar patterns of brain connectivity parameters. This further illustrates that the use of multiple measures when creating more homogeneous subgroups might provide better stratification methods compared to stratifying based on a single measure.

A7.6.2. Cross-comparing subgroups

After defining subgroups based on behavioural and neural data, the next questions are whether these subgroups based on behavioural data show different connectivity patterns, and whether subgroups based on connectivity data shows different behavioural patterns. Figure A7.1C shows the distributions of connectivity data for the behavioural clusters suggesting that there are differences between groups. Overall, children in clusters A, C, and D with higher symptom severity at both ages or at childhood show lower global connectivity parameters compared to the children in cluster B with low severity of symptoms throughout childhood. Exploratory analyses using a multivariate GLM with 4 behavioural phenotype subgroups as factor and the 3 connectivity parameters as dependent variables suggested that there is a medium sized effect of group, $V = .25$, $F(9,147) = 1.46$, $p = .167$, $\eta_p^2 = .082$ (and a large sized effect when excluding the outlier in cluster C: $V = .42$, $F(9,144) = 2.63$, $p = .008$, $\eta_p^2 = .141$). Although subgroups displayed similar clustering coefficients, global alpha across all connections was higher in cluster B than in both cluster A and D, and higher across fronto-central connections in cluster B than cluster A. Small sample sizes for the groups however do not allow for further group analyses.

For the neural phenotype subgroups, SRS-2 data are presented in figure A7.1D. One might suggest that participants in cluster 1 characterised by relatively low normalised clustering also show strong increases in severity for SRS-2 SCI and RRB measures, which is in line with the earlier observed association between normalised clustering and severity of symptoms during childhood. Participants in cluster 2 with medium values of normalised clustering show medium increases in severity of symptoms, while participants in clusters 3 and 4 show more stable trajectories. Results from the multivariate GLM with 4 neural phenotype subgroups as factor and the 6 variables derived from SRS-2 measures as

dependent variables suggested that there is a medium sized effect of group, $V = .37$, $F(18,138) = 1.07$, $p = .392$, $\eta_p^2 = .122$.

Together the exploratory findings suggest that deriving subgroups based on behavioural and neural phenotypes using multiple measures is possible. The data suggest that subgroups showing lower values on alpha band connectivity parameters also showed higher severity and less stability of ASD traits during toddlerhood and childhood. Specifically, the cluster exhibiting relatively low normalised clustering coefficients also displayed increased levels of severity during childhood.

It should be noted however that the results of the exploratory analyses in this section should be interpreted with caution due to a small sample of participants. It has been suggested that samples should include 2^m participants, where m is the number of variables (Dolnicar, 2002). In the cluster analyses based on behavioural data, 6 variables were included. This analysis thus required $2^6 = 64$ participants, whereas data were available for only 53 participants. Studies including larger samples will be able to further clarify how individuals with ASD might be stratified into different subgroups of ASD based on behavioural and neural phenotypes.

A7.7. Associations between SRS-2 and ADI-R measures of ASD traits at toddlerhood

Results for correlations between SRS-2 and ADI-R scores are reported in Table A7.19. For the social communication and interactions domains, Pearson correlations were calculated between SRS-2 T-scores on DSM-V compatible subscale for Social Communication and Interactions, and ADI-R sum of scores on the Social Total and Communication Total algorithms. For the restricted and repetitive behaviour domain, Pearson correlations were calculated between SRS-2 T-scores on DSM-V compatible subscale for Restricted and Repetitive Behaviours, and ADI-R Restricted and Repetitive Behaviours Total algorithm (bivariate correlation in table A7.19).

For the partial correlations, the same measures were included, and each of the 3 alpha connectivity parameters were the third variable correlations would be accounted for (partial correlations in table A7.19).

Table A7.19. Associations between SRS-2 and ADI-R scores at toddlerhood

Bivariate correlation	*Social communication and interaction domain*	*Restricted and repetitive behaviour domain*
SRS-2 and ADI-R scores	r = .84, p < .001, [.68, .94]	r = .70, p < .001, [.42, .86]
Partial correlations controlling for:		
Global alpha connectivity across all connections	r = .84, p < .001, [.68, .93]	r = .69, p < .001, [.45, .83]
Global alpha connectivity across fronto-central connections	r = .85, p < .001, [.69, .94]	r = .69, p < .001, [.44, .86]
Normalised clustering coefficient	r = .84, p < .001, [.65, .94]	r = .70, p < .001, [.42, .87]

Pearson correlation values, with p-values, and bias corrected and accelerated bootstrap 95% confidence intervals in square brackets.

A7.8. Associations between SRS-2 and alpha connectivity measures of ASD traits at toddlerhood

None of the associations between SRS-2 Subscales and alpha connectivity parameters reached significance, even though one would expect that connectivity across fronto-central connections would be related to SRS-2 T-scores for the Restricted and Repetitive Behaviours domain.

Table A7.20. Associations between alpha connectivity parameters at infancy and SRS-2 scores at toddlerhood

	SRS-2 Subscale	
All HR participants (N = 33)	*SCI T-scores*	*RRB T-scores*
Global alpha connectivity across all connections	r = .11, p = .555, [-.26, .47]	r = .10, p = .598, [-.24, .44]
Global alpha connectivity across fronto-central connections	r = .07, p = .707, [-.29, .41]	r = 0, p = .999, [-.37, .37]

Normalised clustering coefficient	r = .02, p = .932, [-.36, .41]	r = -.11, p = .555, [-.41, .23]

HR-TD participants (N = 17)	*SCI T-scores*	*RRB T-scores*
Global alpha connectivity across all connections	r = .12, p = .638, [-.42, .66]	r = .10, p = .703, [-.46, .61]
Global alpha connectivity across fronto-central connections	r = .16, p = .553, [-.32, .66]	r = .02, p = .947, [-.47, .59]
Normalised clustering coefficient	r = .11, p = .669, [-.42, .65]	r = .09, p = .739, [-.46, .60]

HR-Atyp participants (N = 7)	*SCI T-scores*	*RRB T-scores*
Global alpha connectivity across all connections	r = .09, p = .667, [-1, .97]	r = -.37, p = .413, [-1, .78]
Global alpha connectivity across fronto-central connections	r = -.13, p = .786, [-1, 1]	r = -.44, p = .317, [-1, .87]
Normalised clustering coefficient	r = -.15, p = .756, [-1, 1]	r = -.22, p = .632, [-1, .87]

HR-ASD participants (N = 9)	*SCI T-scores*	*RRB T-scores*
Global alpha connectivity across all connections	r = .15, p = .700, [-.89, .90]	r = .22, p = .569, [-.84, 1]
Global alpha connectivity across fronto-central connections	r = -.02, p = .966, [-.88, .79]	r = .09[+], p = .828, [-.87, .90]
Normalised clustering coefficient	r = -.10, p = .798, [-.82, .84]	r = -.20, p = .600, [-.94, .82]

Spearman correlation values, with p-values, and bias corrected and accelerated bootstrap 95% confidence intervals in square brackets.

[+] Expected to reach significance based on previous findings by Orekhova and colleagues (2014), and in Chapter 4.